An Evaluation of the Bubble Point Method for Determining Pore Size Distributions of Nonwoven Geotextiles

by

David William Hayes

A thesis submitted to the Graduate Faculty of
Auburn University
in partial fulfillment of the
requirements for the Degree of
Master of Science

Auburn, Alabama
August 3, 2013

Keywords: ASTM D6767, bubble point, pore size distribution, nonwoven geotextile, filtration, residual fluid

Approved by

David J. Elton, Chair, Professor of Civil Engineering
J. Brian Anderson, Associate Professor of Civil Engineering
Jacob H. Dane, Emeritus Professor of Agronomy and Soils

Abstract

Nonwoven geotextiles are commonly used in soil filtration applications. A geotextile filter must retain soil particles, while allowing permeability to water and being resistant to clogging. Geotextile filter performance is related to the pore sizes of the geotextile. Therefore, knowledge of the size of geotextile pores is necessary for filtration design. The most common method for evaluating geotextile pore size is the AOS test, which uses a single number that only reflects the larger pore sizes of the geotextile. Methods for measuring all of the pore sizes of a geotextile and determining the distribution of pore sizes have been studied in recent years. Among these methods is the capillary flow porometry method, known commonly in the geotextile field as the bubble point method or test, which has been standardized by ASTM International as method D6767.

This thesis presents a study of the bubble point method and related observations by the author. Methods for quantifying geotextile pore structure are discussed, along with a detailed description of bubble point method theory and background. A review of the contact angle, an important parameter needed to calculate pore size, is presented. A detailed description of a bubble point testing apparatus developed at Auburn University is presented and the procedure used to conduct the bubble point test is discussed. An automated spreadsheet for reducing bubble point test data is described. The results of multiple bubble point tests performed on a nonwoven geotextile are presented along with various statistical analyses. The influence of three parameters used to calculate pore size

(i.e., the contact angle, the capillary constant, and surface tension) are examined. Residual fluid is investigated as a source of error for pore size distributions determined using the bubble point method.

Acknowledgments

It is a pleasure to acknowledge several individuals for their contributions to this work. To my parents, Jim and Mary Hayes, and my brother, Jonathan, thank you for all of your love, support, and encouragement, both during my work on this thesis and through the years. To my amazing wife, Amanda, thank you for your constant love, patience, and understanding during the entire thesis process. This would not have been possible without your support. It was an honor to have three outstanding faculty members serve on my graduate committee. To Dr. Brian Anderson, thank you for your keen input and the dedication you show to Civil Engineering students at Auburn University. To Dr. Jacob Dane, thank you for your insightful comments and your wonderful Soil Physics class. To my committee chair, Dr. David Elton, I cannot say enough to express my gratitude and appreciation for your dedication, support, encouragement, and everything you have taught me over the years.

I would like to thank the following individuals and publishers for granting permission to use copyrighted material in this thesis: Dr. Shobha Bhatia, Dr. Greg Fischer, Paul Webb of Micromeritics Instrument Corporation, ASTM International, Institution of Civil Engineers (ICE) Publishing, and Taylor and Francis Group LLC Books.

Table of Contents

List of Tables

List of Figures

List of Abbreviations

2-EH	2-ethyl hexanol
AOS	Apparent Opening Size
ASTM	American Society for Testing and Materials, now known as ASTM International
CI	confidence interval
DCA	dynamic contact angle, as in the Dynamic Contact Angle Analyzer
ft	feet
in	inches
L	liters
LCL	lower confidence limit
LTL	lower tolerance limit
m	meters
MARV	minimum average roll value
MaxARV	maximum average roll value
min	minutes
mm	millimeters
mN	milli-Newtons
N	Newtons
No.	number
O_n	the nth % opening size of a porous media; for example, O_{95} would be the 95% opening size; O_n is equivalent to n % finer
Pa	Pascals

PSD	pore size distribution
psig	gage pressure, pounds per square inch
s	seconds
TI	tolerance interval
UCL	upper confidence limit
UTL	upper tolerance limit
μm	micrometers
U.S.	United States
USD	United States dollars
USEPA	United States Environmental Protection Agency

Chapter 1: Introduction

1.1 Geotextiles

Geotextiles are synthetic, porous fabrics that are used in a variety of engineering applications. Major engineering applications of geotextiles include separation of dissimilar materials, reinforcement of weak soils and other materials, filtration (cross-plane flow), and drainage (in-plane flow) (Koerner 2005). Common polymers used to create geotextiles include polypropylene and polyethylene. Geotextiles are classified into two general types based upon their manufacturing process: woven and nonwoven. Examples of woven and nonwoven geotextiles are shown in Figure 1.1. Woven geotextiles, as the name indicates, are woven in a regular pattern much like a basket. Nonwoven geotextiles are much more fabric-like, with a random pattern and heterogeneous structure. Nonwoven geotextiles are composed of fibers bonded together mechanically (needlepunched), thermally (heat bonded), or chemically (resin bonded), creating a "network of interconnected pores" (Elsharief and Lovell 1996). Needlepunched nonwovens are "subdivided into continuous filament (long fibers) and staple (short fibers)" (Marino 2006). Nonwoven geotextiles, which are commonly used in soil filtration applications, are the focus of this thesis.

Figure 1.1: Examples of geotextiles, showing four nonwoven samples (left) and three woven samples (right). *Source:* Wikipedia Commons 2008.

1.2 Geotextiles as Filters

One of the major applications of geotextiles is filtration. In fact, filtration was the first intended application. According to Koerner (2005), "geotextiles were initially intended to be an alternative to granular soil filters, and thus the original (and still sometimes used) term for geotextiles is 'filter fabrics'." Filters must perform the conflicting mechanisms of retaining one medium while being permeable to another medium. In the case of geotextile filters, soil particles are the medium that must be retained and water is the medium that must be allowed to permeate. Filtration refers to water flow perpendicular to the plane of the geotextile, whereas water flow within the

geotextile plane is referred to as drainage. A schematic of a geotextile filter is shown in Figure 1.2.

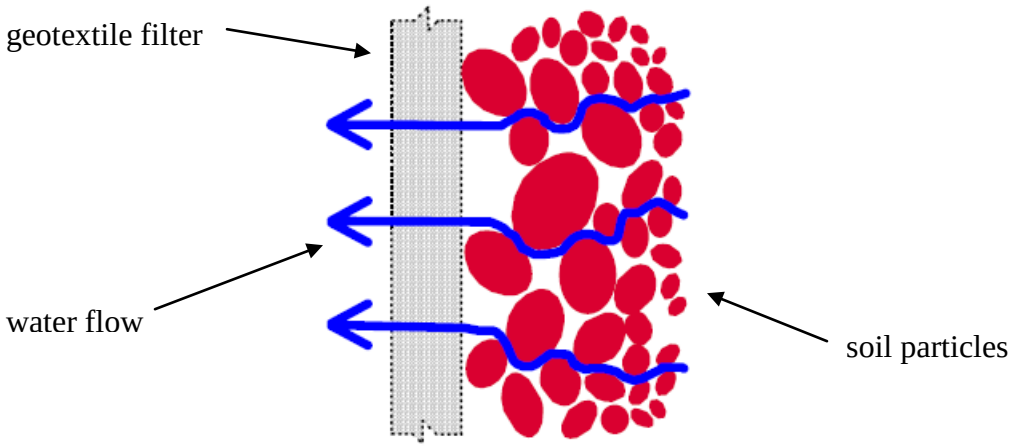

Figure 1.2: A schematic of a geotextile filter retaining soil particles while allowing water to permeate. Note that water flow is perpendicular to the plane of the geotextile. *Source:* Gourc and Palmeira, undated leaflet.

"Nonwoven geotextiles are more frequently used as filters than woven geotextiles due to their high permittivity and non-uniform pore structure … and this heterogeneous pore structure provides a better retention capability" (Aydilek et al. 2005). Geotextile filters are commonly used "in conventional pipe underdrains, behind rigid retaining walls, in earth dams, beneath erosion-control structures, and in landfill leachate collection systems" (Bhatia and Smith 1994). In addition to the basic requirements of adequate retention of soil particles and permeability to water, geotextile filters must maintain adequate permeability to water throughout their design lifetime. In other words, geotextile filters must resist clogging. Resistance to clogging is an important consideration, since the design lifetime of geotextile filters is normally many years and they typically cannot be easily replaced without disruption of a larger engineered system. As with conventional graded granular soil filters, geotextile filters are "generally selected

such that enough larger soil particles are retained to develop a soil 'bridge' leading to the development of a stable soil structure which is able to prevent further migration" (Christopher and Fischer 1992). In this sense, "it has been suggested that the geotextile serves as a *catalyst* to promote the upstream [retained] soil … to generate its own internal filter system" (Koerner 2005).

1.3 Nonwoven Geotextile Pore Structure

In order to properly select a geotextile for a specific filtration application, some measurement of the pore sizes of the geotextile must be made to compare to the soil particle sizes that are to be retained. However, quantifying the pore sizes of nonwoven geotextiles is challenging because the pores are relatively small (pores cannot generally be discerned without magnification), and the pore structure is complex and non-uniform. A photograph of a typical nonwoven geotextile viewed with magnification is shown in Figure 1.3. For an image of a nonwoven geotextile magnified using an electron microscope, see Korkut (2003). Figure 1.3 demonstrates the complexity of nonwoven geotextile pore structure.

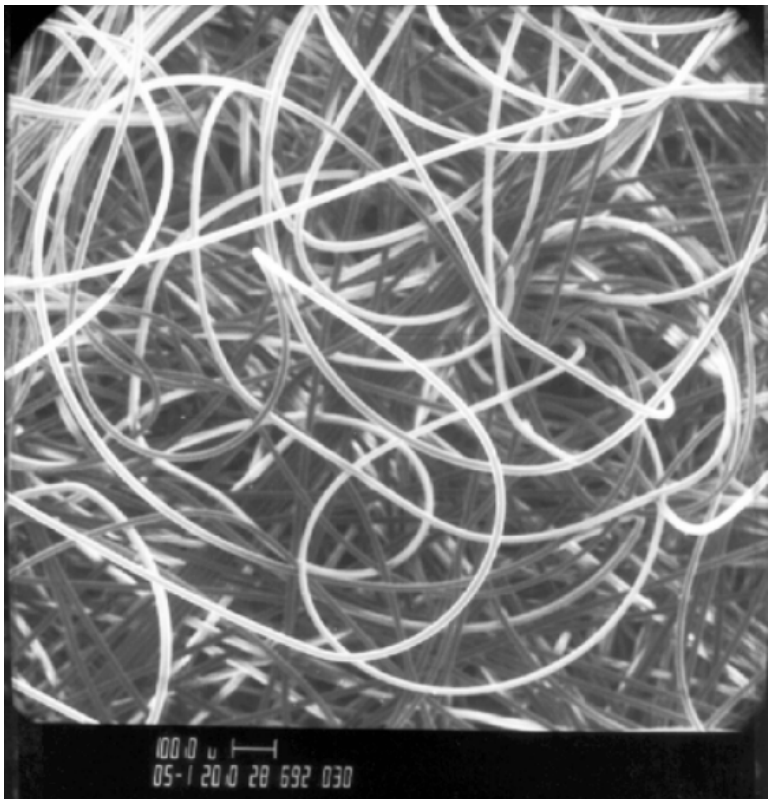

Figure 1.3: A typical nonwoven geotextile, magnified 40x. *Source:* Bhatia and Smith 1996a. Used with permission.

One of the first steps toward quantifying or modeling a real-world system is to develop a conceptual model of the system. Two examples of conceptual models for nonwoven geotextile pore structure are provided in Figures 1.4 and 1.5. Two important aspects of conceptualized nonwoven geotextile pore structure are identified in Figures 1.4 and 1.5. First, the pore channel opening or pore size varies throughout the pore channel, with the minimum opening identified as the "pore channel constriction", "constriction size", or "pore constriction". Secondly, some pore channels may be fully transmissive across the plane of the geotextile while others, known as "dead-end pores", are not. In liquid intrusion and extrusion techniques for determining pore size, pores are typically idealized as cylindrical capillary tubes.

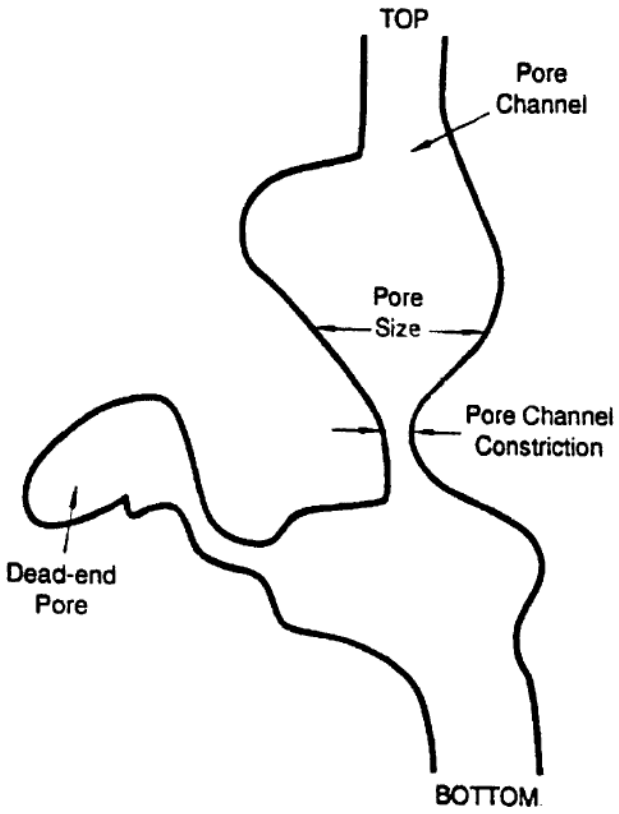

Figure 1.4: A conceptual model of nonwoven geotextile pore structure. *Source:* Fischer 1994. Used with permission.

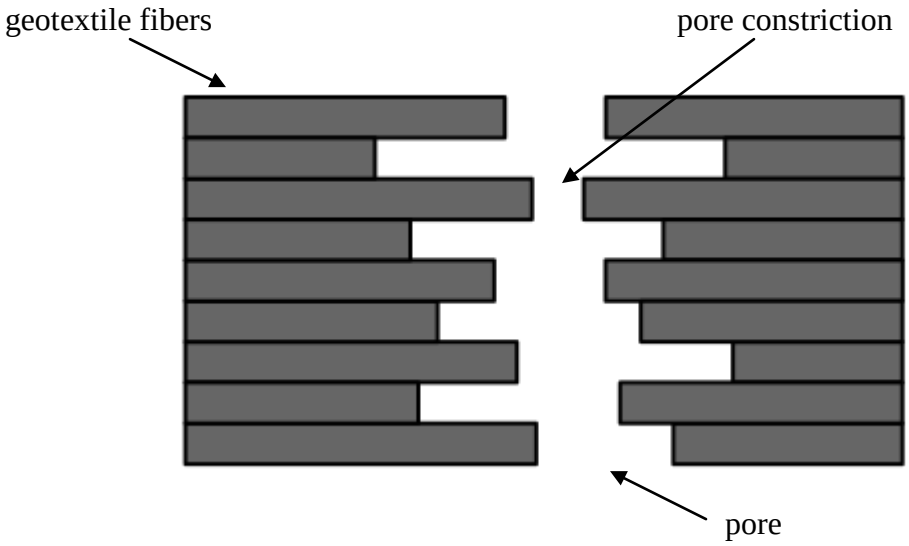

Figure 1.5: A conceptual model of a nonwoven geotextile pore cross-section. Adapted from Aydilek et al. 2005.

1.4 Geotextile Filter Design Criteria

A variety of geotextile filter design criteria have been presented over the years by those in academia, consulting, and geotextile manufacturing. In general, most design methods have traditionally consisted of the evaluation of three primary criteria: retention of soil particles, permeability to water flow, and resistance to clogging. However, specific design recommendations vary and there are no universally accepted criteria. Conventional design criteria are presented by Koerner (2005). More recently, Giroud (undated paper[1]) proposed the additional criteria of a minimum porosity and a minimum thickness of the geotextile.

"There are many formulas that can be applied to soil-retention design, most of which use the soil particle size characteristics and compare them to the 95% opening size of the geotextile," or "O_{95}" (Koerner 2005). In the United States, a dry sieving method known as the Apparent Opening Size (AOS) test is used to determine the O_{95} value (Koerner 2005). The AOS test is standardized by ASTM International as standard D4751, with the most recent version published in 2012 as D4751-12. The "AOS" value of a geotextile is typically provided by the manufacturer along with other basic properties such as weight, thickness, various strength characteristics, and permittivity. Despite the widespread industry use of the AOS test, there are several problems and shortcomings associated with the test. One of the principal shortcomings is that the AOS test yields a single numerical value to characterize the complex pore structure of nonwoven geotextiles.

While the AOS and permeability satisfy the basic design requirements of soil particle retention and water flow, "these properties do not relate directly to the clogging

[1] The paper is undated; however, the text indicates it was written between 2008 and 2010

potential of a geotextile" (Carroll 1987). "Christopher and Holtz (1985) suggested that clogging was related to the ability of the geotextile to pass fine soil particles while retaining the larger particles … [and they proposed] a criterion based on a minimum pore size to allow fines to pass through the filter" (Fischer et al. 1990). "Although relationships between clogging, porosity, and pore size distribution have been clearly recognized (e.g., Wates 1980, Rollin et al. 1982, Gourc & Faure 1990, Fischer et al. 1990), these relationships have not been fully developed to the standard of practice such that clogging can be thoroughly addressed by simple criteria" (Christopher and Fischer 1992). Thus, the recommended use of clogging criteria based on porosity and pore size distribution has been limited to "less critical applications" (Christopher and Fischer 1992). To evaluate clogging, filtration tests are typically performed with site-specific soil; however, these tests "are not easily performed, are expensive, and only provide results for one specific soil and geotextile system," which can result in limited attempts by designers to evaluate the criterion (Christopher and Fischer 1992).

1.5 The Bubble Point Method

In recent years, the bubble point method has emerged as a means for determining the pore size distribution of geotextiles. A pore size distribution, which reflects the complete range of pore sizes, is a more complete description of geotextile pore structure compared to the single value of the AOS test. Fischer et al. (1990) provided recommendations for filter criteria based on pore size distributions. More recently, TenCate Geosynthetics, a geosynthetics manufacturer, reported plans to develop soil filtration guidance utilizing pore size distributions for geotextiles determined using the

bubble point method (TenCate 2011). The bubble point method has been standardized by ASTM International for use with geotextiles as the "Standard Test Method for Pore Size Characteristics of Geotextiles by Capillary Flow Test", designation D6767, with the most recent version published in 2011 as D6767-11. The bubble point method described in this thesis can also be referred to as the capillary flow porometry method. According to ASTM (2011c), "the bubble point method is based on the principle that a wetting liquid[2] is held in the continuous pores of a geotextile by capillary attraction and surface tension, and the minimum pressure required to force liquid from these pores is a function of pore diameter." The bubble point method measures the narrowest openings of geotextile pores, known as pore constrictions. Pore size distributions obtained using the bubble point method are "probably the best … to represent filtration behavior of geotextiles, because it is the size of the pore constrictions that determines whether a soil particle will pass (de Mello 1977, Wates 1980, Kenney et al. 1985)" (Fischer et al. 1996).

1.6 Scope of Study

This thesis presents an evaluation of the bubble point method for determining pore size distributions of nonwoven geotextiles. This evaluation includes reviews of methods for quantifying geotextile pore structure along with the bubble point method and associated parameters, discussions of bubble point test apparatus design, data reduction, analysis of results, and investigations of the influence of test parameters on results. A custom-built bubble point testing apparatus was constructed at Auburn University for the purpose of performing tests on geotextiles. To facilitate the processing and analysis of bubble point test results, an automated data reduction spreadsheet was developed. The

[2] The terms "liquid" and "fluid" are used synonymously in this thesis

data provided by the automated data reduction spreadsheet made it possible to analyze bubble point test results using a variety of statistical methods. The results of multiple bubble point tests performed on a nonwoven geotextile are analyzed and discussed. An observed trend was that different wetting fluids used to perform the bubble point test result in different pore size distributions for the same nonwoven geotextile. This study includes investigations of the contact angle and residual fluid as causes of wetting fluid-based differences in pore size distributions determined using the bubble point method.

The primary objectives of this thesis are to:

- Review methods for quantifying geotextile pore structure;
- Review the bubble point method and associated parameters;
- Describe a custom-built apparatus for conducting bubble point tests;
- Describe how the apparatus is used to conduct bubble point tests;
- Describe how bubble point test data are reduced to yield pore size distributions using an automated spreadsheet;
- Demonstrate various statistical methods for analyzing bubble point test results; and
- Discuss the influences of the contact angle, the capillary constant, surface tension, and residual fluid on pore size distributions determined using the bubble point test.

A review of methods for quantifying geotextile pore structure, including the AOS test and the bubble point method, are presented in Chapter 2. A review of the contact

angle, an important parameter needed to calculate pore sizes using the bubble point method, and methods for measuring the contact angle are presented in Chapter 3. Chapter 4 provides a detailed description of the bubble point testing apparatus developed at Auburn University, along with detailed descriptions of how the test is performed and how test data is processed using the automated data reduction spreadsheet to determine pore size distributions. Chapter 5 presents various experiments, analysis, and results, including results and statistical analysis of multiple bubble point tests performed on a nonwoven geotextile using different wetting fluids, the measurement of the contact angle and its influence on pore size distributions, the influence of the capillary constant on pore size distributions, the influence of surface tension on pore size distributions, and the influence of residual fluid on bubble point test results. Conclusions and recommendations for future research are presented in Chapter 6.

Chapter 2: Quantification of Geotextile Pore Structure

2.1 Introduction

The most common method for quantifying geotextile pore structure for filtration design is the Apparent Opening Size (AOS) test, ASTM D4751-12. As an ASTM test that is considered easy to perform with widespread, historical industry use, the AOS test remains the most-used method despite several problems and shortcomings. Two of the primary problems associated with the AOS test are: 1) only one number is used to characterize the complex structure of nonwoven geotextiles, and 2) this number is a reflection of only the largest pore sizes.

Several methods exist for computing pore size distributions, which give information regarding multiple pore sizes of a porous medium. However, research has shown that different methods for determining pore size distribution yield different pore size distributions for the same geotextile. Among these methods is the bubble point test. The bubble point test is an ASTM standard (ASTM D6767-11) that has been studied as a possible improvement to the AOS test for quantifying the pore structure of geotextiles. One of the important advantages of the bubble point test is that it measures pore constrictions. "Vermeersch and Mlynarek (1996) and Giroud et al. (1998) have confirmed that constriction sizes of a geotextile impact filtration performance, and if they can be accurately measured, they should be used for the design of geotextile filters" (Aydilek et al. 2007). Although the bubble point test is an ASTM standard that has been

researched by many, questions remain regarding the validity of the test and the variables needed to calculate accurate pore size distributions.

2.2 The AOS Test (ASTM D4751-12)

2.2.1 Background and Method

The Apparent Opening Size (AOS) test was developed in the 1970s by the U.S. Army Corps of Engineers to evaluate woven geotextiles, and the test was later extended to include nonwovens (Koerner 2005). Despite its shortcomings, the AOS test remains the industry standard for quantifying geotextile pore size for use in filtration applications. The continued use of the AOS test is attributed to the simplicity of the test and to long, widespread industry use (Koerner 2005).

The AOS test is a dry sieving method that involves sieving sets of glass beads of known, uniform diameter through a geotextile via mechanical shaking for ten minutes and recording the percent of beads by weight that pass the geotextile. A bead size expected to yield greater than 5% passing is tested first, followed by sets of progressively larger bead sizes until a value of 5% or less passing the geotextile by bead weight is obtained. According to ASTM D4751-12, a bead size that yields 5% or less passing may be used as the AOS, or a 5% passing bead size may be interpolated from a plot of percent passing versus bead size. The AOS is also known as the "O_{95}" value, which stands for the 95% opening size. The AOS (O_{95}) is defined by ASTM D4751-12 as "a property that indicates the approximate largest particle that would effectively pass through the geotextile." The AOS of a geotextile can be expressed in terms of bead size (diameter) in millimeters, or in terms of an equivalent U.S. sieve size (e.g., No. 40, No. 100, etc.). The

AOS of five geotextile specimens are averaged to determine the AOS for the geotextile sample.

2.2.2 Associated Problems and Shortcomings

There are several problems and shortcomings associated with the AOS test. Fischer et al. (1996) note that the process of a bead falling through a pore is a somewhat random event and that bead weight may influence the percent of beads which pass through the geotextile. Water used to clean the geotextile prior to testing, as described in ASTM D4751-12, may remain in pores and possibly hinder bead passage. Dierickx and Myles (1996) question the accuracy of measuring pore sizes less than 0.1 mm by dry sieving; a cause for concern considering that many geotextiles contain a significant number of pore sizes smaller than 0.1 mm. The following list of problems is presented by Koerner (2005):

- The test is conducted dry, whereas filtration and drainage always involve liquids.
- The glass beads can easily get trapped in the geotextile itself (particularly in thick nonwovens) and not pass through at all.
- Electrostatic charges often result in the finer glass beads clinging to the inside of the sieve and not participating in the test at all.
- Yarns in some geotextiles easily move with respect to one another during vibratory sieving, thereby allowing the beads to pass through an enlarged void not representative of the total geotextile specimen.

- Slight changes in fabric structure do not result in different O_{95} values. This is perplexing since structure, temperature, humidity, bead size variation, and test duration all potentially influence the test results.
- The test only allows for determination of the O_{95} value (95% passing size). The remainder of the pore size curve is not defined.

The last point made by Koerner highlights one of the main criticisms of the AOS test: one pore size is used to characterize geotextile pore structure, which is composed of a distribution of pore sizes. In addition, the AOS value for a geotextile indicates "the approximate largest particle that would effectively pass through the geotextile" (ASTM D4751-12), which is a reflection of larger pore sizes. As noted in Section 1.4 of this thesis, the AOS does not relate directly to clogging potential, which is believed to be influenced by the smaller, fine soil particles.

2.3 Pore Size Distributions

2.3.1 Definition of a Pore Size Distribution

A pore size distribution is an expression of the various pore sizes of a porous medium. ASTM D6767-11 defines a pore size distribution as the "percent cumulative distribution of the complete range of pore sizes with in a given geotextile based on the surface occupied by the pores." As presented by ASTM D6767-11, a pore size distribution consists of a plot of percent finer versus pore size, with the percent finer ranging from 0 to 100%. For a particular pore size on the plot, the percent finer gives the percentage of pores in the medium "based on the surface occupied by the pores" that are

smaller or equal to that particular pore size (ASTM 2011c). An example of a pore size distribution is shown in Figure 2.1.

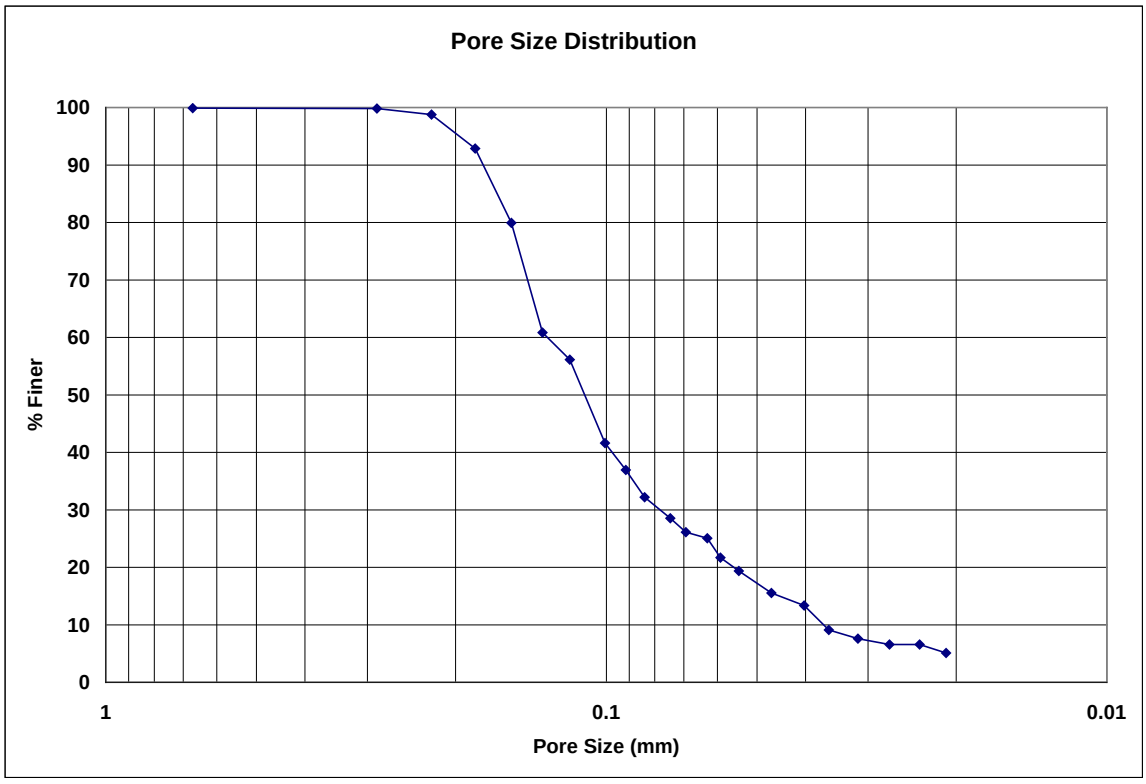

Figure 2.1: An example of a pore size distribution.

2.3.2 Methods for Calculating Pore Size Distributions

2.3.2.1 Overview of Methods

There are several methods available for calculating pore size distributions of geotextiles. These methods include dry sieving, wet sieving, hydrodynamic sieving, image analysis, mercury intrusion porosimetry, and liquid extrusion methods (e.g., bubble point). However, it is well documented that different methods yield different pore size distributions for the same geotextile (Falsye 1985, Bhatia and Smith 1995, Fischer et al. 1996, Bhatia et al. 1996, D'Hondt 2005). An example of this phenomenon is shown in Figure 2.2.

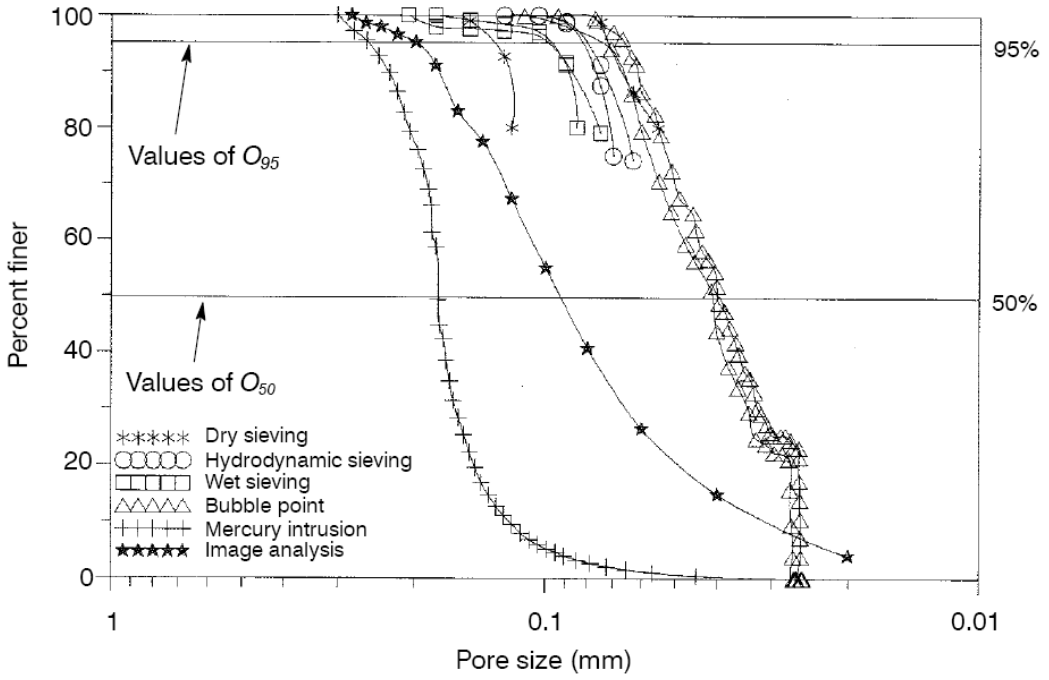

Figure 2.2: Pore size distributions for a nonwoven geotextile (needlepunched, staple fiber) determined using various methods. The wetting fluid used for the bubble point method was Porewick™. *Source:* Bhatia et al. 1996. Used with permission.

As Fischer et al. (1996) noted, each pore size distribution method "provides pore sizes and distributions that are not necessarily a unique property of the geotextile, but instead depend on the method of measurement." The three primary categories of pore size measurement are sieving methods, image analysis, and liquid intrusion and extrusion techniques.

2.3.2.2 Sieving Methods

Sieving methods included dry, wet, and hydrodynamic sieving. All sieving methods involve sieving glass beads of known size through a geotextile to determine pore size. Dry sieving extends the AOS procedure of determining the O_{95} value to several

different opening sizes (e.g., O_{75}, O_{50}, etc.). Wet sieving and hydrodynamic sieving involve the addition of water to the sieving process, which is believed to lessen the effect of static electricity. The primary differences in wet sieving and dry sieving are that, in wet sieving, "a continuous water spray is applied to the particles and the geotextile during shaking; and particle mixtures are used as the testing particles rather than fractions" (Bhatia and Smith 1996b). "The hydrodynamic sieving method is based on hydrodynamic filtration (Fayoux 1977), where glass bead mixtures are sieved through geotextiles by alternating water flow, which occurs as the result of the repeated immersion of the geotextiles in water" (Bhatia and Smith 1996b). The dry, wet, and hydrodynamic sieving methods provide indirect measurements of pore size that do not correlate directly to the constriction sizes of geotextile pores. Because these methods involve sieving glass beads, the tests are subject to some of the same problems as the AOS test (as discussed in Section 2.2.2 of this thesis), such as beads becoming trapped within the geotextile.

2.3.2.3 Image Analysis

Image analysis has been the focus of research in recent years (Aydilek 2005, D'Hondt 2005). Image analysis basically involves photographing a geotextile and then processing the image using a computer program to determine the pore size distribution. In addition to evaluating constriction sizes, image analysis is considered one of the more direct methods of pore size measurement, as pores are visualized and pore size distributions are calculated from photographs of the geotextile. However, no standard

method exists and results can be dependent upon photographic conditions (e.g. glare) and image processing (e.g., thresholding) (Aydilek 2005, D'Hondt 2005).

The two dimensional structure of woven geotextiles seems to lend itself well to the image analysis method, as the structure can be completely captured by a photograph. A study by Aydilek et al. (2007) showed that, for wovens, the O_{95} values determined using image analysis compared "reasonably well" to the manufacturer-reported AOS values. The use of image analysis with nonwovens is met with limitation, due to their three-dimensional nature. D'Hondt (2005) noted that it may not be possible to measure a pore constriction using image analysis if the axis of a pore is skewed. Similarly, the constriction size of a tortuous pore may not be apparent from a photograph of a nonwoven geotextile surface. Given the reported success of the use of image analysis with wovens and the limitations associated with its use on nonwovens, it appears that image analysis may be better suited for analysis of woven geotextiles.

2.3.2.4 Liquid Intrusion and Extrusion Methods

Liquid intrusion and extrusion methods were first developed in the early 20th century to measure pore sizes in porous media. These methods involve either forcing a non-wetting fluid into an initially evacuated porous medium or extruding a wetting fluid from an initially saturated porous medium, using controlled pressure in both cases. As shown in Figure 2.3, wetting fluids will spontaneously wick into pores, whereas non-wetting fluids must be forced into pores using applied pressure (Zeman and Zydney 1996). Non-wetting fluids are those with contact angles between 90° and 180° and wetting fluids are those with contact angles (θ) less than 90° (Zeman and Zydney 1996,

Lowell et al. 2006, Berg 2010). The concepts of contact angles and wetting are discussed in detail in Chapter 3 of this thesis. Intrusion and extrusion methods include mercury intrusion porosimetry, liquid extrusion porosimetry, and liquid extrusion porometry (aka capillary flow porometry). These methods are based on the same capillary theory which relates the pressure required to intrude or extrude a fluid to the diameter of the pores. However, differences in test methodologies yield different measurements of pore size distributions.

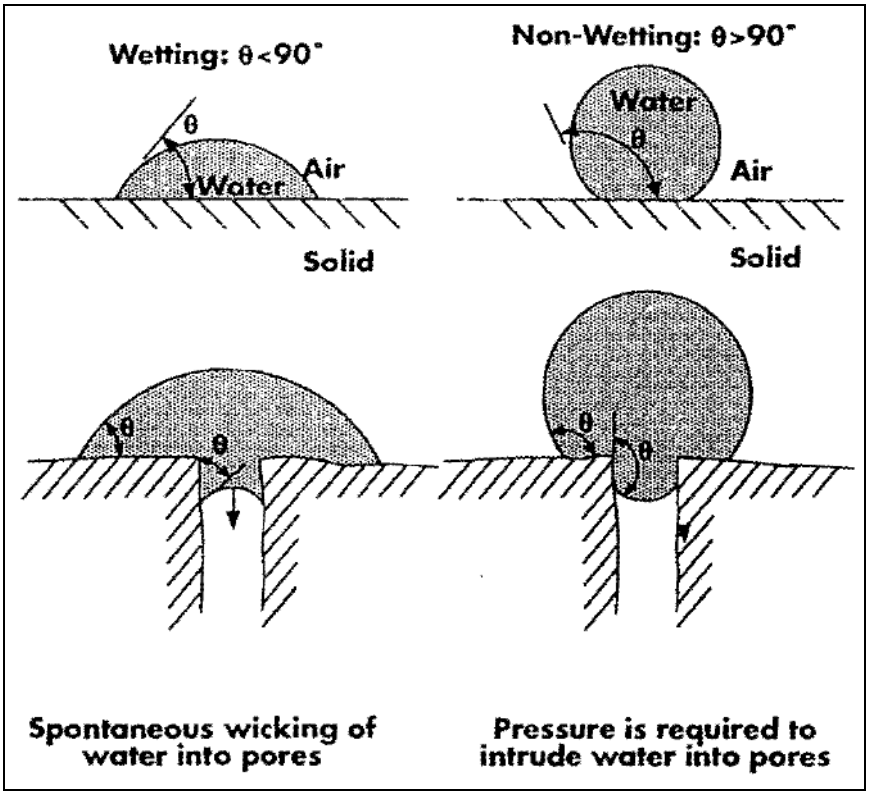

Figure 2.3: Examples of wetting (θ<90°) and non-wetting (θ>90°) behavior (θ = contact angle). *Source:* Zeman and Zydney 1996. Used with permission.

Mercury intrusion porosimetry involves forcing mercury into pores by controlled pressure. During the test, "the volume of intruded pores is determined by measuring the volume of mercury forced into them at various pressures" (ASTM 2010). Mercury is uniquely suited for use in liquid intrusion porosimetry because it is non-wetting on most

solids due to its high surface tension (Lowell et al. 2006). A non-wetting fluid will not spontaneously permeate into pores, but instead, it must be forced into pores using applied pressure (Zeman and Zydney 1996, Lowell et al. 2006, Berg 2010). Edward Washburn (1921) pioneered the mercury intrusion porosimetry method and was the first to propose using the following equation for relating the pressure needed to force mercury into pores to the pore diameter (Miller and Tyomkin 1986, Calvo et al. 1995, Lowell et al. 2006):

$$d = -\frac{4\gamma \cos\theta}{P} \qquad \text{(Equation 2.1)}$$

where:

d = pore diameter (m)

γ = surface tension (N/m)

P = applied pressure (Pa)

θ = contact angle (degrees)

In the field of mercury porosimetry, Equation 2.1 is commonly referred to as the Washburn equation. Derivations of the Washburn equation are presented by Lowell et al. (2006). The negative sign in Equation 2.1 is due to the negative value of $\cos(\theta)$ associated with non-wetting (i.e., $90° < \theta < 180°$) mercury. The mercury intrusion method has been standardized by ASTM International for use with soil and rock as designation D4404-10, "Standard Test Method for Determination of Pore Volume and Pore Volume Distribution of Soil and Rock by Mercury Intrusion Porosimetry." In regards to filtration characterization, one problem with the mercury intrusion method is that mercury will begin to intrude pores based on the diameter of pores at the *surface* of the porous medium, meaning that these pore sizes are measured and included in the pore

size distribution. However, as illustrated by Figure 2.4, the exterior pore size is not necessarily the same as the constriction size of the pore channel, which is of interest for filtration. In addition, the mercury intrusion method determines pore size distributions based on pore volumes, which includes dead-end pores that do not contribute to filtration. Studies of mercury intrusion porosimetry in conjunction with geotextiles have been performed by many, including Prapaharan (1989), Bhatia and Smith (1994, 1996), Fischer et al. (1996), and Elsharief and Lovell (1996). When compared to other methods of calculating pore size distributions on the same geotextile, mercury intrusion typically yields the largest pore size values (Prapaharan 1989, Bhatia and Smith 1994, Elsharief and Lovell 1996). Possible reasons for this effect include the enlargement of the geotextile pores due to the high compressive forces of mercury (Miller and Tyomkin 1986), inclusion of dead-end pores in the pore size distribution, and the inclusion of pore sizes other than the constriction size in the pore size distribution. The use of mercury to perform the test is a general disadvantage, as mercury is a hazardous material that requires special handling and disposal considerations.

Liquid extrusion methods include extrusion porosimetry and capillary flow porometry. Whereas the liquid intrusion method requires the use of a non-wetting liquid (e.g., mercury) that must be forced into pores, liquid extrusion methods use wetting fluids (i.e., $\theta < 90°$) that spontaneously imbibe the pores, are held in pores by capillarity, and require applied pressure to be forced out. Liquid extrusion methods use a similar form of the Washburn equation (Equation 2.1, but without the negative sign) to relate the pressure required to force fluid out of a pore to the diameter of the pore. The name difference of *porosimetry* vs. *porometry* is subtle, but they refer to two distinct test methods which

yield different measurements of pore size distribution. Liquid extrusion porosimetry determines pore size distributions based on the volume of fluid expelled at each pressure interval. In contrast, capillary flow porometry determines pore size distributions by comparing the airflow rates of the wetted sample at each pressure interval to those of the dry sample (see Section 2.4.2.2.4). As shown in Figure 2.4, the capillary flow porometry method measures only pore constrictions, while the liquid extrusion porosimetry method (as with mercury intrusion porosimetry) includes measurements of other, larger diameters of a pore channel in the pore size distribution. Recall that pore constrictions control geotextile filtration.

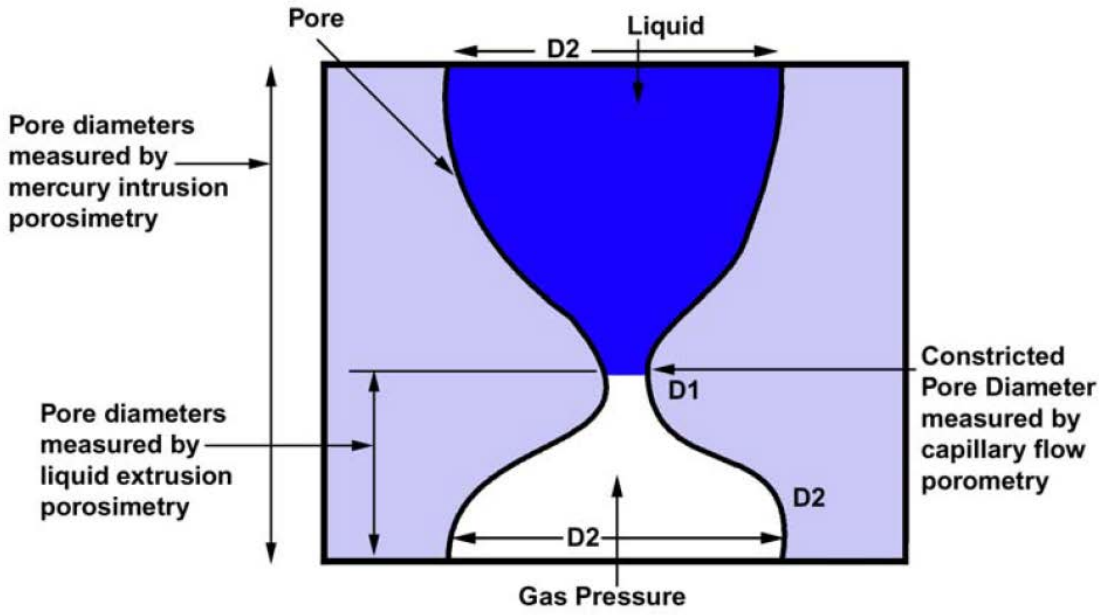

Figure 2.4: Schematic of pore sizes measured using different methods. *Source:* Jena and Gupta 2002. Used with permission.

Both liquid extrusion porosimetry and capillary flow porometry can generally be referred to as "bubble point" methods, tests, techniques, procedures, etc., because they evolved from the general bubble point method pioneered by Bechhold (1908). In the field of geotextile testing, the names "bubble point method" or "bubble point test" are

commonly used to refer to the more specific method of capillary flow porometry. For example, Bhatia and Smith (1994), Fischer (1994), Bhatia et al. (1996), and Aydilek et al. (2007) describe the capillary flow porometry method for measuring pore sizes of geotextiles but refer to them only as "bubble point" methods. Unless otherwise noted, the terms "bubble point method" or "bubble point test" in this thesis refer to the capillary flow porometry method of measuring a complete pore size distribution. In other work, a "bubble point test" often refers to a test to measure only the largest pore size instead of a pore size distribution.

The bubble point method (i.e., capillary flow porometry method) measures the pore constrictions of geotextiles and provides a method for calculating pore size distributions. The use of the bubble point method to measure pore size distributions of geotextiles has been studied and well-documented by Bhatia and Smith (1994, 1995, 1996b), Bhatia et al. (1996), Elton et al. (2007), Elton and Hayes (2007, 2008a, 2008b, 2009), Fischer (1994), Fischer et al. (1996), D'Hondt (2005), Aydilek et al. (2007), and others. Of methods available for determining pore size distributions, the bubble point method has the distinct advantage of theoretically being able to determine pore constrictions in the tortuous pores of nonwoven geotextiles. In their study of image analysis and the bubble point method, Aydilek et al. (2007) concluded that the bubble point method is the "best available test to determine constriction sizes in a nonwoven geotextile." The theoretical basis of the bubble point method is discussed in detail in the following section.

2.4 The Bubble Point Method

2.4.1 Historical Background

2.4.1.1 Capillarity

The physical and mathematical theory associated with the bubble point method is based in the field of capillarity. As noted by de Gennes et al. (2004), "one of the most well-known and vivid manifestations of capillarity is the phenomenon of fluid rise (i.e., capillary rise) in narrow tubes, and it is the foundation of the field." Leonardo da Vinci was an early investigator and some credit him as being the first to observe and document the phenomenon (de Gennes et al. 2004, Berg 2010). A complete mathematical understanding of the phenomenon was gained by Young and Laplace in the early 19th century (de Gennes et al. 2004). An example of capillary rise is shown in Figure 2.5.

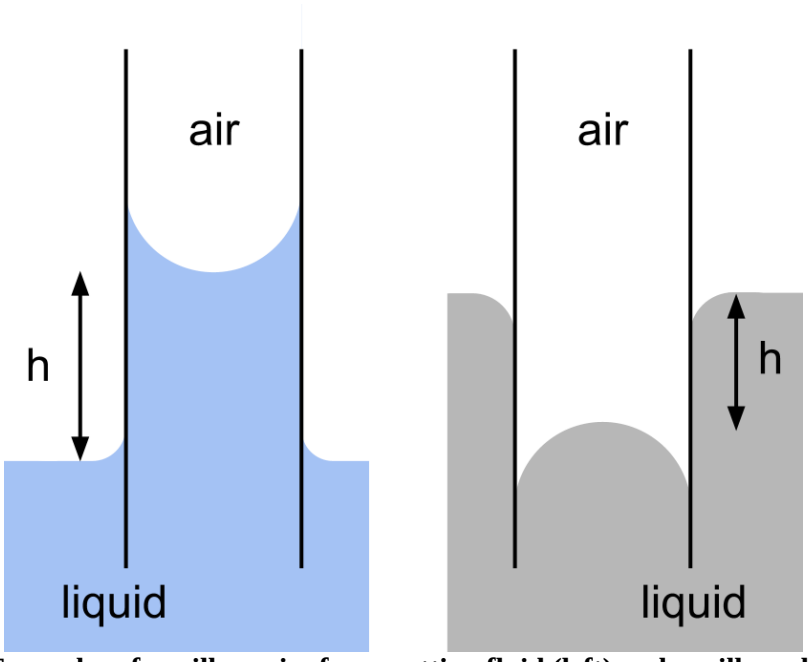

Figure 2.5: Examples of capillary rise for a wetting fluid (left) and capillary depression for a non-wetting fluid (right) in capillary tubes. Adapted from Lowell et al. 2006.

The height of capillary rise for the classic case of a circular tube and a hemispherical meniscus is described by the following equation (de Gennes et al. 2004):

$$h = \frac{2\gamma \cos\theta}{\rho g r} \qquad \text{Equation 2.2}$$

where:

h = height of capillary rise

θ = contact angle

ρ = fluid density

g = gravitational constant

γ = fluid surface tension

r = radius of the capillary tube

Equation 2.2 is familiar to those in the soil sciences as describing the height of capillary rise of groundwater above the water table, which forms the capillary fringe. There are multiple ways to derive Equation 2.2, including the use of energy, pressure, and force equilibrium arguments. Derivations using each of these arguments are presented by de Gennes et al. (2004). Although the phenomenon is commonly referred to as capillary rise, the opposite effect of capillary depression can also occur, as shown in Figure 2.5. Capillary rise occurs when the cosine of the contact angle is positive (i.e., $0° < \theta < 90°$) and depression occurs when the cosine of the contact angle is negative (i.e., $90° < \theta < 180°$). Water and mercury serve as two typical examples of capillary rise and depression, respectively. Water is known to be wetting on glass and exhibits capillary rise in glass

tubes, whereas mercury is known to be nonwetting on glass (and most surfaces) and exhibits capillary depression in glass tubes.

2.4.1.2 Bubble Point Methodology

Bechhold (1908) is credited as being the first to measure the air pressure needed to blow air through a water-filled porous membrane and for introducing the bubble point test to determine the pores sizes of membranes (Cuperus and Smolders 1991, Calvo et al. 1995, Zeman and Zydney 1996, Cheryan 1998). Thus, the bubble point method has its origin in the field of membrane filtration. Since the pioneering work of Bechhold, many have researched the bubble point method and applied the theory to various porous materials. The bubble point method has been used with various materials such as membranes (Bechhold 1908, McBain and Kistler 1930), porous ceramic bodies (Knoll 1940), and textile fabrics (Schwertz 1949, Miller and Tyomkin 1986), just to name a few (Bhatia and Smith 1994). Zeman and Zydney (1996) note that Albert Einstein contributed to bubble point methodology by publishing a paper in 1923 (two years after receiving his Nobel Prize for the discovery of the photoelectric effect) that involved bubble point testing of clay microfilters. The bubble point test has been used extensively for measuring pore sizes and testing the integrity of membranes (Zeman and Zydney 1996, Cheryan 1998).

In its most basic form, the bubble point test involves a fluid-filled porous membrane with a fluid reservoir on top of the membrane, as shown in Figure 2.6. The wetting fluid is held in the pores of the membrane by capillarity.

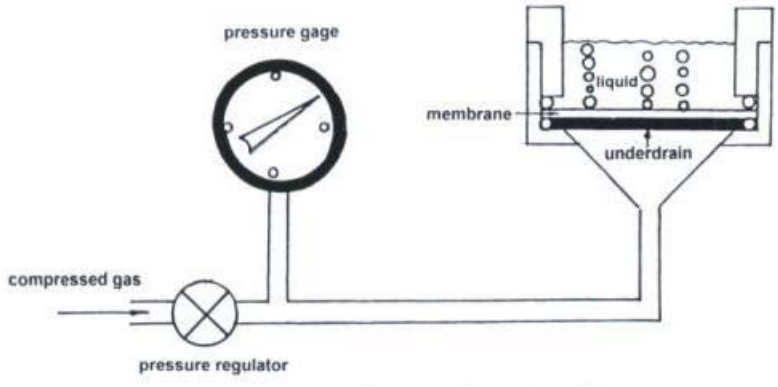

Figure 2.6: Schematic of a basic bubble point test. *Source:* Zeman and Zydney 1996. Used with permission.

Air pressure is introduced from beneath the membrane, and bubbles appear in the fluid reservoir once fluid is forced from the membrane pores and they begin to transmit air. The pressure at which bubbles first appear in the reservoir is known as the "bubble point", which is how the method gets its name. The same capillary theory used to derive the Washburn equation (Equation 2.1) for mercury intrusion into pores and Equation 2.2 for the height of capillary rise is used to relate the pressure required to expel fluid held by capillarity in a tube to the diameter of the tube:

$$d = \frac{4\gamma \cos\theta}{P} \qquad \text{Equation 2.3}$$

where:

d = pore diameter

γ = surface tension

P = pressure difference across fluid

θ = contact angle

The pore size related to the bubble point pressure represents the largest pore size of the membrane (Cuperus and Smolders 1991). Some (Hutten 2007, Yu et al. 2010) note that Equation 2.3 should be corrected to account for the hydrostatic pressure from the overbearing fluid in the reservoir. However, Yu et al. (2010) note that this hydrostatic pressure is often negligible compared to the gas pressure needed to expel fluid from membrane pores, because the height of the fluid reservoir is typically very small. In the context of the bubble point method, Equation 2.3 is identified in the literature as the Cantor equation (Cuperus and Smolders 1991, Cheryan 1998), the Washburn equation (Calvo et al. 1995), and the Young-Laplace equation (Zeman and Zydney 1996, Manickam and McCutcheon 2012). Some (e.g., Calvo et al. 1995, Masuelli et al. 2009) further distinguish that Equation 2.3 becomes the Cantor equation when the contact angle is zero. In his pioneering 1908 paper, Bechhold references work by Cantor (1892). Equation 2.3 is sometimes presented in the literature with an additional parameter, referred to as a correction factor or a capillary constant. This factor will be discussed in detail in Section 2.4.2.2.3.

From the most basic form of a bubble point test shown in Figure 2.6, more sophisticated extensions of the method have been developed. As discussed in Section 2.3.2.4, two of the major extensions are liquid extrusion porosimetry and capillary flow porometry. These methods combine the basic bubble point method with techniques to determine not only the largest pore size, but complete pore size distributions. Modern test methods that have been used with geotextiles have been standardized by ASTM International and are discussed in the following section.

2.4.2 Current ASTM Standards for Bubble Point Methods

2.4.2.1 Overview

There are two current ASTM standards for bubble point methods that have been traditionally used by researchers to test geotextiles: 1) "Standard Test Methods for Pore Size Characteristics of Membrane Filters by Bubble Point and Mean Flow Pore Tests" (designation F316), and 2) "Standard Test Method for Pore Size Characteristics of Geotextiles by Capillary Flow Test" (designation D6767). An additional standard, "Standard Test Method for Pore Size Characteristics of Membrane Filters Using Automated Liquid Porosimeter" (designation E1294-89) was introduced in 1989, but was withdrawn by ASTM in 2008.

ASTM F316 has existed in form since 1970, although it has undergone several revisions. ASTM F316 actually describes two separate test methods, identified as Test Methods A and B. Test Method A is a test for measuring the maximum limiting (i.e., constriction) pore diameter of a membrane. The method presented as Test Method A is the basic bubble point test shown in Figure 2.6, which involves observing air bubbles in a fluid reservoir above the membrane to determine the bubble point pressure, which is correlated to the maximum pore diameter. Test Method B measures the relative abundance of a specified limiting pore diameter in a membrane and can be used to determine a pore size distribution. Test Method B is a capillary flow porometry method in which airflow rates of an initially saturated membrane are compared to airflow rates of a dry membrane at the same pressures.

In 2002, ASTM Committee D-35 on Geosynthetics adapted ASTM F316 specifically for geotextiles as method D6767 (Aydilek et al. 2007). Prior to the

introduction of ASTM D6767, researchers such as Fischer (1994) and Bhatia and Smith (1995) referred to the ASTM F316 standard for conducting bubble point tests on geotextiles. Since 2002, most researchers using the bubble point method with geotextiles have referred to ASTM D6767. ASTM D6767-11 is discussed in the following section.

2.4.2.2 ASTM D6767-11

2.4.2.2.1 Overview

The bubble point method described by ASTM D6767 is a capillary flow porometry method that theoretically measures the constriction sizes of geotextile pores. The most recent version was published in 2011 as D6767-11. The test method consists of exposing a geotextile sample to controlled airflow and recording the values of several different airflow rates and corresponding pressure differences across the sample. The airflow rate begins at zero and is gradually increased in increments as the test progresses. As the airflow rate increases, the pressure difference across the sample also increases. Two "runs" (series of sequential airflow rate and pressure difference measurements) must be performed: one with the dry geotextile and one with the geotextile initially saturated by a fluid known as the "wetting fluid". The two runs are named the "dry run" and the "wet run", respectively. In regard to the wet run, capillary theory dictates that fluid will exit the largest pores first, followed by smaller pores as the pressure increases. Capillary theory is used to mathematically relate the pressure differences recorded during the wet run to the pore diameter. The percent finer is calculated through comparison of the wet and dry airflow rates at particular pressure differences. A detailed discussion of the design of an apparatus for performing bubble point tests, apparatus operation, test

procedure, and data reduction needed to generate pore size distributions is presented in Chapter 4.

2.4.2.2.2 Calculation of Pore Size

Pore size is calculated by applying force equilibrium to the fluid held by capillarity in the pores. Assuming the pore shape to be circular, ASTM D6767-11 presents the force balance as:

$$\pi d\gamma B\cos\theta = \left(\frac{\pi}{4}\right)d^2P \qquad \text{(Equation 2.4)}$$

where:

d = pore size (diameter) (μm)

γ = surface tension (mN/m)

P = pressure (Pa)

B = capillary constant

θ = contact angle

The left side of Equation 2.4 represents the resisting force of surface tension acting along the walls of the pore. The right side of Equation 2.4 represents the driving force due to the applied pressure acting over the area of the pore. Expressing Equation 2.4 in terms of pore diameter gives:

$$d = \frac{4\gamma B\cos\theta}{P} \qquad \text{(Equation 2.5)}$$

Note that Equation 2.5 is equivalent to Equation 2.3, except that the capillary constant, B, has been added to Equation 2.5. As discussed in Section 2.4.1.2, Equation 2.3 appears in

the literature both with (i.e., Equation 2.5) and without the capillary constant and the relationship is known by several different names (e.g., Washburn equation, Young-Laplace equation, etc.). Unless otherwise noted, the relationship presented in Equations 2.3 and 2.5 will be referred to as the Washburn equation in this thesis. The capillary constant will be discussed in the following section (Section 2.4.2.2.3).

According to ASTM D6767-11, once pressure conversion factors and the capillary constant are substituted, and assuming that the wetting fluid completely wets the geotextile ($\theta = 0$), Equation 2.5 becomes:

$$d = \frac{C\gamma}{P} \qquad \text{(Equation 2.6)}$$

where:

C = constant, 2860 when P is in Pascals (Pa)

For the purposes of data reduction, it is desirable to express the pore diameter in terms of millimeters (mm) and to be able to input the contact angle in cases where it is not equal to zero. Therefore, the following relationship is used in this thesis to determine the pore diameter:

$$d = \frac{C\gamma \cos\theta}{P} \qquad \text{(Equation 2.7)}$$

where:

d = pore diameter (mm)

γ = surface tension (N/m)

P = pressure difference across the geotextile (Pa)

C = constant, 2860 (mm/m)

θ = contact angle (degrees)

Note that the author has included units of mm/m for the constant, C, which are necessary for the units of the equation to agree. ASTM D6767-11 does not present units with the constant, C. To be consistent with ASTM D6767-11, a constant, C, of 2860 mm/m will be used to compute pore sizes for bubble point test results presented in this thesis, unless otherwise noted. A constant, C, of 2860 mm/m corresponds to using a capillary constant, B, of 0.715. If the capillary constant is omitted, the constant, C, becomes 4000 mm/m.

When a pressure difference, P, from a bubble point test is used in Equation 2.7, d represents the pore diameter in which fluid will be on the threshold of overcoming static equilibrium. Therefore, at that particular pressure during the bubble point test, fluid is considered to have exited all pores larger than d, and fluid is assumed to remain in all pores of size d and smaller. The pressure difference, P, is the only value in Equation 2.7 that is measured while the bubble point test is being performed, and this value can be measured using a device such as a manometer. The surface tension is a property of the fluid and temperature. Information for the surface tension of various fluids at standard temperatures is readily available in the literature and is commonly available from laboratory-grade fluid suppliers. The contact angle is a measure of how the fluid interacts with the geotextile surface and its value is dependent on properties of both the fluid and the geotextile surface. Of the parameters in Equation 2.7, the contact angle is the most difficult to measure accurately. The significance of the contact angle in regard to the bubble point test and methods of contact angle measurement will be discussed in detail in Chapter 3.

2.4.2.2.3 Discussion of the Capillary Constant

The capillary constant included with the Washburn equation in ASTM D6767-11 is a carryover from the equation as presented in ASTM F316. ASTM F316-86 references Bechhold (1908) when presenting the capillary constant. As discussed in Section 2.4.1.2, Bechhold's 1908 paper is considered the pioneering work for the bubble point method. It should be noted that the Bechhold paper was published in the German language, and an English translation does not appear to be readily available. Bechhold (1908) initially presents the pore size equation as:

$$d = \frac{4\beta}{1.033 \times 10^5 P} \qquad \text{(Equation 2.8)}$$

where:

d = capillary diameter (mm)

P = pressure (atmospheres)

β = capillary constant (no units given)

When compared to the Washburn equation in ASTM D6767-11 (Equation 2.5), the capillary constant presented in Bechhold's 1908 paper would also account for the surface tension and the contact angle terms.

Explanations of the capillary constant or an equivalent correction factor vary in the literature. According to Hutten (2007), the capillary constant presented in ASTM F316 is a tortuosity factor developed by Bechhold that has a value of 0.715. Hutten also notes that "many companies and organizations that use the bubble point technique do not make this correction." For example, the capillary constant, B, does not appear in versions

of Equation 2.5 reported by Miller and Tyomkin (1986), Bhatia and Smith (1994), Calvo et al. (1995), and Unsal et al. (2005), but the capillary constant does appear as part of the equation in work by Fischer (1994) and Fischer et al. (1996) (who used ASTM F316 as a standard for performing bubble point tests). Zeman and Zydney (1996) present a factor equivalent to the capillary constant, but identify it as the "adjustment factor", K. According to Zeman and Zydney, the adjustment factor is a shape or "fudge factor" that "covers up all shortcomings" of bubble point theory. Zeman and Zydney note that K = 1 for the case of a hemispherical fluid meniscus. The United States Environmental Protection Agency (USEPA) (2005) describes an equivalent factor, κ, identified as the "pore shape correction factor". According to USEPA, the "pore shape correction factor ranges from 0 – 1 [one for a perfectly cylindrical pore] and is a function of the pore structure, accounting for deviations from perfectly cylindrical pores, as well as for the tortuous flow path across the membrane."

There have been attempts reported in the literature to measure the capillary constant. Fischer (1994) measured the term $\gamma B\cos\theta$ in Equation 2.5 for the case of mineral oil and a small-diameter glass tube using two methods. Fischer notes that the pore size equation (using mineral oil) in ASTM F316-86 assumes a $\gamma B\cos\theta$ value of 0.0248 N/m, based on a surface tension (γ) of 0.0347 N/m, a capillary constant (B) of 0.715, and a contact angle (θ) of zero, yielding a $\cos\theta$ value of 1. The first method involved measuring the capillary rise of mineral oil in the glass tube after placing the end of the tube in a mineral oil bath. The second method involved measuring the net pressure required to force mineral oil from the end of the glass tube, with a portion of the tube immersed in mineral oil. The methods yielded 0.0245 N/m and 0.0220 N/m,

respectively, and Fischer concluded that the ASTM recommended value for $\gamma B\cos\theta$ was "reasonable." In another example, Zeman and Zydney (1996) report that L. Yen of Millipore Corporation (in an undated personal communication) performed bubble point tests (with methanol as the wetting fluid) on a series of track-etched polycarbonate filters of known pore diameter, and developed an experimental relationship between pressure and pore diameter. For a given pore diameter, experimental values of pressure were found to be lower by a factor of 0.6233 than the pressures predicted using the Washburn equation, assuming an adjustment factor (K) of one and a contact angle of zero. However, as Zeman and Zydney explain, the factor of 0.6233 is likely due to a non-zero value of the contact angle as opposed to the adjustment factor. This is because the track-etched filters had cylindrical pores, making it "hard to invoke a 'shape correction' " (Zeman and Zydney 1996). If the value of 0.6233 is attributed to the term $\cos\theta$, then the receding contact angle would be 51.5°. However, this would mean that the "obtained calibration … is valid only for etched polycarbonate and [it] cannot be used (at least not without careful contact angle corrections) for other membranes" (Zeman and Zydney 1996). The same can be said for the measurements of $\gamma B\cos\theta$ by Fischer (1994). Because the glass capillary tube used was cylindrical (an ideal case), it is likely that the capillary constant (as opposed to $\cos\theta$) was equal to one. For the capillary rise method where $\gamma B\cos\theta$ was found to be 0.0245 N/m and assuming a surface tension of 0.0347 N/m and a capillary constant of one, the $\cos\theta$ term is equal to 0.706, yielding a contact angle of approximately 45° for mineral oil on the glass tube. The value of 0.706 would only be valid for the case of mineral oil on glass. Even when a completely wetting fluid ($\cos\theta = 1$) is used on a non-ideal porous medium, the value of K remains unknown. One

approach to this problem is to use a capillary constant of one and analyze pore diameters "in terms of capillary pore equivalents" (Zeman and Zydney 1996). The influence of the capillary constant on bubble point test results will be discussed in Chapter 5.

2.4.2.2.4 Calculation of the Pore Size Distribution

The calculation of the pore size distribution requires use of the dry run and wet run results. The dry run establishes the airflow rate vs. pressure relationship for a dry geotextile sample. The wet run then determines the airflow rate vs. pressure relationship for a sample initially saturated with a wetting fluid. Differences in the two curves are due to the presence of wetting fluid within the geotextile sample. The results of the dry and wet runs are plotted on a graph of flow rate vs. pore size, with the pore sizes calculated from the pressure differences using Equation 2.7. An example of such a graph is shown in Figure 2.7. The percent finer for a particular pore size is calculated by comparing the airflow rates of the wet run to the dry run at that particular pore size. The equation for the percent finer of a pore size is presented in ASTM D6767-11 as:

$$\%\ finer = \left(1 - \frac{Q_W}{Q_D}\right) \times 100 \qquad \text{(Equation 2.9)}$$

where:

Q_w = wet run airflow rate (L/min)

Q_D = dry run airflow rate (L/min)

As an example, consider the results of the bubble point test shown in Figure 2.7. At the 0.1 mm pore size, the dry run airflow rate is 603 L/min and wet run airflow rate is 352 L/min. Applying Equation 2.9, the percent finer for the 0.1 mm pore size is:

$$\% \, finer = \left(1 - \frac{352}{603}\right) \times 100$$

$$\% \, finer = 41.6$$

Therefore, the percent finer for the 0.1 mm pore size would be 41.6. According to ASTM D6767-11, this means that 41.6% of the total pore diameters "based on the surface occupied by the pores" are smaller than or equal to 0.1 mm. Calculating the percent finer for a variety of pore sizes gives a pore size distribution. The pore size distribution for the bubble point results shown in Figure 2.7 is shown in Figure 2.8.

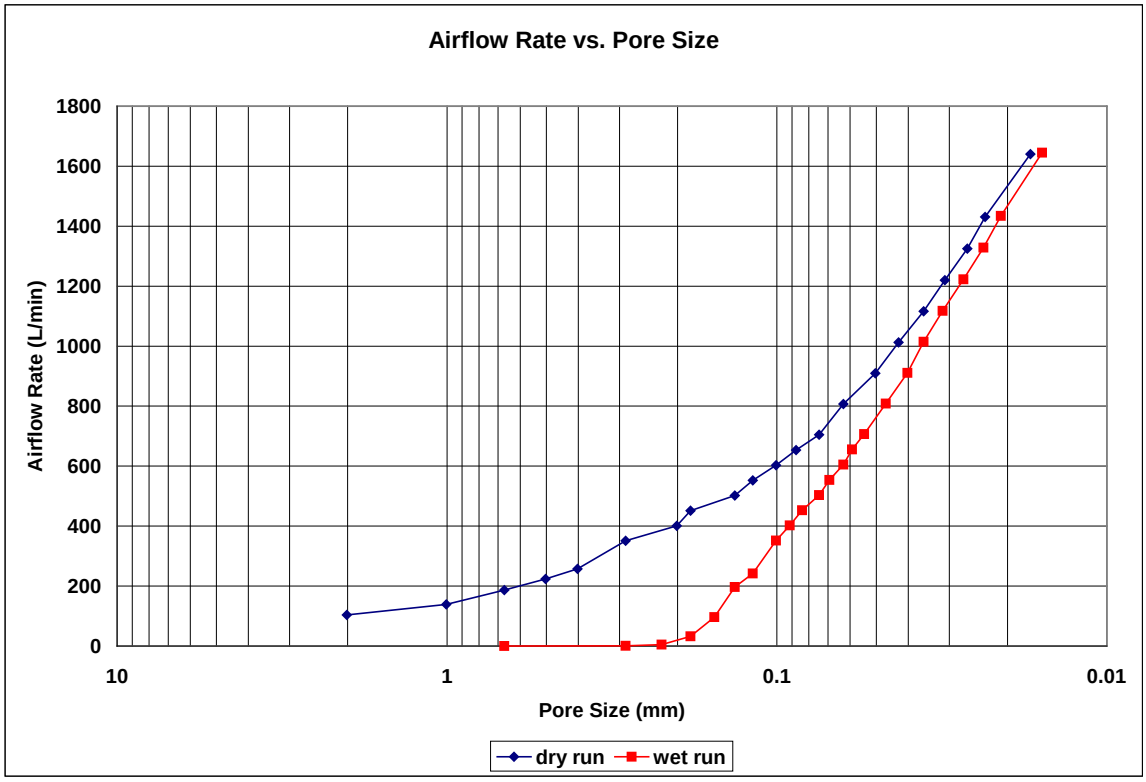

Figure 2.7: An example of bubble point test results, showing the airflow rate vs. pore size for the dry run and the wet run.

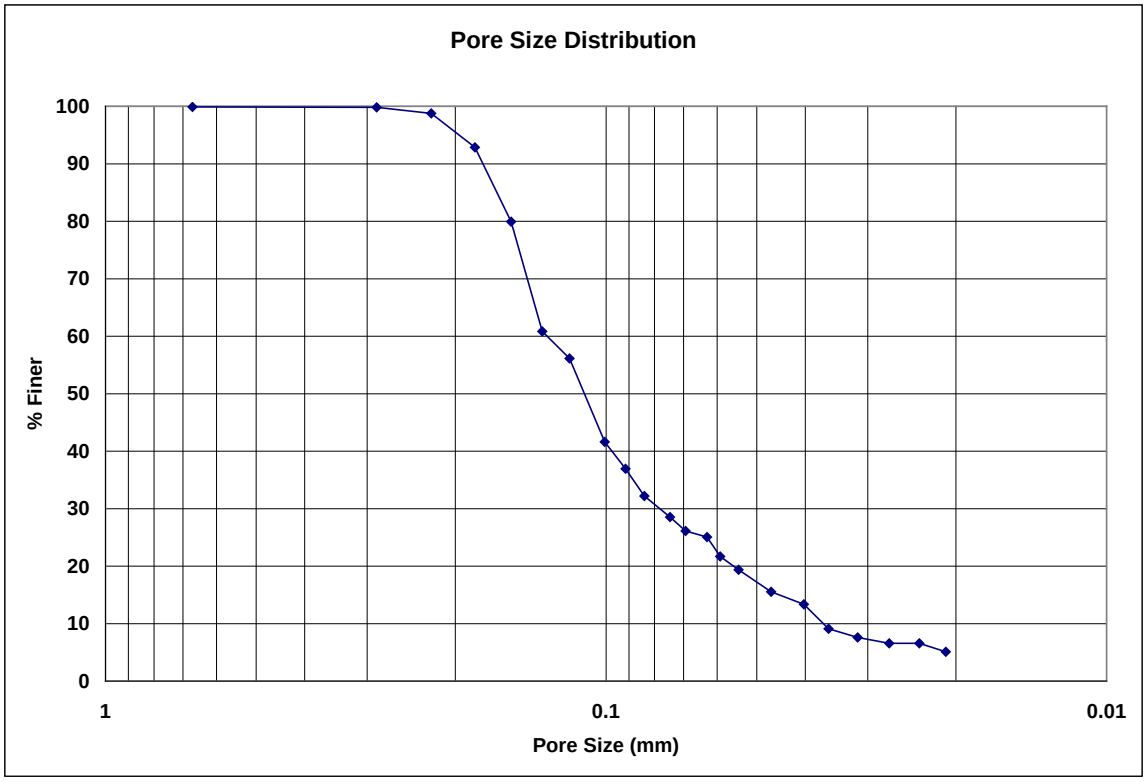

Figure 2.8: Pore size distribution determined for the bubble point test results in Figure 2.7.

2.4.2.2.5 Theoretical Completeness of ASTM D6767-11

Despite the research of many and the establishment of an ASTM standard, questions remain regarding the completeness of ASTM D6767-11 and the validity of pore size distributions determined using the method. The standard was adapted specifically for geotextiles from ASTM F316, and this was done with limited validation (Aydilek et al. 2007, D'Hondt 2005). Therefore, additional validation may be needed to ensure that the theoretical assumptions of ASTM D6767-11 are applicable to geotextiles and to determine if there are other parameters or phenomena that are relevant when measuring pore size distributions of geotextiles. ASTM D6767-11 allows for a variety of wetting fluids to be used, but notes that, "there is a potential influence of the fluid on a measurement of pore size, which should be taken into account by users through

verification tests on materials with known pore size." No explanation is provided in ASTM D6767-11 for *why* there is a potential influence of the wetting fluid on the measurement of pore size.

There are two parameters in the Washburn equation (Equation 2.7), which is the equation in which pore sizes are determined using ASTM D6767-11, that account for the influence of the wetting fluid. One parameter is the surface tension, which is dependent on the type of fluid and the temperature. The other parameter is the contact angle, which is dependent not only on the fluid, but also on the solid that the fluid is contacting. There are two possible reasons that the wetting fluid influences the measurement of pore size. Either incorrect values for the surface tension or the contact angle are being used in the Washburn equation, or there is some other parameter or phenomenon involved in the bubble point test that is not accounted for in ASTM D6767-11. As Berg (2010) notes, "literature values for the surface tension of pure liquids are plentiful and usually reliable, although they are often given for only one temperature." The influence of surface tension on pore size distributions is examined in Section 5.5 of this thesis. The contact angle is discussed further in Chapter 3 of this thesis. The influence of the contact angle on pore size distributions is examined in Section 5.3 of this thesis. The phenomenon of residual fluid is examined in Section 5.6 of this thesis as a potential wetting fluid-based influence on the measurement of pore size distributions.

2.5 Summary

Quantification of geotextile pore size is an essential part of geotextile filter design. Pore size distributions provide information about a range of pore sizes, which

more completely characterizes geotextile pore structure than the single value provided by the AOS test. While there are several methods available for quantifying the pore size distribution of geotextiles, each method is known to yield different pore size distributions for the same geotextile. These differences in pore size distribution are attributable to differences in pore size measurement among the methods. The bubble point test yields pore size distributions and measures pore constrictions, which influence filtration capability. Despite these two major advantages, questions remain regarding to the validity of the bubble point test for geotextiles. Particularly, it has been reported that there is a potential influence of the wetting fluid on the measurement of pore size, indicating that pore size distributions determined using the bubble point test may be a function of the wetting fluid used to perform the test. One possible cause for an influence of the wetting fluid on the measurement of pore size is the use of incorrect values for the fluid-dependent properties involved in the determination of pore size, namely surface tension and the contact angle. The contact angle is discussed in detail in Chapter 3 of this thesis, and an examination of the influence of the contact angle on pore size distributions is presented in Section 5.3. An examination of the influence of surface tension on pore size distributions is presented in Section 5.5. Another possible cause of an influence of the wetting fluid on the measurement of pore size is that there is some other pertinent parameter or phenomenon that affects the determination of pore size distributions that is not accounted for in the current bubble point theory. One such possible phenomenon is residual fluid, which is examined in Section 5.6 of this thesis.

Chapter 3: The Contact Angle – Background and Measurement

3.1 Relevance to the Bubble Point Test

The contact angle is an integral part of bubble point test theory. It is defined in Section 3.2.1 of this chapter. A review of the contact angle, its relevance to the bubble point test, and measurement techniques were discussed by Elton and Hayes (2007 and 2008b). Portions of this chapter have been adapted from Elton and Hayes (2008b) with permission from ICE Publishing. As a parameter of the Washburn equation for determining pore size, the contact angle of the wetting fluid on the geotextile must be known to calculate an accurate pore size distribution in accordance with ASTM D6767-11. The contact angle is unique in that its value is dependent on properties of both the wetting fluid and the solid. The Washburn equation was presented as Equation 2.5 and is presented again here for purposes of this discussion:

$$d = \frac{4\gamma B \cos\theta}{P} \qquad \text{(Equation 3.1)}$$

where:

d = pore size (diameter) (mm)

γ = surface tension (N/m)

P = pressure (Pa)

B = capillary constant

θ = contact angle (degrees)

The contact angle is considered to be a constant in the Washburn equation and the cosine of the contact angle is a multiplier for determining pore size. Therefore, the contact angle will affect the location of the pore size distribution plot along the x-axis (pore size); however, the *shape* of the pore size distribution plot will remain the same regardless of the contact angle. Because the cosine of the contact angle (a non-linear function) is taken in the Washburn equation, changing the contact angle will change the location of the pore size distribution plot in a non-linear manner. Figure 3.1 is provided as an example of how the pore size distribution computed from a single bubble point test can vary depending on the value used for the contact angle in the Washburn equation.

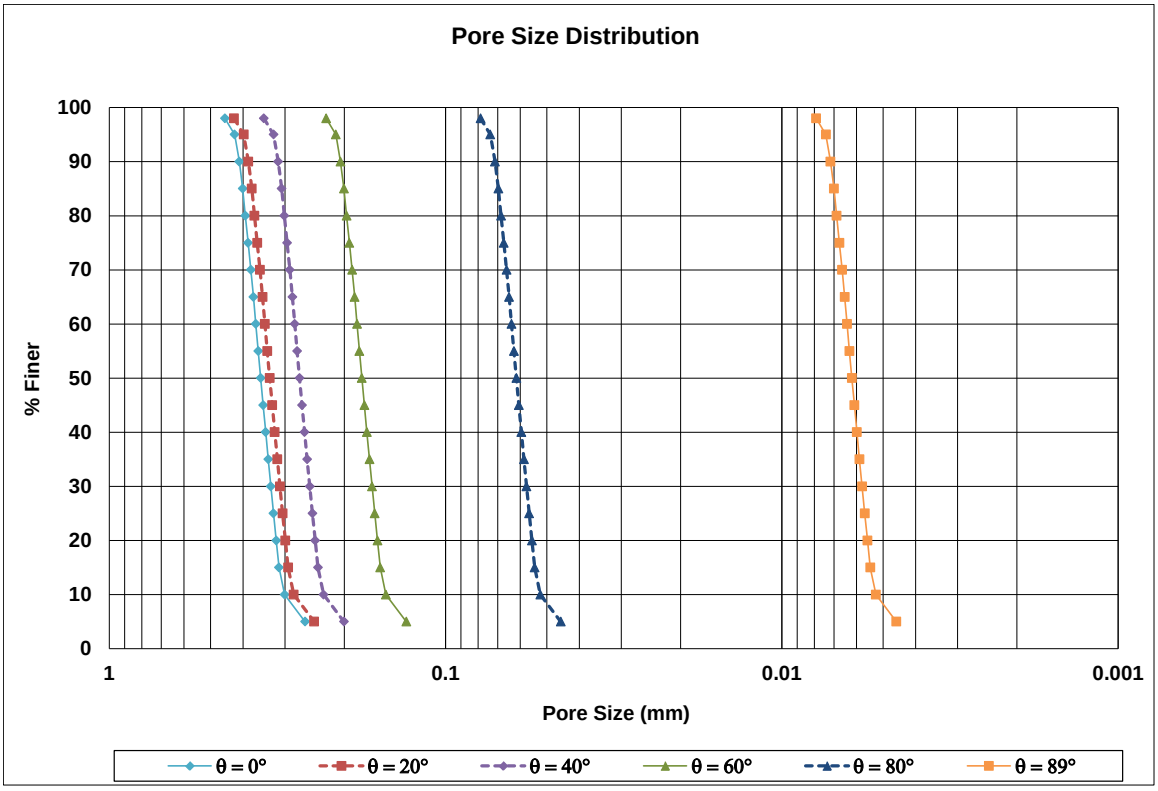

Figure 3.1: Pore size distribution variance as a function of the contact angle (θ), using the Washburn equation.

Bhatia and Smith (1994) show a similar trend for the influence of the contact angle on the pore size distribution obtained using mercury intrusion porosimetry, in which the contact angle is also used in the Washburn equation to determine pore size. Figure 3.1 shows the computed pore sizes from a bubble point test can vary roughly two orders of magnitude when the contact angle ranges from 0° to 89°. Figure 3.1 also demonstrates the influence of the non-linear cosine function on the pore size distribution. In the 0° to 89° range, the effect of the contact angle on the pore size distribution is much more pronounced for higher contact angle values. For example, the effect on the pore size distribution when changing the contact angle from 60° to 80° is much greater than when changing the value from 0° to 20°, even though in both instances the contact angle differs by 20°. This indicates that, in regard to calculating accurate pore size distributions, contact angle accuracy becomes more important for higher contact angle values (within the range of 0 – 90 degrees).

Accurate knowledge of the contact angle is critical to computing an accurate pore size distribution in accordance with ASTM D6767-11. Therefore, it is necessary to understand the definition of the contact angle, associated terminology, the factors that affect the contact angle, and the techniques used to measure the contact angle.

3.2 Definitions

3.2.1 The Contact Angle

An expression for the static contact angle was first derived by Young (1805) (Dussan 1979). The expression, known as Young's equation, "describes the balance of

interfacial tensions at static equilibrium for a drop of liquid on a solid surface" (Starkweather et al. 2000). Young's equation is given as:

$$\gamma_{2,3} \cos \theta = \gamma_{1,3} - \gamma_{1,2} \qquad \text{(Equation 3.2)}$$

where:

$\gamma_{1,2}$ = interfacial tension between the solid and the liquid drop

$\gamma_{2,3}$ = interfacial tension between the wetting liquid and air (surface tension)

$\gamma_{1,3}$ = interfacial tension between the solid and air

θ = contact angle

The diagram in Figure 3.2 shows the contact angle of a drop of liquid resting on a solid and the parameters of Young's equation. The contact angle is defined as the angle between the tangent of the liquid surface taken at the solid surface, measured inside the liquid. The contact angle will be present not only for liquid drops on a solid surface, but any case in which a solid – liquid – air interface occurs. For example, Figure 3.3 shows the contact angle that occurs when a solid is partially immersed in a liquid and Figure 3.4 shows the contact angle for a fluid in a partially-filled capillary tube. If the solid-liquid-air interface in Figures 3.2, 3.3, and 3.4 is stationary relative to the solid, the contact angle formed is known as the static contact angle. For cases where the solid-liquid-air interface is in motion relative to the solid, the contact angle formed is known as the dynamic contact angle.

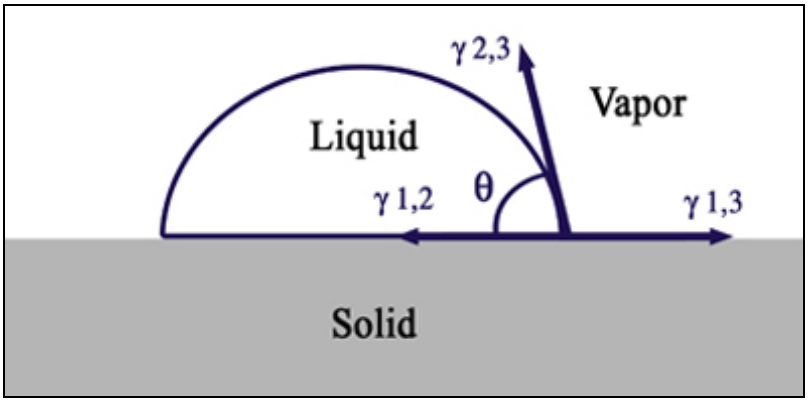

Figure 3.2: Diagram of the contact angle for a drop of liquid resting on a solid, showing the parameters of Young's equation. *Source*: Elton and Hayes 2008b.

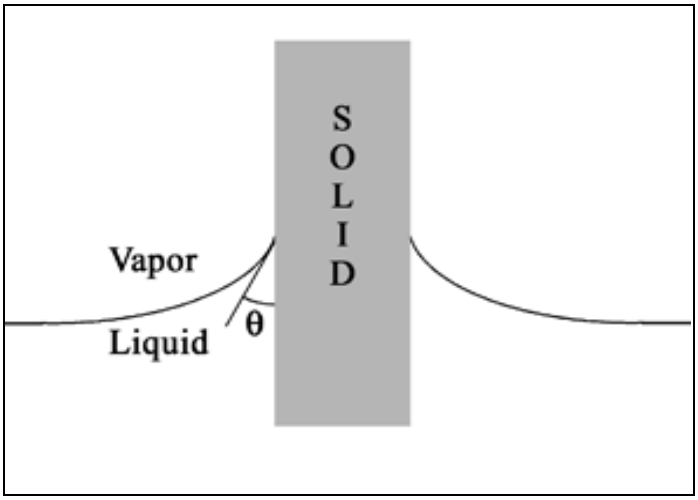

Figure 3.3: A diagram of a solid partially immersed in a liquid, showing the contact angle, θ. *Source*: Elton and Hayes 2008b.

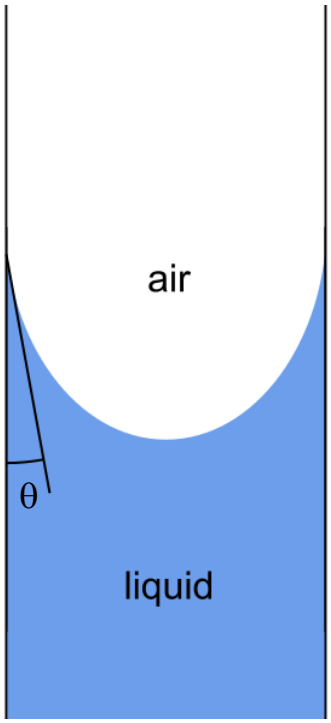

Figure 3.4: A diagram of a capillary tube partially filled with a liquid, showing the contact angle, θ. Adapted from Webb 2001.

3.2.2 Wettability

Qualitatively, the contact angle describes the wettability of a solid by a liquid. The liquid is said to "completely wet" the solid when the contact angle is zero, "partially wet" the solid when the contact angle is between 0° and 90°, and be "non-wetting" (or "partially non-wetting") when the contact angle is between 90° and 180° (Henry and Patton 1998, Van de Velde and Kiekens 1999, Berg 2010). A contact angle of 180° would be classified as "total non-wetting" (Berg 2010). Examples of wettability in terms of the contact angle for drops of liquid on a solid are shown in Figure 3.5.

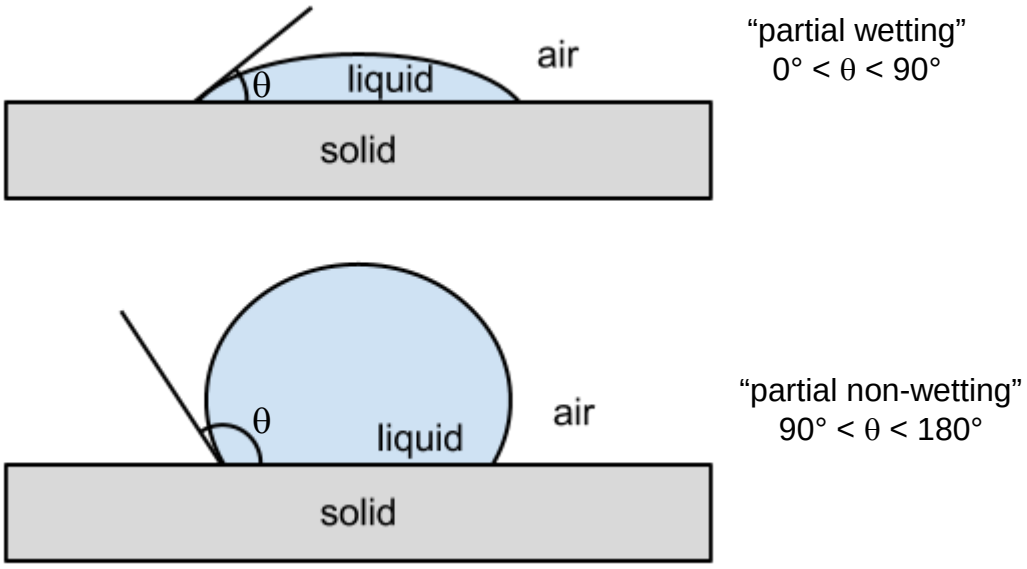

Figure 3.5: Examples of wettability in terms of the contact angle (θ) for drops of liquid on a solid. Adapted from Berg 2010.

Generally, liquids with a high affinity for a solid will result in lower contact angles, and higher contact angles will result when a liquid has a low affinity for a solid. For example, the contact angle of water on glass is typically zero due to hydrogen bonding between water and the glass (SiOH) surface. In contrast, water in contact with non-polar polypropylene has been shown to produce a contact angles between 50° and 90° (Miller and Young 1975).

3.2.3 Contact Angle Hysteresis: Advancing vs. Receding Contact Angles

Contact angles are typically different when a liquid is advancing over a solid compared to when a liquid is receding over a solid. "The angle formed when liquid moves out over a new surface is known as the advancing contact angle (θ_A), and the angle formed when liquid moves off of a previously occupied surface is known as the

receding contact angle (θ_R)" (Mohammad and Kibbey 2005). This difference is known as contact angle hysteresis (Van de Velde and Kiekins 1999). Though there are a variety of explanations for hysteresis (Huang et al. 2006), it is usually attributed to thermodynamic effects such as surface roughness and surface heterogeneity, and kinetic effects such as surface deformation, liquid penetration, surface mobility, and surface reorientation (Tretinnikov and Ikada 1994, Van de Velde and Kiekins 1999). The advancing contact angle, θ_A, is always greater than or equal to the receding contact angle, θ_R (Jenkins and Donald 1999, Berg 2010). Advancing and receding contact angles are shown in Figure 3.6.

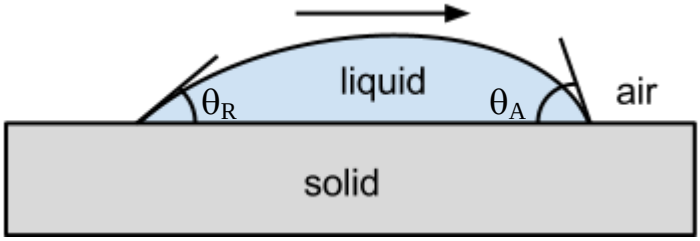

Figure 3.6: Advancing (θ_A) and receding (θ_R) contact angles. Adapted from Berg 2010.

Berg (2010) provides an excellent description of the process that is worth quoting in its entirety:

> When a drop of liquid is deposited on a solid surface, θ may assume some finite value. Then as more liquid is added, the interline remains fixed (or "pinned") so that the apparent contact angle increases. Finally, an angle is reached for which the interline "jumps" to a new position. The angle just before the jump occurs is the "static advanced contact angle" and is generally the value reported in the literature. The reverse situation occurs as liquid is withdrawn from the drop, leading to the "static receded contact angle."

Berg (2010) further describes a scenario where the interline is in motion relative to the solid, forming a "dynamic" contact angle that is a function of velocity. However,

Berg (2010) notes that at low velocity, the observed angle will be the static advanced or receded contact angle.

For a liquid extrusion technique (such as the bubble point method), the receding contact angle is the angle of interest (Miller and Tyomkin 1986). To be more specific, the static receded contact angle is the angle of interest because it is the contact angle formed just as the wetting fluid in pores overcomes equilibrium and begins to exit.

3.2.4 Macroscopic and Microscopic Contact Angles

In addition to advancing and receding, there are two other distinctions for contact angles that should be noted: macroscopic and microscopic. The following discussion of macroscopic and microscopic contact angles is presented by Decker et al. (1998):

> Contact angles measured on the macroscopic level characterize the average wettability of a materials system. In fact, knowledge of the macroscopic contact angle for a materials system allows one to predict not only whether a liquid droplet will bead up or spread out over a solid surface, but also the shape of the macroscopic fluid body in different geometries (e.g., a meniscus in a capillary tube). Thus, in their macroscopic use, contact angles are key in measuring the wettability in a laboratory situation and then predicting the wetting behavior of the same material system in another geometry or technological process. The measured macroscopic contact angle results from an averaging over the spatially varying microscopic contact angles.

Thus, the macroscopic contact angle would be of interest as an input for the Washburn equation.

3.3 Factors Affecting the Contact Angle

The contact angle is the quantitative measure of liquid-solid interactions that occur when a liquid contacts a solid (Van de Velde and Kiekens 1999). Therefore,

properties of both the solid surface and the fluid can affect the contact angle. The primary chemical property of the fluid that can affect the contact angle is the surface tension. Generally, fluids of low surface tension will have contact angles of zero (complete wetting) on solids (Bhatia and Smith 1994). Evidence of this can be seen by examining Equation 3.1. As the surface tension is decreased and the other interfacial tensions are held constant, the contact angle will approach zero. When the interfacial tension between the solid and the liquid ($\gamma_{1,2}$) and the interfacial tension between the solid and air ($\gamma_{1,3}$) are held constant, the contact angle will increase with increasing surface tension. The chemical structure of the fluid can affect the contact angle, as structure can determine characteristics such as polarity, which can influence how a fluid will interact with a solid. Other fluid traits including surfactant concentration, pH, and ionic strength, also affect the contact angle (Starkweather et al. 2000, Mohammad and Kibbey 2005). The array of fluid properties that can affect the contact angle indicates that the contact angle of different fluids on a solid can be different, and that the contact angle of a single fluid under different conditions (e.g., water at varying surface tension) can be different.

With respect to solids, the chemical composition of the solid surface can affect the contact angle (Berg 1989), and the surface roughness of the solid is widely reported to affect the contact angle (Bikerman 1958, Adamson 1976, Good 1984, Berg 1989). Specific to geotextiles, the "exact chemical composition of the fibers, the presence of trace amounts of oils used to lubricate needles during manufacture, calendering, denier, uniformity of curvature, and surface roughness" can affect the contact angle (Henry and Patton 1998).

3.4 Contact Angle Measurement

3.4.1 History

The contact angle has historically been a difficult value to measure (Neumann and Good 1977, Good 1984, Miller and Tyomkin 1986, Berg 1989). Direct observation methods such as drop analysis were primarily used before the advent of computer technology led to more sensitive automated methods. In his pioneering paper on mercury intrusion, Washburn (1921) suggested that the contact angle "could be determined from an X-ray photograph of a mercury meniscus in a capillary," or by the drop analysis method. Bikerman (1958) describes the drop analysis method as placing a drop of liquid on a solid surface and then either enlarging a photograph the drop profile or projecting the drop profile on a screen so that the tangent line of the liquid surface at the liquid – solid interface can be drawn manually. An example of a drop profile is shown in Figure 3.2. This manual method of contact angle measurement is subject to a considerable degree of operator dependence, which may explain variations in measurement by different observers, such as those reported by Good (1984).

3.4.2 Current Methods: Image Analysis and the Dynamic Contact Angle Analyzer

Improved methods of contact angle measurement now exist due to the advent of computer technology. One method, image analysis, involves digital image processing on photographs of sessile drops (Mohammad and Kibbey 2005, ASTM 1999), and digital image processing of electron microscope images (Jenkins and Donald 1999). Another current device for measuring contact angles is the Dynamic Contact Angle (DCA)

Analyzer. The DCA Analyzer measures the force of interaction at the liquid – solid – air interface as a solid sample is slowly lowered or raised in a liquid (see Figure 3.3), considers the effects of buoyancy, surface tension, sample size, and liquid density, and invokes force equilibrium at the solid-liquid interface to obtain the contact angle (Cahn 1996). This method is known as the Wilhelmy method and it evaluates dynamic wetting (Cahn 1996, Huang et al. 2006), yielding advancing and receding contact angles.

3.4.3 Contact Angle Measurement on Geotextiles and Other Textiles

There is limited information available regarding contact angle measurements on geotextiles. Henry and Patton (1998) reported measuring the contact angle of water on individual nonwoven geotextile fibers using a DCA Analyzer manufactured by the Cahn Instruments Corporation. In regard to other fabrics, Unsal et al. (2005) reported measuring the macroscopic contact angle of water and four other fluids at the surface of polypropylene nonwoven fabrics using a DCA Analyzer manufactured by the Cahn Instruments Corporation. Elton and Hayes (2007 and 2008b) measured macroscopic receding contact angles of a variety of fluids on nonwoven geotextile samples using a similar DCA Analyzer. The Elton and Hayes results are discussed further in Chapter 5.

3.5 Summary

As a parameter of the Washburn equation, the contact angle of the wetting fluid on the geotextile must be known to accurately determine pore sizes using the bubble point test, especially for larger contact angles. The contact angle is influenced by both the fluid and the solid surface, and it follows that different fluids on a solid can yield

different contact angles and the same fluid on different solids can result in different contact angles. There are several properties of the solid surface that can vary among geotextiles, including the chemical composition of the fibers, the presence of trace oils from the geotextile manufacturing process, and surface roughness, each of which can influence the contact angle. The contact angle has historically been a difficult parameter to measure. Limited information exists in the literature regarding the measurement of contact angles on geotextiles. However, with the advent of computer technology, improved contact angle measurement tools exist, such as the Dynamic Contact Angle Analyzer.

Chapter 4: The Bubble Point Test: Apparatus Design, Test Procedure, and Data Reduction

4.1 Introduction

An apparatus for performing bubble point tests in accordance with ASTM D6767-11 was developed and constructed at Auburn University by Dr. David Elton and others (Elton et al. 2007). Portions of this chapter have been adapted from Elton et al. (2007) with permission from ASTM International. This chapter presents a description of the apparatus design, the procedure for performing bubble point tests, and the data reduction needed to calculate pore size distributions.

4.2 Apparatus Design

4.2.1 General Design Requirements

In order to perform a bubble point test in accordance with ASTM D6767-11, the following general apparatus design requirements are needed:

- Subject a representative geotextile sample to controlled airflow;
- Measure the pressure difference across a geotextile sample;
- Measure the airflow rate; and
- Produce a pressure difference across a geotextile sample that is high enough to expel the wetting fluid from the smallest pores of the geotextile.

The bubble point test apparatus was designed based on these general requirements.

4.2.2 Overview of the Bubble Point Test Apparatus

A schematic of the bubble point test apparatus is shown in Figure 4.1. A photograph of the apparatus is shown in Figure 4.2 and a close-up photograph of the apparatus is shown in Figure 4.3. During operation, pressurized air (note: pressure source not shown in Figure 4.1) first passes through a filter and then through a series of valves, which control the airflow rate. Air then travels through a series of rotameters that measure the airflow rate, and then through the geotextile sample, where the pressure difference across the sample is measured with a manometer.

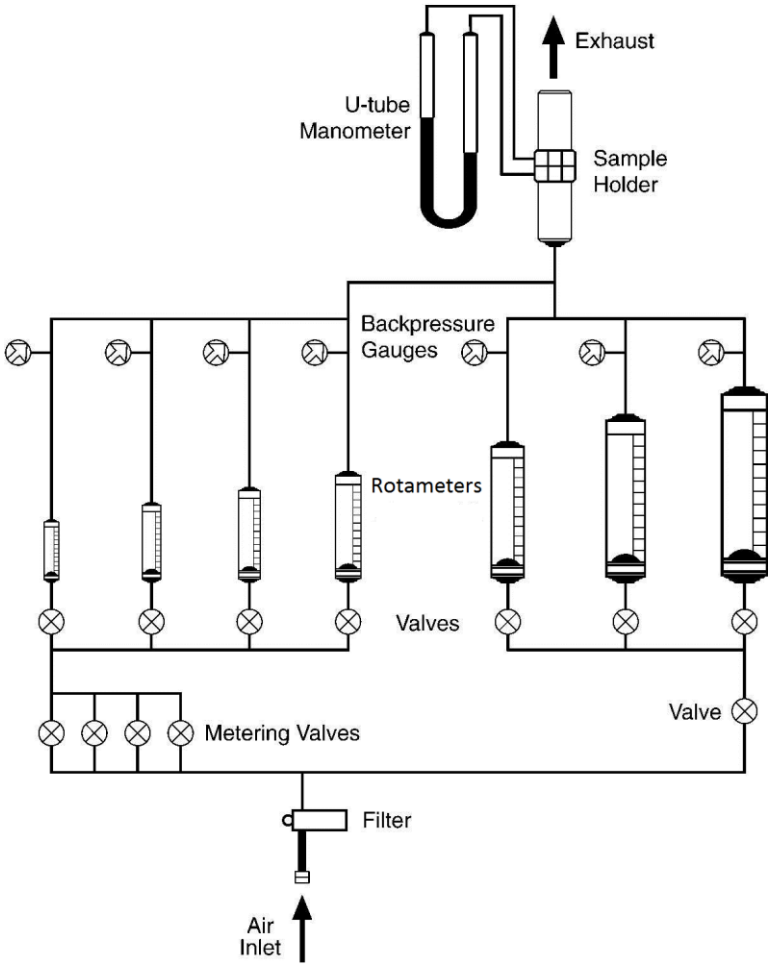

Figure 4.1: Schematic of the bubble point test apparatus. *Source:* Elton et al. 2007.

Figure 4.2: Photograph of the bubble point apparatus. *Source:* Elton et al. 2007.

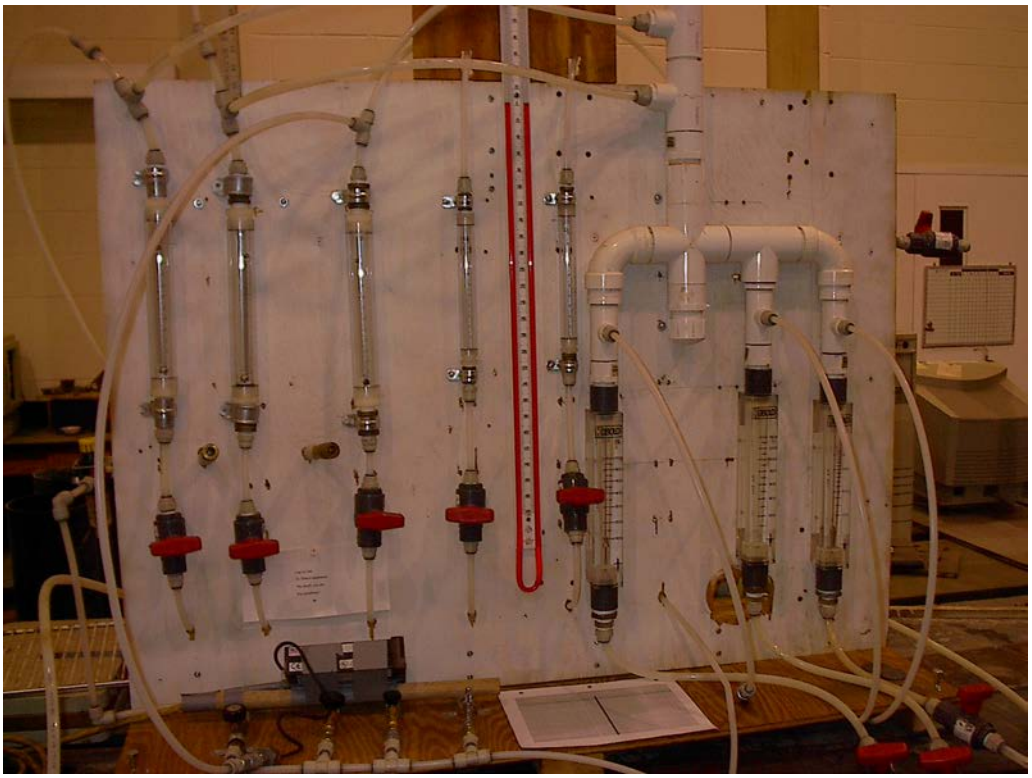

Figure 4.3: Close-up of the bubble point test apparatus. Photograph by David Howie.

4.2.3 The Effect of Head Loss

According to the Washburn equation, the higher the pressure difference across the geotextile sample, the smaller the pore size that can be measured. In order to maximize the available airflow rate and pressure difference across the geotextile sample, efforts must be taken to minimize head loss of the airflow, beginning at the pressure source and ending at the geotextile sample. The Darcy-Weisbach equation can be used to calculate the head loss of air and other fluids (both incompressible and compressible) in a pipe (Menon 2004):

$$h_f = \frac{fL}{d}\frac{v^2}{2g} \qquad \text{(Equation 4.1)}$$

where:

h_f = friction loss (m of head)

f = Darcy friction factor (dimensionless)

L = pipe length (m)

d = inside pipe diameter (m)

v = flow velocity (m/s)

g = gravitational acceleration (m/s^2)

Expressing the Darcy-Weisbach equation in terms of flow rate, Q, gives (Menon 2004):

$$h_f = \frac{8 f L Q^2}{g \pi^2 d^5} \qquad \text{(Equation 4.2)}$$

where:

h_f = friction loss (m of head)

f = Darcy friction factor (dimensionless)

L = pipe length (m)

d = inside pipe diameter (m)

Q = flow rate (m^3/s)

g = gravitational acceleration (m/s^2)

Examining Equation 4.2 gives insight into how head loss relates to the bubble point test apparatus. In regard to airflow conduits, head loss is proportional to the airflow conduit length and the inverse of the 5^{th} power of the conduit diameter. Therefore, decreasing the conduit length will lower head loss and increasing the conduit diameter will lower head loss. Head loss is particularly sensitive to the conduit diameter, as it is raised to the 5^{th}

power in the equation. Head loss is also proportional to the square of the airflow rate, indicating that higher airflow rates will result in higher head losses.

4.2.4 Components of the Bubble Point Test Apparatus

The following description of the bubble point test apparatus components is presented to explain the functions of various apparatus components and to provide insight into various design features. The rationale for the use of the components and design features was obtained by Dr. David Elton and others (e.g., Elton et al. 2007) through several years of developing, testing, and improving the bubble point test apparatus.

4.2.4.1 Air Filter

As air enters the bubble point test apparatus, it passes through a filter. The purpose of the filter is to minimize the entry of particulates (oil, dust, etc.) into the apparatus. Because the bubble point test apparatus uses very large volumes of air, even small concentrations of particulates in the airflow could have a significant cumulative affect on the flow of air through the apparatus. These particulates could also introduce error into the bubble point test by clogging and contaminating the geotextile sample.

4.2.4.2 Airflow Conduits

The conduits of airflow through the bubble point test apparatus are designed to reduce head loss wherever possible. A rubber hose is used as the airflow conduit from the air compressor to the bubble point test apparatus and a combination of plastic tubing and PVC pipe is used as the airflow conduit through the apparatus. Two important

concepts for minimizing head loss through the conduits are 1) the use of larger diameter (as opposed to smaller diameter) conduits to direct air from the air compressor to and through the apparatus, and 2) minimizing conduit length from the air compressor to and through the apparatus.

One specific design improvement to reduce head loss was increasing the diameter of the apparatus tubing. The apparatus was originally built with 9.5 mm (3/8 in) diameter tubing. When most of the original tubing was later upgraded to 12 mm (1/2 in) diameter tubing, higher airflow rates were obtained, indicating a decrease in head loss. Another specific design improvement was creating a direct conduit from the air filter to the high-airflow rotameters. This allows air to travel a shorter distance to high-flow rotameters, which reduces the elevated head losses that are associated with higher airflows.

4.2.4.3 Valves

Valves are used to control airflow through the apparatus. Metering valves are used for lower airflow rates (less than approximately 300 L/min) because precise airflow control is needed, as very small changes in airflow can make a large difference in the pressure drop across the sample, particularly at lower airflow rates. Cutoff valves are used to restrict airflow to rotameters that are not being used to measure a particular airflow rate. The rotameter cutoff valves are used in either the completely open or completely closed position. The rotameter cutoff valves used are ball valves, as they produce less head loss than gate valves.

4.2.4.4 Rotameters

Rotameters are used to measure the airflow rate of air entering the sample holder. A rotameter is a variable area flow meter in which an internal float balances to indicate the flow rate of a liquid or gas on a scale (OMEGA® 2013). The apparatus uses several rotameters covering different airflow ranges such that airflow rates ranging from 0.00838 L/min to 3400 L/min can be measured. All rotameters exhaust into a 4.00 cm (1.57 in) inside diameter PVC pipe. Two types of rotameters are used with the bubble point test apparatus: indirect reading rotameters and direct reading rotameters. Indirect reading rotameters display a scale of 0 – 100. A calibration of the scale to the corresponding flow rate is provided by the manufacturer. Indirect reading rotameters are used to measure the lower airflow rates (less than approximately 300 L/min). Direct reading rotameters display flow rate in units of L/min, so their values give a direct measurement of the airflow during a bubble point test. Direct reading rotameters are used to measure higher airflow rates (greater than 300 L/min).

4.2.4.5 Backpressure Gauge

Backpressure is the difference between the pressure at the exhaust of the rotameters and atmospheric pressure. Backpressure must be accounted for to correct the rotameter measurement, which is calibrated at atmospheric pressure at the exhaust. The adjusted measurement is then used with the rotameter calibration to determine the airflow rate. All rotameters have backpressure gauge ports connected at their exhausts. A digital pressure gauge connected to the desired rotameter port measures the pressure at the exhaust, which is used to correct the rotameter flow rate measurement.

4.2.4.6 Manometer

A manometer measures the pressure head loss, also referred to as the "pressure difference" or the "pressure drop", across the geotextile sample. Plastic tubing connects the manometer to two ports on the sample holder; one on the inlet side of the geotextile sample and one on the exhaust side. While some bubble point test apparatuses simply assume the pressure at the exhaust to be atmospheric, measuring the pressure at the inlet and the exhaust provides a more accurate pressure difference (Fischer 1994). The manometer must have the capacity to measure the maximum pressure difference created during a test. The apparatus uses a manometer that displays pressure difference in units of mm H_2O. A manometer with a pressure difference capacity of at least 1000 mm H_2O is recommended.

4.2.4.7 Sample Holder

The sample holder is a key component of the bubble point test apparatus. Proper design is critical to performing the bubble point test correctly. The sample holder connects just above the common rotameter exhaust pipe. A photograph of the sample holder is shown in Figure 4.4.

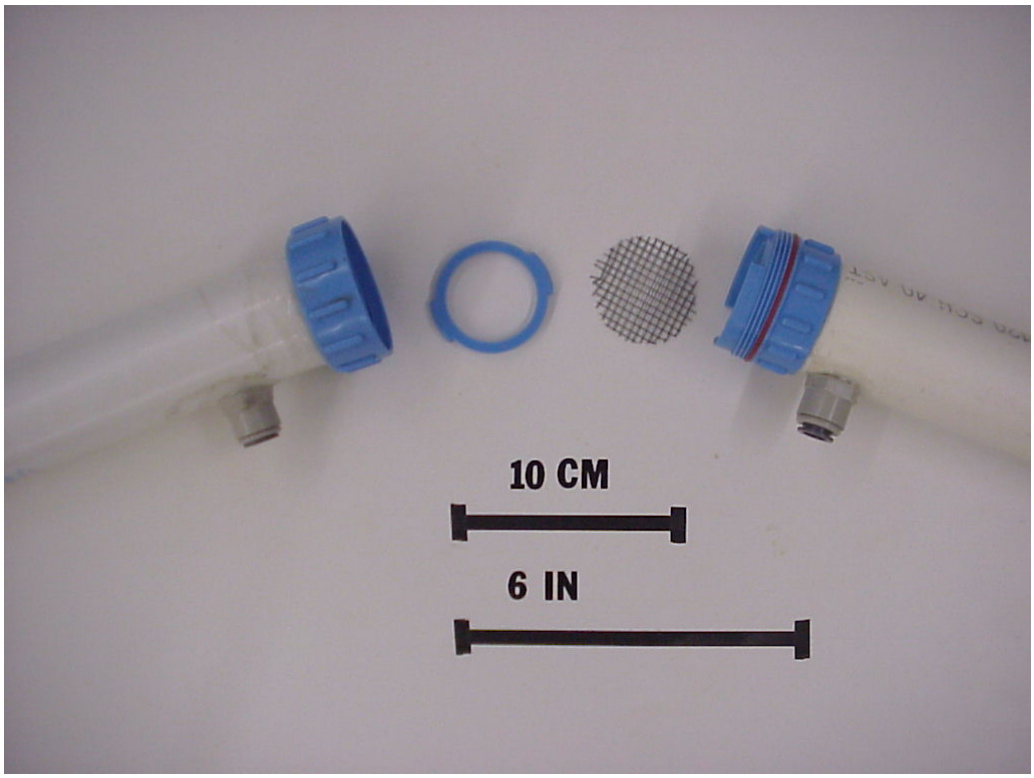

Figure 4.4: The sample holder, including the inlet pipe, wire screen, keyed washer, exhaust pipe, and manometer connection ports. *Source:* Elton et al. 2007.

The sample holder is composed of five general parts: an inlet pipe, a wire screen, a keyed washer, an exhaust pipe, and manometer connection ports. The inlet and exhaust pipe are both 30 cm (12 in) in length. The inside diameter of the inlet pipe and the exhaust pipe is 4.00 cm (1.57 in), which exposes 12.57 cm^2 (1.94 in^2) of the geotextile sample to airflow. The extended lengths and uniform diameters of the inlet and exhaust pipes are intended to keep pressure and airflow as uniform as possible as airflow enters and exits the geotextile sample. Uniformity of the inlet pipe diameter and the diameter of the geotextile sample exposed to airflow are important, as Fischer (1994) showed that differences in these can produce incorrect results. The geotextile sample is supported by the inlet pipe. A wire screen with a wire diameter of 0.045 cm and opening areas (holes) of 0.084 cm^2 is placed on top of the geotextile sample to prevent deformation during the bubble point test due to

airflow. The wire screen is considered to have negligible head loss. The keyed washer is placed on top of the wire screen – geotextile combination to prevent twisting of the geotextile sample when the inlet and exhaust pipes are screwed together. The exhaust pipe screws to the inlet pipe where the geotextile is supported and capped by the wire screen and the keyed washer. O-rings are used to seal the connection between the inlet pipe and the exhaust pipe and to ensure that air flows through the geotextile sample and not around it. The two manometer ports are positioned as close as possible to the geotextile sample. The ports consist of "quick connect" fittings that are glued into holes drilled in the PVC sample holder. To help reduce head loss, the quick connect fittings are cut flush with the inside of the sample holder. For convenience, two separate sample holders are used to perform the bubble point test: one for use with dry geotextile samples (the "dry run") and one for use with samples that have been saturated with a wetting fluid (the "wet run").

4.2.5 Design Summary

The bubble point test apparatus was constructed primarily with off-the-shelf components such as PVC pipe, plastic tubing, and valves. The total cost to construct the apparatus was approximately $3,000 USD (1999) (excluding the air compressor), which is a fraction of the cost of commercial apparatuses that sell for thousands more. Measures taken to reduce head loss, such as increasing the airflow conduit diameter and shortening airflow conduit length, have allowed higher airflow rates to be achieved. The higher airflows obtained through these design improvements allow for measurements of smaller geotextile pore sizes. Mitigation of head losses allows airflows of up to 1600

L/min to be maintained. This airflow capability has allowed for measurements of smaller pores comparable to some other apparatuses in the literature. For example, the Auburn University apparatus has measured pores an order of magnitude smaller than the minimum 0.1 mm measured by Vermeersch and Mlynarek (1996).

4.3 Test Procedure

4.3.1 Sample Preparation

4.3.1.1 Cutting the Geotextile Sample

A circular geotextile sample is cut from a geotextile sheet by hammering a 4.6 cm (1.81 in) diameter steel die into the sheet. The die allows for cutting reproducible geotextile samples faster and with greater precision, accuracy, and with less distortion than other methods of cutting, such as with a knife or with scissors. A diameter of 4.6 cm (1.81 in) is used so that the sample is small enough to lie flat in the sample holder (maximum diameter of 4.86 cm (1.91 in), yet is large enough to overlap the sample holder O-rings (minimum diameter of 4.00 cm (1.57 in)) which prevent air from flowing around the sample during the test.

4.3.1.2 Issue of Cleaning the Geotextile Sample

ASTM D6767-11 states that the geotextile sample should be soaked in water for one hour and allowed to dry prior to performing the test for the purposes of cleaning the sample. However, the author and others at Auburn University omit this step due to the possibility of residual water remaining in the pores and consequently introducing error. Due to the small pore sizes associated with nonwoven geotextiles, all water soaked in a

geotextile sample may not evaporate readily at room temperature. Residual water within the sample will affect pressure – airflow rate readings during the dry run. Furthermore, residual water remaining within the geotextile when a different wetting fluid is used for the bubble point test may result in a "hybrid" wetting fluid. If the wetting fluid used is miscible in water, residual water may mix with the wetting fluid and potentially alter wetting fluid properties, such as surface tension. If the wetting fluid used is not miscible in water, residual water and the wetting fluid may exist within the geotextile sample as two separate fluids, each with different properties. These effects have the potential to introduce error into the bubble point test results. For example, neither an altering of a property such as the wetting fluid surface tension nor the existence of two distinct surface tensions is accounted for in the data reduction (Washburn equation).

4.3.1.3 Sample Holder Assembly

After cutting the geotextile sample, the sample is immediately placed in the appropriate sample holder (i.e., either the dry run sample holder or the wet run sample holder). The wire screen and the washer are then placed on top of the geotextile sample and the exhaust pipe of the sample holder is screwed to the inlet pipe, enclosing the geotextile sample. The sample holder is then attached to the inlet and exhaust pipes of the apparatus and the manometer tubes are attached to their inlet and outlet ports on the sample holder.

4.3.2 Performing the Dry Run

Performing a bubble point test on a geotextile sample involves two "runs"; a "dry run" and a "wet run". A "run" involves exposing a geotextile sample to a series of airflow rates, which yield a series of pressure differences across the geotextile sample. The airflow rates are increased at sequential intervals, beginning with no airflow and ending at the maximum airflow rate of the apparatus. A "dry run" is a run performed on a geotextile sample that has not been exposed to a wetting fluid. A "wet run" is performed on a geotextile sample that is initially saturated with a wetting fluid. The dry run is performed first to ensure that the geotextile sample being used is not influenced by wetting fluid from the wet run.

To conduct the dry run, a dry geotextile sample is first loaded into the dry run sample holder and the sample holder is connected to the apparatus. All valves are initially closed at the beginning of the dry run. The main valve to the pressure source is opened fully and an inline air pressure regulator is adjusted to allow approximately 139 kPa (20 psi) of air pressure to the apparatus. Next, the cutoff valve for the first (smallest) rotameter is opened completely and the corresponding metering valve is opened slowly, allowing air to pass though the first rotameter and through the geotextile sample. The metering valve is opened slowly, typically until the manometer shows a pressure difference of 4 mm H_2O, which is essentially the minimum positive pressure difference that can be read from the manometer. To simplify data recording and reduce the possibility of error, the manometer reading is recorded as the direct reading on one side of the manometer u-tube (half of the actual pressure difference) and is later multiplied by two during data reduction (i.e., a manometer reading of 2 mm H_2O corresponds to a total

pressure difference of 4 mm H_2O). At this point, the rotameter value, backpressure, and the manometer value are recorded. These values are recorded by hand on a form and transferred later to a Microsoft Excel® spreadsheet for processing.

Once the first set of rotameter, backpressure, and manometer values are recorded, airflow to the geotextile sample is increased by adjusting the metering valves. As the airflow capacity of each rotameter is reached, the cutoff valve to the next largest rotameter is opened *before* closing the cutoff valve to the rotameter that has just reached capacity. The purpose of this is to allow for continuity and steady increase of airflow, as completely cutting off airflow may allow air to compress in the lines and result in a pulse of higher-than-expected airflow when airflow is resumed, which may remove wetting fluid prematurely. Additional sets of rotameter, backpressure, and manometer values are recorded at steps of approximately 2 to 6 mm H_2O (i.e., readings are taken at 4 mm H_2O, 6 mm H_2O, etc.). Once the airflow capacity of the indirect reading rotameters has been reached, airflow is directed to the larger, direct reading rotameters. Sets of rotameter, backpressure, and manometer readings are recorded at 50 L/min intervals from 350 to 700 L/min, and every 100 L/min from 700 to the maximum airflow, which is typically 1400 to 1600 L/min. Once the maximum airflow has been reached, the main valve to the pressure source is closed, which stops all airflow to the bubble point test apparatus. All cutoff valves are then opened to clear compressed air from the lines (all metering valves are already open). All metering valves are closed in order from largest to smallest rotameter in order to avoid compressing air, and all cutoff valves are closed.

4.3.3 Saturating the Geotextile Sample with the Wetting Fluid

To prepare the geotextile sample for the wet run, the sample must be saturated with the wetting fluid. The geotextile sample is saturated by slowly immersing it into the wetting fluid at an approximately 45° angle and allowing the fluid to absorb into the sample by capillary rise. This method was found by Dr. David Elton and others at Auburn University (Elton et al. 2007) to be more effective than immersing the entire geotextile sample in the wetting fluid at once or using vacuum saturation. After the wetting fluid has been allowed to enter the geotextile sample by capillary rise, the entire sample is immersed in the wetting fluid for approximately five minutes. No procedure to evaluate saturation has been developed.

4.3.4 Performing the Wet Run

The procedure for performing the wet run is nearly identical to the procedure for performing the dry run. The wet run sample holder is first loaded with a geotextile sample saturated with a wetting fluid and connected to the bubble point test apparatus. Operation of the valves and the recording of the rotameter, backpressure, and manometer values proceed as described for the dry run, however, more care must be taken when increasing the airflow rate during the wet run. Unlike the dry run where the manometer value continues to steadily increase as the airflow rate is increased, the manometer value will increase as the airflow rate is increased at beginning of wet run, but the value will suddenly begin to drop once a critical pressure difference is reached. The exact pressure difference at which this occurs varies for different geotextile samples and depends on the type of wetting fluid. The rate at which the manometer value decreases seems to be

dependent on the viscosity of the wetting fluid. The manometer value will drop more rapidly with wetting fluids of lower viscosity and more slowly with wetting fluids of higher viscosity.

The point during the wet run at which the manometer value, or pressure difference, begins to decrease is the point at which fluid begins to exit the largest pores of the geotextile sample. When fluid is expelled from any of the geotextile pores, there is less resistance to airflow, resulting in a decrease in the pressure difference across the geotextile sample. This effect has also been noted by Fischer (1994) and D'Hondt (2005). As the pressure difference decreases, it will eventually reach a point of equilibrium, as no additional fluid is being expelled from the geotextile pores. Readings of the rotameter, backpressure, and manometer values should not be recorded once the manometer reading begins to drop. This is because the pressure difference that motivated fluid to begin exiting pores is the pressure difference just before the manometer reading began to drop. *To record an accurate airflow rate which represents airflow through pores that have opened due to the motivating pressure difference, the airflow rate should be increased until the manometer reading returns to the level at which it began to drop*. Once the manometer reading returns to this level, readings of the rotameter, backpressure, and manometer are recorded. The process of noting when the manometer reading begins to drop, increasing the airflow rate until the manometer reading returns to that value, and then recording the rotameter, backpressure, and manometer readings is repeated throughout the wet run.

4.3.5 Summary of the Bubble Point Test Procedure

The primary steps for performing a bubble point test are summarized as follows:

1. Cut the geotextile sample
2. Place the geotextile sample in the dry run sample holder
3. Perform the dry run
4. Saturate the geotextile with the wetting fluid
5. Place the sample in the wet run sample holder
6. Perform the wet run

4.4 Data Reduction

4.4.1 Background

Once the dry run and the wet run have been completed, the bubble point test is complete and the next step is to perform the data reduction required to yield the pore size distribution. For bubble point tests performed at Auburn University, this originally involved a three-step process. First, the data recorded during the dry and wet runs were entered into a Microsoft Excel® spreadsheet for the purposes of calculating geotextile pore sizes and true airflow rates. Next, line graphs of the true airflow rate versus the pore size were plotted for both the dry run and the wet run on the same graph so that values of airflow rate at particular pore sizes could be read manually and the percent finer could be calculated at several pore sizes using the following equation (ASTM 2011c):

$$\%\ finer = \left(1 - \frac{Q_W}{Q_D}\right) \times 100 \qquad \text{(Equation 4.3)}$$

where:

Q_w = wet run airflow rate (L/min)

Q_D = dry run airflow rate (L/min)

Finally, a line graph of the percent finer versus the pore size was plotted, yielding a pore size distribution for the geotextile sample.

The original three-step method was adequate for producing a pore size distribution. However, the process of manually reading airflow rates at particular pore sizes from line graphs was time-consuming and tedious. Originally, the airflow rate versus pore size plot was constructed using Excel®. Manually reading airflow rates at particular pore sizes required adjusting the scale of the airflow rate (y-axis) several times, essentially "zooming in" on the plot in order to discern exact airflow rates. Reading enough airflow rates needed to produce the pore size distribution took approximately thirty minutes. To make manually reading airflow rates and pore sizes easier, the author began using the computer graphing program TableCurve 2D® (Systat Software Inc. 2000). Unlike Excel®, TableCurve 2D® provides x-y coordinates of the cursor location on graphs. This allowed the author to simply place the cursor along the line graph at the desired pore size and record the displayed airflow rate. This was much less tedious than manually reading airflow rates on Excel® graphs. However, the procedure was still time-consuming, as the process of manually setting up the graphs in TableCurve 2D® and manually recording pore sizes and airflow rates took approximately twenty minutes.

The author eventually developed a robust data reduction spreadsheet using Excel® that performs all of the necessary data reduction automatically. The automated data reduction spreadsheet requires only the input of basic pore size calculation parameters (i.e., contact angle, surface tension, and the constant, C) and raw data recorded during the

bubble point test. The pore size distribution is instantly displayed in a standardized format. In addition, pore sizes at twenty standard values of percent finer are automatically displayed in a table, which provides the pore size distribution in tabular form. Prior to the automated data reduction spreadsheet, generating such a table would have required manually reading the pore sizes at twenty different values of percent finer from the graphical form of the pore size distribution.

In addition to eliminating the need to read data points from the pore size distribution graph, the ease of which the tabular pore size distribution is generated with the automated data reduction spreadsheet has facilitated new methods of data analysis that were not previously considered. These new analyses include generating an average pore size distribution for a geotextile based on the pore size distributions of several individual samples, displaying the standard deviation of the average pore sizes as error bars to provide a graphical representation of sample variance, and computing tolerance intervals of pore size for each standard value of percent finer (opening size) (see, for example, Figures 5.4 – 5.8). The key to automatically generating the graphical and tabular forms of the pore size distribution is a piecewise linear interpolation method that allows any point on a line graph to be interpolated between known data points. With the automated data reduction spreadsheet, generating pore size distributions both in graphical and tabular format involves simply inputting basic parameters and the raw bubble point test data into the spreadsheet, which takes approximately ten minutes.

4.4.2 Automated Data Reduction Spreadsheet

An overview of the basic functions of the automated data reduction spreadsheet is presented in this section. An in-depth discussion of how the automated data reduction spreadsheet generates the pore size distribution in graphical and tabular form, including the formulas used perform the automated piecewise linear interpolation, is provided in Appendix A. The automated data reduction spreadsheet is an Excel® file containing several worksheets. All data input occurs on a single worksheet, the "Data Entry Sheet". Other worksheets provide the output data, which is a series of standardized reports based on the input data. Having all bubble point test input data and output data contained in one Excel® file is advantageous, as all data is stored together in one place and it can all be easily copied or saved to different locations.

4.4.2.1 Data Entry Sheet

An example of a completed Data Entry Sheet for a bubble point test is shown in Figure 4.5. All data entry cells are white, while non-data entry cells are either grey or green. The types of input data and calculations featured in the Data Entry Sheet are discussed in the following sections.

Bubble Point Test

Auburn University - Department of Civil Engineering

date of test:	3/23/2007	Pore Size Calculation Parameters:			
test identification:	2EH-8	constant, C:	2860	mm/m	● Lock Data Entry Cells
test performed by:	David Hayes	contact angle:	0	degrees	● Unlock Data Entry Cells
wetting fluid:	2-ethyl hexanol	surface tension:	0.0276	N/m	
ambient air temperature:	21.3 °C				
porous media:	NG-1 Nonwoven Geotextile				
comments:	testing to determine geotextile pore size distribution				

Dry Run

Recorded Data							Calculations				
Indirect Reading Rotameters				Direct Reading Rotameter Value (L/min)	Pressure at Rotameter Exit (psig)	Half of Manometer Reading (mm H20)	Manometer Reading (mm H20)	Manometer Pressure (Pa)	Pore Size (Diameter) (mm)	Indicated Airflow Rate (L/min)	True Airflow Rate (L/min)
First Rotameter Used		Second Rotameter Used									
Rotameter ID Number	Rotameter Value	Rotameter ID Number	Rotameter Value								
5	69				0.24	2	4	39.24	2.0116208	103	103.8374
5	90				0.41	4	8	78.48	1.0058104	137	138.8974
5	55	5	69		0.27	6	12	117.72	0.6705403	184.8	186.4894
5	66	5	81		0.38	8	16	156.96	0.5029052	220.7	223.5344
5	75	5	92		0.49	10	20	196.2	0.4023242	253	257.1821
				350	0.06	14	28	274.68	0.2873744	350	350.7136
				400	0.08	20	40	392.4	0.2011621	400	401.087
				450	0.09	22	44	431.64	0.1828746	450	451.3754
				500	0.11	30	60	588.6	0.1341081	500	501.8673
				550	0.12	34	68	667.08	0.1183306	550	552.2403
				600	0.14	40	80	784.8	0.100581	600	602.8504
				650	0.16	46	92	902.52	0.0874618	650	653.5278
				700	0.19	54	108	1059.48	0.0745045	700	704.5093
				800	0.25	64	128	1255.68	0.0628631	800	806.774
				900	0.3	80	160	1569.6	0.0502905	900	909.1373
				1000	0.36	94	188	1844.28	0.0428004	1000	1012.171
				1100	0.43	112	224	2197.44	0.0359218	1100	1115.972
				1200	0.49	130	260	2550.6	0.030948	1200	1219.836
				1300	0.58	152	304	2982.24	0.0264687	1300	1325.398
				1400	0.66	172	344	3374.64	0.0233909	1400	1431.084
				1600	0.75	236	472	4630.32	0.0170476	1600	1640.309

Wet Run

Recorded Data							Calculations				
Indirect Reading Rotameters				Direct Reading Rotameter Value (L/min)	Pressure at Rotameter Exit (psig)	Half of Manometer Reading (mm H20)	Manometer Reading (mm H20)	Manometer Pressure (Pa)	Pore Size (Diameter) (mm)	Indicated Airflow Rate (L/min)	True Airflow Rate (L/min)
First Rotameter Used		Second Rotameter Used									
Rotameter ID Number	Rotameter Value	Rotameter ID Number	Rotameter Value								
2	16					6	12	117.72	0.6705403	0.202	0.202
2	37					14	28	274.68	0.2873744	0.631	0.631
4	15				0.1	18	36	353.16	0.2235134	4.74	4.756095
4	83				0.54	22	44	431.64	0.1828746	31.7	32.27699
5	64				0.27	26	52	510.12	0.1547401	95.6	96.47396
5	58	5	72		0.34	30	60	588.6	0.1341081	194.3	196.5342
5	71	5	87		0.52	34	68	667.08	0.1183306	238	242.1729
				350	0.16	40	80	784.8	0.100581	350	351.8996
				400	0.17	44	88	863.28	0.0914373	400	402.3063
				450	0.18	48	96	941.76	0.0838175	450	452.7467
				500	0.2	54	108	1059.48	0.0745045	500	503.3899
				550	0.21	58	116	1137.96	0.0693662	550	553.9146
				600	0.23	64	128	1255.68	0.0628631	600	604.6757
				650	0.25	68	136	1334.16	0.0591653	650	655.5039
				700	0.27	74	148	1451.88	0.0543681	700	706.3993
				800	0.32	86	172	1687.32	0.0467819	800	808.6606
				900	0.35	100	200	1962	0.0402324	900	910.6513
				1000	0.42	112	224	2197.44	0.0359218	1000	1014.185
				1100	0.48	128	256	2511.36	0.0314316	1100	1117.815
				1200	0.56	148	296	2903.76	0.0271841	1200	1222.644
				1300	0.65	170	340	3335.4	0.0236661	1300	1328.431
				1400	0.73	192	384	3767.04	0.0209544	1400	1434.341
				1600	0.84	256	512	5022.72	0.0157158	1600	1645.079

Figure 4.5: An example of a completed Data Entry Sheet.

4.4.2.1.1 Input Data

The Data Entry Sheet is the sole location for data input. All non-data entry cells, including cells used to perform calculations, are locked to prevent unneeded input and the accidental changing of calculation formulas. An option to lock all data cells is also provided, so that inputted data can be protected from accidental changes. The Data Entry Sheet allows for the entry of test information such as the date and operator, and requires the entry of basic pore size calculation parameters such as the contact angle in addition to the raw data recorded during the bubble point test. The input data are as follows:

- Test Information Inputs:
    - Date of Test: allows the date the test was performed to be input
    - Test Identification: allows a test identification name or number to be input
    - Test Performed By: allows the name of the test operator to be input
    - Wetting Fluid: allows the name of the wetting fluid to be input
    - Ambient Air Temperature: allows the ambient air temperature to be input in degrees centigrade
    - Porous Media: allows a description of the tested porous media to be input
    - Comments: allows desired comments or other test information to be input
- Pore Size Calculation Parameter Inputs:
    - Constant, C: requires the input of the constant, C. According to ASTM D6767-11, C = 2860 mm/m, which corresponds to using a capillary constant, B = 0.715 in the Washburn equation. If the capillary constant, B, is omitted, then C = 4000 mm/m. See Section 2.4.2.2.2.

- Contact Angle: requires the input of the contact angle of the wetting fluid on the porous media in degrees.
- Surface Tension: requires the input of the surface tension of the wetting fluid in units of N/m.

- Bubble Point Test Raw Data Inputs (for both the dry and wet runs):
  - Indirect Reading Rotameter ID: requires the input of the indirect reading rotameter identification number. This number is used to correlate the rotameter value (scale of 0-100) to the calibrated airflow rate supplied by the manufacturer for a particular rotameter.
  - Indirect Reading Rotameter Value: requires the input of the indirect reading rotameter value (scale of 0-100). This number is used to correlate the rotameter value to the calibrated airflow rate supplied by the manufacturer for a particular rotameter.
  - Direct Reading Rotameter Value: requires the input of the direct reading rotameter flow rate in units of L/min.
  - Pressure at Rotameter Exit: requires the input of the pressure at the exit of the rotameter, also known as the backpressure, in units of psig. This value is used to correct the rotameter airflow rate readings, which are calibrated at a backpressure of atmospheric pressure.
  - Half of Manometer Reading: requires the input of the value of half of the manometer reading in units of mm H_2O. The value is read directly from one side of the U-tube manometer and represents half of the total pressure difference across the geotextile sample.

4.4.2.1.2 Calculations

Based on the input data, the following calculations are performed in the Data Entry Sheet for both the dry run and the wet run:

- Manometer Reading: the manometer reading in mm H_2O is calculated by multiplying the Half of Manometer Reading by a factor of two.
- Manometer Pressure: the Manometer Reading in mm H_2O is converted to units of Pa by multiplying the Manometer Reading by 9.81 (1 mm H_2O = 9.81 Pa).
- Pore Size (diameter): the pore diameter is calculated using the following form of the Washburn equation:

$$d = \frac{C\gamma \cos\theta}{P} \qquad \text{(Equation 4.4)}$$

where:

d = pore diameter (mm)

γ = surface tension (N/m)

P = pressure difference across the geotextile (Pa)

C = constant (mm/m)

θ = contact angle

- Indicated Airflow Rate: For indirect reading rotameter values, the scale values are converted to airflow rates in units of L/min using the VLOOKUP function. This function returns the airflow rate in L/min for a particular rotameter number and scale value based on a correlation table provided by the rotameter manufacturer that has been entered into the spreadsheet. For direct reading

rotameter values, the indicated airflow rate is the airflow rate in L/min read directly from the rotameter.

- True Airflow Rate: The rotameters providing the Indicated Airflow Rate are calibrated at atmospheric pressure at the rotameter exit, and therefore the readings must be corrected if this pressure is not atmospheric. Using the Pressure at Rotameter Exit (backpressure) value, the True Airflow Rate is calculated using the following equation (Elton et al. 2007):

$$Q_{True} = Q_{Indicated}\sqrt{\frac{P_{Exit} + 14.7}{14.7}} \qquad \text{(Equation 4.5)}$$

where:

Q_{True} = True (corrected) Airflow Rate (L/min)

$Q_{Indicated}$ = Indicated (uncorrected) Airflow Rate (L/min)

P_{Exit} = Pressure at the Rotameter Exit (backpressure) (psig)

4.4.2.2 Standardized Reports

Based on the input data and calculations from the Data Entry Sheet, several standardized reports are automatically generated. These reports are presented on additional worksheets within the automated data reduction spreadsheet Excel® file. The reports include the following:

- Airflow Rate vs. Pore Size Plot
- Pore Size Distribution Plot
- Pore Size Distribution Report
- Printable Data Entry Sheet

The standardized reports for the bubble point test results provided in the Figure 4.5 Data Entry Sheet are shown in Figures 4.6 – 4.9. Figure 4.6 shows the Airflow Rate vs. Pore Size Plot, which is a line graph of the True Airflow Rate vs. Pore Size for both the dry and wet runs. The Pore Size Distribution Plot is shown in Figure 4.7. To generate this plot, the percent finer is calculated at the pore size from each wet run data point shown on the Airflow Rate vs. Pore Size Plot that lies within the range of dry run data points. Recall that the percent finer is calculated using the following equation:

$$\%\ finer = \left(1 - \frac{Q_W}{Q_D}\right) \times 100 \qquad \text{(Equation 4.6)}$$

where:

Q_w = wet run airflow rate (L/min)

Q_D = dry run airflow rate (L/min)

If there is not a dry run data point with the same pore size of a particular wet run data point, the dry run airflow rate for that pore size is found by piecewise linear interpolation. Once the percent finer at the pore size of each wet run data point has been calculated, the percent finer versus the pore size is plotted as the Pore Size Distribution Plot. The Pore Size Distribution Report is shown in Figure 4.8. This report provides a summary of test information and pore size calculation parameters used in the data reduction, as well as the pore size distribution in graphical and tabular form. To generate the tabular form of the pore size distribution, the pore sizes corresponding to selected values of percent finer are obtained by piecewise linear interpolation between data points on the Pore Size Distribution Plot (the graphical form of the pore size distribution). The Printable Data Entry Sheet is shown in Figure 4.9. The Printable Data Entry sheet displays all values

input into the Data Entry Sheet but without the colors, making it efficient to print in black-and-white.

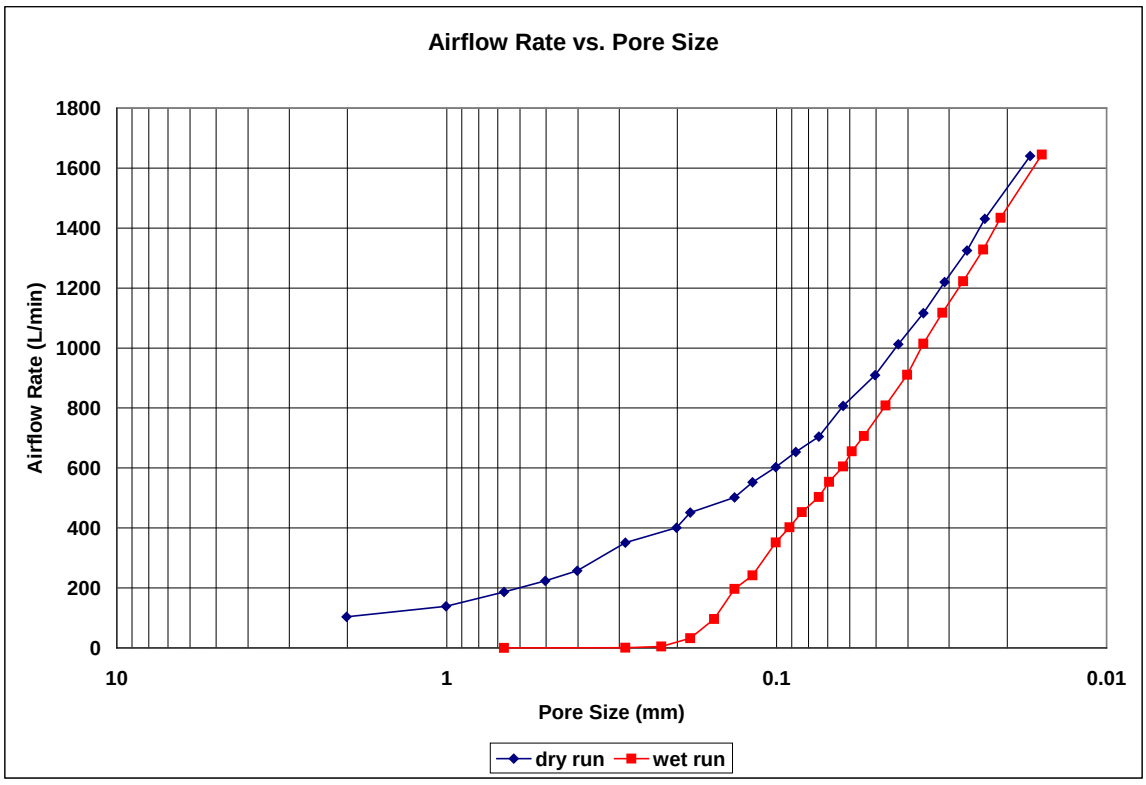

Figure 4.6: Airflow Rate vs. Pore Size Plot for the test results in Figure 4.5.

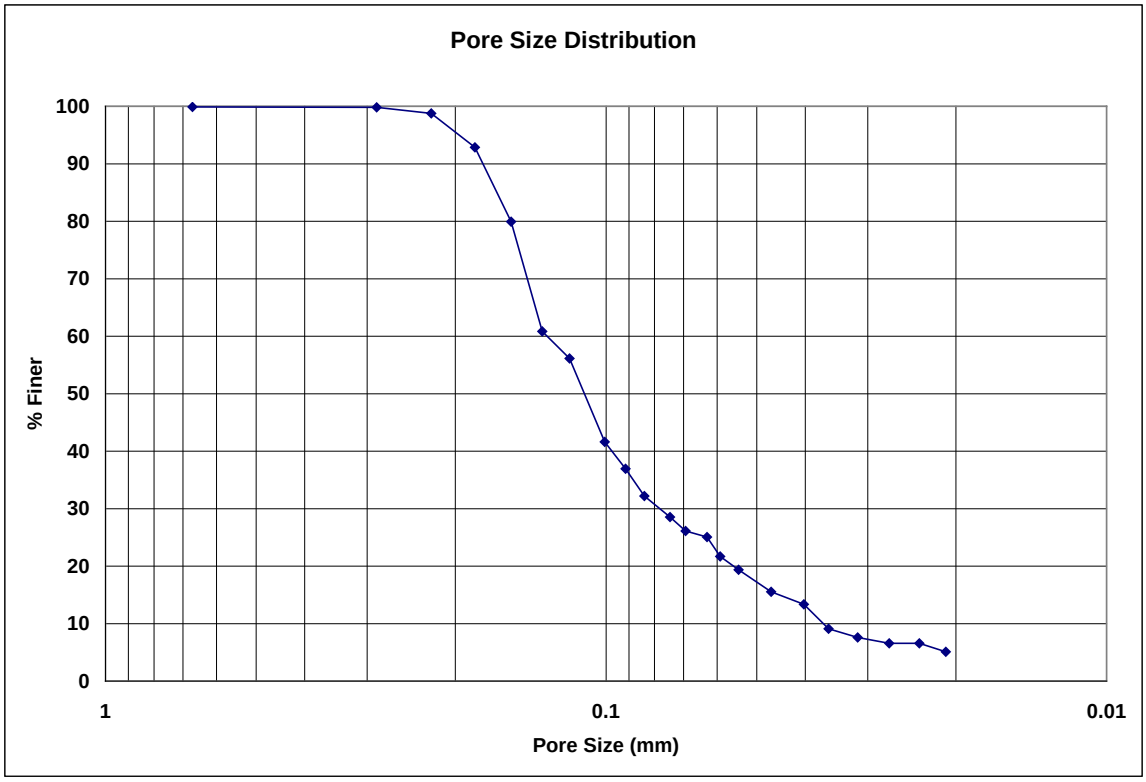

Figure 4.7: Pore Size Distribution Plot for the test results in Figures 4.5 and 4.6.

Bubble Point Test
Auburn University - Department of Civil Engineering

date of test:	3/23/2007	Pore Size Calculation Parameters:		
test identification:	2EH-8	constant, C:	2860	mm/m
test performed by:	David Hayes	contact angle:	0	degrees
wetting fluid:	2-ethyl hexanol	surface tension:	0.0276	N/m
air temperature:	21.3 °C			
porous media:	NG-1 Nonwoven Geotextile			
comments:	testing to determine geotextile pore size distribution			

Pore Size at Selected % Finer

% finer	pore size (mm)
98	0.21820
95	0.19763
90	0.17667
85	0.16579
80	0.15491
75	0.14942
70	0.14401
65	0.13861
60	0.13129
55	0.11693
50	0.11082
45	0.10470
40	0.09739
35	0.08829
30	0.07820
25	0.06281
20	0.05570
15	0.04518
10	0.03682
5	---

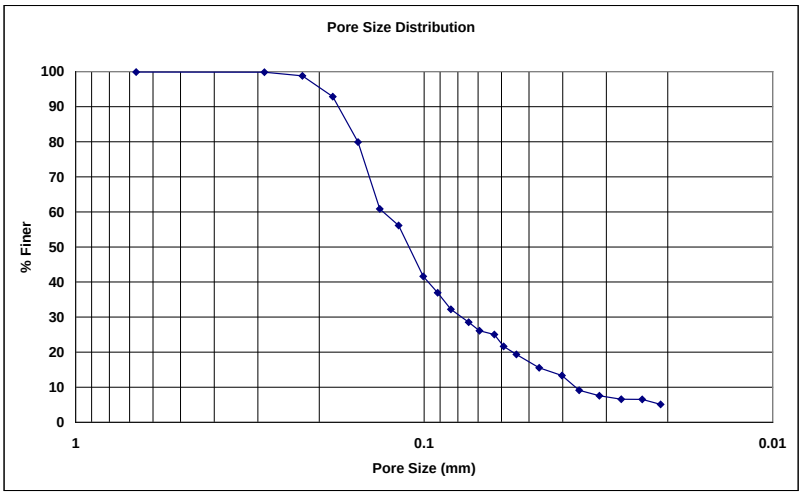

Figure 4.8: Pore Size Distribution Report for the test results shown in Figures 4.5-4.7.

Bubble Point Test

Auburn University - Department of Civil Engineering

date of test:	3/23/2007	Pore Size Calculation Parameters:	
test identification:	2EH-8	constant, C:	2860 mm/m
test performed by:	David Hayes	contact angle:	0 degrees
wetting fluid:	2-ethyl hexanol	surface tension:	0.0276 N/m
ambient air temperature:	21.3 °C		
porous media:	NG-1 Nonwoven Geotextile		
comments:	testing to determine geotextile pore size distribution		

Dry Run

Recorded Data							Calculations				
Indirect Reading Rotameters				Direct Reading Rotameter Value (L/min)	Pressure at Rotameter Exit (psig)	Half of Manometer Reading (mm H20)	Manometer Reading (mm H20)	Manometer Pressure (Pa)	Pore Size (Diameter) (mm)	Indicated Airflow Rate (L/min)	True Airflow Rate (L/min)
First Rotameter Used		Second Rotameter Used									
Rotameter ID Number	Rotameter Value	Rotameter ID Number	Rotameter Value								
5	69				0.24	2	4	39.24	2.0116208	103	103.8374
5	90				0.41	4	8	78.48	1.0058104	137	138.8974
5	55	5	69		0.27	6	12	117.72	0.6705403	184.8	186.4894
5	66	5	81		0.38	8	16	156.96	0.5029052	220.7	223.5344
5	75	5	92		0.49	10	20	196.2	0.4023242	253	257.1821
				350	0.06	14	28	274.68	0.2873744	350	350.7136
				400	0.08	20	40	392.4	0.2011621	400	401.087
				450	0.09	22	44	431.64	0.1828746	450	451.3754
				500	0.11	30	60	588.6	0.1341081	500	501.8673
				550	0.12	34	68	667.08	0.1183306	550	552.2403
				600	0.14	40	80	784.8	0.100581	600	602.8504
				650	0.16	46	92	902.52	0.0874618	650	653.5278
				700	0.19	54	108	1059.48	0.0745045	700	704.5093
				800	0.25	64	128	1255.68	0.0628631	800	806.774
				900	0.3	80	160	1569.6	0.0502905	900	909.1373
				1000	0.36	94	188	1844.28	0.0428004	1000	1012.171
				1100	0.43	112	224	2197.44	0.0359218	1100	1115.972
				1200	0.49	130	260	2550.6	0.030948	1200	1219.836
				1300	0.58	152	304	2982.24	0.0264687	1300	1325.398
				1400	0.66	172	344	3374.64	0.0233909	1400	1431.084
				1600	0.75	236	472	4630.32	0.0170476	1600	1640.309

Wet Run

Recorded Data							Calculations				
Indirect Reading Rotameters				Direct Reading Rotameter Value (L/min)	Pressure at Rotameter Exit (psig)	Half of Manometer Reading (mm H20)	Manometer Reading (mm H20)	Manometer Pressure (Pa)	Pore Size (Diameter) (mm)	Indicated Airflow Rate (L/min)	True Airflow Rate (L/min)
First Rotameter Used		Second Rotameter Used									
Rotameter ID Number	Rotameter Value	Rotameter ID Number	Rotameter Value								
2	16					6	12	117.72	0.6705403	0.202	0.202
2	37					14	28	274.68	0.2873744	0.631	0.631
4	15				0.1	18	36	353.16	0.2235134	4.74	4.756095
4	83				0.54	22	44	431.64	0.1828746	31.7	32.27699
5	64				0.27	26	52	510.12	0.1547401	95.6	96.47396
5	58	5	72		0.34	30	60	588.6	0.1341081	194.3	196.5342
5	71	5	87		0.52	34	68	667.08	0.1183306	238	242.1729
				350	0.16	40	80	784.8	0.100581	350	351.8996
				400	0.17	44	88	863.28	0.0914373	400	402.3063
				450	0.18	48	96	941.76	0.0838175	450	452.7467
				500	0.2	54	108	1059.48	0.0745045	500	503.3899
				550	0.21	58	116	1137.96	0.0693662	550	553.9146
				600	0.23	64	128	1255.68	0.0628631	600	604.6757
				650	0.25	68	136	1334.16	0.0591653	650	655.5039
				700	0.27	74	148	1451.88	0.0543681	700	706.3993
				800	0.32	86	172	1687.32	0.0467819	800	808.6606
				900	0.35	100	200	1962	0.0402324	900	910.6513
				1000	0.42	112	224	2197.44	0.0359218	1000	1014.185
				1100	0.48	128	256	2511.36	0.0314316	1100	1117.815
				1200	0.56	148	296	2903.76	0.0271841	1200	1222.644
				1300	0.65	170	340	3335.4	0.0236661	1300	1328.431
				1400	0.73	192	384	3767.04	0.0209544	1400	1434.341
				1600	0.84	256	512	5022.72	0.0157158	1600	1645.079

Figure 4.9: Printable Data Entry Sheet for the test results in Figures 4.5-4.8.

4.5 Summary

The design and components of a custom bubble point testing apparatus have been presented and described, along with the complete procedure used to perform bubble point tests. The bubble point test apparatus design and test procedures have been refined through years of research under the direction of Dr. David Elton at Auburn University. The method for reducing bubble point test data to produce a pore size distribution using an automated Microsoft Excel® data reduction spreadsheet developed by the author has also been described. The automated data reduction spreadsheet significantly reduces the time and effort required to generate pore size distributions from the bubble point test data. The addition of a tabular pore size distribution generated by the automated data reduction spreadsheet has made it possible to present and analyze bubble point test results using statistical methods that were not considered previously. Examples of these methods, which are discussed in Chapter 5 of this thesis, include the calculation of the mean pore size distribution for a series of bubble point tests, calculation of the standard deviation and 95% confidence interval for mean pore sizes, calculation of tolerance intervals, the use of outlier tests, and the use of analysis of variance (ANOVA) tests.

Chapter 5: Experiments, Results, and Analysis

5.1 Introduction

In order for the bubble point test to be used to determine geotextile pore size distributions for use in real-world filtration design, there must be confidence in the ability of the bubble point test to measure precise and accurate pore size distributions. As such, the initial goal of this research was to examine the precision and accuracy of bubble point testing on nonwoven geotextiles. Prior to the author's involvement with this research project, initial testing had been performed at Auburn University in regard to both precision and accuracy for bubble point tests. This initial testing showed that bubble point test results were generally reproducible (identified by visual inspection of several pore size distribution plots on a graph) for a variety of nonwoven geotextiles, and that different wetting fluids used to perform bubble point tests on a nonwoven geotextile resulted in different (identified by visual inspection) pore size distributions. Under the direction of Dr. David Elton, the author sought to expand the number of bubble point tests for a particular nonwoven geotextile using various wetting fluids, analyze bubble point test results using statistical methods, and investigate the influence of the wetting fluid on the pore size distribution.

To investigate the influence of the wetting fluid on the pore size distribution, the author began by focusing on the contact angle. After reviewing available literature as discussed in Chapter 3 of this thesis, the author measured the contact angle of each wetting fluid used to perform bubble point tests on samples of the tested nonwoven

geotextile using a Dynamic Contact Angle Analyzer manufactured by the Cahn Instruments Corporation. The use of different values of the capillary constant in the data reduction was examined in an effort to better understand its influence on pore size distributions. The influence of surface tension was examined by inputting water surface tension values for a range of typical indoor air temperatures in the data reduction. The influence of residual fluid remaining in pores after reaching the critical pressure was investigated in an effort to explain large variations in calculated pore sizes among wetting fluids for smaller values of percent finer.

5.2 Analysis of Bubble Point Test Results for a Nonwoven Geotextile

5.2.1 Introduction

The results of sixty bubble point tests performed on a nonwoven geotextile using six different wetting fluids (ten tests per fluid) were assembled for the purpose of analyzing the results using statistical methods. The bubble point tests were performed as described in Chapter 4 of this thesis by the author and previous researchers at Auburn University working under the direction of Dr. David Elton. All of the test results were processed using the automated data reduction spreadsheet developed by the author, as described in Chapter 4. The bubble point tests were performed on samples of a continuous filament, needlepunched, polypropylene nonwoven geotextile. For identification purposes in this thesis, this nonwoven geotextile will be referred to as NG-1. Selected material properties for the NG-1 nonwoven geotextile reported by the manufacturer are presented in Table 5.1. The six wetting fluids used were distilled water (hereinafter “water”), Porewick® (hereinafter “Porewick”), mineral oil, 2-ethyl hexanol,

Drakeol® 600 (hereinafter "Drakeol"), and glycerin. These wetting fluids were selected due to their wide range of fluid properties. The wetting fluids and selected fluid properties, which were tabulated by previous researchers at Auburn University working under the direction of Dr. David Elton, are listed in Table 5.2.

Table 5.1: Selected material properties for the NG-1 nonwoven geotextile.

Property	Test Procedure	Minimum Average Roll Value (MARV)
Weight	ASTM D5261	4.0 oz/yd^2
Thickness	ASTM D5199	45 mil
Grab Strength	ASTM D4632	120 lbs
Tear Strength	ASTM D4533	45 lbs
AOS	ASTM D4751	0.3 mm
Permittivity	ASTM D4491	2.4 sec^{-1}

Table 5.2: Selected properties of wetting fluids. *Sources*: Elton and Hayes (2007 and 2008b).

Property	water	Porewick	mineral oil	2-ethyl-hexanol	Drakeol	glycerin
Density (g/mL)	1	1.9	0.838	0.834	0.87	1.173
Surface Tension (N/m)	0.07225	0.016	0.0347	0.0276	0.0347	0.0634
Kinematic Viscosity (cSt)	1	2.1	25	11.8	90	741

The pore size distributions presented were determined using a Constant, C of 2860 mm/m (per ASTM D6767-11) and contact angles determined using the DCA Analyzer, as discussed in Section 5.3. For each wetting fluid, the following summary results are presented:

- A table of pore sizes at selected percent finer (tabular pore size distributions) for all ten tests

- A table of the statistics for pore sizes at selected percent finer. The statistics include the mean pore size, standard deviation, coefficient of variation, 95% confidence interval of the mean, maximum and minimum average roll values, and 95% tolerance interval with 95% coverage for pore sizes at selected percent finer. Statistical methods are described in Section 5.2.2.
- A graph of the pore size distributions from each of the ten individual tests
- A graph of the mean pore size distribution
- A graph of the mean pore size distribution, showing the standard deviation with error bars
- A graph of the mean pore size distribution, showing the 95% confidence interval of the mean
- A graph of the mean pore size distribution, showing the MaxARV, MARV, and the 95% tolerance interval with 95% coverage

These tables and graphs are presented in Sections 5.2.3 – 5.2.8 as Tables 5.4 – 5.15 and Figures 5.4 – 5.33. The complete results of each individual bubble point test used are presented in Appendix B. The bubble point test summary results presented in Sections 5.2.3 – 5.2.8 are discussed in Section 5.2.9. The identification of outlying measured pore sizes, their potential cause, and the influence of outlier removal on the summary results are discussed in Section 5.2.10. The use of characteristic (mean) pore size distributions for each wetting fluid to evaluate wetting fluid-based differences in pore size distribution is discussed in Sections 5.2.11 and 5.2.12.

5.2.2 Statistical Methods

Several statistical methods used to analyze bubble point test data are described in the following sections. Some of the methods described are based on the assumption that the data follows a normal distribution. The assumption that geotextile properties follow a normal distribution is common in the geotextile industry, and this practice will be discussed further in Section 5.2.2.5. The author found two statistics references to be particularly useful: 1) Statistics Manual by Crow et al. (1960), and 2) Statistics for Environmental Engineers, 2nd Edition, by Berthouex and Brown (2002).

5.2.2.1 Mean

The arithmetic mean or average is often used to describe where values of a data set are centered. In other words, the mean is used to describe the central tendency or central location of a data set. For a normally-distributed population, the mean is equal to the median, representing the 50% percentile value of the population. A sample mean is distinguished from the population mean in that the sample mean is computed from a limited number of observations collected from the total population, whereas the population mean is the true mean based on all or large numbers of observations from the population. The sample mean is "generally the best estimate" of the population mean (Crow et al. 1960). In the case of bubble point testing, the sample would represent the pieces of geotextile that bubble point tests were performed on and the population would be the entire geotextile of interest. The arithmetic mean or average of a sample is given by the following equation (Berthouex and Brown 2002):

$$\bar{x} = \frac{1}{n}\sum_{i=1}^{n} x_i \qquad \text{(Equation 5.1)}$$

where:

$\bar{x}$ = the mean of a sample of n observations

x_i = the ith observation

n = the number of observations

The population mean is commonly denoted as μ.

5.2.2.2 Standard Deviation

The standard deviation is "often used as an index of precision (or imprecision)" (Berthouex and Brown 2002). The standard deviation of a sample is given by the following equation (Berthouex and Brown 2002):

$$s = \left[\frac{1}{n-1} \sum_{i=1}^{n} \left(x_i - \bar{x} \right)^2 \right]^{1/2} \qquad \text{(Equation 5.2)}$$

where:

s = the standard deviation of a sample of n observations

$\bar{x}$ = the mean of a sample of n observations

x_i = the ith observation

n = the number of observations

The standard deviation of a population is commonly denoted as σ.

5.2.2.3 Coefficient of Variation

The coefficient of variation is the standard deviation expressed as a percentage of the mean. Expressing the standard deviation this way is useful for understanding the magnitude of the standard deviation in relation to the mean and for comparing the variance of different data sets. It is a particularly useful index of precision for comparing populations with very different means (Minitab Inc. 2010b). The coefficient of variation is given by the following equation (Berthouex and Brown 2002):

$$CV = \frac{s}{\bar{x}} \times 100 \qquad \text{(Equation 5.3)}$$

where:

CV = the coefficient of variation (%)

s = the standard deviation of a sample of n observations

$\bar{x}$ = the mean of a sample of n observations

5.2.2.4 Confidence Interval of the Mean

When a sample mean is calculated from a limited number of observations, there is some uncertainty in how accurately the sample mean reflects the population mean. The uncertainty exists because the sample mean is computed using a limited number of observations taken from the larger population. The confidence interval of the mean can be thought of as an interval that is likely to contain the unknown population mean (Minitab Inc. 2010b). For a normally-distributed population, the confidence interval of the sample mean is given by the following equation (Berthouex and Brown 2002):

$$\bar{x} \pm \frac{t_{\alpha/2,n-1}}{\sqrt{n}} s \qquad \text{(Equation 5.4)}$$

where:

$\bar{x}$ = the mean of a sample of n observations

$t_{\alpha/2,n-1}$ = Student's t distribution value for a given significance level, α, and n-1 degrees of freedom

n = the number of observations

s = the standard deviation of a sample of n observations

Confidence intervals can be calculated by looking-up values of the t-distribution from tables found in standard statistics books, by using the t-distribution function in Microsoft Excel®, or through the use of statistical software such as Minitab® (Minitab Inc. 2010a).

Table 5.3 conveniently lists values of $\frac{t_{\alpha/2,n-1}}{\sqrt{n}}$ for the two-sided 95% confidence interval (significance level, $\alpha = 0.05$). "Two-sided" indicates that there is a 95% degree of confidence that the population mean will be contained *between* the upper and lower confidence limit, as opposed to "one sided" which would indicate that, for the specified degree of confidence, the population mean is either below the upper confidence limit or above the lower confidence limit. It can be seen from Table 5.3 that, as the number of observations approaches infinity, the confidence interval will approach zero. This is because, for large values of n, the calculated sample mean approaches the true population mean.

Table 5.3: Factors for two-sided 95% ($\alpha = 0.05$) confidence intervals and tolerance intervals for the mean of a normal distribution. *Source*: Berthouex and Brown 2002.

n	Confidence Intervals $(t_{n-1,\,\alpha/2}/\sqrt{n})$	$K_{1-\alpha,p,n}$ for Tolerance Intervals $p = 0.90$	$p = 0.95$	$p = 0.99$
4	1.59	5.37	6.34	8.22
5	1.24	4.29	5.08	6.60
6	1.05	3.73	4.42	5.76
7	0.92	3.39	4.02	5.24
8	0.84	3.16	3.75	4.89
9	0.77	2.99	3.55	4.63
10	0.72	2.86	3.39	4.44
12	0.64	2.67	3.17	4.16
15	0.50	2.49	2.96	3.89
20	0.47	2.32	2.76	3.62
25	0.41	2.22	2.64	3.46
30	0.37	2.15	2.55	3.35
40	0.32	2.06	2.45	3.22
60	0.26	1.96	2.34	3.07
∞	0.00	1.64	1.96	2.58

Source: Hahn, G. J. (1970). *J. Qual. Tech.*, 3, 18–22.

5.2.2.5 Maximum and Minimum Average Roll Values

The concepts of Maximum and Minimum Average Roll Values (MaxARV and MARV, respectively) are commonly used in the geotextile industry to describe geotextile properties. MaxARV and MARV are defined as follows (Koerner and Koerner 2011):

$$MARV = \bar{x} - 2s \qquad \text{(Equation 5.5)}$$

where:

MARV = minimum average roll value

$\bar{x}$ = the mean of a sample of n observations

s = the standard deviation of a sample of n observations

$$MaxARV = \bar{x} + 2s \qquad \text{(Equation 5.6)}$$

where:

MaxARV = maximum average roll value

$\bar{x}$ = the mean of a sample of n observations

s = the standard deviation of a sample of n observations

As Koerner and Koerner (2011) explain, "the minimum average roll value (MARV) concept was jointly developed by geotextile users and manufacturers while crafting acceptance protocols in the early 1980's," with the concept serving as a "negotiated middle-ground between the user (often a civil engineer) accustomed to requiring absolute minimum values [of properties] and the textile manufacturers accustomed to providing average values in their product listing of numeric test values." In the case of most geotextile properties (e.g., strength characteristics), it is desired that measured properties will exceed some value, making MARV an appropriate benchmark. If a maximum value is of interest, such as a maximum-allowable AOS opening size, the MaxARV is used (Koerner 2005). "As defined in ASTM D4439 [(ASTM 2011b)], the MARV value yields a 97.7% degree of confidence that any samples taken from quality assurance testing will exceed the value reported" (Propex 2011). The definitions of MaxARV and MARV are derived based on percentiles of a normal distribution. As shown in Figure 5.1, the range of 95% of the observations of a normally-distributed population fall between the limits of the population mean +/- 1.96 times the standard deviation of the population. The value of 1.96 is known as the "z-score". The z-score is "the value of a normally distributed

random variable that has been standardized to have a mean of zero and a standard deviation of one by the transformation" (USEPA 2001):

$$z = \frac{x - \mu}{\sigma} \qquad \text{(Equation 5.7)}$$

where:

z = z-score

x = value of a normally distributed random variable

μ = population mean

σ = population standard deviation

The z-score is the number of standard deviations that a value deviates from the population mean. Tables of the z-score and corresponding distribution coverage are commonly included in statistics books. Rounding 1.96 to 2, Figure 5.2 shows that approximately 5% of the observed values (2.5% on each end) will be outside the limits of the population mean +/- 2 times the population standard deviation. The lower limit is defined as the MARV, as indicated in Figure 5.2, and the upper limit would be the MaxARV. Approximately 97.5% of observed values from the population will be greater than the MARV (or less than the MaxARV). An inherent assumption when calculating MARV or MaxARV is that the *population* mean and the *population* standard deviation are known, which is only the case when large numbers of observations are available.

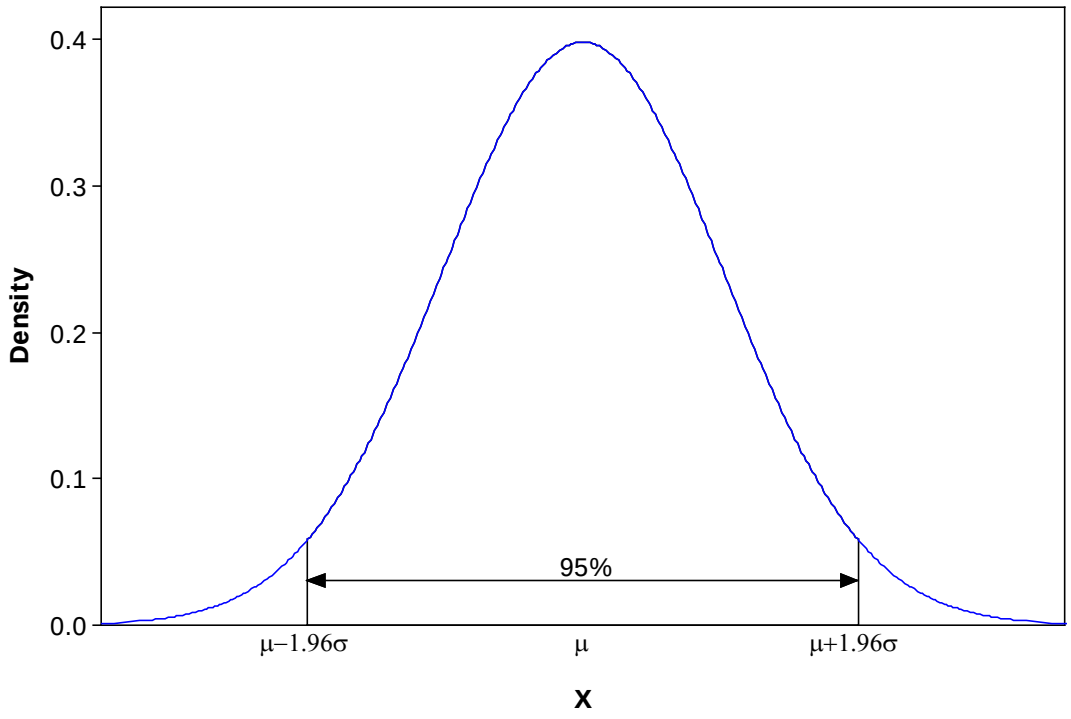

Figure 5.1: Normal distribution of a population showing 95% coverage in terms of the mean (μ) and the standard deviation (σ). The number of standard deviations from the mean is also known as the z-score.

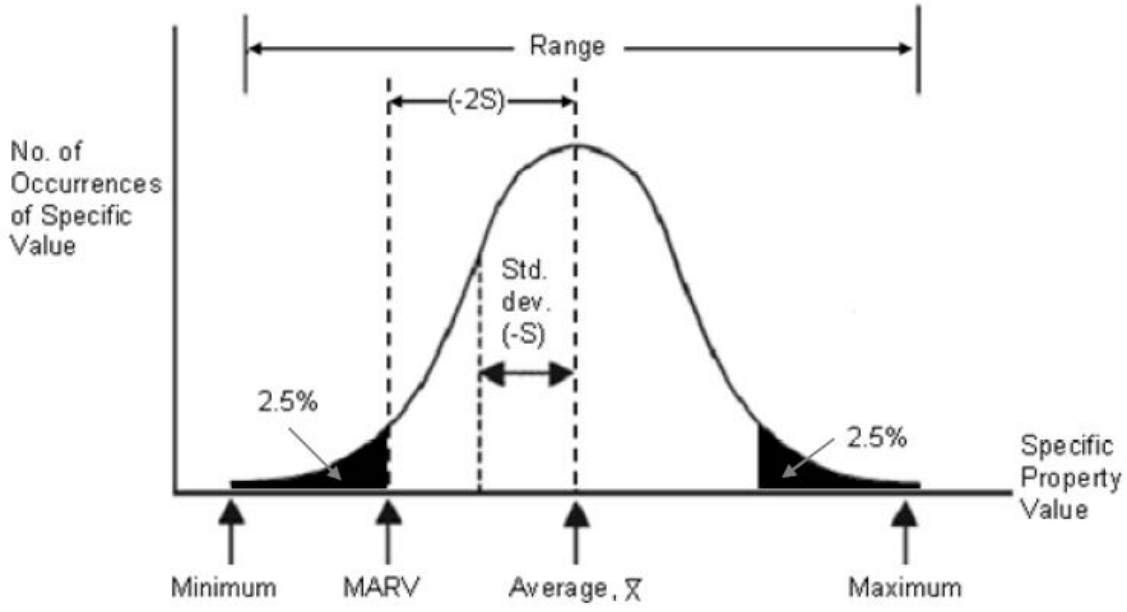

Figure 5.2: Normal distribution, showing MARV. *Source:* Koerner and Koerner 2011.

5.2.2.6 Tolerance Interval

Tolerance intervals enclose some percentage of the population with a given level of confidence (Crow et al. 1960). The MARV and MaxARV enclose a percentage of the population, assuming that the true values of the population mean and standard deviation are known. However, a tolerance interval can be computed in the case where only the sample mean and sample standard deviation are known. For a normally-distributed population, the tolerance interval for a sample of observations is given by (Berthouex and Brown 2002):

$$\bar{x} \pm Ks \qquad \text{(Equation 5.8)}$$

where:

$\bar{x}$ = the mean of a sample of n observations

K = tolerance factor

s = the standard deviation of a sample of n observations

Note in Table 5.3 that, as the number of observations approaches infinity (the population), the tolerance value for the two-sided 95% coverage approaches the z-score of 1.96.

5.2.2.7 Outlier Test

An outlier, or outlying value, can be defined as "an observation that appears to deviate markedly in value from other members of the sample in which it appears" (ASTM E178-08). Outliers can be problematic in data sets because they distort statistics (USEPA 2011b). However, in deciding whether to include or discard an extreme value

from a data set, one must attempt to determine why the extreme value is present. An observation that is not believed to have come from the population of interest could be considered for exclusion (Crow et al. 1960). Such a case would be experimental or equipment error causing inaccurate readings. On the other hand, an extreme value may be a legitimate observation from the population of interest, in which case it should be included in statistical calculations.

Statistical tests can be used to aid in the identification of outliers. One such test is known as Dixon's Extreme Value test, or simply Dixon's test. Dixon's test can be used for smaller data sets (i.e., a sample size less than or equal to 25) that are drawn from a normally-distributed population (Crow et al. 1960, USEPA 2011b). Either the largest or smallest value of such a data set can be tested to determine if it is a statistical outlier (USEPA 2011b). To perform Dixon's test, the observations must first be placed in ascending order: x_1, x_2,...x_n, where x_n is the largest value. The formula for performing Dixon's test varies according to sample size. For example, for a sample of size of n = 8 to n = 10, the following two equations are used (ASTM E178-08):

If the smallest value is suspected: $$r_{11} = \frac{(x_2 - x_1)}{(x_{n-1} - x_1)}$$ (Equation 5.9)

If the largest value is suspected: $$r_{11} = \frac{(x_n - x_{n-1})}{(x_n - x_2)}$$ (Equation 5.10)

If the r value exceeds the tabulated "critical value" for a given level of significance and number of observations, the extreme value is considered to be an outlier. It should be noted that some variations were observed among sources regarding the forms of the equations and the tabulated critical values (see ASTM E178-08, Crow et al. 1960, USEPA 2011b). Dixon's test can be performed rapidly on data sets using USEPA

ProUCL software (USEPA 2011a). ProUCL is a free statistical software package developed by USEPA that is commonly used to calculate statistics related to environmental site investigations. ProUCL version 4.1.01 was used to perform outlier tests on data in this thesis.

5.2.2.8 One-Way Analysis of Variance (ANOVA)

"Analysis of variance (ANOVA) is a method for testing two or more treatments to determine whether their sample means could have been obtained from populations with the same true mean" (Berthouex and Brown 2002). "One-way" indicates that one type of treatment is varied. A "treatment" refers to a particular test condition. ANOVA compares the variance between treatments to the variance within treatments to determine if the treatment means are different (Mintab Inc. 2010). ANOVA is used in this thesis to compare mean pore sizes computed using different wetting fluids to determine if a statistical difference exists. Calculations needed to perform ANOVA are shown in Equations 5.11 – 5.14 (Berthouex and Brown 2002). The pooled within-treatment variance is given by:

$$s_w^2 = \frac{\sum_{t=1}^{k}(n_t - 1)s_t^2}{\sum_{t=1}^{k}(n_t - 1)} \qquad \text{(Equation 5.11)}$$

where:

s^2_w = the pooled within-treatment variance

n_t = the number of observations for a treatment

s^2_t = the treatment variance

k = the number of treatments

The between-treatment variance is given by:

$$s_b^2 = \frac{\sum_{t=1}^{k} n_t \left(\bar{y}_t - \bar{y}\right)^2}{k-1} \qquad \text{(Equation 5.12)}$$

where:

s^2_b = the between-treatment variance

n_t = the number of observations for a treatment

$\bar{y}_t$ = the treatment mean

$\bar{y}_t$ = the grand average of all observations

k = the number of treatments

"Ratios of sample variances are distributed according to the F distribution … whose exact shape depends on the degrees of freedom involved" (Berthouex and Brown 2002). An example of an F distribution with pertinent ANOVA parameters is shown in Figure 5.3. The F ratio is the ratio of between-treatment variance to within-treatment variance:

$$F_{ratio} = \frac{s_b^2}{s_w^2} \qquad \text{(Equation 5.13)}$$

The critical F value (from the F distribution) is given as:

$$F_{v_1, v_2, \alpha} \qquad \text{(Equation 5.14)}$$

where:

v_1 = between-treatment degrees of freedom: $(k - 1)$

v_2 = within-treatment degrees of freedom: $\sum_{t=1}^{k} \left(n_t - 1\right)$

α = level of significance

$F_{v_1,v_2,\alpha}$ will also be denoted as "F critical" at a given level of significance. If the calculated F ratio is greater than F critical, then, at the given level of significance (or confidence level of (1-α) x 100), the means of the treatments are not all equal. If F ratio is less than F critical, then there is no statistical difference in the means at the given level of significance.

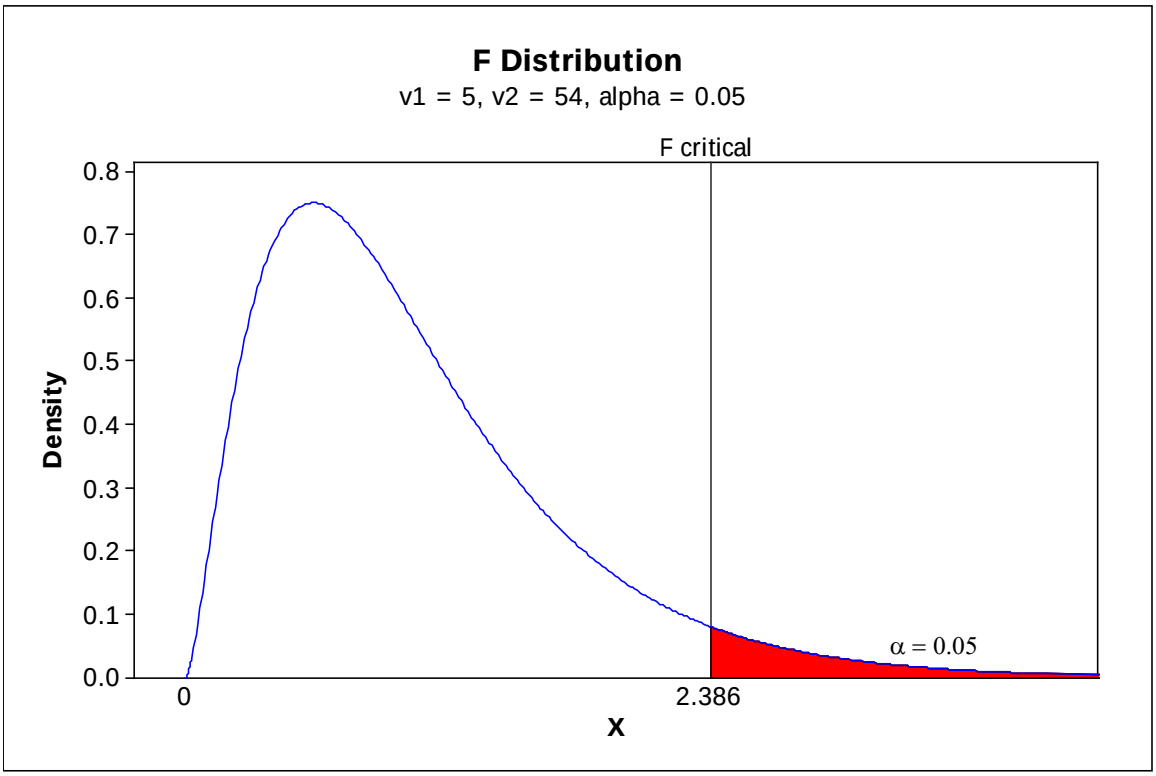

Figure 5.3: Example of an F Distribution, showing F critical for the given degrees of freedom and level of significance. If the F ratio exceeds F critical, the null hypothesis that the sample means are equal is rejected.

5.2.3 Water Summary Results for the NG-1 Nonwoven Geotextile

Table 5.4: Water results for pore sizes at selected % finer.

% Finer	Water-1 Pore Size (mm)	Water-2 Pore Size (mm)	Water-3 Pore Size (mm)	Water-4 Pore Size (mm)	Water-5 Pore Size (mm)	Water-6 Pore Size (mm)	Water-7 Pore Size (mm)	Water-8 Pore Size (mm)	Water-9 Pore Size (mm)	Water-10 Pore Size (mm)
98	0.12191	---	0.20251	0.16537	0.23077	0.16887	0.18402	0.14265	0.49580	0.16847
95	0.11836	0.16849	0.20095	0.12366	0.20028	0.16694	0.18173	0.13427	0.16761	0.15747
90	0.11677	0.16771	0.19836	0.11130	0.19622	0.16371	0.17793	0.13256	0.16520	0.13915
85	0.11518	0.16692	0.19576	0.10906	0.19217	0.16049	0.17412	0.13085	0.16279	0.12496
80	0.11358	0.16614	0.19317	0.10681	0.18811	0.15726	0.17031	0.12914	0.16039	0.11961
75	0.11199	0.16535	0.19057	0.10456	0.18406	0.15403	0.16650	0.12742	0.15798	0.11426
70	0.11040	0.16457	0.18798	0.10231	0.18000	0.15081	0.16269	0.12571	0.15557	0.10891
65	0.10881	0.16378	0.18539	0.10006	0.17595	0.14758	0.15888	0.12400	0.15316	0.10640
60	0.10722	0.16300	0.18279	0.09781	0.17189	0.14436	0.15508	0.12229	0.15075	0.10595
55	0.10562	0.16221	0.18020	0.09556	0.16784	0.14113	0.15127	0.12058	0.14834	0.10549
50	0.10403	0.16143	0.17761	0.09332	0.16378	0.13790	0.14746	0.11887	0.14593	0.10504
45	0.10244	0.16064	0.17501	0.09107	0.15973	0.13468	0.14365	0.11716	0.14352	0.10459
40	0.10085	0.15986	0.17242	0.08882	0.15567	0.13145	0.13984	0.11544	0.14111	0.10413
35	0.09926	0.15907	0.16983	0.08657	0.15162	0.12823	0.13603	0.11373	0.13871	0.10368
30	0.09766	0.15829	0.16723	0.08432	0.14756	0.12500	0.13223	0.11202	0.13630	0.10323
25	0.09607	0.15750	0.16464	0.08207	0.14350	0.12177	0.12842	0.11031	0.13389	0.10277
20	0.09448	0.15672	0.16204	0.07983	0.13945	0.11855	0.12461	0.10860	0.13148	0.10232
15	0.09289	0.15593	0.15945	0.07758	0.13539	0.11532	0.12080	0.10689	0.12907	0.10187
10	0.09130	0.13524	0.15686	0.07533	0.13134	0.10989	0.11699	0.10518	0.12666	0.10141
5	0.08970	---	0.12741	---	0.12728	---	0.11318	0.10346	---	0.03890

Table 5.5: Water statistics for pore sizes at selected % finer.

% Finer	Sample Size	Mean Pore Size (mm)	Standard Deviation (mm)	Coefficient of Variation (%)	95% CI of Mean UCL (mm)	95% CI of Mean LCL (mm)	MaxARV (mm)	MARV (mm)	95% TI with 95% Coverage UTL (mm)	95% TI with 95% Coverage LTL (mm)
98	9	0.20893	0.11211	53.66	0.29525	0.12261	0.43314	-0.01528	0.60690	-0.18905
95	10	0.16198	0.02912	17.98	0.18295	0.14101	0.22022	0.10373	0.26070	0.06325
90	10	0.15689	0.03080	19.63	0.17906	0.13472	0.21849	0.09530	0.26129	0.05249
85	10	0.15323	0.03126	20.40	0.17573	0.13072	0.21574	0.09072	0.25919	0.04727
80	10	0.15045	0.03109	20.66	0.17283	0.12807	0.21263	0.08828	0.25584	0.04506
75	10	0.14767	0.03098	20.98	0.16998	0.12537	0.20963	0.08572	0.25269	0.04266
70	10	0.14490	0.03093	21.34	0.16716	0.12263	0.20675	0.08304	0.24973	0.04006
65	10	0.14240	0.03055	21.45	0.16440	0.12040	0.20350	0.08130	0.24597	0.03883
60	10	0.14011	0.02994	21.37	0.16167	0.11856	0.19999	0.08024	0.24160	0.03862
55	10	0.13782	0.02936	21.30	0.15896	0.11668	0.19655	0.07910	0.23736	0.03829
50	10	0.13554	0.02882	21.27	0.15629	0.11478	0.19318	0.07789	0.23325	0.03783
45	10	0.13325	0.02832	21.26	0.15364	0.11285	0.18990	0.07660	0.22927	0.03723
40	10	0.13096	0.02787	21.28	0.15102	0.11089	0.18670	0.07522	0.22543	0.03649
35	10	0.12867	0.02746	21.34	0.14844	0.10890	0.18358	0.07376	0.22175	0.03559
30	10	0.12638	0.02709	21.44	0.14589	0.10688	0.18057	0.07220	0.21822	0.03454
25	10	0.12410	0.02677	21.58	0.14337	0.10482	0.17765	0.07055	0.21486	0.03333
20	10	0.12181	0.02651	21.76	0.14089	0.10272	0.17482	0.06879	0.21167	0.03194
15	10	0.11952	0.02629	22.00	0.13845	0.10059	0.17211	0.06693	0.20866	0.03038
10	10	0.11502	0.02360	20.52	0.13201	0.09803	0.16221	0.06783	0.19501	0.03503
5	6	0.09999	0.03323	33.23	0.13488	0.06510	0.16645	0.03353	0.24687	-0.04688

CI = confidence interval
UCL = upper confidence limit
LCL = lower confidence limit
MaxARV = maximum average roll value
MARV = minimum average roll value
TI = tolerance interval
UTL = upper tolerance limit
LTL = lower tolerance limit

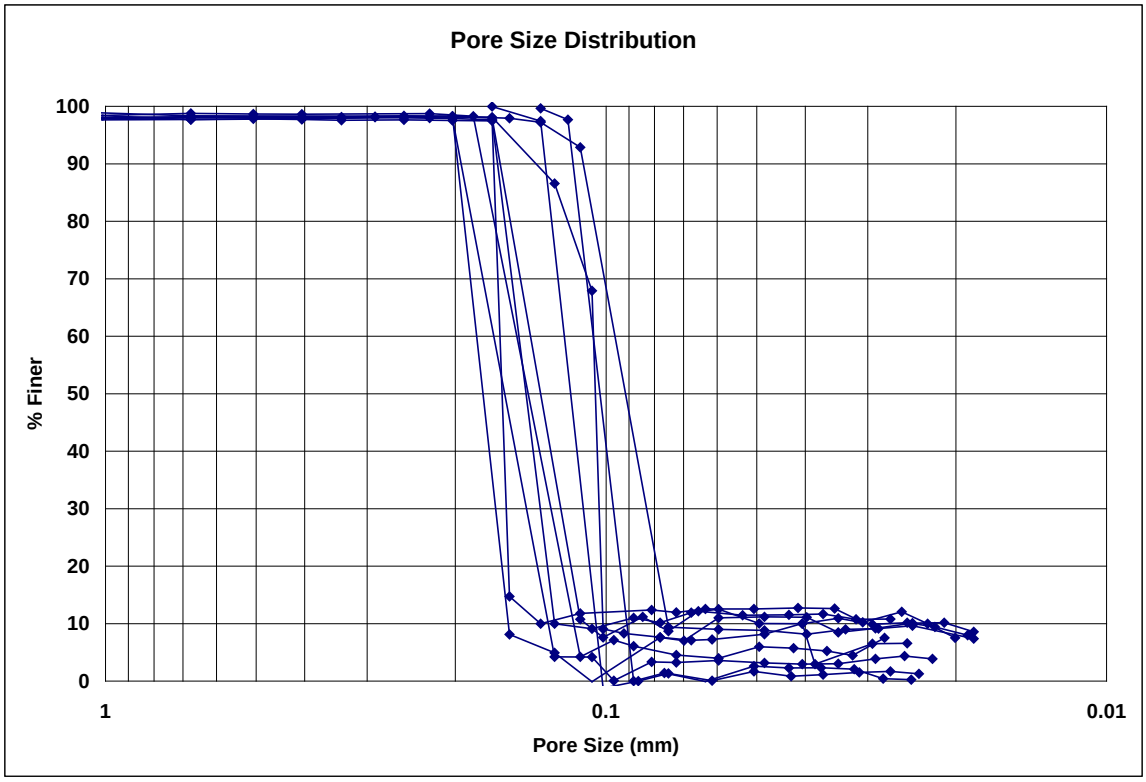

Figure 5.4: Water pore size distributions for individual tests on the NG-1 nonwoven geotextile.

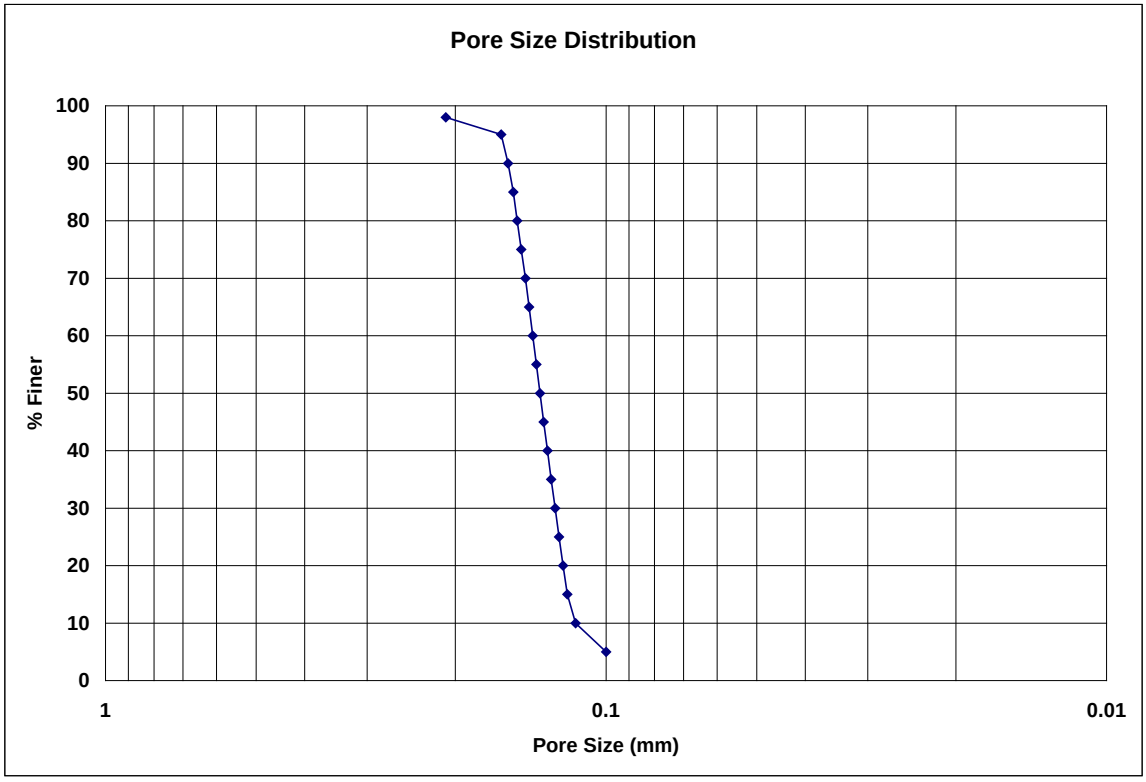

Figure 5.5: Water mean pore size distribution for tests in Figure 5.4.

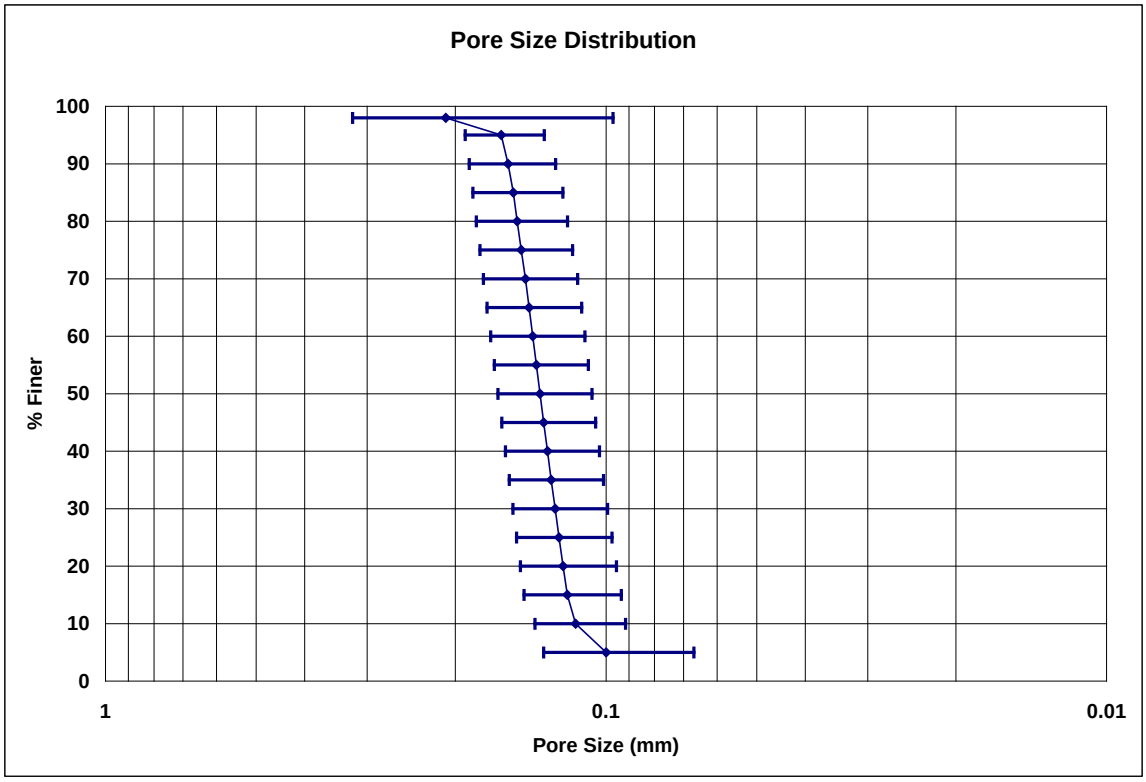

Figure 5.6: Water mean pore size distribution +/- standard deviation for tests in Figure 5.4.

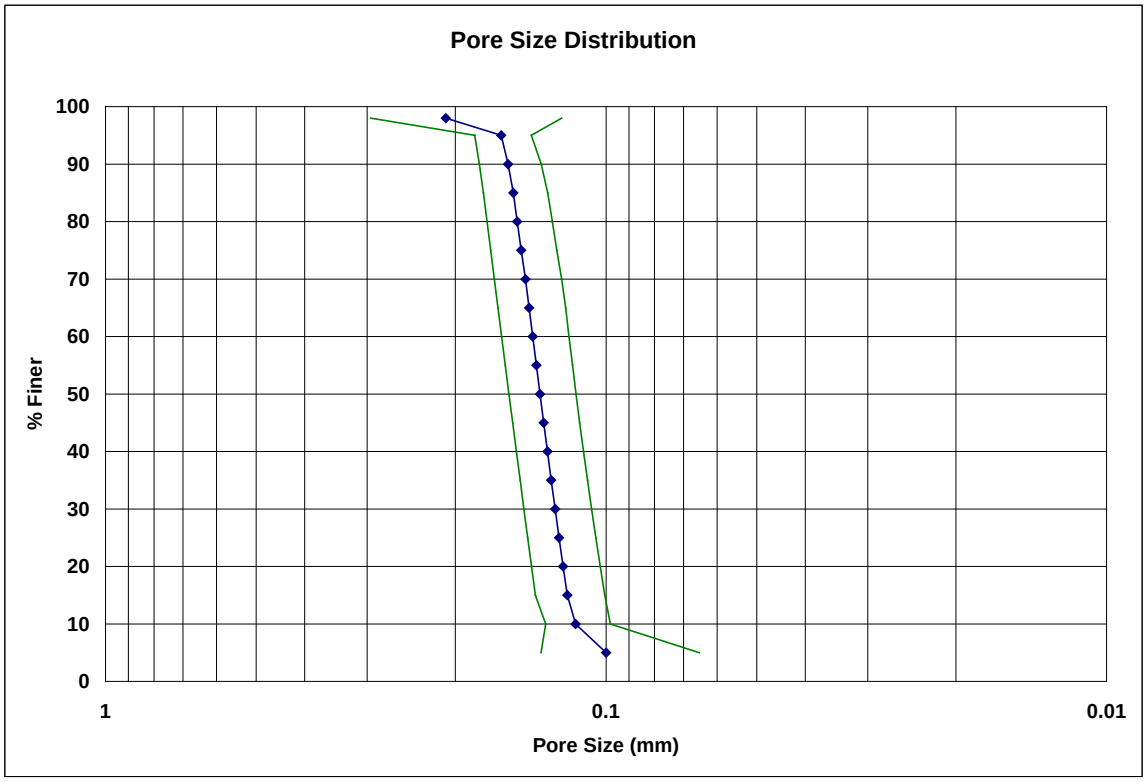

Figure 5.7: Water mean pore size distribution with 95% confidence interval for tests in Figure 5.4.

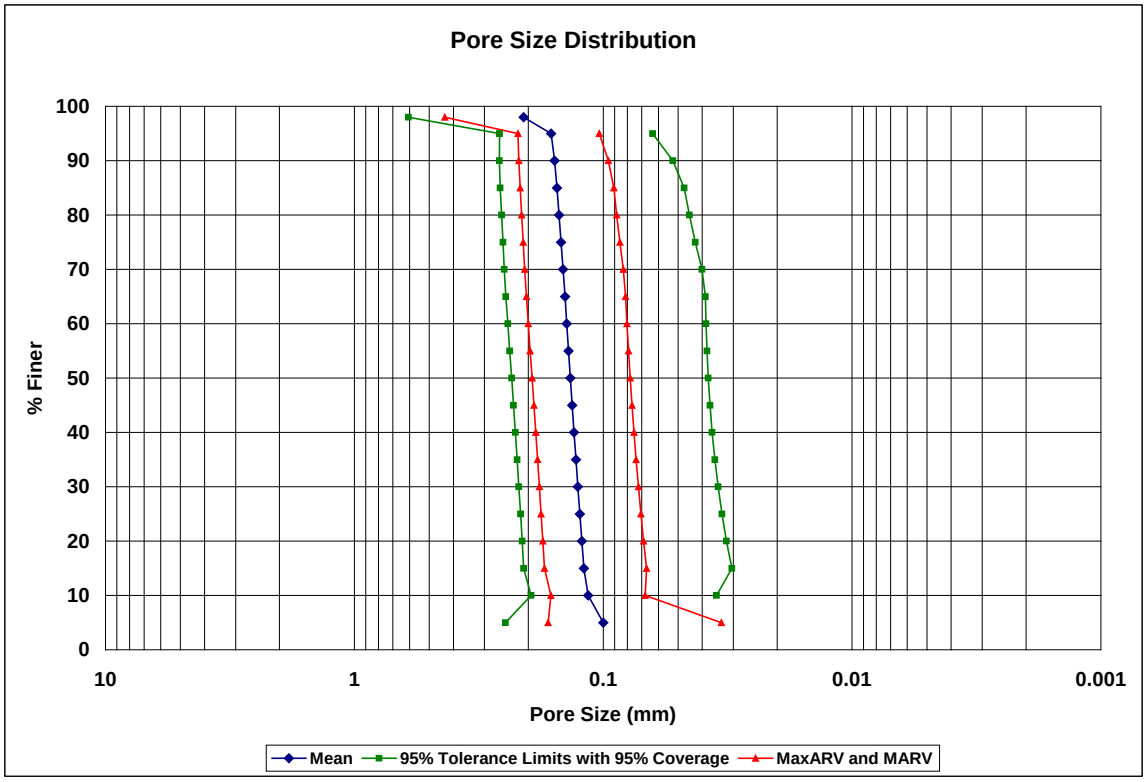

Figure 5.8: Water mean pore size distribution, showing MaxARV, MARV, and the 95% tolerance interval with 95% coverage for tests in Figure 5.4.

5.2.4 Porewick Summary Results for the NG-1 Nonwoven Geotextile

Table 5.6: Porewick results for pore sizes at selected % finer.

% Finer	Porewick-1 Pore Size (mm)	Porewick-2 Pore Size (mm)	Porewick-3 Pore Size (mm)	Porewick-4 Pore Size (mm)	Porewick-5 Pore Size (mm)	Porewick-6 Pore Size (mm)	Porewick-7 Pore Size (mm)	Porewick-8 Pore Size (mm)	Porewick-9 Pore Size (mm)	Porewick-10 Pore Size (mm)
98	0.54505	---	---	---	0.18347	0.16269	0.19233	0.21304	0.21666	0.22593
95	0.16527	0.19192	1.02870	0.23171	0.16511	0.15100	0.18328	0.18913	0.19149	0.20678
90	0.15104	0.17466	0.18388	0.18936	0.15402	0.14506	0.16818	0.17241	0.18094	0.18795
85	0.14070	0.15741	0.17005	0.16157	0.14518	0.14409	0.16474	0.16029	0.17039	0.17746
80	0.13265	0.14304	0.15622	0.15070	0.14287	0.14312	0.16267	0.15063	0.16451	0.16697
75	0.12459	0.13467	0.14240	0.13984	0.14057	0.14215	0.16061	0.14522	0.16126	0.16501
70	0.11655	0.12630	0.12914	0.12898	0.13827	0.14119	0.15854	0.14412	0.15801	0.16338
65	0.10975	0.11793	0.12319	0.11811	0.13596	0.14022	0.15647	0.14302	0.15476	0.16174
60	0.10295	0.11163	0.11723	0.11398	0.13366	0.13925	0.15440	0.14192	0.15151	0.16010
55	0.09615	0.10571	0.11128	0.11092	0.13135	0.13828	0.15233	0.14081	0.14826	0.15846
50	0.08935	0.09979	0.10533	0.10786	0.12905	0.13731	0.15026	0.13971	0.14501	0.15682
45	0.08256	0.09387	0.09937	0.10480	0.12674	0.13634	0.14819	0.13861	0.14176	0.15518
40	0.07732	0.08795	0.09342	0.10174	0.12444	0.13537	0.14612	0.13751	0.13851	0.15354
35	0.07587	0.08270	0.08747	0.09868	0.12213	0.13441	0.14405	0.13640	0.13526	0.15190
30	0.07441	0.07994	0.08151	0.09562	0.11983	0.13344	0.14199	0.13530	0.13202	0.15027
25	0.07296	0.07717	0.07602	0.09256	0.11752	0.13247	0.13992	0.13420	0.12856	0.14863
20	0.07151	0.07440	0.07131	0.08951	0.11522	0.13150	0.13785	0.13310	0.12451	0.14699
15	0.07006	0.07163	0.06660	0.08645	0.11291	0.13053	0.13578	0.13200	0.12045	0.14408
10	0.06861	0.06887	0.06190	0.08339	0.11061	0.12929	0.13371	0.13089	0.11640	0.13748
5	0.04105	---	0.05719	0.05062	0.10830	0.10432	0.13164	0.12979	0.11234	0.13088

Table 5.7: Porewick statistics for pore sizes at selected % finer

% Finer	Sample Size	Mean Pore Size (mm)	Standard Deviation (mm)	Coefficient of Variation (%)	95% CI of Mean		MaxARV (mm)	MARV (mm)	95% TI with 95% Coverage	
					UCL (mm)	LCL (mm)			UTL (mm)	LTL (mm)
98	7	0.24845	0.13258	53.36	0.37043	0.12648	0.51361	-0.01671	0.78143	-0.28452
95	10	0.27044	0.26740	98.88	0.46297	0.07791	0.80524	-0.26437	1.17693	-0.63606
90	10	0.17075	0.01589	9.30	0.18219	0.15931	0.20252	0.13898	0.22460	0.11690
85	10	0.15919	0.01240	7.79	0.16812	0.15026	0.18399	0.13438	0.20123	0.11715
80	10	0.15134	0.01120	7.40	0.15940	0.14328	0.17374	0.12894	0.18930	0.11338
75	10	0.14563	0.01286	8.83	0.15489	0.13637	0.17136	0.11991	0.18924	0.10203
70	10	0.14045	0.01567	11.16	0.15173	0.12916	0.17179	0.10910	0.19358	0.08731
65	10	0.13611	0.01826	13.41	0.14926	0.12297	0.17263	0.09960	0.19801	0.07422
60	10	0.13266	0.02006	15.12	0.14711	0.11822	0.17279	0.09253	0.20068	0.06465
55	10	0.12936	0.02180	16.85	0.14505	0.11366	0.17295	0.08576	0.20324	0.05547
50	10	0.12605	0.02360	18.72	0.14304	0.10906	0.17325	0.07885	0.20605	0.04605
45	10	0.12274	0.02545	20.74	0.14107	0.10442	0.17365	0.07183	0.20903	0.03645
40	10	0.11959	0.02708	22.64	0.13909	0.10009	0.17375	0.06543	0.21140	0.02779
35	10	0.11689	0.02802	23.97	0.13706	0.09672	0.17293	0.06085	0.21187	0.02190
30	10	0.11443	0.02869	25.07	0.13509	0.09378	0.17181	0.05706	0.21168	0.01718
25	10	0.11200	0.02934	26.20	0.13313	0.09088	0.17068	0.05332	0.21146	0.01254
20	10	0.10959	0.02989	27.28	0.13111	0.08807	0.16937	0.04981	0.21092	0.00826
15	10	0.10705	0.03031	28.31	0.12887	0.08523	0.16767	0.04643	0.20979	0.00430
10	10	0.10411	0.03027	29.08	0.12591	0.08232	0.16466	0.04357	0.20674	0.00149
5	9	0.09624	0.03657	38.00	0.12440	0.06808	0.16938	0.02309	0.22607	-0.03360

CI = confidence interval
UCL = upper confidence limit
LCL = lower confidence limit
MaxARV = maximum average roll value
MARV = minimum average roll value

TI = tolerance interval
UTL = upper tolerance limit
LTL = lower tolerance limit

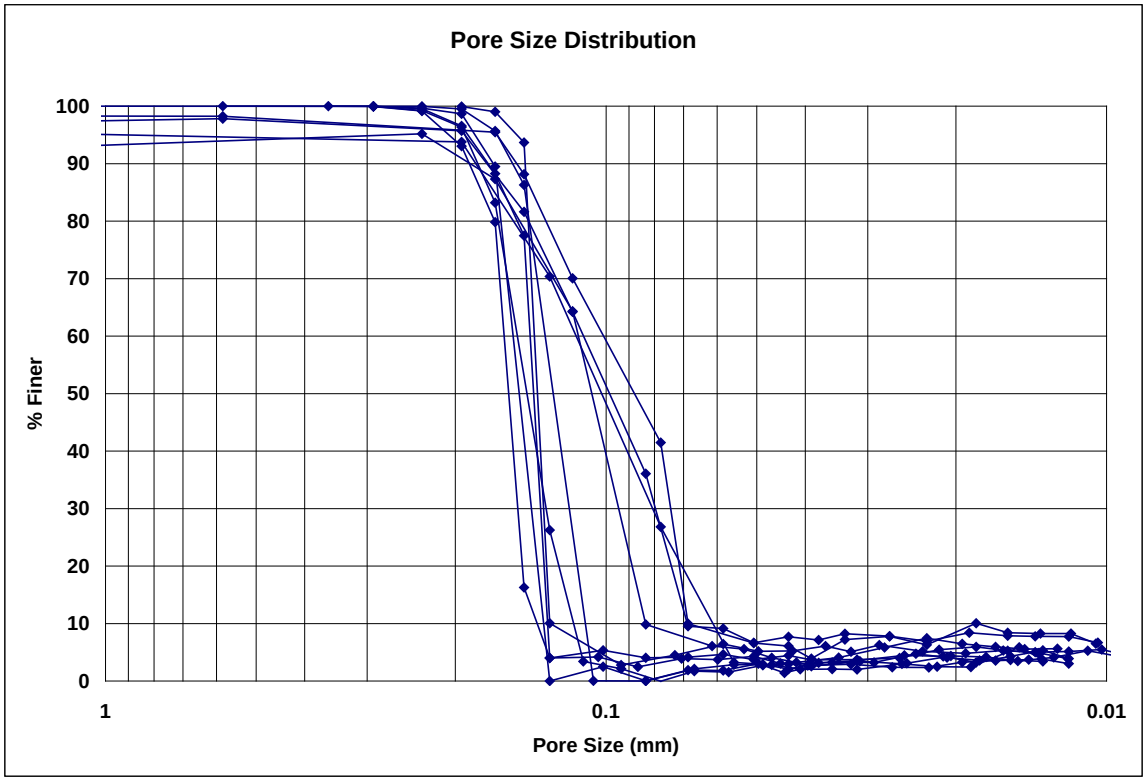

Figure 5.9: Porewick pore size distributions for individual tests on the NG-1 nonoven geotextile.

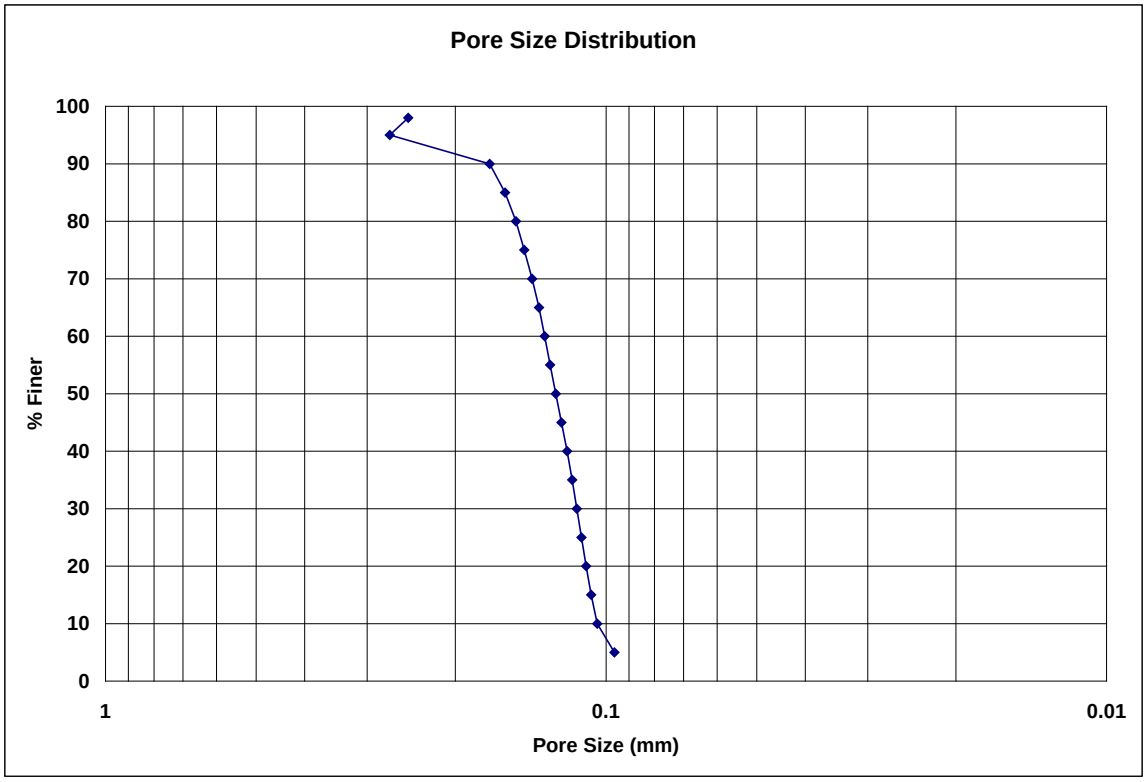

Figure 5.10: Porewick mean pore size distribution for the tests in Figure 5.9.

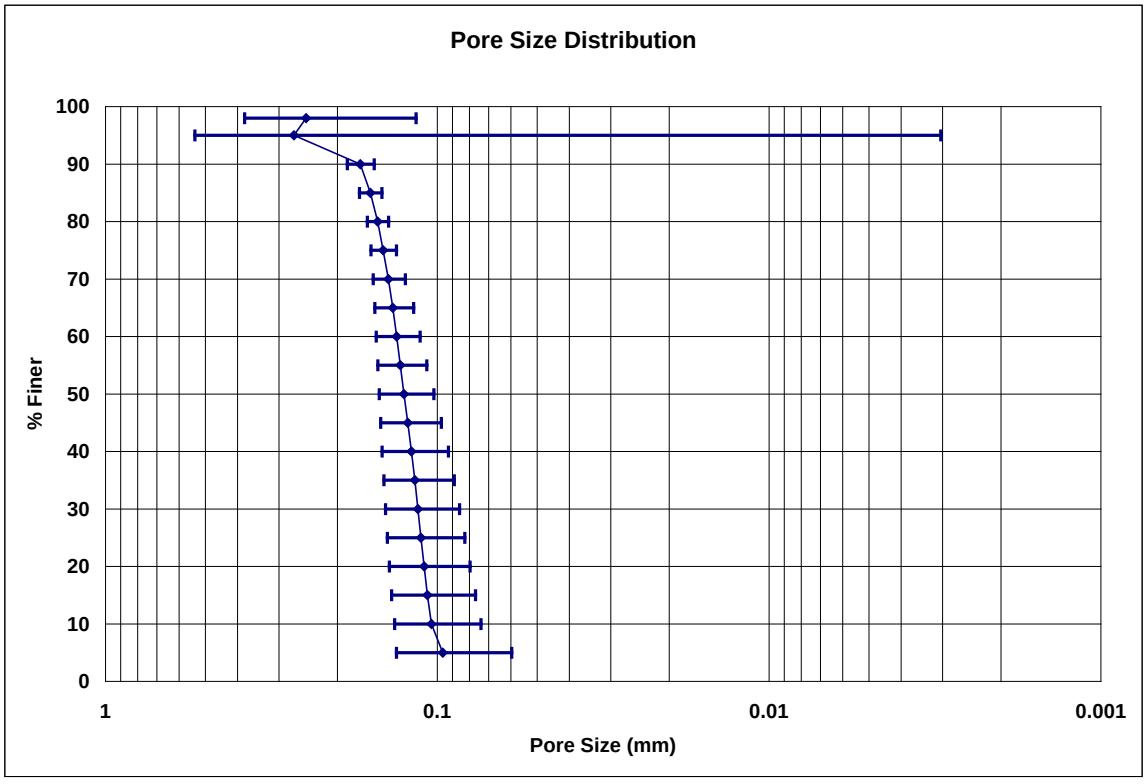

Figure 5.11: Porewick mean pore size distribution +/- standard deviation for the tests in Figure 5.9.

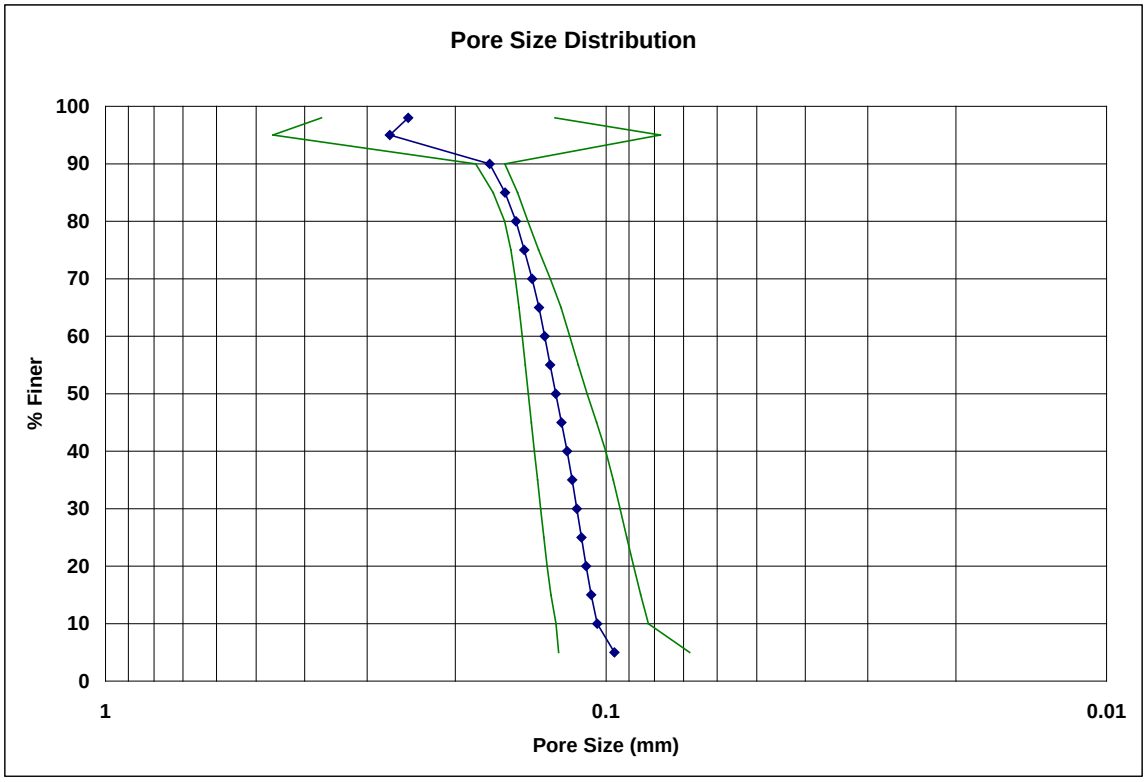

Figure 5.12: Porewick mean pore size distribution with 95% confidence interval for the tests in Figure 5.9.

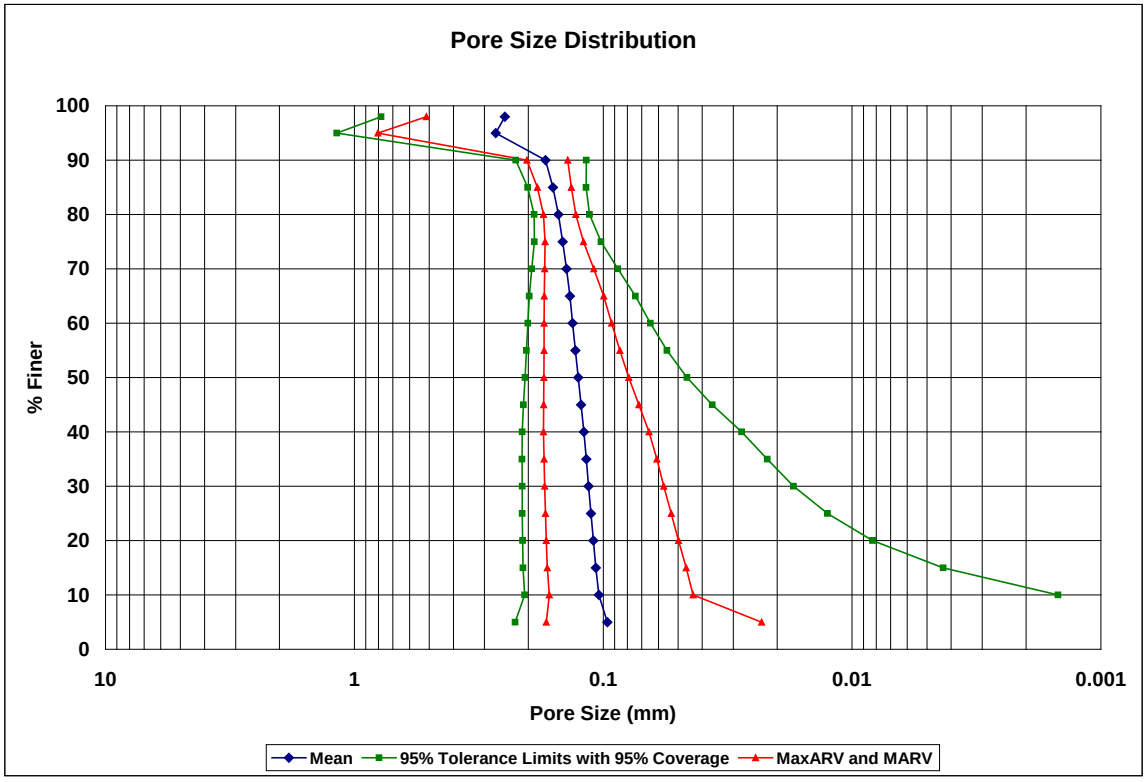

Figure 5.13: Porewick mean pore size distribution, showing MaxARV, MARV, and the 95% tolerance interval with 95% coverage for the tests in Figure 5.9.

5.2.5 Mineral Oil Summary Results for the NG-1 Nonwoven Geotextile

Table 5.8: Mineral oil results for pore sizes at selected % finer.

% Finer	MinOil-1 Pore Size (mm)	MinOil-2 Pore Size (mm)	MinOil-3 Pore Size (mm)	MinOil-4 Pore Size (mm)	MinOil-5 Pore Size (mm)	MinOil-6 Pore Size (mm)	MinOil-7 Pore Size (mm)	MinOil-8 Pore Size (mm)	MinOil-9 Pore Size (mm)	MinOil-10 Pore Size (mm)
98	---	0.21405	0.18212	0.22170	0.23077	0.20917	0.22264	0.16646	0.19285	0.23217
95	0.16894	0.19612	0.17067	0.19916	0.21918	0.18991	0.20360	0.15818	0.17215	0.19626
90	0.14966	0.18355	0.16070	0.18428	0.19985	0.17219	0.18546	0.14438	0.15787	0.16382
85	0.13736	0.16929	0.14821	0.17132	0.18117	0.15913	0.17143	0.13315	0.14511	0.15271
80	0.12595	0.15993	0.13926	0.16043	0.16918	0.14970	0.16095	0.12382	0.13543	0.14407
75	0.11808	0.15184	0.13096	0.14980	0.15802	0.14047	0.15086	0.11594	0.12618	0.13620
70	0.11020	0.14381	0.12350	0.14091	0.15044	0.13233	0.14286	0.10861	0.11882	0.12833
65	0.10259	0.13578	0.11529	0.13201	0.14286	0.12396	0.13504	0.10226	0.11132	0.11864
60	0.09526	0.12776	0.10771	0.12298	0.13040	0.11530	0.12707	0.09549	0.10341	0.11014
55	0.08964	0.12027	0.10099	0.11454	0.12129	0.10716	0.11861	0.08794	0.09656	0.10423
50	0.08627	0.11211	0.09364	0.10841	0.11335	0.10033	0.10901	0.08226	0.08994	0.10023
45	0.08289	0.10225	0.08535	0.10055	0.10899	0.09428	0.10034	0.07658	0.08332	0.09624
40	0.06916	0.09072	0.07581	0.09191	0.09617	0.08823	0.09411	0.06823	0.07331	0.07703
35	0.06185	0.08254	0.06780	0.08176	0.08478	0.07535	0.08394	0.05931	0.06395	0.06833
30	0.05293	0.07210	0.05629	0.06999	0.07397	0.06305	0.07108	0.05213	0.05308	0.05940
25	0.04262	0.06232	0.04575	0.05698	0.05980	0.05181	0.05902	0.03605	0.04379	0.04431
20	0.02631	0.05005	0.03534	0.04315	0.04702	0.03681	0.04579	0.03017	0.02626	0.03855
15	0.01789	0.03617	0.02734	0.03181	0.03458	0.02721	0.03377	0.02504	0.02482	0.03445
10	---	---	---	0.02516	---	---	---	0.01682	---	---
5	---	---	---	---	---	---	---	---	---	---

Table 5.9: Mineral oil statistics for pore sizes at selected % finer.

% Finer	Sample Size	Mean Pore Size (mm)	Standard Deviation (mm)	Coefficient of Variation (%)	95% CI of Mean		MaxARV (mm)	MARV (mm)	95% TI with 95% Coverage	
					UCL (mm)	LCL (mm)			UTL (mm)	LTL (mm)
98	9	0.20799	0.02282	10.97	0.22557	0.19042	0.25364	0.16234	0.28902	0.12696
95	10	0.18742	0.01909	10.18	0.20116	0.17367	0.22559	0.14925	0.25212	0.12272
90	10	0.17018	0.01784	10.48	0.18302	0.15733	0.20585	0.13450	0.23065	0.10970
85	10	0.15689	0.01614	10.29	0.16851	0.14527	0.18917	0.12461	0.21161	0.10217
80	10	0.14687	0.01572	10.70	0.15819	0.13555	0.17831	0.11543	0.20017	0.09358
75	10	0.13783	0.01483	10.76	0.14851	0.12716	0.16749	0.10817	0.18811	0.08756
70	10	0.12998	0.01460	11.23	0.14049	0.11947	0.15918	0.10078	0.17947	0.08049
65	10	0.12198	0.01428	11.71	0.13226	0.11169	0.15054	0.09341	0.17040	0.07356
60	10	0.11355	0.01321	11.63	0.12306	0.10404	0.13997	0.08714	0.15833	0.06878
55	10	0.10612	0.01239	11.67	0.11504	0.09720	0.13090	0.08135	0.14812	0.06413
50	10	0.09956	0.01115	11.20	0.10759	0.09152	0.12186	0.07725	0.13737	0.06174
45	10	0.09308	0.01048	11.26	0.10062	0.08553	0.11404	0.07212	0.12860	0.05756
40	10	0.08247	0.01081	13.11	0.09025	0.07469	0.10408	0.06085	0.11911	0.04583
35	10	0.07296	0.00985	13.51	0.08006	0.06586	0.09267	0.05325	0.10637	0.03955
30	10	0.06240	0.00876	14.03	0.06871	0.05610	0.07991	0.04489	0.09208	0.03272
25	10	0.05024	0.00894	17.78	0.05668	0.04381	0.06812	0.03237	0.08054	0.01995
20	10	0.03795	0.00855	22.54	0.04410	0.03179	0.05505	0.02084	0.06694	0.00895
15	10	0.02931	0.00582	19.85	0.03350	0.02512	0.04094	0.01767	0.04903	0.00959

CI = confidence interval
UCL = upper confidence limit
LCL = lower confidence limit
MaxARV = maximum average roll value
MARV = minimum average roll value
TI = tolerance interval
UTL = upper tolerance limit
LTL = lower tolerance limit

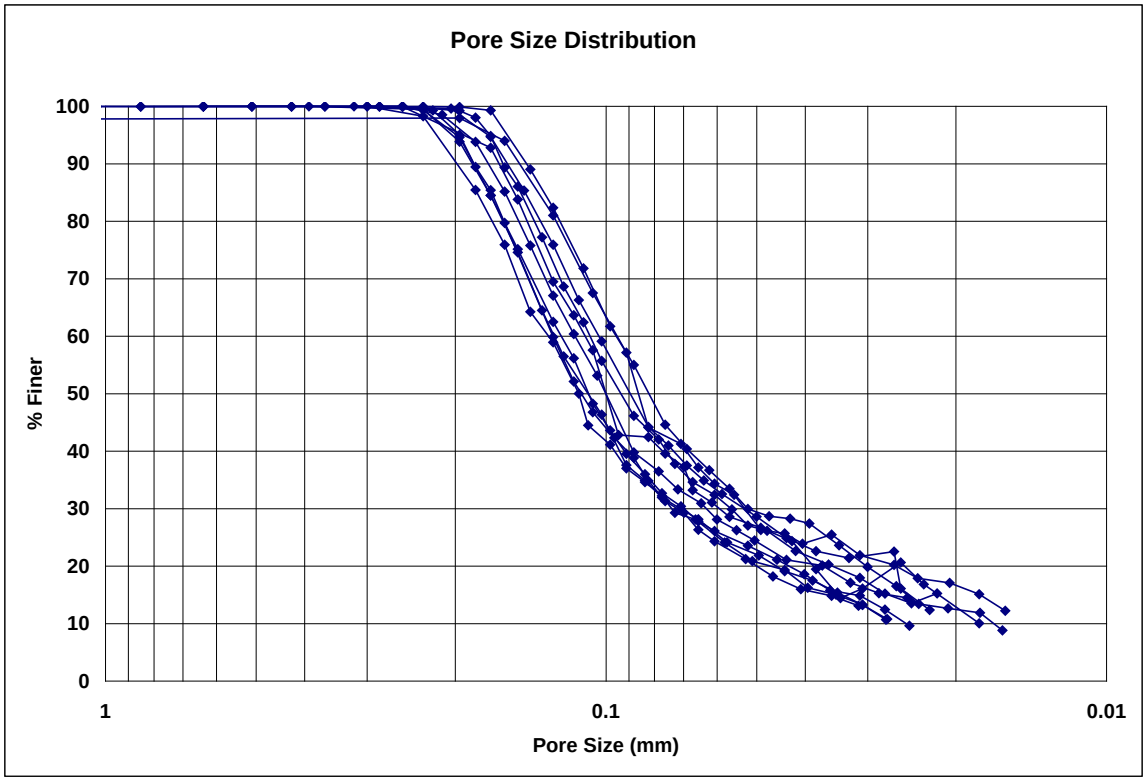

Figure 5.14: Mineral oil pore size distributions for individual tests on the NG-1 nonwoven geotextile.

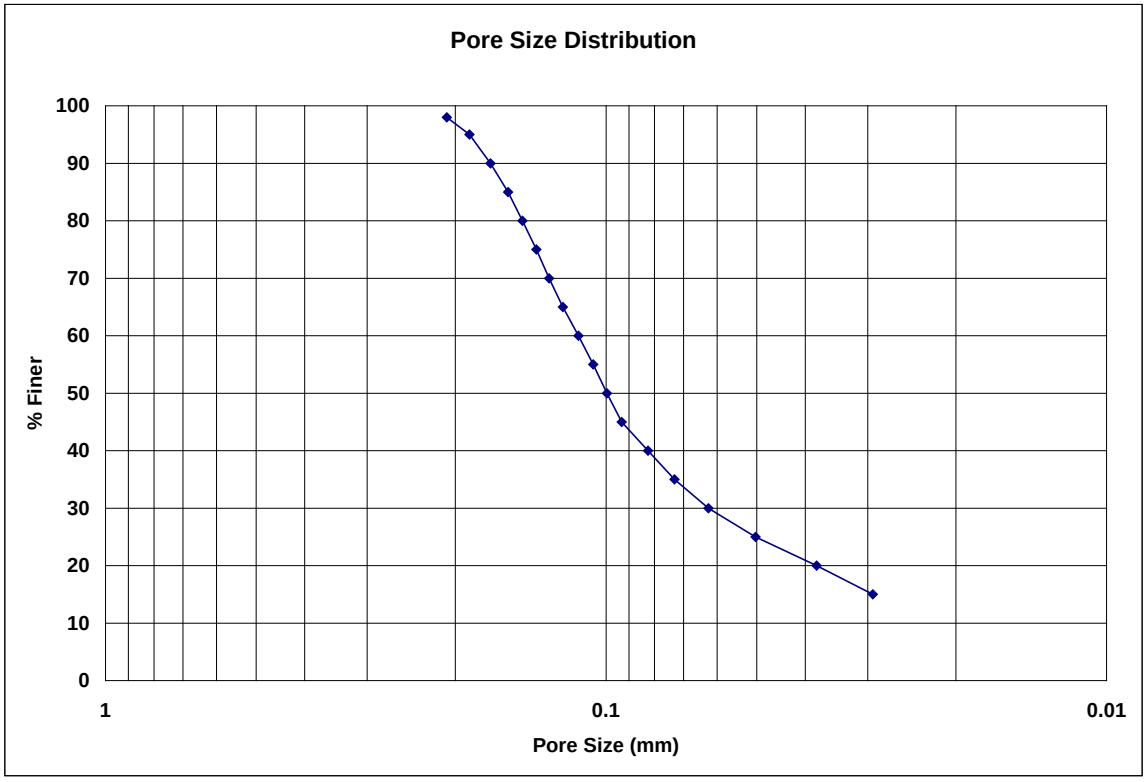

Figure 5.15: Mineral oil mean pore size distribution for the tests in Figure 5.14.

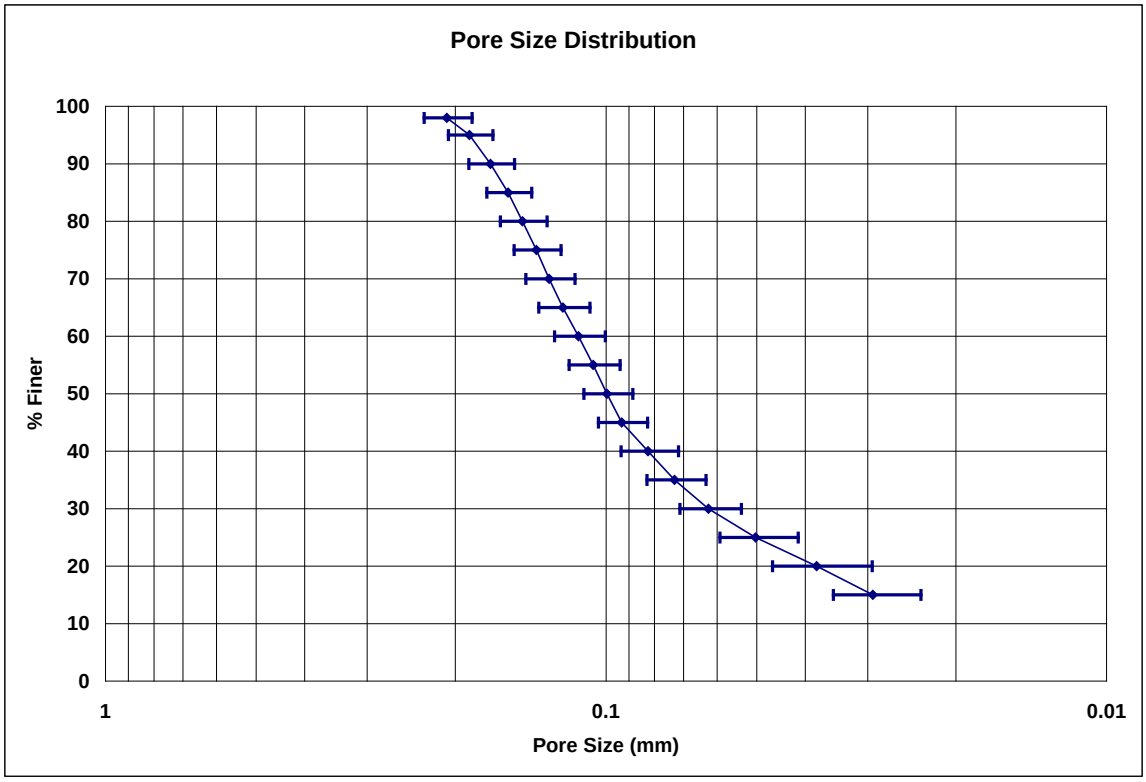

Figure 5.16: Mineral oil mean pore size distribution +/- standard deviation for the tests in Figure 5.14.

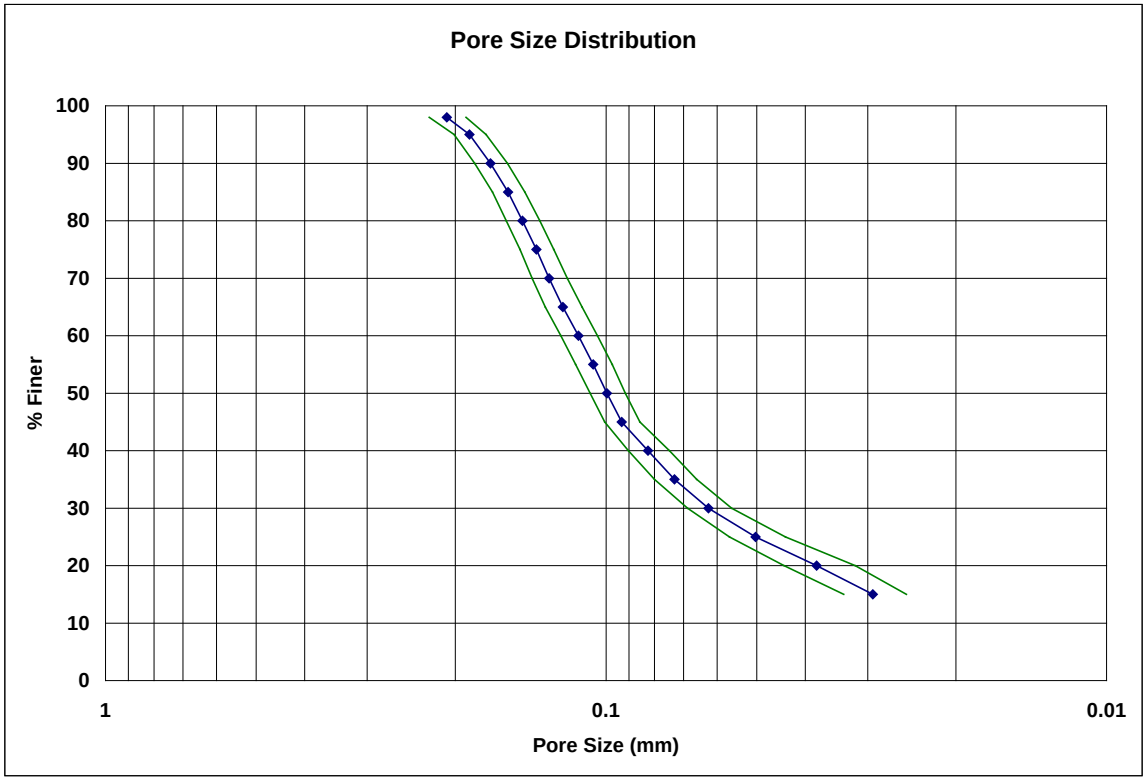

Figure 5.17: Mineral oil mean pore size distribution with 95% confidence interval for the tests in Figure 5.14.

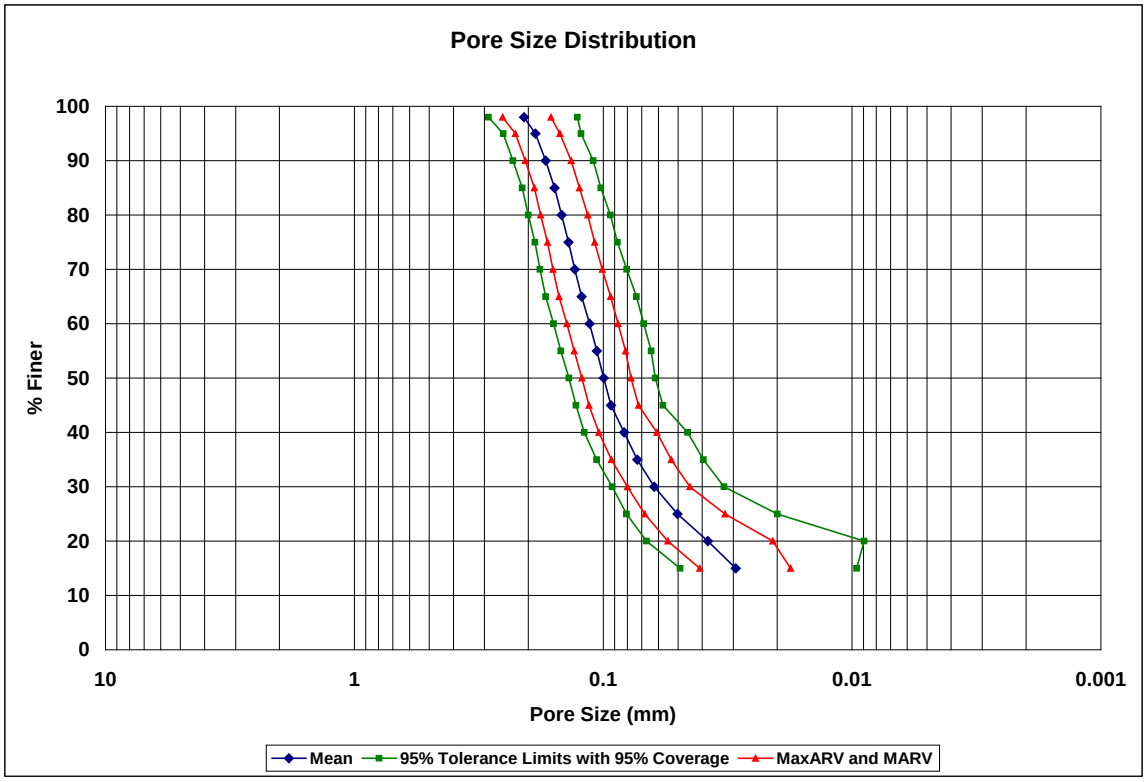

Figure 5.18: Mineral oil mean pore size distribution, showing MaxARV, MARV, and the 95% tolerance interval with 95% coverage for the tests in Figure 5.14.

5.2.6 2-Ethyl Hexanol Summary Results for the NG-1 Nonwoven Geotextile

Table 5.10: 2-ethyl hexanol results for pore sizes at selected % finer.

% Finer	2EH-1 Pore Size (mm)	2EH-2 Pore Size (mm)	2EH-3 Pore Size (mm)	2EH-4 Pore Size (mm)	2EH-5 Pore Size (mm)	2EH-6 Pore Size (mm)	2EH-7 Pore Size (mm)	2EH-8 Pore Size (mm)	2EH-9 Pore Size (mm)	2EH-10 Pore Size (mm)
98	0.97590	0.20485	0.26752	0.28414	0.23710	0.28403	0.20531	0.21820	0.19120	0.20841
95	0.19955	0.17950	0.21908	0.21911	0.21672	0.20085	0.19440	0.19763	0.17727	0.18794
90	0.19384	0.16561	0.20688	0.19763	0.20349	0.19036	0.18171	0.17667	0.16457	0.17399
85	0.18813	0.15216	0.19137	0.18285	0.19027	0.17987	0.16902	0.16579	0.15572	0.16356
80	0.18243	0.14025	0.17294	0.16808	0.17888	0.16937	0.15633	0.15491	0.14818	0.15374
75	0.17672	0.12856	0.15449	0.16158	0.16981	0.16076	0.14366	0.14942	0.14131	0.14727
70	0.17101	0.11710	0.13431	0.15533	0.16075	0.15251	0.13583	0.14401	0.13521	0.14052
65	0.15907	0.10868	0.11413	0.14909	0.15168	0.14427	0.12800	0.13861	0.12911	0.13342
60	0.13809	0.10292	0.10960	0.14060	0.14177	0.13603	0.12017	0.13129	0.12301	0.12633
55	0.12307	0.09271	0.10715	0.11827	0.12553	0.12641	0.11225	0.11693	0.11691	0.11923
50	0.11662	0.08251	0.10319	0.11581	0.11389	0.11704	0.10480	0.11082	0.11081	0.11214
45	0.11017	0.07854	0.09756	0.11336	0.10590	0.11040	0.09938	0.10470	0.10471	0.10504
40	0.10225	0.07456	0.09346	0.10762	0.09779	0.10085	0.09279	0.09739	0.09861	0.09795
35	0.09192	0.06654	0.07900	0.09273	0.08975	0.09006	0.08453	0.08829	0.09153	0.08547
30	0.08217	0.05249	0.06963	0.08531	0.08066	0.08258	0.07770	0.07820	0.08094	0.07516
25	0.06696	0.04265	0.06065	0.06692	0.06753	0.07264	0.06534	0.06281	0.06862	0.07102
20	0.05730	0.03495	0.04450	0.05714	0.05413	0.05628	0.05410	0.05570	0.05249	0.06260
15	0.04482	0.02578	0.03373	0.04678	0.04556	0.04786	0.04962	0.04518	0.04609	0.05738
10	0.03118	---	0.02049	0.03650	0.03026	0.03685	0.04169	0.03682	0.03539	0.04797
5	---	---	---	---	---	---	0.02764	---	---	0.02652

Table 5.11: 2-ethyl hexanol statistics for pore sizes at selected % finer.

% Finer	Sample Size	Mean Pore Size (mm)	Standard Deviation (mm)	Coefficient of Variation (%)	95% CI of Mean		MaxARV (mm)	MARV (mm)	95% TI with 95% Coverage	
					UCL (mm)	LCL (mm)			UTL (mm)	LTL (mm)
98	10	0.30767	0.23728	77.12	0.47851	0.13683	0.78222	-0.16689	1.11204	-0.49671
95	10	0.19920	0.01536	7.71	0.21026	0.18815	0.22992	0.16849	0.25127	0.14714
90	10	0.18548	0.01520	8.20	0.19642	0.17453	0.21588	0.15508	0.23700	0.13395
85	10	0.17387	0.01450	8.34	0.18431	0.16344	0.20286	0.14488	0.22301	0.12473
80	10	0.16251	0.01384	8.52	0.17248	0.15254	0.19020	0.13482	0.20944	0.11558
75	10	0.15336	0.01433	9.34	0.16367	0.14304	0.18201	0.12470	0.20192	0.10479
70	10	0.14466	0.01557	10.76	0.15587	0.13345	0.17579	0.11353	0.19742	0.09189
65	10	0.13561	0.01621	11.96	0.14728	0.12393	0.16803	0.10318	0.19057	0.08064
60	10	0.12698	0.01321	10.41	0.13649	0.11747	0.15341	0.10055	0.17177	0.08219
55	10	0.11585	0.01001	8.64	0.12305	0.10864	0.13586	0.09584	0.14977	0.08193
50	10	0.10876	0.01034	9.51	0.11621	0.10132	0.12944	0.08808	0.14381	0.07371
45	10	0.10298	0.00985	9.57	0.11007	0.09589	0.12268	0.08328	0.13637	0.06959
40	10	0.09633	0.00875	9.08	0.10263	0.09003	0.11382	0.07883	0.12598	0.06667
35	10	0.08598	0.00801	9.31	0.09175	0.08022	0.10199	0.06997	0.11312	0.05885
30	10	0.07648	0.00951	12.43	0.08333	0.06964	0.09550	0.05747	0.10871	0.04425
25	10	0.06451	0.00845	13.10	0.07060	0.05843	0.08141	0.04762	0.09315	0.03587
20	10	0.05292	0.00779	14.73	0.05853	0.04731	0.06851	0.03733	0.07934	0.02650
15	10	0.04428	0.00868	19.61	0.05053	0.03803	0.06165	0.02691	0.07372	0.01484
10	9	0.03524	0.00766	21.73	0.04114	0.02934	0.05056	0.01992	0.06243	0.00805

CI = confidence interval
UCL = upper confidence limit
LCL = lower confidence limit
MaxARV = maximum average roll value
MARV = minimum average roll value

TI = tolerance interval
UTL = upper tolerance limit
LTL = lower tolerance limit

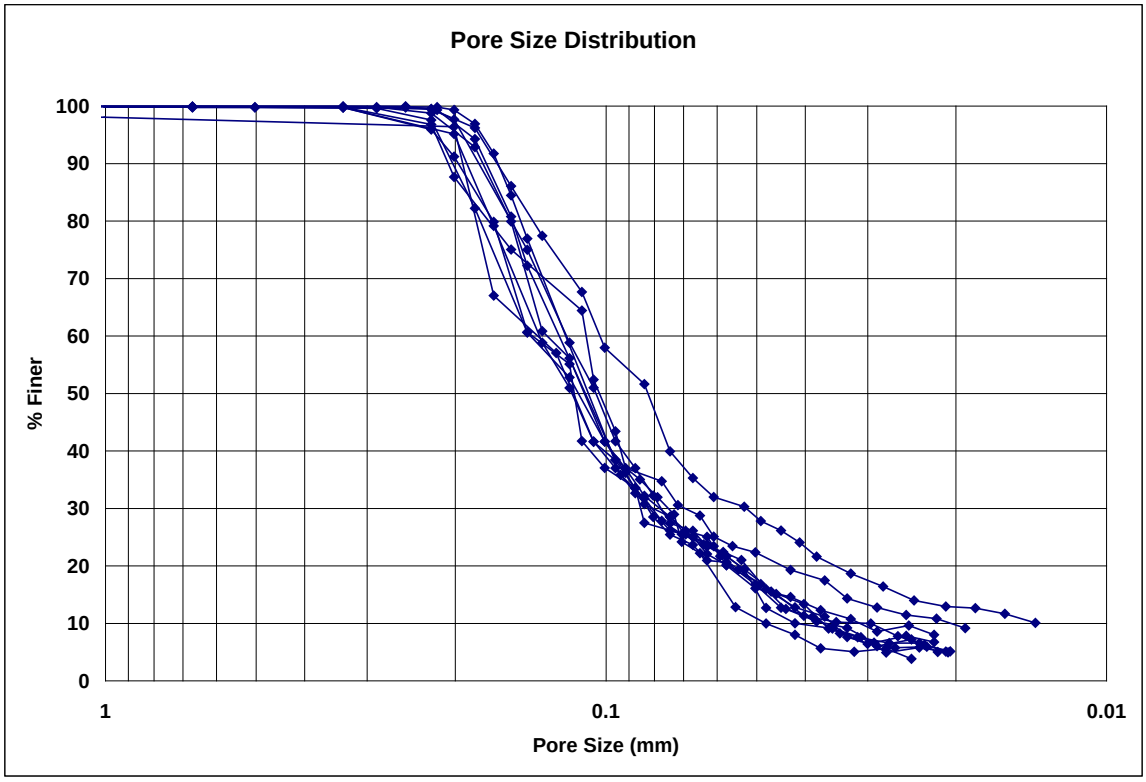

Figure 5.19: 2-ethyl hexanol pore size distributions for individual tests on the NG-1 nonwoven geotextile.

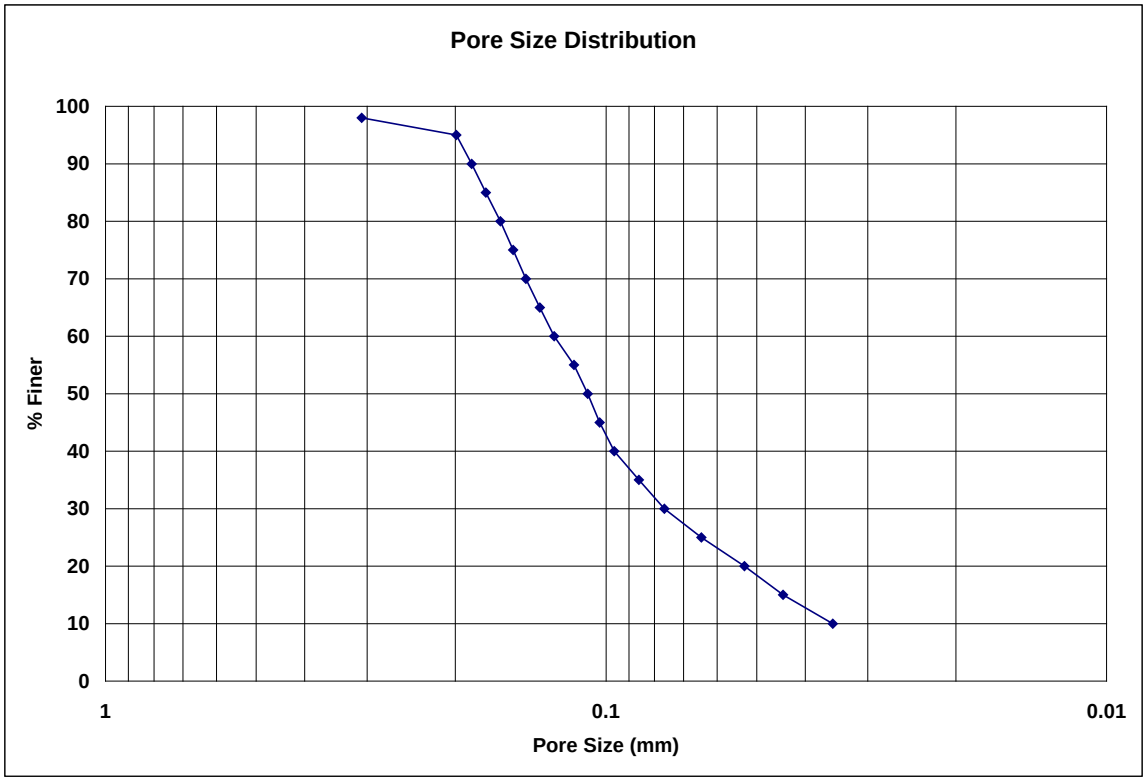

Figure 5.20: 2-ethyl hexanol mean pore size distribution for the tests in Figure 5.19.

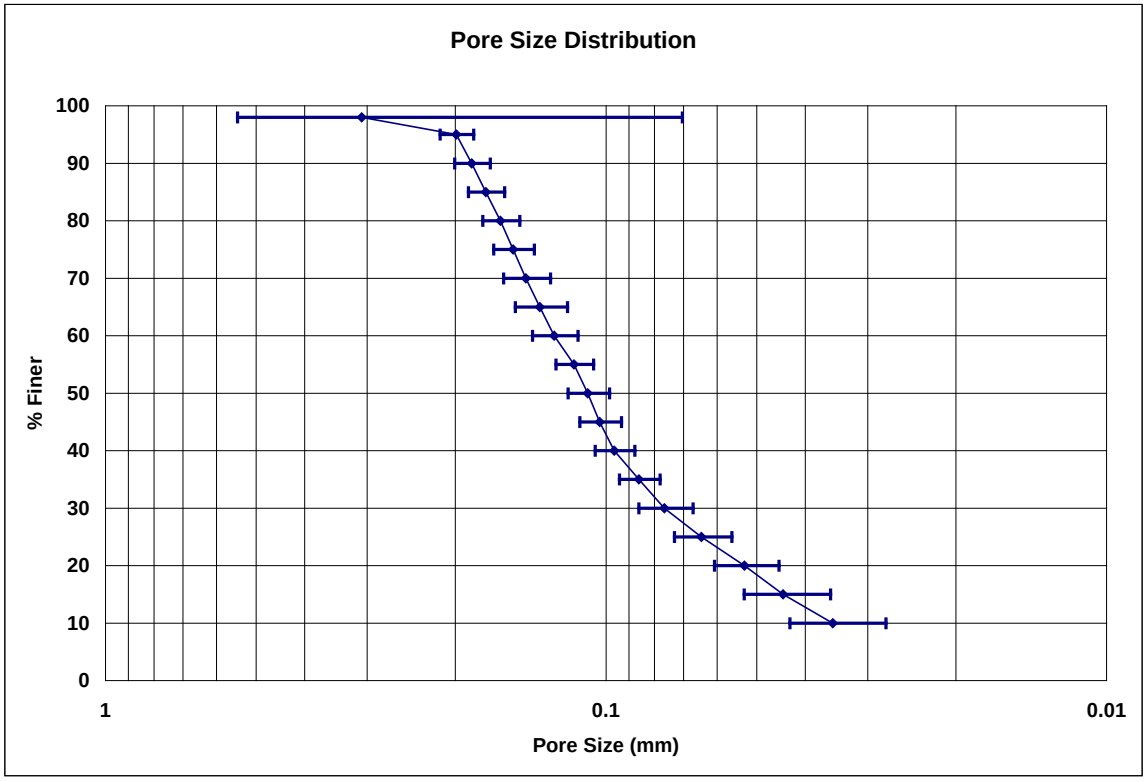

Figure 5.21: 2-ethyl hexanol mean pore size distribution +/- standard deviation for the tests in Figure 5.19.

Figure 5.22: 2-ethyl hexanol mean pore size distribution with 95% confidence interval for the tests in Figure 5.19.

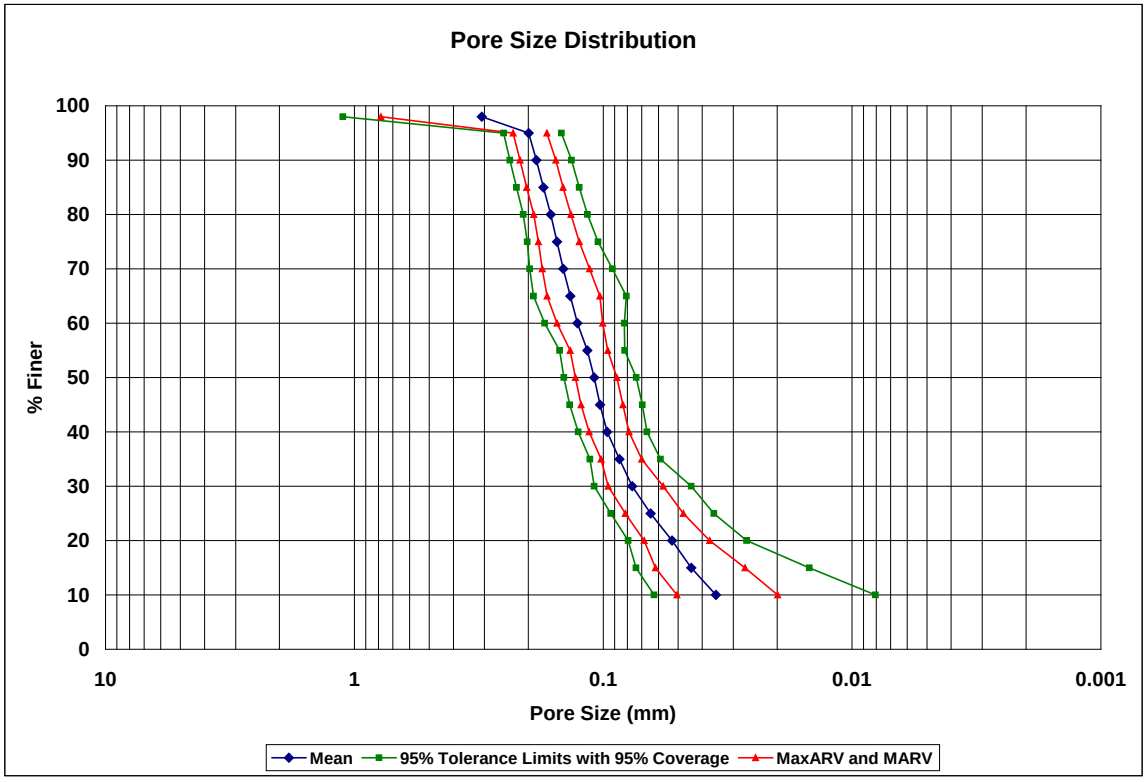

Figure 5.23: 2-ethyl hexanol mean pore size distribution, showing MaxARV, MARV, and the 95% tolerance interval with 95% coverage for the tests in Figure 5.19.

5.2.7 Drakeol Summary Results for the NG-1 Nonwoven Geotextile

Table 5.12: Drakeol results for pore sizes at selected % finer.

% Finer	Drakeol-1 Pore Size (mm)	Drakeol-2 Pore Size (mm)	Drakeol-3 Pore Size (mm)	Drakeol-4 Pore Size (mm)	Drakeol-5 Pore Size (mm)	Drakeol-6 Pore Size (mm)	Drakeol-7 Pore Size (mm)	Drakeol-8 Pore Size (mm)	Drakeol-9 Pore Size (mm)	Drakeol-10 Pore Size (mm)
98	---	0.22688	---	0.25288	0.24899	0.22870	---	---	0.18981	0.23566
95	0.16504	0.18070	0.17730	0.20070	0.16723	0.19625	0.20427	0.22034	0.16266	0.20937
90	0.14749	0.14903	0.14704	0.15204	0.15628	0.16513	0.16089	0.15688	0.14671	0.16717
85	0.13199	0.13688	0.13543	0.14027	0.14533	0.15799	0.14395	0.14546	0.13959	0.14649
80	0.12579	0.12603	0.12383	0.13017	0.13188	0.14709	0.12886	0.13404	0.13247	0.12623
75	0.11951	0.11517	0.10445	0.12019	0.11936	0.13619	0.12044	0.11579	0.12550	0.11898
70	0.11267	0.10758	0.09946	0.11332	0.11521	0.12540	0.11328	0.10006	0.11853	0.11174
65	0.10433	0.09997	0.09448	0.10644	0.11106	0.11553	0.10612	0.09802	0.11021	0.10449
60	0.09501	0.09198	0.08752	0.09933	0.10040	0.10867	0.09819	0.09598	0.10037	0.09804
55	0.08652	0.08509	0.08018	0.09141	0.08915	0.10571	0.09003	0.09394	0.08992	0.09227
50	0.08229	0.07982	0.07382	0.08217	0.08394	0.10275	0.08843	0.09190	0.08618	0.08649
45	0.07587	0.07506	0.05848	0.06927	0.07872	0.08991	0.08345	0.08977	0.08244	0.08071
40	0.06521	0.05739	0.04441	0.06103	0.06292	0.06814	0.07170	0.08735	0.07839	0.07304
35	0.05250	0.04457	0.03687	0.04811	0.05831	0.06129	0.06054	0.07252	0.06459	0.06364
30	0.04096	0.03687	0.02653	0.03738	0.04454	0.05054	0.04640	0.05625	0.04535	0.05385
25	0.03272	---	---	0.02763	0.03629	0.04605	0.04075	0.04610	0.03837	0.04561
20	0.02488	---	---	0.02222	0.02815	---	0.02706	0.04248	0.02917	0.03993
15	---	---	---	---	0.01887	---	0.02217	0.03220	0.02006	0.03340
10	---	---	---	---	---	---	---	---	---	---
5	---	---	---	---	---	---	---	---	---	---

Table 5.13: Drakeol statistics for pore sizes at selected % finer.

% Finer	Sample Size	Mean Pore Size (mm)	Standard Deviation (mm)	Coefficient of Variation (%)	95% CI of Mean UCL (mm)	95% CI of Mean LCL (mm)	MaxARV (mm)	MARV (mm)	95% TI with 95% Coverage UTL (mm)	95% TI with 95% Coverage LTL (mm)
98	6	0.23048	0.02255	9.78	0.25416	0.20681	0.27557	0.18539	0.33014	0.13083
95	10	0.18839	0.02045	10.86	0.20311	0.17366	0.22929	0.14749	0.25771	0.11906
90	10	0.15487	0.00763	4.92	0.16036	0.14938	0.17012	0.13961	0.18072	0.12901
85	10	0.14234	0.00730	5.13	0.14760	0.13708	0.15694	0.12773	0.16710	0.11758
80	10	0.13064	0.00668	5.11	0.13545	0.12583	0.14399	0.11729	0.15327	0.10801
75	10	0.11956	0.00799	6.69	0.12531	0.11380	0.13555	0.10357	0.14666	0.09246
70	10	0.11172	0.00785	7.03	0.11738	0.10607	0.12743	0.09602	0.13834	0.08511
65	10	0.10507	0.00635	6.05	0.10964	0.10049	0.11777	0.09236	0.12660	0.08353
60	10	0.09755	0.00562	5.76	0.10159	0.09350	0.10878	0.08631	0.11659	0.07850
55	10	0.09042	0.00668	7.38	0.09523	0.08561	0.10377	0.07707	0.11305	0.06779
50	10	0.08578	0.00775	9.03	0.09136	0.08020	0.10127	0.07028	0.11204	0.05952
45	10	0.07837	0.00947	12.08	0.08519	0.07155	0.09730	0.05944	0.11046	0.04628
40	10	0.06696	0.01184	17.68	0.07548	0.05843	0.09064	0.04328	0.10710	0.02682
35	10	0.05629	0.01069	19.00	0.06399	0.04859	0.07768	0.03490	0.09255	0.02004
30	10	0.04387	0.00886	20.20	0.05025	0.03749	0.06159	0.02615	0.07390	0.01383
25	8	0.03919	0.00679	17.33	0.04490	0.03348	0.05277	0.02560	0.06466	0.01372
20	7	0.03055	0.00766	25.06	0.03760	0.02351	0.04587	0.01524	0.06133	-0.00023
15	5	0.02534	0.00692	27.32	0.03392	0.01675	0.03919	0.01149	0.06051	-0.00983

CI = confidence interval
UCL = upper confidence limit
LCL = lower confidence limit
MaxARV = maximum average roll value
MARV = minimum average roll value
TI = tolerance interval
UTL = upper tolerance limit
LTL = lower tolerance limit

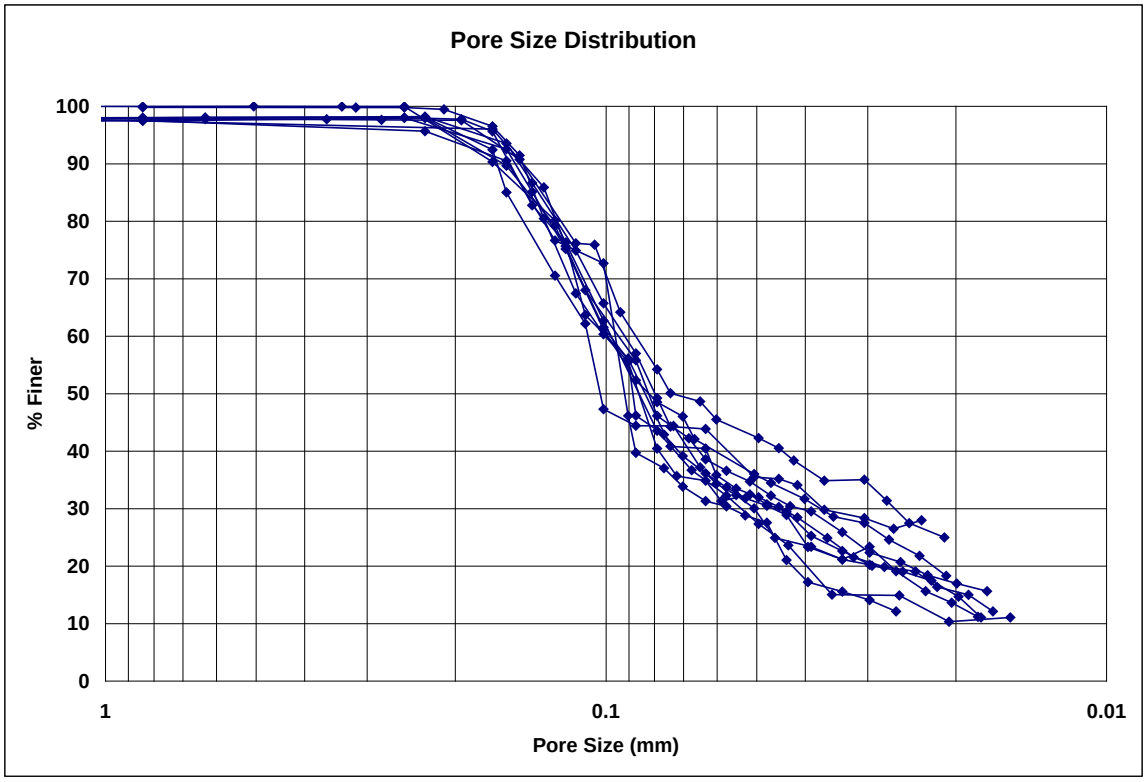

Figure 5.24: Drakeol pore size distributions for individual tests on the NG-1 nonwoven geotextile.

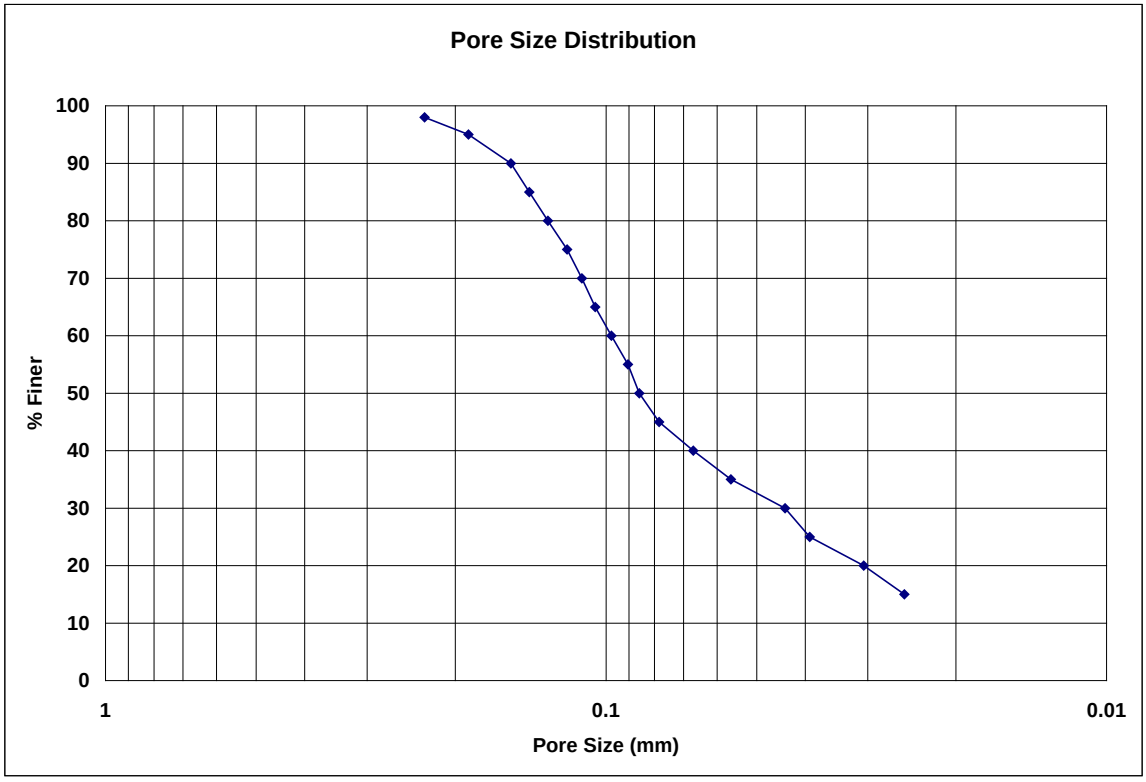

Figure 5.25: Drakeol mean pore size distribution for tests in Figure 5.24.

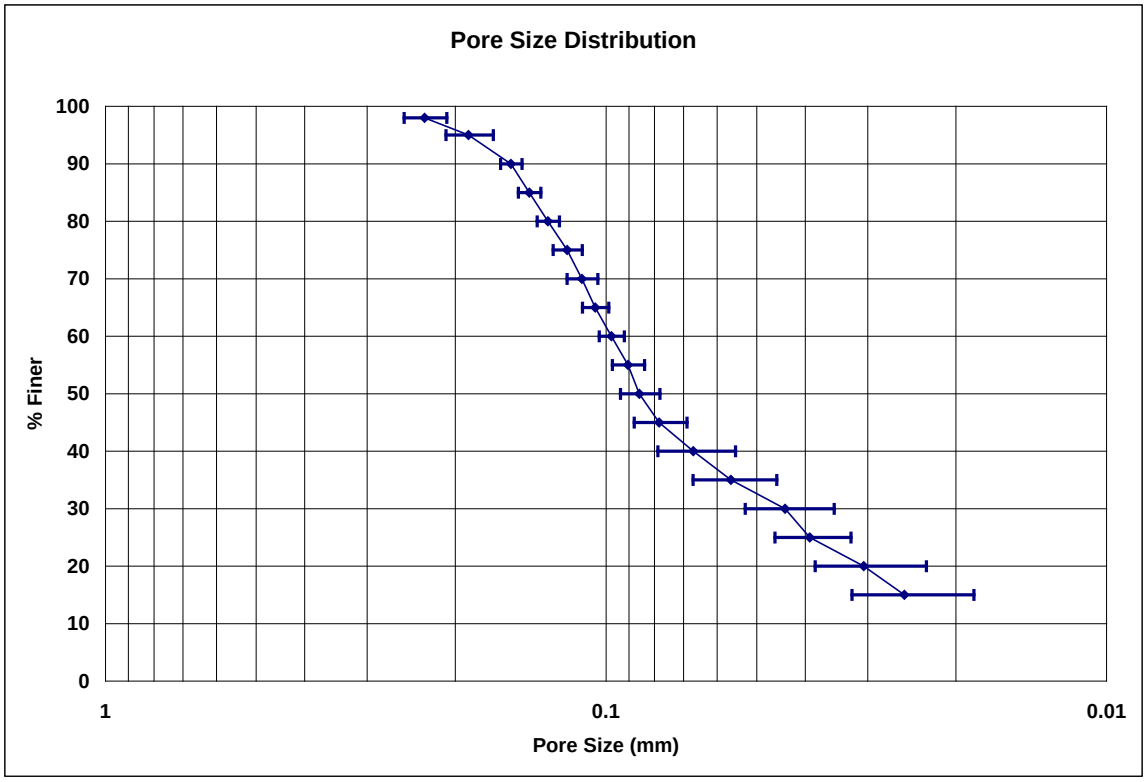

Figure 5.26: Drakeol mean pore size distribution +/- standard deviation for tests in Figure 5.24.

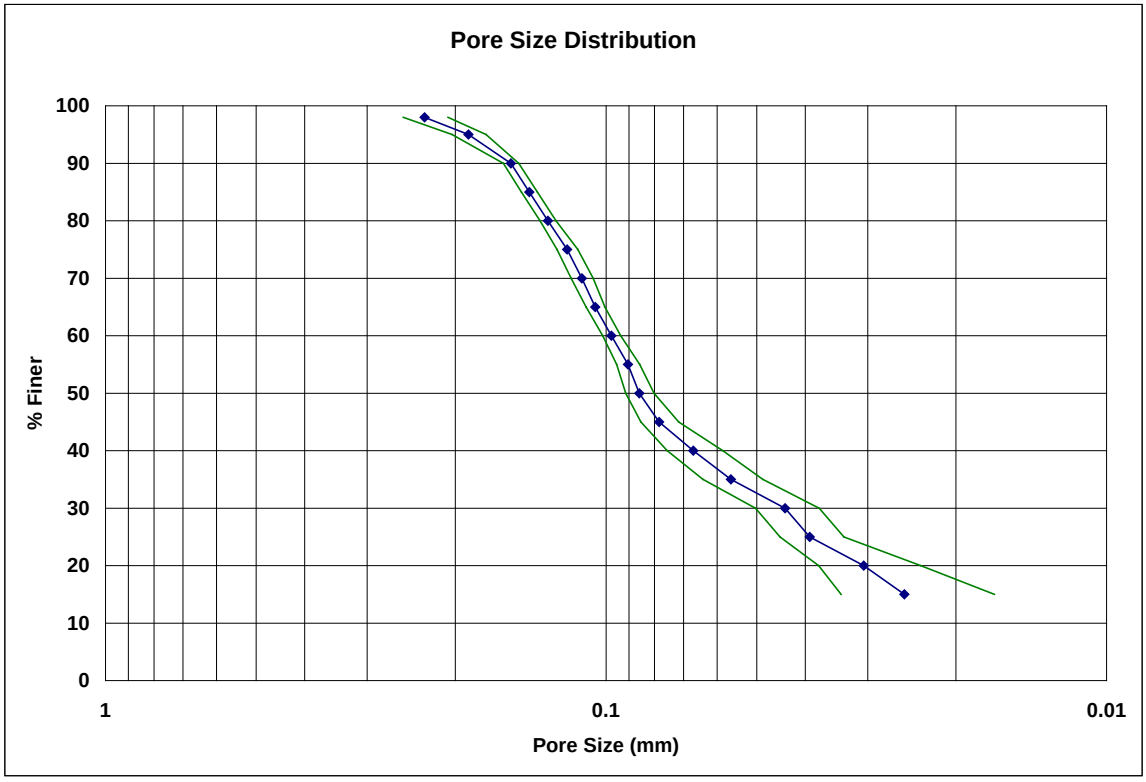

Figure 5.27: Drakeol mean pore size distribution with 95% confidence interval for tests in Figure 5.24.

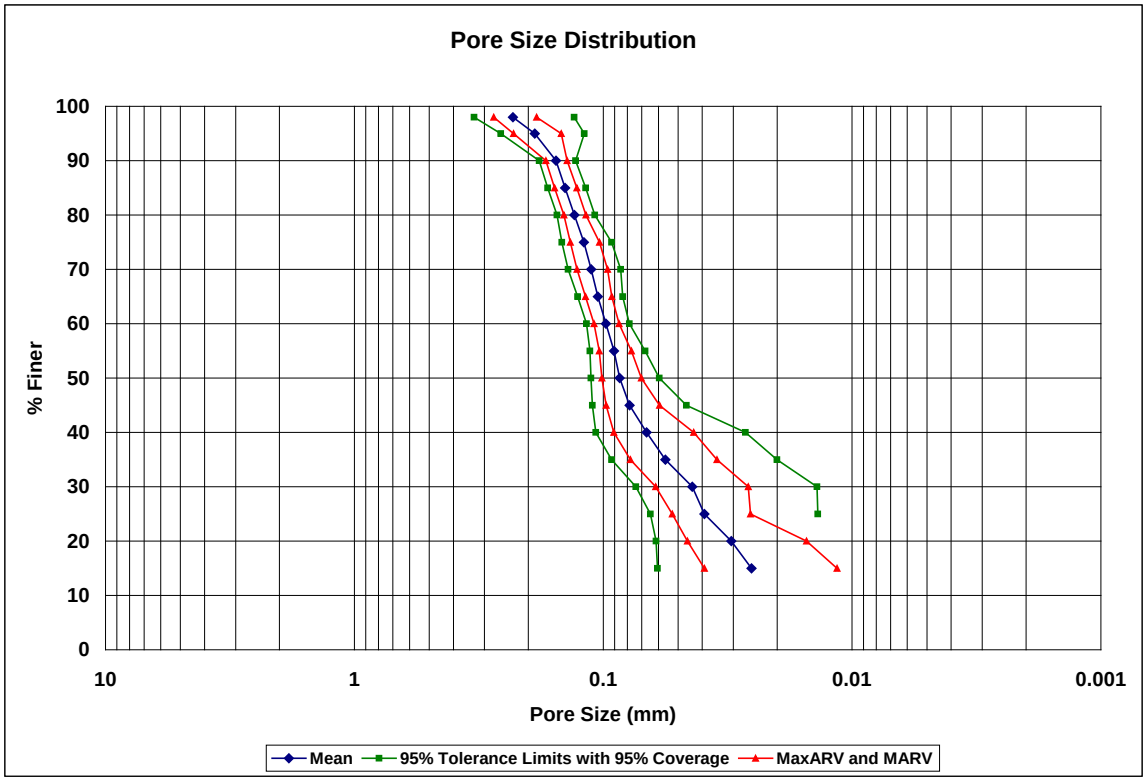

Figure 5.28: Drakeol mean pore size distribution, showing MaxARV, MARV, and the 95% tolerance interval with 95% coverage for tests in 5.24.

5.2.8 Glycerin Summary Results for the NG-1 Nonwoven Geotextile

Table 5.14: Glycerin results for pore sizes at selected % finer.

% Finer	Glycerin-1 Pore Size (mm)	Glycerin-2 Pore Size (mm)	Glycerin-3 Pore Size (mm)	Glycerin-4 Pore Size (mm)	Glycerin-5 Pore Size (mm)	Glycerin-6 Pore Size (mm)	Glycerin-7 Pore Size (mm)	Glycerin-8 Pore Size (mm)	Glycerin-9 Pore Size (mm)	Glycerin-10 Pore Size (mm)
98	0.25852	0.21772	0.16920	0.20857	1.12559	0.17732	0.21889	0.17974	0.21463	0.21900
95	0.15098	0.15834	0.14975	0.20338	0.50817	0.15948	0.20956	0.16156	0.18479	0.18414
90	0.13659	0.14281	0.14329	0.19473	0.18875	0.13962	0.19400	0.14471	0.16058	0.17835
85	0.12220	0.13269	0.13683	0.18609	0.16868	0.12551	0.17844	0.13377	0.14451	0.17524
80	0.11648	0.12425	0.12977	0.17744	0.16008	0.12219	0.16289	0.12283	0.13985	0.16388
75	0.11325	0.11804	0.11913	0.17027	0.15148	0.11888	0.14733	0.11519	0.13298	0.14291
70	0.10791	0.11182	0.10864	0.16460	0.14300	0.11556	0.13120	0.10857	0.11539	0.12859
65	0.10482	0.10654	0.10311	0.15893	0.13451	0.09519	0.11357	0.10720	0.11059	0.11741
60	0.10173	0.10215	0.09759	0.15327	0.12824	0.09519	0.10265	0.10583	0.10884	0.10659
55	0.09865	0.09777	0.08772	0.14851	0.12331	0.09075	0.09707	0.10446	0.10710	0.09700
50	0.09556	0.09338	0.07992	0.14395	0.11839	0.05875	0.07974	0.10310	0.09045	0.08033
45	0.07883	0.08899	0.07133	0.13938	0.11346	0.05287	0.06820	0.07292	0.06342	0.07239
40	0.07478	0.08456	0.06456	0.13482	0.10734	0.04620	0.05499	0.04836	0.05238	0.05502
35	0.05782	0.06397	0.05380	0.10688	0.08666	0.04246	0.04432	0.04112	0.04564	0.04616
30	0.04748	0.05694	0.04616	0.09095	0.06587	0.03446	0.04081	0.03675	0.03942	0.03857
25	0.03910	0.04899	---	0.07259	0.06180	0.03057	---	---	---	---
20	0.03287	0.03896	---	0.06607	0.05805	---	---	---	---	---
15	---	---	---	0.06098	0.04862	---	---	---	---	---
10	---	---	---	0.05475	0.03954	---	---	---	---	---
5	---	---	---	0.04441	0.02882	---	---	---	---	---

Table 5.15: Glycerin statistics for pore sizes at selected % finer.

% Finer	Sample Size	Mean Pore Size (mm)	Standard Deviation (mm)	Coefficient of Variation (%)	95% CI of Mean		MaxARV (mm)	MARV (mm)	95% TI with 95% Coverage	
					UCL (mm)	LCL (mm)			UTL (mm)	LTL (mm)
98	10	0.29892	0.29164	97.56	0.50890	0.08894	0.88220	-0.28436	1.28758	-0.68974
95	10	0.20701	0.10793	52.14	0.28473	0.12930	0.42288	-0.00885	0.57291	-0.15888
90	10	0.16234	0.02414	14.87	0.17972	0.14497	0.21062	0.11407	0.24417	0.08052
85	10	0.15040	0.02412	16.04	0.16776	0.13303	0.19863	0.10216	0.23216	0.06864
80	10	0.14197	0.02206	15.54	0.15785	0.12609	0.18608	0.09786	0.21673	0.06720
75	10	0.13295	0.01931	14.53	0.14685	0.11904	0.17157	0.09432	0.19842	0.06747
70	10	0.12353	0.01858	15.04	0.13691	0.11015	0.16069	0.08637	0.18651	0.06054
65	10	0.11519	0.01858	16.13	0.12857	0.10181	0.15235	0.07802	0.17818	0.05220
60	10	0.11021	0.01761	15.98	0.12289	0.09753	0.14543	0.07499	0.16991	0.05050
55	10	0.10523	0.01812	17.22	0.11828	0.09219	0.14147	0.06900	0.16665	0.04382
50	10	0.09436	0.02361	25.03	0.11136	0.07735	0.14158	0.04713	0.17440	0.01431
45	10	0.08218	0.02585	31.45	0.10079	0.06357	0.13388	0.03048	0.16981	-0.00545
40	10	0.07230	0.02906	40.20	0.09323	0.05138	0.13043	0.01418	0.17082	-0.02622
35	10	0.05888	0.02176	36.96	0.07455	0.04321	0.10241	0.01536	0.13266	-0.01489
30	10	0.04974	0.01745	35.09	0.06231	0.03718	0.08465	0.01484	0.10890	-0.00942
25	5	0.05061	0.01692	33.43	0.07159	0.02963	0.08445	0.01677	0.13656	-0.03535

CI = confidence interval
UCL = upper confidence limit
LCL = lower confidence limit
MaxARV = maximum average roll value
MARV = minimum average roll value
TI = tolerance interval
UTL = upper tolerance limit
LTL = lower tolerance limit

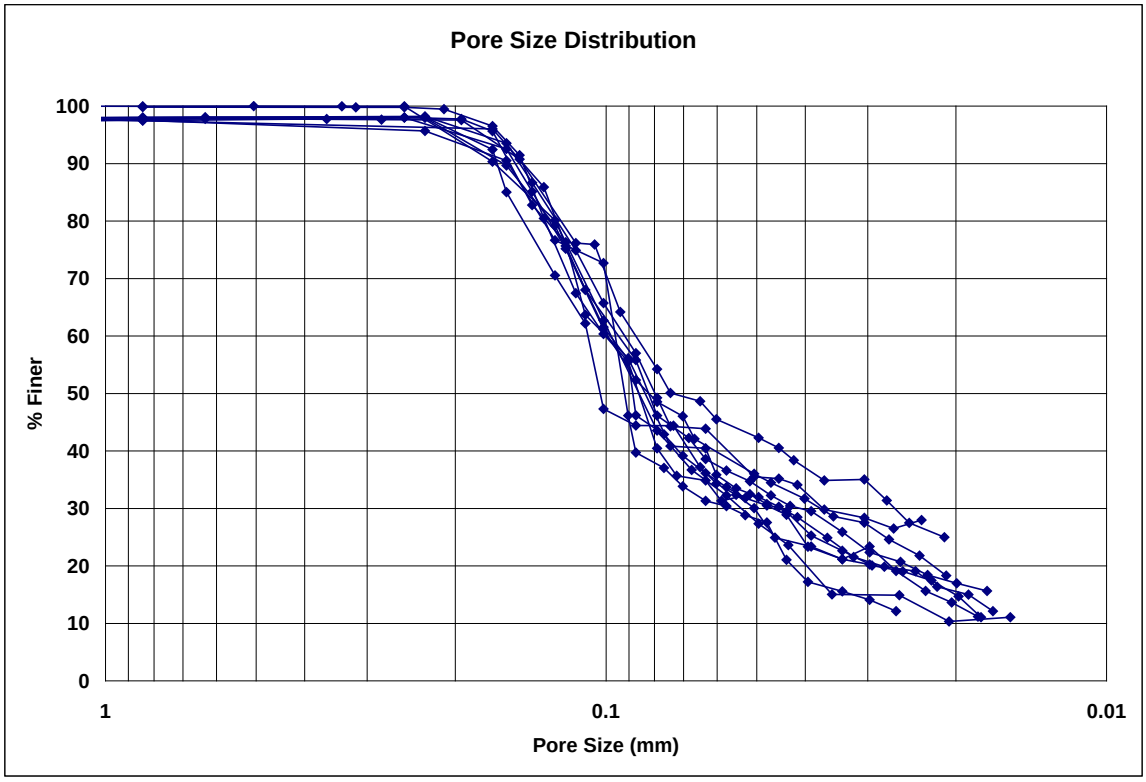

Figure 5.29: Glycerin pore size distributions for individual tests on the NG-1 nonwoven geotextile.

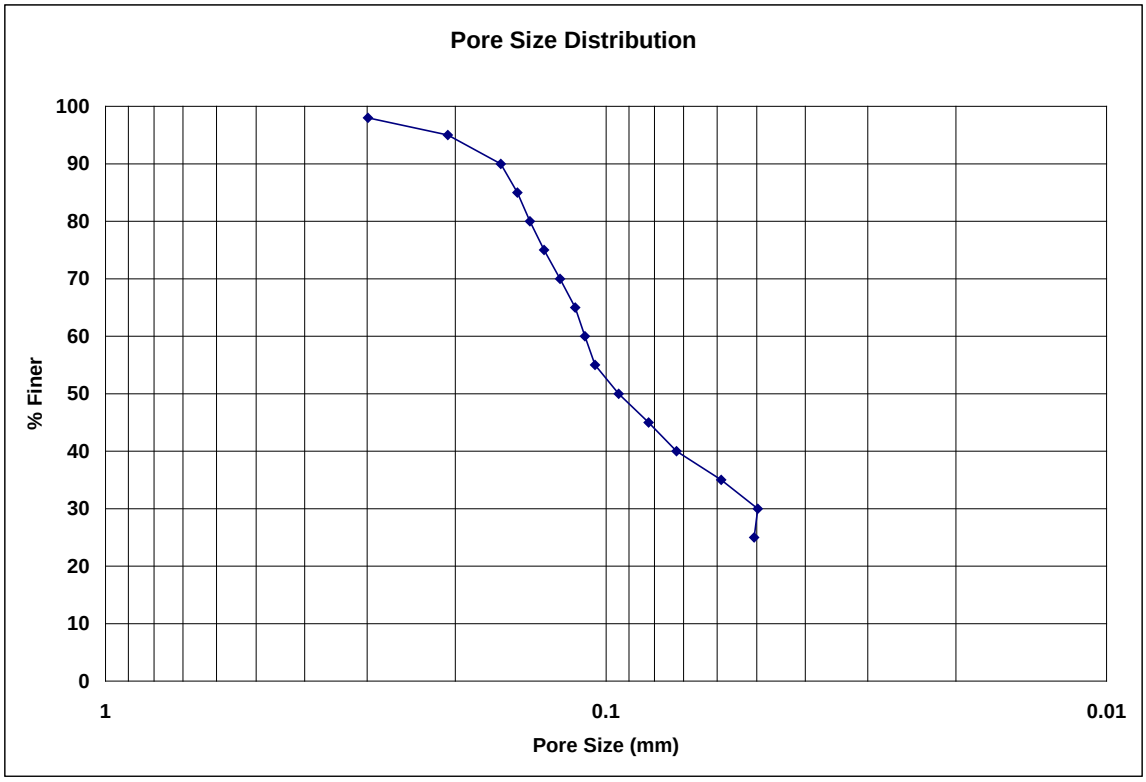

Figure 5.30: Glycerin mean pore size distribution for tests in Figure 5.29.

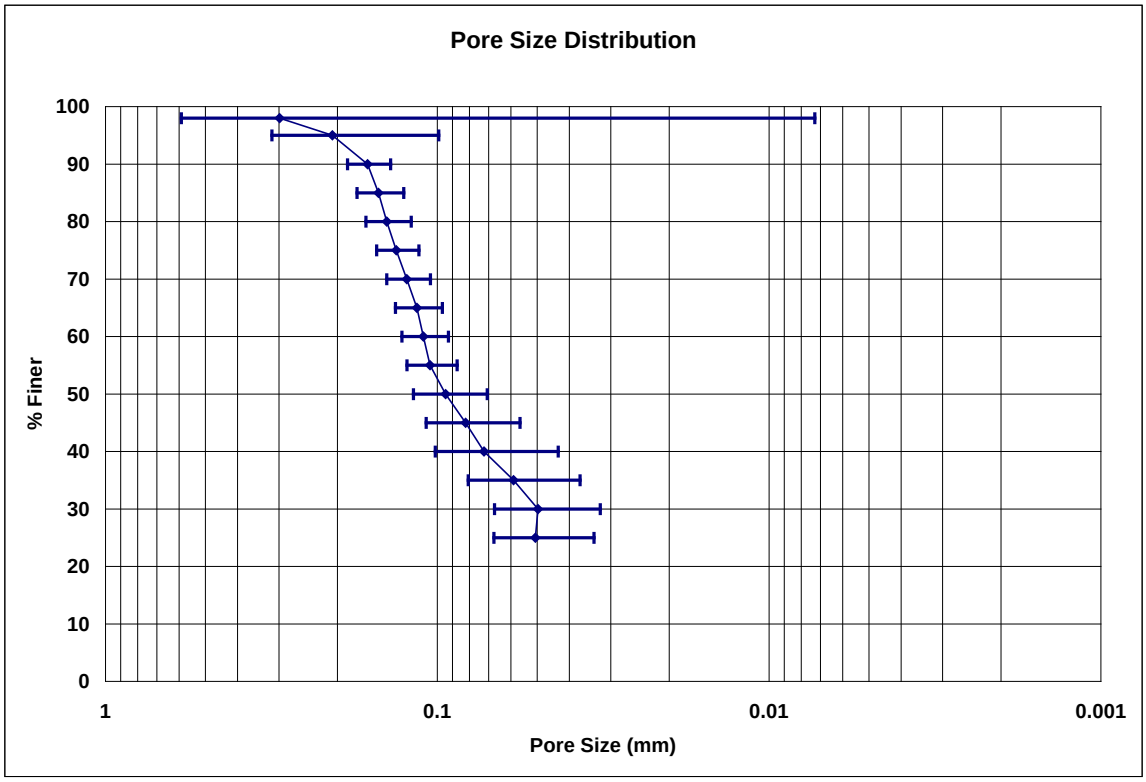

Figure 5.31: Glycerin mean pore size distribution +/- standard deviation for tests in Figure 5.29.

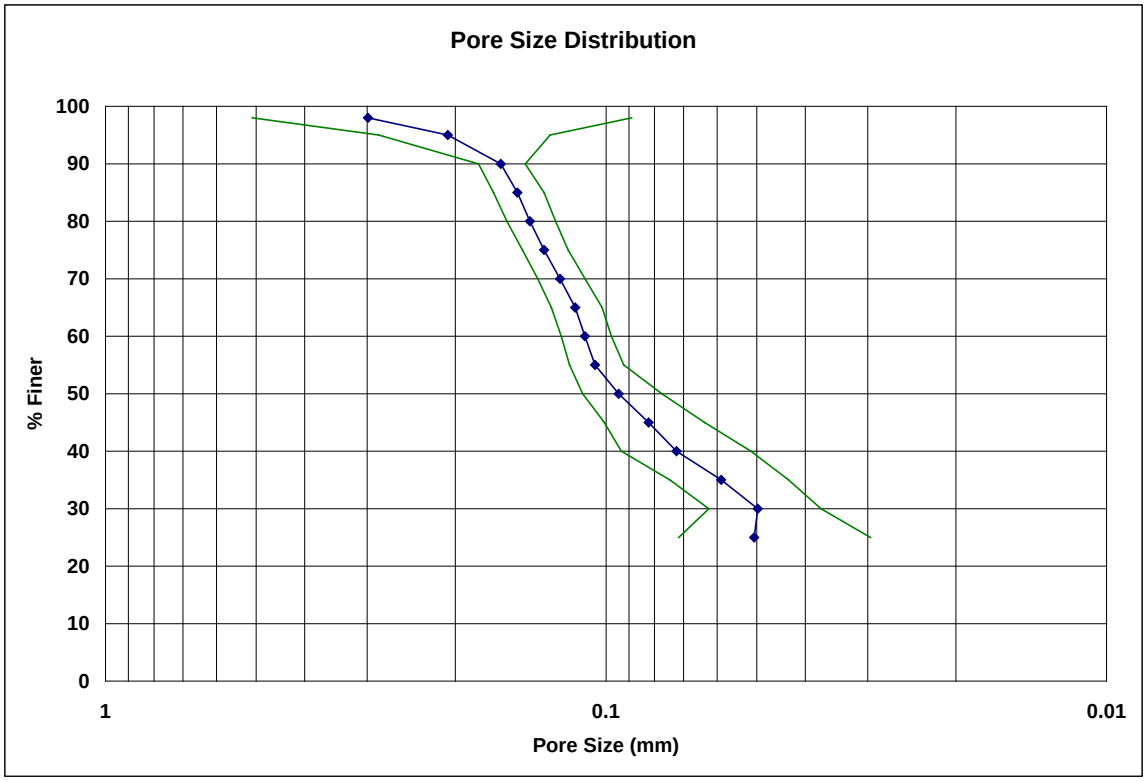

Figure 5.32: Glycerin mean pore size distribution with 95% confidence interval for tests in Figure 5.29.

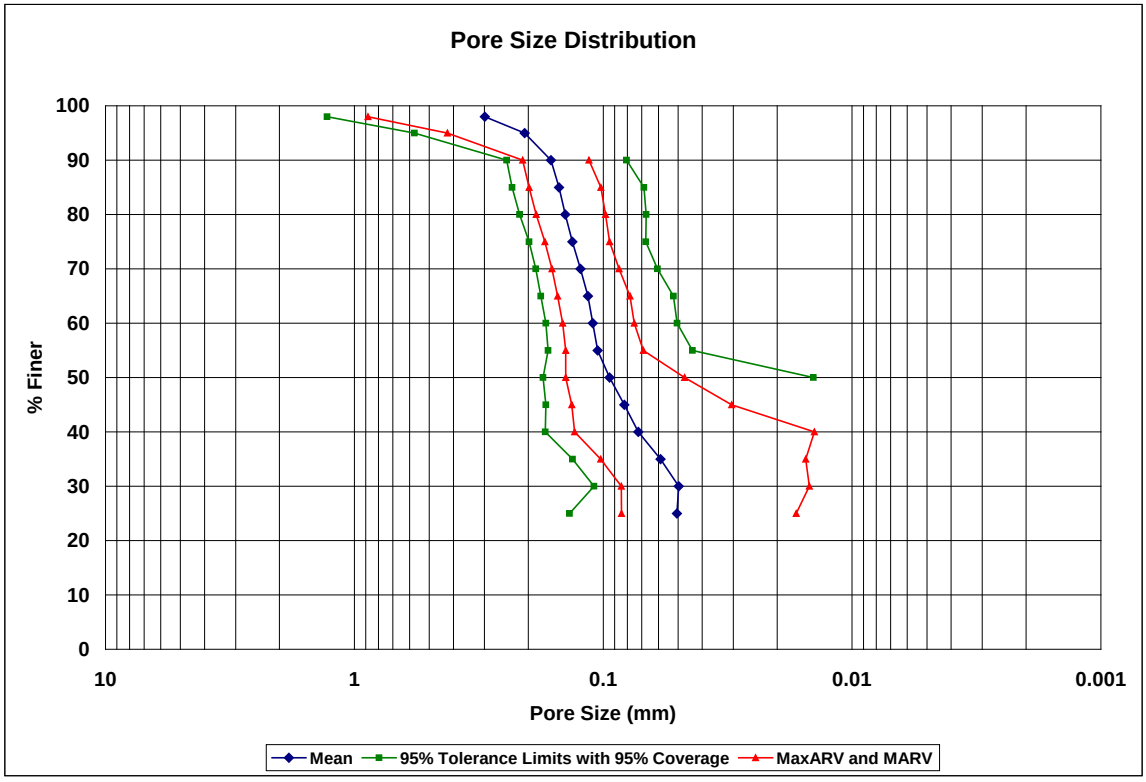

Figure 5.33: Glycerin mean pore size distribution, showing MaxARV, MARV, and the 95% tolerance interval with 95% coverage for the tests in Figure 5.29.

5.2.9 Discussion of Summary Results for the NG-1 Nonwoven Geotextile

Results of bubble point tests performed on the NG-1 nonwoven geotextile are shown in Tables 5.4 – 5.15 and Figures 5.4 –5.33. The standard deviation of the pore size was relatively large (indicating relatively low precision) at O_{98} and O_{95} for all fluids except water and Drakeol. This effect appeared to be caused by outlying data points and it will be discussed in more detail in Section 5.2.10. The standard deviation is reflected in other statistics (coefficient of variation, confidence interval of the mean, MARV, MaxARV, and tolerance intervals) since it is used calculate these parameters. A larger standard deviation (lower precision) results in a larger coefficient of variation, a larger confidence interval of the mean, a larger interval between MARV and MaxARV, and larger tolerance intervals. The standard deviation of the pore size generally tended to increase as the opening size decreases from O_{90}, an effect which is particularly evident in Figure 5.11 for the results of bubble point tests performed using Porewick as the wetting fluid. In some cases, large standard deviations at either ends of the pore size distribution resulted in values of MARV and the lower tolerance limit that were negative and therefore could not be plotted on the log-scale (see for example, Table 5.15 and Figure 5.33).

The coefficient of variation can be used to compare the precision of tests using different fluids. A table listing the coefficient of variation for each fluid at selected values of percent finer is presented as Table 5.16. A line graph of the coefficient of variation vs. percent finer for each fluid is shown in Figure 5.34. A bar graph of the coefficient of variation for selected percent finer grouped by fluid is shown in Figure 5.35. Table 5.16 and Figures 5.34 and 5.35 show the relatively high coefficient of

variation at O_{98} and/or O_{95} for water, Porewick, mineral oil, 2-ethyl hexanol, and glycerin, and also show the general trend for all fluids of an increasing coefficient of variation as the percent finer decreases from O_{90}. Mineral oil, 2-ethyl hexanol, and Drakeol appeared to generally show the best precision (lowest coefficients of variation), although 2-ethyl hexanol yielded a high coefficient of variation (77.12%) at O_{98} and Drakeol showed a more marked trend of an increasing coefficient of variation with decreasing percent finer.

Table 5.16: Coefficient of variation at selected % finer by wetting fluid.

	Coefficient of Variation (%)					
% Finer	water	Porewick	mineral oil	2-ethyl hexanol	Drakeol	glycerin
98	53.66	53.36	10.97	77.12	9.78	97.56
95	17.98	98.88	10.18	7.71	10.86	52.14
90	19.63	9.30	10.48	8.20	4.92	14.87
85	20.40	7.79	10.29	8.34	5.13	16.04
80	20.66	7.40	10.70	8.52	5.11	15.54
75	20.98	8.83	10.76	9.34	6.69	14.53
70	21.34	11.16	11.23	10.76	7.03	15.04
65	21.45	13.41	11.71	11.96	6.05	16.13
60	21.37	15.12	11.63	10.41	5.76	15.98
55	21.30	16.85	11.67	8.64	7.38	17.22
50	21.27	18.72	11.20	9.51	9.03	25.03
45	21.26	20.74	11.26	9.57	12.08	31.45
40	21.28	22.64	13.11	9.08	17.68	40.20
35	21.34	23.97	13.51	9.31	19.00	36.96
30	21.44	25.07	14.03	12.43	20.20	35.09
25	21.58	26.20	17.78	13.10	17.33	33.43
20	21.76	27.28	22.54	14.73	25.06	---
15	22.00	28.31	19.85	19.61	27.32	---
10	20.52	29.08	---	21.73	---	---
5	33.23	38.00	---	---	---	---

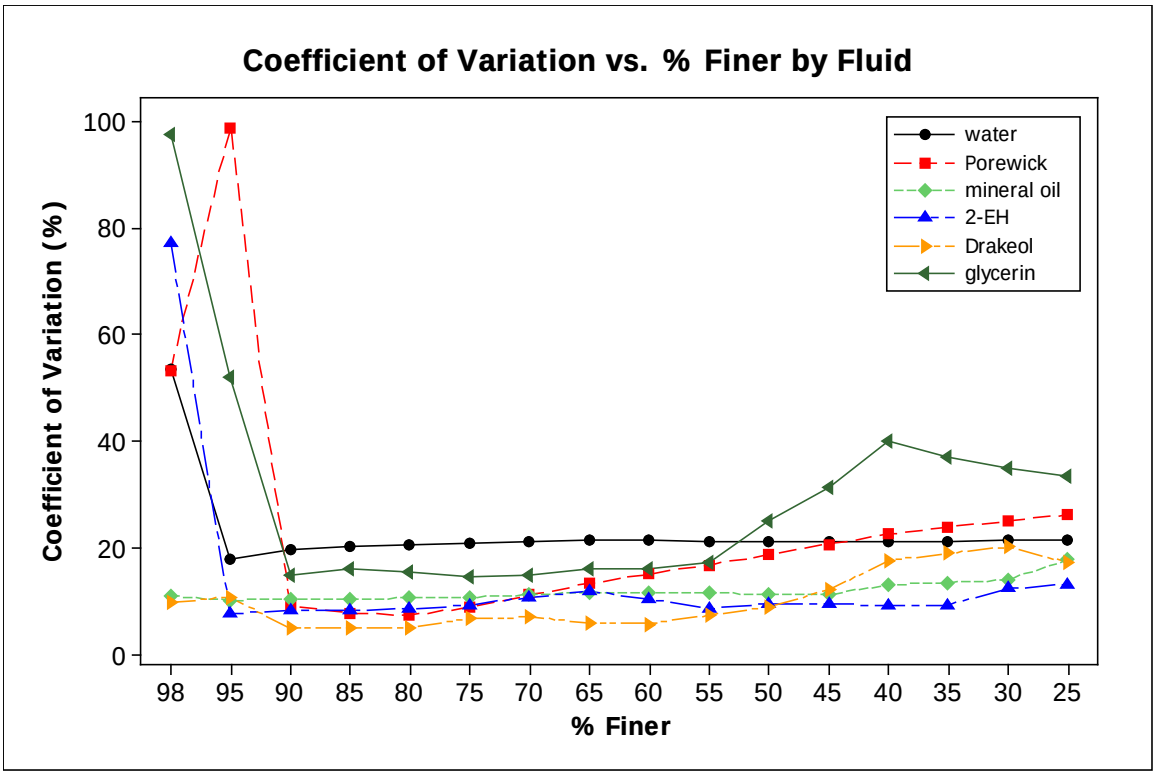

Figure 5.34: Coefficient of variation vs. % finer.

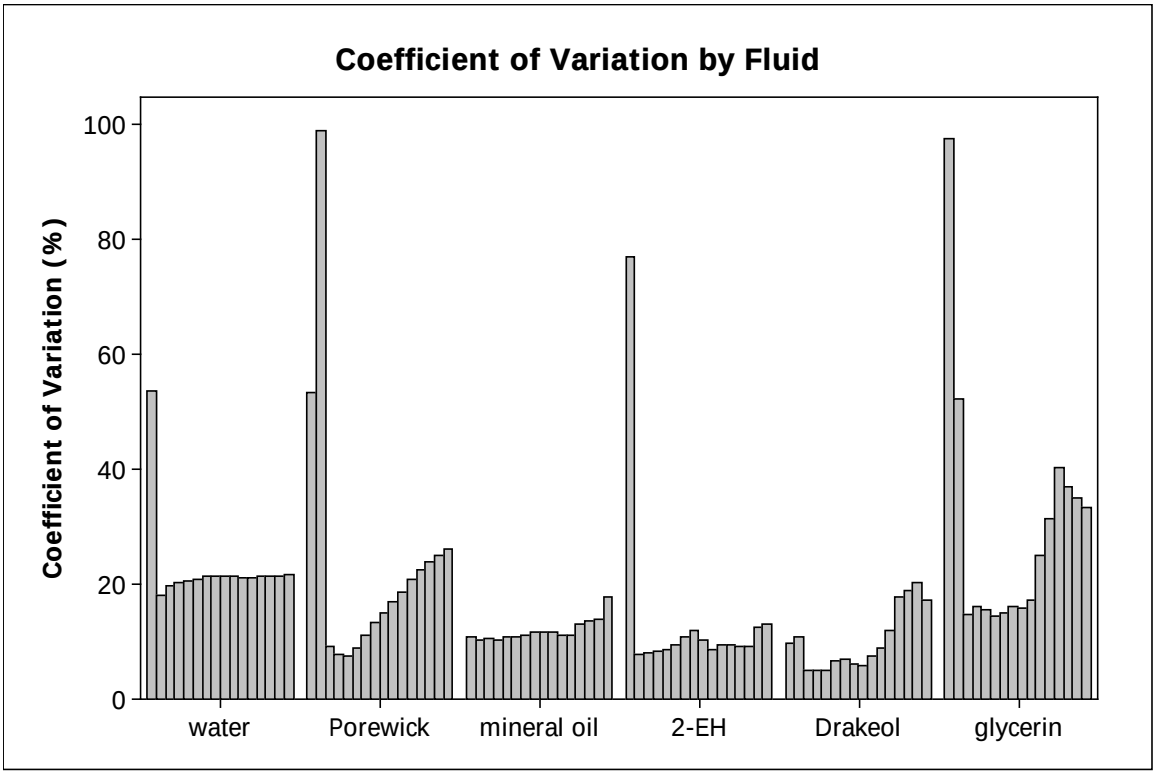

Figure 5.35: Coefficient of variation for % finer (decreasing % finer from left to right), grouped by fluid.

5.2.10 Identification and Removal of Outliers at O_{98} and O_{95}

As discussed in the previous section, relatively high values of the coefficient of variation were observed at O_{98} and/or O_{95} for several fluids, indicating relatively low precision for the calculated pore sizes. However, inspection of the datasets revealed that for each of these cases, there was a single extreme value for pore size that appeared to be skewing the coefficient of variation high. Review of the associated pore size distributions indicated that these extreme values of pore size were caused by the initial baseline values of the pore size distribution being less than 100% finer and associated variation or "noise" in the baseline of the pore size distribution. In these cases, the percent finer was calculated as being less than 100% at the beginning of the test, before fluid began to be effectively expelled from pores. An example of this effect is shown in Figure 5.36.

It is suspected that this "baseline effect" is a result of either equipment or operator error as opposed to being an accurate reflection pore size. The rationale for this belief is that the baseline is less than 100% finer early in the test before fluid begins to be effectively expelled from pores. If the baseline falls below O_{98} or O_{95}, an extreme value of pore size for these opening sizes may result. It should be noted that in some cases, the initial baseline was below O_{98} and thus the pore size for O_{98} could not be determined. However, even when the initial baseline was below 100% finer, once the fluid does begin to be effectively expelled from pores, the measured pore sizes more closely resemble the results other tests. One potential cause could be the geotextile sample not being completely saturated at the beginning of the test.

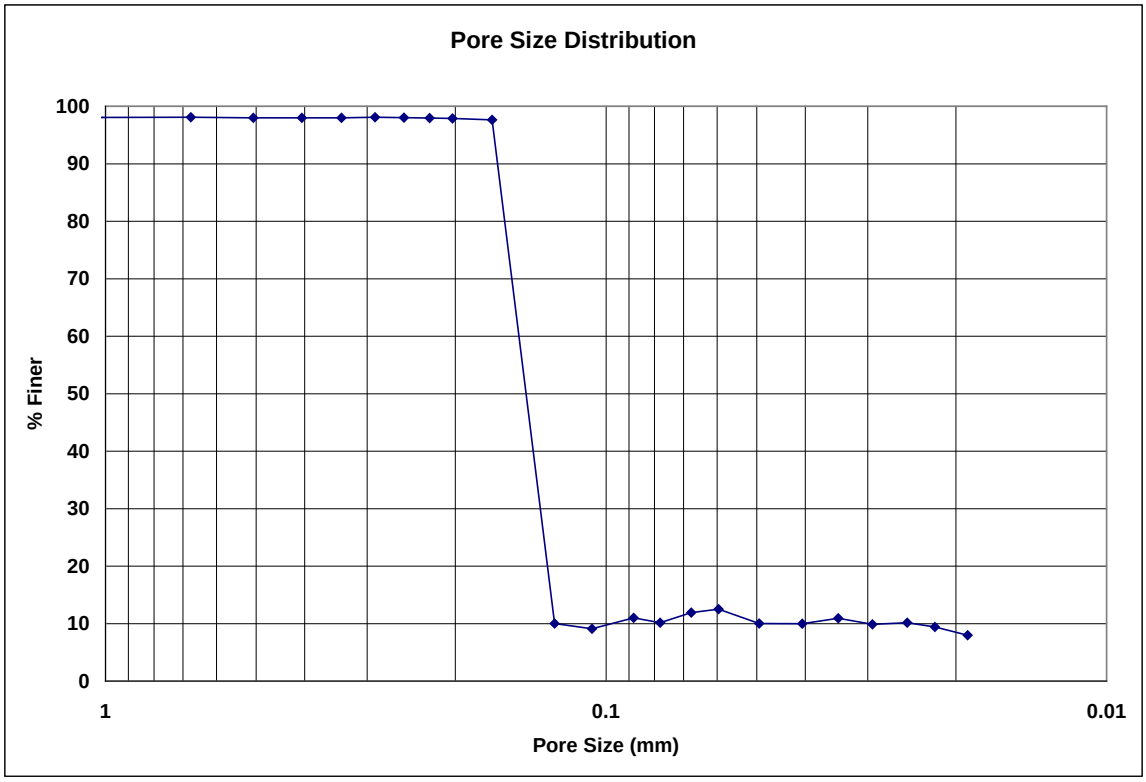

Figure 5.36: Example of a pore size distribution with an initial baseline less than 100% finer.

To identify if the extreme pore size values were indeed statistical outliers, the relevant O_{98} and O_{95} pore size data sets were subjected to Dixon's outlier test using USEPA ProUCL software (USEPA 2011a). In all cases, the extreme values were identified as statistical outliers. Since the statistical outliers were believed to be due to test error and therefore not representative of the population being tested, they were removed from the data sets, yielding lower coefficients of variation and better-behaved statistics. The identification of O_{98} and O_{95} outliers and the effect of their removal on the data set statistics are shown in Tables 5.17 – 5.31 and Figures 5.37 – 5.56. Note that no outliers were identified at O_{98} or O_{95} for mineral oil.

5.2.10.1 Water Summary Results with Outlier Correction

Table 5.17: O_{98} and O_{95} water results with outlier highlighted.

% Finer	Water-1 Pore Size (mm)	Water-2 Pore Size (mm)	Water-3 Pore Size (mm)	Water-4 Pore Size (mm)	Water-5 Pore Size (mm)	Water-6 Pore Size (mm)	Water-7 Pore Size (mm)	Water-8 Pore Size (mm)	Water-9 Pore Size (mm)	Water-10 Pore Size (mm)
98	0.12191	---	0.20251	0.16537	0.23077	0.16887	0.18402	0.14265	0.49580	0.16847
95	0.11836	0.16849	0.20095	0.12366	0.20028	0.16694	0.18173	0.13427	0.16761	0.15747

Table 5.18: O_{98} and O_{95} water statistics with outlier included.

% Finer	Sample Size	Mean Pore Size (mm)	Standard Deviation (mm)	Coefficient of Variation (%)	95% CI of Mean		MaxARV (mm)	MARV (mm)	95% TI with 95% Coverage	
					UCL (mm)	LCL (mm)			UTL (mm)	LTL (mm)
98	9	0.20893	0.11211	53.66	0.29525	0.12261	0.43314	-0.01528	0.60690	-0.18905
95	10	0.16198	0.02912	17.98	0.18295	0.14101	0.22022	0.10373	0.26070	0.06325

Table 5.19: O_{98} and O_{95} water statistics with outlier removed.

% Finer	Sample Size	Mean Pore Size (mm)	Standard Deviation (mm)	Coefficient of Variation (%)	95% CI of Mean		MaxARV (mm)	MARV (mm)	95% TI with 95% Coverage	
					UCL (mm)	LCL (mm)			UTL (mm)	LTL (mm)
98	8	0.17307	0.03372	19.48	0.20139	0.14475	0.24050	0.10564	0.29950	0.04664
95	10	0.16198	0.02912	17.98	0.18295	0.14101	0.22022	0.10373	0.26070	0.06325

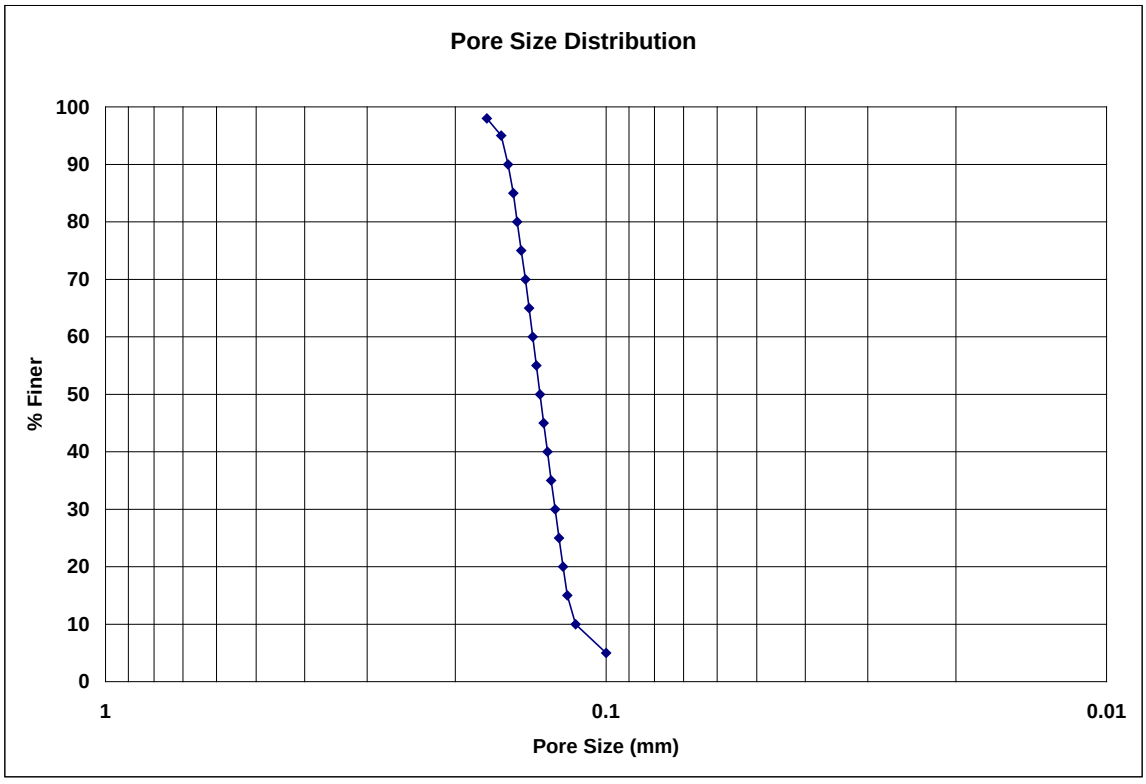

Figure 5.37: Water mean pore size distribution with O_{98} outlier removed.

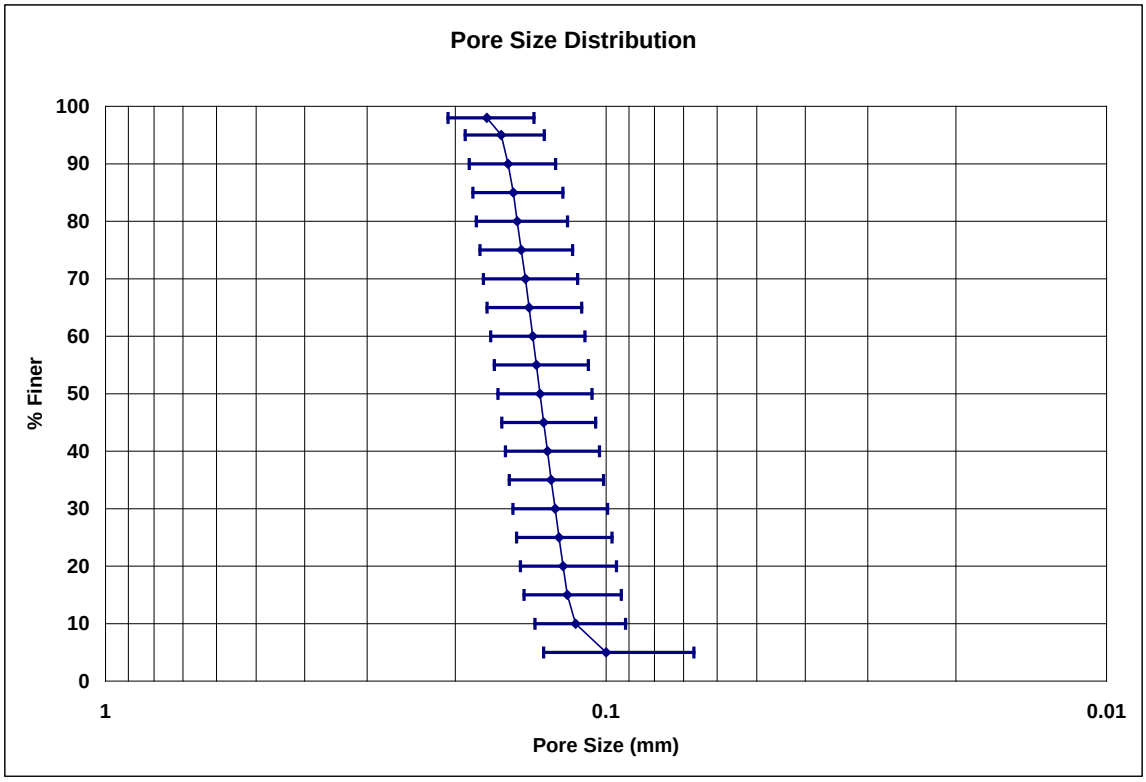

Figure 5.38: Water mean pore size distribution +/- standard deviation with O_{98} outlier removed.

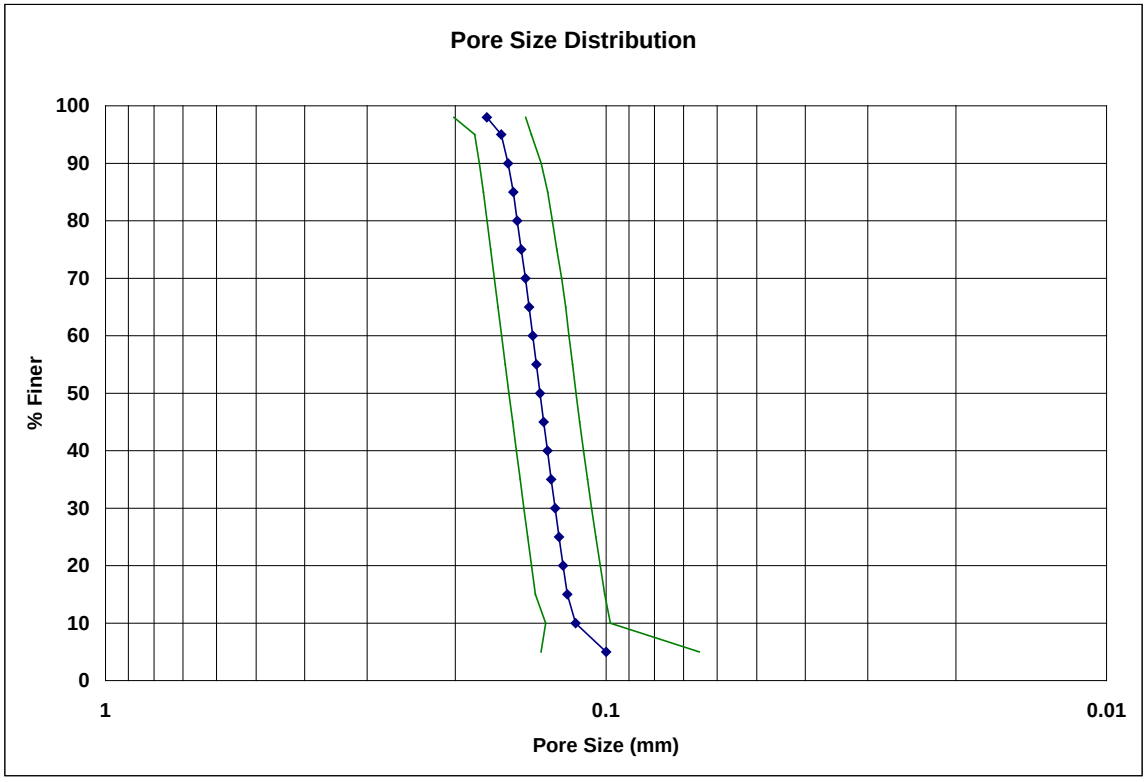

Figure 5.39: Water mean pore size distribution and 95% confidence interval with O_{98} outlier removed.

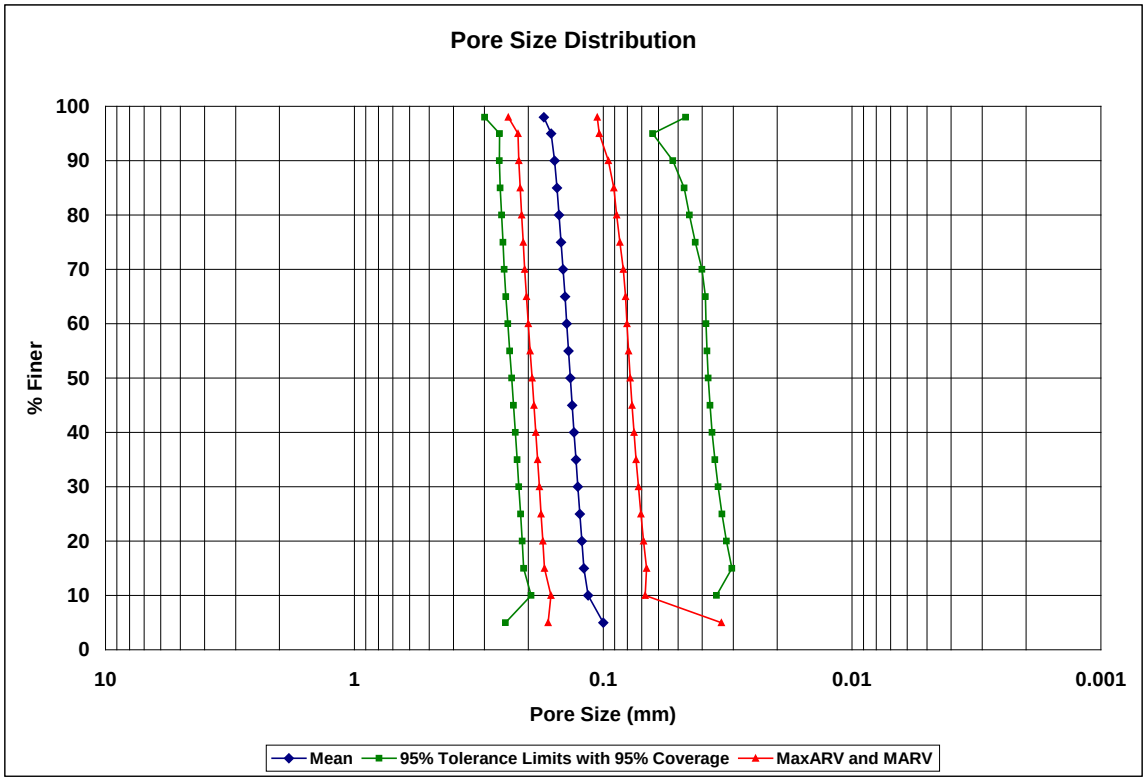

Figure 5.40: Water mean pore size distribution, MaxARV, MARV, and 95% tolerance interval with 95% coverage with O_{98} outlier removed.

5.2.10.2 Porewick Summary Results with Outlier Correction

Table 5.20: O_{98} and O_{95} Porewick results with outliers highlighted.

% Finer	Porewick-1 Pore Size (mm)	Porewick-2 Pore Size (mm)	Porewick-3 Pore Size (mm)	Porewick-4 Pore Size (mm)	Porewick-5 Pore Size (mm)	Porewick-6 Pore Size (mm)	Porewick-7 Pore Size (mm)	Porewick-8 Pore Size (mm)	Porewick-9 Pore Size (mm)	Porewick-10 Pore Size (mm)
98	0.54505	---	---	---	0.18347	0.16269	0.19233	0.21304	0.21666	0.22593
95	0.16527	0.19192	1.02870	0.23171	0.16511	0.15100	0.18328	0.18913	0.19149	0.20678

Table 5.21: O_{98} and O_{95} Porewick statistics with outliers included.

% Finer	Sample Size	Mean Pore Size (mm)	Standard Deviation (mm)	Coefficient of Variation (%)	95% CI of Mean		MaxARV (mm)	MARV (mm)	95% TI with 95% Coverage	
					UCL (mm)	LCL (mm)			UTL (mm)	LTL (mm)
98	7	0.24845	0.13258	53.36	0.37043	0.12648	0.51361	-0.01671	0.78143	-0.28452
95	10	0.27044	0.26740	98.88	0.46297	0.07791	0.80524	-0.26437	1.17693	-0.63606

Table 5.22: O_{98} and O_{95} Porewick statistics with outliers removed.

% Finer	Sample Size	Mean Pore Size (mm)	Standard Deviation (mm)	Coefficient of Variation (%)	95% CI of Mean		MaxARV (mm)	MARV (mm)	95% TI with 95% Coverage	
					UCL (mm)	LCL (mm)			UTL (mm)	LTL (mm)
98	6	0.19902	0.02382	11.97	0.22404	0.17401	0.24667	0.15137	0.30432	0.09372
95	9	0.18619	0.02422	13.01	0.20484	0.16754	0.23464	0.13774	0.27218	0.10019

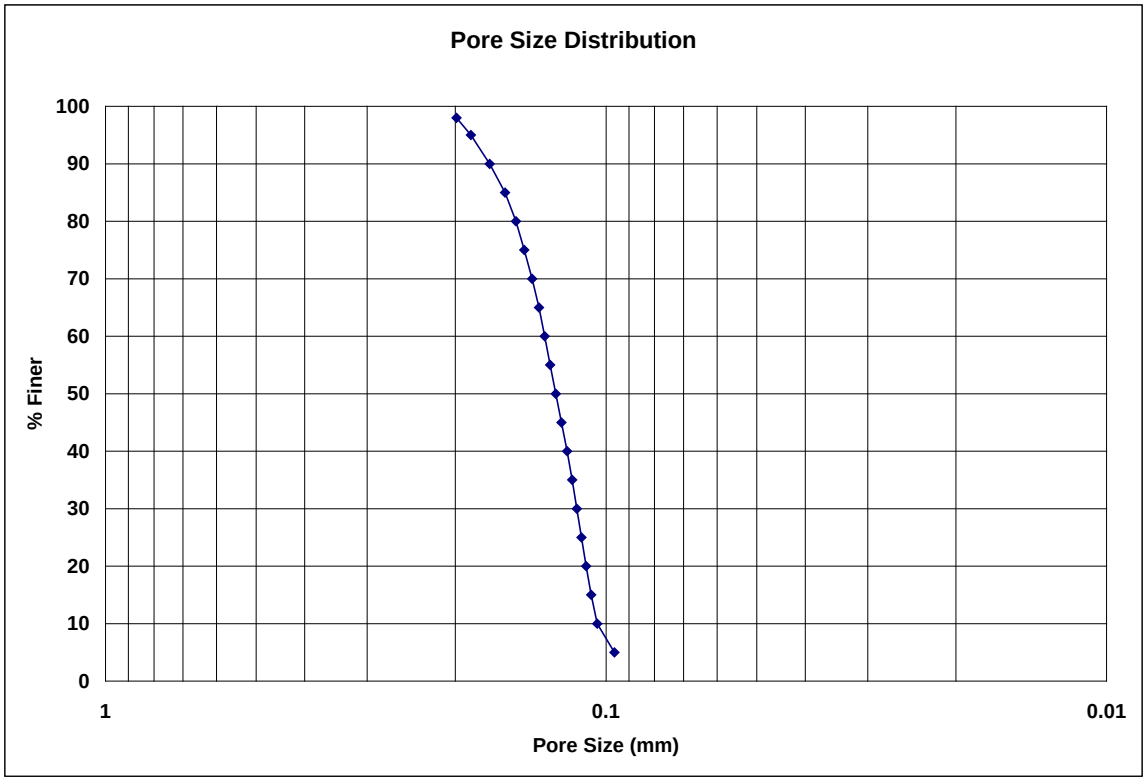

Figure 5.41: Porewick mean pore size distribution with O_{98} and O_{95} outliers removed.

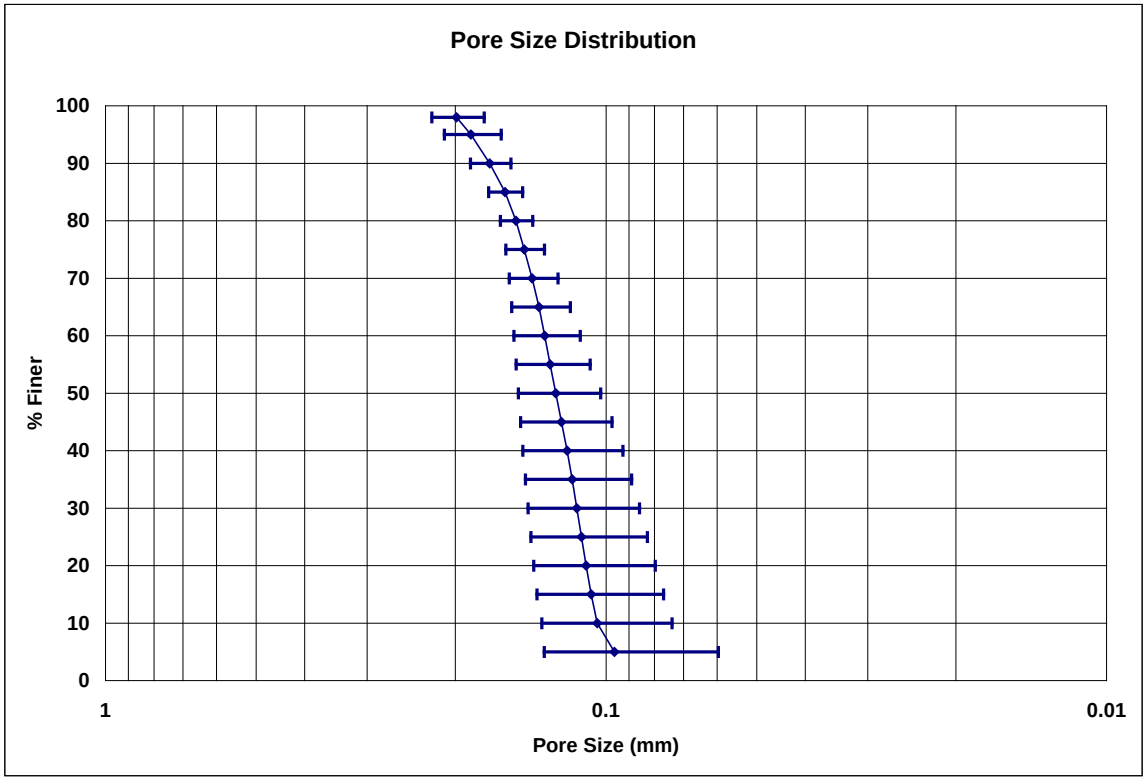

Figure 5.42: Porewick mean pore size distribution +/- standard deviation with O_{98} and O_{95} outliers removed.

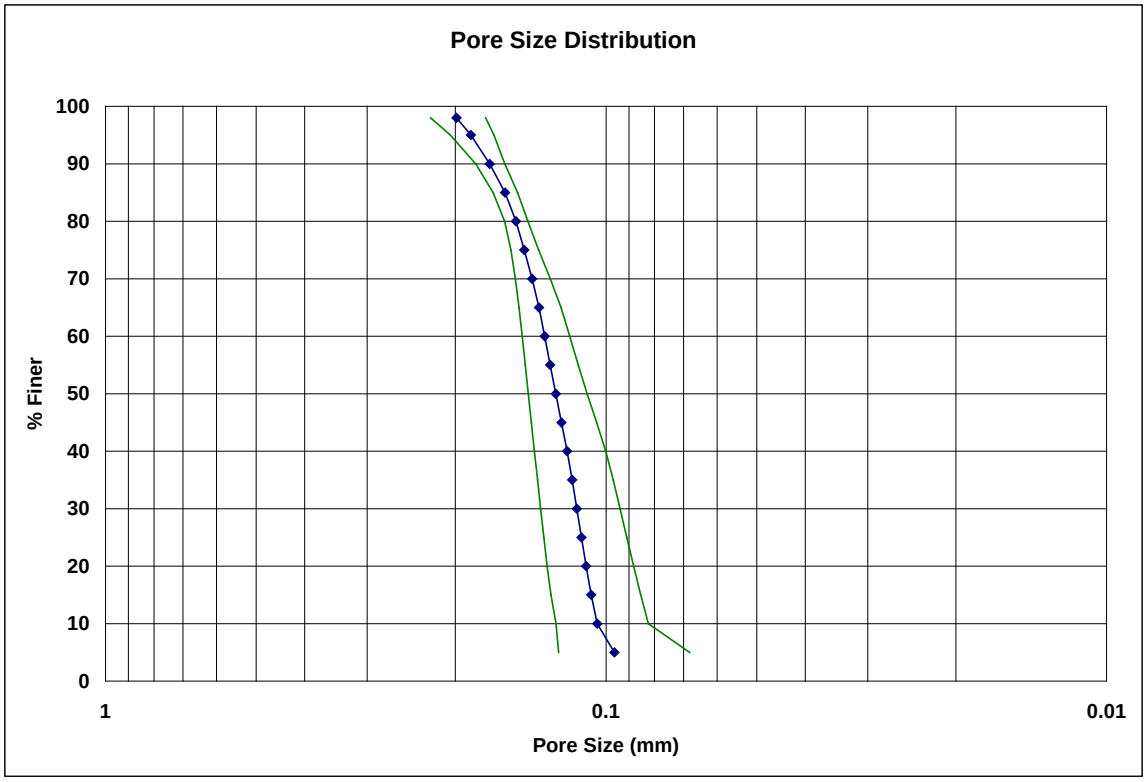

Figure 5.43: Porewick mean pore size distribution and 95% confidence interval with O_{98} and O_{95} outliers removed.

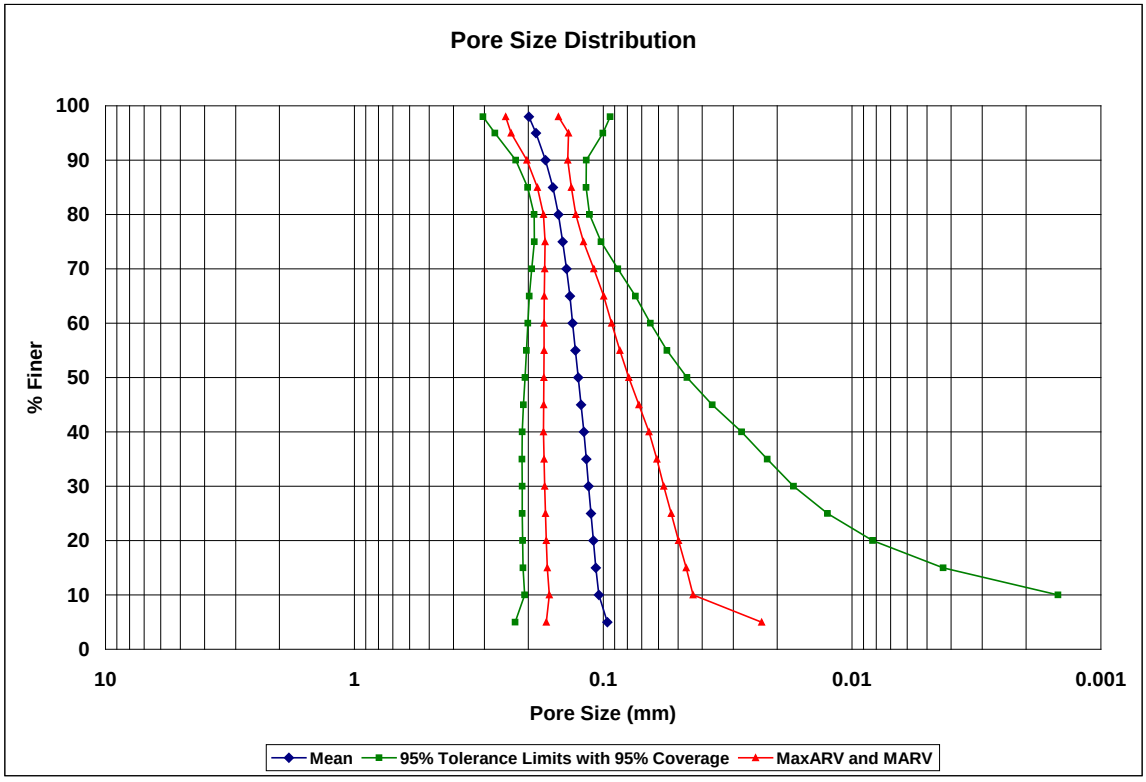

Figure 5.44: Porewick mean pore size distribution showing MaxARV, MARV, and 95% tolerance interval with 95% coverage with O_{98} and O_{95} outliers removed.

5.2.10.3 2-Ethyl Hexanol Summary Results with Outlier Correction

Table 5.23: O_{98} and O_{95} 2-ethyl hexanol results with outlier highlighted.

% Finer	2EH-1 Pore Size (mm)	2EH-2 Pore Size (mm)	2EH-3 Pore Size (mm)	2EH-4 Pore Size (mm)	2EH-5 Pore Size (mm)	2EH-6 Pore Size (mm)	2EH-7 Pore Size (mm)	2EH-8 Pore Size (mm)	2EH-9 Pore Size (mm)	2EH-10 Pore Size (mm)
98	0.97590	0.20485	0.26752	0.28414	0.23710	0.28403	0.20531	0.21820	0.19120	0.20841
95	0.19955	0.17950	0.21908	0.21911	0.21672	0.20085	0.19440	0.19763	0.17727	0.18794

Table 5.24: O_{98} and O_{95} 2-ethyl hexanol statistics with outlier included.

% Finer	Sample Size	Mean Pore Size (mm)	Standard Deviation (mm)	Coefficient of Variation (%)	95% CI of Mean UCL (mm)	95% CI of Mean LCL (mm)	MaxARV (mm)	MARV (mm)	95% TI with 95% Coverage UTL (mm)	95% TI with 95% Coverage LTL (mm)
98	10	0.30767	0.23728	77.12	0.47851	0.13683	0.78222	-0.16689	1.11204	-0.49671
95	10	0.19920	0.01536	7.71	0.21026	0.18815	0.22992	0.16849	0.25127	0.14714

Table 5.25: O_{98} and O_{95} 2-ethyl hexanol results with outlier removed.

% Finer	Sample Size	Mean Pore Size (mm)	Standard Deviation (mm)	Coefficient of Variation (%)	95% CI of Mean UCL (mm)	95% CI of Mean LCL (mm)	MaxARV (mm)	MARV (mm)	95% TI with 95% Coverage UTL (mm)	95% TI with 95% Coverage LTL (mm)
98	9	0.23342	0.03633	15.56	0.26139	0.20545	0.30607	0.16077	0.36237	0.10446
95	10	0.19920	0.01536	7.71	0.21026	0.18815	0.22992	0.16849	0.25127	0.14714

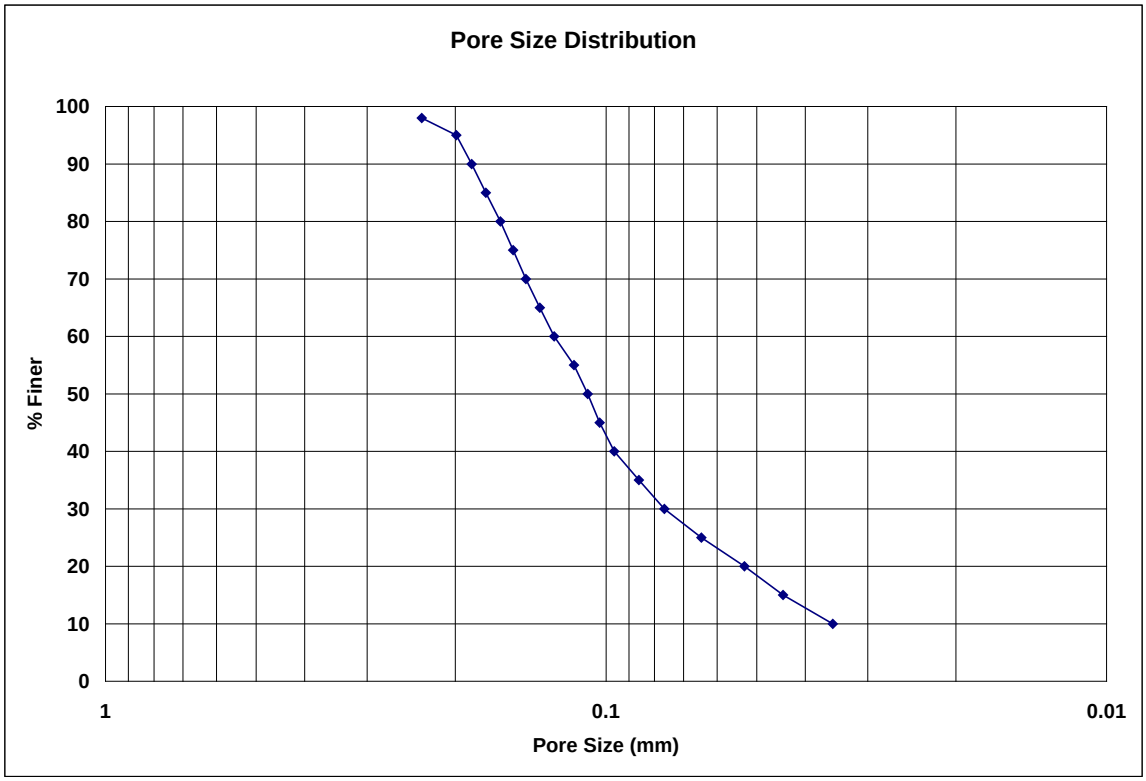

Figure 5.45: 2-ethyl hexanol mean pore size distribution with O_{98} outlier removed.

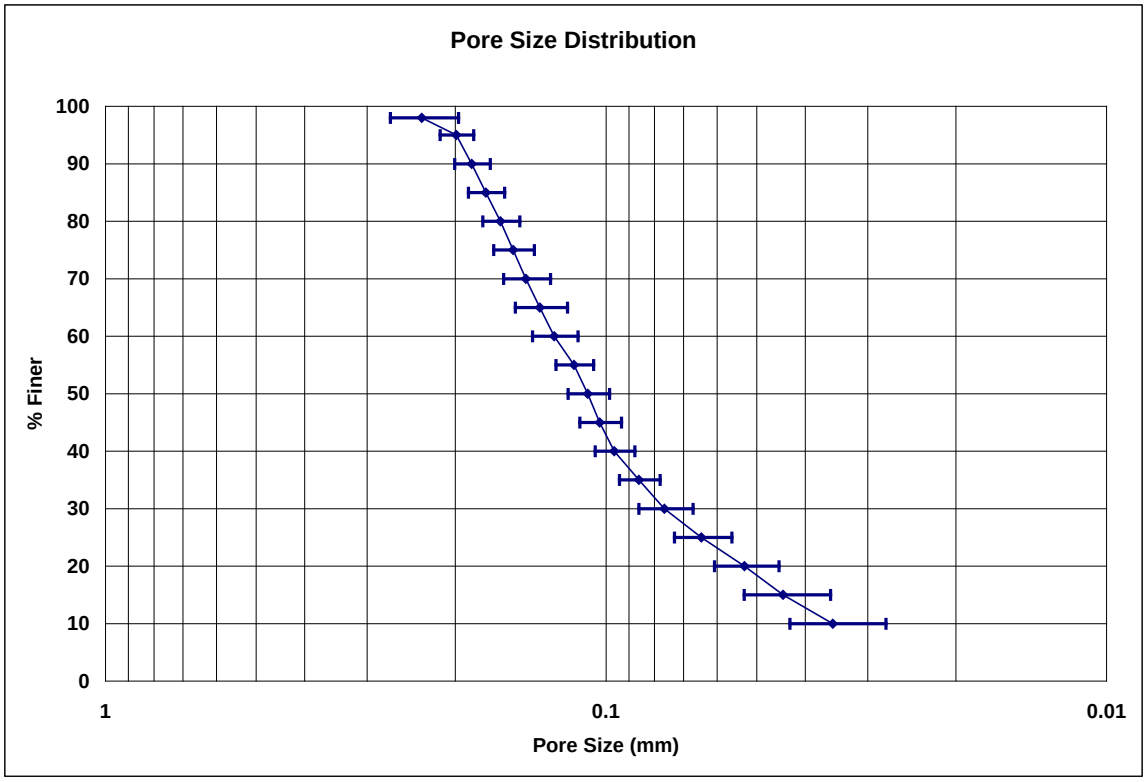

Figure 5.46: 2-ethyl hexanol mean pore size distribution +/- standard deviation with O_{98} outlier removed.

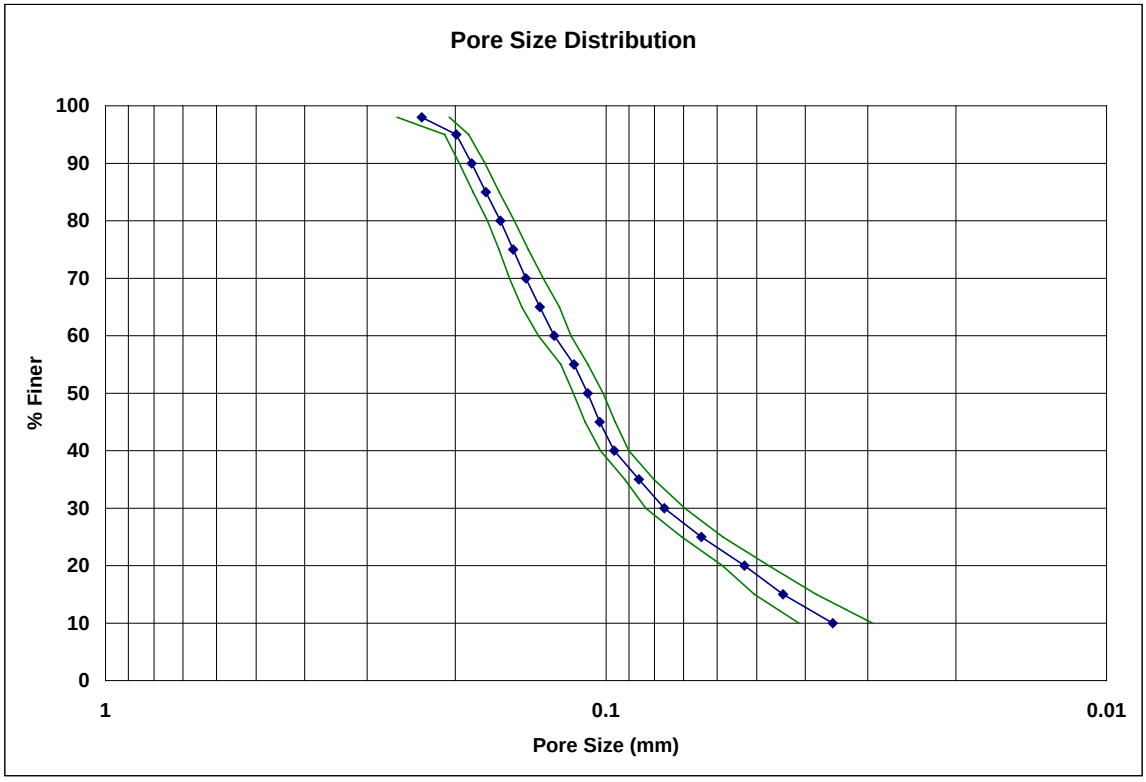

Figure 5.47: 2-ethyl hexanol mean pore size distribution and 95% confidence interval with O_{98} outlier removed.

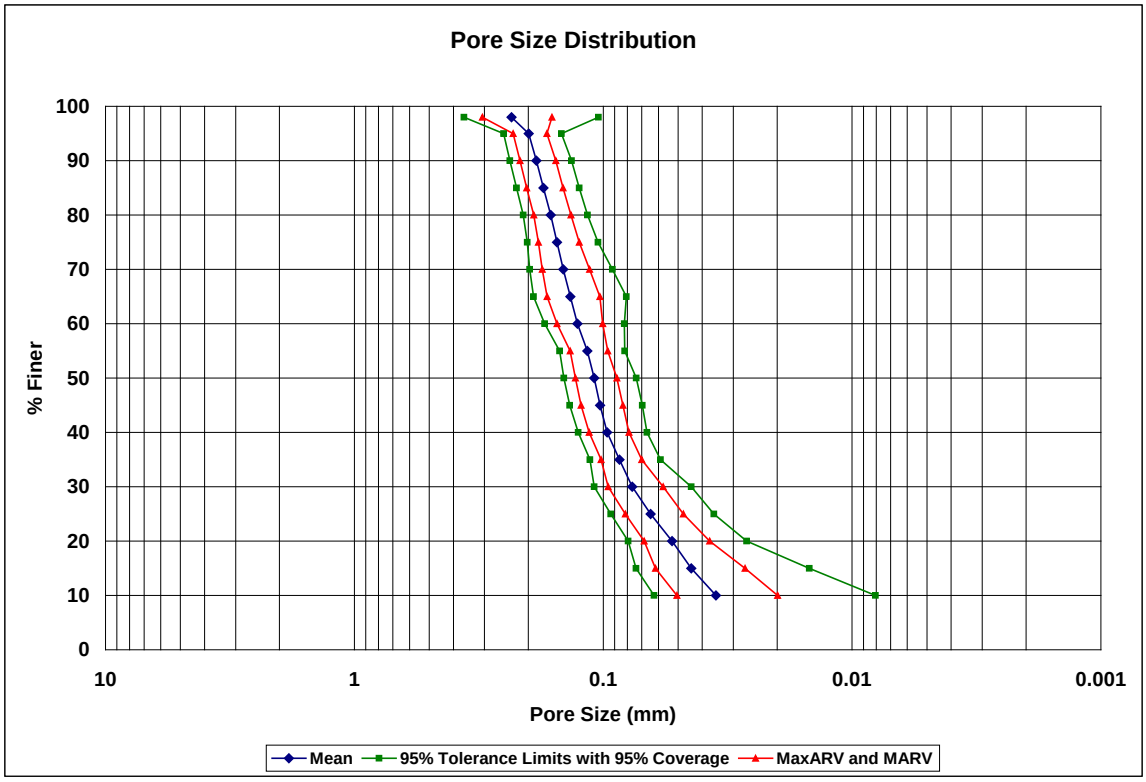

Figure 5.48: 2-ethyl hexanol mean pore size distribution, MaxARV, MARV, and 95% tolerance interval with 95% coverage with O_{98} outlier removed.

5.2.10.4 Drakeol Summary Results with Outlier Correction

Table 5.26: O_{98} and O_{95} Drakeol results with outlier highlighted.

% Finer	Drakeol-1 Pore Size (mm)	Drakeol-2 Pore Size (mm)	Drakeol-3 Pore Size (mm)	Drakeol-4 Pore Size (mm)	Drakeol-5 Pore Size (mm)	Drakeol-6 Pore Size (mm)	Drakeol-7 Pore Size (mm)	Drakeol-8 Pore Size (mm)	Drakeol-9 Pore Size (mm)	Drakeol-10 Pore Size (mm)
98	---	0.22688	---	0.25288	0.24899	0.22870	---	---	0.18981	0.23566
95	0.16504	0.18070	0.17730	0.20070	0.16723	0.19625	0.20427	0.22034	0.16266	0.20937

Table 5.27: O_{98} and O_{95} Drakeol statistics with outlier included.

% Finer	Sample Size	Mean Pore Size (mm)	Standard Deviation (mm)	Coefficient of Variation (%)	95% CI of Mean		MaxARV (mm)	MARV (mm)	95% TI with 95% Coverage	
					UCL (mm)	LCL (mm)			UTL (mm)	LTL (mm)
98	6	0.23048	0.02255	9.78	0.25416	0.20681	0.27557	0.18539	0.33014	0.13083
95	10	0.18839	0.02045	10.86	0.20311	0.17366	0.22929	0.14749	0.25771	0.11906

Table 5.28: O_{98} and O_{95} Drakeol statistics with outlier removed.

% Finer	Sample Size	Mean Pore Size (mm)	Standard Deviation (mm)	Coefficient of Variation (%)	95% CI of Mean		MaxARV (mm)	MARV (mm)	95% TI with 95% Coverage	
					UCL (mm)	LCL (mm)			UTL (mm)	LTL (mm)
98	5	0.23862	0.01179	4.94	0.25324	0.22400	0.26220	0.21504	0.29851	0.17872
95	10	0.18839	0.02045	10.86	0.20311	0.17366	0.22929	0.14749	0.25771	0.11906

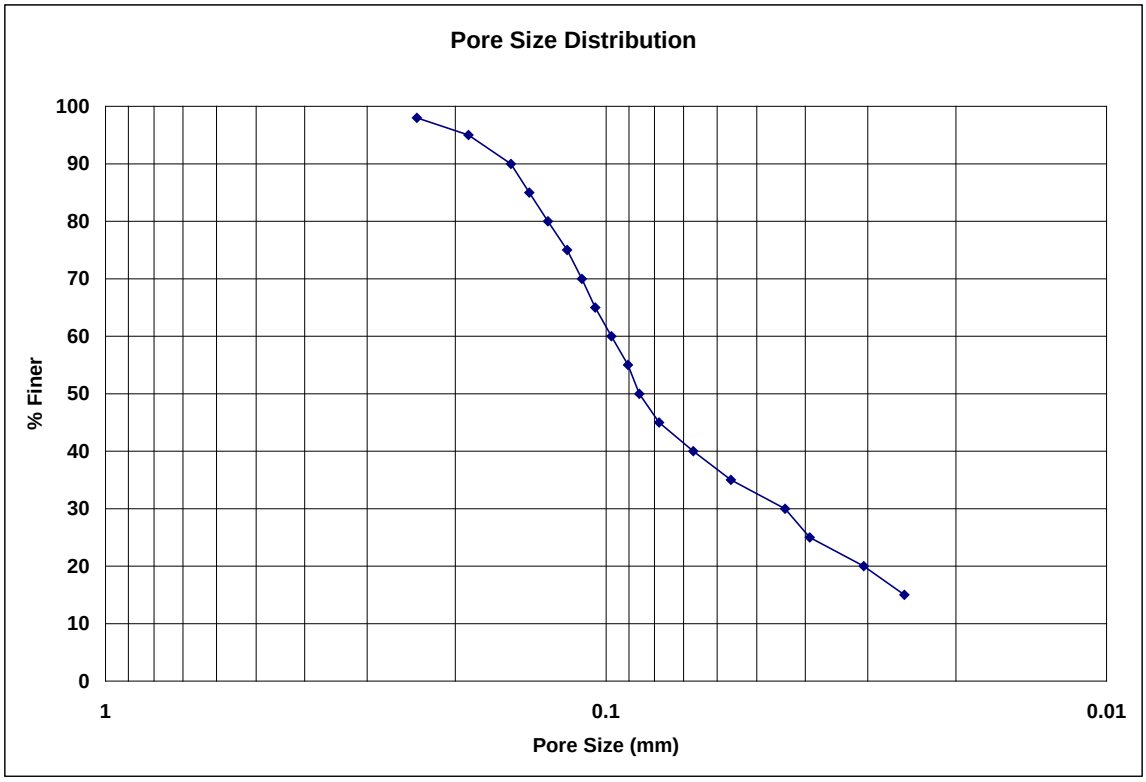

Figure 5.49: Drakeol mean pore size distribution with O_{98} outlier removed.

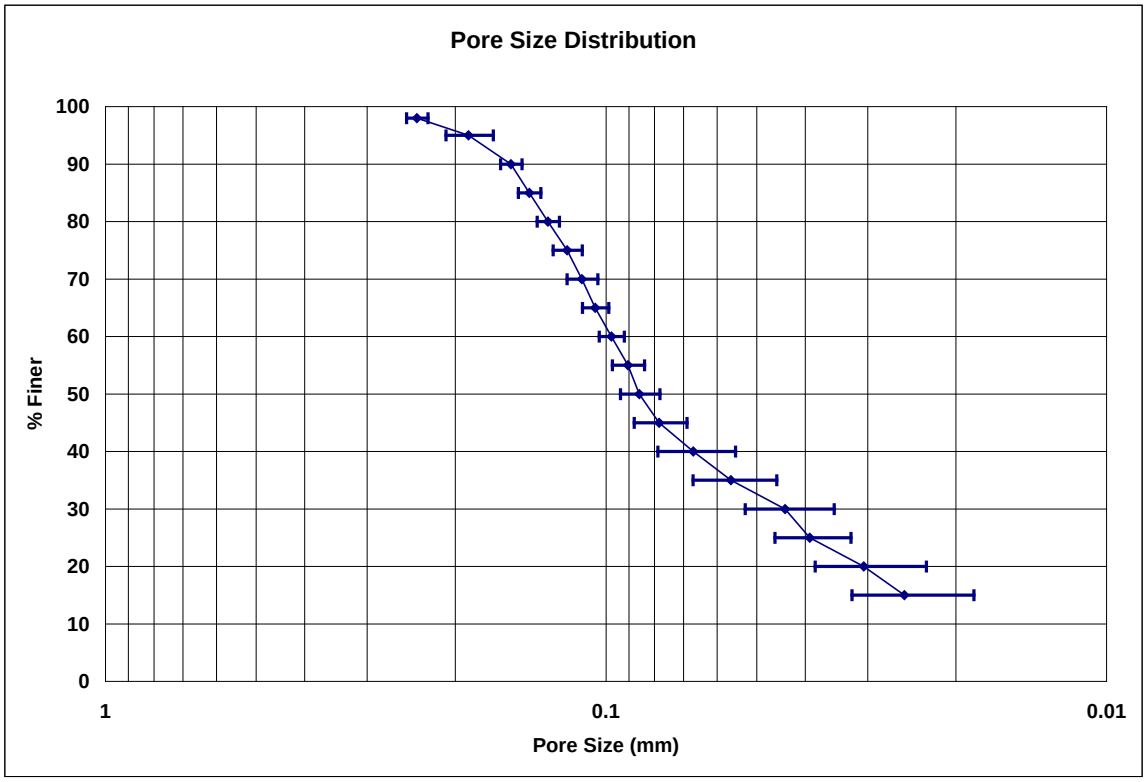

Figure 5.50: Drakeol mean pore size distribution +/- standard deviation with O_{98} outlier removed.

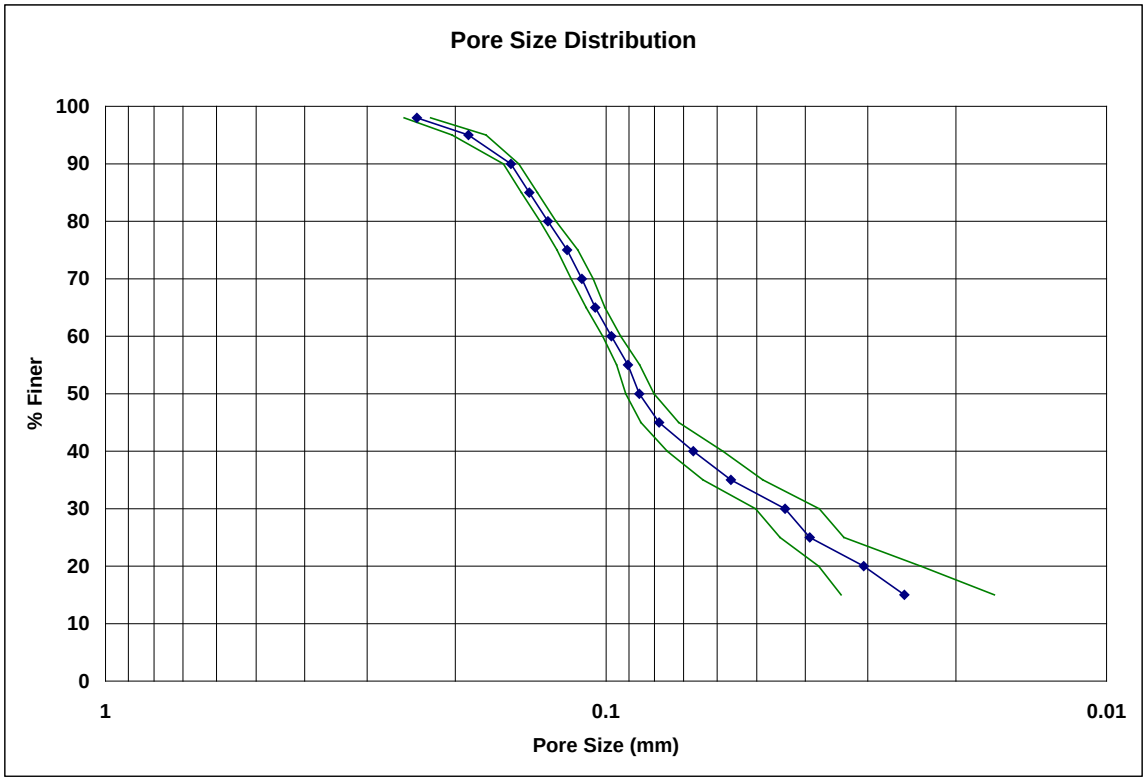

Figure 5.51: Drakeol mean pore size distribution and 95% confidence interval with O_{98} outlier removed.

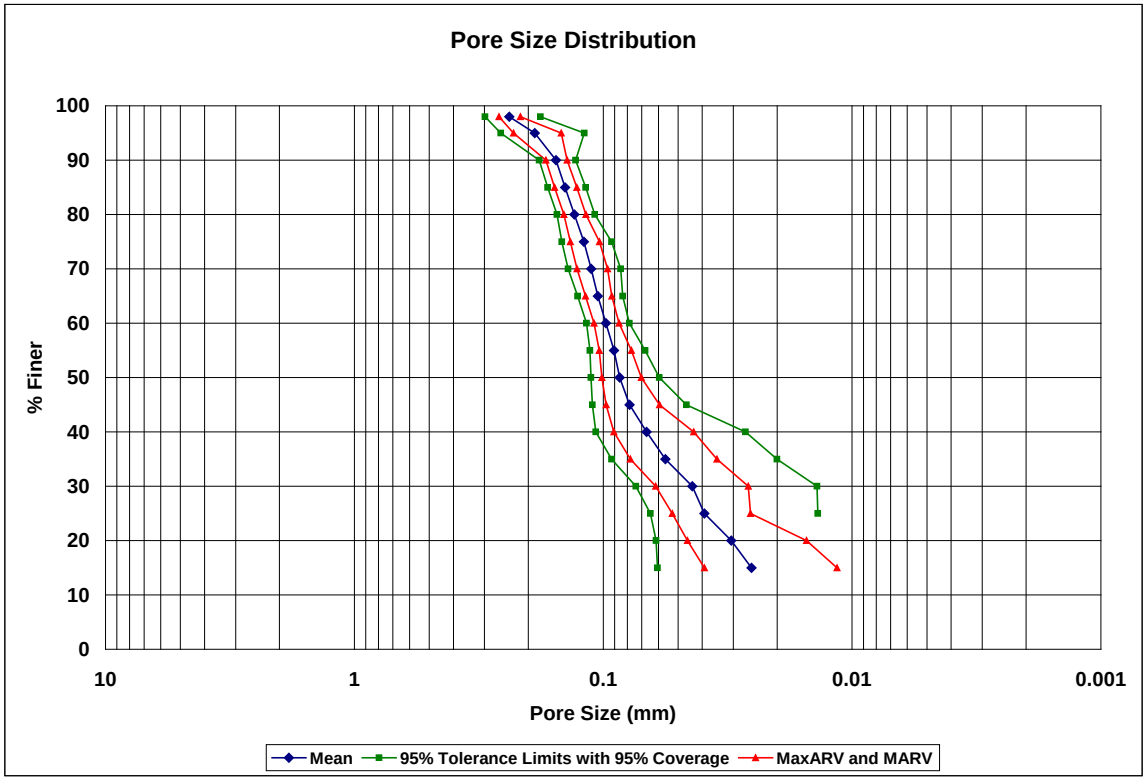

Figure 5.52: Drakeol mean pore size distribution showing MaxARV, MARV, and 95% tolerance interval with 95% coverage with O_{98} outlier removed.

5.2.10.5 Glycerin Summary Results with Outlier Correction

Table 5.29: O_{98} and O_{95} glycerin results with outliers highlighted.

% Finer	Glycerin-1 Pore Size (mm)	Glycerin-2 Pore Size (mm)	Glycerin-3 Pore Size (mm)	Glycerin-4 Pore Size (mm)	Glycerin-5 Pore Size (mm)	Glycerin-6 Pore Size (mm)	Glycerin-7 Pore Size (mm)	Glycerin-8 Pore Size (mm)	Glycerin-9 Pore Size (mm)	Glycerin-10 Pore Size (mm)
98	0.25852	0.21772	0.16920	0.20857	1.12559	0.17732	0.21889	0.17974	0.21463	0.21900
95	0.15098	0.15834	0.14975	0.20338	0.50817	0.15948	0.20956	0.16156	0.18479	0.18414

Table 5.30: O_{98} and O_{95} glycerin statistics with outliers included.

% Finer	Sample Size	Mean Pore Size (mm)	Standard Deviation (mm)	Coefficient of Variation (%)	95% CI of Mean		MaxARV (mm)	MARV (mm)	95% TI with 95% Coverage	
					UCL (mm)	LCL (mm)			UTL (mm)	LTL (mm)
98	10	0.29892	0.29164	97.56	0.50890	0.08894	0.88220	-0.28436	1.28758	-0.68974
95	10	0.20701	0.10793	52.14	0.28473	0.12930	0.42288	-0.00885	0.57291	-0.15888

Table 5.31: O_{98} and O_{95} glycerin statistics with outliers removed.

% Finer	Sample Size	Mean Pore Size (mm)	Standard Deviation (mm)	Coefficient of Variation (%)	95% CI of Mean		MaxARV (mm)	MARV (mm)	95% TI with 95% Coverage	
					UCL (mm)	LCL (mm)			UTL (mm)	LTL (mm)
98	9	0.20707	0.02777	13.41	0.22845	0.18569	0.26260	0.15153	0.30564	0.10849
95	9	0.17355	0.02257	13.00	0.19093	0.15618	0.21868	0.12842	0.25366	0.09345

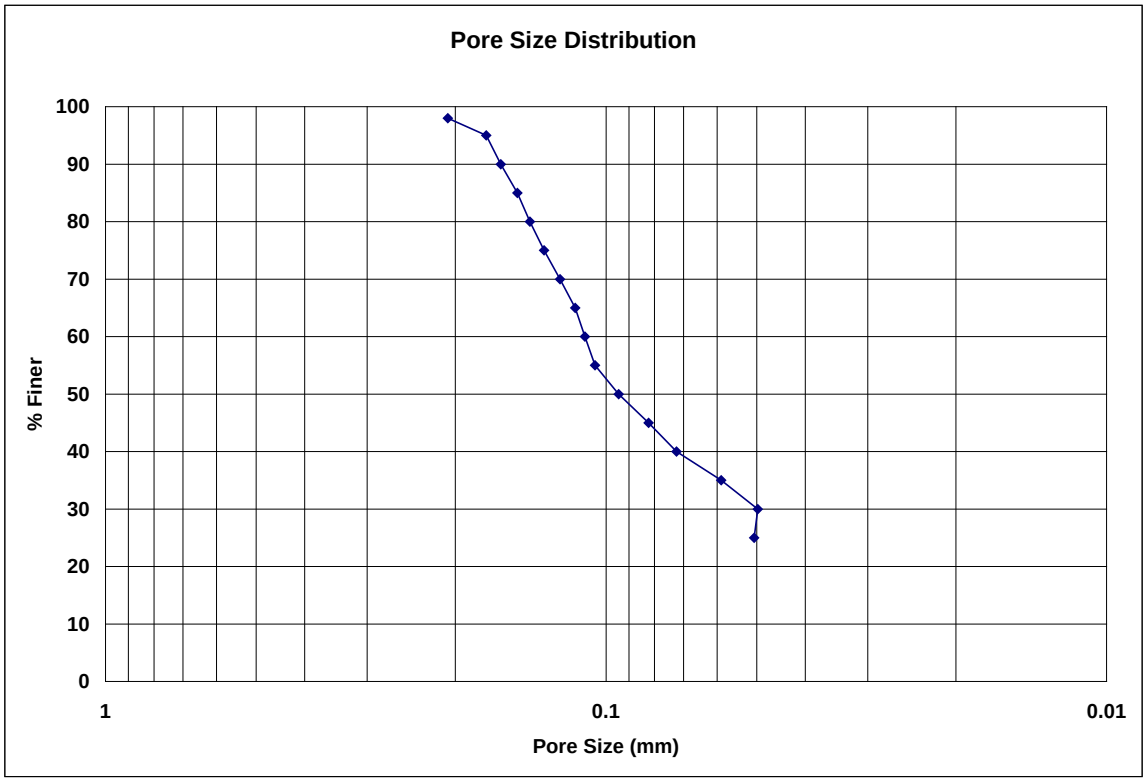

Figure 5.53: Glycerin mean pore size distribution with O_{98} and O_{95} outliers removed.

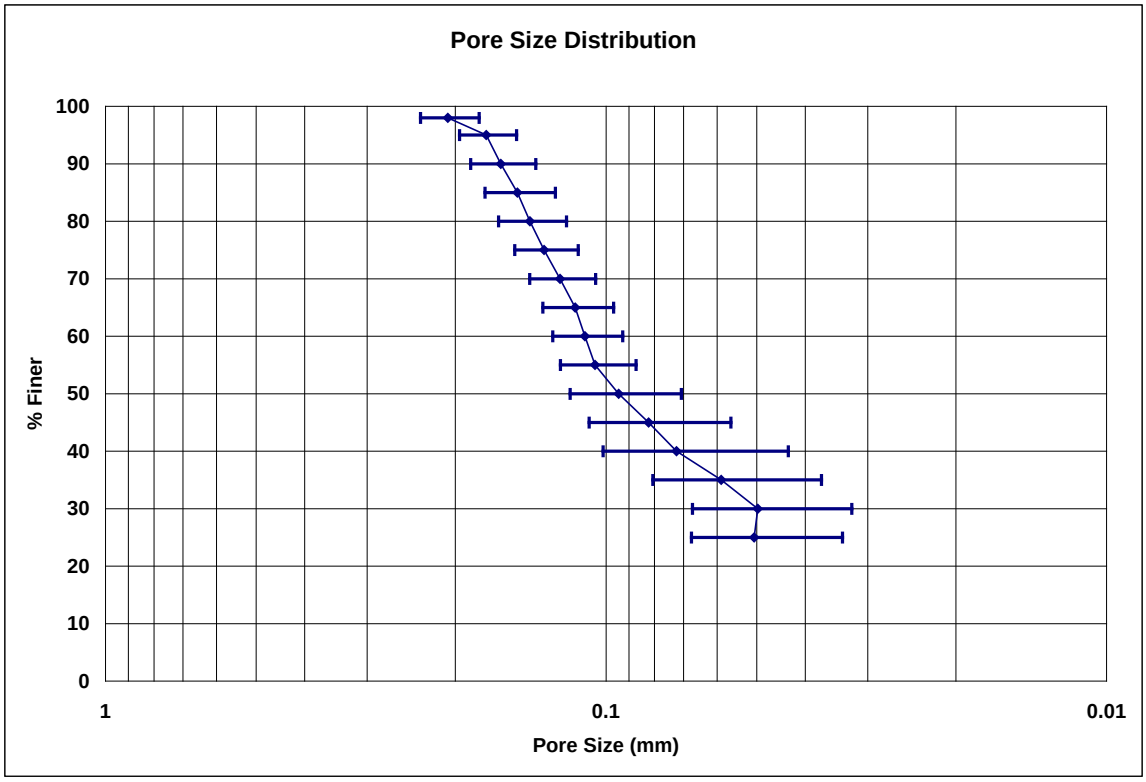

Figure 5.54: Glycerin mean pore size distribution +/- standard deviation with O_{98} and O_{95} outliers removed.

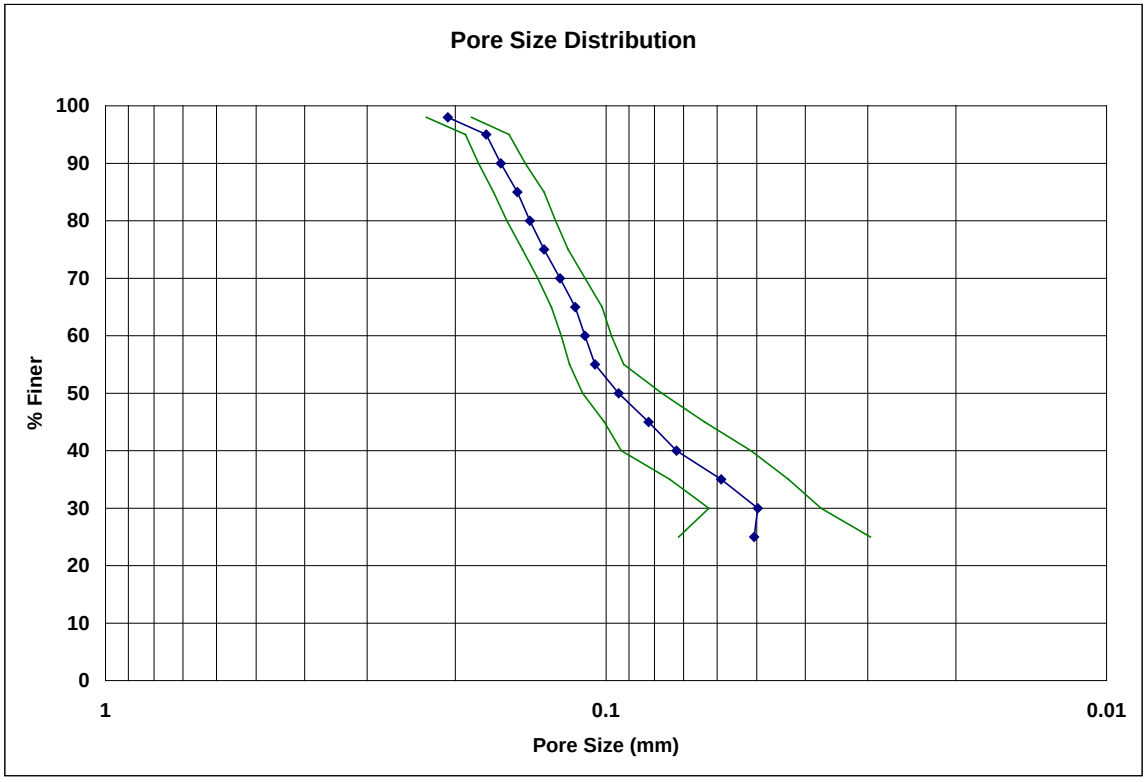

Figure 5.55: Glycerin mean pore size distribution and 95% confidence interval with O_{98} and O_{95} outliers removed.

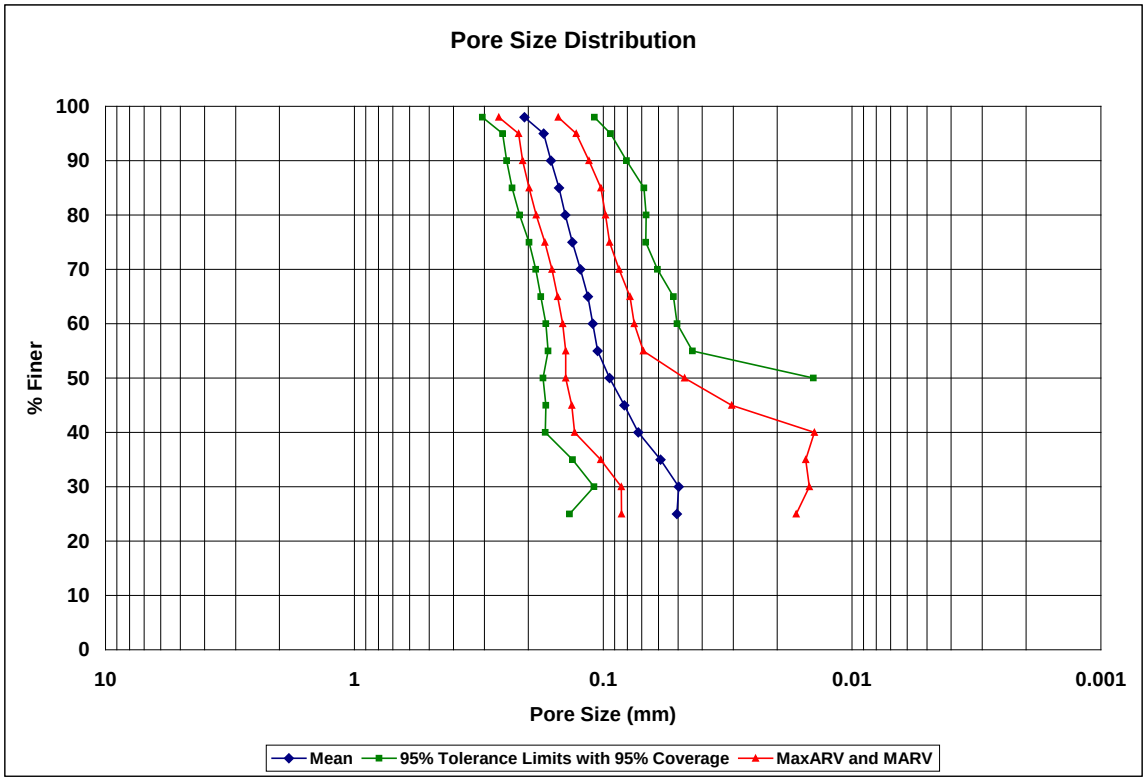

Figure 5.56: Glycerin mean pore size distribution showing MaxARV, MARV, and 95% tolerance interval with 95% coverage with O_{98} and O_{95} outliers removed.

5.2.10.6 Precision of Summary Results with Outlier Correction

Once O_{98} and O_{95} outliers were removed, the coefficients of variation for these opening sizes lowered substantially and were similar to coefficients of variation at other values of percent finer. This can be seen by comparing Figures 5.57 and 5.58, which show coefficients of variation with O_{98} and O_{95} outliers removed, to the original data in Figures 5.34 and 5.35.

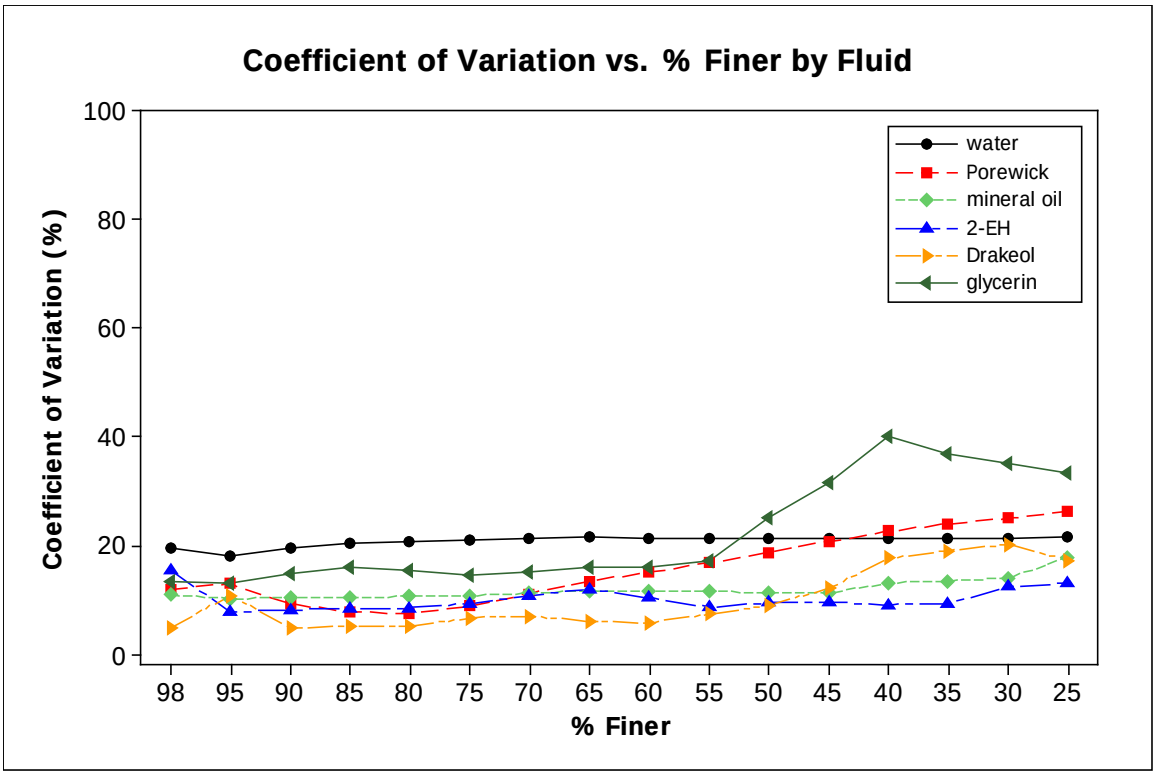

Figure 5.57: Coefficient of variation vs. % finer by fluid, with O_{98} and O_{95} outlier corrections.

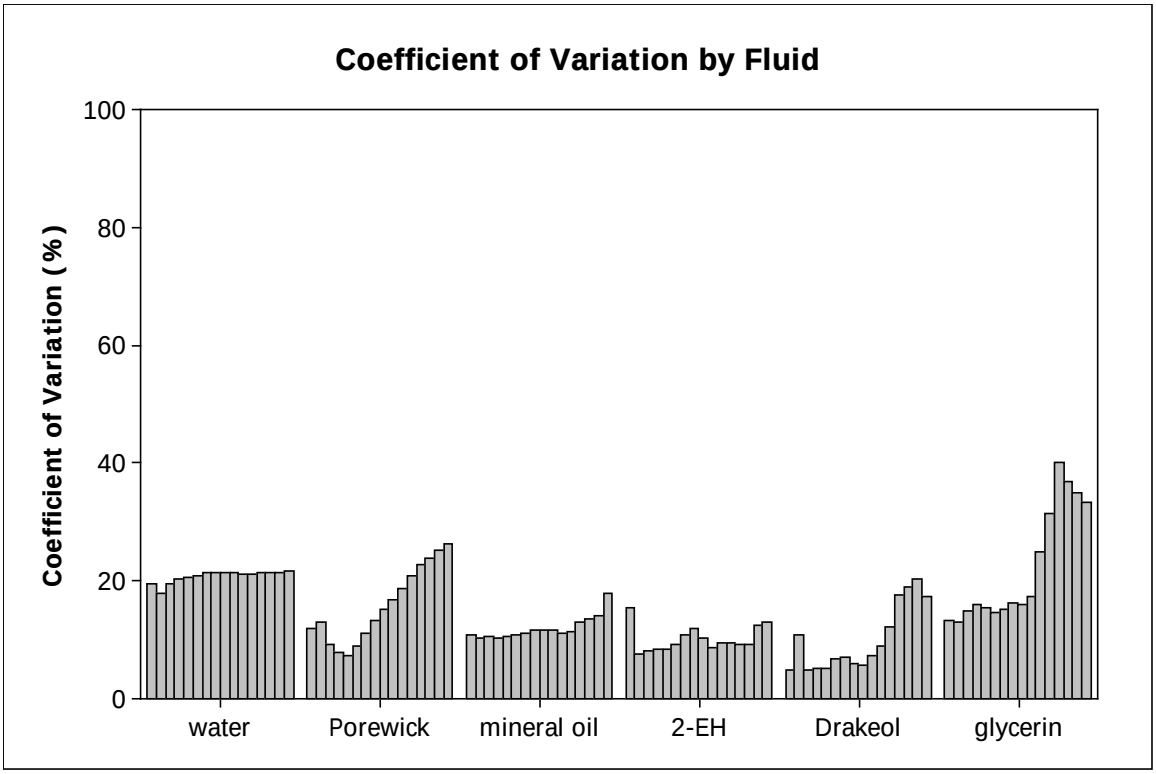

Figure 5.58: Coefficient of variation (decreasing % finer from left to right) grouped by fluid, with O_{98} and O_{95} outlier corrections.

5.2.11 Characteristic Geotextile Pore Size Distributions by Wetting Fluid

The mean pore size distributions for each wetting fluid (with O_{98} and O_{95} statistical outliers removed) are presented in Figure 5.59 as characteristic pore size distributions for the NG-1 nonwoven geotextile. As demonstrated by the 95% confidence intervals of the means in Figures 5.17, 5.39, 5.43, 5.47, 5.51, and 5.55, there is good statistical confidence that these mean pore size distributions, although based on a limited number of observations, are reasonably reflective of the "true" mean pore size distributions that would be calculated if a large number of bubble point tests were repeated using each fluid. Therefore, these characteristic pore size distributions will be used to evaluate the effect of the wetting fluid and other parameters on pore size distributions.

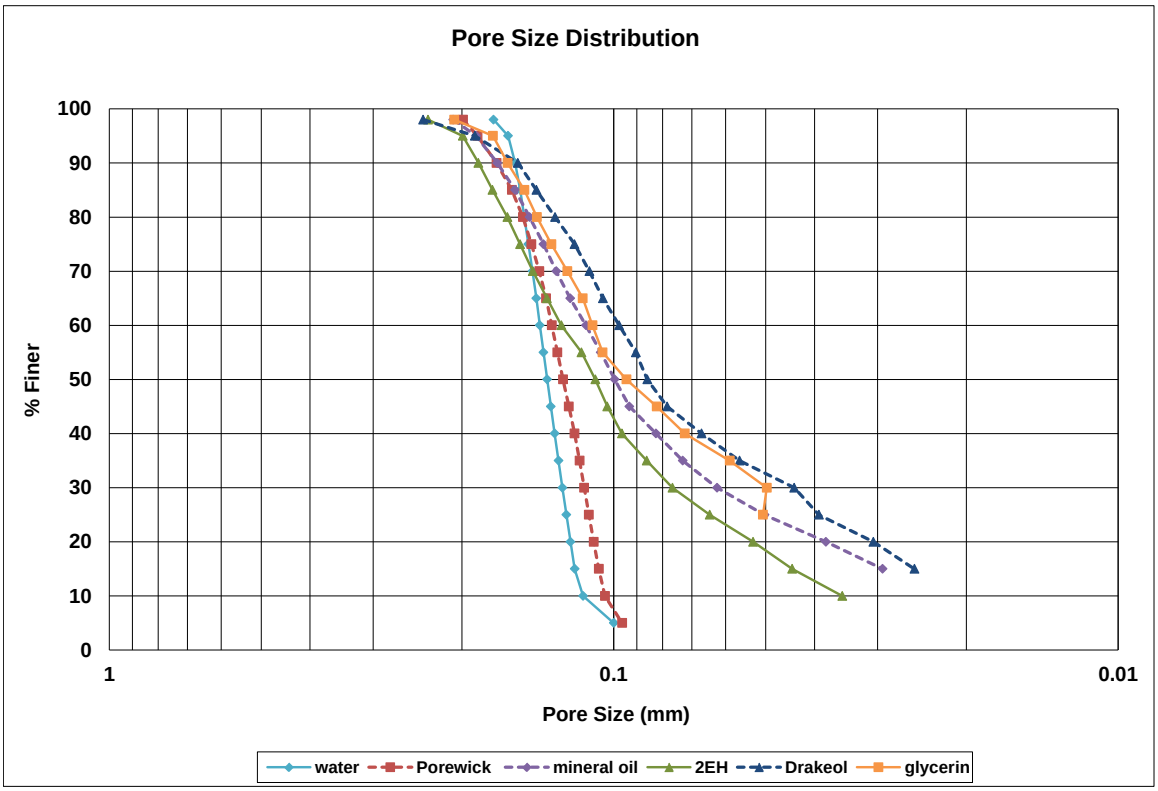

Figure 5.59: Characteristic pore size distributions by wetting fluid for the NG-1 nonwoven geotextile.

5.2.12 Analysis of Variance (ANOVA) for Characteristic Pore Size Distributions

ANOVA tests were used to determine if characteristic (mean) pore sizes determined at selected values of percent finer for different wetting fluids were statistically different. A summary of the ANOVA test results are shown in Table 5.32. ANOVA tests were performed for pore sizes at each of the selected values of percent finer shown in Table 5.32 at levels of significance, α, of 0.01 and 0.05. Graphical summaries of the ANOVA test results are shown in Figures 5.60 and 5.61.

Table 5.32: Analysis of variance results for the NG-1 nonwoven geotextile characteristic pore size distributions shown in Figure 5.59.

% Finer	F ratio	F critical (α = 0.01)	F critical (α = 0.05)
98	5.14	3.51	2.45
95	3.43	3.39	2.39
90	3.19	3.38	2.39
85	2.98	3.38	2.39
80	3.28	3.38	2.39
75	4.47	3.38	2.39
70	5.13	3.38	2.39
65	5.86	3.38	2.39
60	7.57	3.38	2.39
55	9.18	3.38	2.39
50	9.85	3.38	2.39
45	12.12	3.38	2.39
40	14.99	3.38	2.39
35	23.92	3.38	2.39
30	33.45	3.38	2.39
25	32.05	3.43	2.41

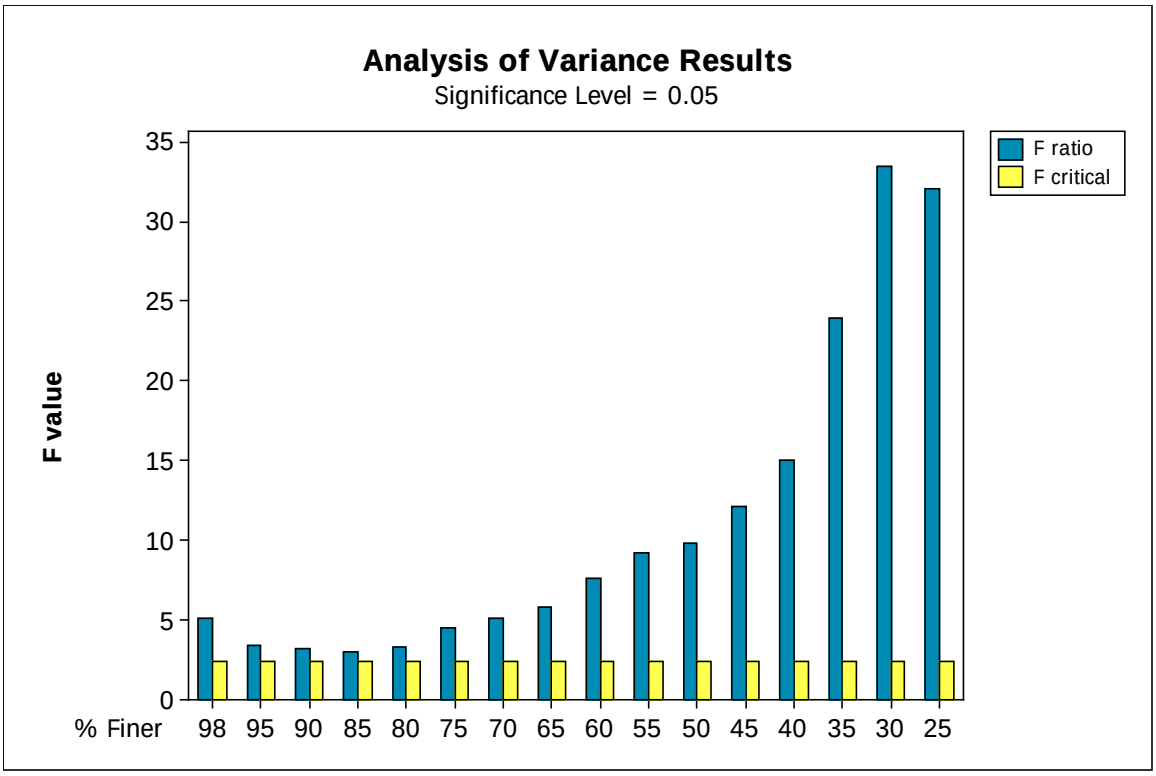

Figure 5.60: ANOVA results (α = 0.05) for the NG-1 nonwoven geotextile characteristic pore size distributions shown in Figure 5.59.

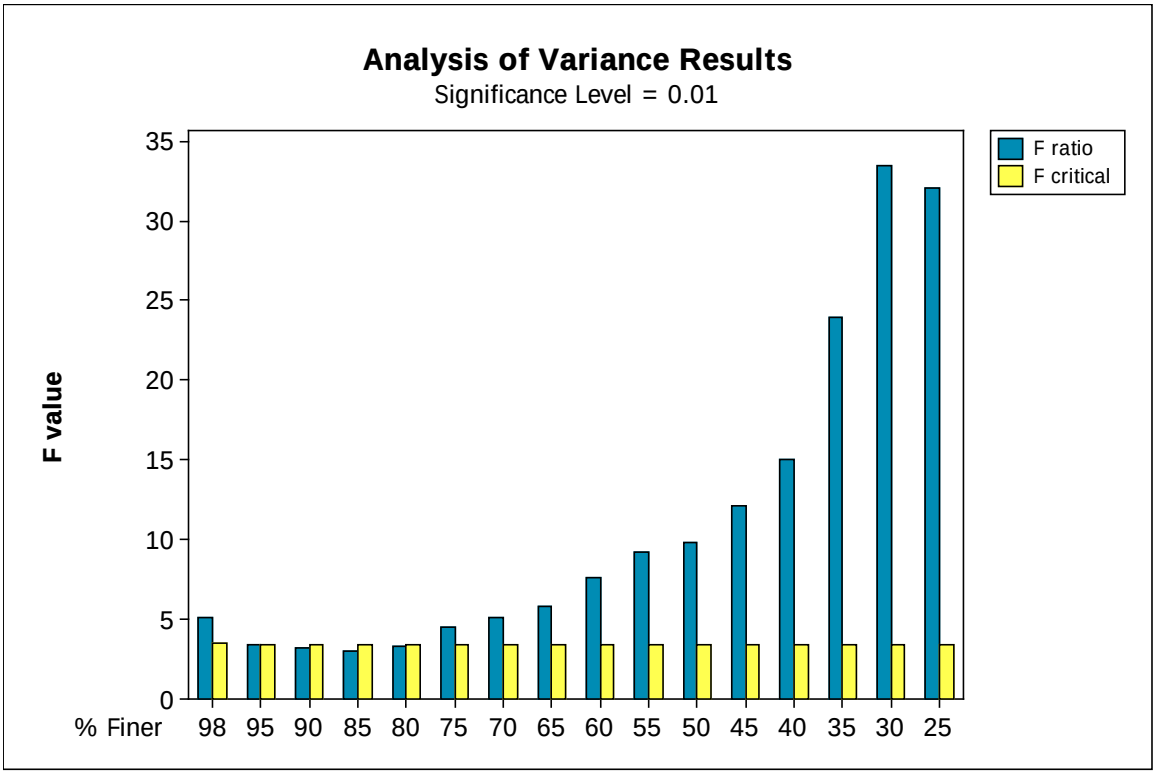

Figure 5.61: ANOVA results (α = 0.01) for the NG-1 nonwoven geotextile characteristic pore size distributions shown in Figure 5.59.

Recall from Section 5.2.2.8 that when the calculated F ratio exceeds the critical F value, the mean pore sizes are significantly different at the given level of significance. When the F ratio is less than F critical, the variation in means can be attributed to the variation within treatments; in this case, variations among individual bubble point tests for each wetting fluid. At the 0.05 significance level, the F ratio exceeds F critical for each value of percent finer, so the mean pore sizes at each percent finer can be considered to be different. At the 0.01 significance level, the F ratio is less than F critical at O_{90}, $O_{85,}$ and O_{80}, so there is not a significant difference between these mean pore sizes. The smallest F ratio was 2.98 at O_{85}, indicating the best agreement among the mean pore sizes at this opening size. The F ratios generally increased for values of percent finer smaller than O_{85}. This indicates that the differences among the mean pore sizes also increased as values of percent finer decreased below O_{85}. At the smaller values of percent finer, the F ratio is much larger than the F critical values, indicating the mean pore sizes in this region are far from being statistically similar.

5.3 Analysis of the Influence of Contact Angle

As discussed in Chapter 3, the contact angle is an important parameter of the Washburn equation for calculating pore size and the contact angle can be dependent on the wetting fluid as well as characteristics of the solid surface. It is tempting to simply assume that the contact angle, θ, is equal to zero, meaning that the wetting fluid "completely wets" the geotextile. This simplifies the Washburn equation by making the factor of $\cos \theta = 1$. However, it will be demonstrated in this section that, although the contact angle may indeed be zero in some cases, making this assumption when it is not

the case can lead to significantly incorrect results. Elton and Hayes (2008b) discussed the measurement of contact angles for the selected wetting fluids by drop analysis and with a Dynamic Contact Angle (DCA) Analyzer. These experiments and results are discussed further in this section. A description of the drop analysis method and the resulting contact angles are presented in Section 5.3.1. A description of the DCA Analyzer method and the resulting contact angles are presented in Section 5.3.2. The influence of contact angles obtained using these different methods on the characteristic geotextile pore size distributions is examined in Section 5.3.3.

5.3.1 Measurement of Contact Angles by Drop Analysis

In an effort to approximate the contact angle of the selected wetting fluids on the polypropylene NG-1 nonwoven geotextile, Dr. David Elton and previous researchers working under his direction at Auburn University measured contact angles of the selected wetting fluids on a sheet of polypropylene using the drop analysis method. Individual drops of the wetting fluids were placed on the polypropylene sheet and magnified photographs of the drop profiles were taken using a microscope / camera apparatus. The contact angle for a drop of fluid on a surface is illustrated in Figures 3.2 and 3.5. The contact angles of the drops in the photographs were then measured using a protractor. The results of these contact angle measurements are in Table 5.33.

Table 5.33: Results of contact angle measurements by drop analysis on a polypropylene sheet. *Source*: Elton and Hayes 2008b.

Contact Angle	Water	Porewick	Mineral oil	2-ethyl-hexanol	Drakeol	Glycerin
θ (deg)	81	18	31.1	24.5	40	92

5.3.2 Measurement of Contact Angles using a Cahn DCA Analyzer

The author used a Cahn Dynamic Contact Angle (DCA) Analyzer model 322 to measure contact angles of the selected wetting fluids on samples of the NG-1 nonwoven geotextile. Rectangular samples of the geotextile were cut using scissors. Latex or nitrile gloves were worn when handling the geotextile samples. Sample dimensions were measured using digital calipers and were typically on the order of 12 mm wide, 20 mm long, and 2.5 mm thick. The DCA Analyzer consists of a highly sensitive balance and a moving stage mechanism, which are controlled via a computer using WinDCA software version 2.04 (Cahn 1996). The DCA Analyzer scale was calibrated in accordance with the Cahn WinDCA manual at the beginning of each day, prior to measuring contact angles. To set up each test, the geotextile sample dimensions and the wetting fluid density and surface tension were entered into the WinDCA software. A beaker containing the wetting fluid was then placed on the stage mechanism and the geotextile sample was suspended from the balance above the stage mechanism using a metal clip. The test was initiated using the WinDCA software, causing the stage to automatically rise to immerse the geotextile sample in the wetting fluid and then lower to remove it at a slow, constant pace throughout the test. During the test, force and position are recorded by the WinDCA software. Once the stage returns to its original position the test is complete and the WinDCA software automatically reports the advancing and receding contact angles. Recall from Section 3.2.3 of this thesis that, for a liquid extrusion method

such as the bubble point method, the receding contact angle is the contact angle of interest.

A summary of the results of the receding contact angle measurements measured with the DCA Analyzer are shown in Table 5.34. For each wetting fluid, the receding contact angle was measured on five samples of the geotextile, and the measurements were averaged. The average receding contact angle for water of 67.53° is similar to the value of 54° reported by Miller and Young (1975) for water and polypropylene textile fibers, and to the results of Henry and Patton (1998) for water on nonwoven continuous filament polypropylene geotextile fibers. Porewick, which is generally considered to have a contact angle of zero due to its low surface tension (Bhatia and Smith 1995), displayed a receding contact angle of zero as expected.

Table 5.34: Receding contact angles of fluids on NG-1 nonwoven geotextile samples, measured with the DCA Analyzer. *Sources*: Elton and Hayes 2007 and 2008b.

parameter	water	Porewick	mineral oil	2-ethyl hexanol	Drakeol	glycerin
Average (of five samples) θ (deg)	67.53	0.00	0.00	0.00	0.00	34.51
Standard Deviation	5.57	0.00	0.00	0.00	0.00	26.15

5.3.3 Influence on Geotextile Characteristic Pore Size Distributions

The characteristic pore size distributions presented in Figure 5.59 were used to demonstrate the influence of using contact angles derived by 1) assuming all contact

angles to be zero, 2) the results of drop analysis as described in Section 5.3.1, and 3) the results of DCA Analyzer testing as described in Section 5.3.2. Characteristic pore size distributions using contact angles of zero for each wetting fluid are shown in Figure 5.62. Characteristic pore size distributions using contact angles determined by drop analysis are shown in Figure 5.63. Note that the drop analysis contact angle for glycerin of 92° is a non-wetting contact angle and therefore the pore size distribution cannot be plotted because it results in a negative value for pore size. Characteristic pore size distributions using contact angles determined from DCA Analyzer testing were shown in Figure 5.59 and are presented again here for convenience as Figure 5.64.

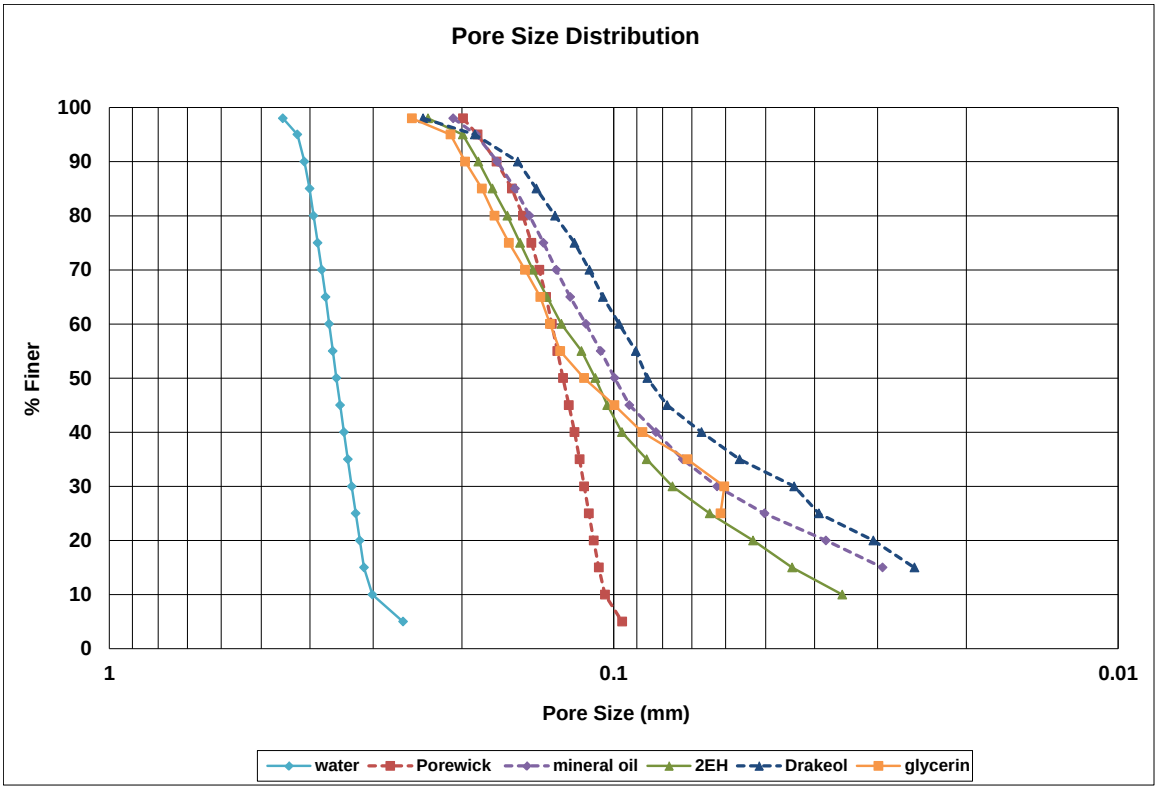

Figure 5.62: Characteristic pore size distributions, with the contact angle set to zero for all wetting fluids.

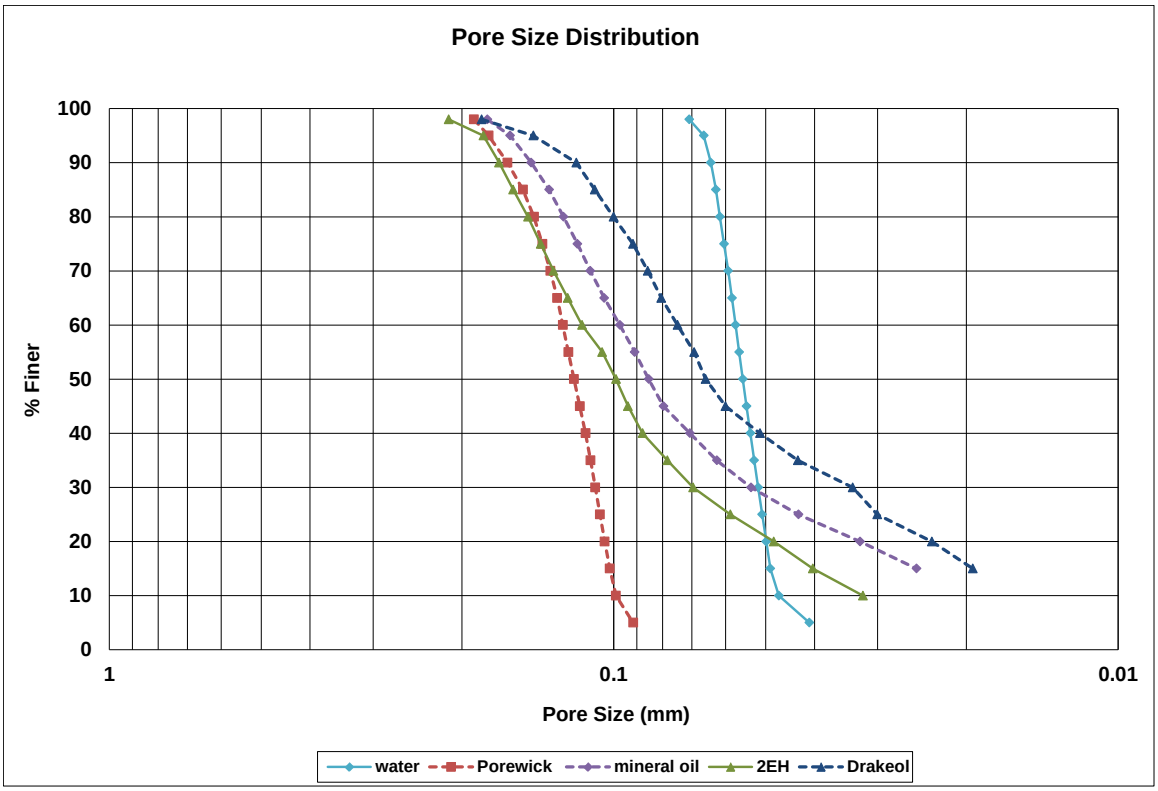

Figure 5.63: Characteristic pore size distributions, using contact angles determined by drop analysis, as listed in Table 5.33 (glycerin data could not be plotted).

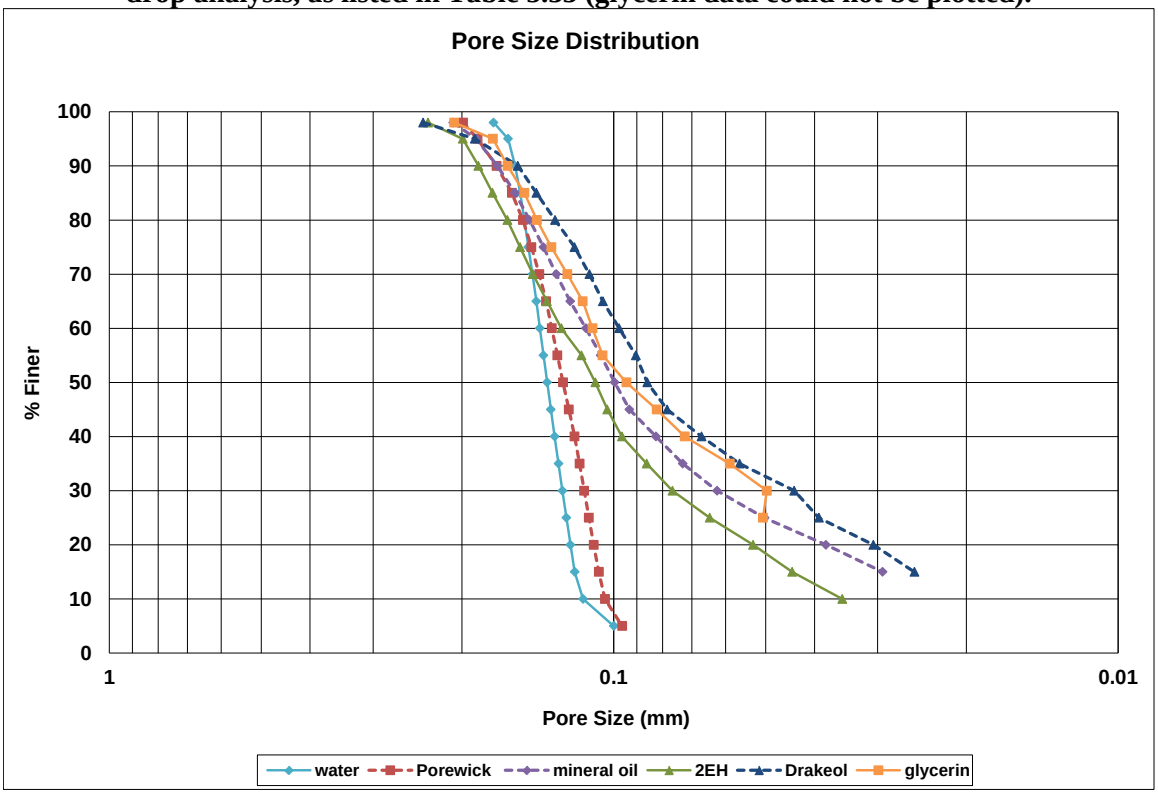

Figure 5.64: Characteristic pore size distributions, using contact angles determined with the DCA Analyzer, as listed in Table 5.34.

It is clear from comparison of Figures 5.62 – 5.64 that the contact angles obtained with the DCA Analyzer yield the best agreement among the characteristic pore size distributions. This indicates that the contact angles determined using the DCA Analyzer are more accurate than those determined using the drop analysis method. Reasons for the better accuracy of the DCA Analyzer contact angles include the fact that *receding* contact angles were measured and the measurements were performed on samples of the actual geotextile as opposed to a sheet of polypropylene. The DCA Analyzer method also employed an automated process using highly sensitive equipment, arguably reducing the chance for human error. It is interesting that a non-wetting contact angle of 92° was obtained for glycerin on polypropylene using the drop analysis method. This contact angle is not possible for glycerin on the geotextile sample, because glycerin exhibits wicking or spontaneous entering of the geotextile and is held by capillarity, meaning that glycerin exhibits wetting behavior and the contact angle must be less than 90°. If the contact angle of glycerin on the geotextile sample was actually 92°, an applied pressure would be necessary to force glycerin into the pores.

It is also interesting to note that, in some cases, it may be valid to use a contact angle of zero. Of the six wetting fluids tested, four of the fluids (Porewick, mineral oil, 2-ethyl hexanol, and Drakeol) were found to have receding contact angles of zero using the DCA Analyzer. The characteristic pore size distributions using these contact angles in Figures 5.62 and 5.64 show good agreement. Knowing that a particular wetting fluid will have a receding contact angle of zero on a geotextile is a beneficial attribute, as the $\cos(\theta)$ term of the Washburn equation becomes one and the need for substantial testing may be reduced. However, as discussed in Section 3.3, it is important to verify the

contact angle of fluids on a particular solid since characteristics of the solid surface influence the contact angle.

5.4 Analysis of the Influence of the Capillary Constant

5.4.1 Influence on Geotextile Characteristic Pore Size Distributions

The influence of the capillary constant on the characteristic pore size distributions determined in Section 5.2.11 is discussed in this section. These characteristic pore size distributions were calculated in accordance with ASTM D6767-11, which recommends using a constant, C, of 2860 mm/m. Recall from Section 2.4.2.2.2 that the constant, C, accounts for a factor of four, a unit conversion from meters to millimeters (1000 mm/m), and the capillary constant, B. The ASTM recommended constant, C, of 2860 mm/m assumes a capillary constant, B, of 0.715. If the capillary constant is set to one, the constant, C, becomes 4000. Figure 5.65 shows the characteristic pore size distributions using a capillary constant, B, of 0.715 and the manufacturer-reported AOS (0.3 mm) of the geotextile. Figure 5.66 shows the same characteristic pore size distributions using a capillary constant of one, along with the AOS of 0.3 mm. As demonstrated in Figures 5.65 and 5.66, changing the capillary constant changes the position of the pore size distributions along the x-axis (i.e., pore sizes) by a constant factor. The shapes of the pore size distribution curves are not affected. Additionally, the O_{95} values of the characteristic pore size distributions determined using a capillary constant of one agree better with the manufacturer-provided AOS than those using the ASTM-recommended value of 0.715. It should be noted that the manufacturer-provided AOS is not necessarily the "correct" value for O_{95}. As discussed in Chapter 2, there are problems and

shortcomings associated with the AOS that have the potential to affect the measured pore size. Nevertheless, the manufacturer-provided AOS is a convenient benchmark for comparison purposes, since no "correct" measurement of pore size is known for a geotextile. The difference between the O_{95} and AOS values can be quantified using the % difference (Equation 5.15), as shown in Table 5.35. A distinction is made here between the % difference and the % error. The % difference is used to compare two experimental quantities, whereas the % error is used to compare an experimental quantity to a "correct" theoretical quantity (Wenning 2012). The % difference is calculated as (Wenning 2012):

$$\%\ \textit{difference} = \frac{\left|E_1 - E_2\right|}{\frac{1}{2}\left(E_1 + E_2\right)} \times 100 \qquad \text{(Equation 5.15)}$$

where:

E_1 = experimental quantity one

E_2 = experimental quantity two

Table 5.35 shows lower values of % difference for all fluids when the capillary constant is set equal to one, indicating better agreement between the bubble point O_{95} values and the manufacturer-provided AOS.

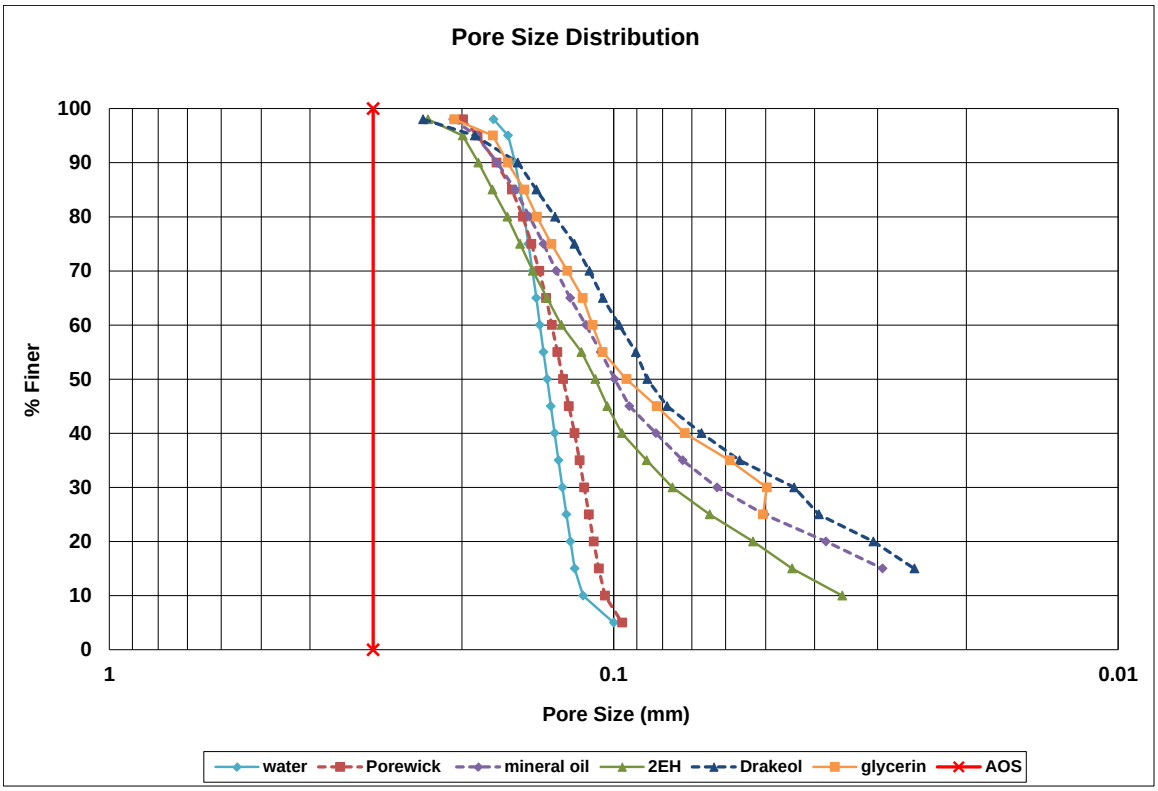

Figure 5.65: Characteristic pore size distributions and the manufacturer-reported AOS, with B = 0.715.

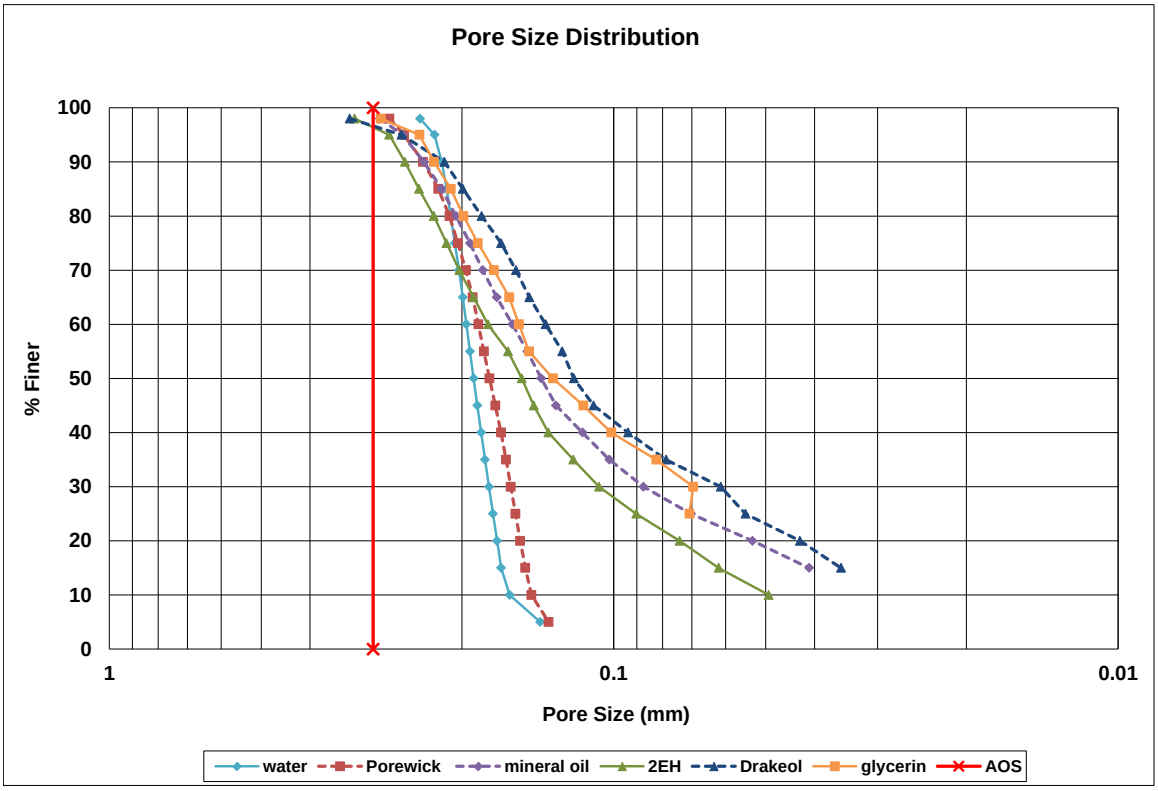

Figure 5.66: Characteristic pore size distributions and the manufacturer-reported AOS, with B = 1.

Table 5.35: Values of O95 with B = 0.715 and B = 1, AOS, and percent differences for characteristic pore size distributions.

Fluid	O95 (mm)		AOS (mm)	% Difference	
	B=0.715	B=1		O95(B=0.715), AOS	O95(B=1), AOS
water	0.1620	0.2265	0.3	59.75	27.90
Porewick	0.1862	0.2604	0.3	46.82	14.13
mineral oil	0.1874	0.2621	0.3	46.20	13.48
2EH	0.1992	0.2786	0.3	40.38	7.39
Drakeol	0.1884	0.2635	0.3	45.71	12.96
glycerin	0.1736	0.2427	0.3	53.40	21.10

5.4.2 Influence on a Typical Pore Size Distribution of a No. 100 Sieve Screen

The influence of the capillary constant on a typical pore size distribution of a No. 100 sieve screen is discussed in this section. Bubble point tests were performed on metal screens of known opening size to assess the accuracy of the test results. A typical pore size distribution for a No. 100 sieve screen determined using mineral oil is shown in Figure 5.67. Figure 5.68 shows the typical pore size distribution using both values of B = 0.715 and B = 1. As with the characteristic geotextile pore size distributions, the larger capillary constant value of one results in a shift of the pore size distribution to the left on the graph. However, unlike the geotextile characteristic pore size distributions, where the capillary constant of one yields better agreement with the reference pore size (the manufacturer-provided AOS), the typical pore size distribution using the capillary constant of 0.715 results in better agreement with the reference pore size; in this case, the theoretical opening size of the No. 100 sieve screen of 0.15 mm. This effect is shown in Figure 5.68 and Table 5.36. Since the theoretical opening size of the No. 100 sieve screen is the "correct" value for the pore size, the % error (Equation 5.16) is used to quantify the difference in the measured and theoretical values.

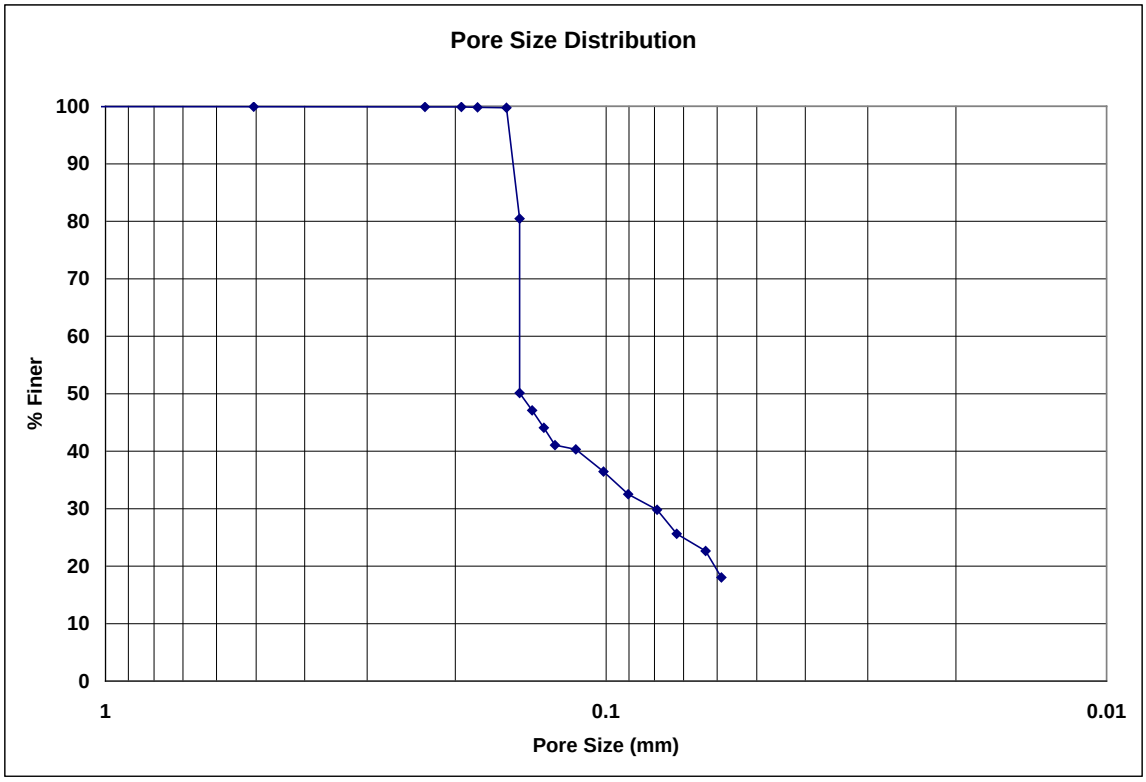

Figure 5.67: A typical pore size distribution for a No. 100 sieve screen determined using mineral oil.

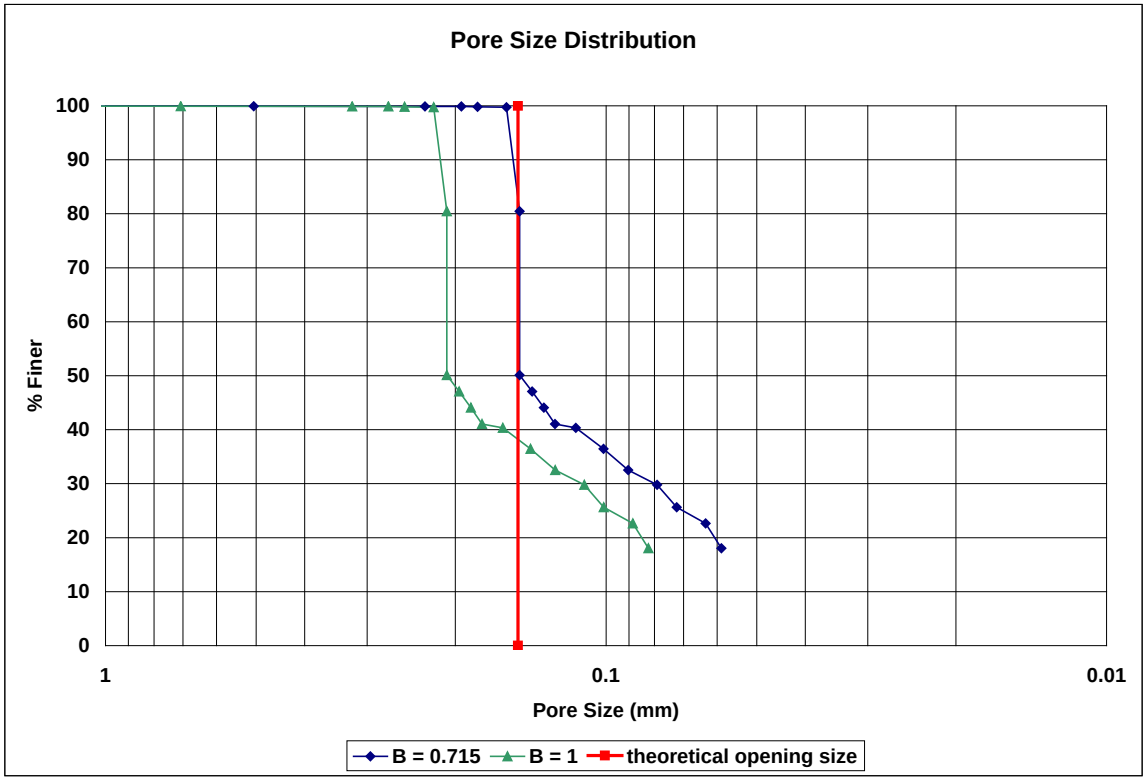

Figure 5.68: A typical pore size distribution for a No. 100 sieve screen determined using mineral oil, shown using B = 0.715 and B = 1, and the theoretical opening size.

Table 5.36: Pore sizes at selected % finer for pore size distributions shown in Figure 5.68, showing the theoretical opening size and the percent error.

	Pore Size (mm)			% Error	
% Finer	B=0.715	B=1	Theoretical	B=0.715	B=1
98	0.1572	0.2199	0.15	3.29	46.60
95	0.1558	0.2179	0.15	2.65	45.25
90	0.1534	0.2145	0.15	1.57	43.00
85	0.1510	0.2111	0.15	0.45	40.75
80	0.1488	0.2081	0.15	0.59	38.71
75	0.1488	0.2081	0.15	0.59	38.71
70	0.1488	0.2081	0.15	0.59	38.71
65	0.1488	0.2081	0.15	0.59	38.71
60	0.1488	0.2081	0.15	0.59	38.71
55	0.1488	0.2081	0.15	0.59	38.71
50	0.1484	0.2076	0.15	0.75	38.41
45	0.1354	0.1894	0.15	7.72	26.24
40	0.1138	0.1591	0.15	22.76	6.09
35	0.0972	0.1359	0.15	38.84	9.37
30	0.0799	0.1117	0.15	62.75	25.51
25	0.0703	0.0984	0.15	80.96	34.41
20	0.0607	0.0849	0.15	105.18	43.40
15	---	---	0.15	---	---
10	---	---	0.15	---	---
5	---	---	0.15	---	---

The % error is calculated as (Wenning 2012):

$$\%\ error = \left| \frac{T - E}{T} \right| \times 100 \qquad \text{(Equation 5.16)}$$

where:

E = experimental quantity

T = theoretical quantity

Note that when a capillary constant of 0.715 is used, the % error from O_{85} to O_{50} is less than 1%, representing a particularly high degree of accuracy within this range.

5.5 Analysis of the Influence of Surface Tension

The wetting fluid surface tension is a constant in the Washburn equation along with the contact angle and the capillary constant. Surface tension values used to calculate pore sizes in this study were obtained from either literature values or from the fluid suppliers, and these values are often reported only for a single temperature. Since surface tension is known to vary with temperature, it is important to consider the effect of using a surface tension value reported at a particular temperature, when the temperature during the bubble point test (and thus the surface tension) may be different than the reported value.

Of the wetting fluids used in this study, the influence of varying water surface tension on the calculated pore size is examined here because surface tension values for water are readily available in the literature for a range of temperatures. A water surface tension value of 0.07275 N/m was used in this study to calculate pore size, which is a literature value at approximately 20 °C (68 °F) (The Engineering Toolbox 2013). To examine how the calculated pore size will be influenced over a range of expected surface tensions, consider the surface tension of water at 10 °C (0.0742 N/m) and 30 °C (0.0712 N/m) (Engineering Toolbox 2013). The range of 10 °C (50 °F) to 30 °C (86 °F) is likely an extreme range of temperatures for any climate-controlled indoor setting. Indeed, for the bubble point tests performed on the NG-1 nonwoven geotextile over a range of years, temperatures varied only from 19.4 °C to 22.5 °C, or approximately 3 °C. Recall the form of the Washburn equation used for data reduction in this thesis:

$$d = \frac{C\gamma \cos\theta}{P} \qquad \text{(Equation 5.17)}$$

where:

d = pore diameter (mm)

γ = surface tension (N/m)

P = pressure difference across the geotextile (Pa)

C = constant (mm/m)

θ = contact angle (degrees)

From Equation 5.17 the resulting pore size using a different surface tension (or any different constant) can be determined from the initial pore size by using a ratio:

$$d_1\left(\frac{\gamma_2}{\gamma_1}\right) = \frac{C\gamma_1\cos\theta}{P}\left(\frac{\gamma_2}{\gamma_1}\right) = d_2 \qquad \text{(Equation 5.18)}$$

where:

d_1 = initial pore diameter using γ_1

d_2 = new pore diameter using γ_2

γ_1 = initial surface tension

γ_2 = new surface tension

Equation 5.18 reduces to:

$$d_2 = d_1\left(\frac{\gamma_2}{\gamma_1}\right) \qquad \text{(Equation 5.19)}$$

Table 5.37 shows the effect of changing the surface tension from 0.07275 N/m to both 0.0742 N/m and 0.0712 N/m on the pore sizes of the characteristic pore size

distribution for the NG-1 nonwoven geotextile determined using water. The characteristic pore size distributions using all three surface tensions are shown in Figure 5.69.

Table 5.37: Characteristic pore size distributions for the NG-1 nonwoven geotextile determined using water, showing the pore sizes determined using a surface tension of 0.07275 N/m and the influence of changing the surface tension to 0.0742 N/m and 0.0712 N/m.

	γ = 0.07275 N/m (20 °C)	γ = 0.0742 N/m (10 °C)		γ = 0.0712 N/m (30 °C)	
% Finer	Pore Size (mm)	Pore Size (mm)	% Change	Pore Size (mm)	% Change
98	0.17307	0.17652	1.99	0.16938	2.13
95	0.16198	0.16521	1.99	0.15853	2.13
90	0.15689	0.16002	1.99	0.15355	2.13
85	0.15323	0.15628	1.99	0.14996	2.13
80	0.15045	0.15345	1.99	0.14725	2.13
75	0.14767	0.15062	1.99	0.14453	2.13
70	0.14490	0.14778	1.99	0.14181	2.13
65	0.14240	0.14524	1.99	0.13937	2.13
60	0.14011	0.14291	1.99	0.13713	2.13
55	0.13782	0.14057	1.99	0.13489	2.13
50	0.13554	0.13824	1.99	0.13265	2.13
45	0.13325	0.13590	1.99	0.13041	2.13
40	0.13096	0.13357	1.99	0.12817	2.13
35	0.12867	0.13124	1.99	0.12593	2.13
30	0.12638	0.12890	1.99	0.12369	2.13
25	0.12410	0.12657	1.99	0.12145	2.13
20	0.12181	0.12423	1.99	0.11921	2.13
15	0.11952	0.12190	1.99	0.11697	2.13
10	0.11502	0.11731	1.99	0.11257	2.13
5	0.09999	0.10198	1.99	0.09786	2.13

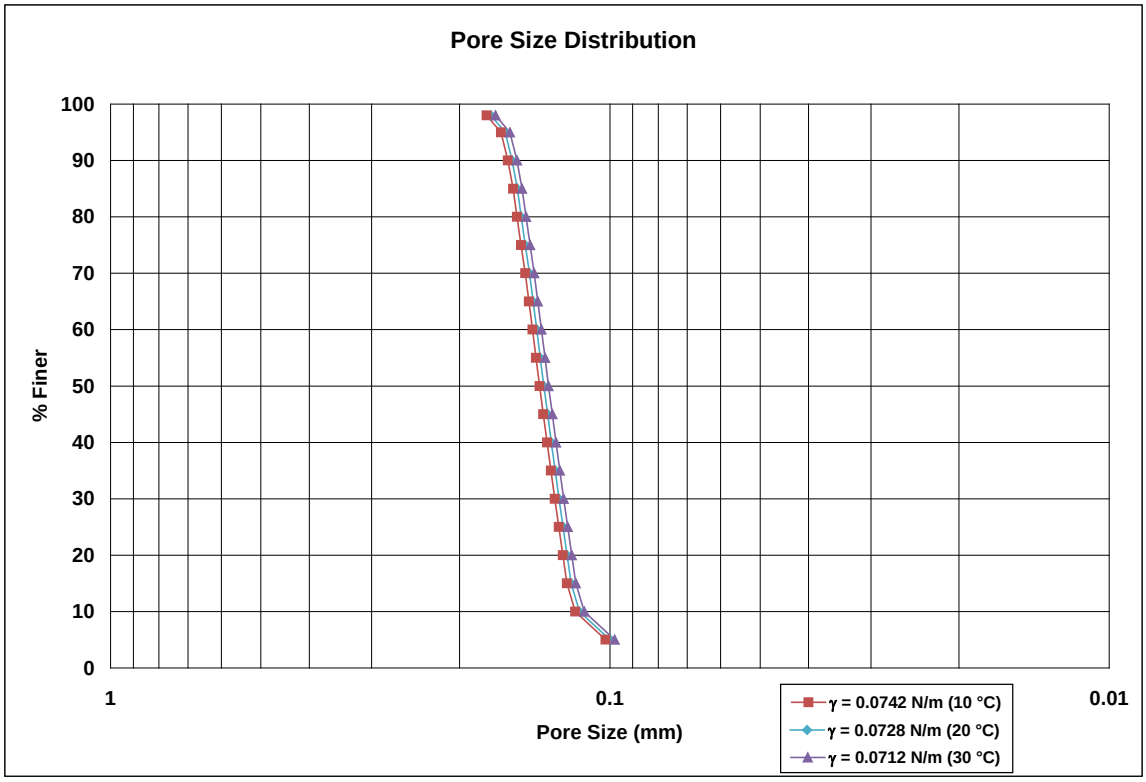

Figure 5.69: Characteristic pore size distributions from Table 5.37 for the NG-1 nonwoven geotextile, showing the influence of using a range of surface tensions for water.

Table 5.37 and Figure 5.69 show that changing the surface tension of water from the value at 20 °C to the values at 10 and 30 °C resulted in pore size changes of approximately 2%. Therefore, using a single surface tension for water at 20 °C appears to be a reasonable assumption for bubble point tests performed over a range of typical indoor air temperatures. However, the change of surface tension with temperature for other fluids used in this study (e.g., mineral oil, Porewick, etc.) should be investigated, as their surface tensions at different temperatures were not readily available. It is interesting to note that since pore size changes by the ratio of surface tensions, a unit change in surface tension for a lower surface tension fluid will result in a greater change in pore size compared to a unit change for a higher surface tension fluid. This effect is shown in

Figure 5.70, which shows values of γ_2/γ_1 as a function of γ_1 where $\gamma_2 = \gamma_1 + 0.001$ N/m over the range of fluid surface tensions used in this thesis to conduct bubble point tests.

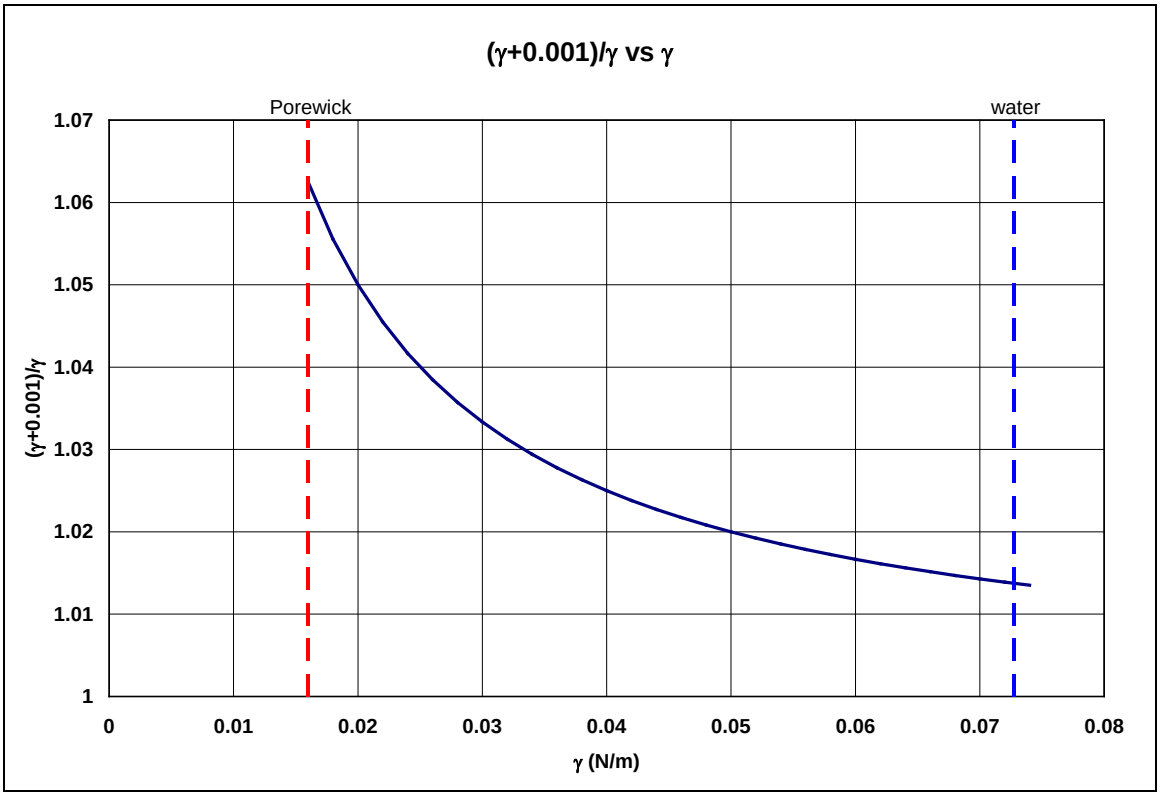

Figure 5.70: Effect of changing the surface tension by 0.001 N/m on the ratio of γ_2/γ_1 as a function of γ_1 (where $\gamma_2 = \gamma_1 + 0.001$ N/m) for the range of surface tensions of fluids used to conduct bubble point tests in this thesis.

Figure 5.70 shows that changing the surface tension by 0.001 N/m with have a greater influence on the ratio of γ_2/γ_1 at lower surface tensions. For the wetting fluids used in this thesis to conduct bubble point tests, this influence is the smallest for water and the greatest for Porewick, with the influence for other fluids falling somewhere in between. It should be stressed that this trend is for a unit change in surface tension. Although a change of 0.001 N/m in the surface tension of water is a reasonable benchmark since water surface tension changes by 0.003 N/m over the range of 10 °C – 30 °C, the surface tension of other fluids may vary more or less in this temperature range.

Further investigation is needed to evaluate the influence of surface tension changes with temperature for the other wetting fluids. For perhaps the most accurate pore size calculations with regard to surface tension, one could measure the surface tension of a wetting fluid over a range of expected laboratory temperatures, fit a trendline to a plot of surface tension vs. temperature, and use the trendline equation to calculate the surface tension for the particular temperature at which a bubble point test is conducted. The approach of fitting trendlines to plots of surface tension vs. temperature is demonstrated by Stan et al. (2009).

5.6 Analysis of the Influence of Residual Fluid

5.6.1 A Problem with No. 100 Sieve Screen Test Results

A confounding trait of the typical pore size distribution for the No. 100 sieve screen shown in Figure 5.71 is the fact that a "distribution" of pore sizes is represented for percent finer values smaller than O_{50}. There is only one theoretical opening size for a No. 100 sieve screen, which is 0.15 mm. Some small variances among individual openings are to be expected, but the distribution below O_{50} appears to be excessive for a sieve screen of a single theoretical opening size. Indeed, Table 5.36 indicates that, when B = 0.715, roughly 25% of the distribution contains pore sizes smaller than 0.075 mm, which is the theoretical opening size for a *No. 200* sieve screen. Since the tested No. 100 sieve screen is not believed to be defective, there must be some error associated with the bubble point test results.

Examination of the airflow rate vs. pore size plots of the dry and wet runs provides insight into the shape of the calculated pore size distribution. Figure 5.72 shows the dry and wet run plots used to generate the pore size distribution in Figure 5.71. At the

theoretical opening size, the wet run plot begins to sharply converge toward the dry run plot, but it does not fully converge. This sharp change in the wet run plot yields the sharp (and seemingly accurate) drop in the pore size distribution between 100% and 50% finer. At subsequent smaller pore sizes, the wet run plot moves only slightly closer to the dry run plot and there remains a distinct difference in the two plots. This non-convergence is responsible for the broadening of the pore size distribution below 50% finer. To further demonstrate the effect of the dry and wet run plots on the pore size distribution, the plots in Figure 5.72 were manipulated to force convergence at the theoretical opening size. This forced convergence is shown in Figure 5.73. The resulting pore size distribution shown in Figure 5.74 agrees much better with the theoretical opening size, showing essentially a uniform distribution from 100% to 0% finer, without the trailing effect away from the theoretical opening size that the pore size distribution in Figure 5.71 shows. Non-convergence of the airflow rate vs. pore size plots for the dry and wet runs indicates that the dry and wet samples are responding differently during the bubble point test. Specifically, non-convergence means that different airflow rates are associated with the same pressure differences across the samples during the test, as shown in Figure 5.75.

The dry and wet screen samples respond differently during the bubble point test due to the presence of the wetting fluid. In fact, it is this principle that makes it possible to determine a pore size distribution. The problem with the No. 100 sieve screen results is that, even after the critical pressure has been reached, the wet run plot does not converge to the dry run plot, which would indicate dry screen conditions. This means that fluid must be remaining on the No. 100 sieve screen at pressures greater than the critical pressure.

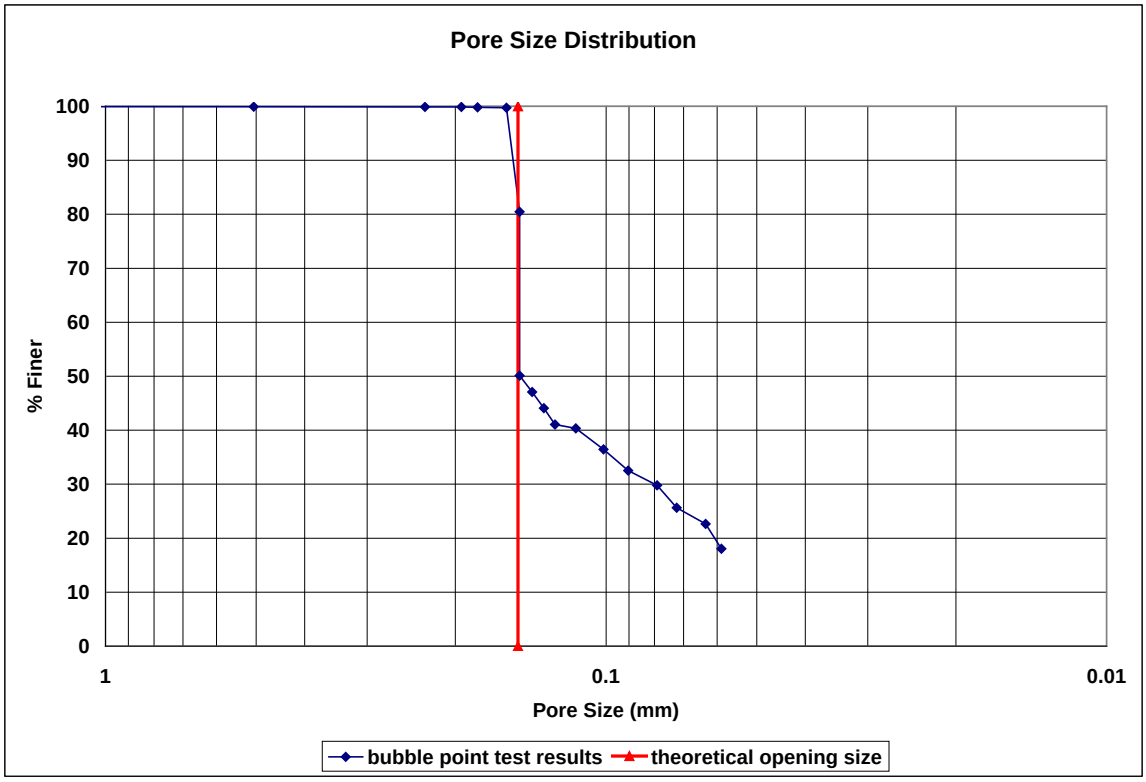

Figure 5.71: A typical pore size distribution for a No. 100 sieve screen using mineral oil, showing the theoretical opening size of the screen.

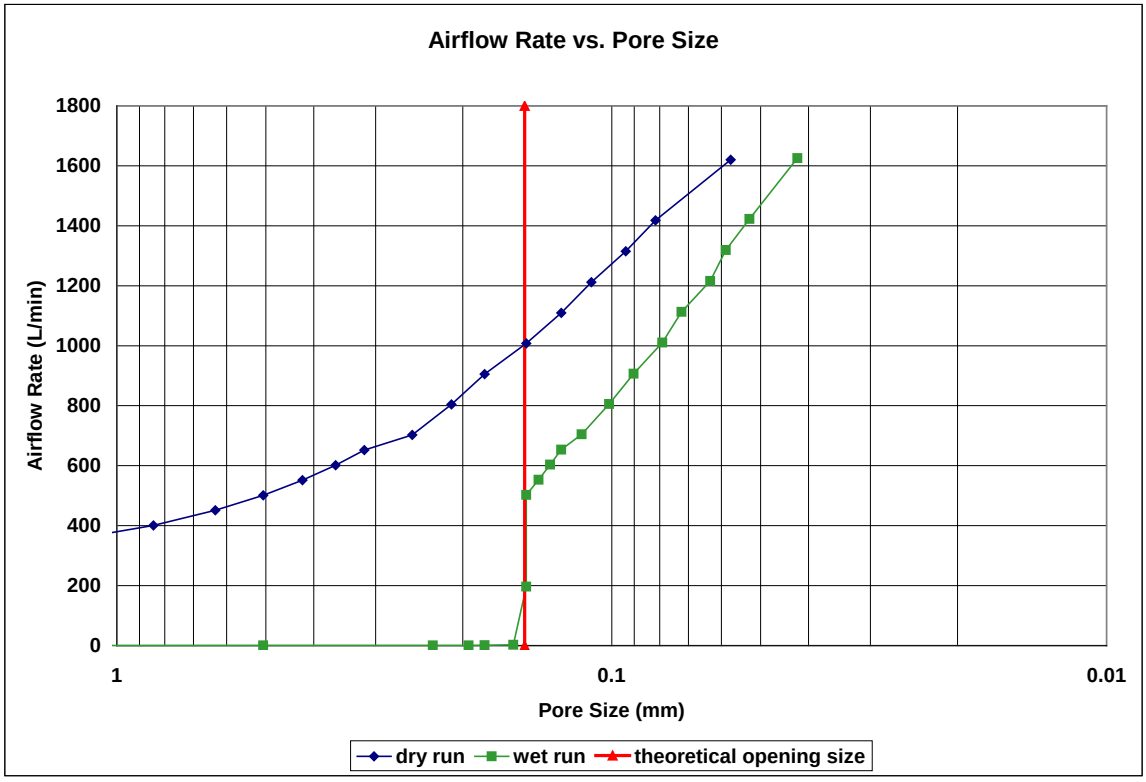

Figure 5.72: Plots of the actual dry and wet runs for the pore size distribution in Figure 5.71, showing the theoretical opening size (theoretical convergence point).

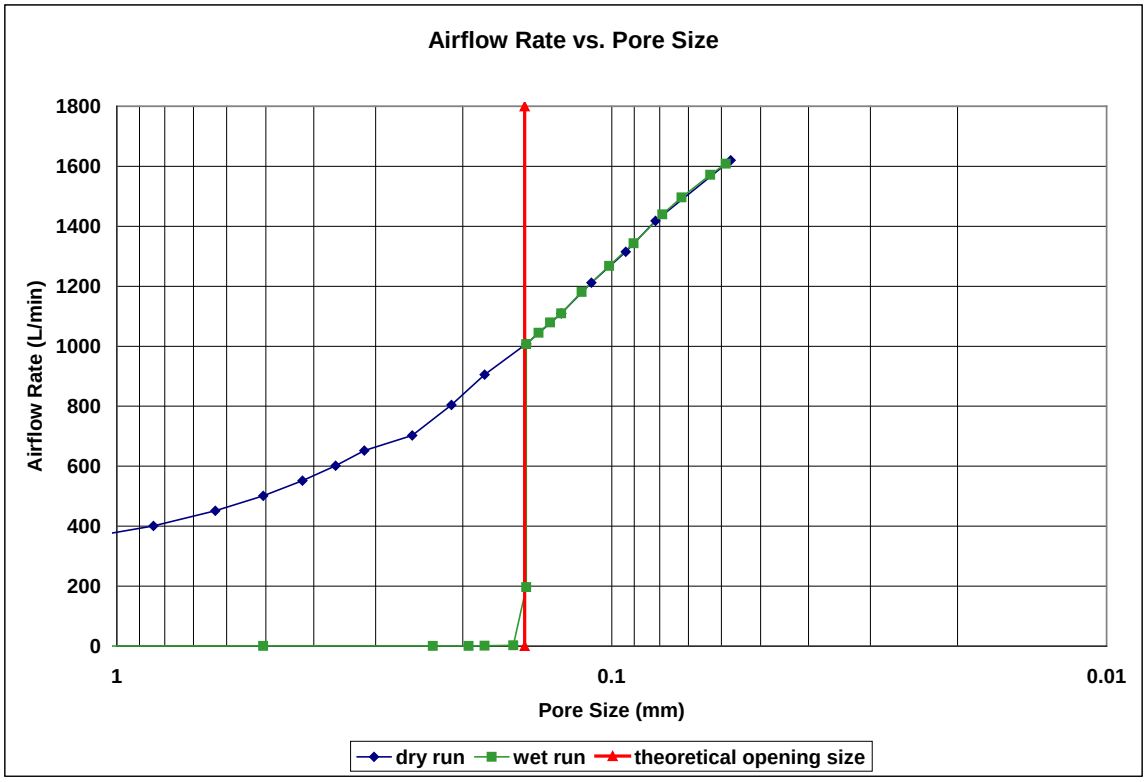

Figure 5.73: Forced convergence of the dry and wet run plots from Figure 5.72 at the theoretical opening size (theoretical convergence point).

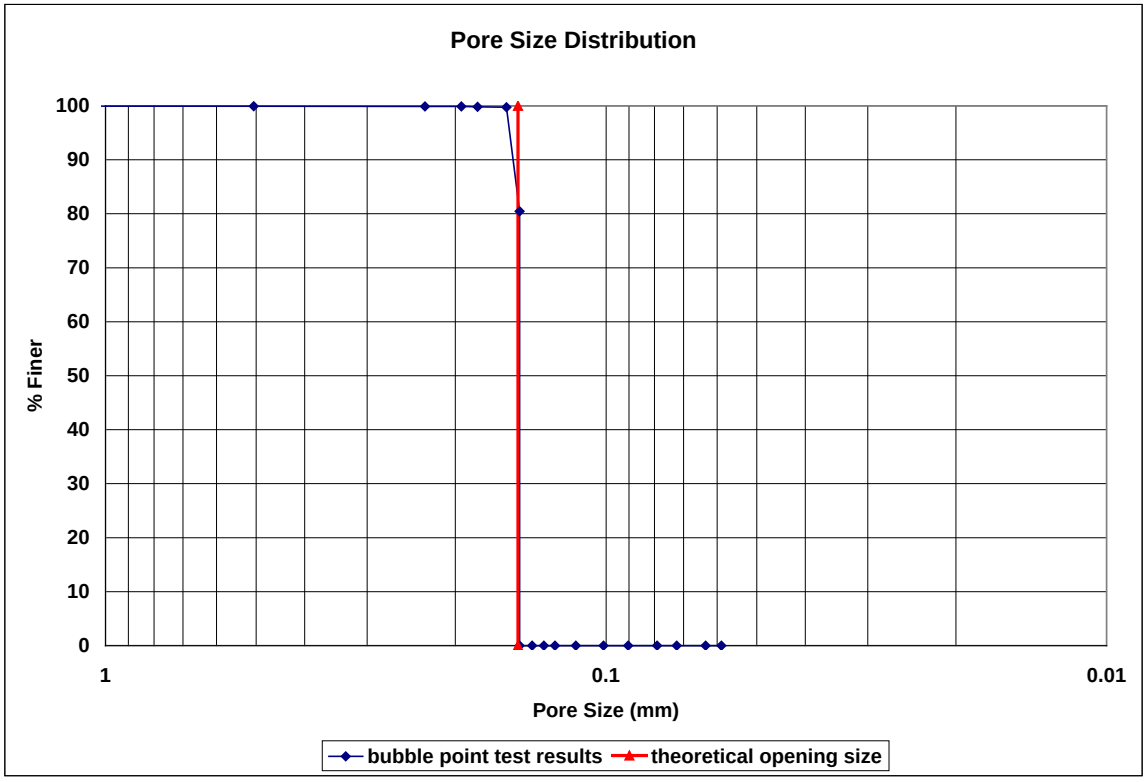

Figure 5.74: The resulting pore size distribution for the No. 100 sieve screen when the dry and wet runs converge at the theoretical opening size, as in Figure 5.73.

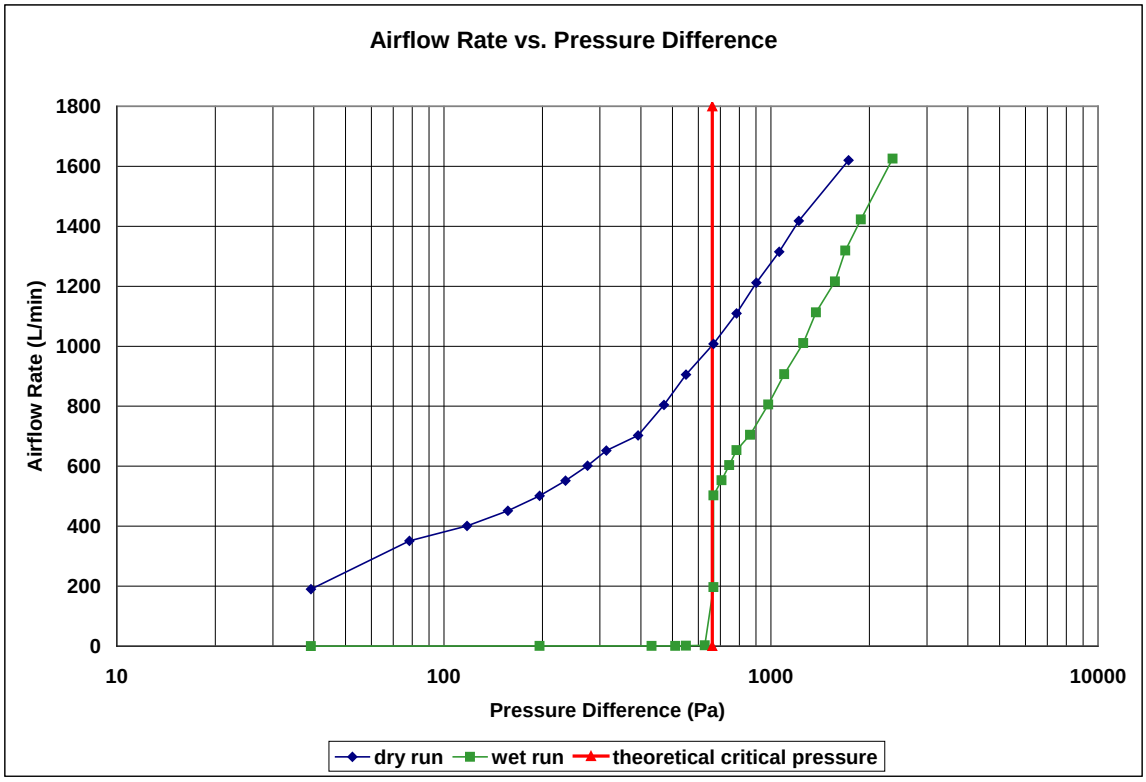

Figure 5.75: Airflow rate vs. pressure difference for the No. 100 sieve screen results shown in Figure 5.72.

Any fluid remaining on the screen after the critical pressure has been reached represents a source of error, since bubble point theory assumes that fluid completely exits a pore after overcoming the critical pressure. In other words, if the fluid does not exit completely once the critical pressure has been reached, the bubble point test results will be inaccurate. The presence of fluid remaining on metal screens after bubble point testing was observed by Fischer (1994). Elton and Hayes (2009) discussed this effect, identified as "residual fluid". Residual fluid is discussed further in Sections 5.6.2, 5.6.3, and 5.6.4.

5.6.2 Investigation of Residual Fluid on a No. 100 Sieve Screen

To investigate the presence of residual fluid remaining on an initially saturated No. 100 sieve screen after the critical pressure has been reached, sieve screens were

observed under a microscope both before and immediately after being exposed to airflow. A digital camera attached to the microscope was used to photograph images of the screens. A dry No. 100 sieve screen is shown in Figure 5.76. Note the generally square appearance of the dry screen holes. A No. 100 sieve screen saturated with mineral oil is shown in Figure 5.77. The mineral oil saturating the screen significantly reduces the light transmitted through the screen. A photograph of an initially saturated sieve screen after being exposed to airflow is shown in Figure 5.78. Two distinct features are common in photographs of initially saturated screens after being exposed to airflow. First, some holes appear to be transmitting light just as the dry screen, except the holes appear circular instead of square. The circular-appearing holes indicate that the holes are open to airflow, but some fluid is remaining along the walls of the hole. The second distinct feature is indicated by the bright squares in Figure 5.78. These holes appear to still be filled with fluid, but these holes appear much more translucent to light than the initial saturated condition. This suggests that these holes are not open to airflow, but that some of the fluid has been forced out of these holes while being exposed to airflow.

Experiments were conducted to quantify the amount of residual fluid remaining on the No. 100 sieve screen after being exposed to airflow. The amount of residual fluid remaining on the screen was quantified by calculating the percent open area of the screen. Experiments consisted of exposing a No. 100 screen initially saturated with mineral oil to constant airflow for a duration of three minutes. Two different airflow rates were used: 800 L/min and 1400 L/min. As shown in Figure 5.75, both airflow rates correspond to pressure differences greater than the critical pressure for a No. 100 sieve screen. Therefore, according to bubble point theory, all fluid should exit the screens after being

exposed to these airflow rates. After exposing an initially saturated screen to airflow, the screen was photographed at six times magnification using the microscope/camera apparatus. Five sections of the screen were selected at random and photographed. From each digital photograph, an area was selected at random and cropped to 633x633 pixels using digital photograph editing software (Corel Corporation 2005). The number of pixels representing the open area of each cropped image was calculated using image analysis software (Scion Corporation 2005).

The percent open area is calculated as:

$$POA = \frac{A_{open}}{A_{total}} \times 100 \qquad \text{(Equation 5.20)}$$

where:

POA = percent open area

A_{open} = open area of the photograph

A_{total} = total area of the photograph

The experiment was repeated five times (five runs) at both the 800 L/min and 1400 L/min airflow rates. For each run, an average percent open area was calculated by averaging the percent open area from each of the five cropped images. For comparison, the percent open area was also calculated for five cropped images of a dry No. 100 sieve screen. The results of the percent open area calculations for the dry screen are shown in Table 5.38.

The experiments showed that mineral oil remained on the No. 100 sieve screen after being exposed to both the 800 L/min and 1400 L/min airflow rates. This residual fluid can be visually observed in Figures 5.78-5.81. A photograph of the No. 100 sieve

screen following a typical 800 L/min run is shown in Figure 5.78. A cropped image from Figure 5.78 used to compute the percent open area is shown in Figure 5.79. A cropped image of a dry No. 100 screen is also shown in Figure 5.79 for comparison. A photograph of the No. 100 sieve screen following a typical 1400 L/min run is shown in Figure 5.80. A cropped image from Figure 5.80 along with a cropped image of a dry No. 100 screen are shown in Figure 5.81. It can be seen by visual inspection of Figures 5.78 and 5.80 that there is less fluid remaining on the screen following the 1400 L/min of airflow. Quantitatively, the results of percent open area measurements on the wet screens are shown in Tables 5.39 and 5.40. The overall average percent open area for the 800 L/min tests of 27.31% is less than the overall average percent open area for 1400 L/min tests of 32.63%, which is consistent with the presence of more residual fluid on the screens following the 800 L/min tests. The overall coefficient of variation of 14.30% for percent open area measurements following the 800 L/min tests compared to the value of 7.77% for 1400 L/min tests indicates better consistency among the percent open area measurements for the screens following the 1400 L/min tests. The coefficient of variation for the 1400 L/min tests of 7.77% is very close to the value of 4.40% observed for a dry screen, indicating similar consistency among percent open area measurements. The fact that overall averages for percent open area for 800 L/min and 1400 L/min tests are less than the average value for the dry No. 100 screen of 41% is consistent with the presence of residual fluid on the No. 100 sieve screen following both the 800 L/min and 1400 L/min tests.

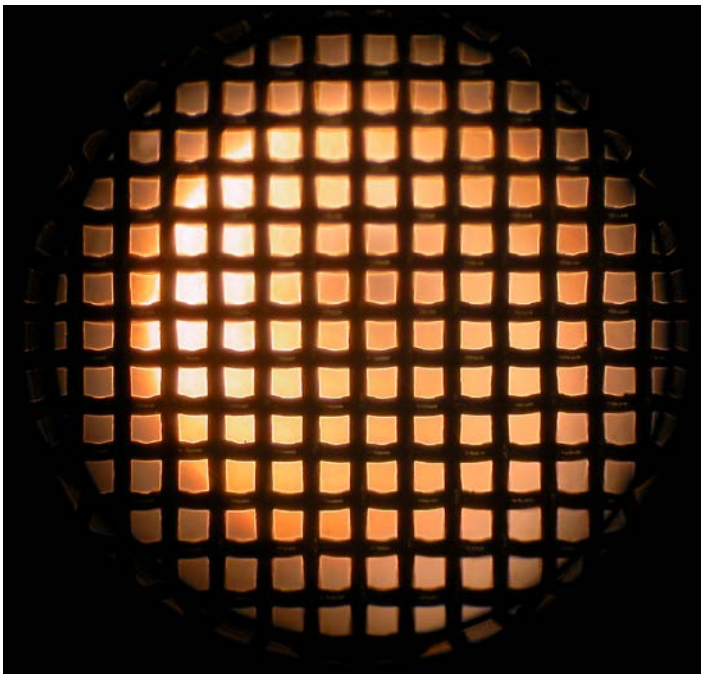

Figure 5.76: Photograph of a dry No. 100 sieve screen.

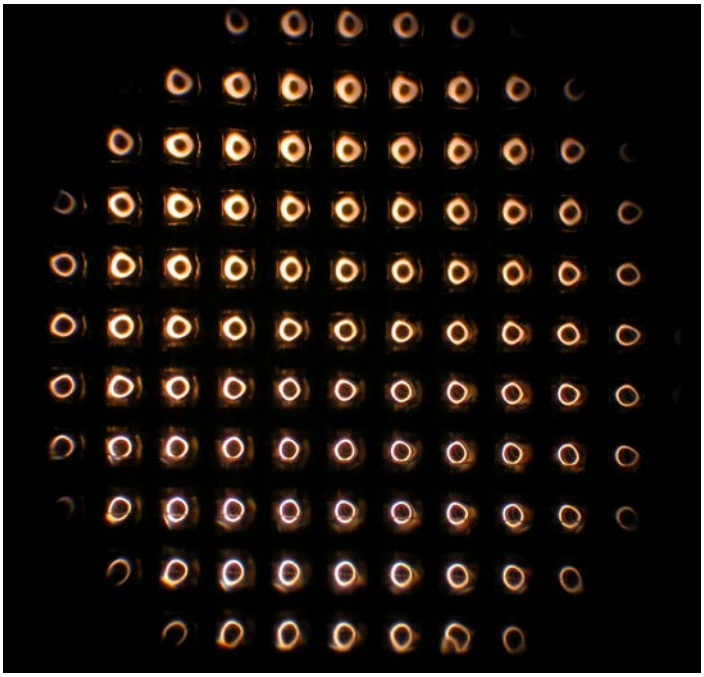

Figure 5.77: Photograph of a No. 100 sieve screen saturated with mineral oil.

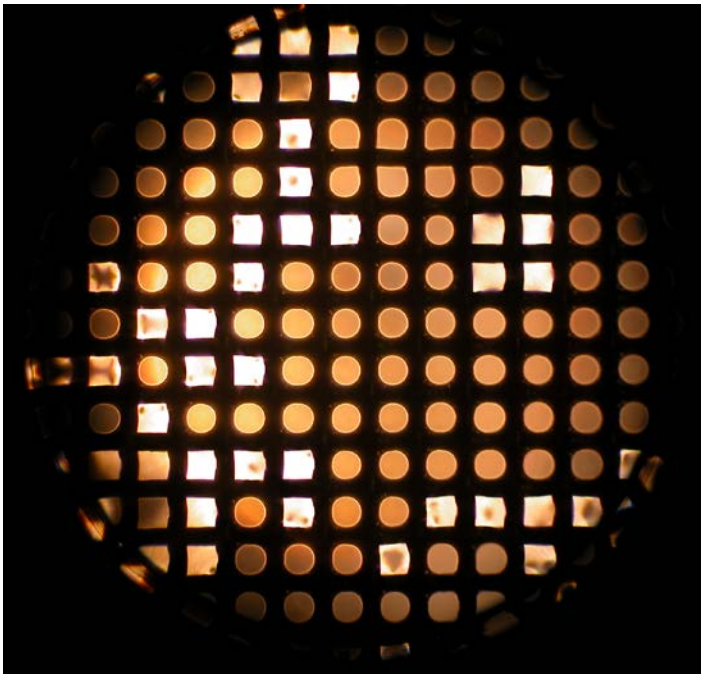

Figure 5.78: Photograph of a No. 100 sieve screen initially saturated with mineral oil, after being exposed to 800 L/min of airflow for three minutes.

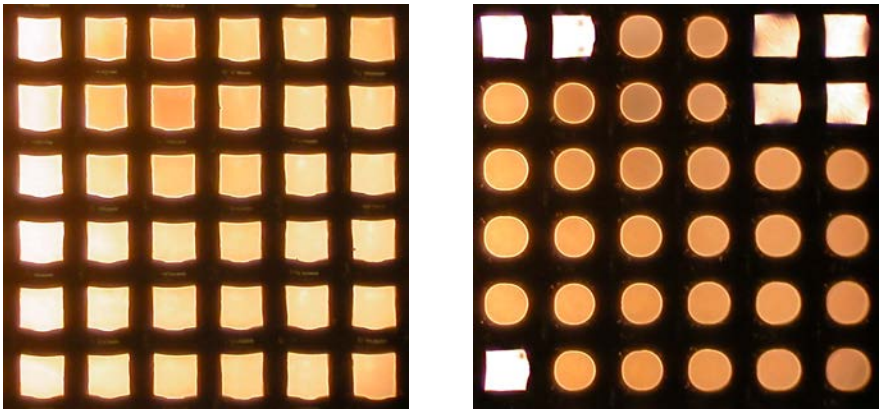

Figure 5.79: Cropped images of a dry screen (left) and a wet screen after being exposed to 800 L/min of airflow for three minutes (right).

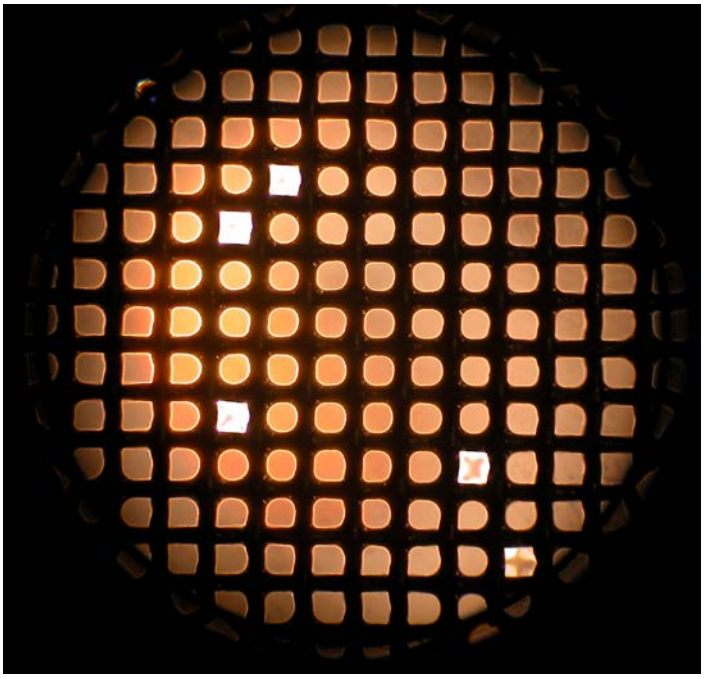

Figure 5.80: Photograph of a No. 100 sieve screen initially saturated with mineral oil, after being exposed to 1400 L/min of airflow for three minutes.

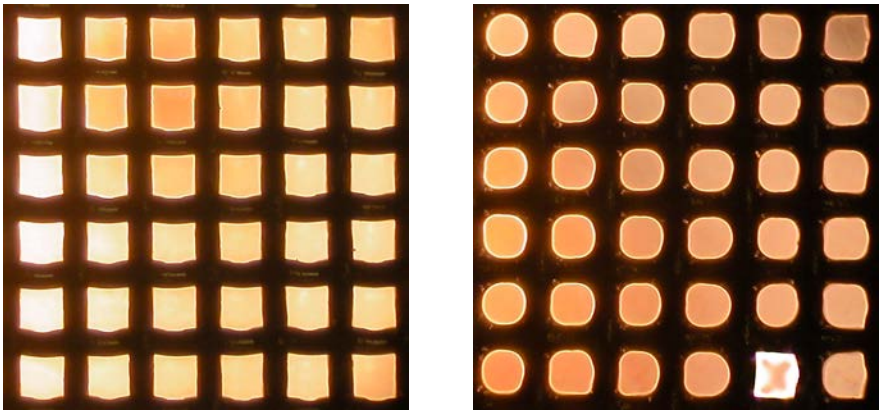

Figure 5.81: Cropped images of a dry screen (left) and a wet screen after being exposed to 1400 L/min of airflow for three minutes (right).

Table 5.38: Percent open area measurements for a dry No. 100 sieve screen.

Measurement	Percent Open Area (%)
1	42.41
2	43.10
3	41.08
4	38.99
5	39.40
Average (%)	41.00
Standard Deviation (%)	1.81
Coefficient of Variation (%)	4.40

Table 5.39: Percent open area measurements for a No. 100 sieve screen initially saturated with mineral oil, after being exposed to 800 L/min of airflow for three minutes.

Run	Average Percent Open Area (%)	Standard Deviation (%)	Coefficient of Variation (%)
1	29.87	4.79	16.04
2	27.88	3.00	10.75
3	25.92	4.30	16.58
4	25.82	4.59	17.79
5	27.08	2.79	10.32
Average	27.31	3.89	14.30

Table 5.40: Percent open area measurements for a No. 100 sieve screen initially saturated with mineral oil, after being exposed to 1400 L/min of airflow for three minutes.

Run	Average Percent Open Area (%)	Standard Deviation (%)	Coefficient of Variation (%)
1	34.66	3.66	10.57
2	32.55	2.53	7.77
3	33.84	1.74	5.15
4	30.47	2.74	8.98
5	31.63	2.02	6.39
Average	32.63	2.54	7.77

5.6.3 Theoretical Basis for Residual Fluid in Capillary Tubes

The effect of residual fluid remaining in capillary tubes and porous media when a fluid is removed is discussed in the literature. A familiar example, as noted by de Gennes et al. (2004), is residual fluid remaining in a pipette after it is drained. In another example, de Gennes et al. (2004) noted that "approximately 40%" of crude oil is retained when oil is extracted from porous rock. According to de Ryck (2002), "coating flows, which are liquid flows leading to a deposited liquid layer on the surface of a solid, have been extensively studied (Ruschak 1985) for their practical importance in many technologies: painting, printing, emulsion deposition in [the] photographic industry, [and] air displacement in wetted porous media." De Ryck (2002) references several early studies of fluid deposition in tubes, including Taylor (1961), Bretherton (1961), and Cox (1962).

A theoretical explanation for the effect of residual fluid is the phenomenon of fluid deposition along the walls of tubes. When a wetting fluid within a capillary tube is displaced by air, a film of wetting fluid remains on the walls of the tube (Aussillous and Quéré 2000). This phenomenon is illustrated in Figure 5.82.

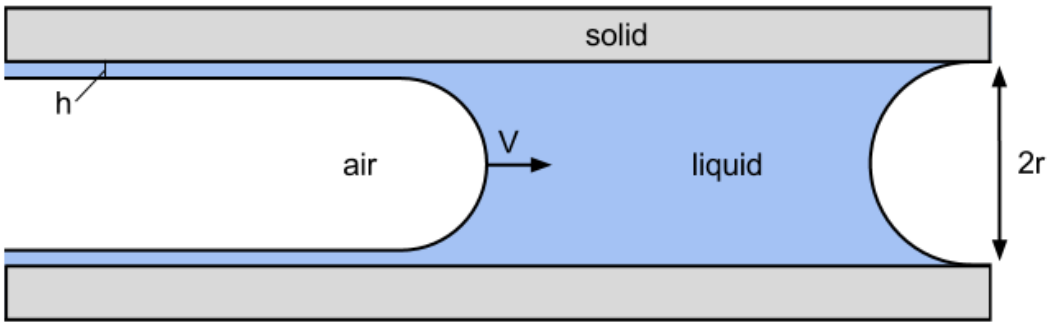

Figure 5.82: "A drop of a wetting liquid moved in a capillary tube leaves behind a film" of thickness, h. Adapted from Aussillous and Quéré 2000.

The thickness of the deposited fluid layer in a tube can be mathematically described by Bretherton's law (de Gennes et al. 2004):

$$h \approx rCa^{2/3} \qquad \text{(Equation 5.21)}$$

where:

h = thickness of the deposited fluid layer

r = radius of the tube

Ca = capillary number

The capillary number is given as (de Gennes et al. 2004):

$$Ca = \frac{\eta V}{\gamma} \qquad \text{(Equation 5.22)}$$

where:

η = viscosity

V = velocity of fluid

γ = surface tension

Substituting Equation 5.22 into Equation 5.21 yields:

$$h \approx r\left(\frac{\eta V}{\gamma}\right)^{2/3} \qquad \text{(Equation 5.23)}$$

Equation 5.23 shows that, for a capillary tube of radius, r, the thickness of the deposited fluid layer will generally be greater for fluids with higher viscosity and lower surface tension (or when the ratio of viscosity to surface tension is higher), provided that fluid velocities are similar.

5.6.4 Influence of Residual Fluid on Geotextile Pore Size Distributions

As discussed in the two preceding sections, residual fluid has been observed on samples of a No. 100 sieve screen following tests where the critical pressure for the theoretical hole size was exceeded, and the effect of residual fluid associated with capillary tubes and porous media has been documented in the literature, with Bretherton's law serving as a theoretical explanation for the deposition of fluids along the walls of capillary tubes. Given these facts, it is reasonable to consider that the same phenomenon may also occur in geotextiles subjected to bubble point tests. A challenge with examining the pore size distributions obtained for geotextiles by the bubble point test is that there is no theoretical pore size distribution to compare to the results. However, insight can be gained by examining the airflow rate vs. pore size graphs and by considering wetting fluid properties in terms of Bretherton's law.

Plots of the airflow rate vs. pore size (or pressure difference) for the wet and dry runs can be useful for indicating the amount of fluid present in the geotextile throughout the bubble point test. Recall that the only difference in test conditions between the wet and dry runs is that the geotextile sample is saturated with a wetting fluid prior to the wet run. Therefore, differences in the plots of airflow rate vs. pore size for these runs can be attributed to the presence of wetting fluid during the wet run. As fluid exits pores during the test, the wet run plot will converge toward the dry run plot. Once the critical pressure for the smallest pore size has been exceeded, the wet and dry run plots should look the same if all of the wetting fluid has indeed exited the geotextile sample, as bubble point theory assumes.

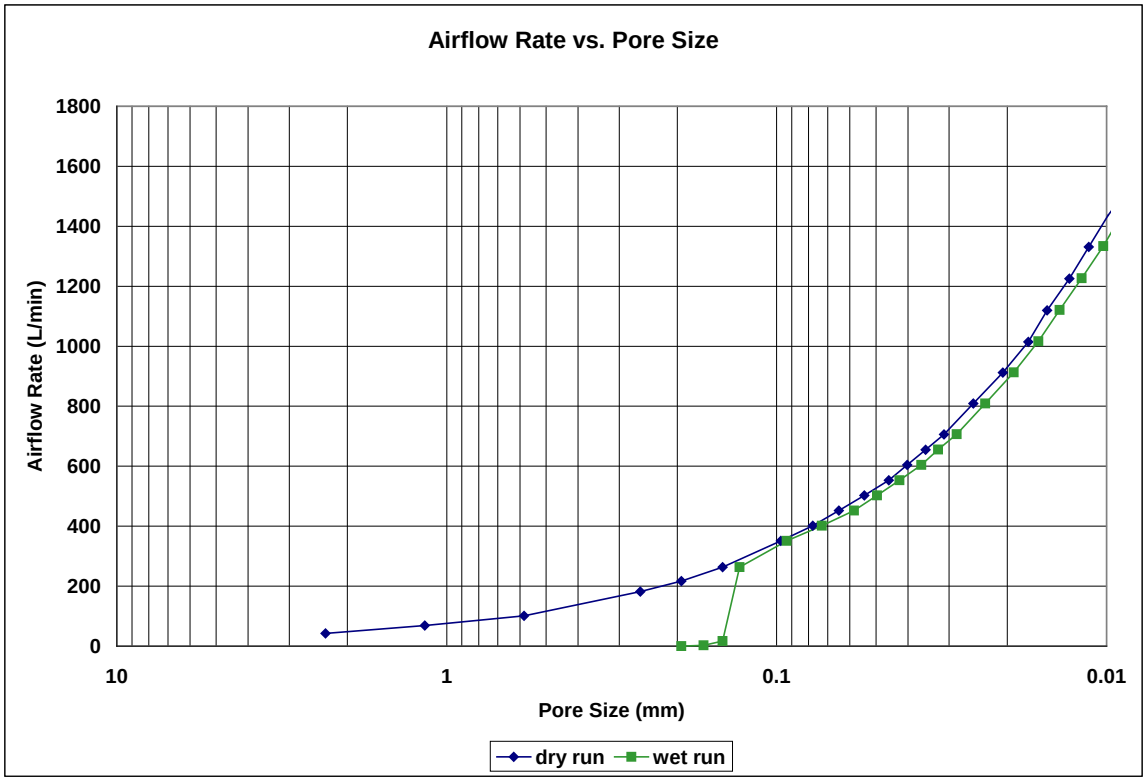

Figure 5.83: Plots of the wet and dry runs for the NG-1 nonwoven geotextile, using Porewick as the wetting fluid, illustrating convergence of the wet and dry runs.

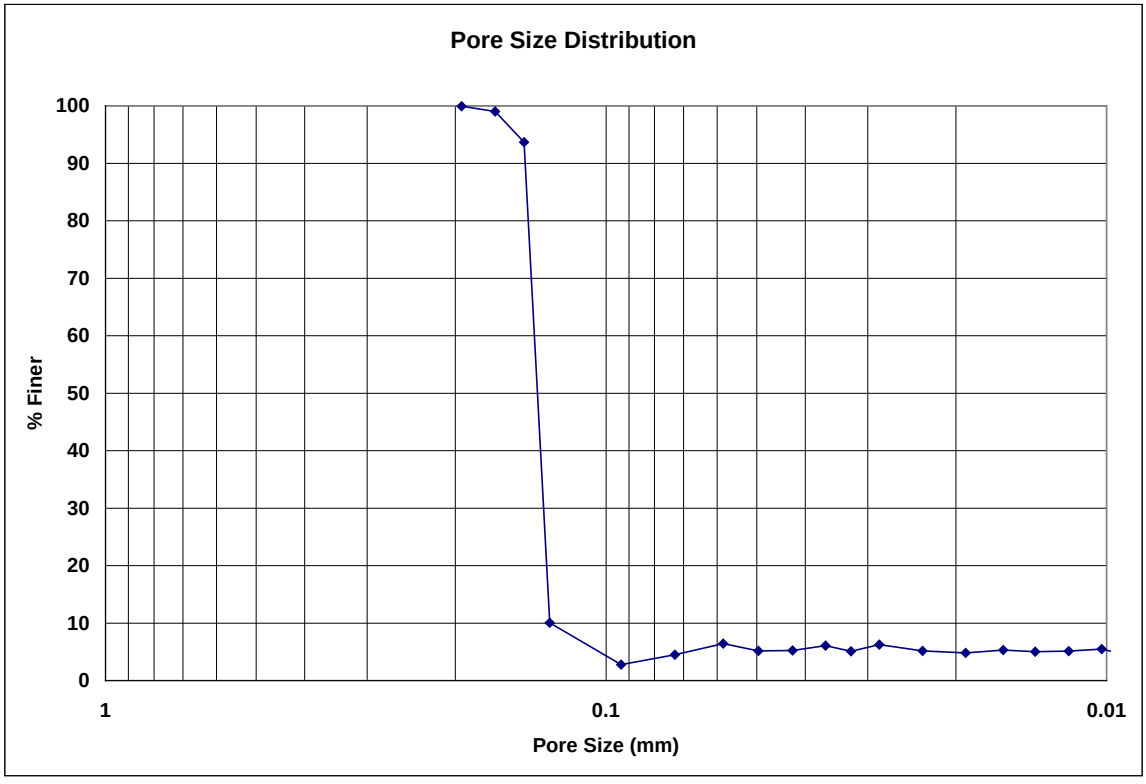

Figure 5.84: The pore size distribution determined from the wet and dry run plots in Figure 5.83 for the NG-1 nonwoven geotextile.

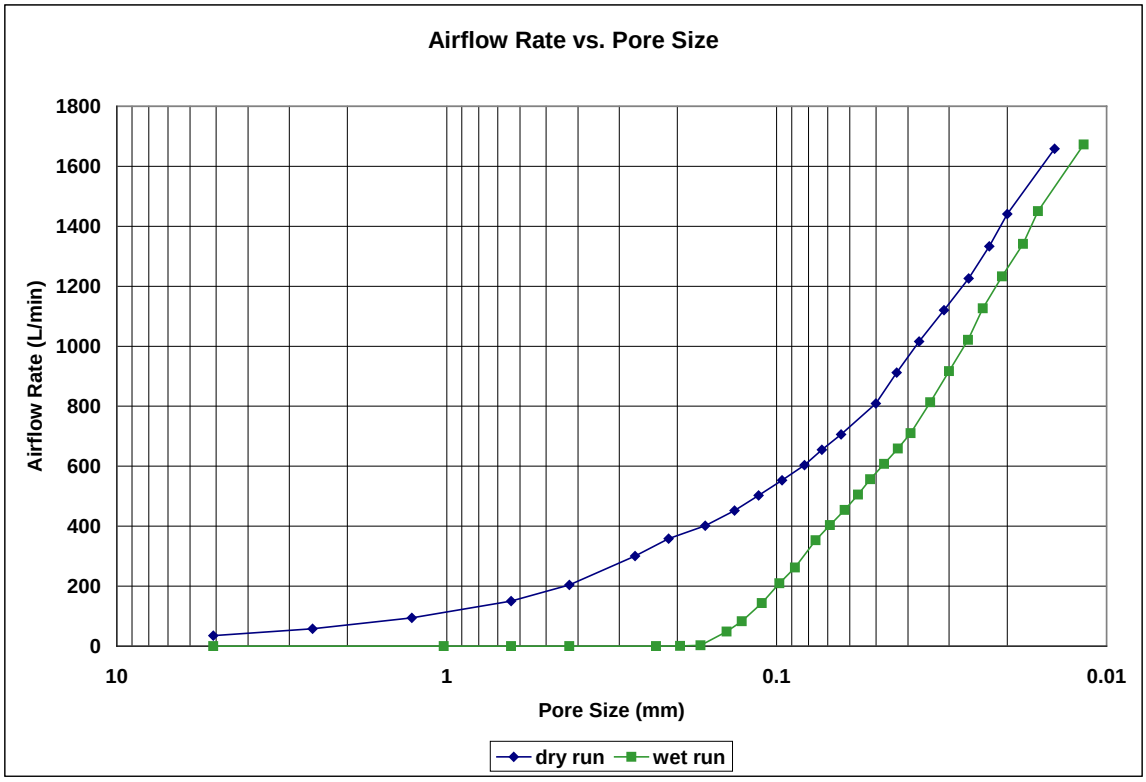

Figure 5.85: Plots of the wet and dry runs for the NG-1 nonwoven geotextile, using mineral oil as the wetting fluid. Note the non-convergence of the wet and dry runs.

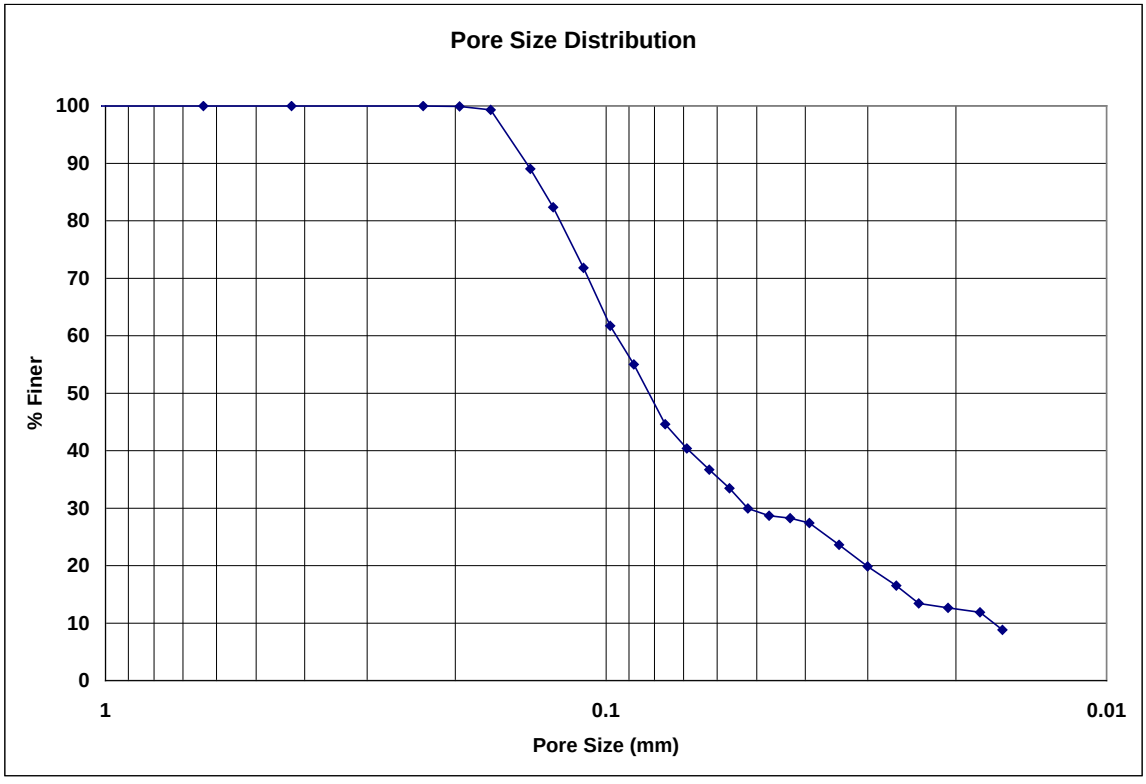

Figure 5.86: The pore size distribution determined from the wet and dry run plots in Figure 5.85 for the NG-1 nonwoven geotextile.

Consider the bubble point test results from two tests performed on the NG-1 nonwoven geotextile in Figures 5.83 – 5.86, in which two different wetting fluids, Porewick and mineral oil, were used. Figure 5.83 shows the plots of the wet and dry run for the test where Porewick was used. Once the plots begin to converge, they converge rather quickly, with the wet run plot closely resembling the dry run plot for pore sizes smaller than 0.1 mm. The resulting pore size distribution in Figure 5.84 is rather steep and essentially reaches a baseline at about O_5, or 5% Finer. Figure 5.85 shows the wet and dry run plots for the test where mineral oil was used. In contrast to the Porewick test, the wet run plot for mineral oil does not converge rapidly to the dry run plot. The wet run plot for the mineral oil test does not converge to the degree that the wet run converges in the Porewick test. The marked gap between the wet and dry run plots for the mineral oil test are reminiscent of the wet and dry run plots for the No. 100 sieve screen in Figure 5.72. The resulting pore size distribution for the mineral oil test is shown in Figure 5.86. The relative non-convergence of the wet and dry runs for the mineral oil test compared to the Porewick test results in a broader pore size distribution for the mineral oil test, with the mineral oil distribution never actually reaching the approximate O_5 baseline displayed by the Porewick test. The relative non-convergence of the mineral oil wet run compared to the Porewick wet run indicates that more wetting fluid remains on the geotextile throughout the mineral oil test compared to the Porewick test.

In regard to which results are more accurate, the answer is not as simple as determining the accuracy of the No. 100 sieve screen results. In the case of the No. 100 sieve screen, a single theoretical hole size is known. Therefore, a distribution showing

multiple hole sizes, as was the case with the mineral oil results, can easily be regarded as inaccurate. In the case of the nonwoven geotextile sample, however, a distribution showing multiple pore sizes is expected. Both geotextile pore size distributions determined using Porewick and mineral oil reflect multiple pore sizes, but to different degrees. The distribution determined using mineral oil (Figure 5.86) is much broader than the distribution determined using Porewick (Figure 5.84), indicating a wider range of pore sizes in the mineral oil distribution. It was shown with the No. 100 sieve screen that the broad portion of the pore size distribution was due to residual mineral oil remaining on the sieve screen. It is reasonable to assume that some residual mineral oil is remaining on the geotextile sample and yielding a similar broadening of the pore size distribution. Barring evaporation of Porewick during the test, there is no particular reason to question the accuracy of the rapid convergence of the wet and dry run plots for the Porewick test. If the Porewick test is considered to be accurate, the differences in the pore size distributions determined using Porewick and mineral oil can be attributed to the presence of more residual fluid with the mineral oil test.

Differences in characteristic geotextile pore size distributions determined using different wetting fluids can be examined in the context of Bretherton's law. The characteristic pore size distributions are shown in Figure 5.87. The distributions are grouped closer together at higher values of percent finer, where the influence of residual fluid is expected to be less, since these values represent the early-stages of the bubble point test where generally less fluid has exited. The most pronounced differences in the pore size distributions occur at the smaller values of percent finer (later stages of the bubble point test), beginning at about O_{70} and generally increasing in difference at

smaller values of percent finer. It has been shown that the differences in pore size distribution curve shape are due to differences in convergence of the wet run plot to the dry run plot. The less the wet run converges to the dry run, the more wetting fluid is present in the geotextile sample and the broader the pore size distribution. According to Bretherton's law (Equation 5.21), the approximate thickness of the deposited fluid layer is proportional to the 2/3 power of the ratio of the dynamic viscosity to the surface tension of the fluid. Table 5.41 shows the dynamic viscosity, surface tension, and associated ratio for the wetting fluids used to determine the characteristic geotextile pore size distributions in Figure 5.87.

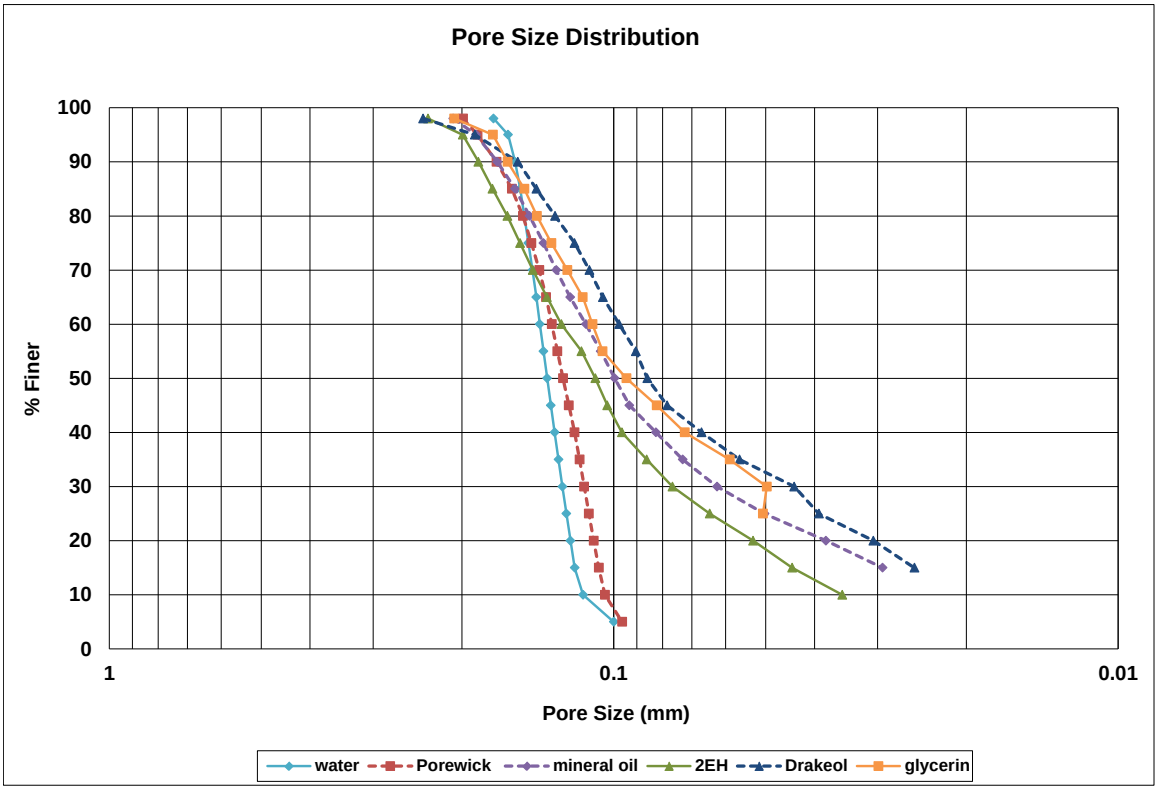

Figure 5.87: Characteristic geotextile pore size distributions for various wetting fluids.

Table 5.41: Wetting fluid properties associated with Bretherton's law.

wetting fluid	dynamic viscosity, η (Pa-s)	surface tension, γ (N/m)	$(\eta/\gamma)^{2/3}$ $(s/m)^{2/3}$
water	0.0010	0.0723	0.06
Porewick	0.0040	0.0160	0.40
2-ethyl hexanol	0.0098	0.0276	0.50
mineral oil	0.0210	0.0347	0.71
Drakeol	0.0783	0.0347	1.72
glycerin	0.8692	0.0634	5.73

A greater value of $(\eta/\gamma)^{2/3}$ will result in a greater value of the Bretherton's law deposited film thickness (assuming fluid velocities are relatively similar) and therefore more residual fluid left on the geotextile. More residual fluid left on the geotextile will result in less convergence of the wet and dry runs and a broader pore size distribution.

Consider the positions of the characteristic geotextile pore size distributions at O_{30}, or 30% finer. The positions of the pore size distributions agree well with the order of $(\eta/\gamma)^{2/3}$. Water, with the lowest value of $(\eta/\gamma)^{2/3}$, yields the largest pore size at O_{30} on the steepest pore size distribution. The next pore size distribution to the right is the Porewick curve, followed by 2-ethyl hexanol, and mineral oil, in order of increasing values of $(\eta/\gamma)^{2/3}$. The only curves that are not in order by values of $(\eta/\gamma)^{2/3}$ are Drakeol and glycerin. The curves for Drakeol and glycerin are very close, with the O_{30} pore size for Drakeol slightly smaller than the O_{30} pore size for glycerin. At O_{20}, the pore size distributions appear in order of $(\eta/\gamma)^{2/3}$ from left to right, with no defined curve for glycerin.

As another example, consider the pore size distribution positions at the 0.1 mm pore size. At this pore size, the water curve shows the smallest value of percent finer, indicating least amount wetting fluid remaining on the geotextile at this point in the bubble point test. Porewick has the next largest value of percent finer, followed by 2-ethyl hexanol and mineral oil, in order of $(\eta/\gamma)^{2/3}$. As with the O_{30} example, the Drakeol and glycerin curves are not in order with respect to $(\eta/\gamma)^{2/3}$.

A potential caveat when examining the pore size distributions in terms of Bretherton's law is the possibility that the velocity at which a fluid exits a pore is likely to be a function of viscosity. Recall from Equation 5.23 that the thickness of the deposited fluid layer in a capillary tube is proportional to $(\eta V/\gamma)^{2/3}$, where V is the velocity of the fluid moving through the capillary tube. Once the critical pressure is reached for fluid in a pore, a lower viscosity fluid would be expected to exit the pore faster than a higher viscosity fluid under similar conditions. During bubble point testing, the pressure difference was observed to drop more rapidly as pores opened for lower-viscosity fluids (water and Porewick) and slower with the higher-viscosity fluids, indicting that the lower-viscosity fluids were exiting the geotextile at a greater velocity. A lower velocity would tend to counteract the affect of a higher viscosity on the deposited film thickness in Bretherton's law (Equation 5.23). This could explain why the glycerin curve in Figure 5.87 is similar to the Drakeol curve even though the $(\eta/\gamma)^{2/3}$ value for glycerin of 5.73 is greater than the Drakeol value of 1.72. Perhaps the velocity of glycerin in the geotextile is reduced due to its relatively high viscosity, reducing the deposited film thickness according to Equation 5.23. Although the velocity of a fluid exiting a geotextile pore may be difficult to measure, it might be possible to approximate

this value by recording the time duration of the drop of the pressure difference during the bubble point test and dividing the thickness of the geotextile by this time.

A potential way to mitigate the effect of residual fluid would be to perform the wet run first, then immediately perform the “dry” run. This way, the wet run would converge to the dry run even if residual fluid is present. Performing the wet run first is actually prescribed by the membrane and filter characterization equipment manufacturer, POROMETER, for use with their commercial porometer devices (POROMETER 2012). Performing the wet run first and then immediately performing the dry run without removing the geotextile sample from the sample holder would have the added benefit of reducing the overall time required to perform the bubble point test. When conducting the dry run after the wet run, it would be important for the critical pressure for the smallest pore size to be exceeded. If the critical pressure is not reached for all of the pore sizes during the wet run and then the dry run is performed on the sample, fluid remaining in pores would incorrectly be considered as residual fluid in the test and these pore sizes would not be included in the pore size distribution. In addition, one would need to verify that evaporation of residual fluid during dry run is not significant. Evaporation of residual fluid during the dry run would alter the airflow rate – pressure relationships from the conditions at the beginning of the dry run, which could affect the results.

Chapter 6: Conclusions and Recommendations for Future Research

This chapter summarizes the work presented in this thesis, highlights important observations, and provides recommendations for future research.

6.1 Conclusions

Key work presented in this thesis along with related observations includes the following:

1. A custom-built apparatus developed at Auburn University for performing bubble point tests on nonwoven geotextiles and other porous materials has been described, along with the procedures used for performing bubble point tests.

2. An automated Microsoft Excel® spreadsheet has been developed by the author for calculating pore size distributions from the raw bubble point test data. The automated spreadsheet significantly reduces the time and effort needed to calculate pore size distributions compared to previous methods, keeps all pertinent data organized together in one file, and generates standardized graphs and reports, all while requiring input of only the basic raw data from the bubble point test and basic pore size calculation parameters. In addition to the standard graphical pore size distribution, the spreadsheet automatically presents a tabular form of the pore size distribution. The tabular pore size distribution eliminates the need to manually read pore sizes and percent finer information from a graph at

standard opening sizes, which saves time and reduces the potential for human error. The tabular pore size distribution facilitates conducting statistical analysis that was not previously considered for multiple bubble point test results for a porous medium.

3. Statistical analysis of multiple bubble point test results performed on samples of a nonwoven geotextile included the calculation of a mean pore size distribution, the standard deviation of pore sizes, the coefficient of variation of pore sizes, the confidence interval of the mean for pore sizes, MARV and MaxARV, and tolerance intervals. ANOVA tests were performed to determine whether mean pore sizes determined using different wetting fluids were statistically different. In most cases, the mean pore sizes determined using different wetting fluids were statistically different, especially at smaller opening sizes. Statistical analyses such as computing a mean pore size distribution, the confidence interval of the mean, and tolerance intervals could potentially be incorporated into methods of quality control and conformance testing for geotextiles. ANOVA tests may be useful in future research where results from different test conditions are studied. One example would be comparing mean pore size distributions obtained by different operators for a geotextile.

4. Using different values for the capillary constant can have a significant influence on the pore size distribution determined using the bubble point test. There is variance in the literature regarding the presence of the capillary constant in the Washburn equation, the physical phenomena accounted for by the capillary constant, and the value that should be used for the capillary constant. Physical

phenomena reported in the literature, such as tortuosity and pore shape, suggest that the capillary constant depends on the specific porous media of interest. In this case, using a single value for all porous media, as prescribed by ASTM, would not be appropriate. Without knowing the value of the capillary constant for a particular porous media, it would seem that a value of unity should be used, which is the same as not including the capillary constant in the pore size calculation. A capillary constant of one yielded O_{95} pore sizes that agreed better (lower % difference) with the manufacturer-supplied AOS value compared to using the ASTM D6767-11 recommended capillary constant value of 0.715. However, the ASTM-recommended value of 0.715 yielded a more accurate (lower % error) pore size distribution for a typical bubble point test using mineral oil on a No. 100 sieve screen. More information should be given in ASTM F316 and ASTM D6767 explaining why a value of 0.715 is recommended.

5. Changing the surface tension of water from a value at 20 °C to values at 10 °C and 30 °C did not greatly change the pore size distribution (only about 2%). Since the temperature values of 10 °C and 30 °C are likely extremes for indoor settings, using a single surface tension for water (e.g., at 20 °C) in the data reduction when water is used as the wetting fluid seems to be reasonable. However, the influence of varying surface tension for other wetting fluids should be evaluated. The lower the surface tension, the more a unit change in surface tension will affect the pore size distribution.

6. The contact angle of the wetting fluid can have a significant influence on the pore size distribution determined using the bubble point test. The results of bubble

point tests on a nonwoven geotextile conducted using several different wetting fluids showed the best agreement when using contact angles determined by a Dynamic Contact Angle Analyzer. The Dynamic Contact Angle Analyzer is believed to yield the most accurate contact angles because it can measure the receding contact angle on the same nonwoven geotextile on which the bubble point test is performed. The receding contact angle is the contact angle of interest for the bubble point test. Measuring the contact angle on the same solid material used in the bubble point test accounts for unique properties of the solid material that can affect the contact angle.

7. The effect of residual wetting fluid appears to be a source of error in bubble point testing. Residual wetting fluid was observed on samples of a No. 100 sieve screen after being exposed to pressures exceeding the theoretical critical pressure from the Washburn equation needed to expel fluid from the screen holes. The presence of this residual fluid results in non-convergence of the airflow rate vs. pore size curve of the wet run to the dry run. This resulted in the erroneous calculation of a distribution pore sizes for the No. 100 sieve screen. A theoretical explanation for the presence of residual fluid is the phenomenon of fluid deposition in capillary tubes, expressed mathematically by Bretherton's law. It is reasonable to consider that the same effect occurs with geotextile samples, and this may be the cause of wetting fluid-based differences in the calculated pore size distribution, particularly for smaller opening sizes.

8. The ideal wetting fluid for the bubble point test would have a low surface tension, a low viscosity, and a low vapor pressure. A low surface tension wetting fluid

will be more likely to have a contact angle of zero. A low viscosity is needed to minimize the Bretherton's law deposited fluid thickness, reducing residual fluid effects. Although not examined experimentally in this thesis, a low vapor pressure reduces the tendency for fluid evaporation. Evaporation of fluid in a pore before the critical pressure for the pore size is reached would be a source of error.

6.2 Recommendations for Future Research

The following recommendations are made for future research:

1. More observations of pore size distributions should be generated on multiple types of nonwoven geotextiles. Particularly, large numbers of observations would help to confirm whether pore sizes determined using the bubble point test for particular opening sizes follow a normal distribution. The automated data reduction spreadsheet will facilitate the generation of additional observations.

2. Operator dependence should be investigated using the results of multiple bubble point tests on geotextiles. Mean pore sizes distributions can be determined from the tests results of each operator, and ANOVA tests can be used to determine if there is a statistical significant difference in the mean pore sizes calculated using different operators.

3. More testing should be conducted on screens of known opening size to test the accuracy of bubble point test results. Both circular and non-circular holed screens should be used. Multiple bubble point tests could be conducted on the same screen and the statistical analyses presented in this thesis could be performed to

analyze the results. Different wetting fluids should be used to give further insight into the influence of the wetting fluid on pore size distributions determined using the bubble point method.

4. Bubble point tests on geotextiles as well as screens of known opening size should be attempted by performing the wet run first, followed by dry run. This may reduce the influence of the wetting fluid on the determined pore size distribution, however, verification is needed. Performing the wet run first and then immediately performing the dry run would have the added benefit of eliminating the need to switch the geotextile sample to a different dry run sample holder, which would reduce testing time.

5. The development of new filtration design criteria based on pore size distributions may be possible. Such criteria could include the specification of maximum pore sizes for larger opening sizes (e.g., O_{95}) to ensure retention of larger soil particles needed to promote bridging in the retained soil and the specification of minimum pore sizes for smaller opening sizes (e.g., O_{50}, O_{15}, etc.) to protect against clogging from fines, as suggested by Fischer et al. (1990). Tolerance limits may be particularly useful for assessing geotextile conformance to such maximum and minimum pore sizes because these limits enclose a percentage of the population at a specified level of confidence based on a limited number of observations. Geotextile filtration tests (e.g., hydraulic conductivity ratio test, ASTM D5567) coupled with the measurement of the smaller geotextile pore sizes using the bubble point method could be used to further investigate the influence of these smaller pore sizes on clogging.

References

Adamson, A. W. (1976). *Physical Chemistry of Surfaces*, 3rd Edition, John Wiley and Sons, New York.

ASTM (1989). *Standard Test Method for Pore Size Characteristics of Membrane Filters Using Automated Liquid Porosimeter*, E1294-89, ASTM International, West Conshohocken, PA.

ASTM (1999). *Standard Test Method for Surface Wettablility and Absorbency of Sheeted Materials Using an Automated Contact Angle Tester*, D5725-99, ASTM International, West Conshohocken, PA.

ASTM (2008). *Standard Practice for Dealing with Outlying Observations*, E178-08, ASTM International, West Conshohocken, PA.

ASTM (2010). *Standard Test Method for Determination of Pore Volume and Pore Volume Distribution of Soil and Rock by Mercury Intrusion Porosimetry*, D4404-10, ASTM International, West Conshohocken, PA.

ASTM (2011a). *Standard Practice for Determining the Specification Conformance of Geosynthetics*, D4759-11, ASTM International, West Conshohocken, PA.

ASTM (2011b). *Standard Terminology for Geosynthetics*, D4439-11, ASTM International, West Conshohocken, PA.

ASTM (2011c). *Standard Test Method for Pore Size Characteristics of Geotextiles by Capillary Flow Test*, D6767-11, ASTM International, West Conshohocken, PA.

ASTM (2011d). *Standard Test Methods for Pore Size Characteristics of Membrane Filters by Bubble Point and Mean Flow Pore Test*, F316-03, ASTM International, West Conshohocken, PA.

ASTM (2012). *Standard Test Method for Determining Apparent Opening Size of a Geotextile*, D4751-12, ASTM International, West Conshohocken, PA.

Aussillous, P., and Quéré, D. (2000). "Quick deposition of a fluid on the wall of a tube." *Physics of Fluids*, 12(10), 2367-2371.

Aydilek, A. H., Oguz, S. H., and Edil, T. B. (2005). "Constriction size of geotextile filters." *Journal of Geotechnical and Geoenvironmental Engineering*, 131(1), 28-38.

Aydilek, A. H., D'Hondt, D., and Holtz, R. D. (2007). "Comparative Evaluation of Geotextile Pore Sizes Using Bubble Point Test and Image Analysis." *ASTM Geotechnical Testing Journal*, 30(3), 1-9.

Bechhold, H. (1908). “The Permeability of Ultrafilters.” *Zeitschrift fuer Physik und Chemie*, 64, 328-342.

Berg, J. C. (1989). “The Use of Single-Fiber Wetting Measurements in the Assessment of Absorbency.” *Nonwovens: An Advanced Tutorial*, Turbak and Vigo, eds., 219-239.

Berg, J. C. (2010). *An introduction to interfaces and colloids, the bridge to nanoscience*, World Scientific Publishing Co. Pte. Ltd, Singapore.

Berthouex, P. M., and Brown, L. C. (2002). *Statistics for Environmental Engineers*, 2nd Edition, CRC Press, Boca Raton, Florida.

Bhatia, S. K., and Smith, J. L. (1994). “Comparative Study of Bubble Point Method and Mercury Intrusion Porosimetry Techniques for Characterizing the Pore-Size Distribution of Geotextiles.” *Geotextiles and Geomembranes*, 13, 679-702.

Bhatia, S. K., and Smith, J. L. (1995). “Application of the Bubble Point Method to the Characterization of the Pore-Size Distribution of Geotextiles.” *ASTM Geotechnical Testing* Journal, 18(1), 94-105.

Bhatia, S. K., and Smith, J. L. (1996a). “Geotextile Characterization and Pore-Size Distribution: Part I. A Review of Manufacturing Processes.” *Geosynthetics International*, 3(1), 85-105, <http://www.geosyntheticssociety.org/Resources/Archive/GI/src/V3I1/GI-V3-N1-Paper6.pdf> (March 25, 2013).

Bhatia, S. K., and Smith, J. L. (1996b). “Geotextile Characterization and Pore-Size Distribution: Part II. A Review of Test Methods and Results.” *Geosynthetics International*, 3(2), 155-180, <http://www.geosyntheticssociety.org/resources/archive/gi/src/v3i2/gi-v3-n2-paper1.pdf> (March 25, 2013).

Bhatia, S. K., Smith, J. L., and Christopher, B. R. (1996). “Geotextile Characterization and Pore-Size Distribution: Part III. Comparison of Methods and Application to Design.” *Geosynthetics International*, 3(3), 301-328, <http://www.geosyntheticssociety.org/Resources/Archive/GI/src/V3I3/GI-V3-N3-Paper1.pdf> (March 25, 2013).

Bikerman, J. J. (1958). *Surface Chemistry, Theory and Applications*, 2nd Edition, Academic Press Inc., New York.

Bretherton, F. P. (1961). ‘‘The motion of long bubbles in tubes,’’ *J. Fluid Mech.*, 10, 166.

Cahn (1996). *DCA Manual*, Cahn Instruments, Inc., Madison, WI.

Calvo, J. I., Hernández, A., Prádanos, P., Martínez, L., and Bowen, W. R. (1995). "Pore Size Distributions in Microporous Membranes, II. Bulk Characterization of Track-Etched Filters by Air Porometry and Mercury Porosimetry." *Journal of Colloid and Interface Science*, 176, 467-478.

Cantor, M. (1892). *Wied. Annalen.*, 47, 399.

Carroll, R. G. (1983). "Geotextile Filter Criteria." *Transportation Research Record 916*, Washington, DC, 46-53.

Carroll, R. G. (1987). "Hydraulic Properties of Geotextiles." *Geotextile Testing and the Design Engineer, ASTM STP 952*, Philadelphia, 7-20.

Cheryan, M. (1998). *Ultrafiltration and Microfiltration Handbook*, 2nd Edition, CRC Press, Boca Raton, FL.

Christopher, B. R., and Fischer, G. R. (1992). "Geotextile Filtration Principles, Practices, and Problems." *Geotextiles and Geomembranes*, 11, 337-353.

Corel Corporation (2005). Corel Photo Album™ (Version 6.3.3) [Software]. Available from <http://www.corel.com/corel/>.

Crow, Edwin L., Davis, Francis A., and Maxfield, Margaret W. (1960). *Statistics Manual*, Dover Publications, Inc., New York.

Cuperus, F. P., and Smolders C. A. (1991). “Characterization of UF Membranes, Membrane Characteristics and Characterization Techniques.” *Advances in Colloid and Interface Science*, 34, 135-173.

Decker, E. L., Frank, B., Suo, Y., and Garoff, S. (1999). *Colloids and Surfaces, A: Physiochemical and Engineering Aspects*, 156, 177-189.

de Gennes, P. G., Brochard-Wyart, F., and Quéré, D. (2004). *Capillarity and wetting phenomena*, Springer, New York.

de Mello, V. F. B. (1977). “Reflections on Design Decisions of Practical Significance to Embankment Dams”, *Geotechique*, 27(3), 279-355.

de Ryck, A. (2002). “The effect of weak inertia on the emptying of a tube.” *Physics of Fluids*, 14(7), 2102-2108.

D’Hondt, D. P. (2005). “An Investigation of the Pore Size Distribution of Geotextiles and Other Materials by the Bubble Point Method.” MSE Thesis, University of Washington, Seattle, WA.

Dierickx, W., and Myles, B. (1996). “Wet Sieving as a European EN-Standard for Determining the Characteristic Opening size of Geotextiles.” *Recent Developments in Geotextile Filters and Prefabricated Drainage Geocomposites*, ASTM Special Technical Publication No. 1281, S. Bhatia, D. Suits, editors, American Society for Testing and Materials, West Conshohocken, PA, 54-64.

Dussan V., E. B. (1979). “On the spreading of liquids on solid surfaces: static and dynamic contact lines.” *Annual Review of Fluid Mechanics*, Vol. 11, pp. 371-400.

Einstein, A., and Muehsam, H. (1923). “Experimental determination of pore size in filters.” *Deut. Med. Wochsch.,* 49(1923) 1012-1013.

Elsharief A. M., and Lovell, C. W. (1996). “Determination and Comparisons of the Pore Structure of Nonwoven Geotextiles.” *Recent Developments in Geotextile Filters and Prefabricated Drainage Geocomposites*, ASTM Special Technical Publication No. 1281, S. Bhatia, D. Suits, editors, American Society for Testing and Materials, West Conshohocken, PA, 35-53.

Elton, D. J., Hayes, D. W., and Adanur, S. (2007). “Bubblepoint Testing of Geotextiles: Apparatus and Operation.” *ASTM Geotechnical Testing Journal*, 30(1), 9-16.

Elton, D. J., and Hayes, D. W. (2007). "The Bubblepoint Method for Characterizing Geotextile Pore Size." *Geosynthetics in Reinforcement and Hydraulic Applications*, GeoDenver 2007, American Society of Civil Engineers, 1-10.

Elton, D. J., and Hayes, D. W. (2008a). "Discussion 'Comparative Evaluation of Geotextile Pore Sizes Using Bubble Point Test and Image Analysis' by Aydilek, A. H., D'Hondt, D., and Holtz, R. D." *ASTM Geotechnical Testing Journal*, 31(4), 1-2.

Elton, D. J., and Hayes, D. W. (2008b). "The significance of the contact angle in characterising the pore size distribution of geotextiles." *Geosynthetics International*, 15(1), 22-30.

Elton, D. J., and Hayes, D. W. (2009). "Residual Fluid as a Source of Error in Bubble Point Testing." *ASTM Geotechnical Testing Journal*, 32(2), 1-7.

Falyse, E., Rollin, A. L., Rigo, J. M., and Gourc, J. P. (1985). "Study of Different Techniques Used to Determine the Filtration Opening Size of Geotextiles." *Proceedings 2nd Canadian Conference Symposium on Geotextiles and Geomembranes*, 45-50.

Fayoux, D. (1977). "Filtration hydrodynamique des sols par des textiles." *Proceedings of the First International Conference on the Use of Fabrics in Geotechnics*, Paris, 329-332.

Fischer, G. R. (1994). “The Influence of Fabric Pore Structure on the Behavior of Geotextile Filters.” Doctoral dissertation, University of Washington, Seattle, WA.

Fischer, G. R., Christopher, B. R., and Holtz, R. D. (1990). “Filter Criteria Based on Pore Size Distribution.” *Fourth International Conference on Geotextiles, Geomembranes and Related Products,* A. A. Balkema Publishers, Brookfield, VT, 289-294.

Fischer, G., Holtz, R. D., and Christopher, B. R. (1996). “Evaluating Geotextile Pore Structure.”, *Recent Developments in Geotextile Filters and Prefabricated Drainage Geocomposites,* ASTM Special Technical Publication, No. 1281, S. Bhatia, D. Suits, editors, American Society for Testing and Materials, West Conshohocken, PA, 3-18.

Giroud, J. P., Delmas, P., and Artières, O. (1998) “Theoretical Basis for the Development of a Two-Layer Geotextile Filter.” *Proceedings of the 6th International Conference on Geosynthetics,* Atlanta, GA, 1037–1044.

Giroud, J. P. (undated paper). “Development of criteria for geotextile and granular filters.” <http://www.igs-uk.org/files/Deveolpment%20of%20criteria%20for%20geotextiles%20&%20granular%20filters.pdf> (September 10, 2012).

Good, R. J. (1984). “The Contact Angle of Mercury on the Internal Surfaces of Porous Bodies.” *Surface and Colloid Science,* Vol. 13, Plenum Press, 283-287.

Gourc, J. P., and Palmeira, E. M. (undated leaflet). “Geosynthetics in Drainage and Filtration.” *International Geosynthetics Society*, <http://www.geosyntheticssociety.org/Resources/Documents/Drainage%20and%20Filtration/English.pdf> (August 12, 2012).

Henry, K. S., and Patton, S. (1998). “Measurement of the Contact Angle of Water on Geotextile Fibers.” *ASTM Geotechnical Testing Journal*, 21(1), March, 11-17.

Huang, F., Wei, Q., Wang, X, and Xu, W. (2006). “Dynamic contact angles and morphology of PP fibres treated with plasma.” *Polymer Testing*, 25, 22-27.

Hutten, I. M. (2007). *Handbook of Nonwoven Filter Media*, Elsevier Science, Oxford, United Kingdom.

Jena, A., and Gupta, K. (2002). “Characterization of Pore Structure of Filtration Media.” Porous Materials, Inc., Ithaca, NY, <http://www.pmiapp.com/publications/docs/Characterization_of_pore_2002.pdf> (August 12, 2012).

Jenkins, L.M., and Donald, A. M. (1999). “Contact Angle Measurements on Fibers in the Environmental Scanning Electron Microscope.” *Langmuir*, Volume 15, 7829-7835.

Kenney, T. C., Chahal, R., Chiu, E., Ofoegbu, G. I., Omange, G.N., and Ume, C. A. (1985). "Controlling Constriction Sizes of Granular Filters." *Canadian Geotechnical Journal*, 22, 32-43.

Knoll, H. (1940). *Kolloid Zhur.*, 90(189).

Koerner, R. M. (2005). *Designing with Geosynthetics*, 5th Edition, Pearson Education, Inc., Upper Saddle River, NJ.

Koerner, R. M., and Koerner, G. R. (2011). *The Dual Roles for Using MARV*, GRI White Paper No. 10, Geosynthetic Institute, Folsom, PA, <http://www.geosynthetic-institute.org/papers/paper10.pdf> (August 12, 2012).

Korkut, E. N. (2003). “Geotextiles as Biofilm Attachment Baffles for Wastewater Treatment.” Doctoral thesis, Drexel University, Philadelphia, PA, <http://hdl.handle.net/1860/158> (March 25, 2013).

Lowell, S., Shields, J. E., Thomas, M. A., and Thommes, M. (2006). *Characterization of Porous Solids and Powders: Surface Area, Pore Size and Density*, Springer, Dordrecht, The Netherlands.

Manickam, S. S., and McCutcheon, J. R. (2012). “Characterization of polymeric nonwovens using porosimetry, porometry and X-ray computed tomography.” *Journal of Membrane Science*, 407-408(2012), 108-115.

Marino, R. J. (2006). “Geotextile Filter Treatment of Combined Sewer Discharges.” Doctoral thesis, Drexel University, Philadelphia, PA, <http://hdl.handle.net/1860/891> (March 25, 2013).

Masuelli, M., Marchese, J., and Ochoa, N. A. (2009). “SPC/PVDF membranes for emulsified oily wastewater treatment.” *Journal of Membrane Science*, 326(2009), 688-693.

McBain, J. W., and Kistler, S. S. (1930). *Transactions of the Faraday Society*, 33(157).

Mehta, T. (2012). “Interpolation.” <http://www.tushar-mehta.com/excel/newsgroups/interpolation/index.html> (March 20, 2013).

Menon, E. S. (2004). *Piping Calculations Manual*, McGraw-Hill, New York.

Microsoft (2013). “Create a dynamic named range on worksheet.” <http://office.microsoft.com/en-us/excel-help/create-a-dynamic-named-range-on-a-worksheet-HA001126115.aspx> (March 20, 2013).

Miller, B., and Young, R. (1975). “Methodology for Studying the Wettability of Filaments.” *Textile Research Journal*, 45(5), 359-365.

Miller, B., and Tyomkin, I. (1986). “An Extended Range Liquid Extrusion Method for Determining Pore Size Distributions.” *Textile Research Journal*, Vol. 56, No. 1, 35-40.

Minitab Inc. (2010a). Minitab® (Version 16.2) [Software]. Available from <http://www.minitab.com>.

Minitab Inc. (2010b). *Help File*, Minitab® (Version 16.2) [Software]. Available from <http://www.minitab.com>.

Mohammad, O. I., and Kibbey, T. C. G. (2005). “Dissolution-Induced Contact Angle Modification in Dense Nonaqueous Phase Liquids.” *Environmental Science and Technology*, Vol. 39, 1698-1706.

Neumann, A. W., and Good, R. J. (1977). “Techniques of Measuring Contact Angles.” *Surface and Colloid Science*, Vol. 11, R.J. Good & R.R. Stromberg, eds., Plenum Press, New York, 1977, 31.

OMEGA® (2013). “Rotameter Home Page.” <http://www.omega.com/prodinfo/rotameters.html> (March 25, 2013).

POROMETER (2012). “The Measurement Principle of Capillary Flow Porometry.” <http://www.porometer.com/porometers/technology/principle.html> (August 25, 2012).

Prapaharan, S., Holtz, R. D., and Luna, J. D. (1989). “Pore Size Distribution of Nonwoven Geotextiles.” *ASTM Geotechnical Testing Journal*, 12(4), 261-268.

Propex (2011). “Understanding Minimum Average Roll Value (MARV), Typical Values, and Minimum Value (MV).” Engineering Bulletin, Propex Operating Company, LLC, Chattanooga, TN, <http://www.geotextile.com/downloads/Propex%20EB-603%20Understanding%20MARV%20and%20Typical%20Values.pdf> (August 12, 2012).

Ruschak, K. J. (1985). ‘‘Coating flows.’’ *Annu. Rev. Fluid Mech.*, 17, 65.

Schwertz, E. A. (1949). *Journal of Applied Physics*, 20(1070).

Stan, C.A., Tang, S.K.Y., and Whitesides, G.M. (2009). *Supporting Information: Independent Control of Drop Size and Velocity in Microfluidic Flow-Focusing Generators Using Variable Temperature and Flow Rate*, <http://gmwgroup.harvard.edu/pubs/Supplemental/1045.pdf> (March 20, 2013).

Starkweather, B. A., Zhang, X., and Counce, R. M. (2000). “An Experimental Study of the Change in the Contact Angle of an Oil on a Solid Surface.” *Industrial and Engineering Chemistry Research*, Vol. 39, 362-366.

Scion Corporation (2005). Scion Image (Beta 4.0.3) [Software]. Available from: <http://scioncorp.com>.

Systat Software Inc. (2000). TableCurve 2D® (Version 5) [Software]. Available from <http://www.sigmaplot.com/products/tablecurve2d/tablecurve2d.php>.

Taylor, G. I. (1961). ‘‘Deposition of a viscous fluid on the wall of a tube,’’ *J. Fluid Mech.*, 10, 161.

TenCate (2011). *Understanding Porometer versus AOS Testing of a Geotextile*, TenCante Geosynthetics North America, August 22, <http://www.tencate.com/TenCate/Geosynthetics/documents/Tech%20Notes/TN_Porometer.pdf> (August 25, 2012).

The Engineering Toolbox (2013). “Surface Tension of Water in contact with Air.” <http://www.engineeringtoolbox.com/water-surface-tension-d_597.html> (March 20, 2013).

Tretinnikov, O. and Ikada, Y. (1994). "Dynamic Wetting and Contact Angle Hysterisis of Polymer Surfaces Studied with the Modified Wilhelmy Balance Technique." *Langmuir*, Vol. 10, No. 5, 1606-1614.

USEPA (2005). *Membrane Filtration Guidance Manual*, EPA 815-R-06-009, November, <http://www.epa.gov/safewater/disinfection/lt2/pdfs/guide_lt2_membranefiltration_final.pdf> (April 2, 2013).

USEPA (2001). *Risk Assessment Guidance for Superfund: Volume III – Part A, Process for Conducting Probabilistic Risk Assessment*, EPA 540-R-02-002, December, <http://www.epa.gov/oswer/riskassessment/rags3adt/index.htm> (February 10, 2013).

USEPA (2011a). ProUCL (Version 4.1.01) [Software]. Available from <http://www.epa.gov/osp/hstl/tsc/software.htm>.

USEPA (2011b). *ProUCL 4.0 Online Help Directory*. ProUCL (Version 4.1.01) [Software]. Available from <http://www.epa.gov/osp/hstl/tsc/software.htm>.

Unsal, E., Schwartz, P., and Dane, J. H. (2005). "Role of Capillarity in Penetration into and Flow Through Fibrous Barrier Materials." *Journal of Applied Polymer Science*, 95(4), 841-846.

Van de Velde, K., and Kiekens, P. (1999). Wettability of Natural Fibres used as Reinforcement for Composites." *Die Angewandte Makromolekulare Chemie,* Vol. 272, Nr. 4761, 97-93.

Vermeersch, O. G., and Mlynarek, J. (1996). "Determination of the Pore Size Distribution of Nonwoven Geotextiles by a Modified Capillary Flow Porometry Technique." *Recent Developments in Geotextile Filters and Prefabricated Drainage Geocomposites*, ASTM Special Technical Publication, No. 1281, S. Bhatia, D. Suits, eds., American Society for Testing and Materials, West Conshohocken, PA.

Washburn, E. W. (1921). "Note on a Method of Determining the Distribution of Pore Sizes in a Porous Material." *Proceedings of National Academy of Sciences,* 7(4), April, 115-116.

Wates, J. A. (1980). "Filtration, An Application of a Statistical Approach to Filters and Filter Fabrics." *Proceedings of the Seventh Regional Conference for Africa on Soil Mechanics and Foundation Engineering*, 433-440.

Webb, P. A. (2001). "An Introduction to the Physical Characterization of Materials by Mercury Intrusion Porosimetry with Emphasis on Reduction and Presentation of Experimental Data." *Micromeritics Instrument Corporation*, <http://www.micromeritics.com/pdf/app_articles/mercury_paper.pdf> (August 12, 2012).

Wenning, C. J. (2012). “Percent Difference – Percent Error.” *Student Laboratory Handbook*, Illinois State University Department of Physics, <http://www.phy.ilstu.edu/slh/Percent%20Difference%20Error.pdf> (August 12, 2012).

Wikipedia Commons (2008). <http://commons.wikimedia.org/wiki/File:Geotextile-GSI.JPG > (August 12, 2012).

Young, T. (1805). “An essay on the cohesion of fluids.” *Philosophical Transactions of the Royal Society of London*, 95, 65-87.

Yu, J., Hu, X., and Huang, Y. (2010). “A modification of the bubble-point method to determine the pore-mouth size distribution of porous materials.” *Separation and Purification Technology*, 70, 314-319.

Zeman, L. J,. and Zydney, A. L. (1996). *Microfiltration and Ultrafiltration: Principles and Applications*, Marcel Dekker, Inc., New York.

Appendix A: Automated Data Reduction Spreadsheet – PSD Calculation Sheet

A.1 Introduction

The automated data entry spreadsheet reduces the raw data recorded during the bubble point test and generates several standardized reports, including the graphical and tabular forms of the pore size distribution. The spreadsheet was developed using Microsoft Excel® 2003 and it is described generally in Section 4.4.2 of this thesis. This appendix describes the PSD Calculation sheet, which is a sheet within the automated data reduction spreadsheet workbook. The PSD Calculation sheet is neither a data entry sheet nor a standardized report, but rather, an intermediate calculation sheet where bubble point test data entered in the Data Entry Sheet is reduced to generate the graphical and tabular forms of the pore size distribution. An overview of the PSD Calculation sheet is shown in Figure A.1. There are four tables of data within the sheet. The tables and their functions are described as follows:

1. *Airflow Rate vs. Pore Size*: This table presents pore sizes and corresponding airflow rates for the wet and dry runs, as determined on the Data Entry Sheet. The table is setup to accommodate data points in rows 10 to 100, for a maximum of 101 data points.
2. *Plotted Pore Size Distribution*: This table calculates the interpolated dry run airflow rate for each wet run pore size and calculates the corresponding percent finer. The graphical pore size distribution is graphed using the wet run pore sizes and the plotted percent finer.

3. *Pore Size at Selected % Finer*: In this table, the tabular pore size distribution is determined by performing piecewise linear interpolation on the plotted (i.e., graphical) pore size distribution to determine the pore sizes at the selected values of percent finer.
4. *Determination of O_{98} Interpolation Point*: In this table, the last value in the Plotted % finer column that is greater than or equal to 98% is determined. This value is used to calculate the interpolated pore size at 98% finer.

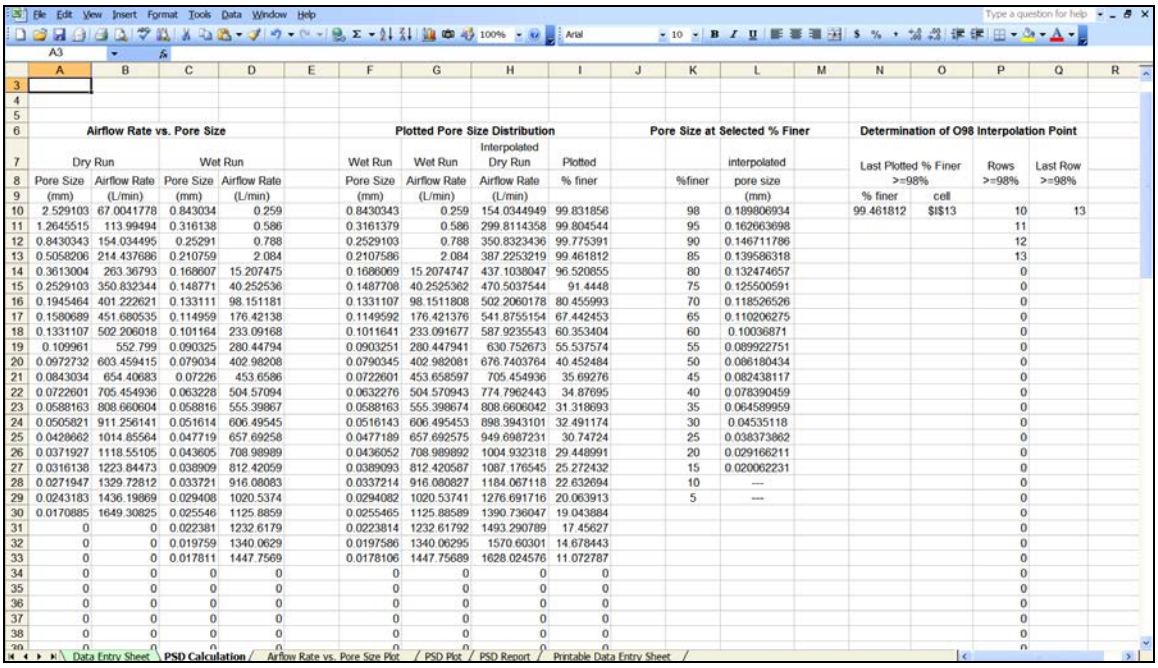

	Airflow Rate vs. Pore Size					Plotted Pore Size Distribution					Pore Size at Selected % Finer		Determination of O98 Interpolation Point			
	Dry Run		Wet Run			Wet Run	Wet Run	Interpolated Dry Run	Plotted			interpolated	Last Plotted % Finer >=98%		Rows >=98%	Last Row >=98%
	Pore Size (mm)	Airflow Rate (L/min)	Pore Size (mm)	Airflow Rate (L/min)		Pore Size (mm)	Airflow Rate (L/min)	Airflow Rate (L/min)	% finer		%finer	pore size (mm)	% finer	cell		
10	2.529103	67.0041778	0.843034	0.259		0.8430343	0.259	154.0344949	99.831856		98	0.189806934	99.461812	$I$13	10	13
11	1.2645515	113.99494	0.316138	0.586		0.3161379	0.586	299.8114358	99.804544		95	0.162663698			11	
12	0.8430343	154.034495	0.25291	0.788		0.2529103	0.788	350.8323436	99.775391		90	0.146711786			12	
13	0.5058206	214.437686	0.210759	2.084		0.2107586	2.084	387.2253219	99.461812		85	0.139586318			13	
14	0.3613004	263.36793	0.168607	15.207475		0.1686069	15.2074747	437.1038047	96.520855		80	0.132474657			0	
15	0.2529103	350.832344	0.148771	40.252536		0.1487708	40.2525362	470.5037544	91.4448		75	0.125500591			0	
16	0.1945464	401.222621	0.133111	98.151181		0.1331107	98.1511808	502.2060178	80.455993		70	0.118526526			0	
17	0.1580689	451.680535	0.114959	176.42138		0.1149592	176.421376	541.8755154	67.442453		65	0.110206275			0	
18	0.1331107	502.206018	0.101164	233.09168		0.1011641	233.091677	587.9235543	60.353404		60	0.10036871			0	
19	0.109961	552.799	0.090325	280.44794		0.0903251	280.447941	630.752673	55.537574		55	0.089922751			0	
20	0.0972732	603.459415	0.079034	402.98208		0.0790345	402.982081	676.7403764	40.452484		50	0.086180434			0	
21	0.0843034	654.40683	0.07226	453.6586		0.0722601	453.658597	705.454936	35.69276		45	0.082438117			0	
22	0.0722601	705.454936	0.063228	504.57094		0.0632276	504.570943	774.7962443	34.87695		40	0.078390459			0	
23	0.0588163	808.660604	0.058816	555.39867		0.0588163	555.398674	808.6606042	31.318693		35	0.064589959			0	
24	0.0505821	911.256141	0.051614	606.49545		0.0516143	606.495453	898.3943101	32.491174		30	0.04535118			0	
25	0.0428662	1014.85564	0.047719	657.69258		0.0477189	657.692575	949.6987231	30.74724		25	0.038373862			0	
26	0.0371927	1118.55105	0.043605	708.98989		0.0436052	708.989892	1004.932318	29.448991		20	0.029166211			0	
27	0.0316138	1223.84473	0.038909	812.42059		0.0389093	812.420587	1087.176545	25.272432		15	0.020062231			0	
28	0.0271947	1329.72812	0.033721	916.08083		0.0337214	916.080827	1184.067118	22.632694		10	---			0	
29	0.0243183	1436.19869	0.029408	1020.5374		0.0294082	1020.53741	1276.691716	20.063913		5	---			0	
30	0.0170885	1649.30825	0.025546	1125.8859		0.0255465	1125.88589	1390.736047	19.043884						0	
31	0	0	0.022381	1232.6179		0.0223814	1232.61792	1493.290789	17.45627						0	
32	0	0	0.019759	1340.0629		0.0197586	1340.06295	1570.60301	14.678443						0	
33	0	0	0.017811	1447.7569		0.0178106	1447.75689	1628.024576	11.072787						0	
34	0	0	0	0		0	0	0	0						0	
35	0	0	0	0		0	0	0	0						0	
36	0	0	0	0		0	0	0	0						0	
37	0	0	0	0		0	0	0	0						0	
38	0	0	0	0		0	0	0	0						0	

Figure A.1: Overview of the PSD Calculation sheet.

There are two key tools that enable the spreadsheet to be fully automated: dynamic named ranges and piecewise linear interpolation. For background information on these topics, see Microsoft (2013) and Mehta (2012), respectively. Dynamic named ranges are discussed in Section A.2. Piecewise linear interpolation is accomplished by the use of formulas within the spreadsheet cells. Specifically, piecewise linear interpolation is used to determine the Interpolated Dry Run Airflow Rate in the Plotted

Pore Size Distribution table and the interpolated pore size in the Pore Size at Selected % Finer table. Each of the formulas used in the sheet, including the piecewise linear interpolation methods, are discussed in Section A.3.

A.2 Dynamic Named Ranges

In Excel® 2003, ranges are defined by selecting (from the toolbar) Insert > Name > Define, as shown in Figure A.2. This displays the Define Name window shown in Figure A.3, where names and cell ranges can be defined. Ranges can be defined as a static range of cells, such as A1:A10, or as a dynamic range in which the size of the named range is a function of cell values. One of the main advantages of dynamic ranges in regard to spreadsheet automation is the ability to define a range as all numbers in a column that are greater than zero. For example, if values in column A will be used as the x-axis for a graph, the source data for the graph can be a dynamic named ranged instead of a static range that may contain values of zero in addition to the data of interest. This way, the graph will only include entered data points, regardless of how many are entered.

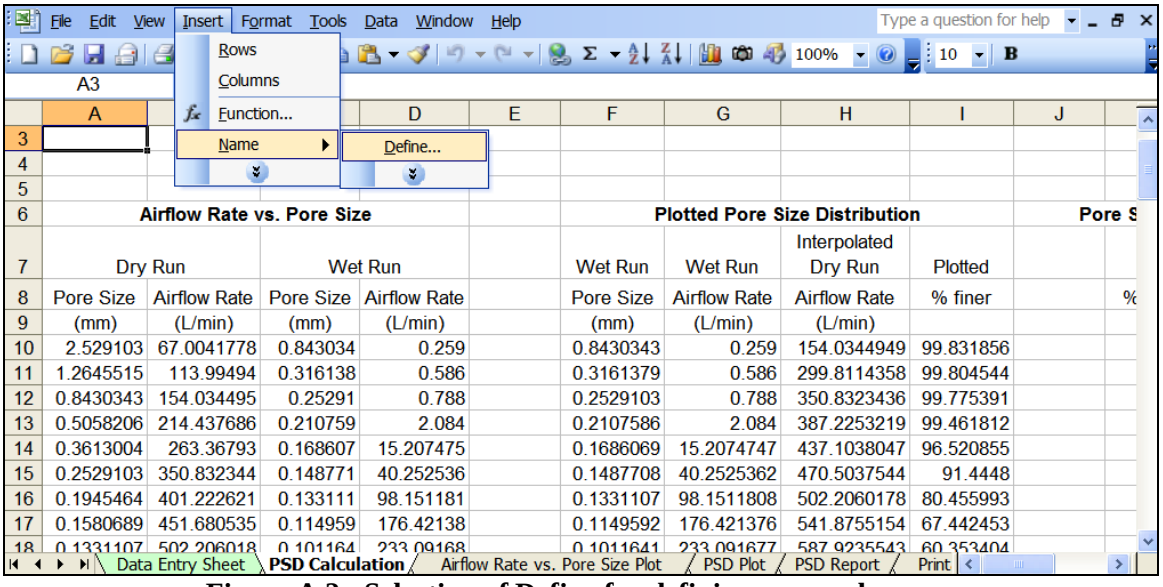

Figure A.2: Selection of Define for defining a named range.

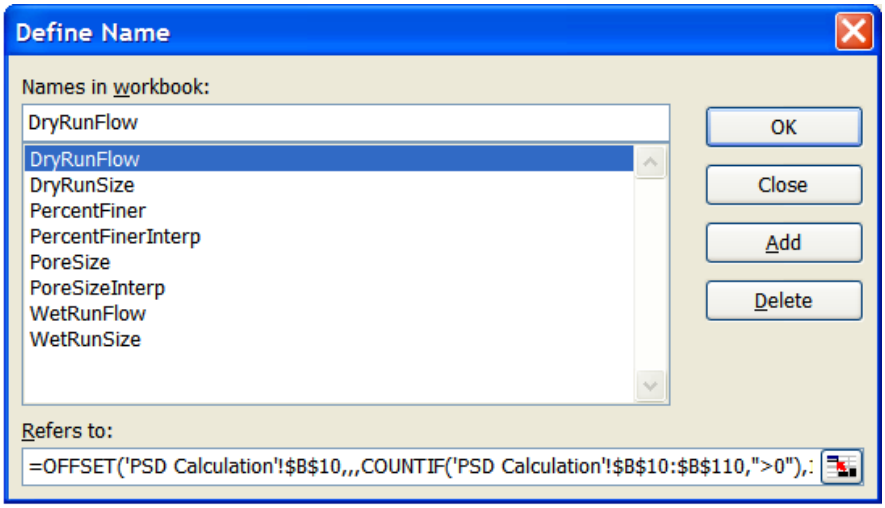

Figure A.3: The Define Name widow.

The dynamic range names, formulas, and purposes are described as follows:

Name: DryRunSize

Formula: =OFFSET('PSD Calculation'!$A$10,,,COUNTIF('PSD Calculation'!$A$10:$A$110,">0"),1)

Purpose: This range defines the dry run pore size range as cell A10 to the last cell in column A with a value greater than zero. This range is used as the x-axis values for the dry run plot on the Airflow Rate vs. Pore Size graph.

Name: DryRunFlow

Formula: =OFFSET('PSD Calculation'!$B$10,,,COUNTIF('PSD Calculation'!$B$10:$B$110,">0"),1)

Purpose: This range defines the dry run airflow rate range as cell B10 to the last cell in column B with a value greater than zero. This range is used as the y-axis values for the dry run plot on the Airflow Rate vs. Pore Size graph.

Name: WetRunSize

Formula: =OFFSET('PSD Calculation'!$C$10,,,COUNTIF('PSD Calculation'!$C$10:$C$110,">0"),1)

Purpose: This range defines the wet run pore size range as cell C10 to the last cell in column C with a value greater than zero. This range is used as the x-axis values for the wet run plot on the Airflow Rate vs. Pore Size graph.

Name: WetRunFlow

Formula: =OFFSET('PSD Calculation'!$D$10,,,COUNTIF('PSD Calculation'!$D$10:$D$110,">0"),1)

Purpose: This range defines the wet run airflow rate range as cell D10 to the last cell in column D with a value greater than zero. This range is used as the y-axis values for the wet run plot on the Airflow Rate vs. Pore Size graph.

Name: PoreSize

Formula: =OFFSET('PSD Calculation'!$F$10,,,COUNTIF('PSD Calculation'!$F$10:$F$110,">0"),1)

Purpose: This range defines the pore sizes for the graphical (plotted) pore size distribution as cell F10 to the last cell in column F with a value greater

than zero. This range is used as the x-axis values for graphical pore size distribution (Plotted PSD report).

Name: PercentFiner

Formula: =OFFSET('PSD Calculation'!$I$10,,,COUNTIF('PSD Calculation'!$I$10:$I$110,">0"),1)

Purpose: This range defines the percent finer for the graphical (plotted) pore size distribution as cell I10 to the last cell in column I with a value greater than zero. This range is used as the y-axis values for the graphical pore size distribution (Plotted PSD report).

Name: PercentFinerInterp

Formula: =OFFSET(INDIRECT('PSD Calculation'!$O$10),,,100,1)

Purpose: This range defines a range in column I beginning at the last plotted % finer value greater than or equal to 98% and includes all other lesser values of the plotted % finer. This range is used in the interpolation formula for the O_{98} pore size in the tabular pore size distribution.

Name: PoreSizeInterp

Formula: =OFFSET(INDIRECT(ADDRESS('PSD Calculation'!$Q$10,6)),,,100,1)

Purpose: This range defines a range in column F beginning at the last row where the plotted % finer value in column I is greater than or equal to 98% and includes all other rows with lesser values of plotted % finer. This range is

used in the interpolation formula for the O_{98} pore size in the tabular pore size distribution.

A.3 Formulas

Range: Column A, Dry Run Pore Size for the Airflow Rate vs. Pore Size graph

Example Formula:

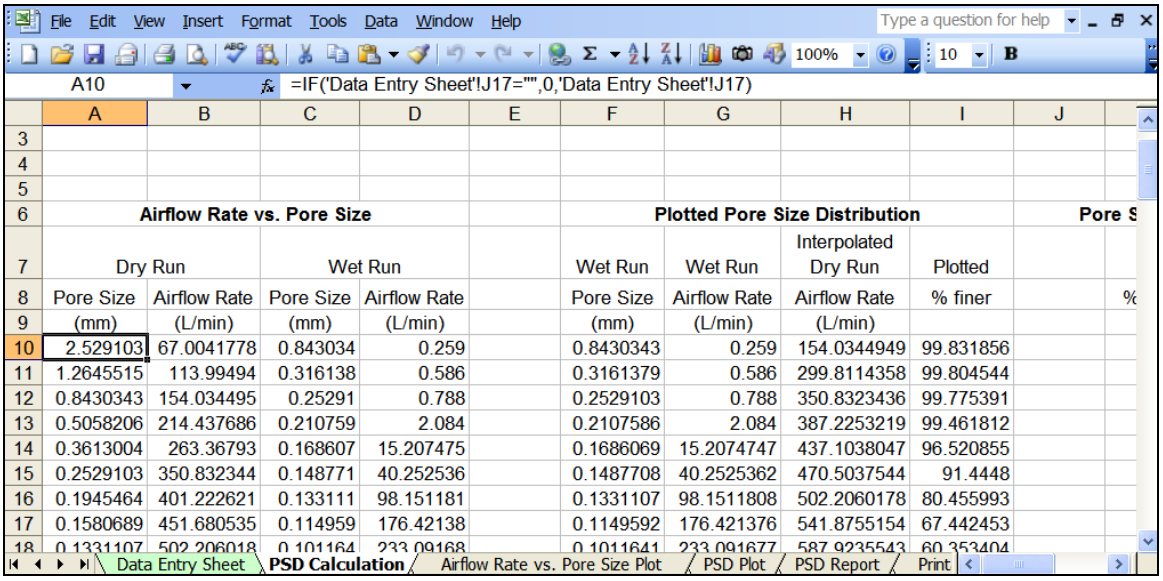

	A	B	C	D	E	F	G	H	I	J
3										
4										
5										
6	**Airflow Rate vs. Pore Size**					**Plotted Pore Size Distribution**				**Pore S**
7	Dry Run		Wet Run			Wet Run	Wet Run	Interpolated Dry Run	Plotted	
8	Pore Size	Airflow Rate	Pore Size	Airflow Rate		Pore Size	Airflow Rate	Airflow Rate	% finer	%
9	(mm)	(L/min)	(mm)	(L/min)		(mm)	(L/min)	(L/min)		
10	2.529103	67.0041778	0.843034	0.259		0.8430343	0.259	154.0344949	99.831856	
11	1.2645515	113.99494	0.316138	0.586		0.3161379	0.586	299.8114358	99.804544	
12	0.8430343	154.034495	0.25291	0.788		0.2529103	0.788	350.8323436	99.775391	
13	0.5058206	214.437686	0.210759	2.084		0.2107586	2.084	387.2253219	99.461812	
14	0.3613004	263.36793	0.168607	15.207475		0.1686069	15.2074747	437.1038047	96.520855	
15	0.2529103	350.832344	0.148771	40.252536		0.1487708	40.2525362	470.5037544	91.4448	
16	0.1945464	401.222621	0.133111	98.151181		0.1331107	98.1511808	502.2060178	80.455993	
17	0.1580689	451.680535	0.114959	176.42138		0.1149592	176.421376	541.8755154	67.442453	
18	0.1331107	502.206018	0.101164	233.09168		0.1011641	233.091677	587.9235543	60.353404	

Figure A.4: Example formula for Column A.

Purpose: This formula displays the Dry Run Pore Size calculated in the Data Entry Sheet. Once all values are displayed, the formula returns a value of zero.

Range: Column B, Dry Run Airflow Rate for the Airflow Rate vs. Pore Size graph

Example Formula:

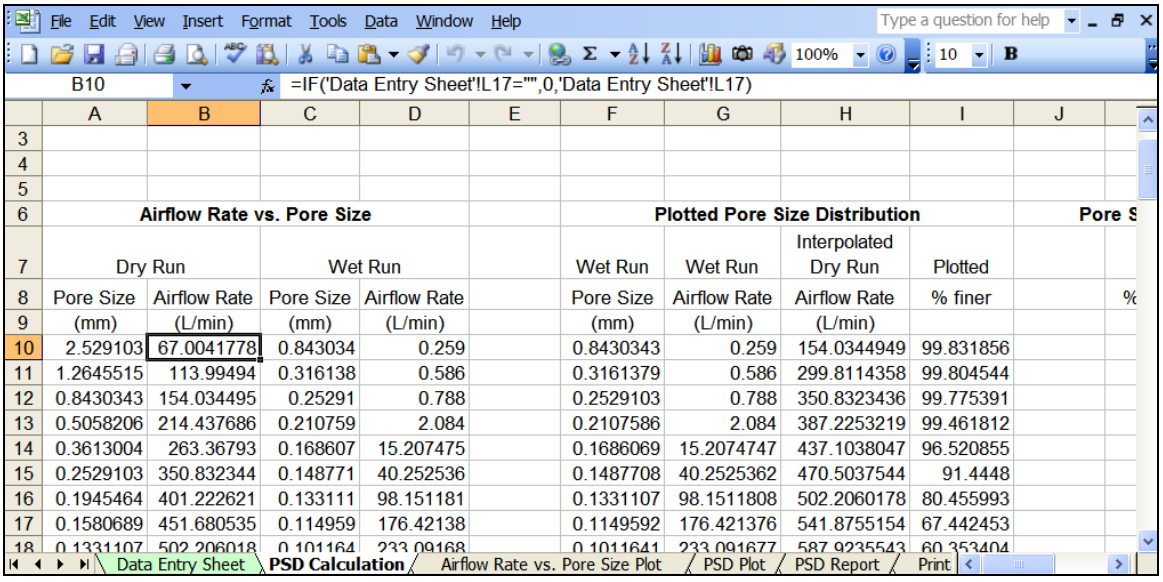

File Edit View Insert Format Tools Data Window Help — Type a question for help

B10 =IF('Data Entry Sheet'!L17="",0,'Data Entry Sheet'!L17)

	A	B	C	D	E	F	G	H	I	J
3										
4										
5										
6	**Airflow Rate vs. Pore Size**					**Plotted Pore Size Distribution**				**Pore S**
7	Dry Run		Wet Run			Wet Run	Wet Run	Interpolated Dry Run	Plotted	
8	Pore Size	Airflow Rate	Pore Size	Airflow Rate		Pore Size	Airflow Rate	Airflow Rate	% finer	%
9	(mm)	(L/min)	(mm)	(L/min)		(mm)	(L/min)	(L/min)		
10	2.529103	67.0041778	0.843034	0.259		0.8430343	0.259	154.0344949	99.831856	
11	1.2645515	113.99494	0.316138	0.586		0.3161379	0.586	299.8114358	99.804544	
12	0.8430343	154.034495	0.25291	0.788		0.2529103	0.788	350.8323436	99.775391	
13	0.5058206	214.437686	0.210759	2.084		0.2107586	2.084	387.2253219	99.461812	
14	0.3613004	263.36793	0.168607	15.207475		0.1686069	15.2074747	437.1038047	96.520855	
15	0.2529103	350.832344	0.148771	40.252536		0.1487708	40.2525362	470.5037544	91.4448	
16	0.1945464	401.222621	0.133111	98.151181		0.1331107	98.1511808	502.2060178	80.455993	
17	0.1580689	451.680535	0.114959	176.42138		0.1149592	176.421376	541.8755154	67.442453	
18	0.1331107	502.206018	0.101164	233.09168		0.1011641	233.091677	587.9235543	60.353404	

Data Entry Sheet | **PSD Calculation** | Airflow Rate vs. Pore Size Plot | PSD Plot | PSD Report | Print

Figure A.5: Example formula for Column B.

Purpose: This formula displays the Dry Run True Airflow Rate calculated in the Data Entry Sheet. Once all values are displayed, the formula returns a value of zero.

Range: Column C, Wet Run Pore Size for the Airflow Rate vs. Pore Size graph

Example Formula:

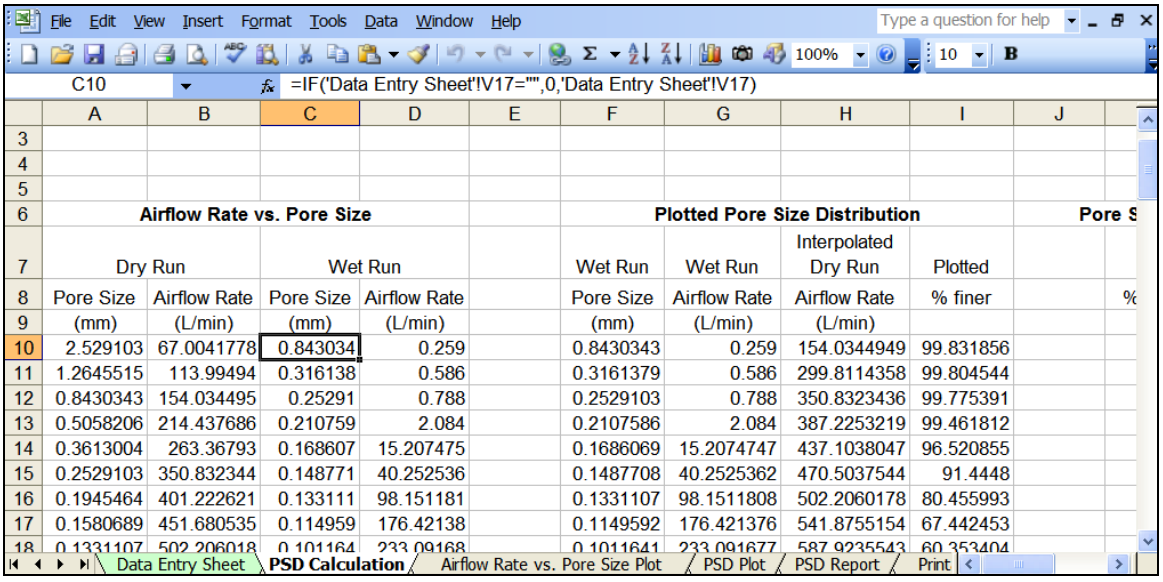

File Edit View Insert Format Tools Data Window Help — Type a question for help

C10 =IF('Data Entry Sheet'!V17="",0,'Data Entry Sheet'!V17)

	A	B	C	D	E	F	G	H	I	J
3										
4										
5										
6	**Airflow Rate vs. Pore Size**					**Plotted Pore Size Distribution**				**Pore S**
7	Dry Run		Wet Run			Wet Run	Wet Run	Interpolated Dry Run	Plotted	
8	Pore Size	Airflow Rate	Pore Size	Airflow Rate		Pore Size	Airflow Rate	Airflow Rate	% finer	%
9	(mm)	(L/min)	(mm)	(L/min)		(mm)	(L/min)	(L/min)		
10	2.529103	67.0041778	0.843034	0.259		0.8430343	0.259	154.0344949	99.831856	
11	1.2645515	113.99494	0.316138	0.586		0.3161379	0.586	299.8114358	99.804544	
12	0.8430343	154.034495	0.25291	0.788		0.2529103	0.788	350.8323436	99.775391	
13	0.5058206	214.437686	0.210759	2.084		0.2107586	2.084	387.2253219	99.461812	
14	0.3613004	263.36793	0.168607	15.207475		0.1686069	15.2074747	437.1038047	96.520855	
15	0.2529103	350.832344	0.148771	40.252536		0.1487708	40.2525362	470.5037544	91.4448	
16	0.1945464	401.222621	0.133111	98.151181		0.1331107	98.1511808	502.2060178	80.455993	
17	0.1580689	451.680535	0.114959	176.42138		0.1149592	176.421376	541.8755154	67.442453	
18	0.1331107	502.206018	0.101164	233.09168		0.1011641	233.091677	587.9235543	60.353404	

Data Entry Sheet | **PSD Calculation** | Airflow Rate vs. Pore Size Plot | PSD Plot | PSD Report | Print

Figure A.6: Example formula for Column C.

Purpose: This formula displays the Wet Run Pore Size calculated in the Data Entry Sheet. Once all values are displayed, the formula returns a value of zero.

Range: Column D, Wet Run Airflow Rate for the Airflow Rate vs. Pore Size graph

Example Formula:

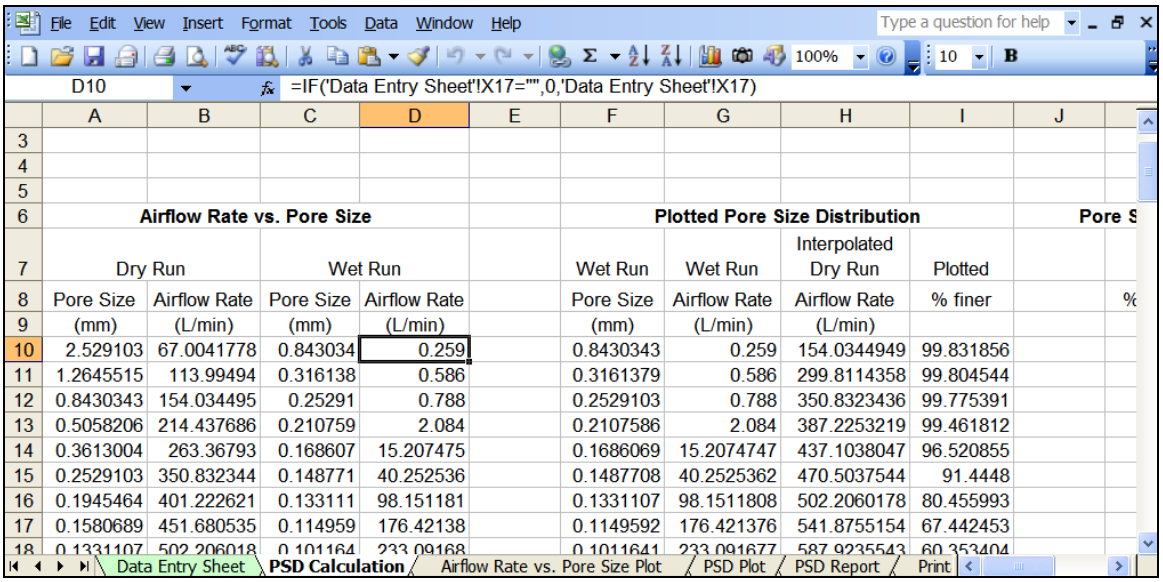

	A	B	C	D	E	F	G	H	I	J
3										
4										
5										
6	**Airflow Rate vs. Pore Size**					**Plotted Pore Size Distribution**				**Pore S**
7	Dry Run		Wet Run			Wet Run	Wet Run	Interpolated Dry Run	Plotted	
8	Pore Size	Airflow Rate	Pore Size	Airflow Rate		Pore Size	Airflow Rate	Airflow Rate	% finer	%
9	(mm)	(L/min)	(mm)	(L/min)		(mm)	(L/min)	(L/min)		
10	2.529103	67.0041778	0.843034	0.259		0.8430343	0.259	154.0344949	99.831856	
11	1.2645515	113.99494	0.316138	0.586		0.3161379	0.586	299.8114358	99.804544	
12	0.8430343	154.034495	0.25291	0.788		0.2529103	0.788	350.8323436	99.775391	
13	0.5058206	214.437686	0.210759	2.084		0.2107586	2.084	387.2253219	99.461812	
14	0.3613004	263.36793	0.168607	15.207475		0.1686069	15.2074747	437.1038047	96.520855	
15	0.2529103	350.832344	0.148771	40.252536		0.1487708	40.2525362	470.5037544	91.4448	
16	0.1945464	401.222621	0.133111	98.151181		0.1331107	98.1511808	502.2060178	80.455993	
17	0.1580689	451.680535	0.114959	176.42138		0.1149592	176.421376	541.8755154	67.442453	
18	0.1331107	502.206018	0.101164	233.09168		0.1011641	233.091677	587.9235543	60.353404	

Figure A.7: Example formula for Column D.

Purpose: This formula displays the Wet Run Airflow Rate calculated in the Data Entry Sheet. Once all values are displayed, the formula returns a value of zero.

Range: Column F, Wet Run Pore Size for the Plotted Pore Size Distribution

Example Formula:

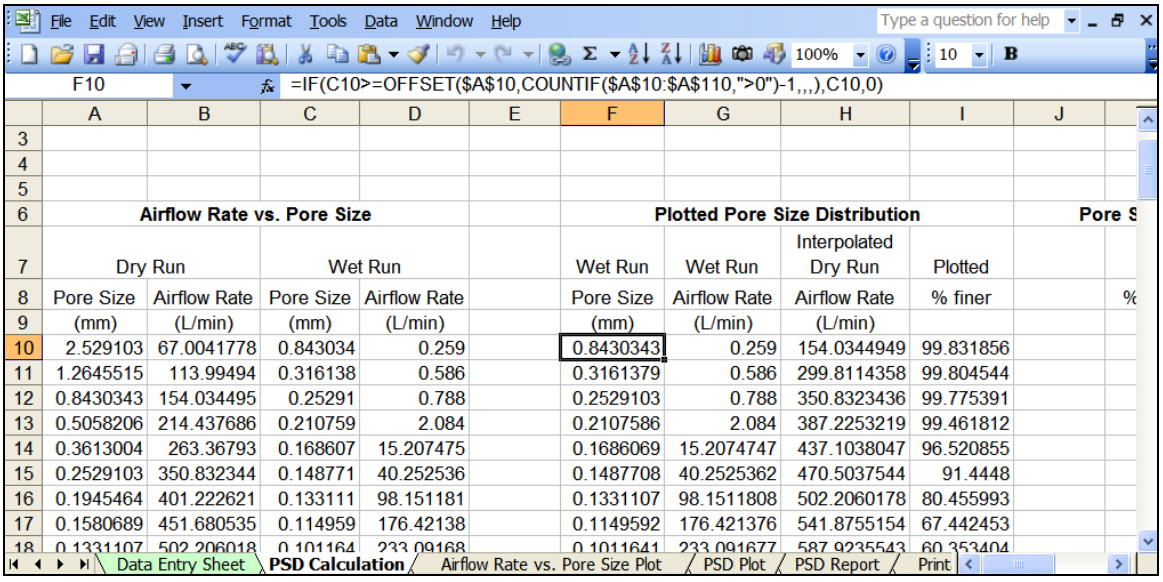

	A	B	C	D	E	F	G	H	I	J
3										
4										
5										
6	**Airflow Rate vs. Pore Size**					**Plotted Pore Size Distribution**				**Pore S**
7	Dry Run		Wet Run			Wet Run	Wet Run	Interpolated Dry Run	Plotted	
8	Pore Size	Airflow Rate	Pore Size	Airflow Rate		Pore Size	Airflow Rate	Airflow Rate	% finer	%
9	(mm)	(L/min)	(mm)	(L/min)		(mm)	(L/min)	(L/min)		
10	2.529103	67.0041778	0.843034	0.259		0.8430343	0.259	154.0344949	99.831856	
11	1.2645515	113.99494	0.316138	0.586		0.3161379	0.586	299.8114358	99.804544	
12	0.8430343	154.034495	0.25291	0.788		0.2529103	0.788	350.8323436	99.775391	
13	0.5058206	214.437686	0.210759	2.084		0.2107586	2.084	387.2253219	99.461812	
14	0.3613004	263.36793	0.168607	15.207475		0.1686069	15.2074747	437.1038047	96.520855	
15	0.2529103	350.832344	0.148771	40.252536		0.1487708	40.2525362	470.5037544	91.4448	
16	0.1945464	401.222621	0.133111	98.151181		0.1331107	98.1511808	502.2060178	80.455993	
17	0.1580689	451.680535	0.114959	176.42138		0.1149592	176.421376	541.8755154	67.442453	
18	0.1331107	502.206018	0.101164	233.09168		0.1011641	233.091677	587.9235543	60.353404	

Figure A.8: Example formula for Column F.

Purpose: This formula displays the Wet Run Pore Size shown in Column C, provided that there is a Dry Run Pore Size of equal or greater value. Otherwise, a value of zero is displayed.

Range: Column G, Wet Run Airflow Rate for the Plotted Pore Size Distribution

Example Formula:

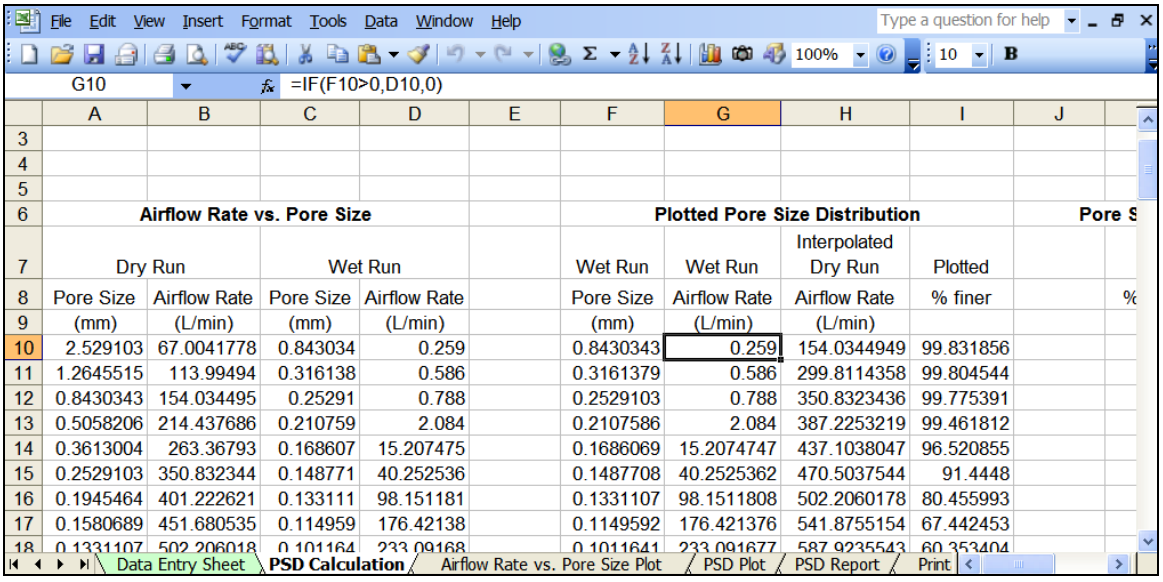

	A	B	C	D	E	F	G	H	I	J
3										
4										
5										
6	**Airflow Rate vs. Pore Size**					**Plotted Pore Size Distribution**				**Pore S**
7	Dry Run		Wet Run			Wet Run	Wet Run	Interpolated Dry Run	Plotted	
8	Pore Size	Airflow Rate	Pore Size	Airflow Rate		Pore Size	Airflow Rate	Airflow Rate	% finer	%
9	(mm)	(L/min)	(mm)	(L/min)		(mm)	(L/min)	(L/min)		
10	2.529103	67.0041778	0.843034	0.259		0.8430343	0.259	154.0344949	99.831856	
11	1.2645515	113.99494	0.316138	0.586		0.3161379	0.586	299.8114358	99.804544	
12	0.8430343	154.034495	0.25291	0.788		0.2529103	0.788	350.8323436	99.775391	
13	0.5058206	214.437686	0.210759	2.084		0.2107586	2.084	387.2253219	99.461812	
14	0.3613004	263.36793	0.168607	15.207475		0.1686069	15.2074747	437.1038047	96.520855	
15	0.2529103	350.832344	0.148771	40.252536		0.1487708	40.2525362	470.5037544	91.4448	
16	0.1945464	401.222621	0.133111	98.151181		0.1331107	98.1511808	502.2060178	80.455993	
17	0.1580689	451.680535	0.114959	176.42138		0.1149592	176.421376	541.8755154	67.442453	
18	0.1331107	502.206018	0.101164	233.09168		0.1011641	233.091677	587.9235543	60.353404	

Figure A.9: Example formula for Column G.

Purpose: This formula displays the Wet Run Airflow Rate shown in Column D, provided that there is a corresponding Wet Run Pore Size displayed in Column F. Otherwise, a value of zero is displayed.

Range: Column H, Dry Run Airflow Rate for the Plotted Pore Size Distribution

Example Formula:

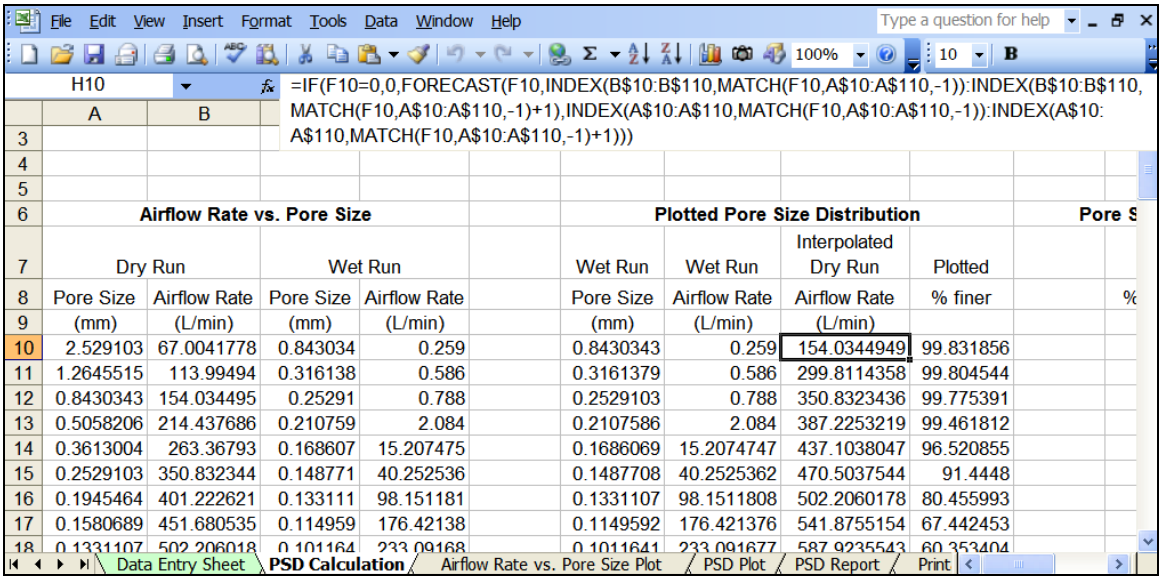

H10 =IF(F10=0,0,FORECAST(F10,INDEX(B$10:B$110,MATCH(F10,A$10:A$110,-1)):INDEX(B$10:B$110,MATCH(F10,A$10:A$110,-1)+1),INDEX(A$10:A$110,MATCH(F10,A$10:A$110,-1)):INDEX(A$10:A$110,MATCH(F10,A$10:A$110,-1)+1)))

	A	B	C	D	E	F	G	H	I	J	K
6	Airflow Rate vs. Pore Size					Plotted Pore Size Distribution				Pore S	
7	Dry Run		Wet Run			Wet Run	Wet Run	Interpolated Dry Run	Plotted		
8	Pore Size	Airflow Rate	Pore Size	Airflow Rate		Pore Size	Airflow Rate	Airflow Rate	% finer		%
9	(mm)	(L/min)	(mm)	(L/min)		(mm)	(L/min)	(L/min)			
10	2.529103	67.0041778	0.843034	0.259		0.8430343	0.259	154.0344949	99.831856		
11	1.2645515	113.99494	0.316138	0.586		0.3161379	0.586	299.8114358	99.804544		
12	0.8430343	154.034495	0.25291	0.788		0.2529103	0.788	350.8323436	99.775391		
13	0.5058206	214.437686	0.210759	2.084		0.2107586	2.084	387.2253219	99.461812		
14	0.3613004	263.36793	0.168607	15.207475		0.1686069	15.2074747	437.1038047	96.520855		
15	0.2529103	350.832344	0.148771	40.252536		0.1487708	40.2525362	470.5037544	91.4448		
16	0.1945464	401.222621	0.133111	98.151181		0.1331107	98.1511808	502.2060178	80.455993		
17	0.1580689	451.680535	0.114959	176.42138		0.1149592	176.421376	541.8755154	67.442453		
18	0.1331107	502.206018	0.101164	233.09168		0.1011641	233.091677	587.9235543	60.353404		

Data Entry Sheet | PSD Calculation | Airflow Rate vs. Pore Size Plot | PSD Plot | PSD Report | Print

Figure A.10: Example formula for Column H.

Purpose: This formula performs piecewise linear interpolation to calculate the Dry Run Airflow Rate for the corresponding Wet Run Pore Size in Column F. A value of zero is displayed if the corresponding cell in Column F is zero.

Example 1:

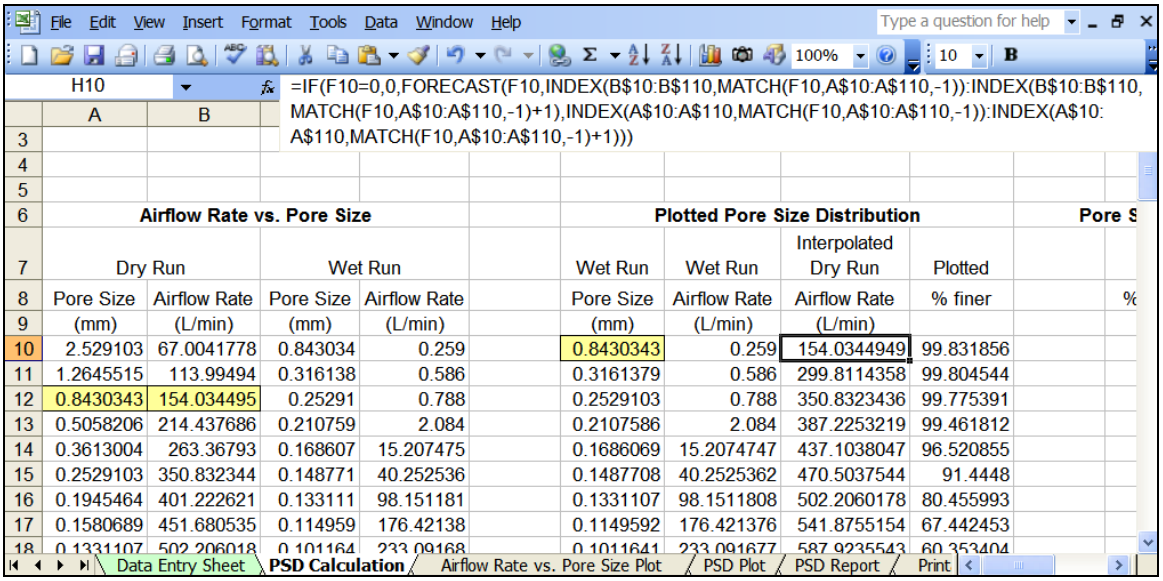

H10 =IF(F10=0,0,FORECAST(F10,INDEX(B$10:B$110,MATCH(F10,A$10:A$110,-1)):INDEX(B$10:B$110,MATCH(F10,A$10:A$110,-1)+1),INDEX(A$10:A$110,MATCH(F10,A$10:A$110,-1)):INDEX(A$10:A$110,MATCH(F10,A$10:A$110,-1)+1)))

	A	B	C	D	E	F	G	H	I	J	K
6	Airflow Rate vs. Pore Size					Plotted Pore Size Distribution				Pore S	
7	Dry Run		Wet Run			Wet Run	Wet Run	Interpolated Dry Run	Plotted		
8	Pore Size	Airflow Rate	Pore Size	Airflow Rate		Pore Size	Airflow Rate	Airflow Rate	% finer		%
9	(mm)	(L/min)	(mm)	(L/min)		(mm)	(L/min)	(L/min)			
10	2.529103	67.0041778	0.843034	0.259		0.8430343	0.259	154.0344949	99.831856		
11	1.2645515	113.99494	0.316138	0.586		0.3161379	0.586	299.8114358	99.804544		
12	0.8430343	154.034495	0.25291	0.788		0.2529103	0.788	350.8323436	99.775391		
13	0.5058206	214.437686	0.210759	2.084		0.2107586	2.084	387.2253219	99.461812		
14	0.3613004	263.36793	0.168607	15.207475		0.1686069	15.2074747	437.1038047	96.520855		
15	0.2529103	350.832344	0.148771	40.252536		0.1487708	40.2525362	470.5037544	91.4448		
16	0.1945464	401.222621	0.133111	98.151181		0.1331107	98.1511808	502.2060178	80.455993		
17	0.1580689	451.680535	0.114959	176.42138		0.1149592	176.421376	541.8755154	67.442453		
18	0.1331107	502.206018	0.101164	233.09168		0.1011641	233.091677	587.9235543	60.353404		

Data Entry Sheet | PSD Calculation | Airflow Rate vs. Pore Size Plot | PSD Plot | PSD Report | Print

Figure A.11: Example 1 for the formula in Column H.

Explanation: In Example 1, the Wet Run Pore Size in Column F has an exact matching Dry Run Pore Size in Column A. Therefore, piecewise linear interpolation is not needed to find the Dry Run Airflow Rate and the value in Column H is simply the value from Column B.

Example 2:

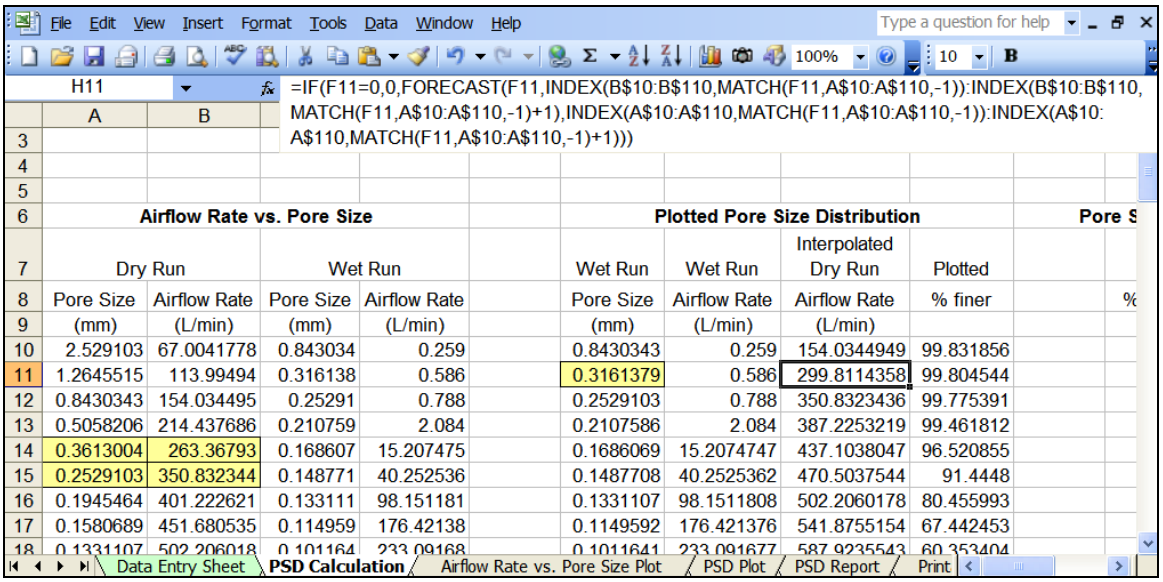

	A	B	C	D	F	G	H	I	
6	Airflow Rate vs. Pore Size				Plotted Pore Size Distribution				Pore S
7	Dry Run		Wet Run		Wet Run	Wet Run	Interpolated Dry Run	Plotted	
8	Pore Size	Airflow Rate	Pore Size	Airflow Rate	Pore Size	Airflow Rate	Airflow Rate	% finer	%
9	(mm)	(L/min)	(mm)	(L/min)	(mm)	(L/min)	(L/min)		
10	2.529103	67.0041778	0.843034	0.259	0.8430343	0.259	154.0344949	99.831856	
11	1.2645515	113.99494	0.316138	0.586	0.3161379	0.586	299.8114358	99.804544	
12	0.8430343	154.034495	0.25291	0.788	0.2529103	0.788	350.8323436	99.775391	
13	0.5058206	214.437686	0.210759	2.084	0.2107586	2.084	387.2253219	99.461812	
14	0.3613004	263.36793	0.168607	15.207475	0.1686069	15.2074747	437.1038047	96.520855	
15	0.2529103	350.832344	0.148771	40.252536	0.1487708	40.2525362	470.5037544	91.4448	
16	0.1945464	401.222621	0.133111	98.151181	0.1331107	98.1511808	502.2060178	80.455993	
17	0.1580689	451.680535	0.114959	176.42138	0.1149592	176.421376	541.8755154	67.442453	
18	0.1331107	502.206018	0.101164	233.09168	0.1011641	233.091677	587.9235543	60.353404	

Figure A.12: Example 2 for the formula in Column H.

Explanation: In Example 2, there is no matching Dry Run Pore Size for the Wet Run Pore Size in Column F, so piecewise linear interpolation is needed to find the Dry Run Airflow Rate at this pore size. The formula identifies the Dry Run Pore Sizes immediately greater and less than the pore size of interest and performs linear interpolation to find the Dry Run Airflow Rate that corresponds to the Wet Run Pore Size. The values in Column A and B being used for interpolation are highlighted.

Range: Column I, Plotted % Finer

Example Formula:

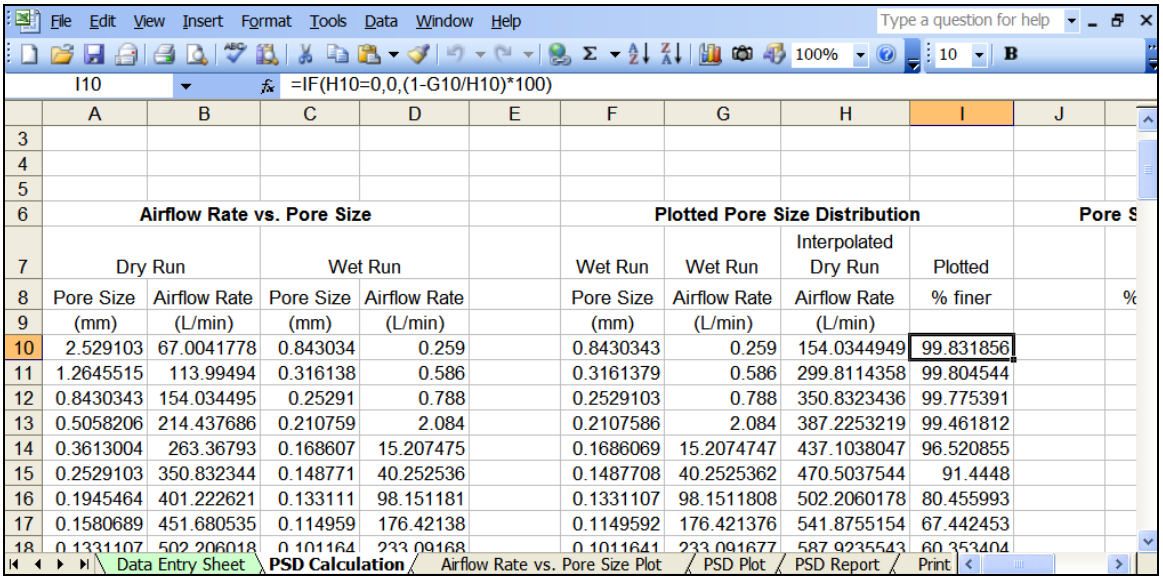

File Edit View Insert Format Tools Data Window Help — Type a question for help

I10 =IF(H10=0,0,(1-G10/H10)*100)

	A	B	C	D	E	F	G	H	I	J
3										
4										
5										
6	**Airflow Rate vs. Pore Size**					**Plotted Pore Size Distribution**				**Pore S**
7	Dry Run		Wet Run			Wet Run	Wet Run	Interpolated Dry Run	Plotted	
8	Pore Size	Airflow Rate	Pore Size	Airflow Rate		Pore Size	Airflow Rate	Airflow Rate	% finer	%
9	(mm)	(L/min)	(mm)	(L/min)		(mm)	(L/min)	(L/min)		
10	2.529103	67.0041778	0.843034	0.259		0.8430343	0.259	154.0344949	99.831856	
11	1.2645515	113.99494	0.316138	0.586		0.3161379	0.586	299.8114358	99.804544	
12	0.8430343	154.034495	0.25291	0.788		0.2529103	0.788	350.8323436	99.775391	
13	0.5058206	214.437686	0.210759	2.084		0.2107586	2.084	387.2253219	99.461812	
14	0.3613004	263.36793	0.168607	15.207475		0.1686069	15.2074747	437.1038047	96.520855	
15	0.2529103	350.832344	0.148771	40.252536		0.1487708	40.2525362	470.5037544	91.4448	
16	0.1945464	401.222621	0.133111	98.151181		0.1331107	98.1511808	502.2060178	80.455993	
17	0.1580689	451.680535	0.114959	176.42138		0.1149592	176.421376	541.8755154	67.442453	
18	0.1331107	502.206018	0.101164	233.09168		0.1011641	233.091677	587.9235543	60.353404	

Data Entry Sheet | **PSD Calculation** | Airflow Rate vs. Pore Size Plot | PSD Plot | PSD Report | Print

Figure A.13: Example formula for Column I.

Purpose: This formula calculates the % Finer for the pore size in Column F based on the Wet and Dry Run Airflow Rates in Columns G and H (using Equation 4.6).

Range: Cell L10, interpolated pore size for 98% Finer

Example Formula:

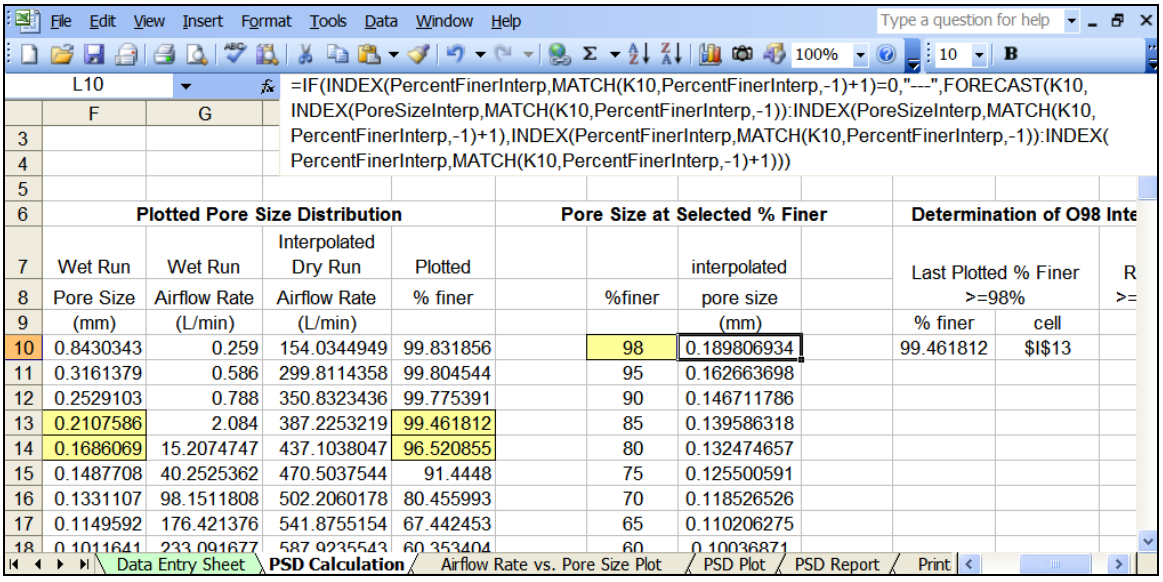

	F	G								
3										
4										
5										
6	**Plotted Pore Size Distribution**					**Pore Size at Selected % Finer**		**Determination of O98 Inte**		
7	Wet Run	Wet Run	Interpolated Dry Run	Plotted			interpolated	Last Plotted % Finer		R
8	Pore Size	Airflow Rate	Airflow Rate	% finer		%finer	pore size	>=98%		>=
9	(mm)	(L/min)	(L/min)				(mm)	% finer	cell	
10	0.8430343	0.259	154.0344949	99.831856		98	0.189806934	99.461812	$I$13	
11	0.3161379	0.586	299.8114358	99.804544		95	0.162663698			
12	0.2529103	0.788	350.8323436	99.775391		90	0.146711786			
13	0.2107586	2.084	387.2253219	99.461812		85	0.139586318			
14	0.1686069	15.2074747	437.1038047	96.520855		80	0.132474657			
15	0.1487708	40.2525362	470.5037544	91.4448		75	0.125500591			
16	0.1331107	98.1511808	502.2060178	80.455993		70	0.118526526			
17	0.1149592	176.421376	541.8755154	67.442453		65	0.110206275			
18	0.1011641	233.091677	587.9235543	60.353404		60	0.10036871			

Figure A.14: Example formula for Cell L10.

Purpose: This formula uses piecewise linear interpolation to calculate the pore size corresponding to 98% Finer. The highlighted values show the pore sizes in Column F and the % finer in Column I being used for interpolation.

Range: Column L (excluding Cell L10), interpolated pore size for selected % finer

Example Formula:

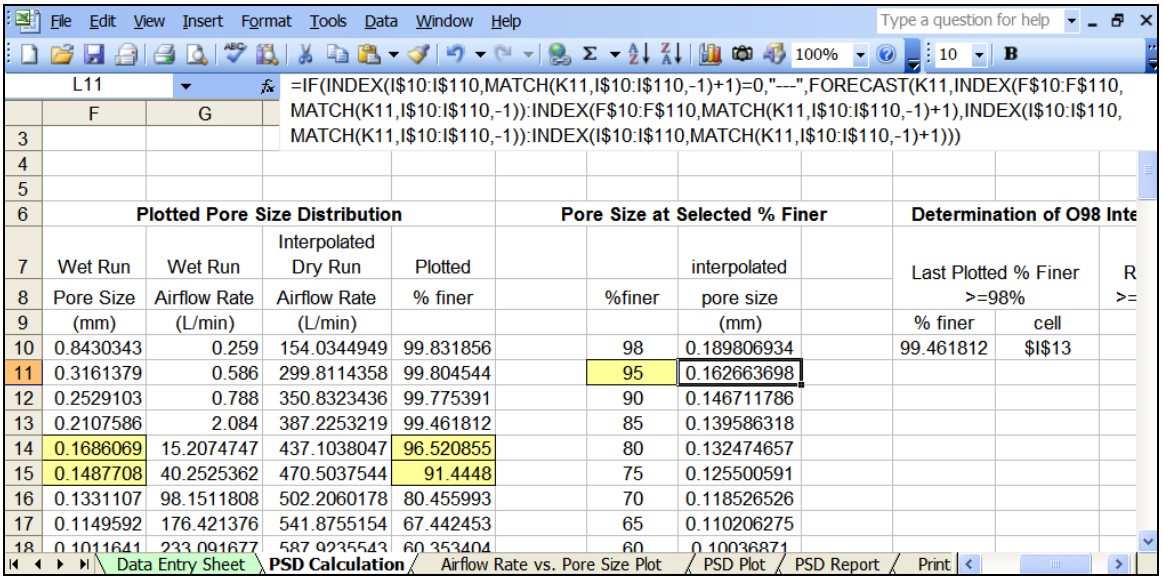

	F	G								
3										
4										
5										
6	**Plotted Pore Size Distribution**					**Pore Size at Selected % Finer**		**Determination of O98 Inte**		
7	Wet Run	Wet Run	Interpolated Dry Run	Plotted			interpolated	Last Plotted % Finer >=98%		R
8	Pore Size	Airflow Rate	Airflow Rate	% finer		%finer	pore size			>=
9	(mm)	(L/min)	(L/min)				(mm)	% finer	cell	
10	0.8430343	0.259	154.0344949	99.831856		98	0.189806934	99.461812	$I$13	
11	0.3161379	0.586	299.8114358	99.804544		95	0.162663698			
12	0.2529103	0.788	350.8323436	99.775391		90	0.146711786			
13	0.2107586	2.084	387.2253219	99.461812		85	0.139586318			
14	0.1686069	15.2074747	437.1038047	96.520855		80	0.132474657			
15	0.1487708	40.2525362	470.5037544	91.4448		75	0.125500591			
16	0.1331107	98.1511808	502.2060178	80.455993		70	0.118526526			
17	0.1149592	176.421376	541.8755154	67.442453		65	0.110206275			
18	0.1011641	233.091677	587.9235543	60.353404		60	0.10036871			

Figure A.15: Example formula for Column L (excluding Cell L10).

Purpose: This formula uses piecewise linear interpolation to calculate the pore size corresponding to the selected values of % Finer. The highlighted values show the pore sizes in Column F and the % Finer in Column I being used for interpolation at 95% Finer.

Range: Cell N10, Last Plotted % Finer >=98%

Example Formula:

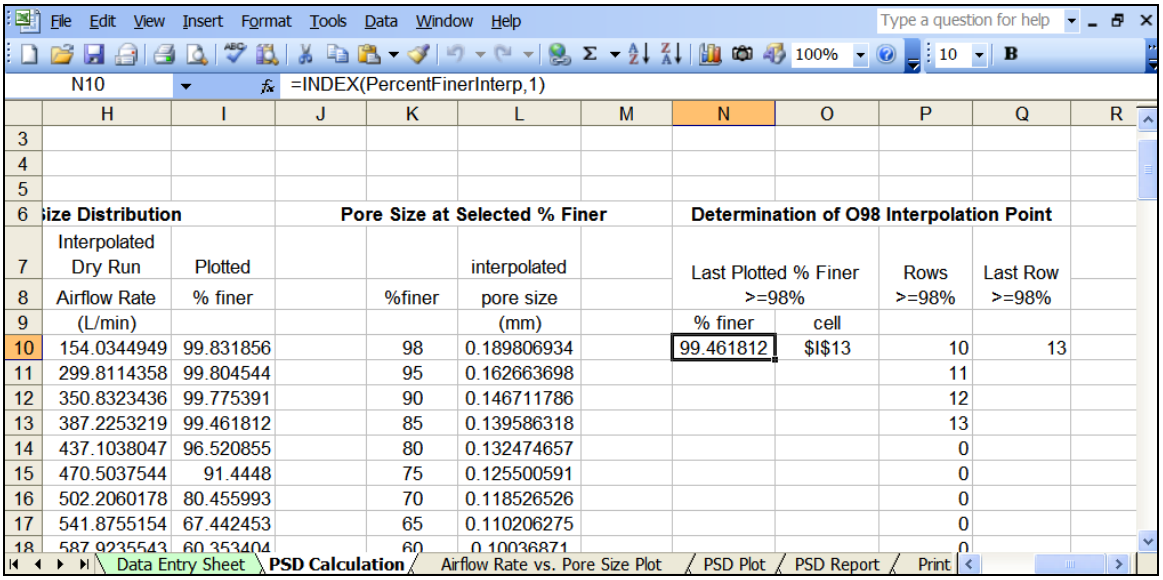

Figure A.16: Example formula for Cell N10.

Purpose: This formula displays the last plotted % finer value in Column I that is greater or equal to 98%. This value is used to determine the interpolated pore size in Column L for the 98% finer value.

Range: Cell O10, cell address for Last Plotted % Finer >=98%

Example Formula:

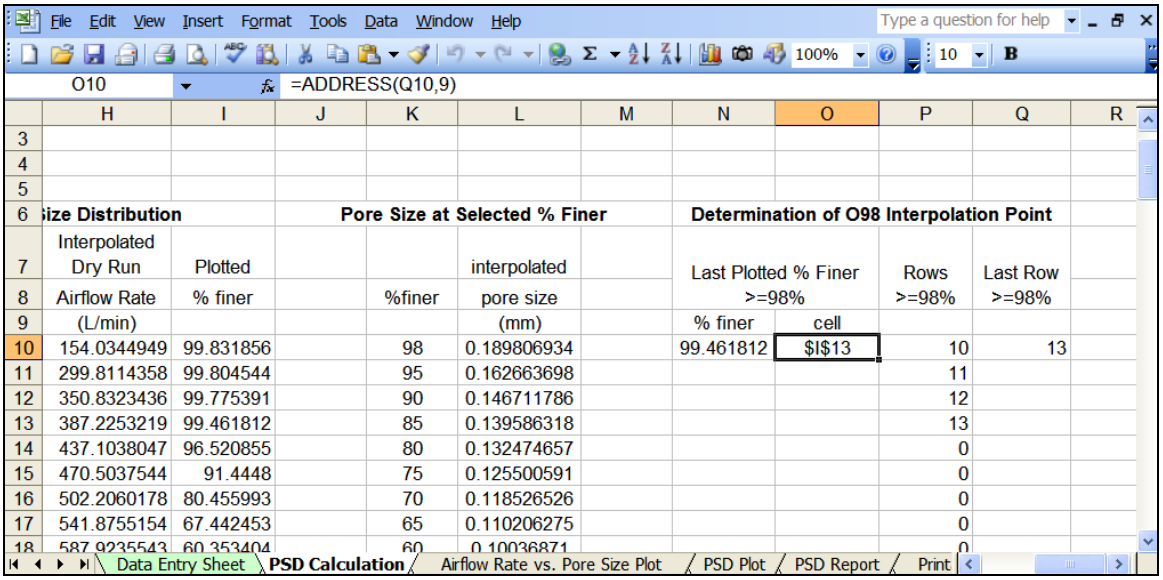

Figure A.17: Example formula for Cell O10.

Purpose: This formula displays the cell address for the last plotted % finer value in Column I that is greater or equal to 98%, according to the row listed in cell Q10.

Range: Column P, Rows with Plotted % Finer values >= 98%

Example Formula:

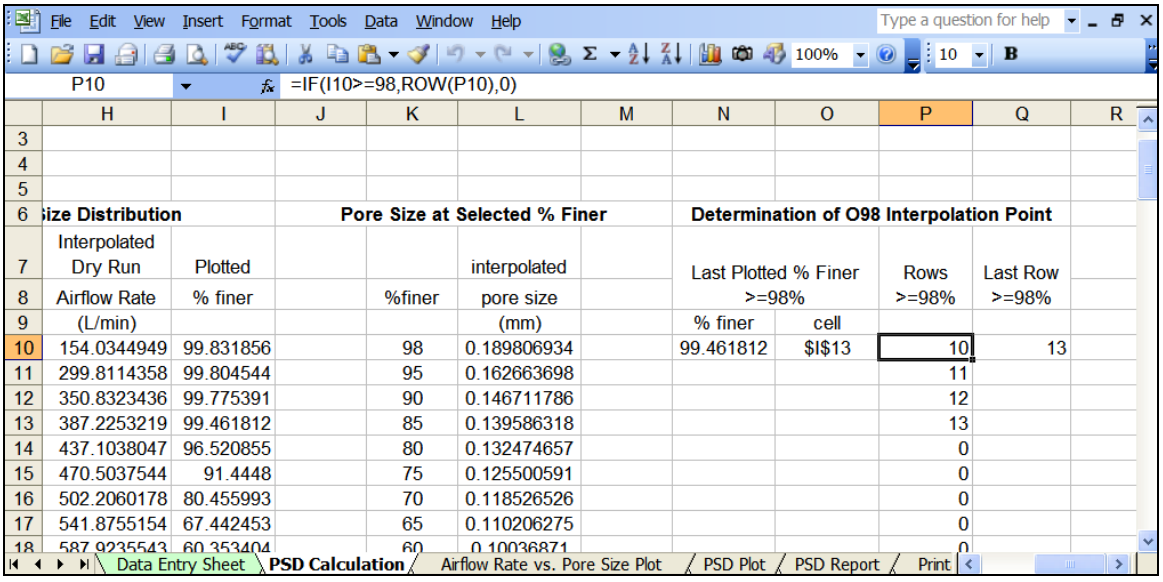

	H	I	J	K	L	M	N	O	P	Q	R
3											
4											
5											
6	**ize Distribution**			**Pore Size at Selected % Finer**			**Determination of O98 Interpolation Point**				
7	Interpolated Dry Run	Plotted			interpolated		Last Plotted % Finer		Rows	Last Row	
8	Airflow Rate	% finer		%finer	pore size		>=98%		>=98%	>=98%	
9	(L/min)				(mm)		% finer	cell			
10	154.0344949	99.831856		98	0.189806934		99.461812	$I$13	10	13	
11	299.8114358	99.804544		95	0.162663698				11		
12	350.8323436	99.775391		90	0.146711786				12		
13	387.2253219	99.461812		85	0.139586318				13		
14	437.1038047	96.520855		80	0.132474657				0		
15	470.5037544	91.4448		75	0.125500591				0		
16	502.2060178	80.455993		70	0.118526526				0		
17	541.8755154	67.442453		65	0.110206275				0		
18	587.9235543	60.353404		60	0.10036871				0		

Data Entry Sheet | PSD Calculation | Airflow Rate vs. Pore Size Plot | PSD Plot | PSD Report | Print

Figure A.18: Example formula for Column P.

Purpose: This formula displays the row value if the value in Column I is greater or equal to 98%.

Range: Column P, Rows with Plotted % Finer values >= 98%

Example Formula:

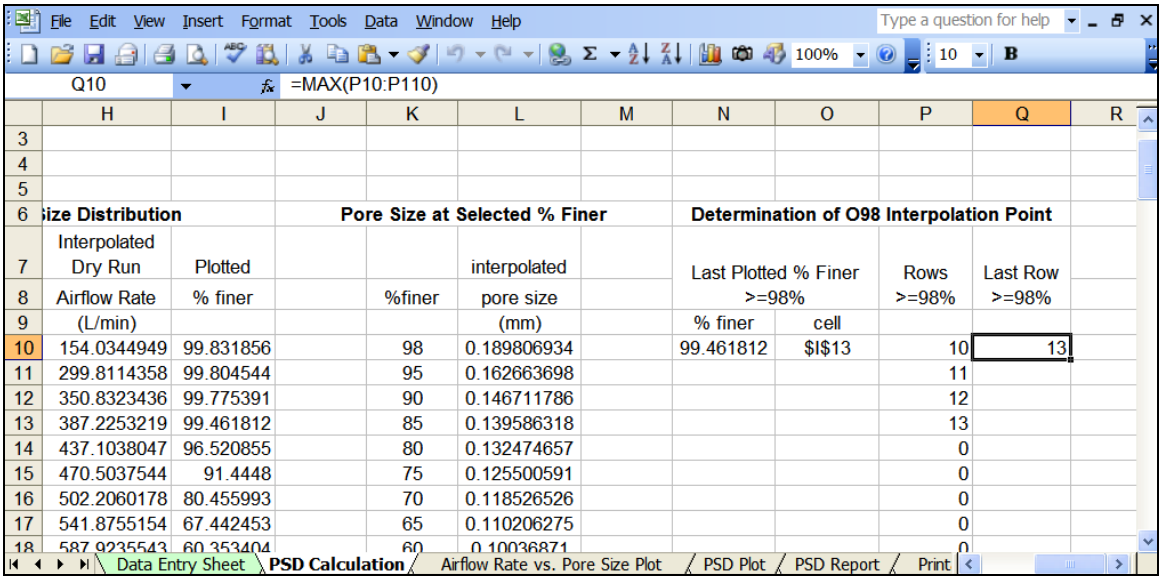

	H	I	J	K	L	M	N	O	P	Q	R
3											
4											
5											
6	**ize Distribution**			**Pore Size at Selected % Finer**			**Determination of O98 Interpolation Point**				
7	Interpolated Dry Run	Plotted			interpolated		Last Plotted % Finer >=98%		Rows >=98%	Last Row >=98%	
8	Airflow Rate	% finer		%finer	pore size						
9	(L/min)				(mm)		% finer	cell			
10	154.0344949	99.831856		98	0.189806934		99.461812	$I$13	10	13	
11	299.8114358	99.804544		95	0.162663698				11		
12	350.8323436	99.775391		90	0.146711786				12		
13	387.2253219	99.461812		85	0.139586318				13		
14	437.1038047	96.520855		80	0.132474657				0		
15	470.5037544	91.4448		75	0.125500591				0		
16	502.2060178	80.455993		70	0.118526526				0		
17	541.8755154	67.442453		65	0.110206275				0		
18	587.9235543	60.353404		60	0.10036871				0		

Data Entry Sheet | PSD Calculation | Airflow Rate vs. Pore Size Plot | PSD Plot | PSD Report | Print

Figure A.19: Example formula for Cell Q10.

Purpose: This formula displays the maximum value in Column P, which is the last row number that has a Column I value greater or equal to 98%.

Appendix B: Bubble Point Test Data for the NG-1 Nonwoven Geotextile

B.1 Tests with Water as the Wetting Fluid

Bubble Point Test
Auburn University - Department of Civil Engineering

date of test: 8/22/2002
test identification: water 1
test performed by: David Howie
wetting fluid: distilled water
ambient air temperature: 22 °C
porous media: NG-1 nonwoven geotextile
comments: testing to determine geotextile pore size distribution

Pore Size Calculation Parameters:
constant, C: 2860 mm/m
contact angle: 67.53 degrees
surface tension: 0.07275 N/m

Dry Run											
Recorded Data							Calculations				
Indirect Reading Rotameters				Direct Reading Rotameter Value (L/min)	Pressure at Rotameter Exit (psig)	Half of Manometer Reading (mm H20)	Manometer Reading (mm H20)	Manometer Pressure (Pa)	Pore Size (Diameter) (mm)	Indicated Airflow Rate (L/min)	True Airflow Rate (L/min)
First Rotameter Used		Second Rotameter Used									
Rotameter ID Number	Rotameter Value	Rotameter ID Number	Rotameter Value								
5	34				0.06	1	2	19.62	4.0531278	50.7	50.80336
5	52				0.14	2	4	39.24	2.0265639	77.2	77.56675
5	83				0.34	4	8	78.48	1.013282	125	126.4373
5	75	5	62		0.31	8	16	156.96	0.506641	205.5	207.6555
5	97	5	80		0.53	12	24	235.44	0.3377607	269	273.8064
				350	0.05	16	32	313.92	0.2533205	350	350.5947
				400	0.07	20	40	392.4	0.2026564	400	400.9512
				450	0.08	25	50	490.5	0.1621251	450	451.2228
				500	0.1	29	58	568.98	0.139763	500	501.6978
				550	0.11	34	68	667.08	0.1192096	550	552.054
				600	0.13	40	80	784.8	0.1013282	600	602.6472
				650	0.15	46	92	902.52	0.0881115	650	653.3079
				700	0.17	52	104	1020.24	0.0779448	700	704.036
				800	0.24	64	128	1255.68	0.0633301	800	806.5042
				900	0.29	77	154	1510.74	0.052638	900	908.8342
				1000	0.34	91	182	1785.42	0.0445399	1000	1011.499
				1100	0.4	105	210	2060.1	0.0386012	1100	1114.866
				1200	0.46	122	244	2393.64	0.0332224	1200	1218.631
				1300	0.54	144	288	2825.28	0.0281467	1300	1323.662
				1400	0.61	164	328	3217.68	0.0247142	1400	1428.752
				1600	0.77	227	454	4453.74	0.0178552	1600	1641.37

Wet Run											
Recorded Data							Calculations				
Indirect Reading Rotameters				Direct Reading Rotameter Value (L/min)	Pressure at Rotameter Exit (psig)	Half of Manometer Reading (mm H20)	Manometer Reading (mm H20)	Manometer Pressure (Pa)	Pore Size (Diameter) (mm)	Indicated Airflow Rate (L/min)	True Airflow Rate (L/min)
First Rotameter Used		Second Rotameter Used									
Rotameter ID Number	Rotameter Value	Rotameter ID Number	Rotameter Value								
2	89					30	60	588.6	0.1351043	1.886	1.886
4	37				0.19	34	68	667.08	0.1192096	12.8	12.88246
				650	0.15	46	92	902.52	0.0881115	650	653.3079
				700	0.18	53	106	1039.86	0.0764741	700	704.2727
				800	0.26	64	128	1255.68	0.0633301	800	807.0438
				900	0.31	80	160	1569.6	0.0506641	900	909.4403
				1000	0.37	94	188	1844.28	0.0431184	1000	1012.507
				1100	0.42	109	218	2138.58	0.0371847	1100	1115.604
				1200	0.49	127	254	2491.74	0.0319144	1200	1219.836
				1300	0.55	145	290	2844.9	0.0279526	1300	1324.096
				1400	0.63	165	330	3237.3	0.0245644	1400	1429.685
				1600	0.77	278	556	5454.36	0.0145796	1600	1641.37

Figure B.1: Water 1 recorded data and calculations.

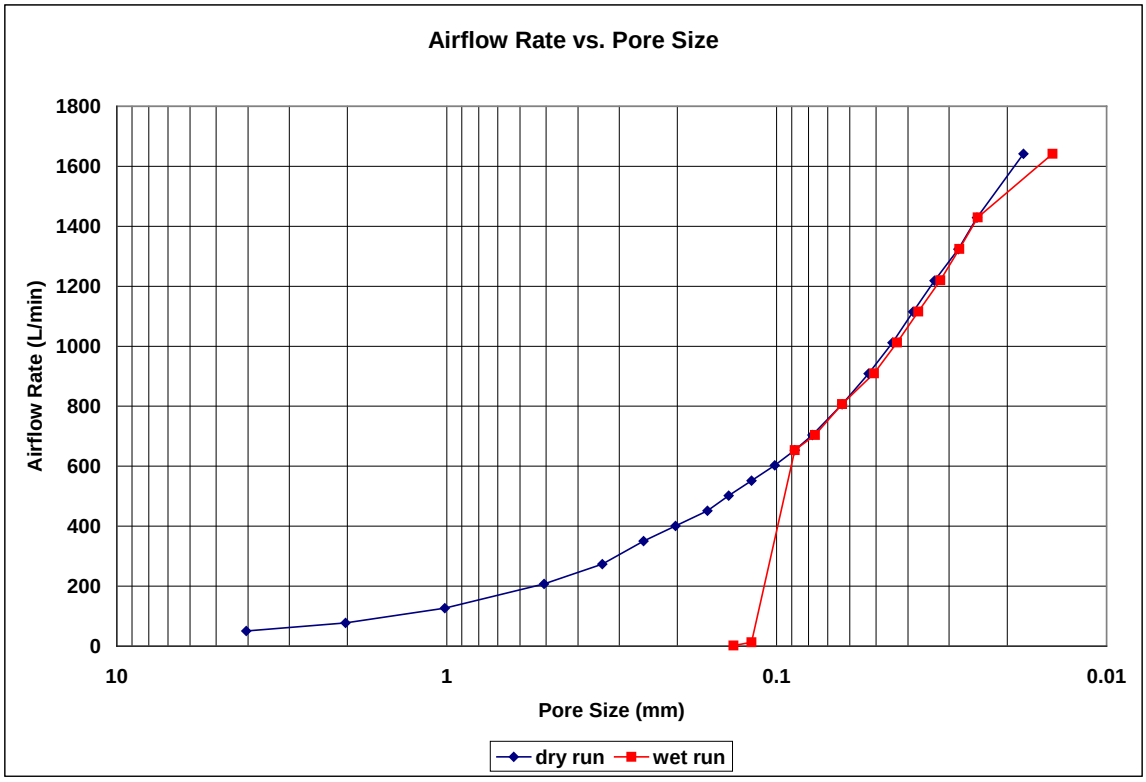

Figure B.2: Water 1 airflow rate vs. pore size for the wet and dry runs.

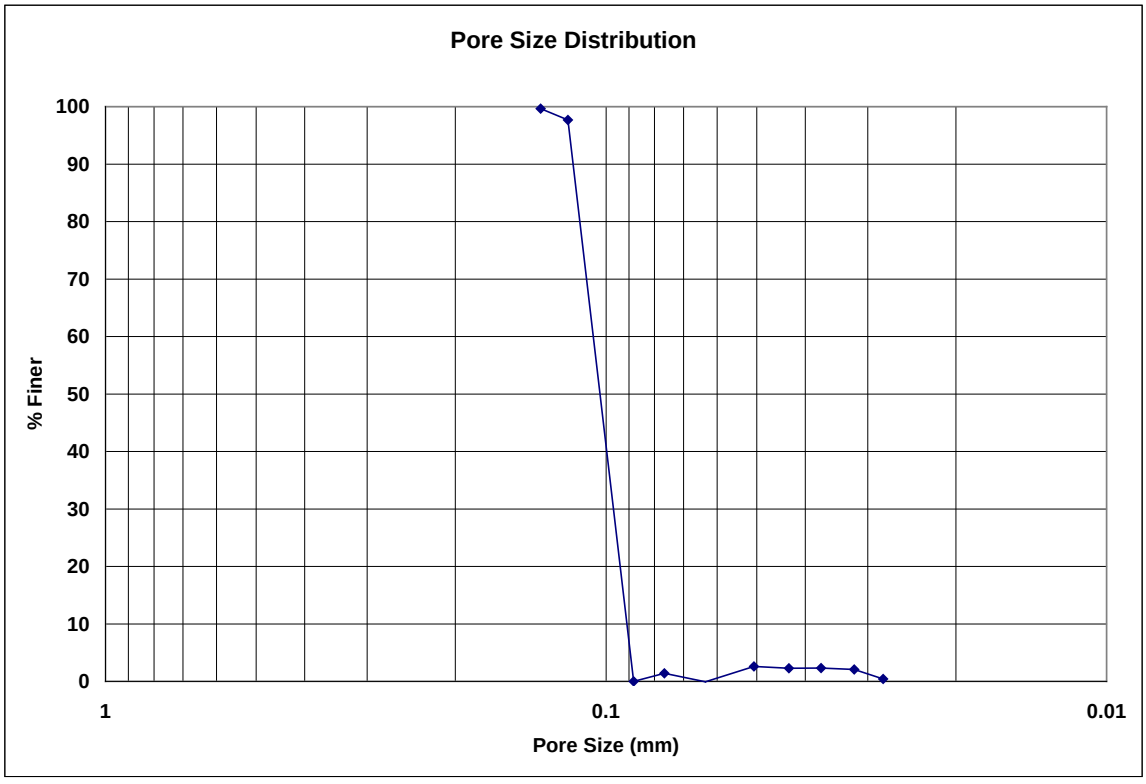

Figure B.3: Water 1 pore size distribution.

Bubble Point Test
Auburn University - Department of Civil Engineering

date of test: 8/22/2002
test identification: water 1
test performed by: David Howie
wetting fluid: distilled water
air temperature: 22 °C
porous media: NG-1 nonwoven geotextile
comments: testing to determine geotextile pore size distribution

Pore Size Calculation Parameters:
constant, C: 2860 mm/m
contact angle: 67.53 degrees
surface tension: 0.07275 N/m

Pore Size at Selected % Finer

% finer	pore size (mm)
98	0.12191
95	0.11836
90	0.11677
85	0.11518
80	0.11358
75	0.11199
70	0.11040
65	0.10881
60	0.10722
55	0.10562
50	0.10403
45	0.10244
40	0.10085
35	0.09926
30	0.09766
25	0.09607
20	0.09448
15	0.09289
10	0.09130
5	0.08970

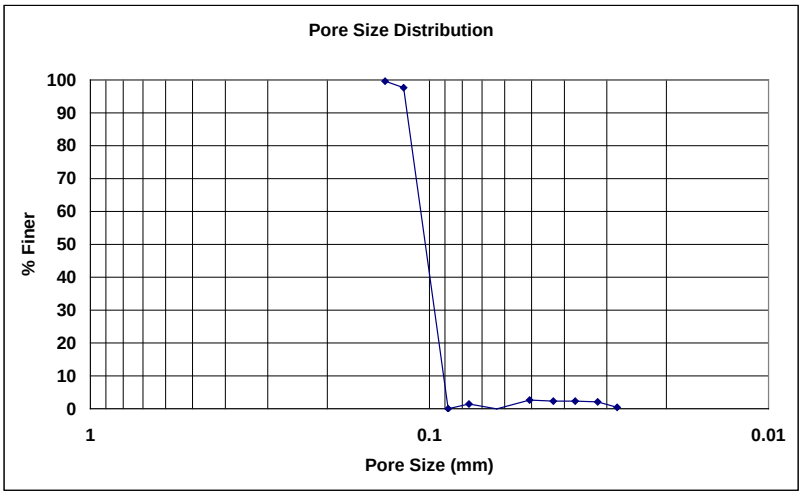

Figure B.4: Water 1 pore size distribution report.

Bubble Point Test

Auburn University - Department of Civil Engineering

date of test: 8/30/2006
test identification: water-2
test performed by: David Hayes
wetting fluid: distilled water
ambient air temperature: 21.3 °C
porous media: NG-1 nonwoven geotextile
comments: testing to determine geotextile pore size distribution

Pore Size Calculation Parameters:
constant, C: 2860 mm/m
contact angle: 67.53 degrees
surface tension: 0.07275 N/m

Dry Run

Recorded Data							Calculations				
Indirect Reading Rotameters				Direct Reading Rotameter Value (L/min)	Pressure at Rotameter Exit (psig)	Half of Manometer Reading (mm H20)	Manometer Reading (mm H20)	Manometer Pressure (Pa)	Pore Size (Diameter) (mm)	Indicated Airflow Rate (L/min)	True Airflow Rate (L/min)
First Rotameter Used		Second Rotameter Used									
Rotameter ID Number	Rotameter Value	Rotameter ID Number	Rotameter Value								
5	59				0.17	2	4	39.24	2.0265639	87.9	88.4068
5	85				0.35	4	8	78.48	1.013282	129	130.5267
5	53	5	66		0.22	6	12	117.72	0.6755213	177.5	178.8233
5	64	5	80		0.32	8	16	156.96	0.506641	216.6	218.9449
5	73	5	91		0.43	10	20	196.2	0.4053128	248	251.6011
5	82	5	100		0.55	12	24	235.44	0.3377607	277	282.1344
				350	0.07	16	32	313.92	0.2533205	350	350.8323
				400	0.08	20	40	392.4	0.2026564	400	401.087
				450	0.1	24	48	470.88	0.1688803	450	451.528
				500	0.11	30	60	588.6	0.1351043	500	501.8673
				600	0.15	40	80	784.8	0.1013282	600	603.0535
				650	0.17	46	92	902.52	0.0881115	650	653.7477
				700	0.19	52	104	1020.24	0.0779448	700	704.5093
				800	0.25	64	128	1255.68	0.0633301	800	806.774
				900	0.31	78	156	1530.36	0.0519632	900	909.4403
				1000	0.36	94	188	1844.28	0.0431184	1000	1012.171
				1100	0.41	108	216	2118.96	0.037529	1100	1115.235
				1200	0.5	128	256	2511.36	0.0316651	1200	1220.238
				1300	0.57	146	292	2864.52	0.0277611	1300	1324.964
				1400	0.65	166	332	3256.92	0.0244164	1400	1430.618
				1600	0.78	240	480	4708.8	0.016888	1600	1641.9

Wet Run

Recorded Data							Calculations				
Indirect Reading Rotameters				Direct Reading Rotameter Value (L/min)	Pressure at Rotameter Exit (psig)	Half of Manometer Reading (mm H20)	Manometer Reading (mm H20)	Manometer Pressure (Pa)	Pore Size (Diameter) (mm)	Indicated Airflow Rate (L/min)	True Airflow Rate (L/min)
First Rotameter Used		Second Rotameter Used									
Rotameter ID Number	Rotameter Value	Rotameter ID Number	Rotameter Value								
2	87					2	4	39.24	2.0265639	1.84	1.84
4	10				0.03	4	8	78.48	1.013282	3.07	3.073131
4	13				0.04	6	12	117.72	0.6755213	4.07	4.075534
4	15				0.05	8	16	156.96	0.506641	4.74	4.748054
4	18				0.06	10	20	196.2	0.4053128	5.75	5.761723
4	21				0.08	12	24	235.44	0.3377607	6.8	6.818478
4	25				0.1	16	32	313.92	0.2533205	8.27	8.298082
4	29				0.13	20	40	392.4	0.2026564	9.76	9.803061
4	33				0.16	24	48	470.88	0.1688803	11.3	11.36133
				400	0.11	26	52	510.12	0.1558895	400	401.4938
				450	0.12	30	60	588.6	0.1351043	450	451.833
				500	0.14	36	72	706.32	0.1125869	500	502.3753
				600	0.18	50	100	981	0.0810626	600	603.6623
				650	0.21	56	112	1098.72	0.0723773	650	654.6264
				700	0.23	64	128	1255.68	0.0633301	700	705.4549
				800	0.31	80	160	1569.6	0.0506641	800	808.3914
				900	0.38	98	196	1922.76	0.0413584	900	911.5584
				1000	0.44	116	232	2275.92	0.0349408	1000	1014.856
				1100	0.5	132	264	2589.84	0.0307055	1100	1118.551
				1200	0.59	158	316	3099.96	0.0256527	1200	1223.845
				1300	0.67	178	356	3492.36	0.0227704	1300	1329.296
				1400	0.76	202	404	3963.24	0.020065	1400	1435.734

Figure B.5: Water-2 recorded data and calculations.

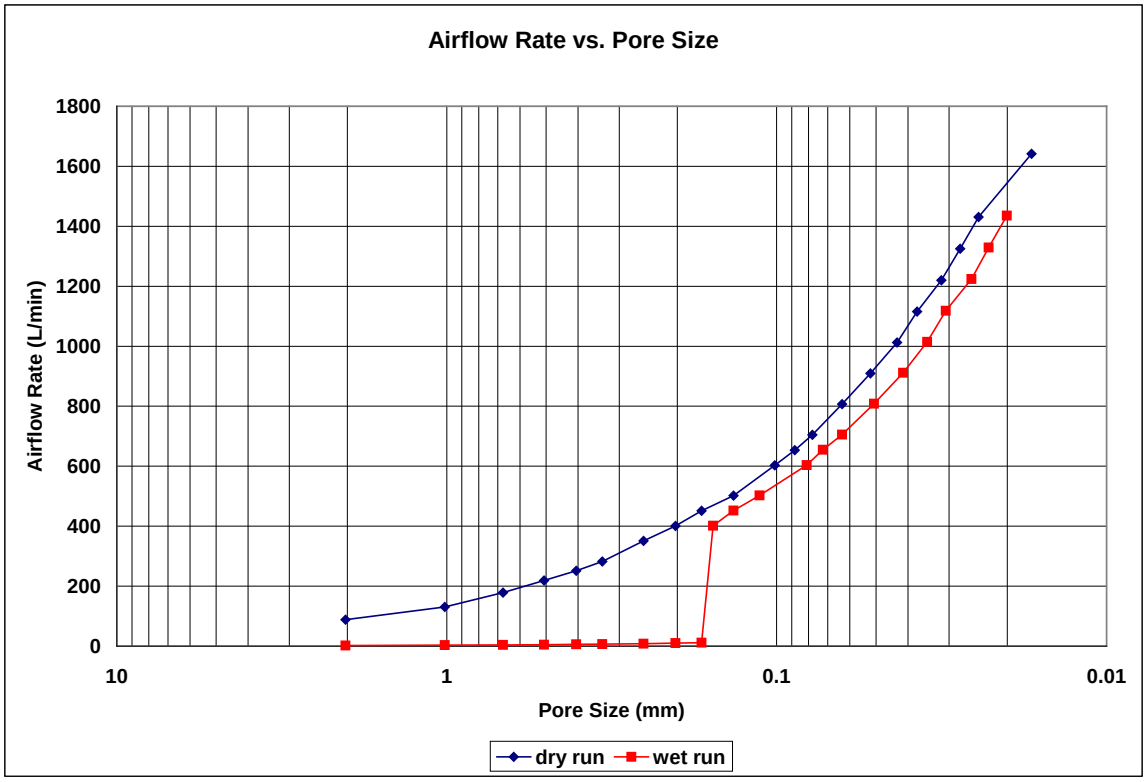

Figure B.6: Water-2 airflow rate vs. pore size for the wet and dry runs.

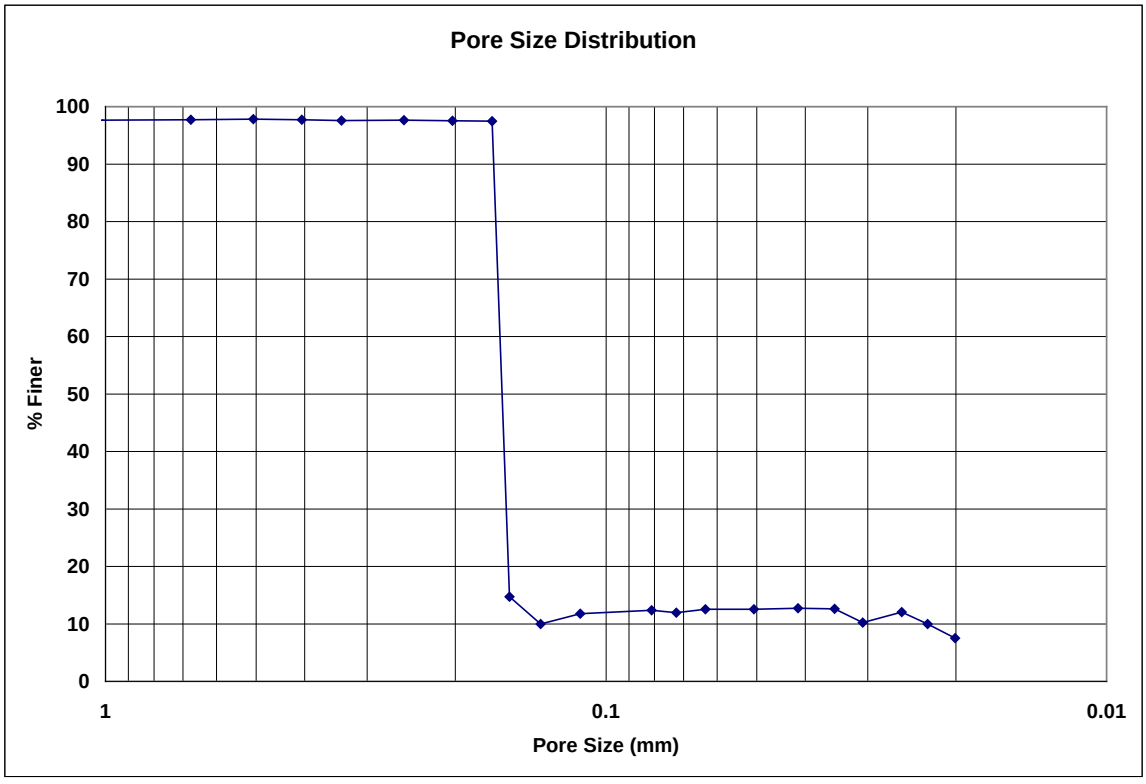

Figure B.7: Water-2 pore size distribution.

Bubble Point Test
Auburn University - Department of Civil Engineering

date of test: 8/30/2006
test identification: water-2
test performed by: David Hayes
wetting fluid: distilled water
air temperature: 21.3 °C
porous media: NG-1 nonwoven geotextile
comments: testing to determine geotextile pore size distribution

Pore Size Calculation Parameters:
constant, C: 2860 mm/m
contact angle: 67.53 degrees
surface tension: 0.07275 N/m

Pore Size at Selected % Finer

% finer	pore size (mm)
98	---
95	0.16849
90	0.16771
85	0.16692
80	0.16614
75	0.16535
70	0.16457
65	0.16378
60	0.16300
55	0.16221
50	0.16143
45	0.16064
40	0.15986
35	0.15907
30	0.15829
25	0.15750
20	0.15672
15	0.15593
10	0.13524
5	---

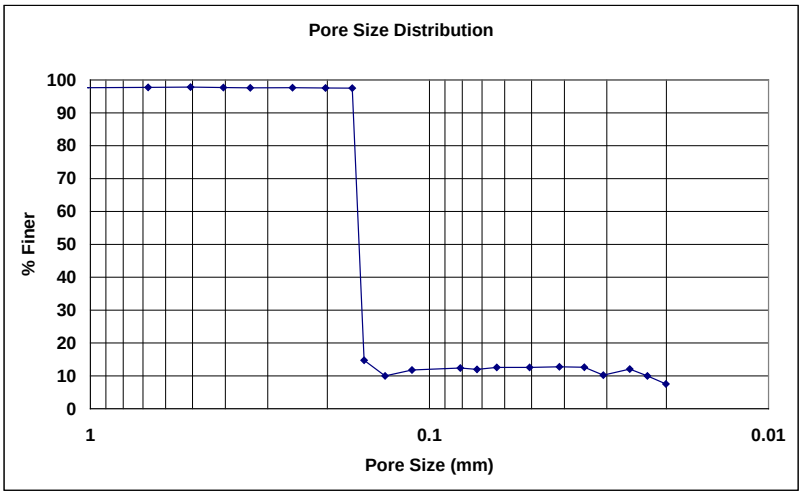

Figure B.8: Water-2 pore size distribution report.

Bubble Point Test

Auburn University - Department of Civil Engineering

date of test: 8/30/2006
test identification: water-3
test performed by: David Hayes
wetting fluid: distilled water
ambient air temperature: 21.3 °C
porous media: NG-1 nonwoven geotextile
comments: testing to determine geotextile pore size distribution

Pore Size Calculation Parameters:
constant, C: 2860 mm/m
contact angle: 67.53 degrees
surface tension: 0.07275 N/m

Dry Run

Recorded Data							Calculations				
Indirect Reading Rotameters				Direct Reading Rotameter Value (L/min)	Pressure at Rotameter Exit (psig)	Half of Manometer Reading (mm H20)	Manometer Reading (mm H20)	Manometer Pressure (Pa)	Pore Size (Diameter) (mm)	Indicated Airflow Rate (L/min)	True Airflow Rate (L/min)
First Rotameter Used		Second Rotameter Used									
Rotameter ID Number	Rotameter Value	Rotameter ID Number	Rotameter Value								
5	47				0.11	2	4	39.24	2.0265639	69.8	70.06067
5	80				0.31	4	8	78.48	1.013282	121	122.2692
5	100				0.51	6	12	117.72	0.6755213	153	155.6315
5	66	5	82		0.37	10	20	196.2	0.4053128	222.7	225.4853
5	82	5	100		0.56	14	28	274.68	0.2895091	277	282.2269
				350	0.04	18	36	353.16	0.2251738	350	350.4759
				400	0.06	22	44	431.64	0.1842331	400	400.8155
				450	0.07	28	56	549.36	0.1447546	450	451.0702
				500	0.11	38	76	745.56	0.1066613	500	501.8673
				600	0.13	44	88	863.28	0.0921165	600	602.6472
				650	0.15	52	104	1020.24	0.0779448	650	653.3079
				700	0.17	58	116	1137.96	0.0698815	700	704.036
				800	0.27	70	140	1373.4	0.0579018	800	807.3135
				900	0.33	84	168	1648.08	0.0482515	900	910.046
				1000	0.38	100	200	1962	0.0405313	1000	1012.843
				1100	0.46	120	240	2354.4	0.0337761	1100	1117.078
				1200	0.53	138	276	2707.56	0.0293705	1200	1221.441
				1300	0.62	160	320	3139.2	0.025332	1300	1327.132
				1400	0.7	180	360	3531.6	0.0225174	1400	1432.946
				1600	0.79	248	496	4865.76	0.0163433	1600	1642.431

Wet Run

Recorded Data							Calculations				
Indirect Reading Rotameters				Direct Reading Rotameter Value (L/min)	Pressure at Rotameter Exit (psig)	Half of Manometer Reading (mm H20)	Manometer Reading (mm H20)	Manometer Pressure (Pa)	Pore Size (Diameter) (mm)	Indicated Airflow Rate (L/min)	True Airflow Rate (L/min)
First Rotameter Used		Second Rotameter Used									
Rotameter ID Number	Rotameter Value	Rotameter ID Number	Rotameter Value								
2	86					2	4	39.24	2.0265639	1.817	1.817
4	8				0.02	4	8	78.48	1.013282	2.43	2.431652
4	10				0.03	6	12	117.72	0.6755213	3.07	3.073131
4	12				0.04	8	16	156.96	0.506641	3.74	3.745085
4	16				0.07	14	28	274.68	0.2895091	5.07	5.082057
4	20				0.1	20	40	392.4	0.2026564	6.44	6.461868
				400	0.1	26	52	510.12	0.1558895	400	401.3582
				450	0.12	32	64	627.84	0.1266602	450	451.833
				500	0.14	38	76	745.56	0.1066613	500	502.3753
				600	0.18	52	104	1020.24	0.0779448	600	603.6623
				650	0.21	58	116	1137.96	0.0698815	650	654.6264
				700	0.23	68	136	1334.16	0.0596048	700	705.4549
				800	0.31	84	168	1648.08	0.0482515	800	808.3914
				900	0.37	102	204	2001.24	0.0397365	900	911.2561
				1000	0.43	118	236	2315.16	0.0343485	1000	1014.52
				1100	0.52	140	280	2746.8	0.0289509	1100	1119.287
				1200	0.6	166	332	3256.92	0.0244164	1200	1224.245
				1300	0.69	192	384	3767.04	0.02111	1300	1330.16
				1400	0.79	220	440	4316.4	0.0184233	1400	1437.127

Figure B.9: Water-3 recorded data and calculations.

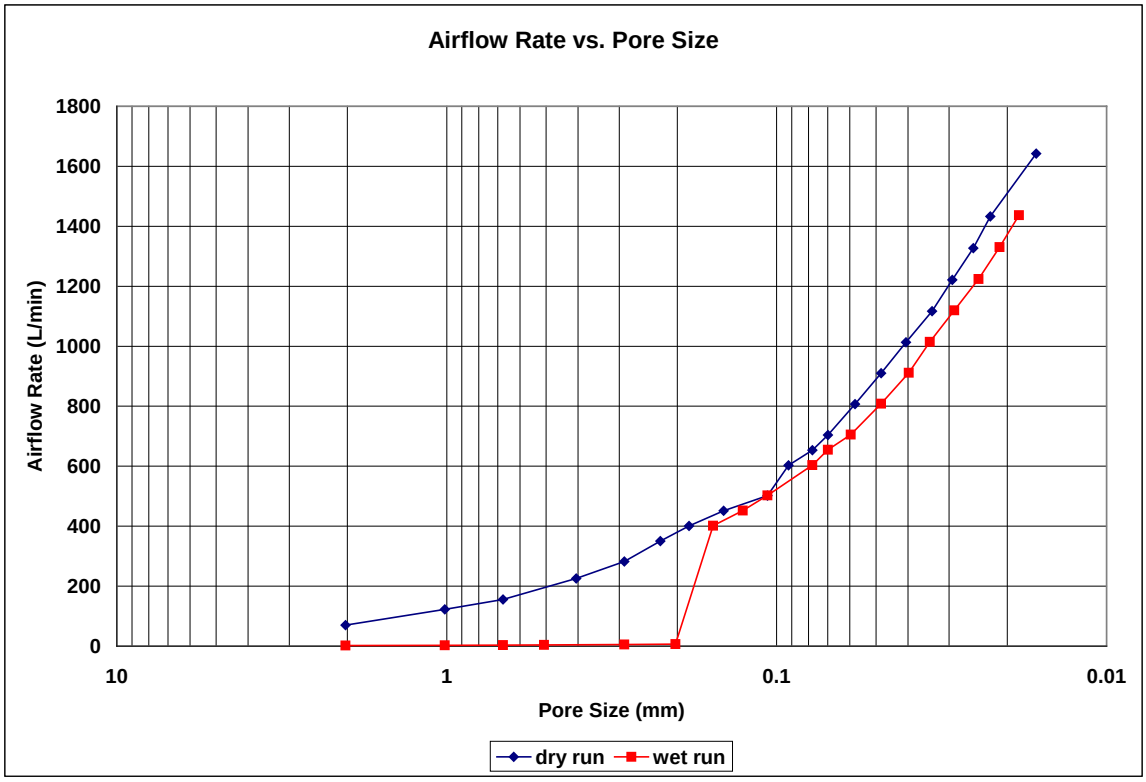

Figure B.10: Water-3 airflow rate vs. pore size for the wet and dry runs.

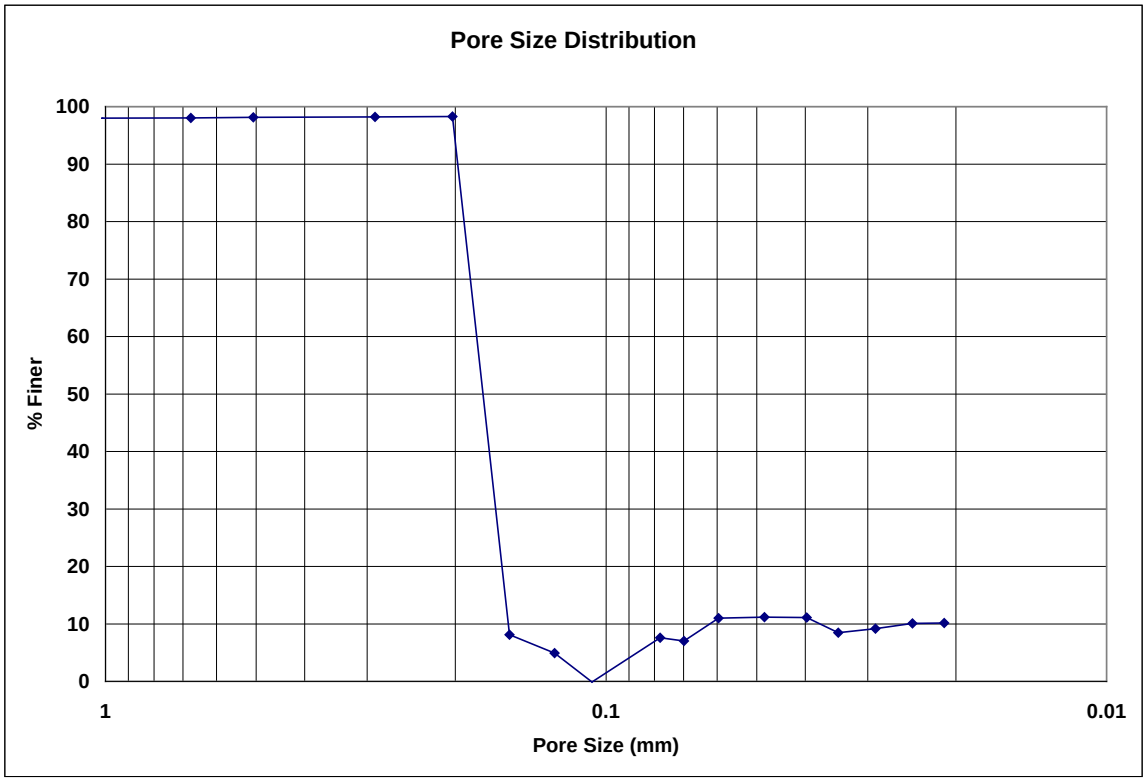

Figure B.11: Water-3 pore size distribution.

Bubble Point Test
Auburn University - Department of Civil Engineering

date of test: 8/30/2006
test identification: water-3
test performed by: David Hayes
wetting fluid: distilled water
air temperature: 21.3 °C
porous media: NG-1 nonwoven geotextile
comments: testing to determine geotextile pore size distribution

Pore Size Calculation Parameters:
constant, C: 2860 mm/m
contact angle: 67.53 degrees
surface tension: 0.07275 N/m

Pore Size at Selected % Finer

% finer	pore size (mm)
98	0.20251
95	0.20095
90	0.19836
85	0.19576
80	0.19317
75	0.19057
70	0.18798
65	0.18539
60	0.18279
55	0.18020
50	0.17761
45	0.17501
40	0.17242
35	0.16983
30	0.16723
25	0.16464
20	0.16204
15	0.15945
10	0.15686
5	0.12741

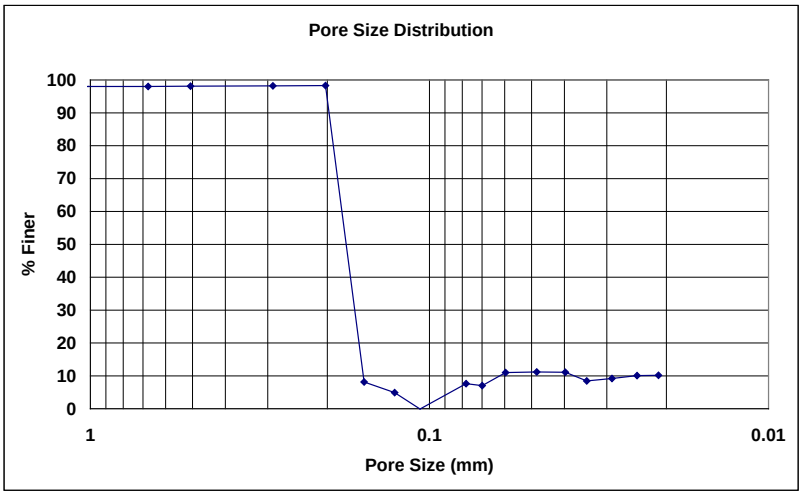

Figure B.12: Water-3 pore size distribution report.

Bubble Point Test

Auburn University - Department of Civil Engineering

date of test: 8/28/2006
test identification: water-4
test performed by: David Hayes
wetting fluid: distilled water
ambient air temperature: 21.5 °C
porous media: NG-1 nonwoven geotextile
comments: testing to determine geotextile pore size distribution

Pore Size Calculation Parameters:
constant, C: 2860 mm/m
contact angle: 67.53 degrees
surface tension: 0.07275 N/m

Dry Run

Recorded Data							Calculations				
Indirect Reading Rotameters				Direct Reading Rotameter Value (L/min)	Pressure at Rotameter Exit (psig)	Half of Manometer Reading (mm H20)	Manometer Reading (mm H20)	Manometer Pressure (Pa)	Pore Size (Diameter) (mm)	Indicated Airflow Rate (L/min)	True Airflow Rate (L/min)
First Rotameter Used		Second Rotameter Used									
Rotameter ID Number	Rotameter Value	Rotameter ID Number	Rotameter Value								
5	54				0.09	2	4	39.24	2.0265639	80.3	80.54544
5	60	5	73		0.23	8	16	156.96	0.506641	199.4	200.9539
5	74	5	90		0.4	12	24	235.44	0.3377607	248	251.3515
5	80	5	100		0.5	14	28	274.68	0.2895091	274	278.6209
				350	0.01	18	36	353.16	0.2251738	350	350.119
				400	0.02	22	44	431.64	0.1842331	400	400.272
				450	0.04	28	56	549.36	0.1447546	450	450.6118
				500	0.05	32	64	627.84	0.1266602	500	500.8496
				550	0.08	40	80	784.8	0.1013282	550	551.4946
				600	0.1	46	92	902.52	0.0881115	600	602.0374
				650	0.12	52	104	1020.24	0.0779448	650	652.6477
				700	0.14	60	120	1177.2	0.0675521	700	703.3254
				800	0.21	72	144	1412.64	0.0562934	800	805.694
				900	0.27	88	176	1726.56	0.0460583	900	908.2277
				1000	0.34	106	212	2079.72	0.0382371	1000	1011.499
				1100	0.4	122	244	2393.64	0.0332224	1100	1114.866
				1200	0.47	140	280	2746.8	0.0289509	1200	1219.033
				1300	0.56	160	320	3139.2	0.025332	1300	1324.53
				1400	0.64	184	368	3610.08	0.0220279	1400	1430.152
				1600	0.74	258	516	5061.96	0.0157098	1600	1639.778

Wet Run

Recorded Data							Calculations				
Indirect Reading Rotameters				Direct Reading Rotameter Value (L/min)	Pressure at Rotameter Exit (psig)	Half of Manometer Reading (mm H20)	Manometer Reading (mm H20)	Manometer Pressure (Pa)	Pore Size (Diameter) (mm)	Indicated Airflow Rate (L/min)	True Airflow Rate (L/min)
First Rotameter Used		Second Rotameter Used									
Rotameter ID Number	Rotameter Value	Rotameter ID Number	Rotameter Value								
1	80					2	4	39.24	2.0265639	0.2245	0.2245
4	10					6	12	117.72	0.6755213	3.07	3.07
4	20				0.09	20	40	392.4	0.2026564	6.44	6.459684
4	27				0.13	26	52	510.12	0.1558895	9.01	9.049752
4	38				0.19	30	60	588.6	0.1351043	13.2	13.28503
4	95				0.73	36	72	706.32	0.1125869	36.9	37.80512
				600	0.2	54	108	1059.48	0.0750579	600	604.0678
				700	0.25	68	136	1334.16	0.0596048	700	705.9273
				800	0.3	84	168	1648.08	0.0482515	800	808.122
				900	0.36	102	204	2001.24	0.0397365	900	910.9538
				1000	0.43	122	244	2393.64	0.0332224	1000	1014.52
				1100	0.5	142	284	2786.04	0.0285432	1100	1118.551
				1200	0.58	166	332	3256.92	0.0244164	1200	1223.444
				1400	0.75	220	440	4316.4	0.0184233	1400	1435.27
				1600	0.91	290	580	5689.8	0.0139763	1600	1648.78

Figure B.13: Water-4 recorded data and calculations.

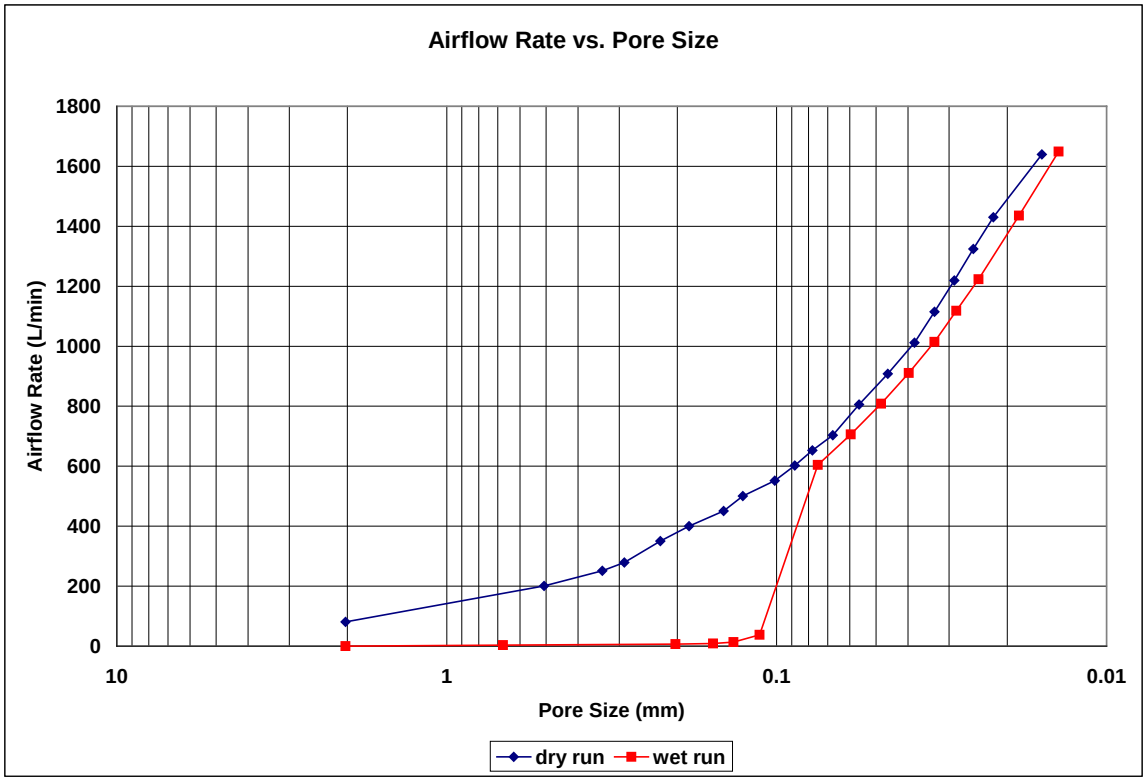

Figure B.14: Water-4 airflow rate vs. pore size for the wet and dry runs.

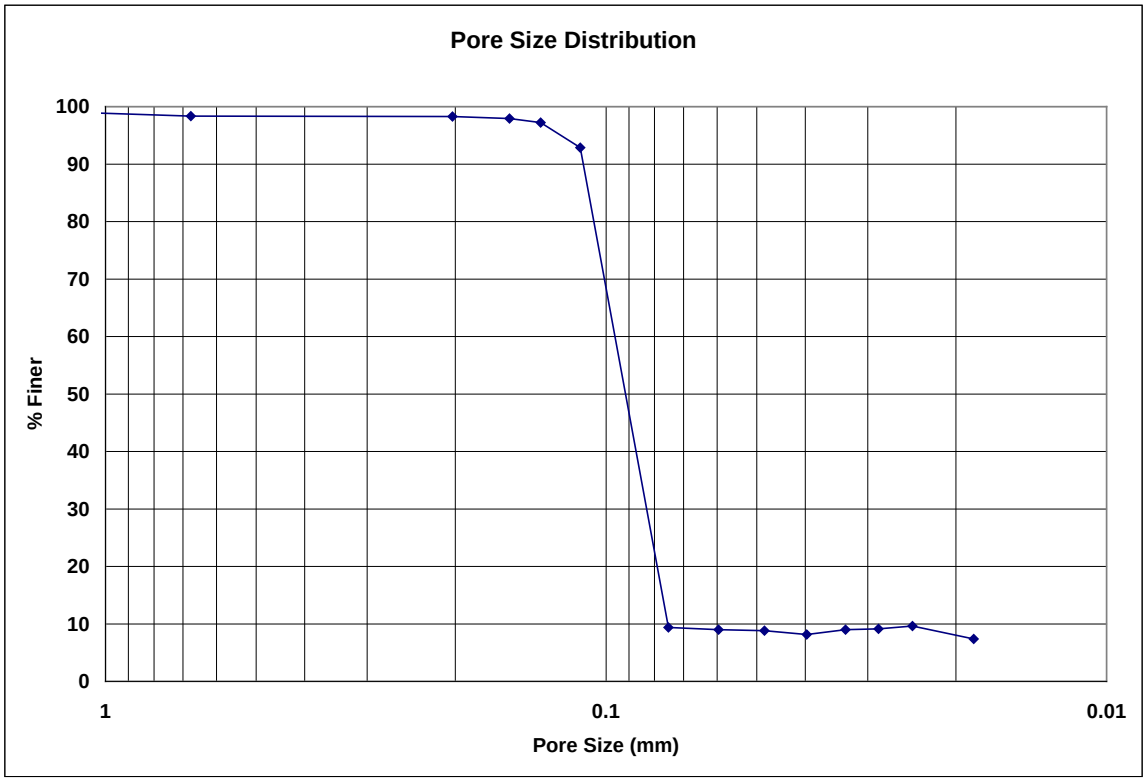

Figure B.15: Water-4 pore size distribution.

Bubble Point Test
Auburn University - Department of Civil Engineering

date of test: 8/28/2006
test identification: water-4
test performed by: David Hayes
wetting fluid: distilled water
air temperature: 21.5 °C
porous media: NG-1 nonwoven geotextile
comments: testing to determine geotextile pore size distribution

Pore Size Calculation Parameters:
constant, C: 2860 mm/m
contact angle: 67.53 degrees
surface tension: 0.07275 N/m

Pore Size at Selected % Finer

% finer	pore size (mm)
98	0.16537
95	0.12366
90	0.11130
85	0.10906
80	0.10681
75	0.10456
70	0.10231
65	0.10006
60	0.09781
55	0.09556
50	0.09332
45	0.09107
40	0.08882
35	0.08657
30	0.08432
25	0.08207
20	0.07983
15	0.07758
10	0.07533
5	---

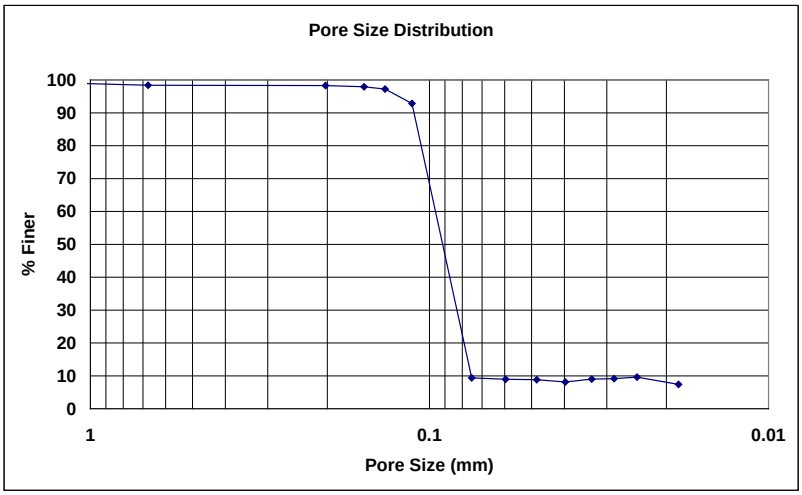

Figure B.16: Water-4 pore size distribution report,

Bubble Point Test

Auburn University - Department of Civil Engineering

date of test: 8/30/2006
test identification: water-5
test performed by: David Hayes
wetting fluid: distilled water
ambient air temperature: 21.3 °C
porous media: NG-1 nonwoven geotextile
comments: testing to determine geotextile pore size distribution

Pore Size Calculation Parameters:
constant, C: 2860 mm/m
contact angle: 67.53 degrees
surface tension: 0.07275 N/m

Dry Run

Recorded Data							Calculations				
Indirect Reading Rotameters				Direct Reading Rotameter Value (L/min)	Pressure at Rotameter Exit (psig)	Half of Manometer Reading (mm H20)	Manometer Reading (mm H20)	Manometer Pressure (Pa)	Pore Size (Diameter) (mm)	Indicated Airflow Rate (L/min)	True Airflow Rate (L/min)
First Rotameter Used		Second Rotameter Used									
Rotameter ID Number	Rotameter Value	Rotameter ID Number	Rotameter Value								
5	52				0	2	4	39.24	2.0265639	77.2	77.2
5	52	5	65		0.23	6	12	117.72	0.6755213	174.3	175.6583
5	70	5	86		0.41	10	20	196.2	0.4053128	235	238.2547
5	80	5	98		0.53	12	24	235.44	0.3377607	270	274.8242
				350	0.06	16	32	313.92	0.2533205	350	350.7136
				400	0.07	20	40	392.4	0.2026564	400	400.9512
				450	0.09	26	52	510.12	0.1558895	450	451.3754
				500	0.1	30	60	588.6	0.1351043	500	501.6978
				600	0.15	42	84	824.04	0.096503	600	603.0535
				700	0.19	54	108	1059.48	0.0750579	700	704.5093
				800	0.24	64	128	1255.68	0.0633301	800	806.5042
				900	0.31	80	160	1569.6	0.0506641	900	909.4403
				1000	0.35	96	192	1883.52	0.0422201	1000	1011.835
				1100	0.42	112	224	2197.44	0.0361886	1100	1115.604
				1200	0.5	132	264	2589.84	0.0307055	1200	1220.238
				1300	0.57	150	300	2943	0.0270209	1300	1324.964
				1400	0.65	168	336	3296.16	0.0241258	1400	1430.618
				1600	0.73	230	460	4512.6	0.0176223	1600	1639.247

Wet Run

Recorded Data							Calculations				
Indirect Reading Rotameters				Direct Reading Rotameter Value (L/min)	Pressure at Rotameter Exit (psig)	Half of Manometer Reading (mm H20)	Manometer Reading (mm H20)	Manometer Pressure (Pa)	Pore Size (Diameter) (mm)	Indicated Airflow Rate (L/min)	True Airflow Rate (L/min)
First Rotameter Used		Second Rotameter Used									
Rotameter ID Number	Rotameter Value	Rotameter ID Number	Rotameter Value								
2	78					2	4	39.24	2.0265639	1.628	1.628
4	8				0.01	4	8	78.48	1.013282	2.43	2.430826
4	13				0.02	6	12	117.72	0.6755213	4.07	4.072768
4	16				0.04	10	20	196.2	0.4053128	5.07	5.076893
4	21				0.08	16	32	313.92	0.2533205	6.8	6.818478
4	25				0.1	20	40	392.4	0.2026564	8.27	8.298082
				500	0.1	32	64	627.84	0.1266602	500	501.6978
				550	0.12	38	76	745.56	0.1066613	550	552.2403
				600	0.13	42	84	824.04	0.096503	600	602.6472
				650	0.16	50	100	981	0.0810626	650	653.5278
				700	0.18	56	112	1098.72	0.0723773	700	704.2727
				800	0.25	68	136	1334.16	0.0596048	800	806.774
				900	0.3	84	168	1648.08	0.0482515	900	909.1373
				1000	0.3	100	200	1962	0.0405313	1000	1010.153
				1100	0.43	118	236	2315.16	0.0343485	1100	1115.972
				1200	0.52	140	280	2746.8	0.0289509	1200	1221.04
				1300	0.6	160	320	3139.2	0.025332	1300	1326.265
				1400	0.69	182	364	3570.84	0.0222699	1400	1432.48

Figure B.17: Water-5 recorded data and calculations.

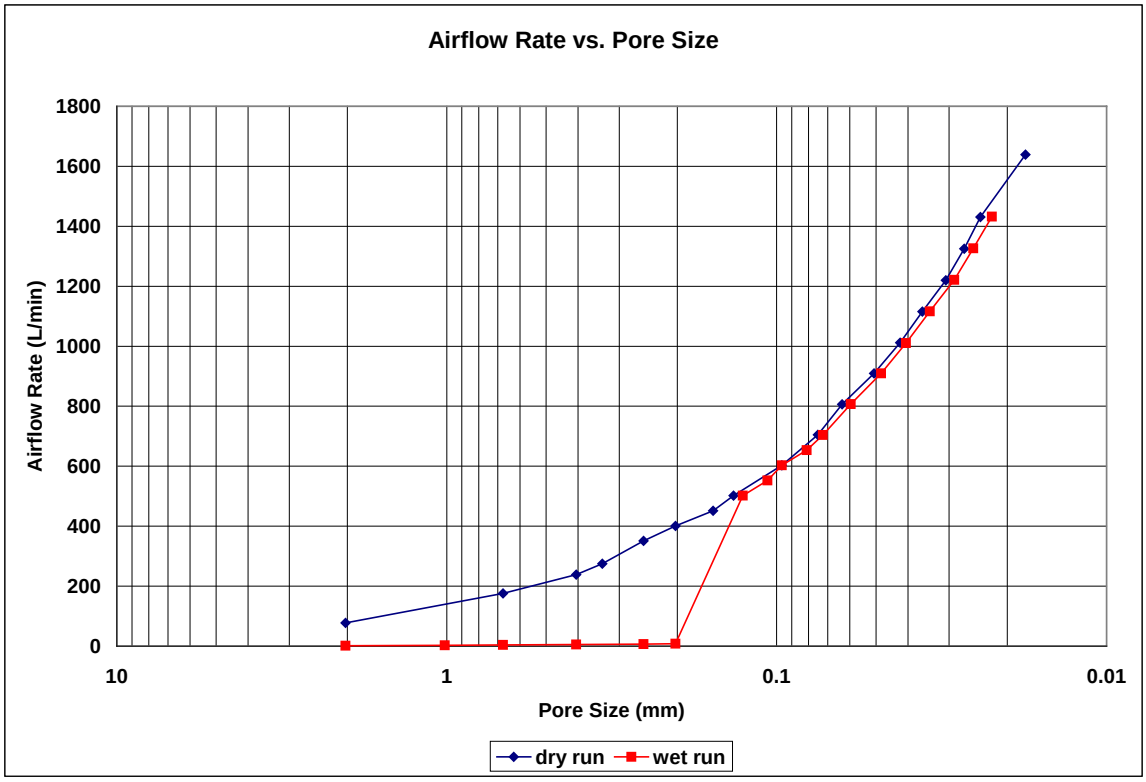

Figure B.18: Water-5 airflow rate vs. pore size for the wet and dry runs.

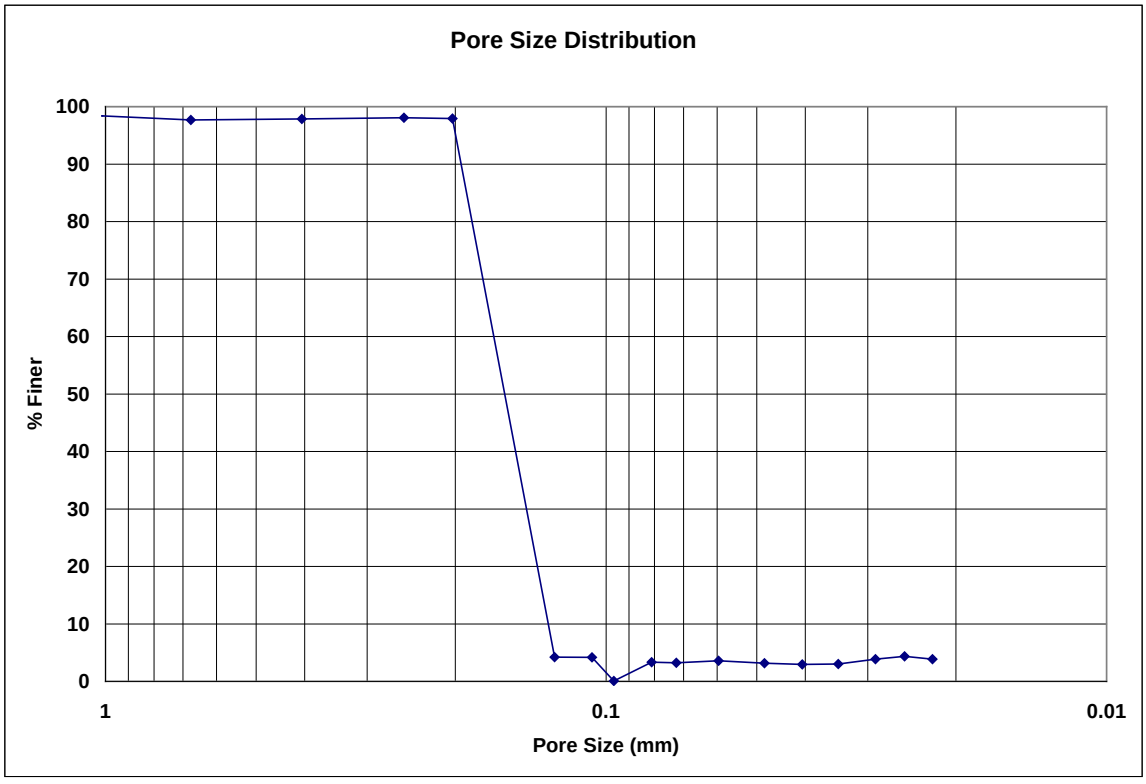

Figure B.19: Water-5 pore size distribution.

Bubble Point Test
Auburn University - Department of Civil Engineering

date of test: 8/30/2006
test identification: water-5
test performed by: David Hayes
wetting fluid: distilled water
air temperature: 21.3 °C
porous media: NG-1 nonwoven geotextile
comments: testing to determine geotextile pore size distribution

Pore Size Calculation Parameters:
constant, C: 2860 mm/m
contact angle: 67.53 degrees
surface tension: 0.07275 N/m

Pore Size at Selected % Finer

% finer	pore size (mm)
98	0.23077
95	0.20028
90	0.19622
85	0.19217
80	0.18811
75	0.18406
70	0.18000
65	0.17595
60	0.17189
55	0.16784
50	0.16378
45	0.15973
40	0.15567
35	0.15162
30	0.14756
25	0.14350
20	0.13945
15	0.13539
10	0.13134
5	0.12728

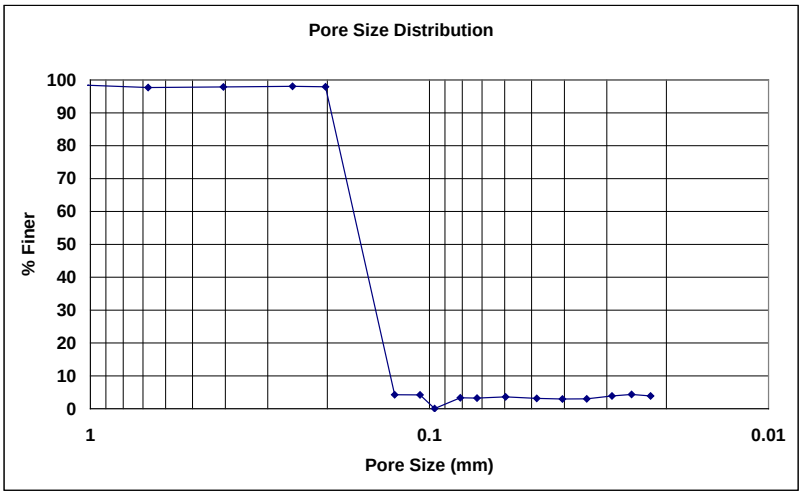

Figure B.20: Water-5 pore size distribution report.

Bubble Point Test

Auburn University - Department of Civil Engineering

date of test: 8/30/2006
test identification: water-6
test performed by: David Hayes
wetting fluid: distilled water
ambient air temperature: 21.3 °C
porous media: NG-1 nonwoven geotextile
comments: testing to determine geotextile pore size distribution

Pore Size Calculation Parameters:
constant, C: 2860 mm/m
contact angle: 67.53 degrees
surface tension: 0.07275 N/m

Dry Run

Recorded Data							Calculations				
Indirect Reading Rotameters				Direct Reading Rotameter Value (L/min)	Pressure at Rotameter Exit (psig)	Half of Manometer Reading (mm H20)	Manometer Reading (mm H20)	Manometer Pressure (Pa)	Pore Size (Diameter) (mm)	Indicated Airflow Rate (L/min)	True Airflow Rate (L/min)
First Rotameter Used		Second Rotameter Used									
Rotameter ID Number	Rotameter Value	Rotameter ID Number	Rotameter Value								
5	46				0.1	2	4	39.24	2.0265639	68.3	68.53192
5	77				0.28	4	8	78.48	1.013282	116	117.0996
5	52	5	63		0.23	6	12	117.72	0.6755213	171.2	172.5341
5	60	5	74		0.3	8	16	156.96	0.506641	200.4	202.4346
5	69	5	85		0.4	10	20	196.2	0.4053128	232	235.1353
5	72	5	95		0.51	12	24	235.44	0.3377607	253	257.3514
				400	0.04	20	40	392.4	0.2026564	400	400.5438
				500	0.62	30	60	588.6	0.1351043	500	510.4353
				550	0.69	36	72	706.32	0.1125869	550	562.7601
				600	0.66	42	84	824.04	0.096503	600	613.3215
				650	0.68	46	92	902.52	0.0881115	650	664.8641
				700	0.7	54	108	1059.48	0.0750579	700	716.4728
				800	0.78	64	128	1255.68	0.0633301	800	820.9502
				900	0.83	78	156	1530.36	0.0519632	900	925.0593
				1000	0.89	94	188	1844.28	0.0431184	1000	1029.827
				1100	0.94	108	216	2118.96	0.037529	1100	1134.625
				1200	1.02	126	252	2472.12	0.0321677	1200	1240.934
				1300	1.1	146	292	2864.52	0.0277611	1300	1347.762
				1400	1.18	166	332	3256.92	0.0244164	1400	1455.106

Wet Run

Recorded Data							Calculations				
Indirect Reading Rotameters				Direct Reading Rotameter Value (L/min)	Pressure at Rotameter Exit (psig)	Half of Manometer Reading (mm H20)	Manometer Reading (mm H20)	Manometer Pressure (Pa)	Pore Size (Diameter) (mm)	Indicated Airflow Rate (L/min)	True Airflow Rate (L/min)
First Rotameter Used		Second Rotameter Used									
Rotameter ID Number	Rotameter Value	Rotameter ID Number	Rotameter Value								
2	79					2	4	39.24	2.0265639	1.652	1.652
4	10				0.05	6	12	117.72	0.6755213	3.07	3.075217
4	12				0.06	8	16	156.96	0.506641	3.74	3.747625
4	15				0.08	12	24	235.44	0.3377607	4.74	4.75288
4	18				0.1	16	32	313.92	0.2533205	5.75	5.769525
4	22				0.12	20	40	392.4	0.2026564	7.17	7.199206
4	27				0.15	24	48	470.88	0.1688803	9.01	9.055853
				500	0.13	36	72	706.32	0.1125869	500	502.206
				550	0.15	40	80	784.8	0.1013282	550	552.799
				600	0.17	48	96	941.76	0.0844402	600	603.4594
				650	0.19	54	108	1059.48	0.0750579	650	654.1872
				700	0.22	62	124	1216.44	0.065373	700	705.2186
				800	0.3	76	152	1491.12	0.0533306	800	808.122
				900	0.36	94	188	1844.28	0.0431184	900	910.9538
				1000	0.42	110	220	2158.2	0.0368466	1000	1014.185
				1100	0.49	128	256	2511.36	0.0316651	1100	1118.183
				1200	0.58	150	300	2943	0.0270209	1200	1223.444
				1300	0.67	174	348	3413.88	0.0232938	1300	1329.296
				1400	0.74	196	392	3845.52	0.0206792	1400	1434.805

Figure B.21: Water-6 recorded data and calculations.

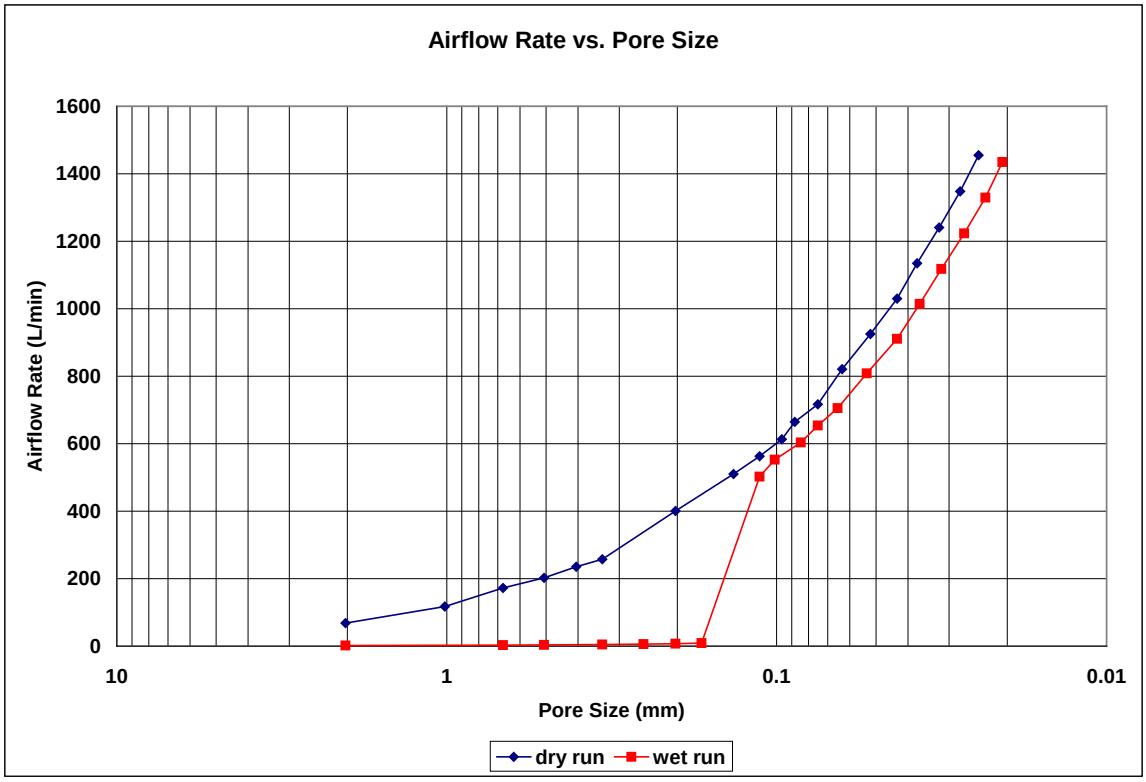

Figure B.22: Water-6 airflow rate vs. pore size for the wet and dry runs.

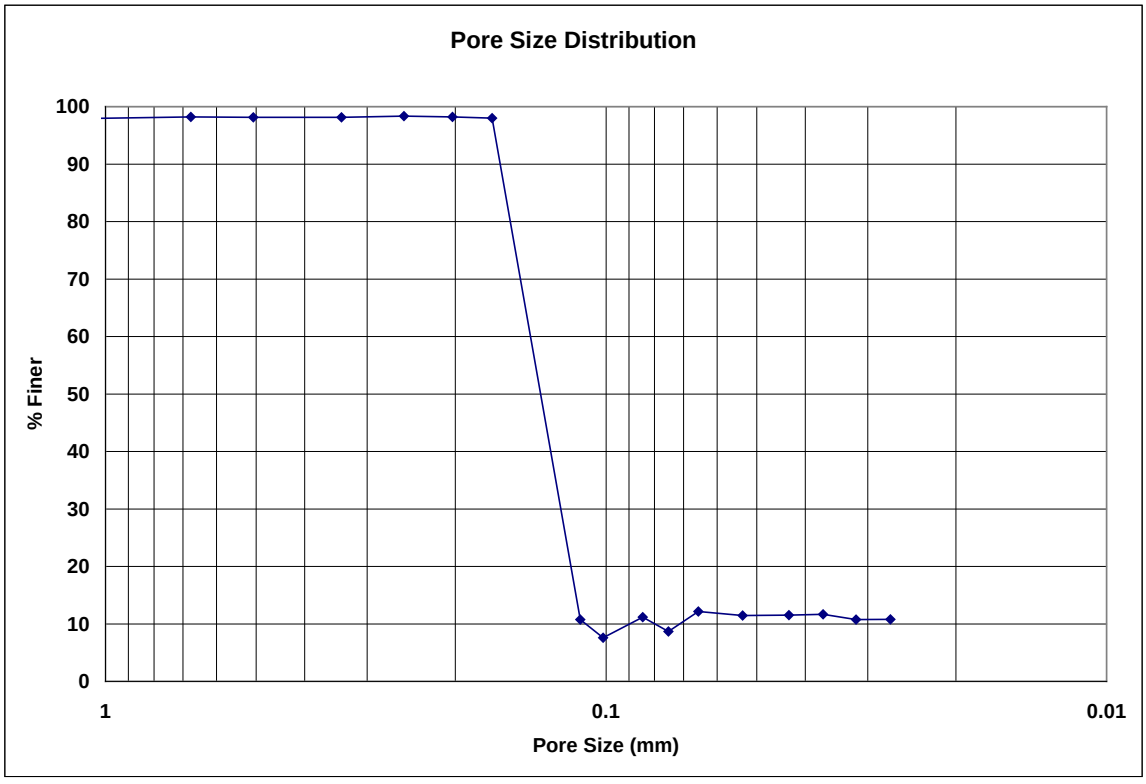

Figure B.23: Water-6 pore size distribution.

Bubble Point Test
Auburn University - Department of Civil Engineering

date of test: 8/30/2006
test identification: water-6
test performed by: David Hayes
wetting fluid: distilled water
air temperature: 21.3 °C
porous media: NG-1 nonwoven geotextile
comments: testing to determine geotextile pore size distribution

Pore Size Calculation Parameters:
constant, C: 2860 mm/m
contact angle: 67.53 degrees
surface tension: 0.07275 N/m

Pore Size at Selected % Finer

% finer	pore size (mm)
98	0.16887
95	0.16694
90	0.16371
85	0.16049
80	0.15726
75	0.15403
70	0.15081
65	0.14758
60	0.14436
55	0.14113
50	0.13790
45	0.13468
40	0.13145
35	0.12823
30	0.12500
25	0.12177
20	0.11855
15	0.11532
10	0.10989
5	---

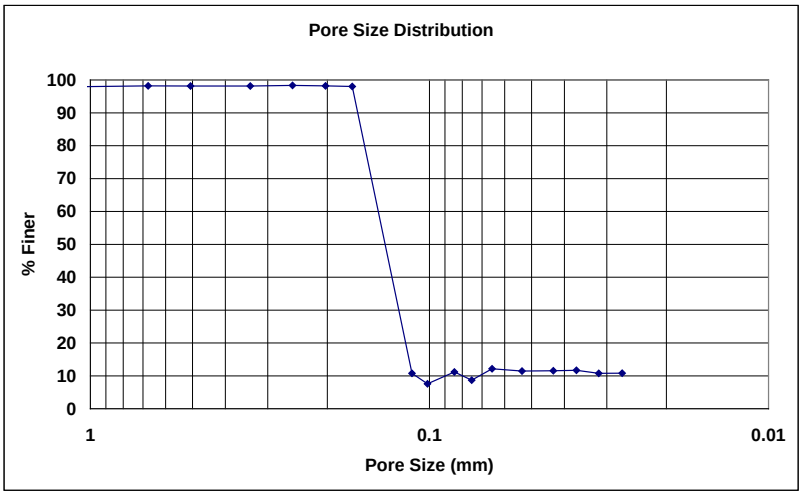

Figure B.24: Water-6 pore size distribution report.

Bubble Point Test

Auburn University - Department of Civil Engineering

date of test: 8/31/2006
test identification: water-7
test performed by: David Hayes
wetting fluid: distilled water
ambient air temperature: 21.2 °C
porous media: NG-1 nonwoven geotextile
comments: testing to determine geotextile pore size distribution

Pore Size Calculation Parameters:
constant, C: 2860 mm/m
contact angle: 67.53 degrees
surface tension: 0.07275 N/m

Dry Run

Recorded Data							Calculations				
Indirect Reading Rotameters				Direct Reading Rotameter Value (L/min)	Pressure at Rotameter Exit (psig)	Half of Manometer Reading (mm H20)	Manometer Reading (mm H20)	Manometer Pressure (Pa)	Pore Size (Diameter) (mm)	Indicated Airflow Rate (L/min)	True Airflow Rate (L/min)
First Rotameter Used		Second Rotameter Used									
Rotameter ID Number	Rotameter Value	Rotameter ID Number	Rotameter Value								
5	50				0.11	2	4	39.24	2.0265639	74.2	74.4771
5	88				0.37	4	8	78.48	1.013282	133	134.6634
5	58	5	72		0.27	6	12	117.72	0.6755213	194.3	196.0763
5	67	5	83		0.37	8	16	156.96	0.506641	225	227.814
5	79	5	97		0.52	10	20	196.2	0.4053128	267	271.6814
				350	0.04	14	28	274.68	0.2895091	350	350.4759
				400	0.04	16	32	313.92	0.2533205	400	400.5438
				450	0.06	20	40	392.4	0.2026564	450	450.9174
				550	0.09	28	56	549.36	0.1447546	550	551.6811
				600	0.1	34	68	667.08	0.1192096	600	602.0374
				650	0.12	38	76	745.56	0.1066613	650	652.6477
				700	0.13	42	84	824.04	0.096503	700	703.0884
				800	0.18	52	104	1020.24	0.0779448	800	804.8831
				900	0.23	64	128	1255.68	0.0633301	900	907.0135
				1000	0.28	76	152	1491.12	0.0533306	1000	1009.479
				1100	0.33	86	172	1687.32	0.0471294	1100	1112.278
				1200	0.39	102	204	2001.24	0.0397365	1200	1215.814
				1300	0.47	118	236	2315.16	0.0343485	1300	1320.619
				1400	0.53	132	264	2589.84	0.0307055	1400	1425.015
				1600	0.51	158	316	3099.96	0.0256527	1600	1627.518

Wet Run

Recorded Data							Calculations				
Indirect Reading Rotameters				Direct Reading Rotameter Value (L/min)	Pressure at Rotameter Exit (psig)	Half of Manometer Reading (mm H20)	Manometer Reading (mm H20)	Manometer Pressure (Pa)	Pore Size (Diameter) (mm)	Indicated Airflow Rate (L/min)	True Airflow Rate (L/min)
First Rotameter Used		Second Rotameter Used									
Rotameter ID Number	Rotameter Value	Rotameter ID Number	Rotameter Value								
2	71				0.01	2	4	39.24	2.0265639	1.455	1.455495
4	7				0.02	4	8	78.48	1.013282	2.15	2.151462
4	8				0.03	6	12	117.72	0.6755213	2.43	2.432478
4	10				0.04	8	16	156.96	0.506641	3.07	3.074174
4	12				0.05	10	20	196.2	0.4053128	3.74	3.746355
4	17				0.09	18	36	353.16	0.2251738	5.41	5.426536
4	25				0.12	22	44	431.64	0.1842331	8.27	8.303686
				600	0.11	36	72	706.32	0.1125869	600	602.2407
				650	0.13	42	84	824.04	0.096503	650	652.8678
				700	0.15	46	92	902.52	0.0881115	700	703.5624
				800	0.2	56	112	1098.72	0.0723773	800	805.4238
				900	0.25	68	136	1334.16	0.0596048	900	907.6208
				1000	0.3	82	164	1608.84	0.0494284	1000	1010.153
				1100	0.36	96	192	1883.52	0.0422201	1100	1113.388
				1200	0.43	112	224	2197.44	0.0361886	1200	1217.425
				1300	0.49	126	252	2472.12	0.0321677	1300	1321.489
				1400	0.57	146	292	2864.52	0.0277611	1400	1426.885
				1600	0.62	198	396	3884.76	0.0204703	1600	1633.393

Figure B.25: Water-7 recorded data and calculations.

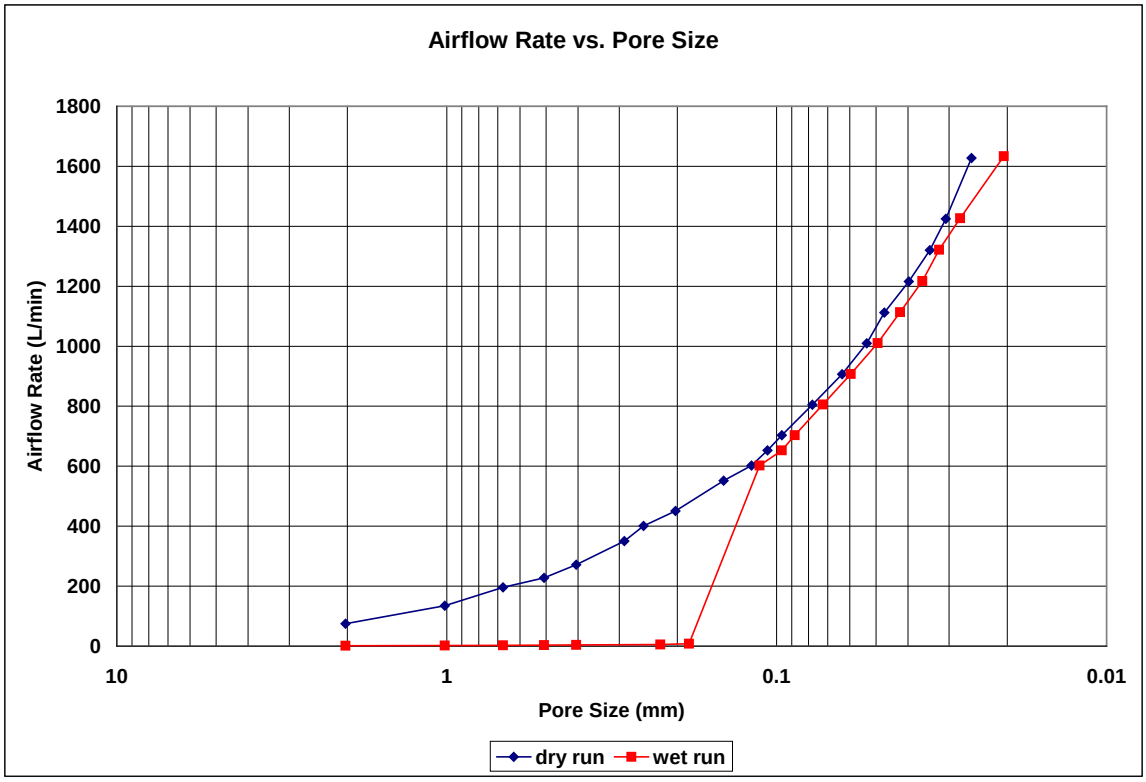

Figure B.26: Water-7 airflow rate vs. pore size for the wet and dry runs.

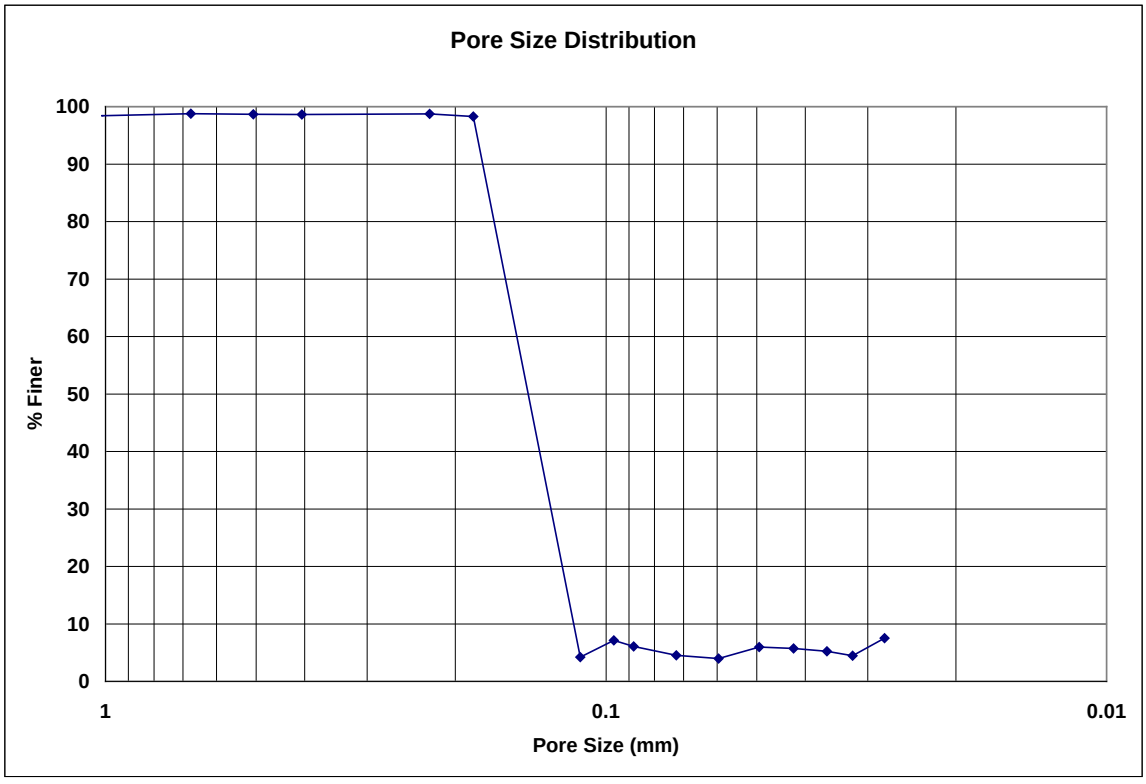

Figure B.27: Water-7 pore size distribution.

Bubble Point Test
Auburn University - Department of Civil Engineering

date of test: 8/31/2006
test identification: water-7
test performed by: David Hayes
wetting fluid: distilled water
air temperature: 21.2 °C
porous media: NG-1 nonwoven geotextile
comments: testing to determine geotextile pore size distribution

Pore Size Calculation Parameters:
constant, C: 2860 mm/m
contact angle: 67.53 degrees
surface tension: 0.07275 N/m

Pore Size at Selected % Finer

% finer	pore size (mm)
98	0.18402
95	0.18173
90	0.17793
85	0.17412
80	0.17031
75	0.16650
70	0.16269
65	0.15888
60	0.15508
55	0.15127
50	0.14746
45	0.14365
40	0.13984
35	0.13603
30	0.13223
25	0.12842
20	0.12461
15	0.12080
10	0.11699
5	0.11318

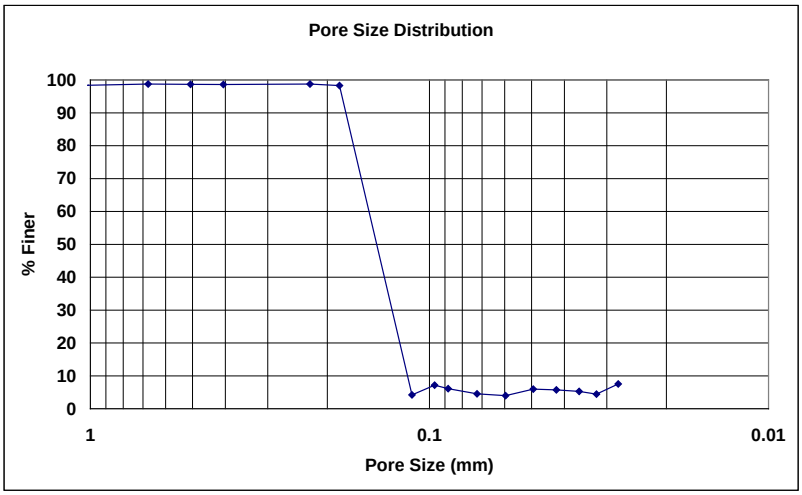

Figure B.28: Water-7 pore size distribution report.

Bubble Point Test

Auburn University - Department of Civil Engineering

date of test: 8/22/2002
test identification: water 8
test performed by: David Howie
wetting fluid: distilled water
ambient air temperature: 22 °C
porous media: NG-1 nonwoven geotextile
comments: testing to determine geotextile pore size distribution

Pore Size Calculation Parameters:
constant, C: 2860 mm/m
contact angle: 67.53 degrees
surface tension: 0.07275 N/m

Dry Run

Recorded Data							Calculations				
Indirect Reading Rotameters				Direct Reading Rotameter Value (L/min)	Pressure at Rotameter Exit (psig)	Half of Manometer Reading (mm H20)	Manometer Reading (mm H20)	Manometer Pressure (Pa)	Pore Size (Diameter) (mm)	Indicated Airflow Rate (L/min)	True Airflow Rate (L/min)
First Rotameter Used		Second Rotameter Used									
Rotameter ID Number	Rotameter Value	Rotameter ID Number	Rotameter Value								
5	44				0.09	1	2	19.62	4.0531278	65.3	65.49959
5	55				0.15	2	4	39.24	2.0265639	81.8	82.21629
5	87				0.37	4	8	78.48	1.013282	132	133.6509
5	79	5	64		0.34	8	16	156.96	0.506641	214.6	217.0676
5	98	5	80		0.53	12	24	235.44	0.3377607	270	274.8242
				350	0.08	16	32	313.92	0.2533205	350	350.9511
				400	0.09	20	40	392.4	0.2026564	400	401.2226
				450	0.11	24.5	49	480.69	0.1654338	450	451.6805
				500	0.12	30	60	588.6	0.1351043	500	502.0367
				550	0.14	35	70	686.7	0.1158037	550	552.6128
				600	0.16	41	82	804.42	0.0988568	600	603.2565
				650	0.18	47	94	922.14	0.0862368	650	653.9675
				700	0.2	53	106	1039.86	0.0764741	700	704.7458
				800	0.25	66	132	1294.92	0.061411	800	806.774
				900	0.3	78	156	1530.36	0.0519632	900	909.1373
				1000	0.35	94	188	1844.28	0.0431184	1000	1011.835
				1100	0.4	108	216	2118.96	0.037529	1100	1114.866
				1200	0.47	127	254	2491.74	0.0319144	1200	1219.033
				1300	0.55	146	292	2864.52	0.0277611	1300	1324.096
				1400	0.63	167	334	3276.54	0.0242702	1400	1429.685
				1600	0.77	235	470	4610.7	0.0172474	1600	1641.37

Wet Run

Recorded Data							Calculations				
Indirect Reading Rotameters				Direct Reading Rotameter Value (L/min)	Pressure at Rotameter Exit (psig)	Half of Manometer Reading (mm H20)	Manometer Reading (mm H20)	Manometer Pressure (Pa)	Pore Size (Diameter) (mm)	Indicated Airflow Rate (L/min)	True Airflow Rate (L/min)
First Rotameter Used		Second Rotameter Used									
Rotameter ID Number	Rotameter Value	Rotameter ID Number	Rotameter Value								
1	72					24	48	470.88	0.1688803	0.195	0.195
4	37				0.15	30	60	588.6	0.1351043	12.8	12.86514
				600	0.16	40	80	784.8	0.1013282	600	603.2565
				650	0.18	47	94	922.14	0.0862368	650	653.9675
				700	0.2	54	108	1059.48	0.0750579	700	704.7458
				800	0.23	66	132	1294.92	0.061411	800	806.2342
				900	0.28	80	160	1569.6	0.0506641	900	908.531
				1000	0.34	95	190	1863.9	0.0426645	1000	1011.499
				1100	0.4	110	220	2158.2	0.0368466	1100	1114.866
				1200	0.47	130	260	2550.6	0.0311779	1200	1219.033
				1300	0.54	150	300	2943	0.0270209	1300	1323.662
				1400	0.6	171	342	3355.02	0.0237025	1400	1428.286

Figure B.29: Water 8 recorded data and calculations.

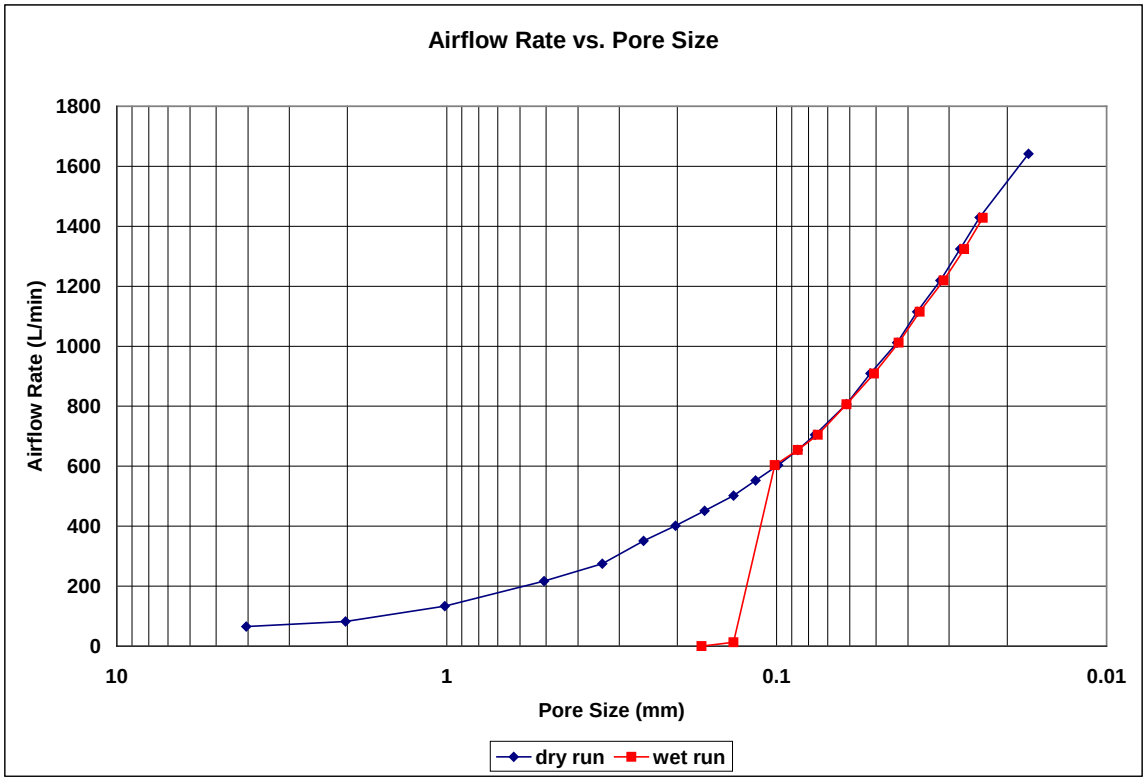

Figure B.30: Water-8 airflow rate vs. pore size for the wet and dry runs.

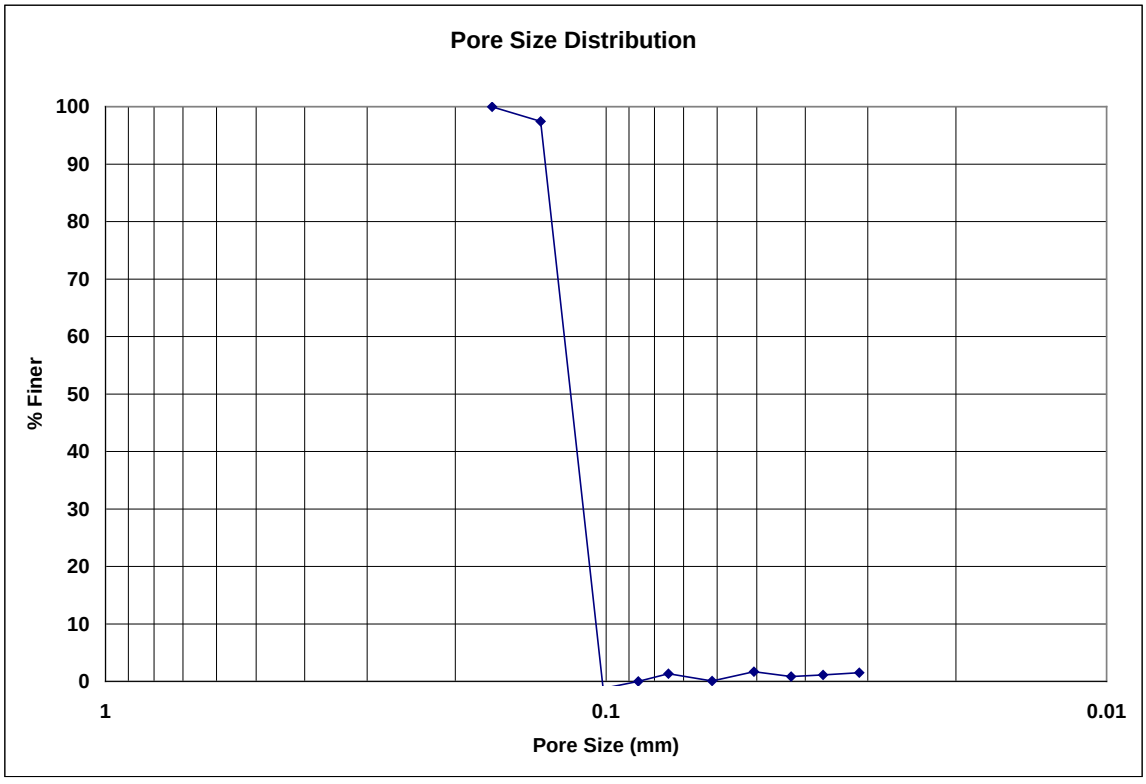

Figure B.31: Water-8 pore size distribution.

Bubble Point Test
Auburn University - Department of Civil Engineering

date of test: 8/22/2002
test identification: water 8
test performed by: David Howie
wetting fluid: distilled water
air temperature: 22 °C
porous media: NG-1 nonwoven geotextile
comments: testing to determine geotextile pore size distribution

Pore Size Calculation Parameters:
constant, C: 2860 mm/m
contact angle: 67.53 degrees
surface tension: 0.07275 N/m

Pore Size at Selected % Finer

% finer	pore size (mm)
98	0.14265
95	0.13427
90	0.13256
85	0.13085
80	0.12914
75	0.12742
70	0.12571
65	0.12400
60	0.12229
55	0.12058
50	0.11887
45	0.11716
40	0.11544
35	0.11373
30	0.11202
25	0.11031
20	0.10860
15	0.10689
10	0.10518
5	0.10346

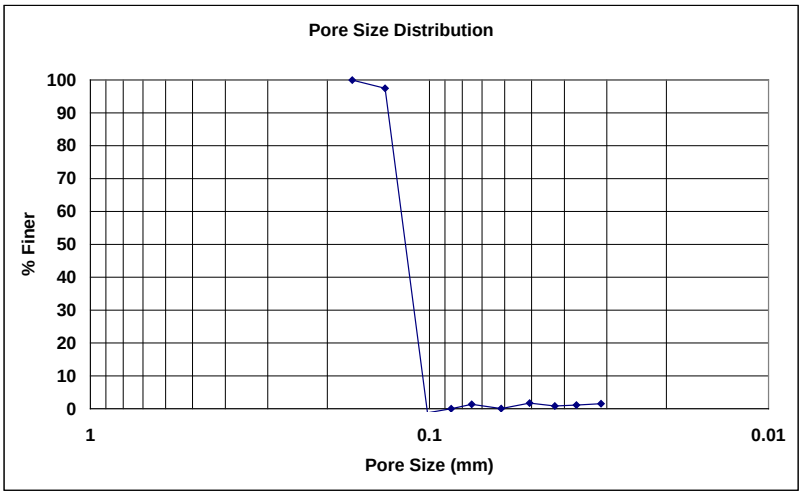

Figure B.32: Water-8 pore size distribution report.

Bubble Point Test
Auburn University - Department of Civil Engineering

date of test: 8/31/2006
test identification: water-9
test performed by: David Hayes
wetting fluid: distilled water
ambient air temperature: 21.3 °C
porous media: NG-1 nonwoven geotextile
comments: testing to determine geotextile pore size distribution

Pore Size Calculation Parameters:
constant, C: 2860 mm/m
contact angle: 67.53 degrees
surface tension: 0.07275 N/m

Dry Run

Recorded Data							Calculations				
Indirect Reading Rotameters				Direct Reading Rotameter Value (L/min)	Pressure at Rotameter Exit (psig)	Half of Manometer Reading (mm H20)	Manometer Reading (mm H20)	Manometer Pressure (Pa)	Pore Size (Diameter) (mm)	Indicated Airflow Rate (L/min)	True Airflow Rate (L/min)
First Rotameter Used		Second Rotameter Used									
Rotameter ID Number	Rotameter Value	Rotameter ID Number	Rotameter Value								
5	56				0.17	2	4	39.24	2.0265639	83.3	83.78028
5	83				0.35	4	8	78.48	1.013282	125	126.4793
5	53	5	66		0.23	6	12	117.72	0.6755213	177.5	178.8832
5	61	5	74		0.29	8	16	156.96	0.506641	201.9	203.8818
5	69	5	85		0.38	10	20	196.2	0.4053128	232	234.9795
5	77	5	97		0.52	12	24	235.44	0.3377607	264	268.6288
				350	0.05	18	36	353.16	0.2251738	350	350.5947
				400	0.06	22	44	431.64	0.1842331	400	400.8155
				450	0.08	26	52	510.12	0.1558895	450	451.2228
				500	0.09	32	64	627.84	0.1266602	500	501.5283
				550	0.11	38	76	745.56	0.1066613	550	552.054
				600	0.13	44	88	863.28	0.0921165	600	602.6472
				650	0.15	50	100	981	0.0810626	650	653.3079
				700	0.17	56	112	1098.72	0.0723773	700	704.036
				800	0.22	68	136	1334.16	0.0596048	800	805.9642
				900	0.28	84	168	1648.08	0.0482515	900	908.531
				1000	0.34	100	200	1962	0.0405313	1000	1011.499
				1100	0.4	114	228	2236.68	0.0355538	1100	1114.866
				1200	0.47	134	268	2629.08	0.0302472	1200	1219.033
				1300	0.56	156	312	3060.72	0.0259816	1300	1324.53
				1400	0.63	174	348	3413.88	0.0232938	1400	1429.685
				1600	0.74	248	496	4865.76	0.0163433	1600	1639.778

Wet Run

Recorded Data							Calculations				
Indirect Reading Rotameters				Direct Reading Rotameter Value (L/min)	Pressure at Rotameter Exit (psig)	Half of Manometer Reading (mm H20)	Manometer Reading (mm H20)	Manometer Pressure (Pa)	Pore Size (Diameter) (mm)	Indicated Airflow Rate (L/min)	True Airflow Rate (L/min)
First Rotameter Used		Second Rotameter Used									
Rotameter ID Number	Rotameter Value	Rotameter ID Number	Rotameter Value								
2	72				0	2	4	39.24	2.0265639	1.48	1.48
4	8				0	4	8	78.48	1.013282	2.43	2.43
4	11				0.01	6	12	117.72	0.6755213	3.41	3.41116
4	13				0.02	8	16	156.96	0.506641	4.07	4.072768
4	15				0.04	10	20	196.2	0.4053128	4.74	4.746445
4	17				0.05	12	24	235.44	0.3377607	5.41	5.419193
4	18				0.06	14	28	274.68	0.2895091	5.75	5.761723
4	20				0.06	16	32	313.92	0.2533205	6.44	6.453129
4	22				0.08	18	36	353.16	0.2251738	7.17	7.189484
4	24				0.09	20	40	392.4	0.2026564	7.91	7.934177
4	30				0.12	24	48	470.88	0.1688803	10.1	10.14114
				450	0.09	32	64	627.84	0.1266602	450	451.3754
				500	0.11	38	76	745.56	0.1066613	500	501.8673
				550	0.14	46	92	902.52	0.0881115	550	552.6128
				600	0.16	52	104	1020.24	0.0779448	600	603.2565
				650	0.18	60	120	1177.2	0.0675521	650	653.9675
				700	0.21	68	136	1334.16	0.0596048	700	704.9823
				800	0.29	82	164	1608.84	0.0494284	800	807.8526
				900	0.35	100	200	1962	0.0405313	900	910.6513
				1000	0.42	118	236	2315.16	0.0343485	1000	1014.185
				1100	0.49	138	276	2707.56	0.0293705	1100	1118.183
				1200	0.59	162	324	3178.44	0.0250193	1200	1223.845
				1300	0.68	184	368	3610.08	0.0220279	1300	1329.728
				1400	0.78	214	428	4198.68	0.0189398	1400	1436.663

Figure B.33: Water-9 recorded data and calculations.

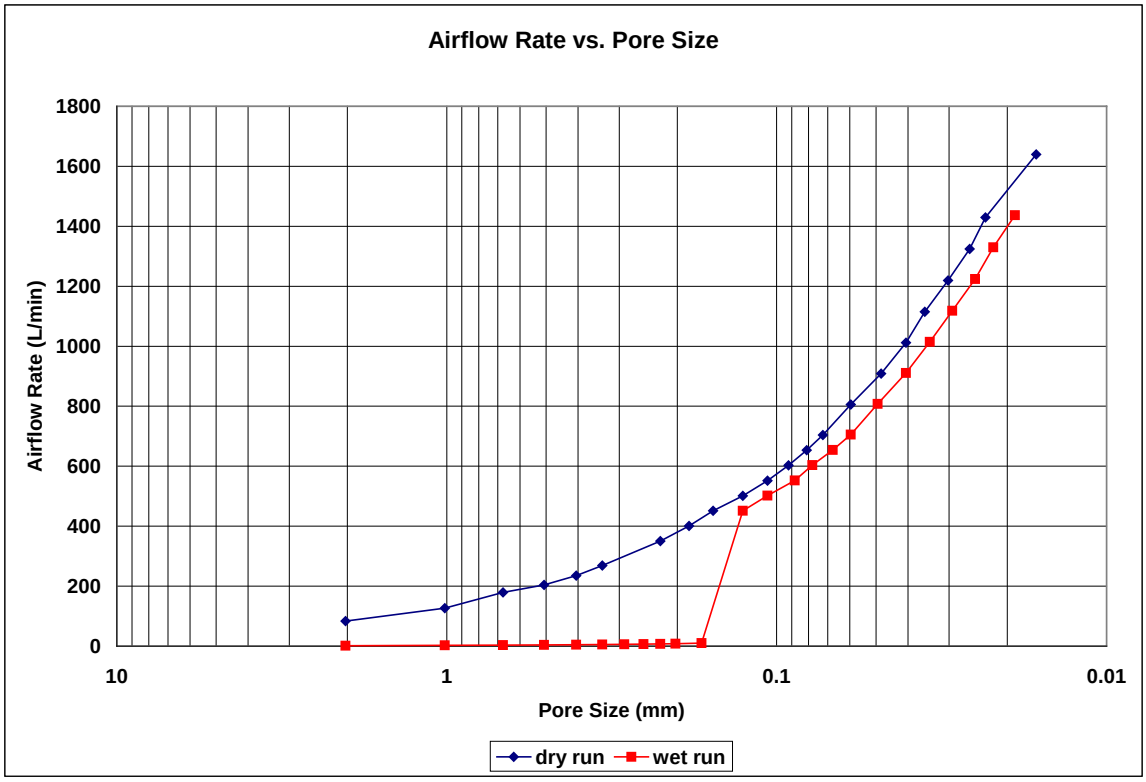

Figure B.34: Water-9 airflow rate vs. pore size for the wet and dry runs.

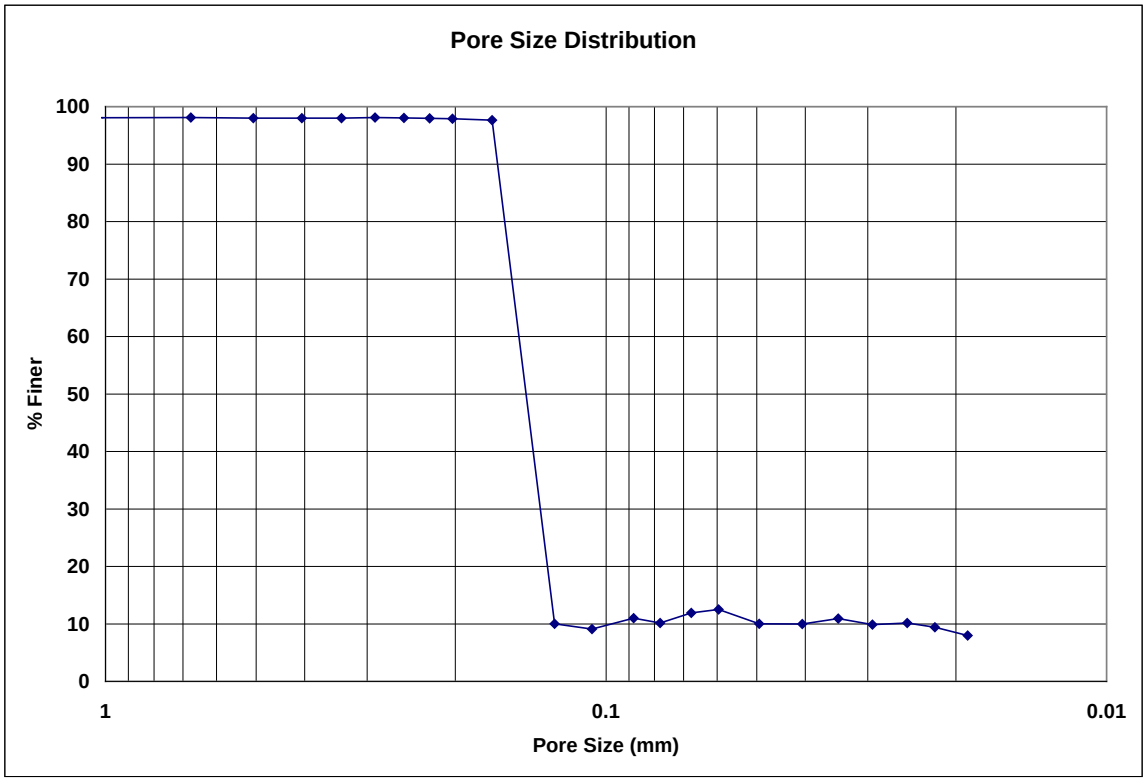

Figure B.35: Water-9 pore size distribution.

Bubble Point Test
Auburn University - Department of Civil Engineering

date of test: 8/31/2006
test identification: water-9
test performed by: David Hayes
wetting fluid: distilled water
air temperature: 21.3 °C
porous media: NG-1 nonwoven geotextile
comments: testing to determine geotextile pore size distribution

Pore Size Calculation Parameters:
constant, C: 2860 mm/m
contact angle: 67.53 degrees
surface tension: 0.07275 N/m

Pore Size at Selected % Finer

% finer	pore size (mm)
98	0.49580
95	0.16761
90	0.16520
85	0.16279
80	0.16039
75	0.15798
70	0.15557
65	0.15316
60	0.15075
55	0.14834
50	0.14593
45	0.14352
40	0.14111
35	0.13871
30	0.13630
25	0.13389
20	0.13148
15	0.12907
10	0.12666
5	---

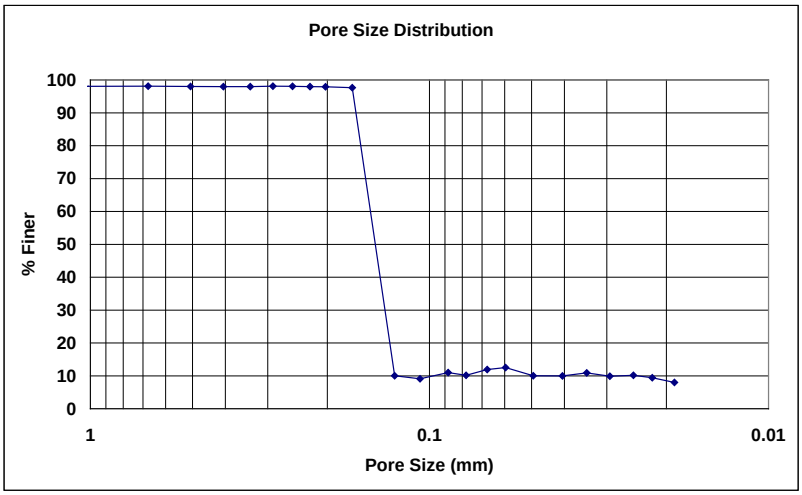

Figure B.36: Water-9 pore size distribution report.

Bubble Point Test
Auburn University - Department of Civil Engineering

date of test: 8/31/2006
test identification: water-10
test performed by: David Hayes
wetting fluid: distilled water
ambient air temperature: 21.2 °C
porous media: NG-1 nonwoven geotextile
comments: testing to determine geotextile pore size distribution

Pore Size Calculation Parameters:
constant, C: 2860 mm/m
contact angle: 67.53 degrees
surface tension: 0.07275 N/m

Dry Run

Recorded Data							Calculations				
Indirect Reading Rotameters				Direct Reading Rotameter Value (L/min)	Pressure at Rotameter Exit (psig)	Half of Manometer Reading (mm H20)	Manometer Reading (mm H20)	Manometer Pressure (Pa)	Pore Size (Diameter) (mm)	Indicated Airflow Rate (L/min)	True Airflow Rate (L/min)
First Rotameter Used		Second Rotameter Used									
Rotameter ID Number	Rotameter Value	Rotameter ID Number	Rotameter Value								
5	36				0.07	2	4	39.24	2.0265639	53.6	53.72747
5	68				0.23	4	8	78.48	1.013282	102	102.7949
5	91				0.42	6	12	117.72	0.6755213	138	139.9575
5	53	5	67		0.23	8	16	156.96	0.506641	178.8	180.1933
5	63	5	78		0.32	10	20	196.2	0.4053128	212	214.2951
5	71	5	87		0.42	12	24	235.44	0.3377607	238	241.3761
5	78	5	97		0.52	14	28	274.68	0.2895091	266	270.6639
				350	0.07	20	40	392.4	0.2026564	350	350.8323
				400	0.08	24	48	470.88	0.1688803	400	401.087
				450	0.1	30	60	588.6	0.1351043	450	451.528
				500	0.12	34	68	667.08	0.1192096	500	502.0367
				550	0.13	40	80	784.8	0.1013282	550	552.4266
				600	0.15	44	88	863.28	0.0921165	600	603.0535
				650	0.17	52	104	1020.24	0.0779448	650	653.7477
				700	0.2	60	120	1177.2	0.0675521	700	704.7458
				800	0.25	72	144	1412.64	0.0562934	800	806.774
				900	0.33	90	180	1765.8	0.0450348	900	910.046
				1000	0.39	100	200	1962	0.0405313	1000	1013.178
				1100	0.46	122	244	2393.64	0.0332224	1100	1117.078
				1200	0.54	144	288	2825.28	0.0281467	1200	1221.842
				1300	0.63	166	332	3256.92	0.0244164	1300	1327.565
				1400	0.7	186	372	3649.32	0.021791	1400	1432.946

Wet Run

Recorded Data							Calculations				
Indirect Reading Rotameters				Direct Reading Rotameter Value (L/min)	Pressure at Rotameter Exit (psig)	Half of Manometer Reading (mm H20)	Manometer Reading (mm H20)	Manometer Pressure (Pa)	Pore Size (Diameter) (mm)	Indicated Airflow Rate (L/min)	True Airflow Rate (L/min)
First Rotameter Used		Second Rotameter Used									
Rotameter ID Number	Rotameter Value	Rotameter ID Number	Rotameter Value								
2	60				0	2	4	39.24	2.0265639	1.173	1.173
4	7				0.02	4	8	78.48	1.013282	2.15	2.151462
4	9				0.03	6	12	117.72	0.6755213	2.74	2.742794
4	11				0.04	8	16	156.96	0.506641	3.41	3.414636
4	13				0.05	10	20	196.2	0.4053128	4.07	4.076916
4	15				0.06	12	24	235.44	0.3377607	4.74	4.749664
4	19				0.09	18	36	353.16	0.2251738	6.09	6.108614
4	23				0.11	24	48	470.88	0.1688803	7.54	7.568158
5	43				0.16	32	64	627.84	0.1266602	63.8	64.14627
5	52	5	63		0.23	38	76	745.56	0.1066613	171.2	172.5341
				500	0.14	40	80	784.8	0.1013282	500	502.3753
				550	0.16	44	88	863.28	0.0921165	550	552.9851
				600	0.19	52	104	1020.24	0.0779448	600	603.8651
				650	0.21	60	120	1177.2	0.0675521	650	654.6264
				700	0.23	66	132	1294.92	0.061411	700	705.4549
				800	0.32	84	168	1648.08	0.0482515	800	808.6606
				900	0.38	100	200	1962	0.0405313	900	911.5584
				1000	0.44	106	212	2079.72	0.0382371	1000	1014.856
				1100	0.51	138	276	2707.56	0.0293705	1100	1118.919
				1200	0.6	162	324	3178.44	0.0250193	1200	1224.245
				1300	0.7	188	376	3688.56	0.0215592	1300	1330.592
				1400	0.8	214	428	4198.68	0.0189398	1400	1437.591

Figure B.37: Water-10 recorded data and calculations.

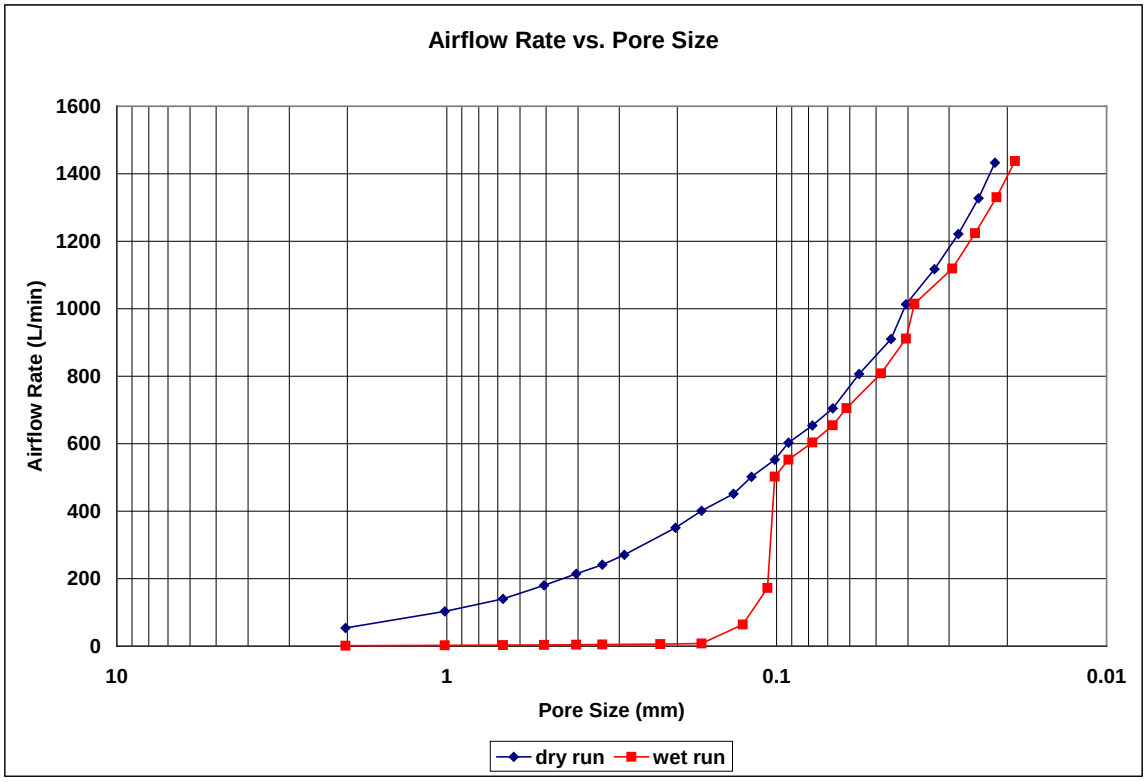

Figure B.38: Water-10 airflow rate vs. pore size for the wet and dry runs.

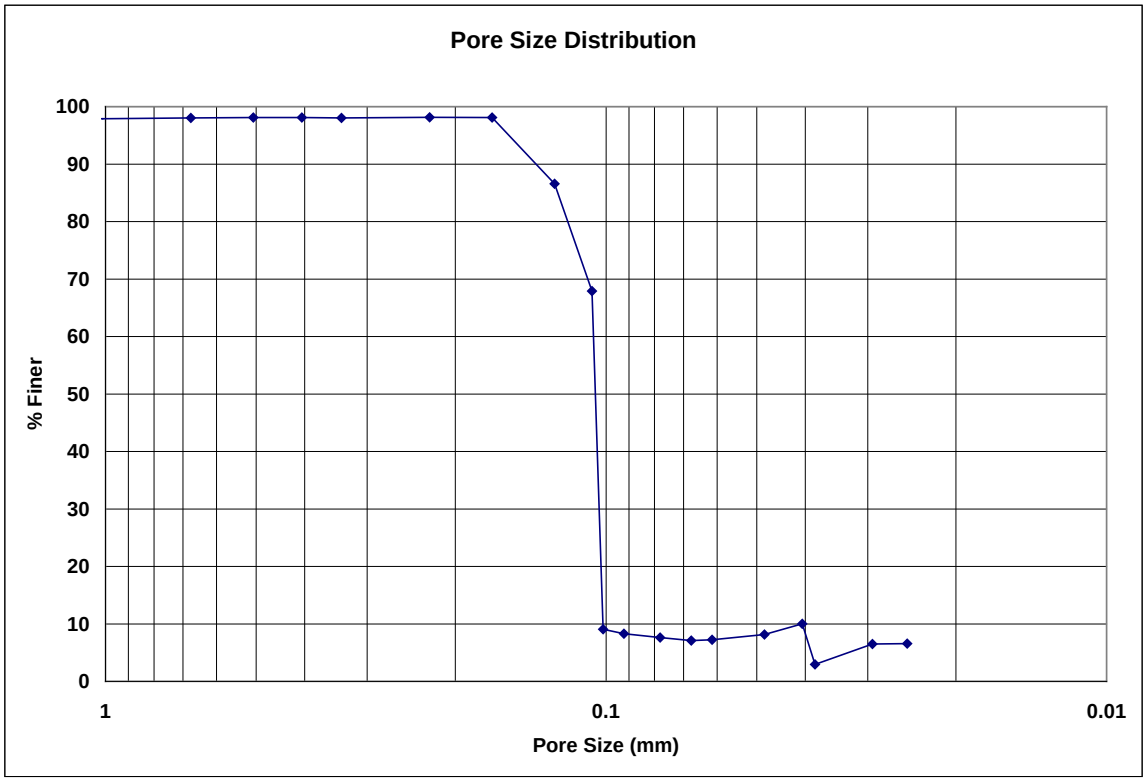

Figure B.39: Water-10 pore size distribution.

Bubble Point Test
Auburn University - Department of Civil Engineering

date of test: 8/31/2006
test identification: water-10
test performed by: David Hayes
wetting fluid: distilled water
air temperature: 21.2 °C
porous media: NG-1 nonwoven geotextile
comments: testing to determine geotextile pore size distribution

Pore Size Calculation Parameters:
constant, C: 2860 mm/m
contact angle: 67.53 degrees
surface tension: 0.07275 N/m

Pore Size at Selected % Finer

% finer	pore size (mm)
98	0.16847
95	0.15747
90	0.13915
85	0.12496
80	0.11961
75	0.11426
70	0.10891
65	0.10640
60	0.10595
55	0.10549
50	0.10504
45	0.10459
40	0.10413
35	0.10368
30	0.10323
25	0.10277
20	0.10232
15	0.10187
10	0.10141
5	0.03890

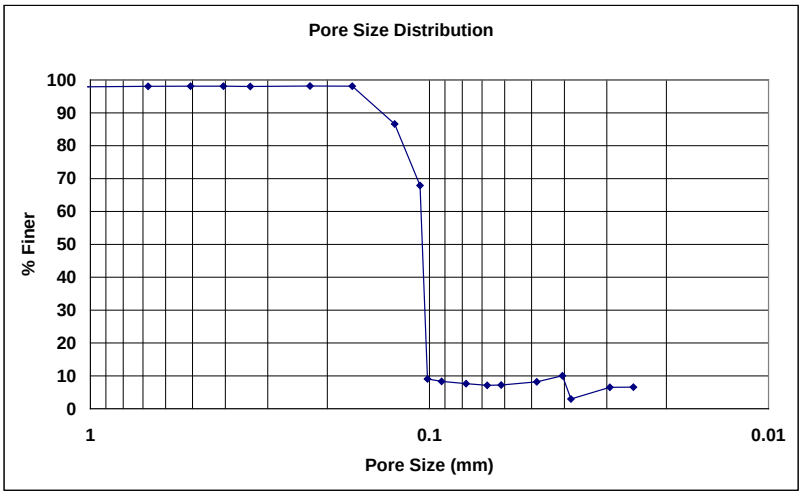

Figure B.40: Water-10 pore size distribution report.

B.2 Tests with Porewick as the Wetting Fluid

Bubble Point Test
Auburn University - Department of Civil Engineering

date of test: 11/1/2006
test identification: porewick 1
test performed by: David Hayes
wetting fluid: porewick
ambient air temperature: 21.3 °C
porous media: NG-1 nonwoven geotextile
comments: testing to determine geotextile pore size distribution

Pore Size Calculation Parameters:
constant, C: 2860 mm/m
contact angle: 0 degrees
surface tension: 0.016 N/m

Dry Run											
Recorded Data							Calculations				
Indirect Reading Rotameters				Direct Reading Rotameter Value (L/min)	Pressure at Rotameter Exit (psig)	Half of Manometer Reading (mm H20)	Manometer Reading (mm H20)	Manometer Pressure (Pa)	Pore Size (Diameter) (mm)	Indicated Airflow Rate (L/min)	True Airflow Rate (L/min)
First Rotameter Used		Second Rotameter Used									
Rotameter ID Number	Rotameter Value	Rotameter ID Number	Rotameter Value								
5	55				0.15	2	4	39.24	1.166157	81.8	82.21629
5	81				0.33	4	8	78.48	0.5830785	122	123.3618
5	100				0.51	6	12	117.72	0.388719	153	155.6315
5	56	5	70		0.29	8	16	156.96	0.2915392	188.3	190.1483
5	65	5	81		0.38	10	20	196.2	0.2332314	219.1	221.9138
5	72	5	90		0.47	12	24	235.44	0.1943595	245	248.8859
				350	0.08	18	36	353.16	0.129573	350	350.9511
				400	0.1	24	48	470.88	0.0971797	400	401.3582
				450	0.12	28	56	549.36	0.0832969	450	451.833
				500	0.13	34	68	667.08	0.0685975	500	502.206
				550	0.15	40	80	784.8	0.0583078	550	552.799
				600	0.17	48	96	941.76	0.0485899	600	603.4594
				650	0.2	56	112	1098.72	0.0416485	650	654.4068
				700	0.22	64	128	1255.68	0.0364424	700	705.2186
				800	0.3	76	152	1491.12	0.0306883	800	808.122
				900	0.36	92	184	1805.04	0.0253512	900	910.9538
				1000	0.43	110	220	2158.2	0.0212029	1000	1014.52
				1100	0.49	126	252	2472.12	0.0185104	1100	1118.183
				1200	0.57	148	296	2903.76	0.0157589	1200	1223.044
				1300	0.6	170	340	3335.4	0.0137195	1300	1326.265
				1400	0.74	194	388	3806.28	0.0120222	1400	1434.805
				1600	0.84	260	520	5101.2	0.0089704	1600	1645.079

Wet Run											
Recorded Data							Calculations				
Indirect Reading Rotameters				Direct Reading Rotameter Value (L/min)	Pressure at Rotameter Exit (psig)	Half of Manometer Reading (mm H20)	Manometer Reading (mm H20)	Manometer Pressure (Pa)	Pore Size (Diameter) (mm)	Indicated Airflow Rate (L/min)	True Airflow Rate (L/min)
First Rotameter Used		Second Rotameter Used									
Rotameter ID Number	Rotameter Value	Rotameter ID Number	Rotameter Value								
2	69				0	2	4	39.24	1.166157	1.404	1.404
4	7				0.04	4	8	78.48	0.5830785	2.15	2.152923
4	38				0.16	14	28	274.68	0.1665939	13.2	13.27164
4	98				0.21	16	32	313.92	0.1457696	38.3	38.5726
5	73				0.31	20	40	392.4	0.1166157	110	111.1538
5	80	5	98		0.62	30	60	588.6	0.0777438	270	275.6351
				450	0.14	34	68	667.08	0.0685975	450	452.1378
				550	0.18	46	92	902.52	0.0507025	550	553.3571
				600	0.2	54	108	1059.48	0.043191	600	604.0678
				650	0.22	60	120	1177.2	0.0388719	650	654.8459
				700	0.26	70	140	1373.4	0.0333188	700	706.1633
				800	0.32	86	172	1687.32	0.0271199	800	808.6606
				900	0.39	102	204	2001.24	0.0228658	900	911.8606
				1000	0.47	128	256	2511.36	0.0182212	1000	1015.861
				1100	0.55	148	296	2903.76	0.0157589	1100	1120.389
				1200	0.64	172	344	3374.64	0.01356	1200	1225.844
				1300	0.73	198	396	3884.76	0.0117794	1300	1331.888
				1400	0.83	222	444	4355.64	0.0105059	1400	1438.981
				1600	0.99	304	608	5964.48	0.0076721	1600	1653

Figure B.41: Porewick-1 recorded data and calculations.

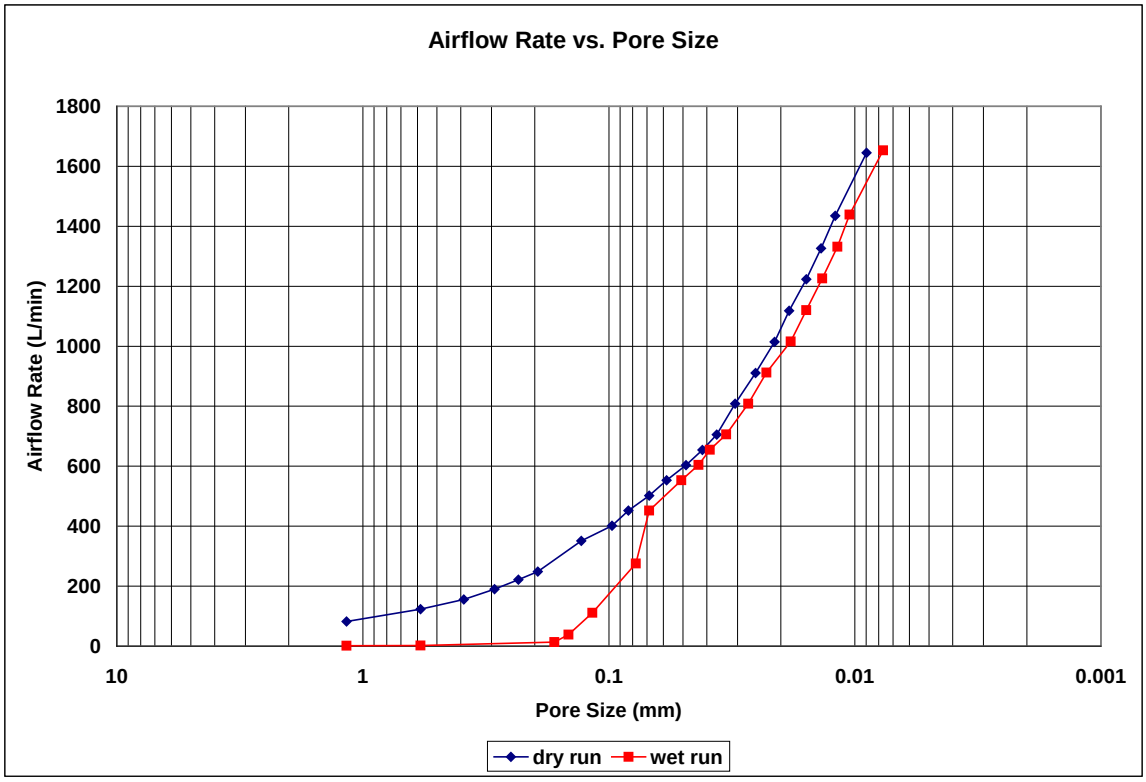

Figure B.42: Porewick-1 airflow rate vs. pore size for the wet and dry runs.

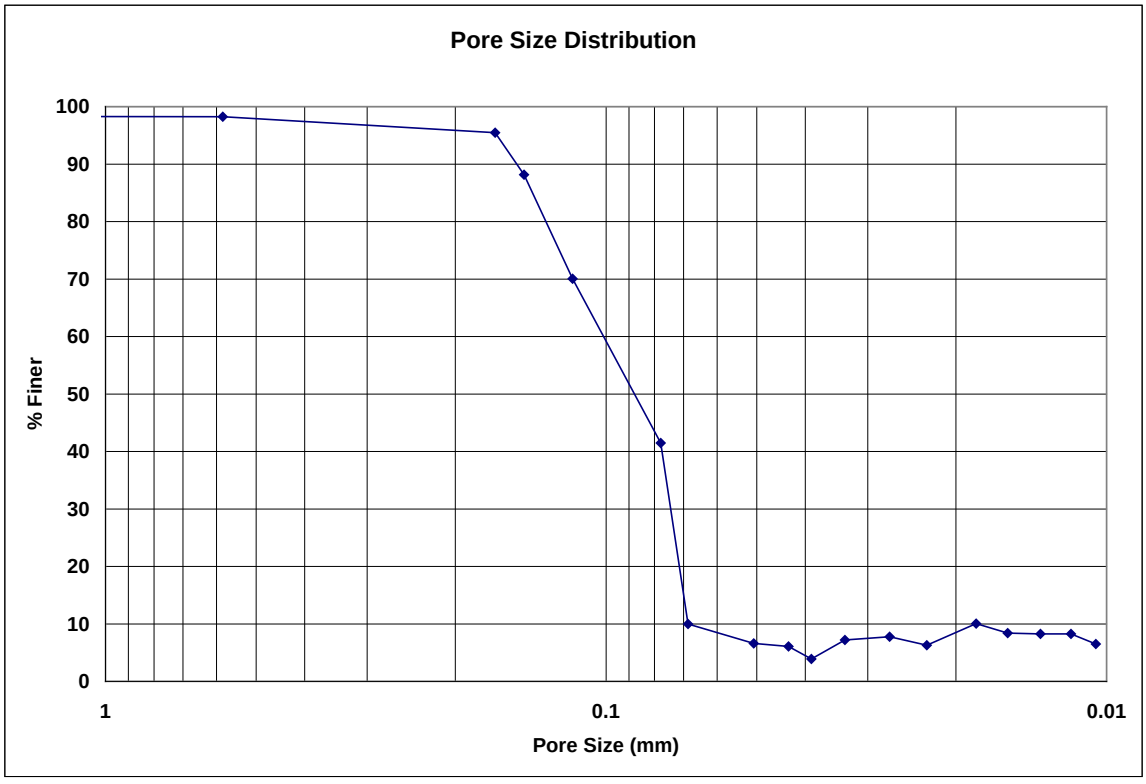

Figure B.43: Porewick-1 pore size distribution.

Bubble Point Test
Auburn University - Department of Civil Engineering

date of test: 11/1/2006
test identification: porewick 1
test performed by: David Hayes
wetting fluid: porewick
air temperature: 21.3 °C
porous media: NG-1 nonwoven geotextile
comments: testing to determine geotextile pore size distribution

Pore Size Calculation Parameters:
constant, C: 2860 mm/m
contact angle: 0 degrees
surface tension: 0.016 N/m

Pore Size at Selected % Finer

% finer	pore size (mm)
98	0.54505
95	0.16527
90	0.15104
85	0.14070
80	0.13265
75	0.12459
70	0.11655
65	0.10975
60	0.10295
55	0.09615
50	0.08935
45	0.08256
40	0.07732
35	0.07587
30	0.07441
25	0.07296
20	0.07151
15	0.07006
10	0.06861
5	0.04105

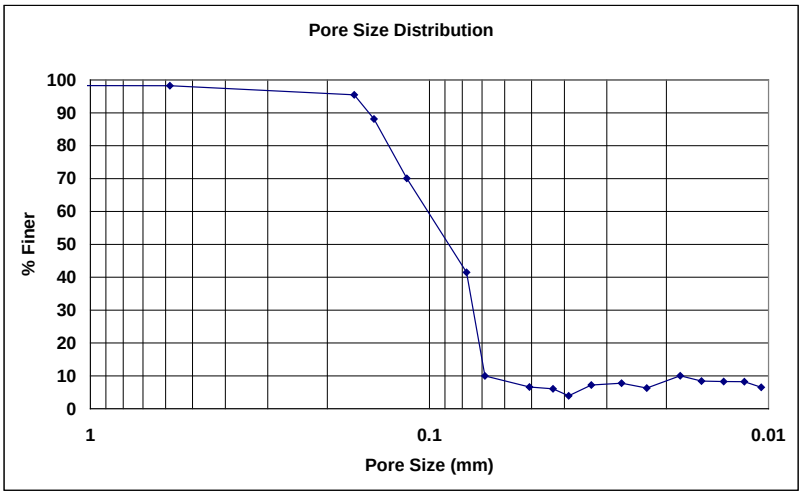

Figure B.44: Porewick-1 pore size distribution report.

Bubble Point Test

Auburn University - Department of Civil Engineering

date of test: 11/1/2006
test identification: porewick 2
test performed by: David Hayes
wetting fluid: porewick
ambient air temperature: 22.5 °C
porous media: NG-1 nonwoven geotextile
comments: testing to determine geotextile pore size distribution

Pore Size Calculation Parameters:
constant, C: 2860 mm/m
contact angle: 0 degrees
surface tension: 0.016 N/m

Dry Run

Recorded Data							Calculations				
Indirect Reading Rotameters				Direct Reading Rotameter Value (L/min)	Pressure at Rotameter Exit (psig)	Half of Manometer Reading (mm H20)	Manometer Reading (mm H20)	Manometer Pressure (Pa)	Pore Size (Diameter) (mm)	Indicated Airflow Rate (L/min)	True Airflow Rate (L/min)
First Rotameter Used		Second Rotameter Used									
Rotameter ID Number	Rotameter Value	Rotameter ID Number	Rotameter Value								
5	44				0.13	2	4	39.24	1.166157	65.3	65.58811
5	73				0.29	4	8	78.48	0.5830785	110	111.0797
5	92				0.47	6	12	117.72	0.388719	140	142.2205
5	53	5	66		0.25	8	16	156.96	0.2915392	177.5	179.003
5	63	5	80		0.36	10	20	196.2	0.2332314	215	217.6167
5	77	5	95		0.52	14	28	274.68	0.1665939	261	265.5762
				350	0.08	20	40	392.4	0.1166157	350	350.9511
				400	0.1	24	48	470.88	0.0971797	400	401.3582
				450	0.12	30	60	588.6	0.0777438	450	451.833
				550	0.15	40	80	784.8	0.0583078	550	552.799
				600	0.17	48	96	941.76	0.0485899	600	603.4594
				650	0.19	54	108	1059.48	0.043191	650	654.1872
				700	0.22	62	124	1216.44	0.037618	700	705.2186
				800	0.29	76	152	1491.12	0.0306883	800	807.8526
				900	0.35	92	184	1805.04	0.0253512	900	910.6513
				1000	0.4	108	216	2118.96	0.0215955	1000	1013.514
				1100	0.48	126	252	2472.12	0.0185104	1100	1117.815
				1200	0.56	150	300	2943	0.0155488	1200	1222.644
				1300	0.64	168	336	3296.16	0.0138828	1300	1327.998
				1400	0.74	194	388	3806.28	0.0120222	1400	1434.805
				1600	0.87	266	532	5218.92	0.0087681	1600	1646.666

Wet Run

Recorded Data							Calculations				
Indirect Reading Rotameters				Direct Reading Rotameter Value (L/min)	Pressure at Rotameter Exit (psig)	Half of Manometer Reading (mm H20)	Manometer Reading (mm H20)	Manometer Pressure (Pa)	Pore Size (Diameter) (mm)	Indicated Airflow Rate (L/min)	True Airflow Rate (L/min)
First Rotameter Used		Second Rotameter Used									
Rotameter ID Number	Rotameter Value	Rotameter ID Number	Rotameter Value								
2	82				0	2	4	39.24	1.166157	1.724	1.724
4	8				0.04	4	8	78.48	0.5830785	2.43	2.433304
4	31				0.13	12	24	235.44	0.1943595	10.5	10.54633
5	37				0.12	16	32	313.92	0.1457696	55.1	55.32444
5	82				0.38	20	40	392.4	0.1166157	124	125.5925
5	80	5	100		0.61	28	56	549.36	0.0832969	274	279.6272
				450	0.12	34	68	667.08	0.0685975	450	451.833
				500	0.14	40	80	784.8	0.0583078	500	502.3753
				550	0.16	46	92	902.52	0.0507025	550	552.9851
				600	0.19	54	108	1059.48	0.043191	600	603.8651
				650	0.22	62	124	1216.44	0.037618	650	654.8459
				700	0.24	70	140	1373.4	0.0333188	700	705.6912
				800	0.3	86	172	1687.32	0.0271199	800	808.122
				900	0.36	102	204	2001.24	0.0228658	900	910.9538
				1000	0.44	124	248	2432.88	0.018809	1000	1014.856
				1100	0.53	148	296	2903.76	0.0157589	1100	1119.654
				1200	0.61	168	336	3296.16	0.0138828	1200	1224.645
				1300	0.71	196	392	3845.52	0.0118996	1300	1331.024
				1400	0.78	224	448	4394.88	0.0104121	1400	1436.663
				1600	0.97	300	600	5886	0.0077744	1600	1651.946

Figure B.45: Porewick-2 recorded data and calculations.

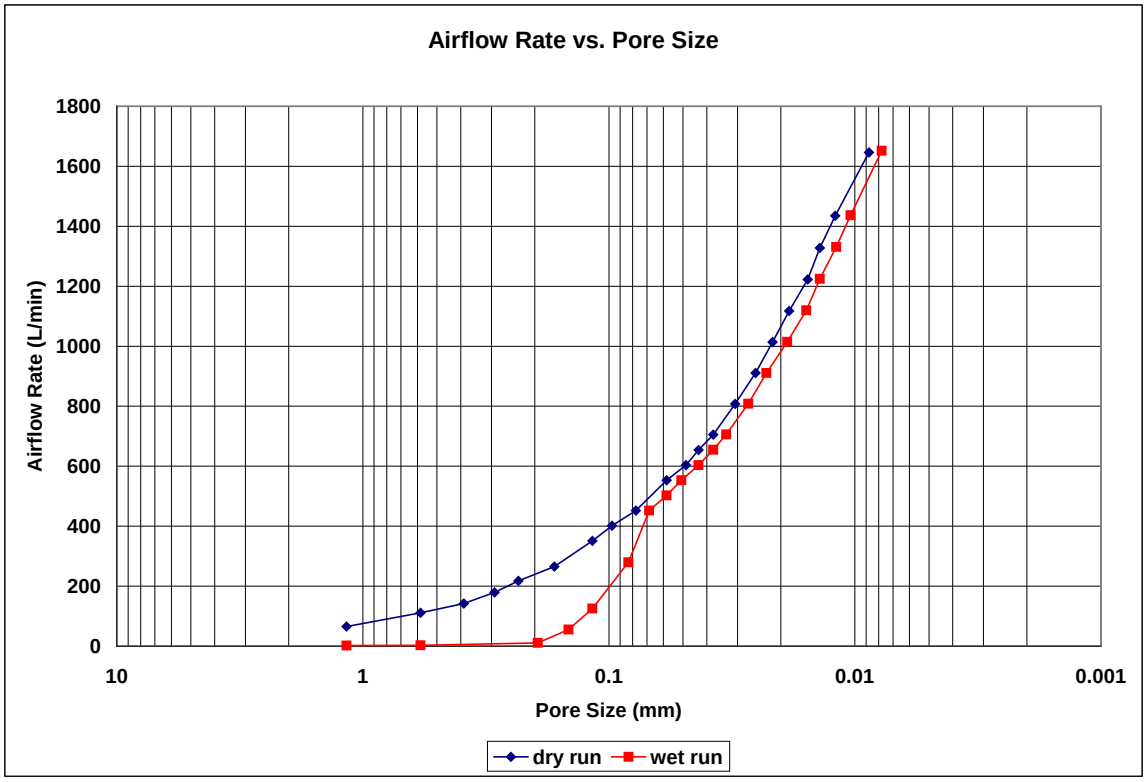

Figure B.46: Porewick-2 airflow rate vs. pore size for the wet and dry runs.

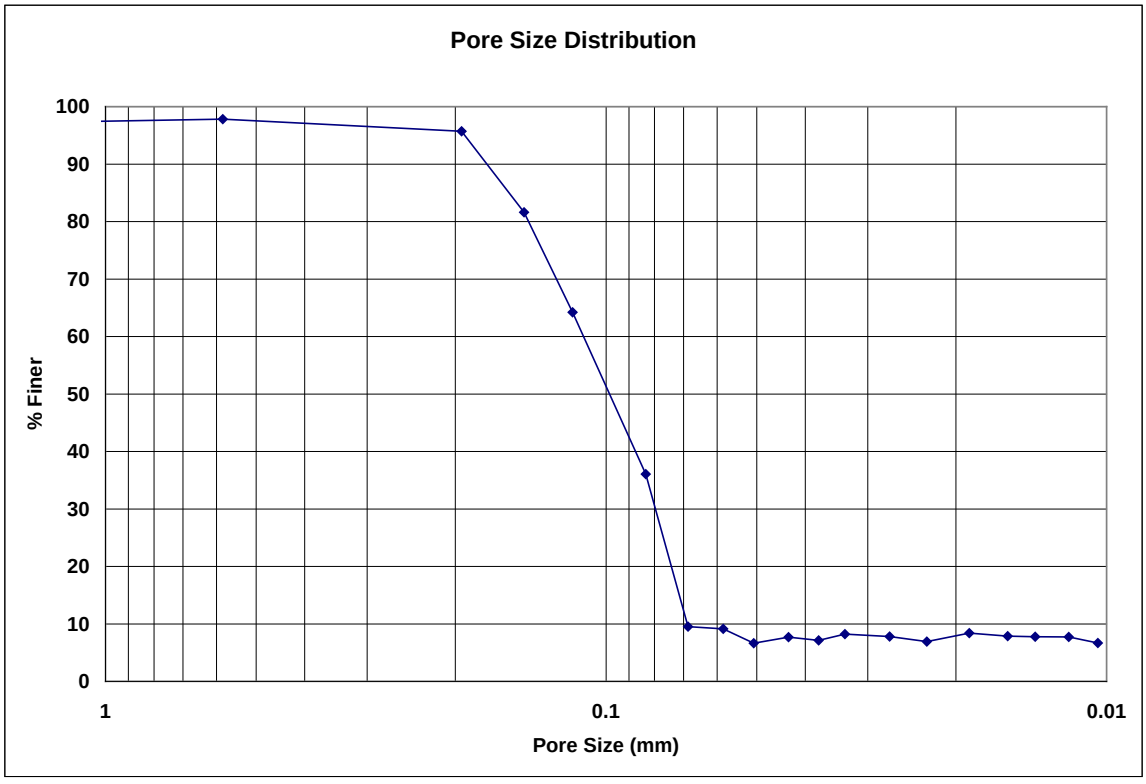

Figure B.47: Porewick-2 pore size distribution.

Bubble Point Test
Auburn University - Department of Civil Engineering

date of test: 11/1/2006
test identification: porewick 2
test performed by: David Hayes
wetting fluid: porewick
air temperature: 22.5 °C
porous media: NG-1 nonwoven geotextile
comments: testing to determine geotextile pore size distribution

Pore Size Calculation Parameters:
constant, C: 2860 mm/m
contact angle: 0 degrees
surface tension: 0.016 N/m

Pore Size at Selected % Finer

% finer	pore size (mm)
98	---
95	0.19192
90	0.17466
85	0.15741
80	0.14304
75	0.13467
70	0.12630
65	0.11793
60	0.11163
55	0.10571
50	0.09979
45	0.09387
40	0.08795
35	0.08270
30	0.07994
25	0.07717
20	0.07440
15	0.07163
10	0.06887
5	---

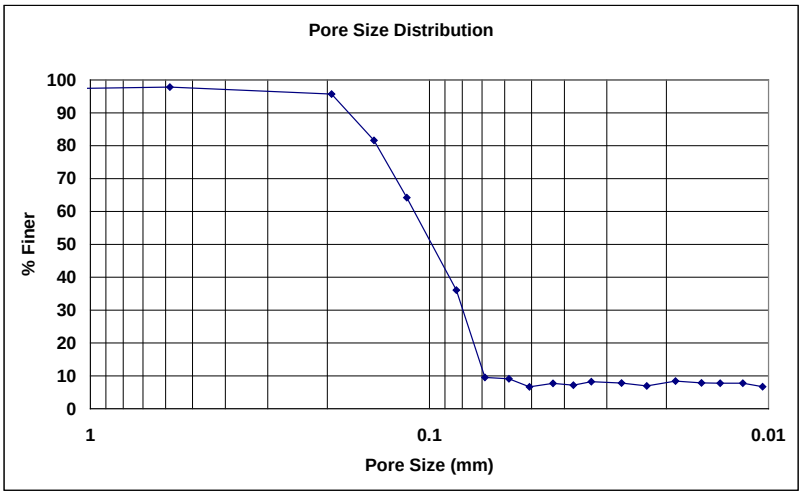

Figure B.48: Porewick-2 pore size distribution report.

Bubble Point Test

Auburn University - Department of Civil Engineering

date of test: 11/1/2006
test identification: porewick 3
test performed by: David Hayes
wetting fluid: porewick
ambient air temperature: 22.5 °C
porous media: NG-1 nonwoven geotextile
comments: testing to determine geotextile pore size distribution

Pore Size Calculation Parameters:
constant, C: 2860 mm/m
contact angle: 0 degrees
surface tension: 0.016 N/m

Dry Run

Recorded Data							Calculations				
Indirect Reading Rotameters				Direct Reading Rotameter Value (L/min)	Pressure at Rotameter Exit (psig)	Half of Manometer Reading (mm H20)	Manometer Reading (mm H20)	Manometer Pressure (Pa)	Pore Size (Diameter) (mm)	Indicated Airflow Rate (L/min)	True Airflow Rate (L/min)
First Rotameter Used		Second Rotameter Used									
Rotameter ID Number	Rotameter Value	Rotameter ID Number	Rotameter Value								
5	43				0.09	2	4	39.24	1.166157	63.8	63.99501
5	75				0.28	4	8	78.48	0.5830785	113	114.0711
5	95				0.45	6	12	117.72	0.388719	145	147.2027
5	65	5	80		0.37	10	20	196.2	0.2332314	218.1	220.8277
5	73	5	90		0.47	12	24	235.44	0.1943595	247	250.9176
				350	0.07	18	36	353.16	0.129573	350	350.8323
				400	0.08	22	44	431.64	0.1060143	400	401.087
				450	0.1	26	52	510.12	0.0897044	450	451.528
				500	0.12	34	68	667.08	0.0685975	500	502.0367
				550	0.14	40	80	784.8	0.0583078	550	552.6128
				600	0.16	46	92	902.52	0.0507025	600	603.2565
				650	0.17	52	104	1020.24	0.0448522	650	653.7477
				700	0.2	60	120	1177.2	0.0388719	700	704.7458
				800	0.27	70	140	1373.4	0.0333188	800	807.3135
				900	0.33	86	172	1687.32	0.0271199	900	910.046
				1000	0.38	102	204	2001.24	0.0228658	1000	1012.843
				1100	0.44	122	244	2393.64	0.0191173	1100	1116.341
				1200	0.52	140	280	2746.8	0.0166594	1200	1221.04
				1300	0.6	160	320	3139.2	0.014577	1300	1326.265
				1400	0.69	180	360	3531.6	0.0129573	1400	1432.48
				1600	0.82	252	504	4944.24	0.0092552	1600	1644.02

Wet Run

Recorded Data							Calculations				
Indirect Reading Rotameters				Direct Reading Rotameter Value (L/min)	Pressure at Rotameter Exit (psig)	Half of Manometer Reading (mm H20)	Manometer Reading (mm H20)	Manometer Pressure (Pa)	Pore Size (Diameter) (mm)	Indicated Airflow Rate (L/min)	True Airflow Rate (L/min)
First Rotameter Used		Second Rotameter Used									
Rotameter ID Number	Rotameter Value	Rotameter ID Number	Rotameter Value								
4	10				0.02	2	4	39.24	1.166157	3.07	3.072088
4	44				0.16	12	24	235.44	0.1943595	15.5	15.58413
5	69				0.28	18	36	353.16	0.129573	103	103.9763
				350	0.11	30	60	588.6	0.0777438	350	351.3071
				550	0.14	42	84	824.04	0.0555313	550	552.6128
				600	0.16	48	96	941.76	0.0485899	600	603.2565
				650	0.18	54	108	1059.48	0.043191	650	653.9675
				700	0.21	62	124	1216.44	0.037618	700	704.9823
				800	0.27	74	148	1451.88	0.0315178	800	807.3135
				900	0.34	92	184	1805.04	0.0253512	900	910.3487
				1000	0.4	110	220	2158.2	0.0212029	1000	1013.514
				1100	0.46	128	256	2511.36	0.0182212	1100	1117.078
				1200	0.55	150	300	2943	0.0155488	1200	1222.243
				1300	0.65	174	348	3413.88	0.0134041	1300	1328.431
				1400	0.74	196	392	3845.52	0.0118996	1400	1434.805
				1600	0.86	270	540	5297.4	0.0086382	1600	1646.138

Figure B.49: Porewick-3 recorded data and calculations.

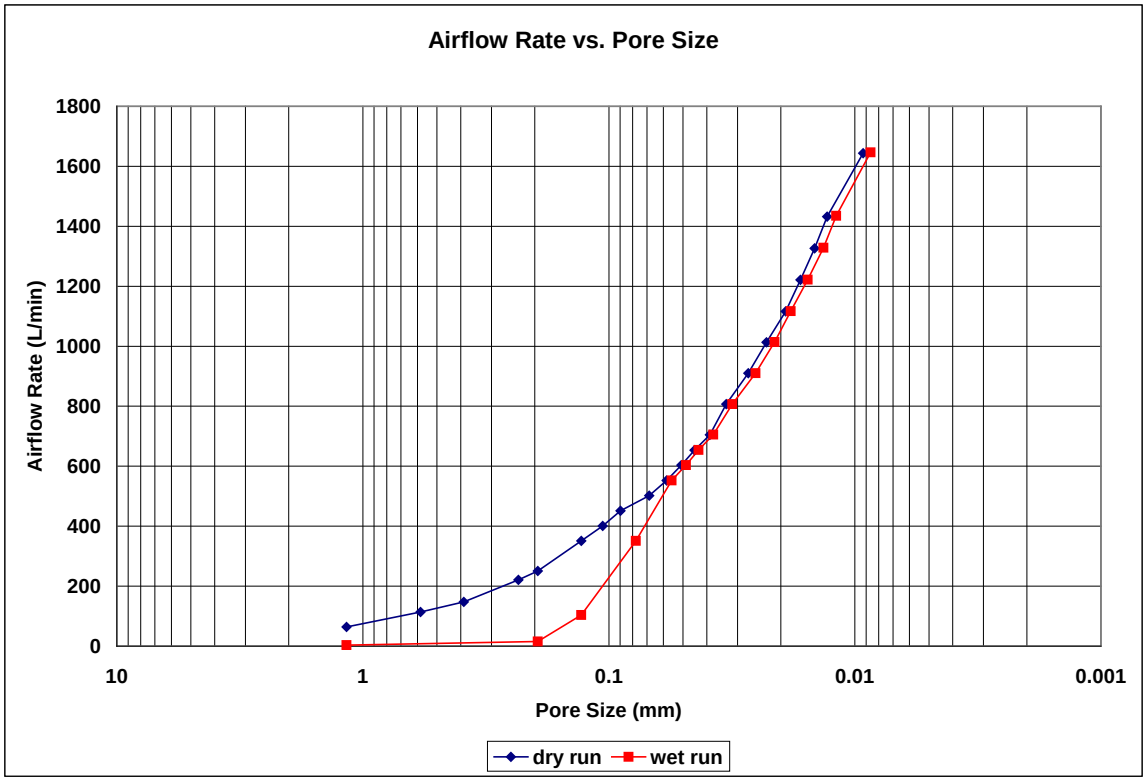

Figure B.50: Porewick-3 airflow rate vs. pore size for the wet and dry runs.

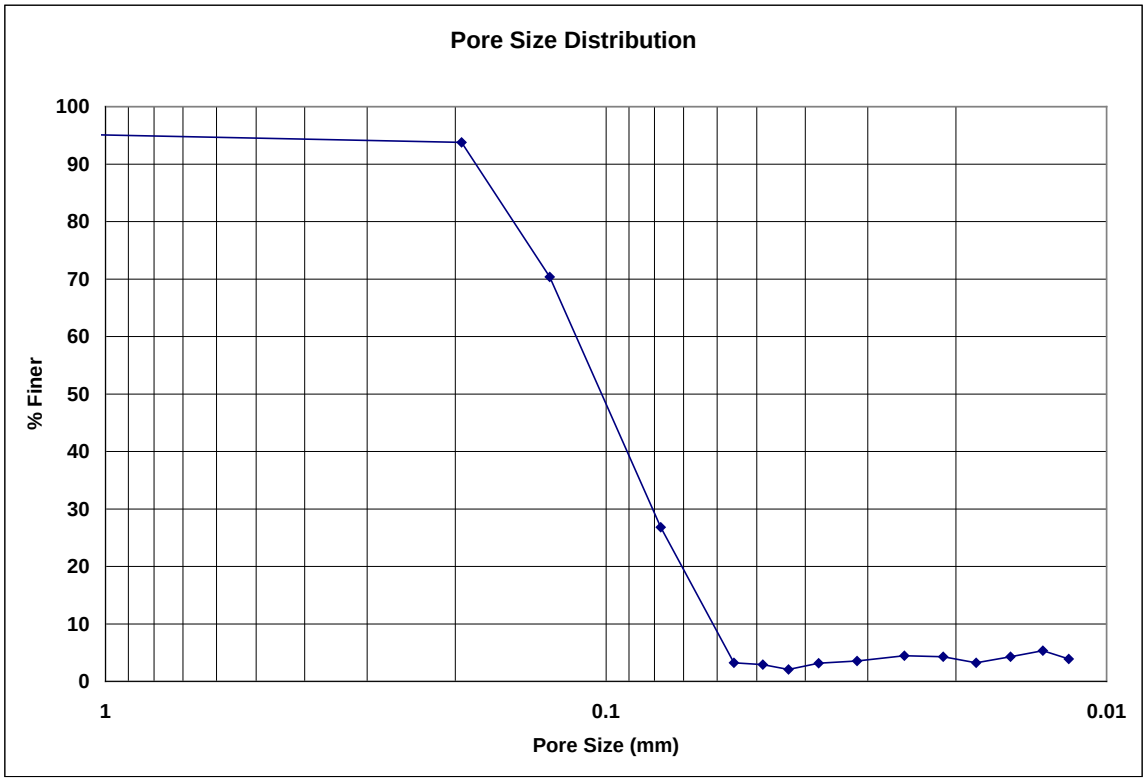

Figure B.51: Porewick-3 pore size distribution.

Bubble Point Test
Auburn University - Department of Civil Engineering

date of test: 11/1/2006
test identification: porewick 3
test performed by: David Hayes
wetting fluid: porewick
air temperature: 22.5 °C
porous media: NG-1 nonwoven geotextile
comments: testing to determine geotextile pore size distribution

Pore Size Calculation Parameters:
constant, C: 2860 mm/m
contact angle: 0 degrees
surface tension: 0.016 N/m

Pore Size at Selected % Finer

% finer	pore size (mm)
98	---
95	1.02870
90	0.18388
85	0.17005
80	0.15622
75	0.14240
70	0.12914
65	0.12319
60	0.11723
55	0.11128
50	0.10533
45	0.09937
40	0.09342
35	0.08747
30	0.08151
25	0.07602
20	0.07131
15	0.06660
10	0.06190
5	0.05719

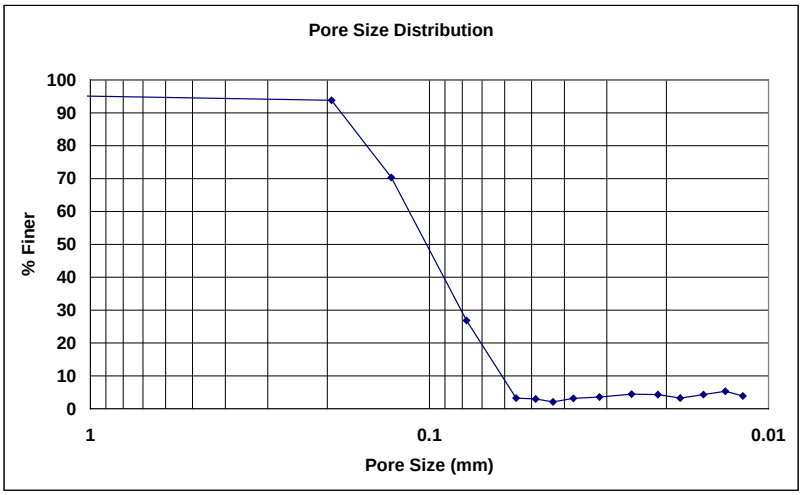

Figure B.52: Porewick-3 pore size distribution report.

Bubble Point Test

Auburn University - Department of Civil Engineering

date of test: 11/1/2006
test identification: porewick 4
test performed by: David Hayes
wetting fluid: porewick
ambient air temperature: 22.5 °C
porous media: NG-1 nonwoven geotextile
comments: testing to determine geotextile pore size distribution

Pore Size Calculation Parameters:
constant, C: 2860 mm/m
contact angle: 0 degrees
surface tension: 0.016 N/m

Dry Run

Recorded Data							Calculations				
Indirect Reading Rotameters				Direct Reading Rotameter Value (L/min)	Pressure at Rotameter Exit (psig)	Half of Manometer Reading (mm H20)	Manometer Reading (mm H20)	Manometer Pressure (Pa)	Pore Size (Diameter) (mm)	Indicated Airflow Rate (L/min)	True Airflow Rate (L/min)
First Rotameter Used		Second Rotameter Used									
Rotameter ID Number	Rotameter Value	Rotameter ID Number	Rotameter Value								
5	39				0.09	2	4	39.24	1.166157	58	58.17728
5	75				0.29	4	8	78.48	0.5830785	113	114.1092
5	50	5	63		0.23	6	12	117.72	0.388719	168.2	169.5107
5	69	5	85		0.42	10	20	196.2	0.2332314	232	235.2909
5	76	5	94		0.51	12	24	235.44	0.1943595	257	261.4202
				350	0.07	16	32	313.92	0.1457696	350	350.8323
				400	0.08	20	40	392.4	0.1166157	400	401.087
				450	0.1	24	48	470.88	0.0971797	450	451.528
				550	0.13	34	68	667.08	0.0685975	550	552.4266
				600	0.15	40	80	784.8	0.0583078	600	603.0535
				650	0.17	46	92	902.52	0.0507025	650	653.7477
				700	0.19	54	108	1059.48	0.043191	700	704.5093
				800	0.24	64	128	1255.68	0.0364424	800	806.5042
				900	0.3	78	156	1530.36	0.0299015	900	909.1373
				1000	0.36	90	180	1765.8	0.0259146	1000	1012.171
				1100	0.42	106	212	2079.72	0.022003	1100	1115.604
				1200	0.49	126	252	2472.12	0.0185104	1200	1219.836
				1300	0.57	146	292	2864.52	0.0159748	1300	1324.964
				1400	0.65	166	332	3256.92	0.0140501	1400	1430.618
				1600	0.75	226	452	4434.12	0.01032	1600	1640.309

Wet Run

Recorded Data							Calculations				
Indirect Reading Rotameters				Direct Reading Rotameter Value (L/min)	Pressure at Rotameter Exit (psig)	Half of Manometer Reading (mm H20)	Manometer Reading (mm H20)	Manometer Pressure (Pa)	Pore Size (Diameter) (mm)	Indicated Airflow Rate (L/min)	True Airflow Rate (L/min)
First Rotameter Used		Second Rotameter Used									
Rotameter ID Number	Rotameter Value	Rotameter ID Number	Rotameter Value								
4	13				0.03	2	4	39.24	1.166157	4.07	4.074151
4	33				0.11	10	20	196.2	0.2332314	11.3	11.3422
4	99				0.73	14	28	274.68	0.1665939	38.7	39.64928
5	93				0.45	20	40	392.4	0.1166157	141	143.1419
				450	0.08	28	56	549.36	0.0832969	450	451.2228
				550	0.12	38	76	745.56	0.0613767	550	552.2403
				600	0.14	44	88	863.28	0.0530071	600	602.8504
				650	0.16	50	100	981	0.0466463	650	653.5278
				700	0.18	56	112	1098.72	0.0416485	700	704.2727
				800	0.22	68	136	1334.16	0.0342987	800	805.9642
				900	0.27	84	168	1648.08	0.0277656	900	908.2277
				1000	0.34	102	204	2001.24	0.0228658	1000	1011.499
				1100	0.41	120	240	2354.4	0.0194359	1100	1115.235
				1200	0.48	140	280	2746.8	0.0166594	1200	1219.434
				1300	0.55	160	320	3139.2	0.014577	1300	1324.096
				1400	0.64	186	372	3649.32	0.0125393	1400	1430.152
				1600	0.79	244	488	4787.28	0.0095587	1600	1642.431

Figure B.53: Porewick-4 recorded data and calculations.

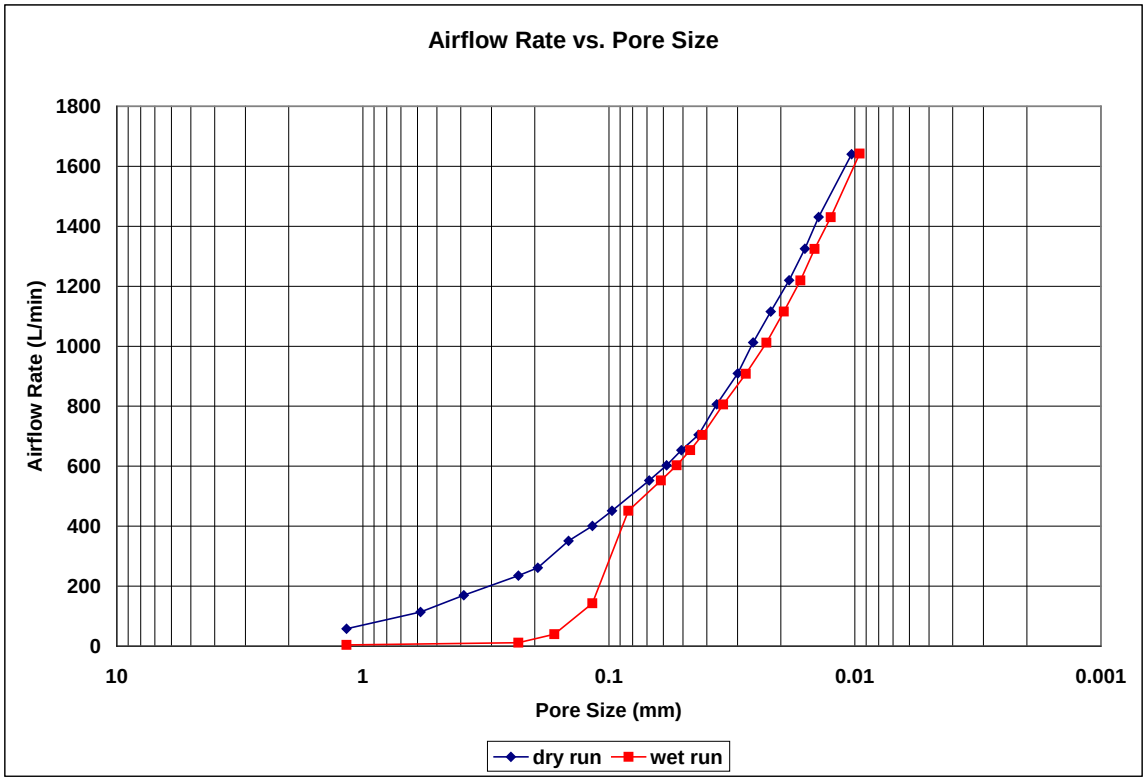

Figure B.54: Porewick-4 airflow rate vs. pore size for the wet and dry runs.

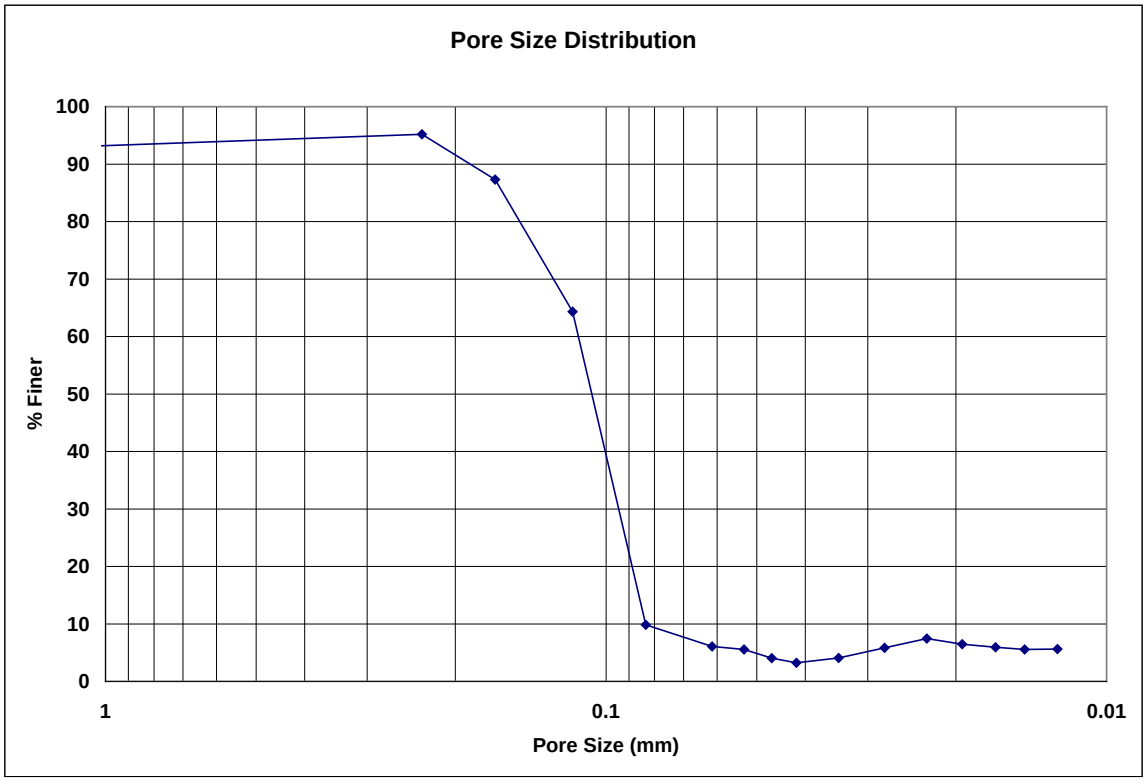

Figure B.55: Porewick-4 pore size distribution.

Bubble Point Test
Auburn University - Department of Civil Engineering

date of test: 11/1/2006
test identification: porewick 4
test performed by: David Hayes
wetting fluid: porewick
air temperature: 22.5 °C
porous media: NG-1 nonwoven geotextile
comments: testing to determine geotextile pore size distribution

Pore Size Calculation Parameters:
constant, C: 2860 mm/m
contact angle: 0 degrees
surface tension: 0.016 N/m

Pore Size at Selected % Finer

% finer	pore size (mm)
98	---
95	0.23171
90	0.18936
85	0.16157
80	0.15070
75	0.13984
70	0.12898
65	0.11811
60	0.11398
55	0.11092
50	0.10786
45	0.10480
40	0.10174
35	0.09868
30	0.09562
25	0.09256
20	0.08951
15	0.08645
10	0.08339
5	0.05062

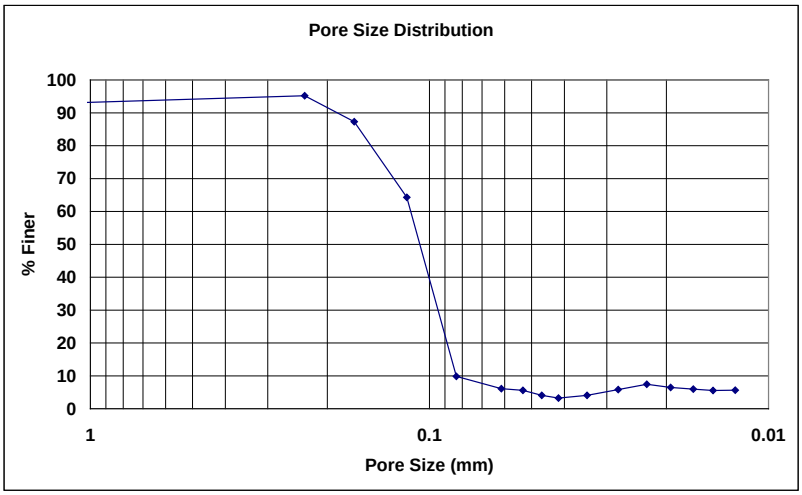

Figure B.56: Porewick-4 pore size distribution report.

Bubble Point Test
Auburn University - Department of Civil Engineering

date of test: 4/11/2002
test identification: Porewick 5
test performed by: David Howie
wetting fluid: Porewick
ambient air temperature: 21 °C
porous media: NG-1 nonwoven geotextile
comments: testing to determine geotextile pore size distribution

Pore Size Calculation Parameters:
constant, C: 2860 mm/m
contact angle: 0 degrees
surface tension: 0.016 N/m

Dry Run

Recorded Data							Calculations				
Indirect Reading Rotameters				Direct Reading Rotameter Value (L/min)	Pressure at Rotameter Exit (psig)	Half of Manometer Reading (mm H20)	Manometer Reading (mm H20)	Manometer Pressure (Pa)	Pore Size (Diameter) (mm)	Indicated Airflow Rate (L/min)	True Airflow Rate (L/min)
First Rotameter Used		Second Rotameter Used									
Rotameter ID Number	Rotameter Value	Rotameter ID Number	Rotameter Value								
4	94				0.6	1	2	19.62	2.332314	36.5	37.23745
5	37				0.08	2	4	39.24	1.166157	55.1	55.24973
5	67				0.22	4	8	78.48	0.5830785	100	100.7455
5	64	5	52		0.24	8	16	156.96	0.2915392	172.8	174.2049
5	82	5	67		0.38	12	24	235.44	0.1943595	224	226.8768
5	97	5	79		0.54	16	32	313.92	0.1457696	267	271.8599
				350	0.09	22	44	431.64	0.1060143	350	351.0698
				400	0.1	28	56	549.36	0.0832969	400	401.3582
				450	0.13	34	68	667.08	0.0685975	450	451.9854
				500	0.15	40	80	784.8	0.0583078	500	502.5445
				550	0.17	48	96	941.76	0.0485899	550	553.1711
				600	0.19	55	110	1079.1	0.0424057	600	603.8651
				650	0.22	64	128	1255.68	0.0364424	650	654.8459
				700	0.25	72	144	1412.64	0.0323932	700	705.9273
				800	0.31	89	178	1746.18	0.0262058	800	808.3914
				900	0.38	107	214	2099.34	0.0217973	900	911.5584
				1000	0.44	126	252	2472.12	0.0185104	1000	1014.856
				1100	0.51	146	292	2864.52	0.0159748	1100	1118.919
				1200	0.59	171	342	3355.02	0.0136393	1200	1223.845
				1300	0.69	196	392	3845.52	0.0118996	1300	1330.16
				1400	0.78	222	444	4355.64	0.0105059	1400	1436.663
				1600	0.99	310	620	6082.2	0.0075236	1600	1653

Wet Run

Recorded Data							Calculations				
Indirect Reading Rotameters				Direct Reading Rotameter Value (L/min)	Pressure at Rotameter Exit (psig)	Half of Manometer Reading (mm H20)	Manometer Reading (mm H20)	Manometer Pressure (Pa)	Pore Size (Diameter) (mm)	Indicated Airflow Rate (L/min)	True Airflow Rate (L/min)
First Rotameter Used		Second Rotameter Used									
Rotameter ID Number	Rotameter Value	Rotameter ID Number	Rotameter Value								
1	7					4	8	78.48	0.5830785	0.00459	0.00459
1	32					10	20	196.2	0.2332314	0.0532	0.0532
2	58					12	24	235.44	0.1943595	1.123	1.123
4	32				0.12	14	28	274.68	0.1665939	10.9	10.9444
4	94				0.65	16	32	313.92	0.1457696	36.5	37.29824
				350	0.08	22	44	431.64	0.1060143	350	350.9511
				400	0.1	28	56	549.36	0.0832969	400	401.3582
				450	0.12	35	70	686.7	0.0666375	450	451.833
				500	0.14	42	84	824.04	0.0555313	500	502.3753
				550	0.17	50	100	981	0.0466463	550	553.1711
				600	0.2	57	114	1118.34	0.0409178	600	604.0678
				650	0.22	66	132	1294.92	0.0353381	650	654.8459
				700	0.25	74	148	1451.88	0.0315178	700	705.9273
				800	0.33	93	186	1824.66	0.0250786	800	808.9298
				900	0.4	114	228	2236.68	0.0204589	900	912.1627
				1000	0.47	134	268	2629.08	0.0174053	1000	1015.861
				1100	0.54	155	310	3041.1	0.0150472	1100	1120.022
				1200	0.64	183	366	3590.46	0.0127449	1200	1225.844
				1300	0.74	214	428	4198.68	0.0108987	1300	1332.319
				1400	0.85	244	488	4787.28	0.0095587	1400	1439.907
				1600	1.08	345	690	6768.9	0.0067603	1600	1657.734

Figure B.57: Porewick-5 recorded data and calculations.

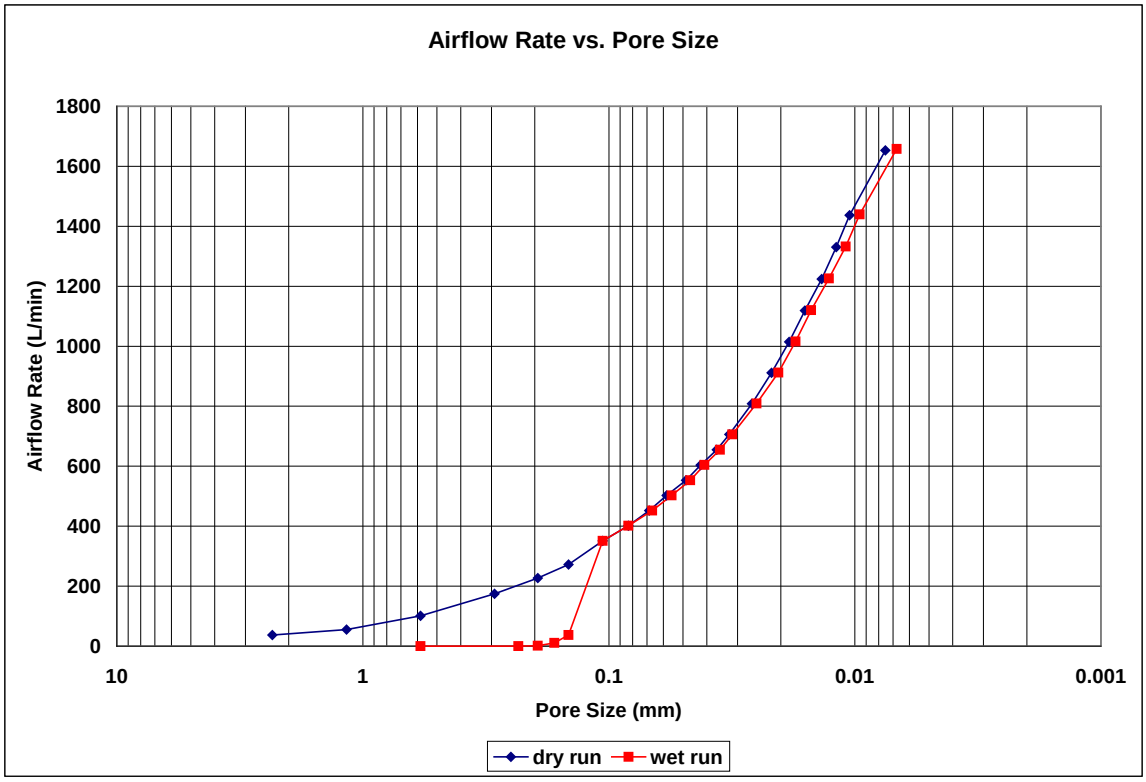

Figure B.58: Porewick-5 airflow rate vs. pore size for the wet and dry runs.

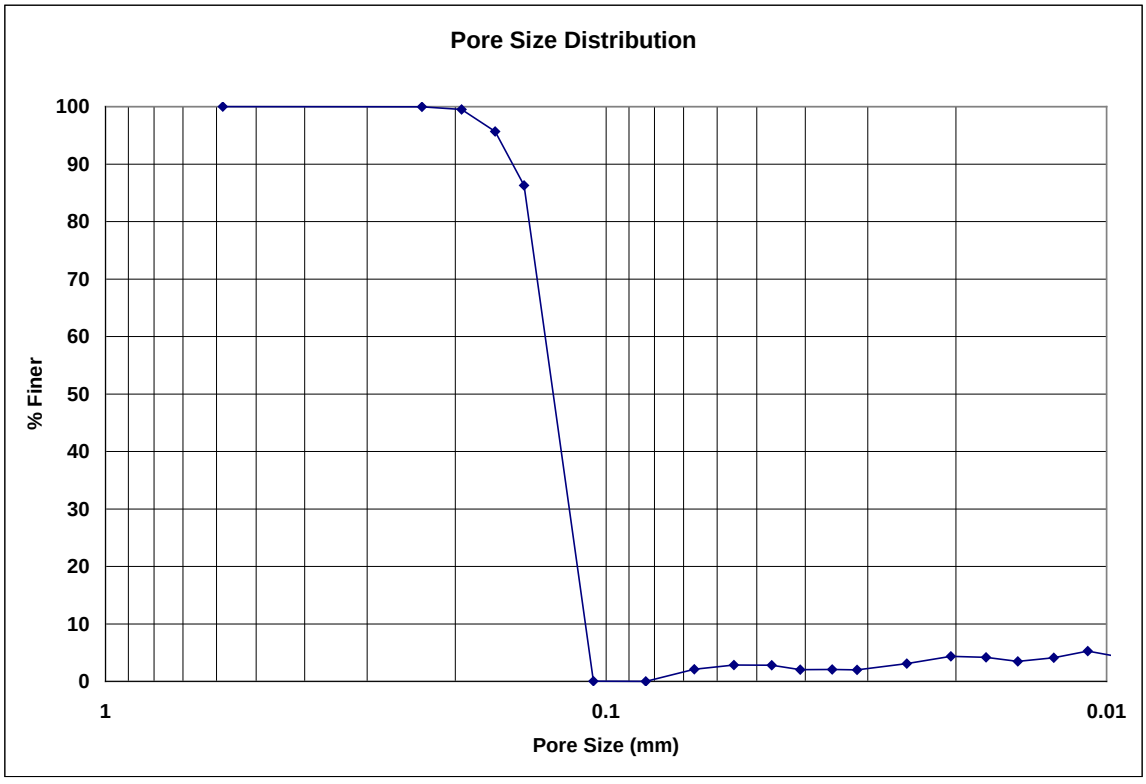

Figure B.59: Porewick-5 pore size distribution.

Bubble Point Test
Auburn University - Department of Civil Engineering

date of test:	4/11/2002	Pore Size Calculation Parameters:		
test identification:	Porewick 5	constant, C:	2860	mm/m
test performed by:	David Howie	contact angle:	0	degrees
wetting fluid:	Porewick	surface tension:	0.016	N/m
air temperature:	21 °C			
porous media:	NG-1 nonwoven geotextile			
comments:	testing to determine geotextile pore size distribution			

Pore Size at Selected % Finer

% finer	pore size (mm)
98	0.18347
95	0.16511
90	0.15402
85	0.14518
80	0.14287
75	0.14057
70	0.13827
65	0.13596
60	0.13366
55	0.13135
50	0.12905
45	0.12674
40	0.12444
35	0.12213
30	0.11983
25	0.11752
20	0.11522
15	0.11291
10	0.11061
5	0.10830

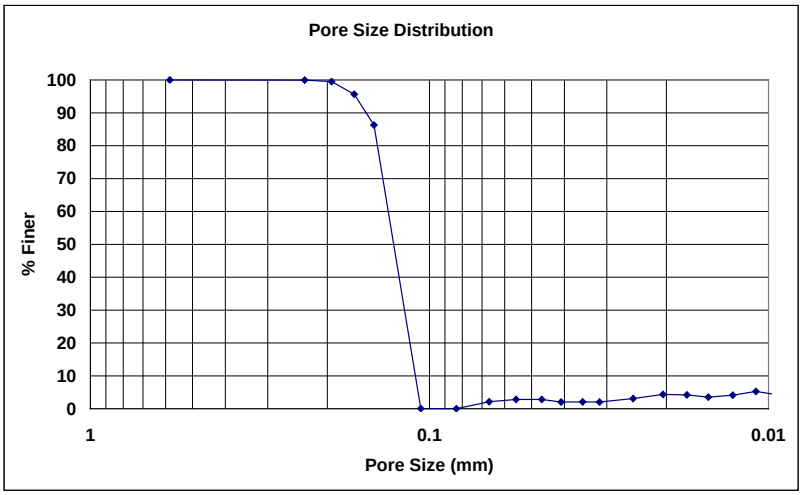

Figure B.60: Porewick-5 pore size distribution report.

Bubble Point Test
Auburn University - Department of Civil Engineering

date of test: 4/11/2002
test identification: Porewick 6
test performed by: David Howie
wetting fluid: Porewick
ambient air temperature: 21 °C
porous media: NG-1 nonwoven geotextile
comments: testing to determine geotextile pore size distribution

Pore Size Calculation Parameters:
constant, C: 2860 mm/m
contact angle: 0 degrees
surface tension: 0.016 N/m

Dry Run

Recorded Data							Calculations				
Indirect Reading Rotameters				Direct Reading Rotameter Value (L/min)	Pressure at Rotameter Exit (psig)	Half of Manometer Reading (mm H20)	Manometer Reading (mm H20)	Manometer Pressure (Pa)	Pore Size (Diameter) (mm)	Indicated Airflow Rate (L/min)	True Airflow Rate (L/min)
First Rotameter Used		Second Rotameter Used									
Rotameter ID Number	Rotameter Value	Rotameter ID Number	Rotameter Value								
5	28				0.06	1	2	19.62	2.332314	42.1	42.18583
5	46				0.12	2	4	39.24	1.166157	68.3	68.57821
5	67				0.24	4	8	78.48	0.5830785	100	100.813
5	67	5	54		0.27	9	18	176.58	0.259146	180.3	181.9483
5	79	5	64		0.36	12	24	235.44	0.1943595	214.6	217.2119
5	94	5	77		0.52	16	32	313.92	0.1457696	259	263.5411
				350	0.09	24	48	470.88	0.0971797	350	351.0698
				400	0.11	30	60	588.6	0.0777438	400	401.4938
				450	0.13	36	72	706.32	0.0647865	450	451.9854
				500	0.15	43	86	843.66	0.0542399	500	502.5445
				550	0.17	51	102	1000.62	0.0457316	550	553.1711
				600	0.2	58	116	1137.96	0.0402123	600	604.0678
				650	0.23	66	132	1294.92	0.0353381	650	655.0653
				700	0.26	75	150	1471.5	0.0310975	700	706.1633
				800	0.33	92	184	1805.04	0.0253512	800	808.9298
				900	0.39	113	226	2217.06	0.0206399	900	911.8606
				1000	0.44	135	270	2648.7	0.0172764	1000	1014.856
				1100	0.53	154	308	3021.48	0.0151449	1100	1119.654
				1200	0.62	180	360	3531.6	0.0129573	1200	1225.045
				1300	0.71	206	412	4041.72	0.0113219	1300	1331.024
				1400	0.78	236	472	4630.32	0.0098827	1400	1436.663
				1600	1.08	334	668	6553.08	0.006983	1600	1657.734

Wet Run

Recorded Data							Calculations				
Indirect Reading Rotameters				Direct Reading Rotameter Value (L/min)	Pressure at Rotameter Exit (psig)	Half of Manometer Reading (mm H20)	Manometer Reading (mm H20)	Manometer Pressure (Pa)	Pore Size (Diameter) (mm)	Indicated Airflow Rate (L/min)	True Airflow Rate (L/min)
First Rotameter Used		Second Rotameter Used									
Rotameter ID Number	Rotameter Value	Rotameter ID Number	Rotameter Value								
1	67					12	24	235.44	0.1943595	0.174	0.174
4	8				0.06	14	28	274.68	0.1665939	2.43	2.434954
4	47				0.2	16	32	313.92	0.1457696	16.6	16.71254
5	94	5	77		0.49	18	36	353.16	0.129573	259	263.2813
				350	0.09	25	50	490.5	0.0932926	350	351.0698
				400	0.11	32	64	627.84	0.0728848	400	401.4938
				450	0.13	40	80	784.8	0.0583078	450	451.9854
				500	0.15	47	94	922.14	0.0496237	500	502.5445
				550	0.18	55	110	1079.1	0.0424057	550	553.3571
				600	0.21	64	128	1255.68	0.0364424	600	604.2705
				650	0.24	72	144	1412.64	0.0323932	650	655.2846
				700	0.27	82	164	1608.84	0.0284429	700	706.3993
				800	0.34	100	200	1962	0.0233231	800	809.1988
				900	0.41	122	244	2393.64	0.0191173	900	912.4647
				1000	0.49	145	290	2844.9	0.0160849	1000	1016.53
				1100	0.57	168	336	3296.16	0.0138828	1100	1121.124
				1200	0.67	196	392	3845.52	0.0118996	1200	1227.042
				1300	0.77	228	456	4473.36	0.0102294	1300	1333.613
				1400	0.88	260	520	5101.2	0.0089704	1400	1441.296
				1600	1.14	365	730	7161.3	0.0063899	1600	1660.882

Figure B.61: Porewick-6 recorded data and calculations.

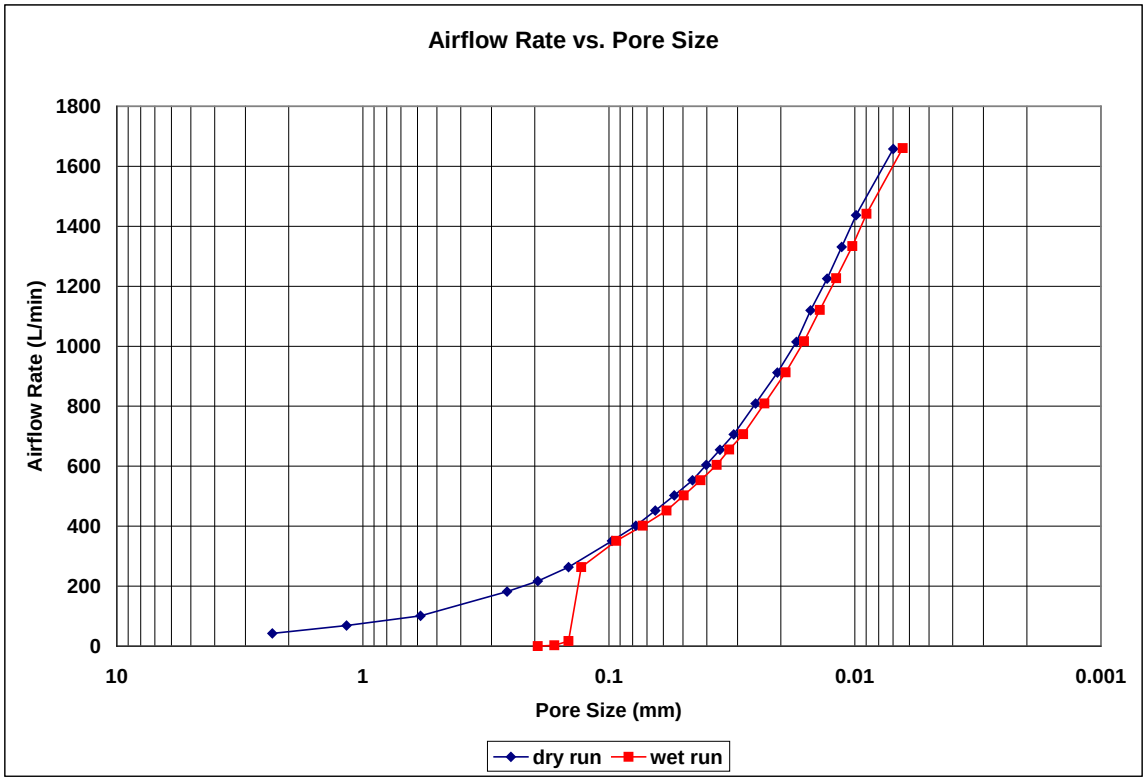

Figure B.62: Porewick-6 airflow rate vs. pore size for the wet and dry runs.

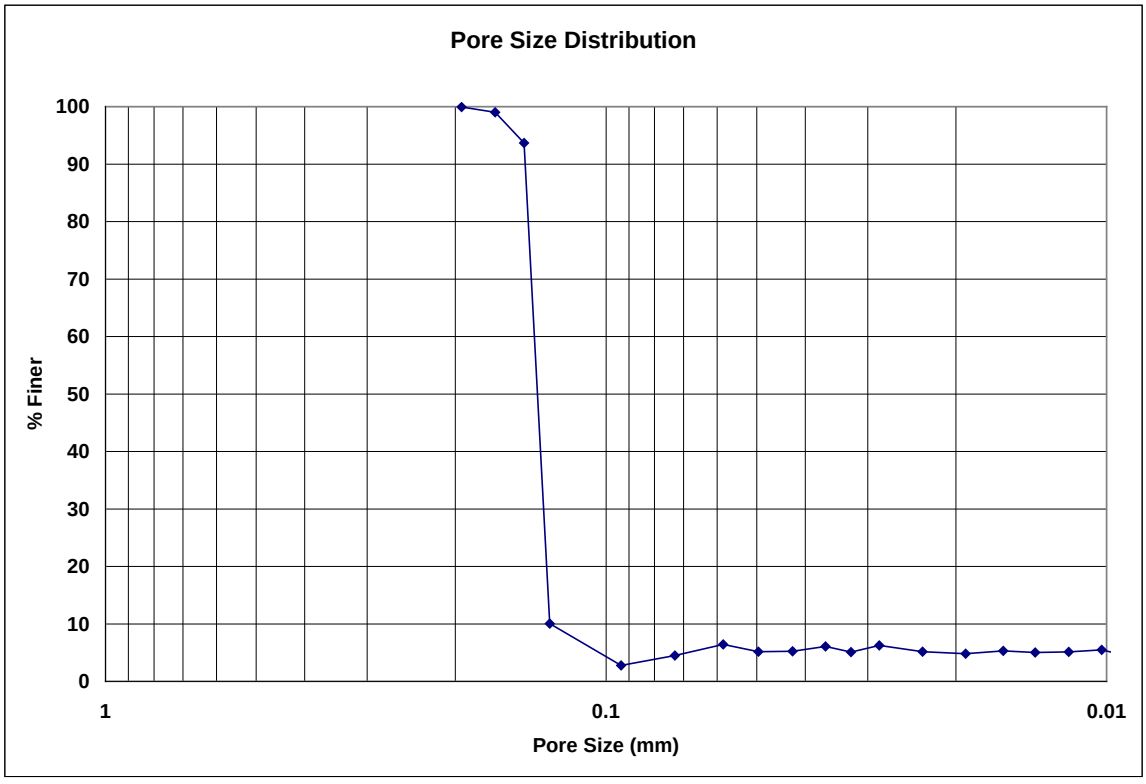

Figure B.63: Porewick-6 pore size distribution.

Bubble Point Test
Auburn University - Department of Civil Engineering

date of test:	4/11/2002	Pore Size Calculation Parameters:		
test identification:	Porewick 6	constant, C:	2860	mm/m
test performed by:	David Howie	contact angle:	0	degrees
wetting fluid:	Porewick	surface tension:	0.016	N/m
air temperature:	21 °C			
porous media:	NG-1 nonwoven geotextile			
comments:	testing to determine geotextile pore size distribution			

Pore Size at Selected % Finer

% finer	pore size (mm)
98	0.16269
95	0.15100
90	0.14506
85	0.14409
80	0.14312
75	0.14215
70	0.14119
65	0.14022
60	0.13925
55	0.13828
50	0.13731
45	0.13634
40	0.13537
35	0.13441
30	0.13344
25	0.13247
20	0.13150
15	0.13053
10	0.12929
5	0.10432

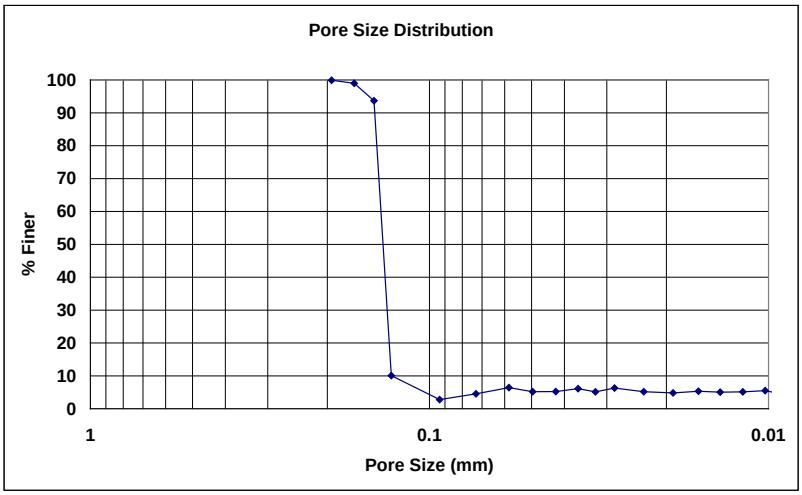

Figure B.64: Porewick-6 pore size distribution report.

Bubble Point Test

Auburn University - Department of Civil Engineering

date of test: 5/4/2002
test identification: Porewick 7
test performed by: David Howie
wetting fluid: Porewick
ambient air temperature: 21.1 °C
porous media: NG-1 nonwoven geotextile
comments: testing to determine geotextile pore size distribution

Pore Size Calculation Parameters:
constant, C: 2860 mm/m
contact angle: 0 degrees
surface tension: 0.016 N/m

Dry Run

Recorded Data							Calculations				
Indirect Reading Rotameters				Direct Reading Rotameter Value (L/min)	Pressure at Rotameter Exit (psig)	Half of Manometer Reading (mm H20)	Manometer Reading (mm H20)	Manometer Pressure (Pa)	Pore Size (Diameter) (mm)	Indicated Airflow Rate (L/min)	True Airflow Rate (L/min)
First Rotameter Used		Second Rotameter Used									
Rotameter ID Number	Rotameter Value	Rotameter ID Number	Rotameter Value								
5	32				0.06	1	2	19.62	2.332314	47.9	47.99766
5	54				0.15	2	4	39.24	1.166157	80.3	80.70865
5	78				0.3	4	8	78.48	0.5830785	118	119.198
5	71	5	57		0.28	8	16	156.96	0.2915392	190.8	192.6086
5	92	5	75		0.49	12	24	235.44	0.1943595	253	257.1821
				350	0.07	18	36	353.16	0.129573	350	350.8323
				400	0.09	22	44	431.64	0.1060143	400	401.2226
				450	0.11	28	56	549.36	0.0832969	450	451.6805
				500	0.12	33	66	647.46	0.0706762	500	502.0367
				550	0.14	39	78	765.18	0.0598029	550	552.6128
				600	0.16	44.5	89	873.09	0.0524115	600	603.2565
				650	0.19	52	104	1020.24	0.0448522	650	654.1872
				700	0.21	58	116	1137.96	0.0402123	700	704.9823
				800	0.26	71	142	1393.02	0.0328495	800	807.0438
				900	0.31	87	174	1706.94	0.0268082	900	909.4403
				1000	0.37	103	206	2020.86	0.0226438	1000	1012.507
				1100	0.43	120	240	2354.4	0.0194359	1100	1115.972
				1200	0.5	140	280	2746.8	0.0166594	1200	1220.238
				1300	0.55	162	324	3178.44	0.014397	1300	1324.096
				1400	0.66	184	368	3610.08	0.0126756	1400	1431.084
				1600	0.83	254	508	4983.48	0.0091823	1600	1644.55

Wet Run

Recorded Data							Calculations				
Indirect Reading Rotameters				Direct Reading Rotameter Value (L/min)	Pressure at Rotameter Exit (psig)	Half of Manometer Reading (mm H20)	Manometer Reading (mm H20)	Manometer Pressure (Pa)	Pore Size (Diameter) (mm)	Indicated Airflow Rate (L/min)	True Airflow Rate (L/min)
First Rotameter Used		Second Rotameter Used									
Rotameter ID Number	Rotameter Value	Rotameter ID Number	Rotameter Value								
1	13					6.5	13	127.53	0.3588175	0.011	0.011
1	25					8	16	156.96	0.2915392	0.0352	0.0352
2	44					10	20	196.2	0.2332314	0.788	0.788
4	11				0.06	12	24	235.44	0.1943595	3.41	3.416952
4	81				0.48	14	28	274.68	0.1665939	30.8	31.29882
				350	0.07	18	36	353.16	0.129573	350	350.8323
				400	0.09	23	46	451.26	0.101405	400	401.2226
				450	0.1	28	56	549.36	0.0832969	450	451.528
				500	0.12	34	68	667.08	0.0685975	500	502.0367
				550	0.14	40	80	784.8	0.0583078	550	552.6128
				600	0.16	47	94	922.14	0.0496237	600	603.2565
				650	0.19	53	106	1039.86	0.0440059	650	654.1872
				700	0.21	60	120	1177.2	0.0388719	700	704.9823
				800	0.29	75	150	1471.5	0.0310975	800	807.8526
				900	0.35	91	182	1785.42	0.0256298	900	910.6513
				1000	0.41	107	214	2099.34	0.0217973	1000	1013.85
				1100	0.47	125	250	2452.5	0.0186585	1100	1117.447
				1200	0.55	156	312	3060.72	0.0149507	1200	1222.243
				1300	0.64	173	346	3394.26	0.0134816	1300	1327.998
				1400	0.72	196	392	3845.52	0.0118996	1400	1433.876
				1600	0.9	274	548	5375.88	0.0085121	1600	1648.252

Figure B.65: Porewick-7 recorded data and calculations.

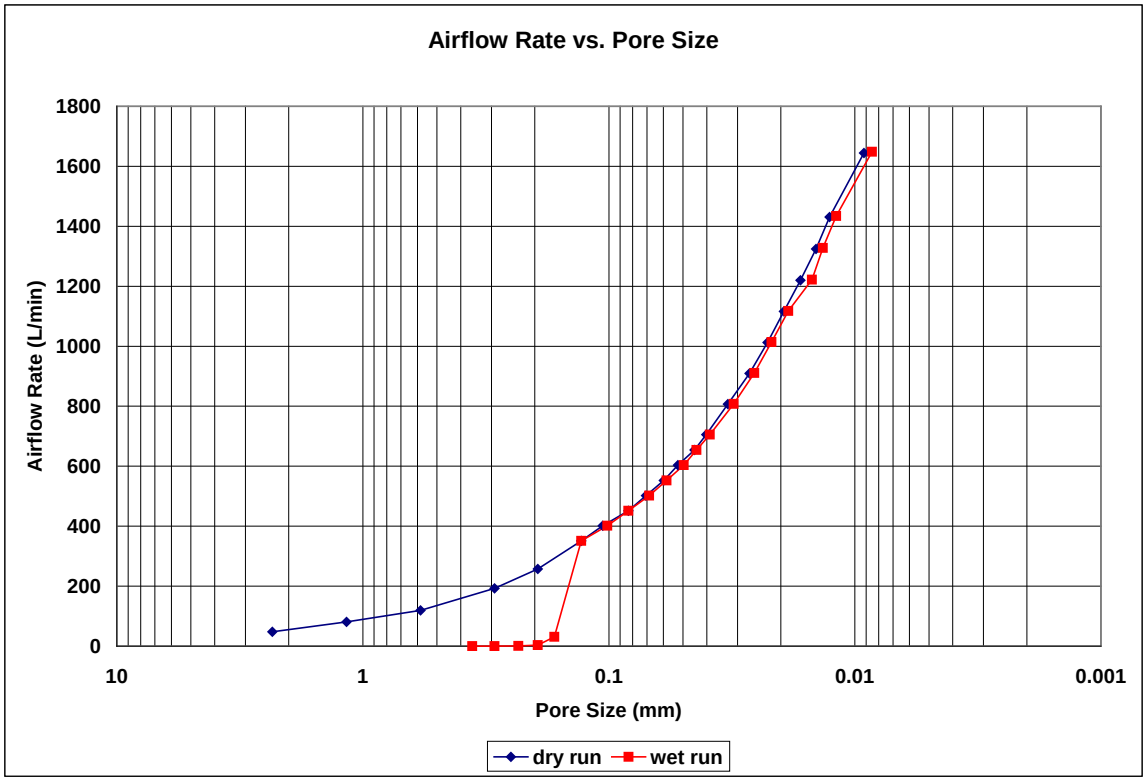

Figure B.66: Porewick-7 airflow rate vs. pore size for the wet and dry runs.

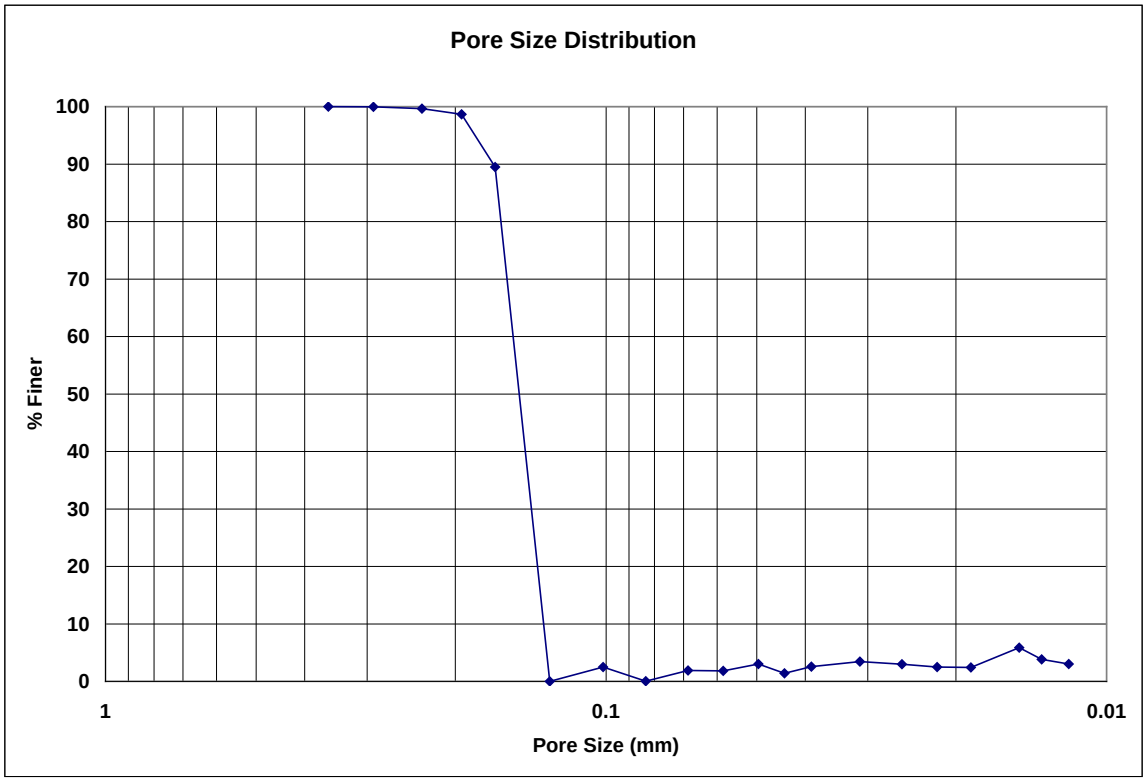

Figure B.67: Porewick-7 pore size distribution.

Bubble Point Test
Auburn University - Department of Civil Engineering

date of test:	5/4/2002	Pore Size Calculation Parameters:		
test identification:	Porewick 7	constant, C:	2860	mm/m
test performed by:	David Howie	contact angle:	0	degrees
wetting fluid:	Porewick	surface tension:	0.016	N/m
air temperature:	21.1 °C			
porous media:	NG-1 nonwoven geotextile			
comments:	testing to determine geotextile pore size distribution			

Pore Size at Selected % Finer

% finer	pore size (mm)
98	0.19233
95	0.18328
90	0.16818
85	0.16474
80	0.16267
75	0.16061
70	0.15854
65	0.15647
60	0.15440
55	0.15233
50	0.15026
45	0.14819
40	0.14612
35	0.14405
30	0.14199
25	0.13992
20	0.13785
15	0.13578
10	0.13371
5	0.13164

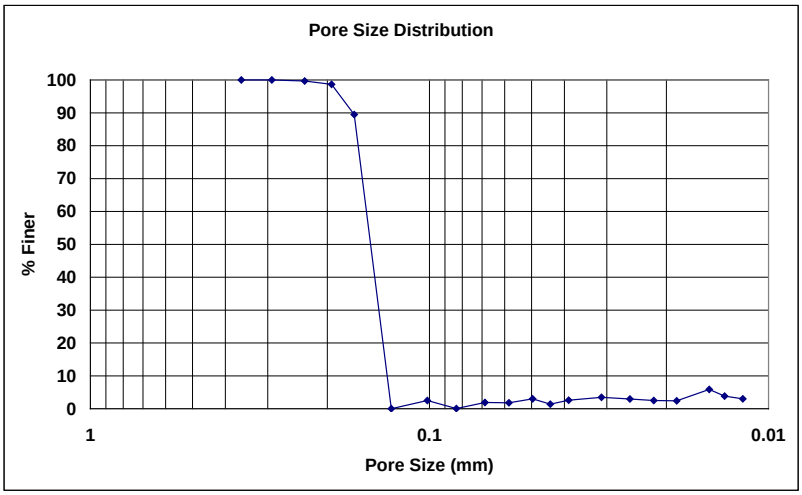

Figure B.68: Porewick-7 pore size distribution report.

Bubble Point Test

Auburn University - Department of Civil Engineering

date of test: 5/4/2002
test identification: Porewick 8
test performed by: David Howie
wetting fluid: Porewick
ambient air temperature: 21.1 °C
porous media: NG-1 nonwoven geotextile
comments: testing to determine geotextile pore size distribution

Pore Size Calculation Parameters:
constant, C: 2860 mm/m
contact angle: 0 degrees
surface tension: 0.016 N/m

Dry Run

Recorded Data							Calculations				
Indirect Reading Rotameters				Direct Reading Rotameter Value (L/min)	Pressure at Rotameter Exit (psig)	Half of Manometer Reading (mm H20)	Manometer Reading (mm H20)	Manometer Pressure (Pa)	Pore Size (Diameter) (mm)	Indicated Airflow Rate (L/min)	True Airflow Rate (L/min)
First Rotameter Used		Second Rotameter Used									
Rotameter ID Number	Rotameter Value	Rotameter ID Number	Rotameter Value								
5	28				0.04	1	2	19.62	2.332314	42.1	42.15724
5	48				0.11	2	4	39.24	1.166157	71.3	71.56627
5	81				0.32	4	8	78.48	0.5830785	122	123.3207
5	74	5	60		0.29	8	16	156.96	0.2915392	200.4	202.3671
5	94	5	77		0.48	12	24	235.44	0.1943595	259	263.1946
				350	0.1	17	34	333.54	0.1371949	350	351.1885
				400	0.11	21	42	412.02	0.1110626	400	401.4938
				450	0.12	26	52	510.12	0.0897044	450	451.833
				500	0.14	31	62	608.22	0.0752359	500	502.3753
				550	0.16	36.5	73	716.13	0.063899	550	552.9851
				600	0.18	43	86	843.66	0.0542399	600	603.6623
				650	0.2	49	98	961.38	0.0475982	650	654.4068
				700	0.22	57	114	1118.34	0.0409178	700	705.2186
				800	0.26	69	138	1353.78	0.0338017	800	807.0438
				900	0.31	84	168	1648.08	0.0277656	900	909.4403
				1000	0.37	100	200	1962	0.0233231	1000	1012.507
				1100	0.42	114	228	2236.68	0.0204589	1100	1115.604
				1200	0.49	132	264	2589.84	0.017669	1200	1219.836
				1300	0.56	152	304	2982.24	0.0153442	1300	1324.53
				1400	0.65	176	352	3453.12	0.0132518	1400	1430.618

Wet Run

Recorded Data							Calculations				
Indirect Reading Rotameters				Direct Reading Rotameter Value (L/min)	Pressure at Rotameter Exit (psig)	Half of Manometer Reading (mm H20)	Manometer Reading (mm H20)	Manometer Pressure (Pa)	Pore Size (Diameter) (mm)	Indicated Airflow Rate (L/min)	True Airflow Rate (L/min)
First Rotameter Used		Second Rotameter Used									
Rotameter ID Number	Rotameter Value	Rotameter ID Number	Rotameter Value								
1	2					1	2	19.62	2.332314	0.00158	0.00158
1	5					2	4	39.24	1.166157	0.00316	0.00316
1	31					8	16	156.96	0.2915392	0.0505	0.0505
2	56					10	20	196.2	0.2332314	1.073	1.073
4	27				0.1	12	24	235.44	0.1943595	9.01	9.040594
4	91				0.6	14	28	274.68	0.1665939	35.2	35.91118
5	51				0.16	16	32	313.92	0.1457696	75.7	76.11086
				350	0.1	18	36	353.16	0.129573	350	351.1885
				400	0.11	22.5	45	441.45	0.1036584	400	401.4938
				450	0.13	27	54	529.74	0.086382	450	451.9854
				500	0.14	33	66	647.46	0.0706762	500	502.3753
				550	0.16	39	78	765.18	0.0598029	550	552.9851
				600	0.18	46	92	902.52	0.0507025	600	603.6623
				650	0.21	52	104	1020.24	0.0448522	650	654.6264
				700	0.23	59	118	1157.58	0.0395307	700	705.4549
				800	0.25	72	144	1412.64	0.0323932	800	806.774
				900	0.31	87	174	1706.94	0.0268082	900	909.4403
				1000	0.37	103	206	2020.86	0.0226438	1000	1012.507
				1100	0.43	120	240	2354.4	0.0194359	1100	1115.972
				1200	0.5	140	280	2746.8	0.0166594	1200	1220.238
				1300	0.59	163	326	3198.06	0.0143087	1300	1325.832
				1400	0.67	186	372	3649.32	0.0125393	1400	1431.549
				1600	0.85	262	524	5140.44	0.008902	1600	1645.608

Figure B.69: Porewick-8 recorded data and calculations.

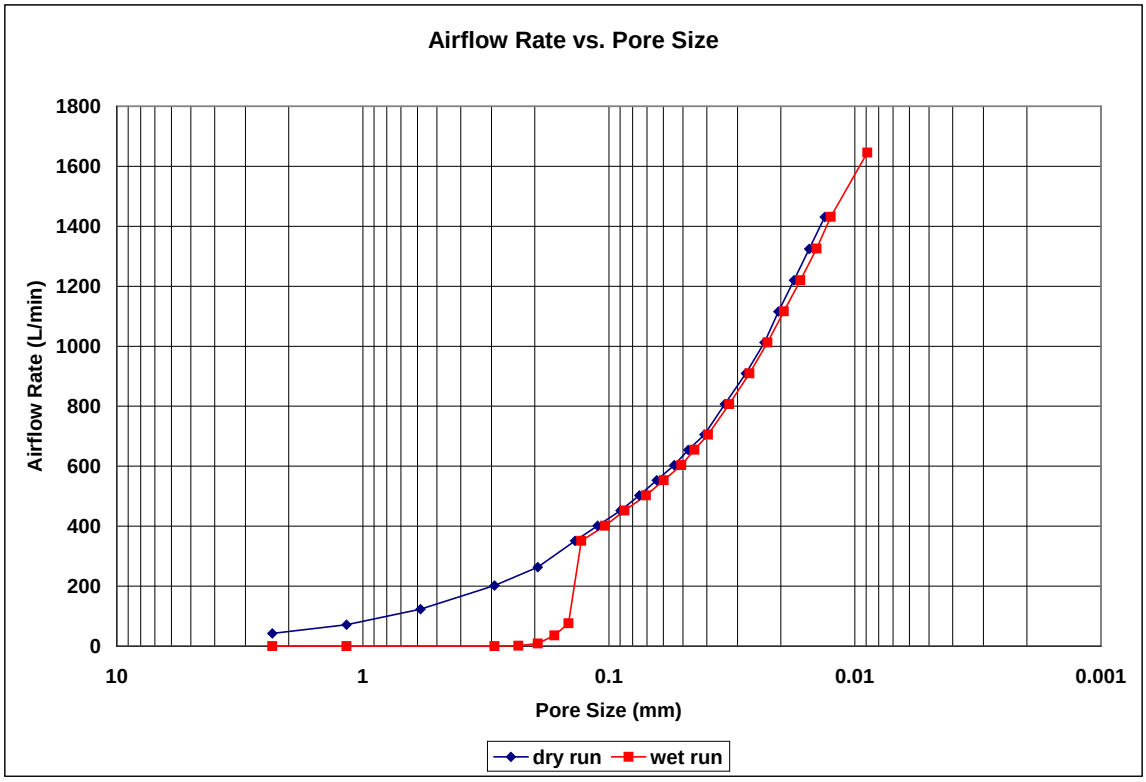

Figure B.70: Porewick-8 airflow rate vs. pore size for the wet and dry runs.

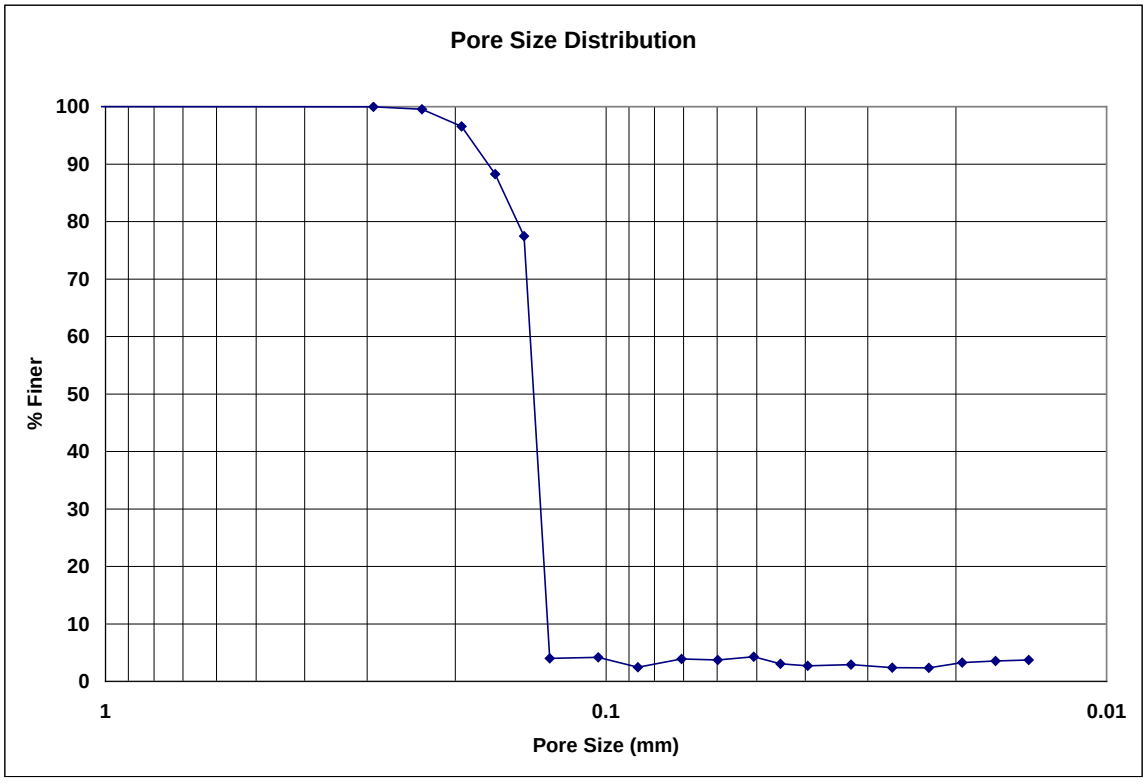

Figure B.71: Porewick-8 pore size distribution.

Bubble Point Test
Auburn University - Department of Civil Engineering

date of test:	5/4/2002	Pore Size Calculation Parameters:		
test identification:	Porewick 8	constant, C:	2860	mm/m
test performed by:	David Howie	contact angle:	0	degrees
wetting fluid:	Porewick	surface tension:	0.016	N/m
air temperature:	21.1 °C			
porous media:	NG-1 nonwoven geotextile			
comments:	testing to determine geotextile pore size distribution			

Pore Size at Selected % Finer

% finer	pore size (mm)
98	0.21304
95	0.18913
90	0.17241
85	0.16029
80	0.15063
75	0.14522
70	0.14412
65	0.14302
60	0.14192
55	0.14081
50	0.13971
45	0.13861
40	0.13751
35	0.13640
30	0.13530
25	0.13420
20	0.13310
15	0.13200
10	0.13089
5	0.12979

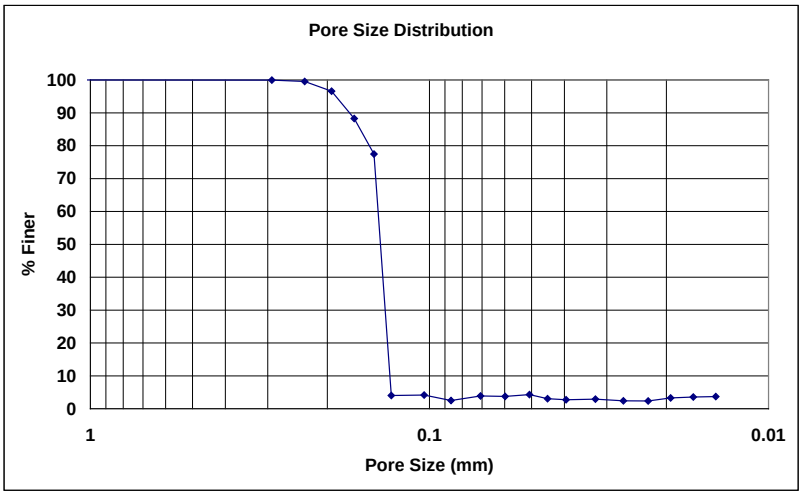

Figure B.72: Porewick-8 pore size distribution report.

Bubble Point Test

Auburn University - Department of Civil Engineering

date of test: 3/19/2002
test identification: Porewick 9
test performed by: David Howie
wetting fluid: Porewick
ambient air temperature: 21.3 °C
porous media: NG-1 nonwoven geotextile
comments: testing to determine geotextile pore size distribution

Pore Size Calculation Parameters:
constant, C: 2860 mm/m
contact angle: 0 degrees
surface tension: 0.016 N/m

Dry Run

Recorded Data							Calculations				
Indirect Reading Rotameters				Direct Reading Rotameter Value (L/min)	Pressure at Rotameter Exit (psig)	Half of Manometer Reading (mm H20)	Manometer Reading (mm H20)	Manometer Pressure (Pa)	Pore Size (Diameter) (mm)	Indicated Airflow Rate (L/min)	True Airflow Rate (L/min)
First Rotameter Used		Second Rotameter Used									
Rotameter ID Number	Rotameter Value	Rotameter ID Number	Rotameter Value								
5	32				0.05	1	2	19.62	2.332314	47.9	47.98139
5	54				0.14	2	4	39.24	1.166157	80.3	80.68147
5	87				0.37	4	8	78.48	0.5830785	132	133.6509
5	79	5	64		0.33	8	16	156.96	0.2915392	214.6	216.9954
				300	0.05	12	24	235.44	0.1943595	300	300.5098
				350	0.06	16	32	313.92	0.1457696	350	350.7136
				400	0.07	20	40	392.4	0.1166157	400	400.9512
				450	0.08	24	48	470.88	0.0971797	450	451.2228
				500	0.1	30	60	588.6	0.0777438	500	501.6978
				550	0.12	34	68	667.08	0.0685975	550	552.2403
				600	0.14	40	80	784.8	0.0583078	600	602.8504
				650	0.16	46	92	902.52	0.0507025	650	653.5278
				700	0.18	52	104	1020.24	0.0448522	700	704.2727
				800	0.23	63	126	1236.06	0.0370209	800	806.2342
				900	0.28	76	152	1491.12	0.0306883	900	908.531
				1000	0.33	91	182	1785.42	0.0256298	1000	1011.162
				1100	0.39	104	208	2040.48	0.0224261	1100	1114.496
				1200	0.45	123	246	2413.26	0.0189619	1200	1218.229
				1300	0.52	140	280	2746.8	0.0166594	1300	1322.793
				1400	0.6	162	324	3178.44	0.014397	1400	1428.286
				1600	0.74	225	450	4414.5	0.0103658	1600	1639.778

Wet Run

Recorded Data							Calculations				
Indirect Reading Rotameters				Direct Reading Rotameter Value (L/min)	Pressure at Rotameter Exit (psig)	Half of Manometer Reading (mm H20)	Manometer Reading (mm H20)	Manometer Pressure (Pa)	Pore Size (Diameter) (mm)	Indicated Airflow Rate (L/min)	True Airflow Rate (L/min)
First Rotameter Used		Second Rotameter Used									
Rotameter ID Number	Rotameter Value	Rotameter ID Number	Rotameter Value								
1	32					8	16	156.96	0.2915392	0.0532	0.0532
2	98					10	20	196.2	0.2332314	2.084	2.084
4	32				0.11	12	24	235.44	0.1943595	10.9	10.94071
5	37				0.11	14	28	274.68	0.1665939	55.1	55.30577
5	100	5	80		0.57	18	36	353.16	0.129573	274	279.2617
				400	0.08	21	42	412.02	0.1110626	400	401.087
				450	0.09	25	50	490.5	0.0932926	450	451.3754
				500	0.11	30	60	588.6	0.0777438	500	501.8673
				550	0.12	35	70	686.7	0.0666375	550	552.2403
				600	0.14	41	82	804.42	0.0568857	600	602.8504
				650	0.16	48	96	941.76	0.0485899	650	653.5278
				700	0.19	54	108	1059.48	0.043191	700	704.5093
				800	0.24	66	132	1294.92	0.0353381	800	806.5042
				900	0.3	80	160	1569.6	0.0291539	900	909.1373
				1000	0.35	97	194	1903.14	0.0240445	1000	1011.835
				1100	0.41	112	224	2197.44	0.0208242	1100	1115.235
				1200	0.48	130	260	2550.6	0.0179409	1200	1219.434
				1300	0.55	150	300	2943	0.0155488	1300	1324.096
				1400	0.64	174	348	3413.88	0.0134041	1400	1430.152
				1600	0.81	240	480	4708.8	0.009718	1600	1643.491
				1800	1	298	596	5846.76	0.0078266	1800	1860.217

Figure B.73: Porewick-9 recorded data and calculations.

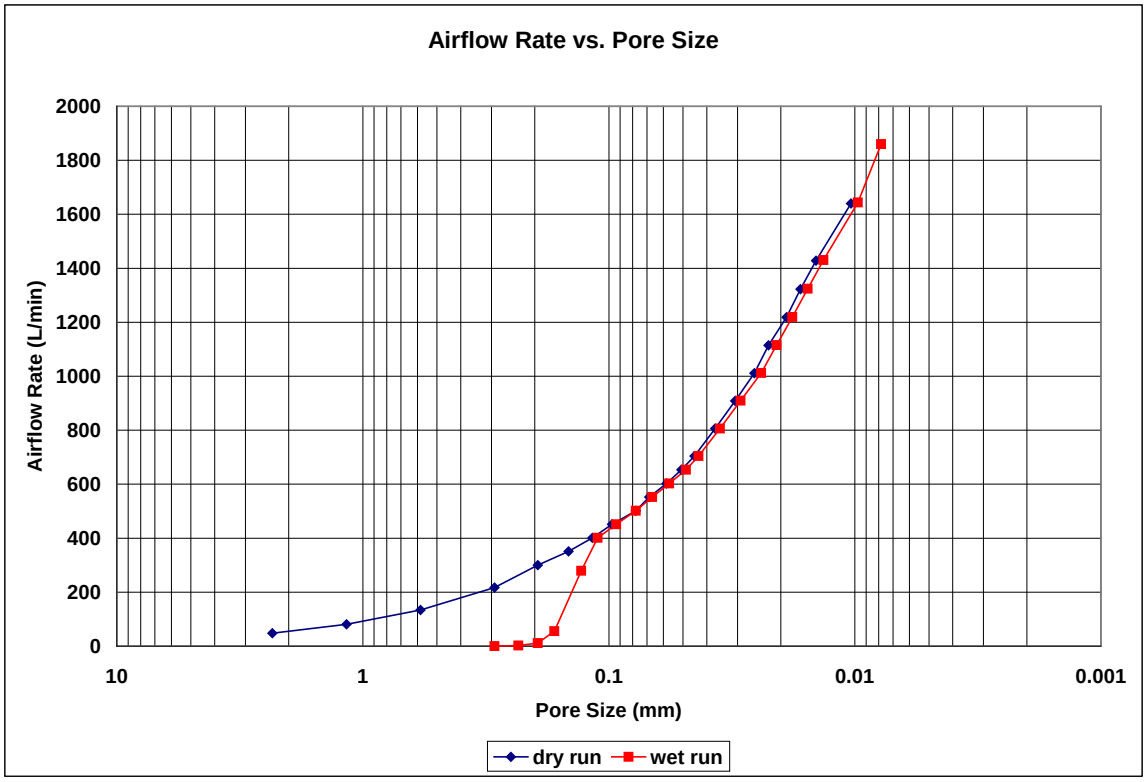

Figure B.74: Porewick-9 airflow rate vs. pore size for the wet and dry runs.

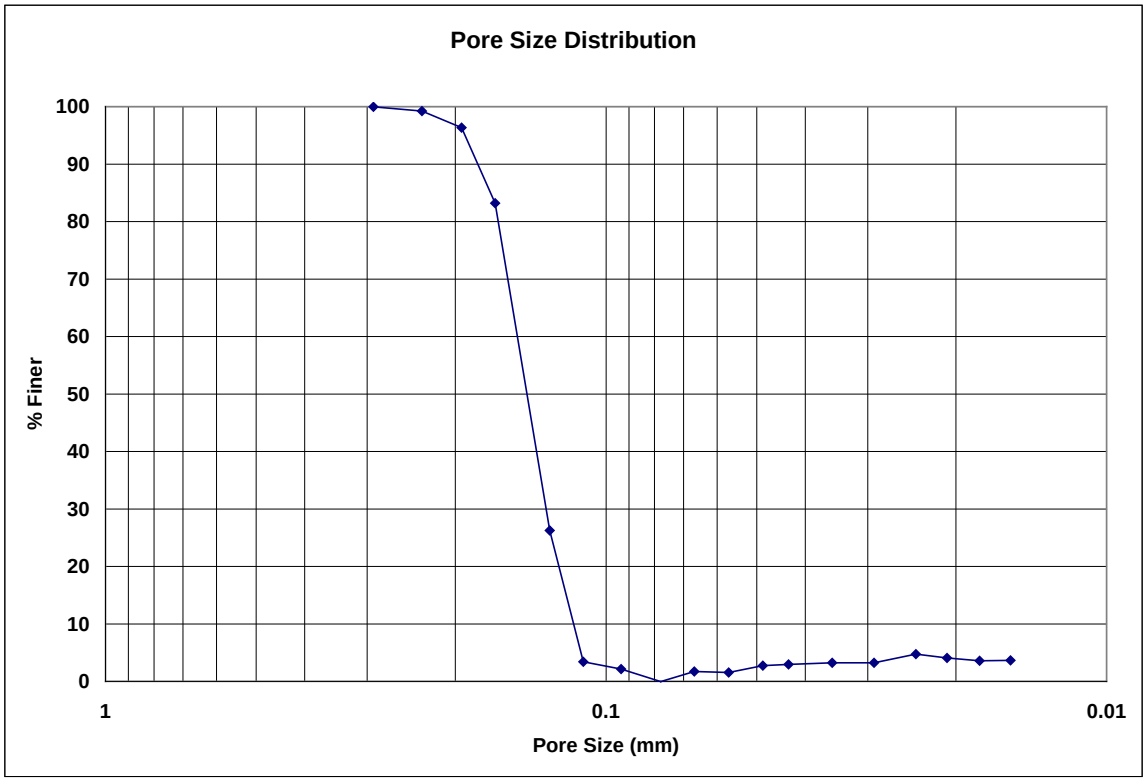

Figure B.75: Porewick-9 pore size distribution.

Bubble Point Test
Auburn University - Department of Civil Engineering

date of test:	3/19/2002	Pore Size Calculation Parameters:		
test identification:	Porewick 9	constant, C:	2860	mm/m
test performed by:	David Howie	contact angle:	0	degrees
wetting fluid:	Porewick	surface tension:	0.016	N/m
air temperature:	21.3 °C			
porous media:	NG-1 nonwoven geotextile			
comments:	testing to determine geotextile pore size distribution			

Pore Size at Selected % Finer

% finer	pore size (mm)
98	0.21666
95	0.19149
90	0.18094
85	0.17039
80	0.16451
75	0.16126
70	0.15801
65	0.15476
60	0.15151
55	0.14826
50	0.14501
45	0.14176
40	0.13851
35	0.13526
30	0.13202
25	0.12856
20	0.12451
15	0.12045
10	0.11640
5	0.11234

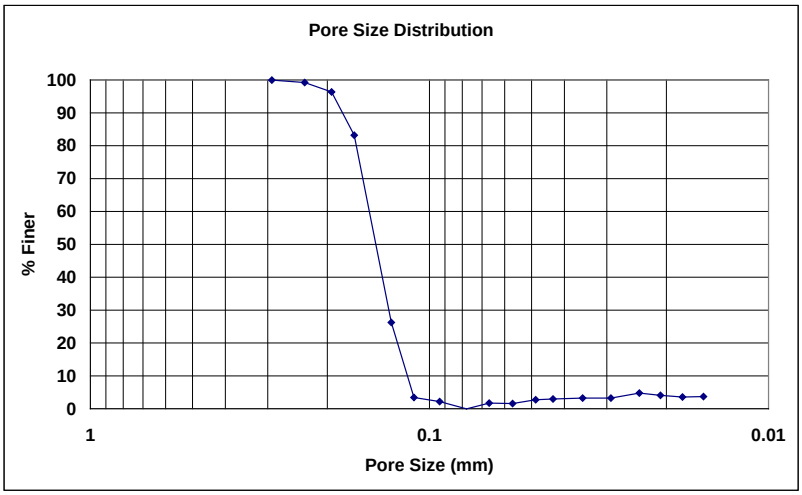

Figure B.76: Porewick-9 pore size distribution report.

Bubble Point Test

Auburn University - Department of Civil Engineering

date of test: 3/19/2002
test identification: Porewick 10
test performed by: David Howie
wetting fluid: Porewick
ambient air temperature: 21.3 °C
porous media: NG-1 nonwoven geotextile
comments: testing to determine geotextile pore size distribution

Pore Size Calculation Parameters:
constant, C: 2860 mm/m
contact angle: 0 degrees
surface tension: 0.016 N/m

Dry Run

Recorded Data							Calculations				
Indirect Reading Rotameters				Direct Reading Rotameter Value (L/min)	Pressure at Rotameter Exit (psig)	Half of Manometer Reading (mm H20)	Manometer Reading (mm H20)	Manometer Pressure (Pa)	Pore Size (Diameter) (mm)	Indicated Airflow Rate (L/min)	True Airflow Rate (L/min)
First Rotameter Used		Second Rotameter Used									
Rotameter ID Number	Rotameter Value	Rotameter ID Number	Rotameter Value								
5	32				0.06	1	2	19.62	2.332314	47.9	47.99766
5	52				0.13	2	4	39.24	1.166157	77.2	77.54061
5	81				0.32	4	8	78.48	0.5830785	122	123.3207
5	74	5	60		0.3	8	16	156.96	0.2915392	200.4	202.4346
5	92	5	76		0.47	12	24	235.44	0.1943595	254	258.0286
				350	0.09	17	34	333.54	0.1371949	350	351.0698
				400	0.1	21	42	412.02	0.1110626	400	401.3582
				450	0.12	26	52	510.12	0.0897044	450	451.833
				500	0.14	32	64	627.84	0.0728848	500	502.3753
				550	0.15	37	74	725.94	0.0630355	550	552.799
				600	0.17	43	86	843.66	0.0542399	600	603.4594
				650	0.2	50	100	981	0.0466463	650	654.4068
				700	0.22	57	114	1118.34	0.0409178	700	705.2186
				800	0.27	70	140	1373.4	0.0333188	800	807.3135
				900	0.32	85	170	1667.7	0.027439	900	909.7432
				1000	0.38	100	200	1962	0.0233231	1000	1012.843
				1100	0.44	115	230	2256.3	0.020281	1100	1116.341
				1200	0.51	135	270	2648.7	0.0172764	1200	1220.639
				1300	0.59	156	312	3060.72	0.0149507	1300	1325.832
				1400	0.67	180	360	3531.6	0.0129573	1400	1431.549
				1600	0.82	248	496	4865.76	0.0094045	1600	1644.02

Wet Run

Recorded Data							Calculations				
Indirect Reading Rotameters				Direct Reading Rotameter Value (L/min)	Pressure at Rotameter Exit (psig)	Half of Manometer Reading (mm H20)	Manometer Reading (mm H20)	Manometer Pressure (Pa)	Pore Size (Diameter) (mm)	Indicated Airflow Rate (L/min)	True Airflow Rate (L/min)
First Rotameter Used		Second Rotameter Used									
Rotameter ID Number	Rotameter Value	Rotameter ID Number	Rotameter Value								
1	54					8	16	156.96	0.2915392	0.126	0.126
2	95					10	20	196.2	0.2332314	2.019	2.019
4	50				0.2	12	24	235.44	0.1943595	17.8	17.92068
5	41				0.14	14	28	274.68	0.1665939	60.9	61.18931
5	100	5	82		0.56	16	32	313.92	0.1457696	277	282.2269
				350	0.09	18	36	353.16	0.129573	350	351.0698
				400	0.11	23	46	451.26	0.101405	400	401.4938
				450	0.13	28	56	549.36	0.0832969	450	451.9854
				500	0.15	34	68	667.08	0.0685975	500	502.5445
				550	0.17	40	80	784.8	0.0583078	550	553.1711
				600	0.19	46	92	902.52	0.0507025	600	603.8651
				650	0.21	54	108	1059.48	0.043191	650	654.6264
				700	0.24	60	120	1177.2	0.0388719	700	705.6912
				800	0.28	74	148	1451.88	0.0315178	800	807.5831
				900	0.33	90	180	1765.8	0.0259146	900	910.046
				1000	0.39	108	216	2118.96	0.0215955	1000	1013.178
				1100	0.47	128	256	2511.36	0.0182212	1100	1117.447
				1200	0.53	148	296	2903.76	0.0157589	1200	1221.441
				1300	0.62	171	342	3355.02	0.0136393	1300	1327.132
				1400	0.7	195	390	3825.9	0.0119606	1400	1432.946
				1600	0.88	274	548	5375.88	0.0085121	1600	1647.195

Figure B.77: Porewick-10 recorded data and calculations.

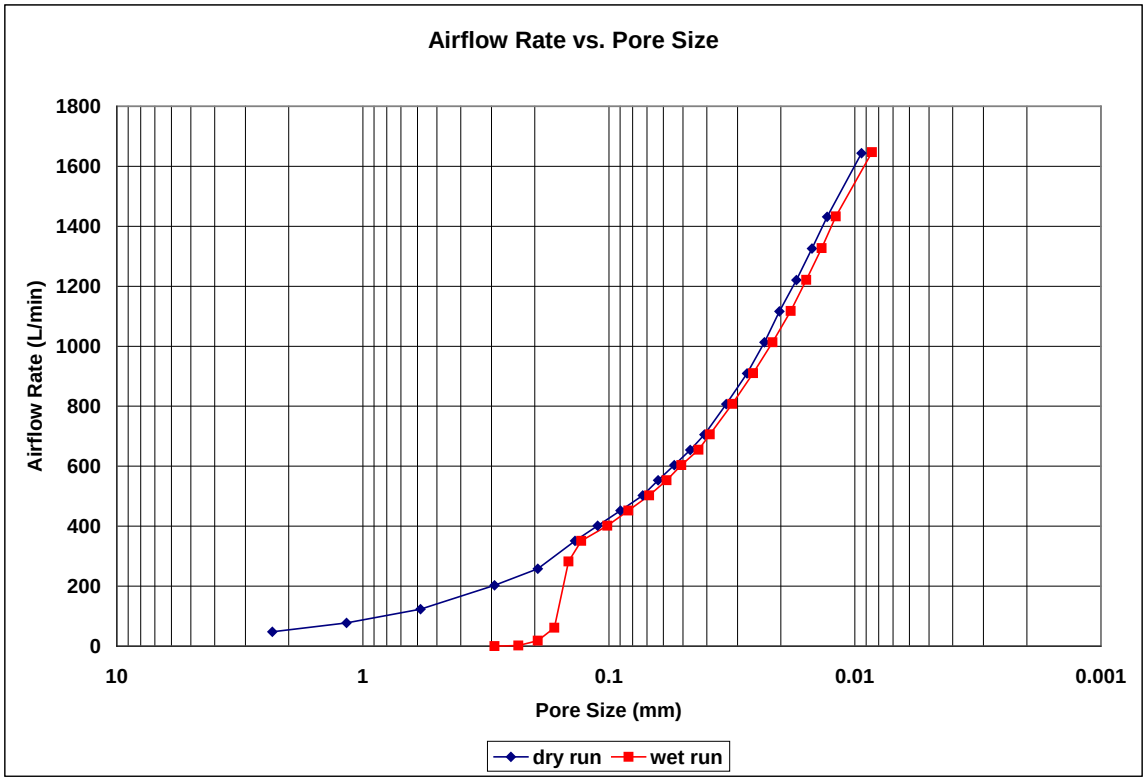

Figure B.78: Porewick-10 airflow rate vs. pore size for the wet and dry runs.

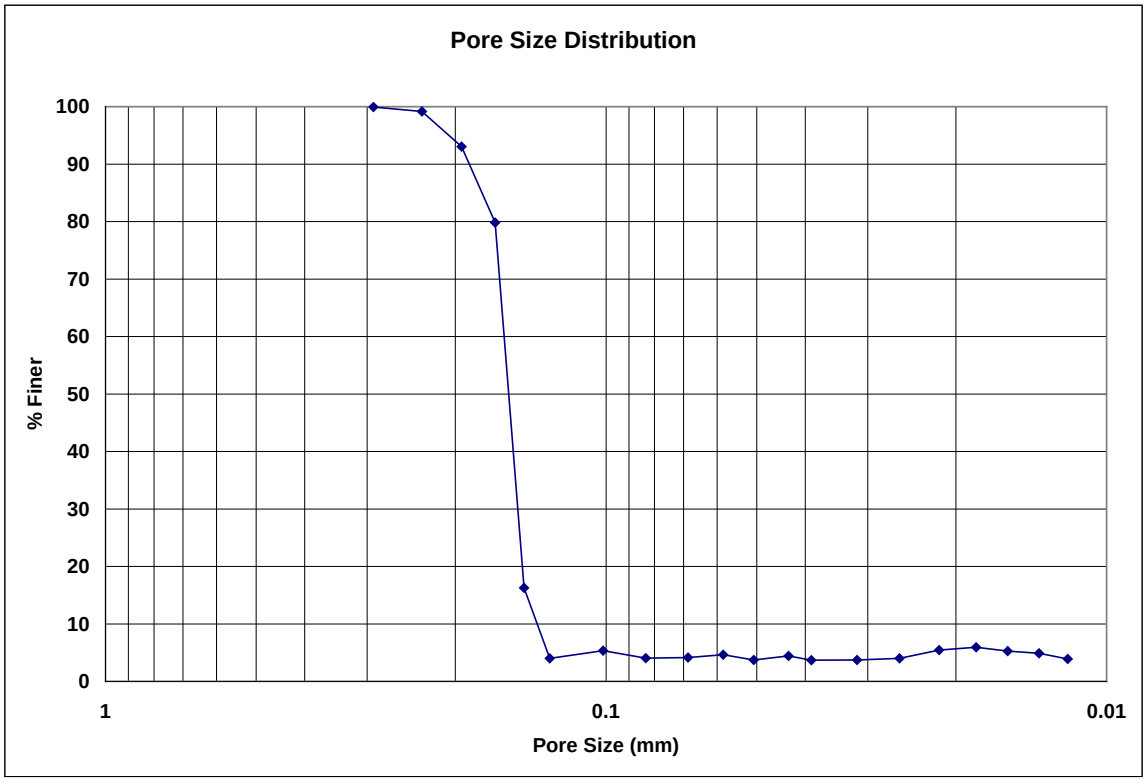

Figure B.79: Porewick-10 pore size distribution.

Bubble Point Test
Auburn University - Department of Civil Engineering

date of test: 3/19/2002
test identification: Porewick 10
test performed by: David Howie
wetting fluid: Porewick
air temperature: 21.3 °C
porous media: NG-1 nonwoven geotextile
comments: testing to determine geotextile pore size distribution

Pore Size Calculation Parameters:
constant, C: 2860 mm/m
contact angle: 0 degrees
surface tension: 0.016 N/m

Pore Size at Selected % Finer

% finer	pore size (mm)
98	0.22593
95	0.20678
90	0.18795
85	0.17746
80	0.16697
75	0.16501
70	0.16338
65	0.16174
60	0.16010
55	0.15846
50	0.15682
45	0.15518
40	0.15354
35	0.15190
30	0.15027
25	0.14863
20	0.14699
15	0.14408
10	0.13748
5	0.13088

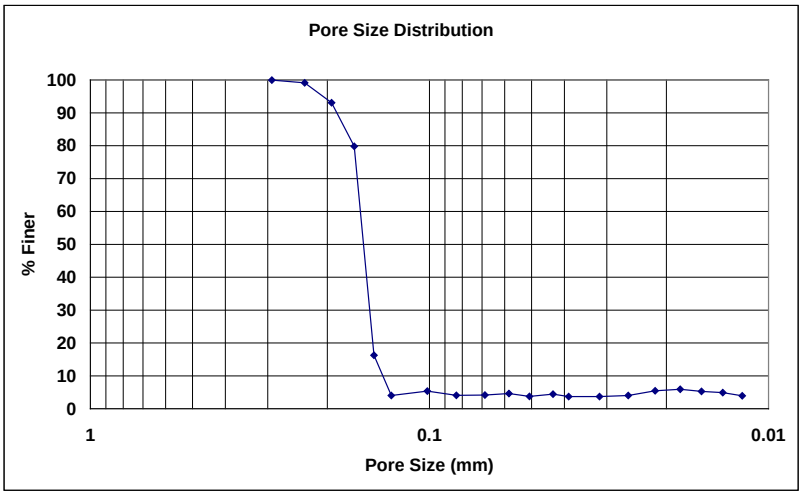

Figure B.80: Porewick-10 pore size distribution report.

B.3 Tests with Mineral Oil as the Wetting Fluid

Bubble Point Test
Auburn University - Department of Civil Engineering

date of test: 11/2/2006
test identification: MinOil-1
test performed by: David Hayes
wetting fluid: mineral oil
ambient air temperature: 22.2 °C
porous media: NG-1 nonwoven geotextile
comments: testing to determine geotextile pore size distribution

Pore Size Calculation Parameters:
constant, C: 2860 mm/m
contact angle: 0 degrees
surface tension: 0.035 N/m

Dry Run

Recorded Data							Calculations				
Indirect Reading Rotameters				Direct Reading Rotameter Value (L/min)	Pressure at Rotameter Exit (psig)	Half of Manometer Reading (mm H20)	Manometer Reading (mm H20)	Manometer Pressure (Pa)	Pore Size (Diameter) (mm)	Indicated Airflow Rate (L/min)	True Airflow Rate (L/min)
First Rotameter Used		Second Rotameter Used									
Rotameter ID Number	Rotameter Value	Rotameter ID Number	Rotameter Value								
5	42				0.07	2	4	39.24	2.5509684	62.4	62.54839
5	82				0.31	6	12	117.72	0.8503228	124	125.3007
5	51	5	64		0.22	8	16	156.96	0.6377421	171.3	172.5771
5	63	5	78		0.33	12	24	235.44	0.4251614	212	214.3664
5	75	5	93		0.48	16	32	313.92	0.318871	254	258.1136
				350	0.07	22	44	431.64	0.2319062	350	350.8323
				400	0.08	28	56	549.36	0.182212	400	401.087
				500	0.12	42	84	824.04	0.1214747	500	502.0367
				550	0.14	50	100	981	0.1020387	550	552.6128
				600	0.17	58	116	1137.96	0.0879644	600	603.4594
				650	0.19	66	132	1294.92	0.0773021	650	654.1872
				700	0.22	76	152	1491.12	0.0671307	700	705.2186
				800	0.32	90	180	1765.8	0.0566882	800	808.6606
				900	0.38	108	216	2118.96	0.0472402	900	911.5584
				1000	0.46	130	260	2550.6	0.0392457	1000	1015.526
				1100	0.52	150	300	2943	0.0340129	1100	1119.287
				1200	0.62	180	360	3531.6	0.0283441	1200	1225.045
				1300	0.71	204	408	4002.48	0.0250095	1300	1331.024
				1400	0.8	232	464	4551.84	0.0219911	1400	1437.591
				1600	0.99	320	640	6278.4	0.0159436	1600	1653

Wet Run

Recorded Data							Calculations				
Indirect Reading Rotameters				Direct Reading Rotameter Value (L/min)	Pressure at Rotameter Exit (psig)	Half of Manometer Reading (mm H20)	Manometer Reading (mm H20)	Manometer Pressure (Pa)	Pore Size (Diameter) (mm)	Indicated Airflow Rate (L/min)	True Airflow Rate (L/min)
First Rotameter Used		Second Rotameter Used									
Rotameter ID Number	Rotameter Value	Rotameter ID Number	Rotameter Value								
2	80				0	2	4	39.24	2.5509684	1.676	1.676
4	8				0.02	4	8	78.48	1.2754842	2.43	2.431652
4	24				0.12	26	52	510.12	0.1962283	7.91	7.94222
4	70				0.4	32	64	627.84	0.1594355	26.1	26.45272
5	62				0.29	40	80	784.8	0.1275484	92.5	93.40796
5	52	5	65		0.27	48	96	941.76	0.1062903	174.3	175.8934
5	73	5	92		0.43	56	112	1098.72	0.091106	250	253.6301
				350	0.2	62	124	1216.44	0.0822893	350	352.3729
				400	0.23	72	144	1412.64	0.0708602	400	403.1171
				450	0.25	78	156	1530.36	0.0654094	450	453.8104
				500	0.28	84	168	1648.08	0.0607373	500	504.7394
				550	0.3	92	184	1805.04	0.0554558	550	555.5839
				650	0.33	104	208	2040.48	0.0490571	650	657.2554
				700	0.37	116	232	2275.92	0.0439822	700	708.7548
				750	0.41	126	252	2472.12	0.0404916	750	760.3873
				800	0.49	144	288	2825.28	0.0354301	800	813.224
				900	0.55	164	328	3217.68	0.0311094	900	916.6821
				1000	0.66	192	384	3767.04	0.0265726	1000	1022.203
				1100	0.73	214	428	4198.68	0.0238408	1100	1126.982
				1200	0.84	248	496	4865.76	0.0205723	1200	1233.809
				1300	0.97	284	568	5572.08	0.0179646	1300	1342.206
				1400	1.09	320	640	6278.4	0.0159436	1400	1450.977

Figure B.81: MinOil-1 recorded data and calculations.

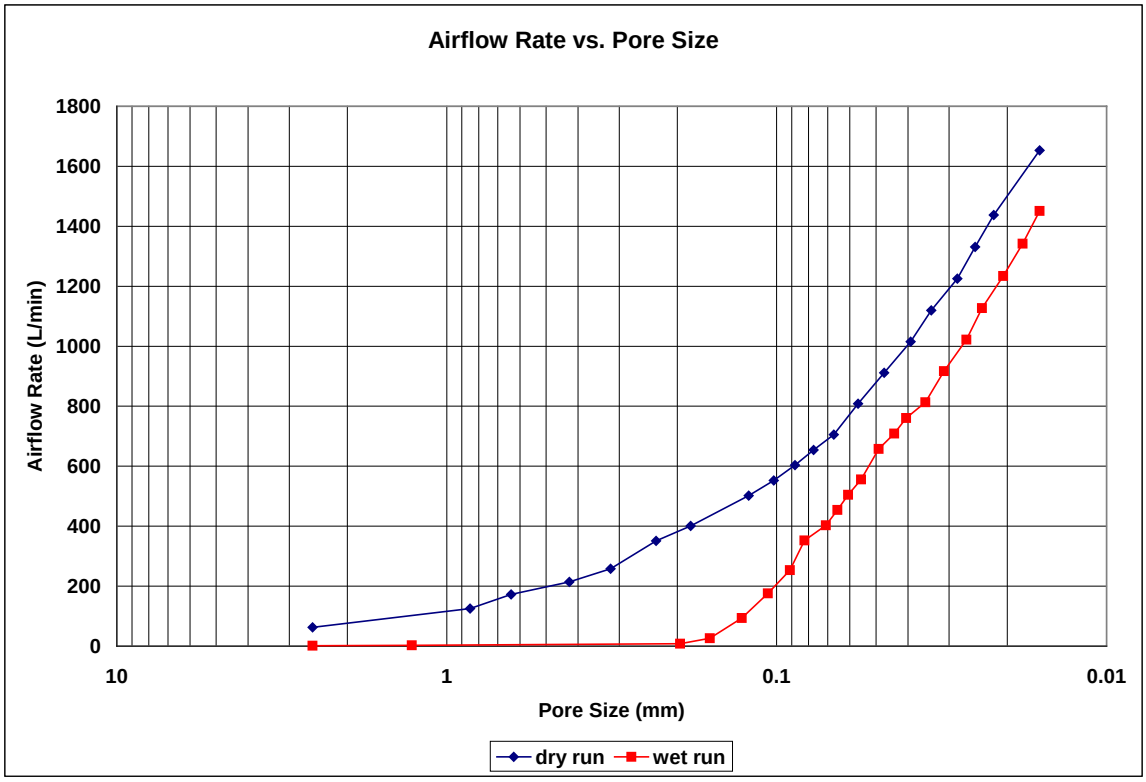

Figure B.82: MinOil-1 airflow rate vs. pore size for the wet and dry runs.

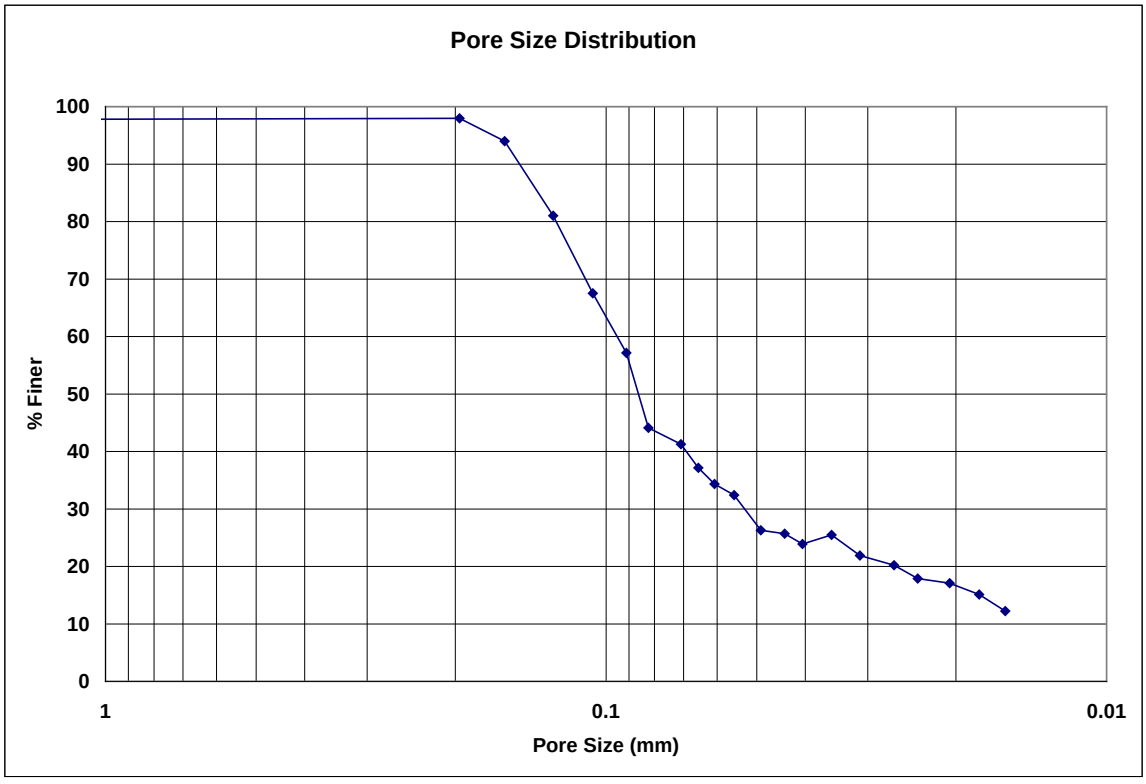

Figure B.83: MinOil-1 pore size distribution.

Bubble Point Test
Auburn University - Department of Civil Engineering

date of test: 11/2/2006
test identification: MinOil-1
test performed by: David Hayes
wetting fluid: mineral oil
air temperature: 22.2 °C
porous media: NG-1 nonwoven geotextile
comments: testing to determine geotextile pore size distribution

Pore Size Calculation Parameters:
constant, C: 2860 mm/m
contact angle: 0 degrees
surface tension: 0.035 N/m

Pore Size at Selected % Finer

% Finer	Pore Size (mm)
98	---
95	0.16894
90	0.14966
85	0.13736
80	0.12595
75	0.11808
70	0.11020
65	0.10259
60	0.09526
55	0.08964
50	0.08627
45	0.08289
40	0.06916
35	0.06185
30	0.05293
25	0.04262
20	0.02631
15	0.01789
10	---
5	---

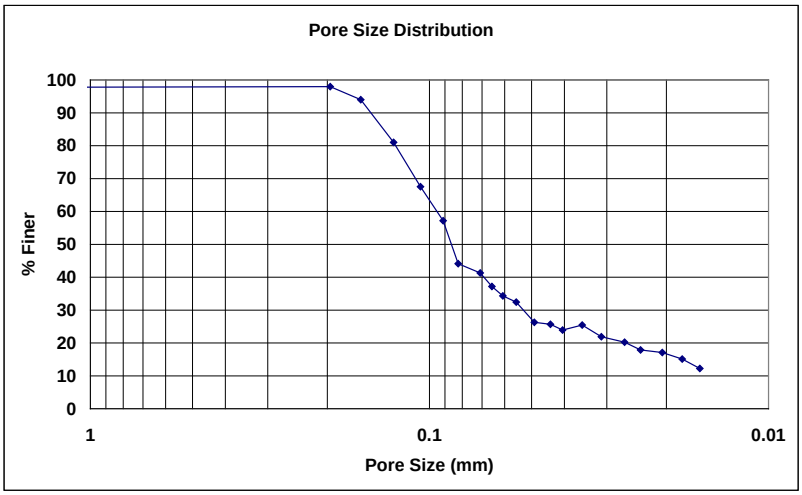

Figure B.84: MinOil-1 pore size distribution report.

Bubble Point Test

Auburn University - Department of Civil Engineering

date of test: 4/10/2002
test identification: MinOil-2
test performed by: David Howie
wetting fluid: mineral oil
ambient air temperature: 21 °C
porous media: NG-1 nonwoven geotextile
comments: testing to determine geotextile pore size distribution

Pore Size Calculation Parameters:
constant, C: 2860 mm/m
contact angle: 0 degrees
surface tension: 0.035 N/m

Dry Run

Recorded Data							Calculations				
Indirect Reading Rotameters				Direct Reading Rotameter Value (L/min)	Pressure at Rotameter Exit (psig)	Half of Manometer Reading (mm H20)	Manometer Reading (mm H20)	Manometer Pressure (Pa)	Pore Size (Diameter) (mm)	Indicated Airflow Rate (L/min)	True Airflow Rate (L/min)
First Rotameter Used		Second Rotameter Used									
Rotameter ID Number	Rotameter Value	Rotameter ID Number	Rotameter Value								
4	94				0.61	1	2	19.62	5.1019368	36.5	37.24962
5	50				0.13	2	4	39.24	2.5509684	74.2	74.52737
5	83				0.34	4	8	78.48	1.2754842	125	126.4373
5	77	5	62		0.33	8	16	156.96	0.6377421	208.5	210.8273
5	97	5	79		0.54	12	24	235.44	0.4251614	267	271.8599
				350	0.06	16	32	313.92	0.318871	350	350.7136
				400	0.08	20	40	392.4	0.2550968	400	401.087
				450	0.09	25	50	490.5	0.2040775	450	451.3754
				500	0.11	30	60	588.6	0.1700646	500	501.8673
				550	0.12	35	70	686.7	0.1457696	550	552.2403
				600	0.14	41	82	804.42	0.1244375	600	602.8504
				650	0.16	47	94	922.14	0.1085518	650	653.5278
				700	0.18	54	108	1059.48	0.0944803	700	704.2727
				800	0.26	67	134	1314.54	0.0761483	800	807.0438
				900	0.3	81	162	1589.22	0.0629869	900	909.1373
				1000	0.35	95	190	1863.9	0.0537046	1000	1011.835
				1100	0.41	110	220	2158.2	0.0463812	1100	1115.235
				1200	0.47	127	254	2491.74	0.0401727	1200	1219.033
				1300	0.54	146	292	2864.52	0.0349448	1300	1323.662
				1400	0.63	168	336	3296.16	0.0303687	1400	1429.685

Wet Run

Recorded Data							Calculations				
Indirect Reading Rotameters				Direct Reading Rotameter Value (L/min)	Pressure at Rotameter Exit (psig)	Half of Manometer Reading (mm H20)	Manometer Reading (mm H20)	Manometer Pressure (Pa)	Pore Size (Diameter) (mm)	Indicated Airflow Rate (L/min)	True Airflow Rate (L/min)
First Rotameter Used		Second Rotameter Used									
Rotameter ID Number	Rotameter Value	Rotameter ID Number	Rotameter Value								
1	30					16	32	313.92	0.318871	0.0478	0.0478
1	34					20	40	392.4	0.2550968	0.0587	0.0587
4	10				0.08	23	46	451.26	0.2218233	3.07	3.078342
4	62				0.33	26	52	510.12	0.1962283	22.7	22.95338
5	34				0.15	28	56	549.36	0.182212	50.7	50.95802
5	49				0.21	30	60	588.6	0.1700646	72.7	73.21744
5	70				0.33	32	64	627.84	0.1594355	105	106.172
5	86	5	70		0.5	40	80	784.8	0.1275484	235	238.9632
				300	0.16	44	88	863.28	0.1159531	300	301.6282
				350	0.17	48	96	941.76	0.1062903	350	352.018
				400	0.18	53	106	1039.86	0.096263	400	402.4415
				450	0.2	58	116	1137.96	0.0879644	450	453.0509
				500	0.21	62	124	1216.44	0.0822893	500	503.5588
				550	0.23	67	134	1314.54	0.0761483	550	554.286
				600	0.25	73	146	1432.26	0.0698895	600	605.0805
				650	0.27	78	156	1530.36	0.0654094	650	655.9422
				700	0.29	84	168	1648.08	0.0607373	700	706.871
				800	0.34	97	194	1903.14	0.0525973	800	809.1988
				900	0.4	110	220	2158.2	0.0463812	900	912.1627
				1000	0.45	125	250	2452.5	0.0408155	1000	1015.191
				1100	0.51	144	288	2825.28	0.0354301	1100	1118.919
				1200	0.58	163	326	3198.06	0.0313002	1200	1223.444
				1300	0.65	182	364	3570.84	0.0280326	1300	1328.431
				1400	0.74	207	414	4061.34	0.024647	1400	1434.805
				1600	0.91	280	560	5493.6	0.0182212	1600	1648.78

Figure B.85: MinOil-2 recorded data and calculations.

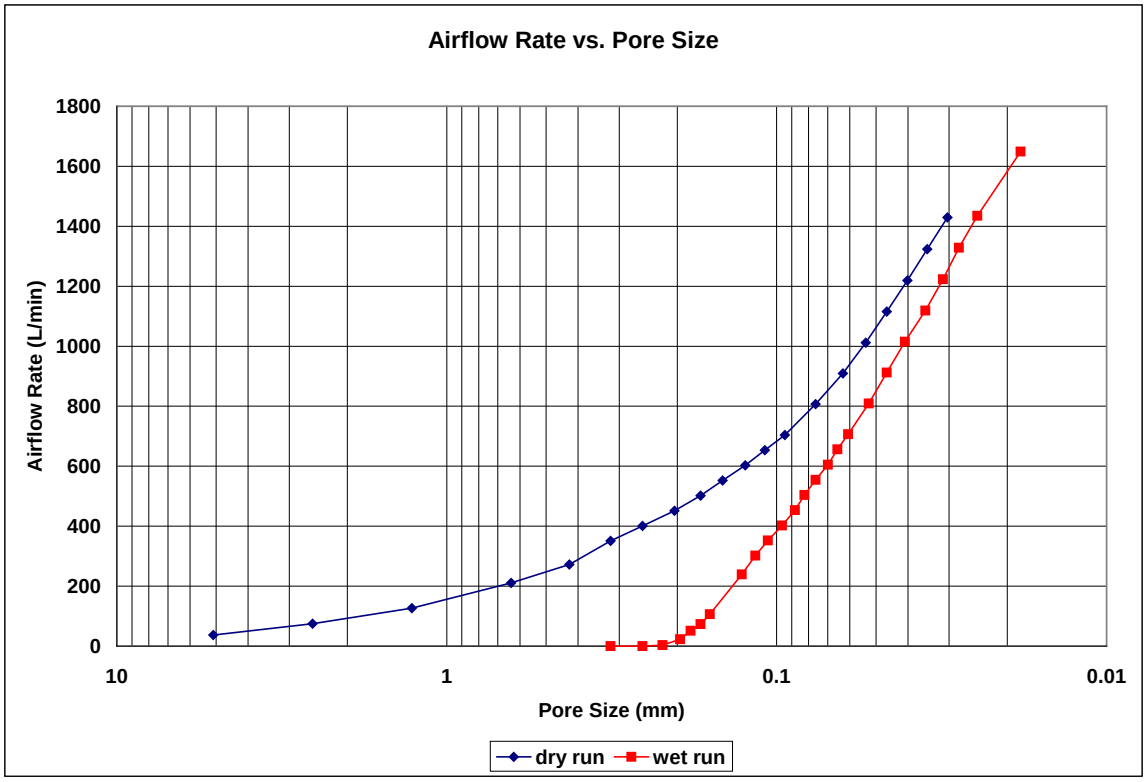

Figure B.86: MinOil-2 airflow rate vs. pore size for the wet and dry runs.

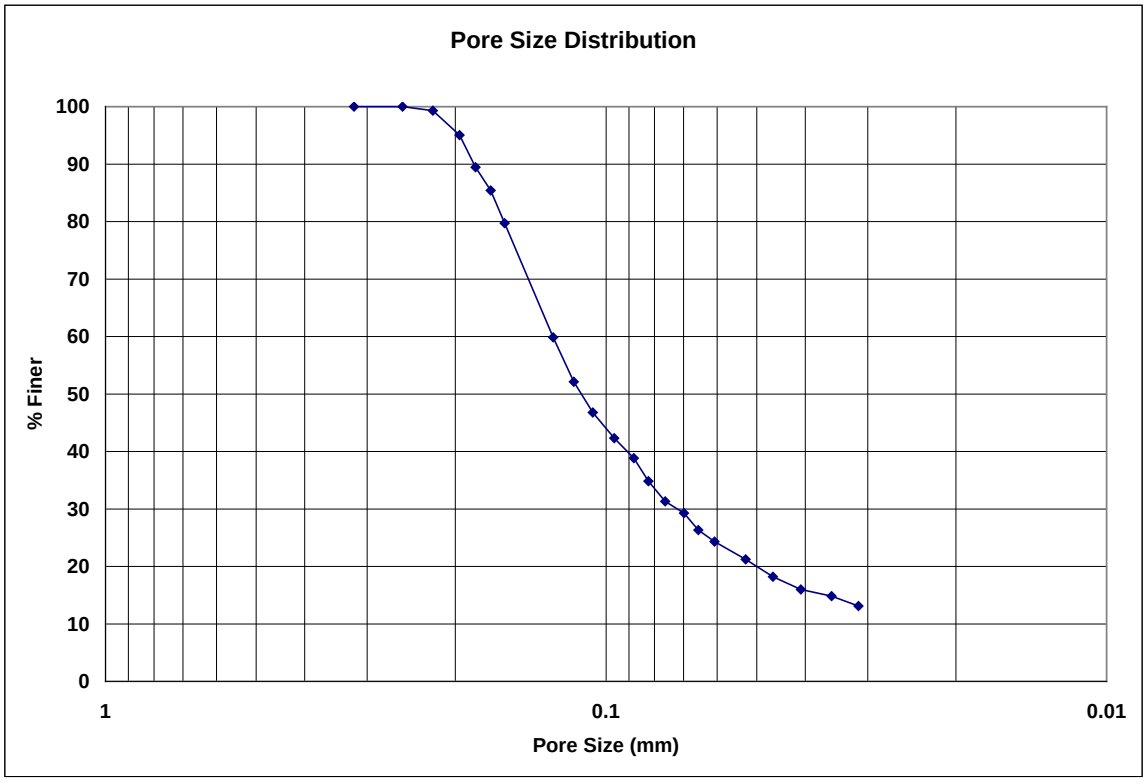

Figure B.87: MinOil-2 pore size distribution.

Bubble Point Test
Auburn University - Department of Civil Engineering

date of test: 4/10/2002
test identification: MinOil-2
test performed by: David Howie
wetting fluid: mineral oil
air temperature: 21 °C
porous media: NG-1 nonwoven geotextile
comments: testing to determine geotextile pore size distribution

Pore Size Calculation Parameters:
constant, C: 2860 mm/m
contact angle: 0 degrees
surface tension: 0.035 N/m

Pore Size at Selected % Finer

% Finer	Pore Size (mm)
98	0.21405
95	0.19612
90	0.18355
85	0.16929
80	0.15993
75	0.15184
70	0.14381
65	0.13578
60	0.12776
55	0.12027
50	0.11211
45	0.10225
40	0.09072
35	0.08254
30	0.07210
25	0.06232
20	0.05005
15	0.03617
10	---
5	---

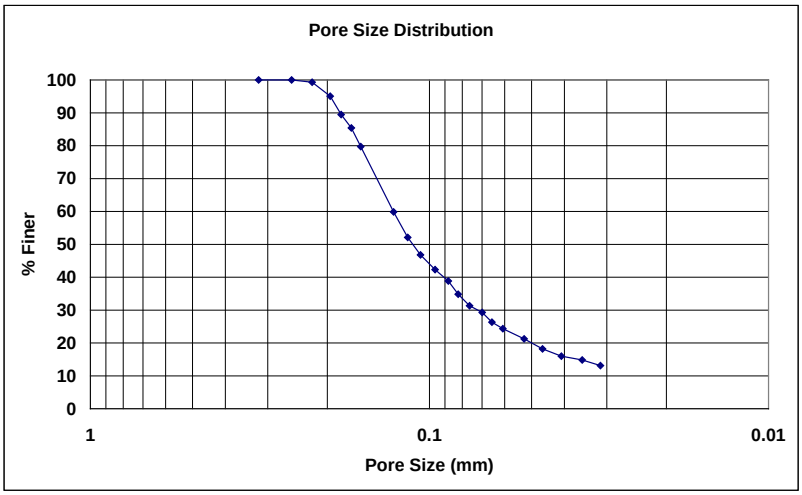

Figure B.88: MinOil-2 pore size distribution report.

Bubble Point Test
Auburn University - Department of Civil Engineering

date of test: 4/10/2002
test identification: MinOil-3
test performed by: David Howie
wetting fluid: mineral oil
ambient air temperature: 21 °C
porous media: NG-1 nonwoven geotextile
comments: testing to determine geotextile pore size distribution

Pore Size Calculation Parameters:
constant, C: 2860 mm/m
contact angle: 0 degrees
surface tension: 0.035 N/m

Dry Run

Recorded Data							Calculations				
Indirect Reading Rotameters				Direct Reading Rotameter Value (L/min)	Pressure at Rotameter Exit (psig)	Half of Manometer Reading (mm H20)	Manometer Reading (mm H20)	Manometer Pressure (Pa)	Pore Size (Diameter) (mm)	Indicated Airflow Rate (L/min)	True Airflow Rate (L/min)
First Rotameter Used		Second Rotameter Used									
Rotameter ID Number	Rotameter Value	Rotameter ID Number	Rotameter Value								
4	92				0.58	1	2	19.62	5.1019368	35.6	36.29552
5	43				0.09	2	4	39.24	2.5509684	63.8	63.99501
5	71				0.25	4	8	78.48	1.2754842	106	106.8976
5	66	5	53		0.24	8	16	156.96	0.6377421	177.5	178.9431
5	85	5	69		0.4	12	24	235.44	0.4251614	232	235.1353
				300	0.06	16	32	313.92	0.318871	300	300.6116
				350	0.07	20	40	392.4	0.2550968	350	350.8323
				400	0.09	26	52	510.12	0.1962283	400	401.2226
				450	0.11	32	64	627.84	0.1594355	450	451.6805
				500	0.12	38	76	745.56	0.1342615	500	502.0367
				550	0.14	44	88	863.28	0.1159531	550	552.6128
				600	0.17	52	104	1020.24	0.0981142	600	603.4594
				650	0.19	58	116	1137.96	0.0879644	650	654.1872
				700	0.22	67	134	1314.54	0.0761483	700	705.2186
				800	0.29	82	164	1608.84	0.0622187	800	807.8526
				900	0.35	100	200	1962	0.0510194	900	910.6513
				1000	0.41	116	232	2275.92	0.0439822	1000	1013.85
				1100	0.48	136	272	2668.32	0.0375142	1100	1117.815
				1200	0.56	160	320	3139.2	0.0318871	1200	1222.644
				1300	0.65	185	370	3629.7	0.027578	1300	1328.431
				1400	0.74	212	424	4159.44	0.0240657	1400	1434.805
				1600	0.96	248	496	4865.76	0.0205723	1600	1651.419

Wet Run

Recorded Data							Calculations				
Indirect Reading Rotameters				Direct Reading Rotameter Value (L/min)	Pressure at Rotameter Exit (psig)	Half of Manometer Reading (mm H20)	Manometer Reading (mm H20)	Manometer Pressure (Pa)	Pore Size (Diameter) (mm)	Indicated Airflow Rate (L/min)	True Airflow Rate (L/min)
First Rotameter Used		Second Rotameter Used									
Rotameter ID Number	Rotameter Value	Rotameter ID Number	Rotameter Value								
1	11					10	20	196.2	0.5101937	0.00847	0.00847
1	16					17	34	333.54	0.3001139	0.0155	0.0155
1	19					20	40	392.4	0.2550968	0.0212	0.0212
4	10				0.08	26	52	510.12	0.1962283	3.07	3.078342
4	25				0.12	28	56	549.36	0.182212	8.27	8.303686
4	61				0.33	30	60	588.6	0.1700646	22.3	22.54892
5	32				0.14	32	64	627.84	0.1594355	47.9	48.12755
5	44				0.19	34	68	667.08	0.150057	65.3	65.72065
5	75				0.37	38	76	745.56	0.1342615	113	114.4133
5	62	5	50		0.32	42	84	824.04	0.1214747	166.7	168.5047
5	77	5	63		0.43	46	92	902.52	0.1109117	210	213.0493
5	93	5	77		0.61	50	100	981	0.1020387	257	262.2781
				350	0.2	58	116	1137.96	0.0879644	350	352.3729
				400	0.22	65	130	1275.3	0.0784913	400	402.9821
				450	0.24	70	140	1373.4	0.0728848	450	453.6586
				500	0.26	76	152	1491.12	0.0671307	500	504.4024
				550	0.28	84	168	1648.08	0.0607373	550	555.2134
				600	0.3	91	182	1785.42	0.0560652	600	606.0915
				650	0.33	98	196	1922.76	0.0520606	650	657.2554
				700	0.36	107	214	2099.34	0.0476817	700	708.5196
				800	0.42	122	244	2393.64	0.0418192	800	811.3481
				900	0.48	142	284	2786.04	0.0359291	900	914.5758
				1000	0.56	164	328	3217.68	0.0311094	1000	1018.87
				1100	0.63	184	368	3610.08	0.0277279	1100	1123.324
				1200	0.71	208	416	4080.96	0.0245285	1200	1228.638
				1300	0.8	234	468	4591.08	0.0218031	1300	1334.906
				1400	0.9	263	526	5160.06	0.019399	1400	1442.221
				1600	1.13	358	716	7023.96	0.0142512	1600	1660.358

Figure B.89: MinOil-3 recorded data and calculations.

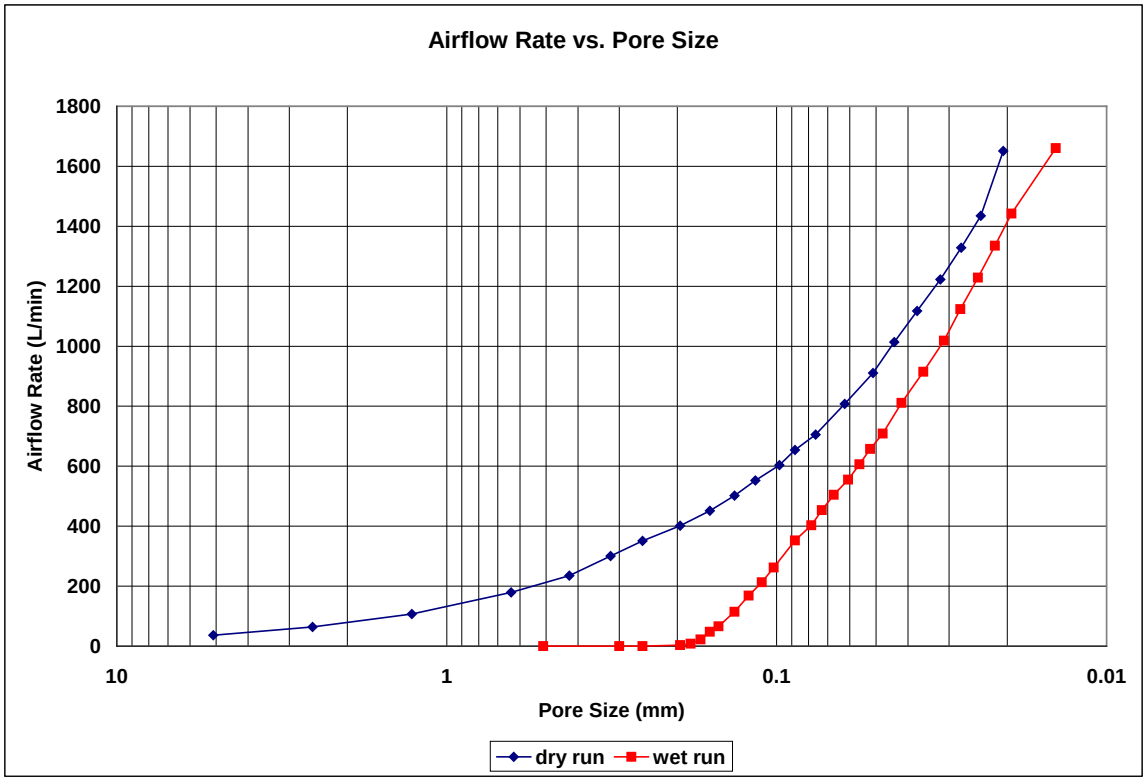

Figure B.90: MinOil-3 airflow rate vs. pore size for the wet and dry runs.

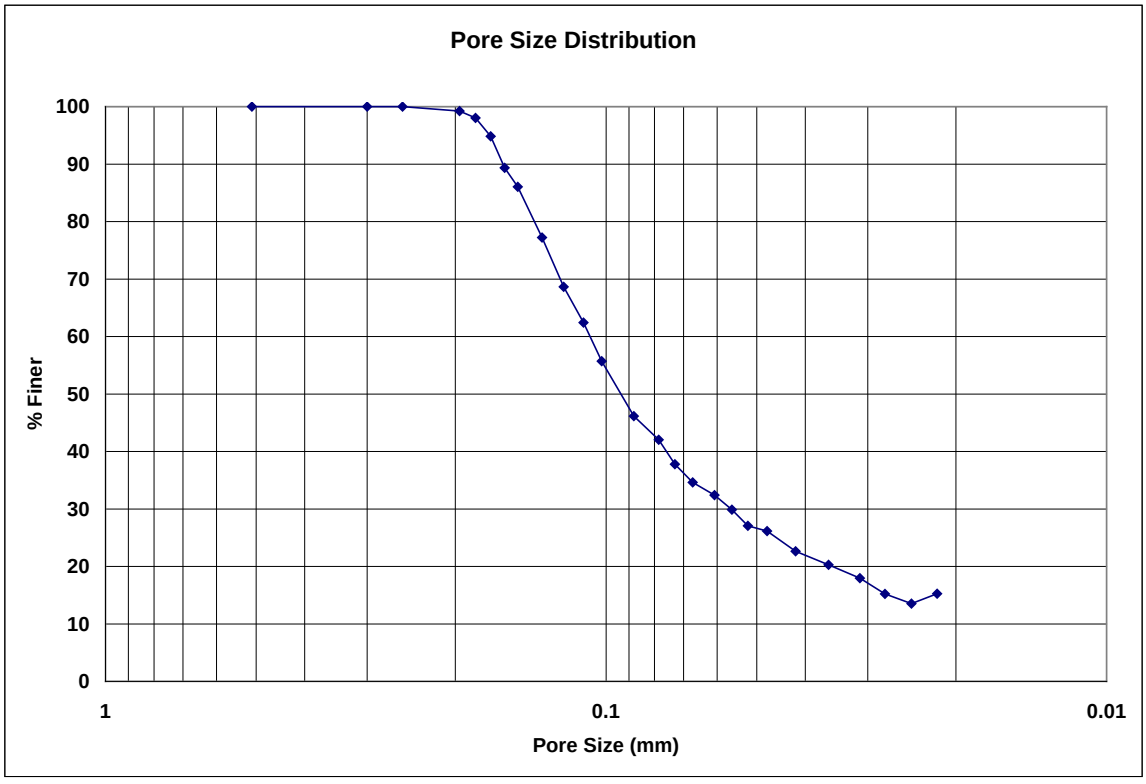

Figure B.91: MinOil-3 pore size distribution.

Bubble Point Test
Auburn University - Department of Civil Engineering

date of test: 4/10/2002
test identification: MinOil-3
test performed by: David Howie
wetting fluid: mineral oil
air temperature: 21 °C
porous media: NG-1 nonwoven geotextile
comments: testing to determine geotextile pore size distribution

Pore Size Calculation Parameters:
constant, C: 2860 mm/m
contact angle: 0 degrees
surface tension: 0.035 N/m

Pore Size at Selected % Finer

% Finer	Pore Size (mm)
98	0.18212
95	0.17067
90	0.16070
85	0.14821
80	0.13926
75	0.13096
70	0.12350
65	0.11529
60	0.10771
55	0.10099
50	0.09364
45	0.08535
40	0.07581
35	0.06780
30	0.05629
25	0.04575
20	0.03534
15	0.02734
10	---
5	---

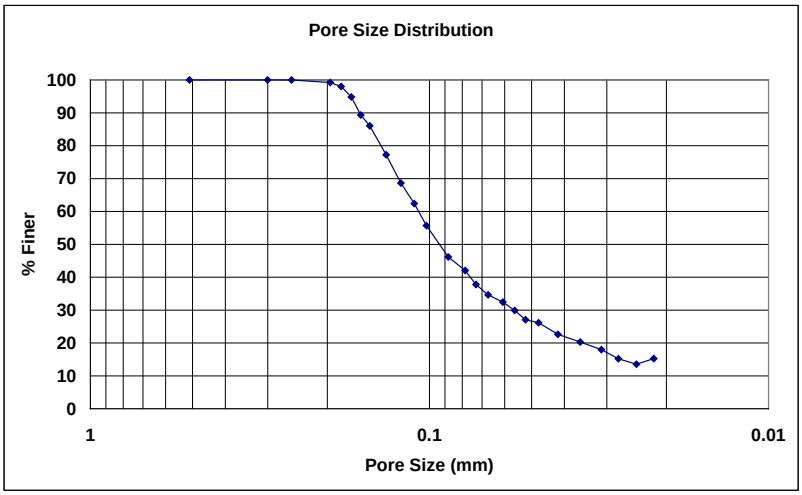

Figure B.92: MinOil-3 pore size distribution report.

Bubble Point Test

Auburn University - Department of Civil Engineering

date of test: 6/19/2000
test identification: MinOil-4
test performed by: David Howie
wetting fluid: mineral oil
ambient air temperature: 21.4 °C
porous media: NG-1 nonwoven geotextile
comments: testing to determine geotextile pore size distribution

Pore Size Calculation Parameters:
constant, C: 2860 mm/m
contact angle: 0 degrees
surface tension: 0.035 N/m

Dry Run

Recorded Data							Calculations				
Indirect Reading Rotameters				Direct Reading Rotameter Value (L/min)	Pressure at Rotameter Exit (psig)	Half of Manometer Reading (mm H20)	Manometer Reading (mm H20)	Manometer Pressure (Pa)	Pore Size (Diameter) (mm)	Indicated Airflow Rate (L/min)	True Airflow Rate (L/min)
First Rotameter Used		Second Rotameter Used									
Rotameter ID Number	Rotameter Value	Rotameter ID Number	Rotameter Value								
5	54				0.14	2	4	39.24	2.5509684	80.3	80.68147
5	65	5	53		0.22	6	12	117.72	0.8503228	175.9	177.2114
5	88	5	72		0.42	10	20	196.2	0.5101937	241	244.4186
				350	0.04	16	32	313.92	0.318871	350	350.4759
				400	0.06	20	40	392.4	0.2550968	400	400.8155
				450	0.07	24	48	470.88	0.2125807	450	451.0702
				500	0.09	29	58	568.98	0.1759289	500	501.5283
				550	0.11	34	68	667.08	0.150057	550	552.054
				600	0.13	39	78	765.18	0.1308189	600	602.6472
				650	0.15	45	90	882.9	0.1133764	650	653.3079
				700	0.17	51	102	1000.62	0.100038	700	704.036
				800	0.23	64	128	1255.68	0.0797178	800	806.2342
				900	0.28	78	156	1530.36	0.0654094	900	908.531
				1000	0.33	92	184	1805.04	0.0554558	1000	1011.162
				1100	0.39	106	212	2079.72	0.0481315	1100	1114.496
				1200	0.45	122	244	2393.64	0.0418192	1200	1218.229
				1300	0.53	142	284	2786.04	0.0359291	1300	1323.228
				1400	0.62	162	324	3178.44	0.0314934	1400	1429.219
				1600	0.75	225	450	4414.5	0.0226753	1600	1640.309

Wet Run

Recorded Data							Calculations				
Indirect Reading Rotameters				Direct Reading Rotameter Value (L/min)	Pressure at Rotameter Exit (psig)	Half of Manometer Reading (mm H20)	Manometer Reading (mm H20)	Manometer Pressure (Pa)	Pore Size (Diameter) (mm)	Indicated Airflow Rate (L/min)	True Airflow Rate (L/min)
First Rotameter Used		Second Rotameter Used									
Rotameter ID Number	Rotameter Value	Rotameter ID Number	Rotameter Value								
1	48					18	36	353.16	0.2834409	0.104	0.104
4	9				0.08	22	44	431.64	0.2319062	2.74	2.747446
4	68				0.38	26	52	510.12	0.1962283	25.2	25.52364
5	53				0.24	30	60	588.6	0.1700646	78.8	79.44066
5	89				0.49	34	68	667.08	0.150057	135	137.2316
5	82	5	68		0.47	40	80	784.8	0.1275484	226	229.5845
5	100	5	82		0.66	44	88	863.28	0.1159531	277	283.1501
				350	0.16	48	96	941.76	0.1062903	350	351.8996
				400	0.18	52	104	1020.24	0.0981142	400	402.4415
				450	0.19	56	112	1098.72	0.091106	450	452.8988
				500	0.21	61	122	1196.82	0.0836383	500	503.5588
				550	0.23	66	132	1294.92	0.0773021	550	554.286
				600	0.25	72	144	1412.64	0.0708602	600	605.0805
				650	0.27	78	156	1530.36	0.0654094	650	655.9422
				700	0.29	84	168	1648.08	0.0607373	700	706.871
				800	0.36	98	196	1922.76	0.0520606	800	809.7367
				900	0.41	112	224	2197.44	0.045553	900	912.4647
				1000	0.46	127	254	2491.74	0.0401727	1000	1015.526
				1100	0.53	143	286	2805.66	0.0356779	1100	1119.654
				1200	0.61	164	328	3217.68	0.0311094	1200	1224.645
				1300	0.69	184	368	3610.08	0.0277279	1300	1330.16
				1400	0.79	206	412	4041.72	0.0247667	1400	1437.127
				1600	0.95	278	556	5454.36	0.0183523	1600	1650.891

Figure B.93: MinOil-4 recorded data and calculations.

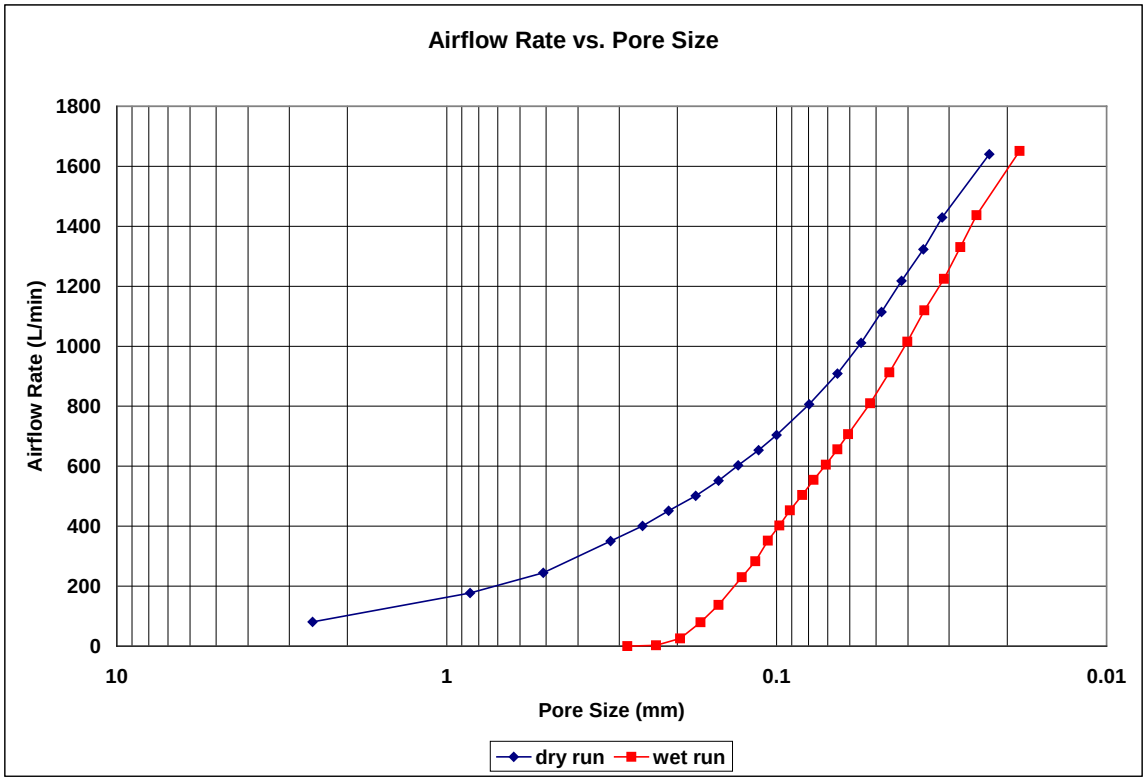

Figure B.94: MinOil-4 airflow rate vs. pore size for the wet and dry runs.

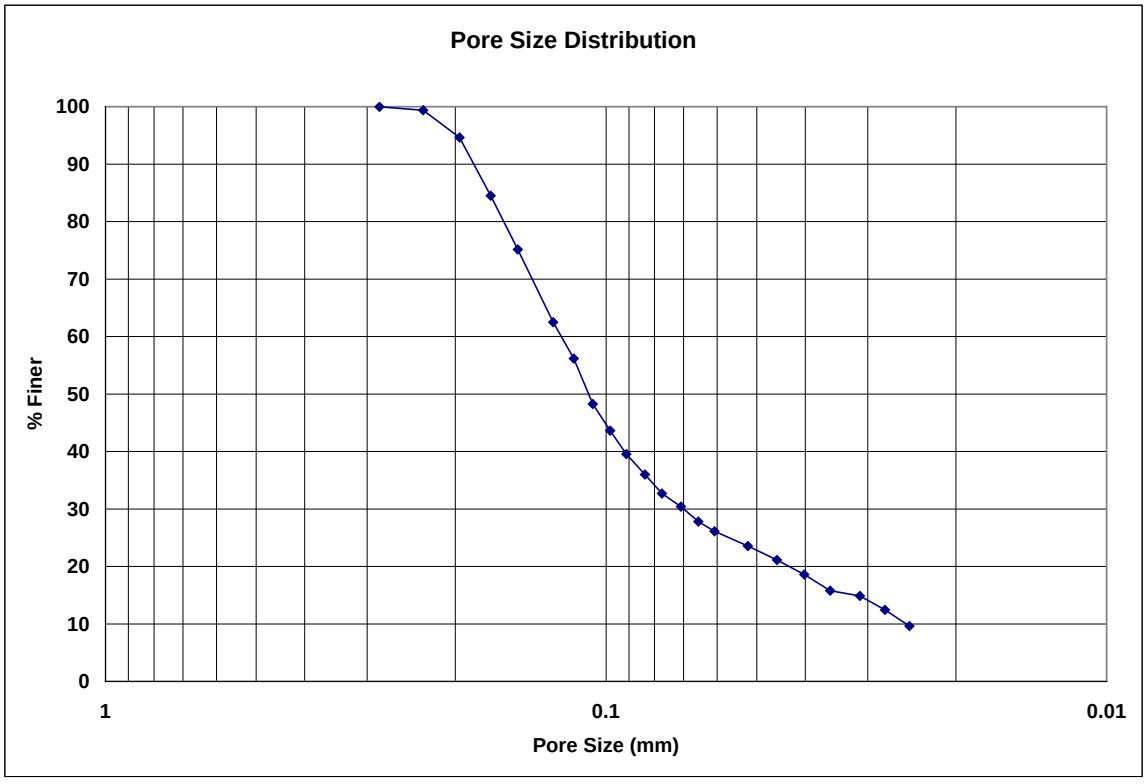

Figure B.95: MinOil-4 pore size distribution.

Bubble Point Test
Auburn University - Department of Civil Engineering

date of test: 6/19/2000
test identification: MinOil-4
test performed by: David Howie
wetting fluid: mineral oil
air temperature: 21.4 °C
porous media: NG-1 nonwoven geotextile
comments: testing to determine geotextile pore size distribution

Pore Size Calculation Parameters:
constant, C: 2860 mm/m
contact angle: 0 degrees
surface tension: 0.035 N/m

Pore Size at Selected % Finer

% Finer	Pore Size (mm)
98	0.22170
95	0.19916
90	0.18428
85	0.17132
80	0.16043
75	0.14980
70	0.14091
65	0.13201
60	0.12298
55	0.11454
50	0.10841
45	0.10055
40	0.09191
35	0.08176
30	0.06999
25	0.05698
20	0.04315
15	0.03181
10	0.02516
5	---

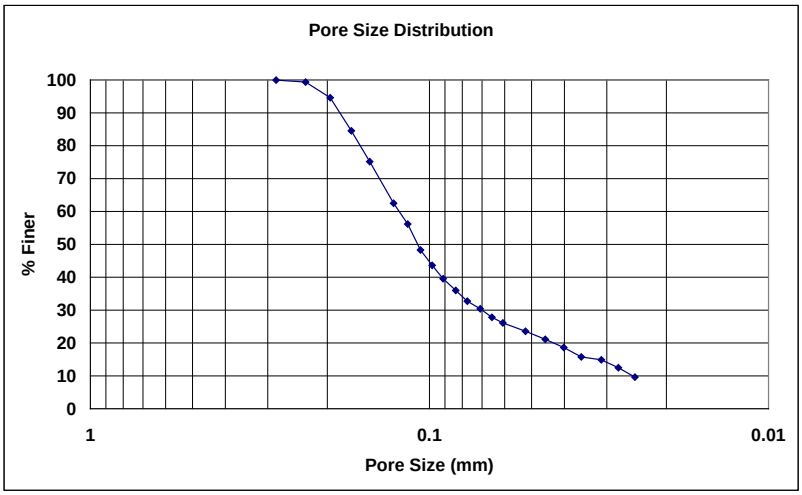

Figure B.96: MinOil-4 pore size distribution report.

Bubble Point Test

Auburn University - Department of Civil Engineering

date of test: 6/19/2000
test identification: MinOil-5
test performed by: David Howie
wetting fluid: mineral oil
ambient air temperature: 21.4 °C
porous media: NG-1 nonwoven geotextile
comments: testing to determine geotextile pore size distribution

Pore Size Calculation Parameters:
constant, C: 2860 mm/m
contact angle: 0 degrees
surface tension: 0.035 N/m

Dry Run

Recorded Data							Calculations				
Indirect Reading Rotameters				Direct Reading Rotameter Value (L/min)	Pressure at Rotameter Exit (psig)	Half of Manometer Reading (mm H20)	Manometer Reading (mm H20)	Manometer Pressure (Pa)	Pore Size (Diameter) (mm)	Indicated Airflow Rate (L/min)	True Airflow Rate (L/min)
First Rotameter Used		Second Rotameter Used									
Rotameter ID Number	Rotameter Value	Rotameter ID Number	Rotameter Value								
5	58				0.17	2	4	39.24	2.5509684	86.3	86.79758
5	70	5	57		0.25	6	12	117.72	0.8503228	189.8	191.4071
5	95	5	78		0.47	10	20	196.2	0.5101937	263	267.1713
				350	0.05	14	28	274.68	0.3644241	350	350.5947
				450	0.07	21	42	412.02	0.2429494	450	451.0702
				500	0.09	25	50	490.5	0.2040775	500	501.5283
				550	0.11	30	60	588.6	0.1700646	550	552.054
				600	0.12	34	68	667.08	0.150057	600	602.444
				650	0.14	40	80	784.8	0.1275484	650	653.0879
				700	0.16	45	90	882.9	0.1133764	700	703.7992
				800	0.21	57	114	1118.34	0.0895077	800	805.694
				900	0.26	68	136	1334.16	0.0750285	900	907.9243
				1000	0.31	81	162	1589.22	0.0629869	1000	1010.489
				1100	0.36	95	190	1863.9	0.0537046	1100	1113.388
				1200	0.43	110	220	2158.2	0.0463812	1200	1217.425
				1300	0.5	127	254	2491.74	0.0401727	1300	1321.924
				1400	0.59	145	290	2844.9	0.0351858	1400	1427.819
				1600	0.69	195	390	3825.9	0.0261638	1600	1637.12

Wet Run

Recorded Data							Calculations				
Indirect Reading Rotameters				Direct Reading Rotameter Value (L/min)	Pressure at Rotameter Exit (psig)	Half of Manometer Reading (mm H20)	Manometer Reading (mm H20)	Manometer Pressure (Pa)	Pore Size (Diameter) (mm)	Indicated Airflow Rate (L/min)	True Airflow Rate (L/min)
First Rotameter Used		Second Rotameter Used									
Rotameter ID Number	Rotameter Value	Rotameter ID Number	Rotameter Value								
1	25					17	34	333.54	0.3001139	0.0352	0.0352
4	24				0.12	22	44	431.64	0.2319062	7.91	7.94222
5	52				0.22	28	56	549.36	0.182212	77.2	77.77554
5	90				0.5	32	64	627.84	0.1594355	137	139.3104
5	77	5	69		0.42	36	72	706.32	0.1417205	219	222.1065
5	95	5	78		0.59	40	80	784.8	0.1275484	263	268.226
				350	0.14	45	90	882.9	0.1133764	350	351.6627
				400	0.15	47	94	922.14	0.1085518	400	402.0356
				450	0.17	52	104	1020.24	0.0981142	450	452.5946
				500	0.18	56	112	1098.72	0.091106	500	503.0519
				550	0.2	61	122	1196.82	0.0836383	550	553.7289
				600	0.22	66	132	1294.92	0.0773021	600	604.4731
				650	0.23	70	140	1373.4	0.0728848	650	655.0653
				700	0.26	77	154	1510.74	0.0662589	700	706.1633
				800	0.33	88	176	1726.56	0.0579766	800	808.9298
				900	0.37	100	200	1962	0.0510194	900	911.2561
				1000	0.43	116	232	2275.92	0.0439822	1000	1014.52
				1100	0.49	129	258	2530.98	0.0395499	1100	1118.183
				1200	0.55	147	294	2884.14	0.0347071	1200	1222.243
				1300	0.63	166	332	3256.92	0.0307346	1300	1327.565
				1400	0.7	185	370	3629.7	0.027578	1400	1432.946
				1600	0.86	248	496	4865.76	0.0205723	1600	1646.138

Figure B.97: MinOil-5 recorded data and calculations.

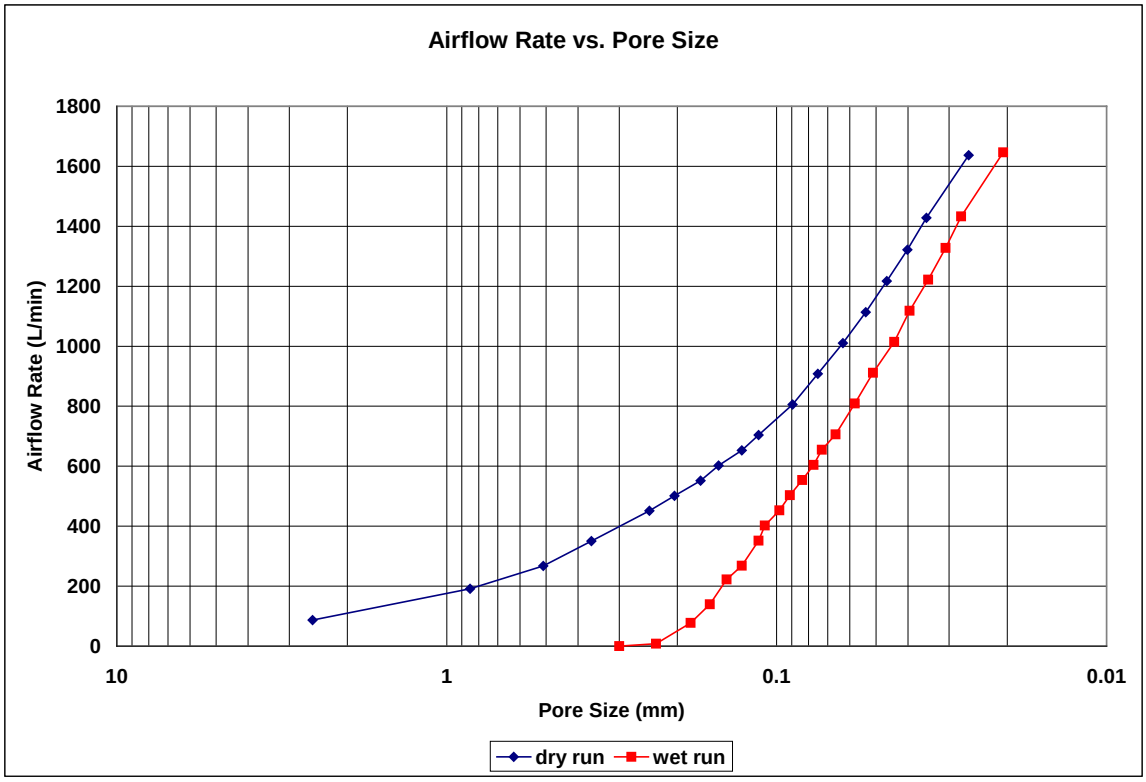

Figure B.98: MinOil-5 airflow rate vs. pore size for the wet and dry runs.

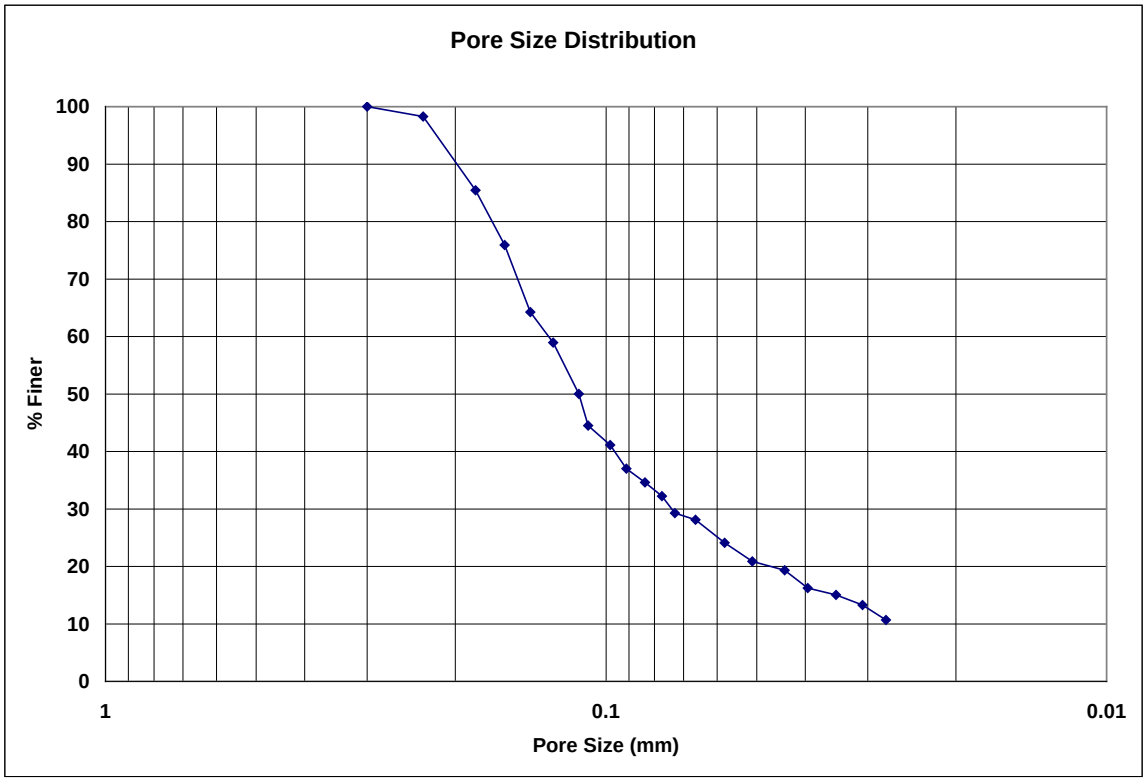

Figure B.99: MinOil-5 pore size distribution.

Bubble Point Test
Auburn University - Department of Civil Engineering

date of test: 6/19/2000
test identification: MinOil-5
test performed by: David Howie
wetting fluid: mineral oil
air temperature: 21.4 °C
porous media: NG-1 nonwoven geotextile
comments: testing to determine geotextile pore size distribution

Pore Size Calculation Parameters:
constant, C: 2860 mm/m
contact angle: 0 degrees
surface tension: 0.035 N/m

Pore Size at Selected % Finer

% Finer	Pore Size (mm)
98	0.23077
95	0.21918
90	0.19985
85	0.18117
80	0.16918
75	0.15802
70	0.15044
65	0.14286
60	0.13040
55	0.12129
50	0.11335
45	0.10899
40	0.09617
35	0.08478
30	0.07397
25	0.05980
20	0.04702
15	0.03458
10	---
5	---

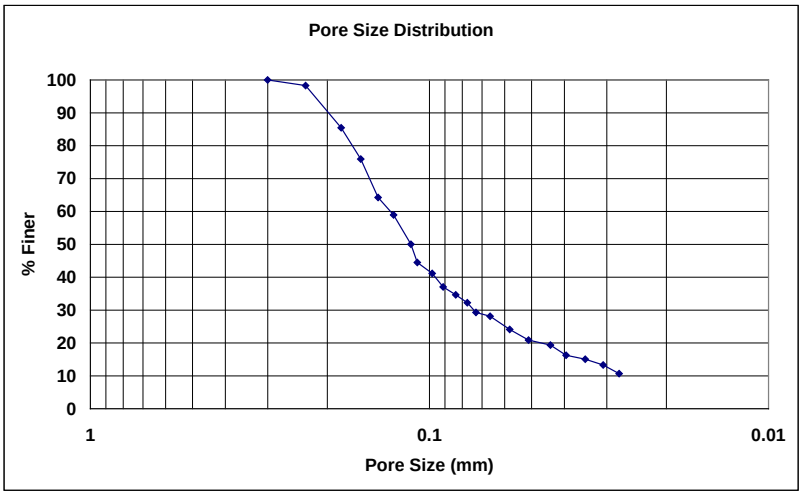

Figure B.100: MinOil-5 pore size distribution report.

Bubble Point Test

Auburn University - Department of Civil Engineering

date of test: 12/7/2000
test identification: MinOil-6
test performed by: David Howie
wetting fluid: mineral oil
ambient air temperature: 19.8 °C
porous media: NG-1 nonwoven geotextile
comments: testing to determine geotextile pore size distribution

Pore Size Calculation Parameters:
constant, C: 2860 mm/m
contact angle: 0 degrees
surface tension: 0.035 N/m

Dry Run

Recorded Data							Calculations				
Indirect Reading Rotameters				Direct Reading Rotameter Value (L/min)	Pressure at Rotameter Exit (psig)	Half of Manometer Reading (mm H20)	Manometer Reading (mm H20)	Manometer Pressure (Pa)	Pore Size (Diameter) (mm)	Indicated Airflow Rate (L/min)	True Airflow Rate (L/min)
First Rotameter Used		Second Rotameter Used									
Rotameter ID Number	Rotameter Value	Rotameter ID Number	Rotameter Value								
5	42				0.1	2	4	39.24	2.5509684	62.4	62.61189
5	90				0.42	6	12	117.72	0.8503228	137	138.9434
5	76	5	62		0.32	10	20	196.2	0.5101937	206.5	208.7355
5	94	5	78		0.53	14	28	274.68	0.3644241	261	265.6634
				350	0.07	20	40	392.4	0.2550968	350	350.8323
				400	0.09	25	50	490.5	0.2040775	400	401.2226
				450	0.1	30	60	588.6	0.1700646	450	451.528
				500	0.12	35	70	686.7	0.1457696	500	502.0367
				550	0.14	42	84	824.04	0.1214747	550	552.6128
				600	0.17	48	96	941.76	0.1062903	600	603.4594
				650	0.19	56	112	1098.72	0.091106	650	654.1872
				700	0.22	64	128	1255.68	0.0797178	700	705.2186
				800	0.3	80	160	1569.6	0.0637742	800	808.122
				900	0.35	97	194	1903.14	0.0525973	900	910.6513
				1000	0.42	115	230	2256.3	0.0443647	1000	1014.185
				1100	0.49	133	266	2609.46	0.0383604	1100	1118.183
				1200	0.57	156	312	3060.72	0.0327047	1200	1223.044
				1300	0.67	180	360	3531.6	0.0283441	1300	1329.296
				1400	0.77	204	408	4002.48	0.0250095	1400	1436.199

Wet Run

Recorded Data							Calculations				
Indirect Reading Rotameters				Direct Reading Rotameter Value (L/min)	Pressure at Rotameter Exit (psig)	Half of Manometer Reading (mm H20)	Manometer Reading (mm H20)	Manometer Pressure (Pa)	Pore Size (Diameter) (mm)	Indicated Airflow Rate (L/min)	True Airflow Rate (L/min)
First Rotameter Used		Second Rotameter Used									
Rotameter ID Number	Rotameter Value	Rotameter ID Number	Rotameter Value								
1	77					20	40	392.4	0.2550968	0.216	0.216
4	18				0.1	24	48	470.88	0.2125807	5.75	5.769525
4	71				0.42	28	56	549.36	0.182212	26.5	26.87591
5	47				0.2	32	64	627.84	0.1594355	69.8	70.27323
5	81				0.41	36	72	706.32	0.1417205	122	123.6897
5	65	5	53		0.33	40	80	784.8	0.1275484	175.9	177.8634
5	82	5	66		0.46	44	88	863.28	0.1159531	222.7	226.1576
5	100	5	84		0.66	49	98	961.38	0.1041212	280	286.2167
				400	0.18	58	116	1137.96	0.0879644	400	402.4415
				450	0.2	65	130	1275.3	0.0784913	450	453.0509
				500	0.22	71	142	1393.02	0.0718583	500	503.7276
				550	0.24	79	158	1549.98	0.0645815	550	554.4716
				600	0.27	85	170	1667.7	0.0600228	600	605.4851
				650	0.29	93	186	1824.66	0.0548595	650	656.3803
				700	0.32	101	202	1981.62	0.0505142	700	707.578
				800	0.39	117	234	2295.54	0.0436063	800	810.5428
				900	0.46	138	276	2707.56	0.0369706	900	913.9732
				1000	0.53	157	314	3080.34	0.0324964	1000	1017.868
				1100	0.61	179	358	3511.98	0.0285024	1100	1122.591
				1200	0.7	204	408	4002.48	0.0250095	1200	1228.239
				1300	0.8	232	464	4551.84	0.0219911	1300	1334.906
				1400	0.92	262	524	5140.44	0.019473	1400	1443.145
				1600	1.16	352	704	6906.24	0.0144941	1600	1661.931

Figure B.101: MinOil-6 recorded data and calculations.

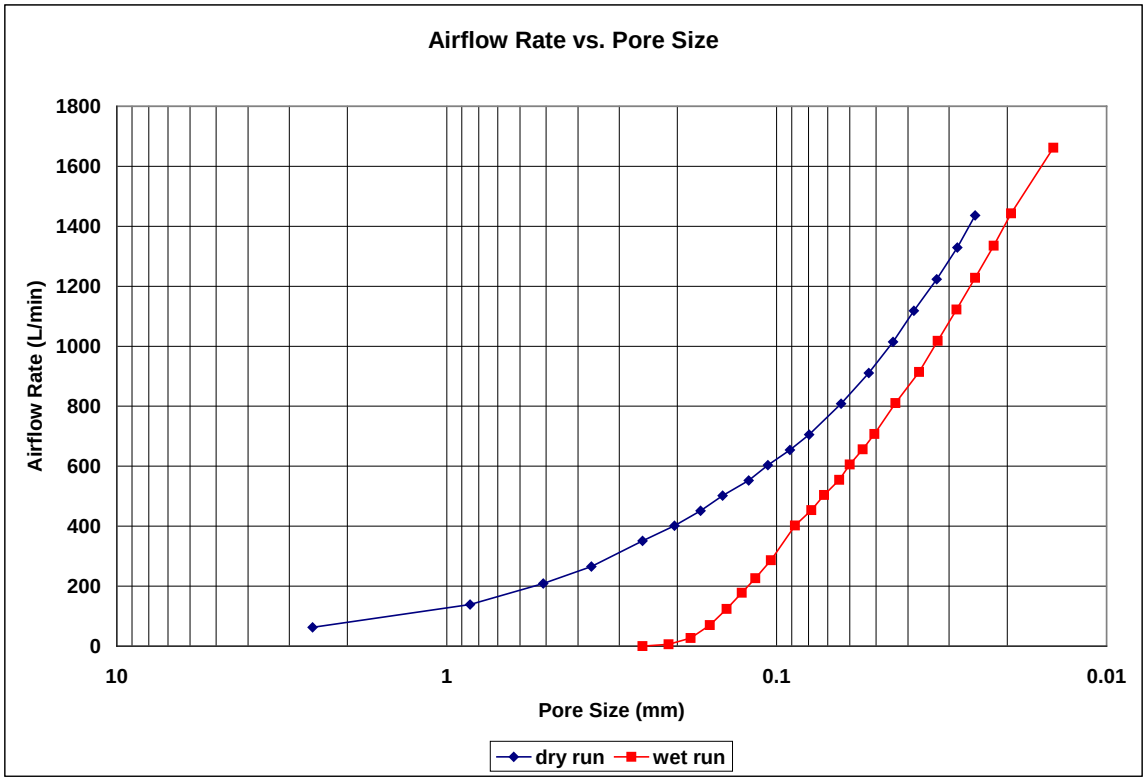

Figure B.102: MinOil-6 airflow rate vs. pore size for the wet and dry runs.

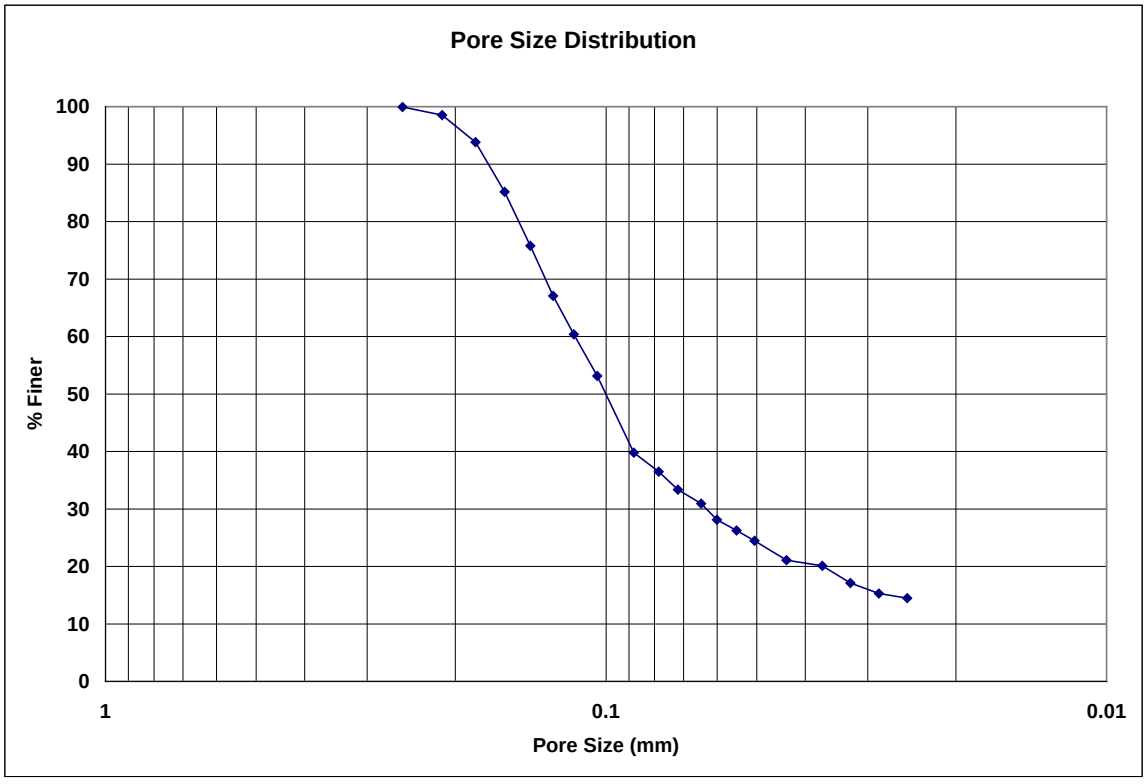

Figure B.103: MinOil-6 pore size distribution.

Bubble Point Test
Auburn University - Department of Civil Engineering

date of test: 12/7/2000
test identification: MinOil-6
test performed by: David Howie
wetting fluid: mineral oil
air temperature: 19.8 °C
porous media: NG-1 nonwoven geotextile
comments: testing to determine geotextile pore size distribution

Pore Size Calculation Parameters:
constant, C: 2860 mm/m
contact angle: 0 degrees
surface tension: 0.035 N/m

Pore Size at Selected % Finer

% Finer	Pore Size (mm)
98	0.20917
95	0.18991
90	0.17219
85	0.15913
80	0.14970
75	0.14047
70	0.13233
65	0.12396
60	0.11530
55	0.10716
50	0.10033
45	0.09428
40	0.08823
35	0.07535
30	0.06305
25	0.05181
20	0.03681
15	0.02721
10	---
5	---

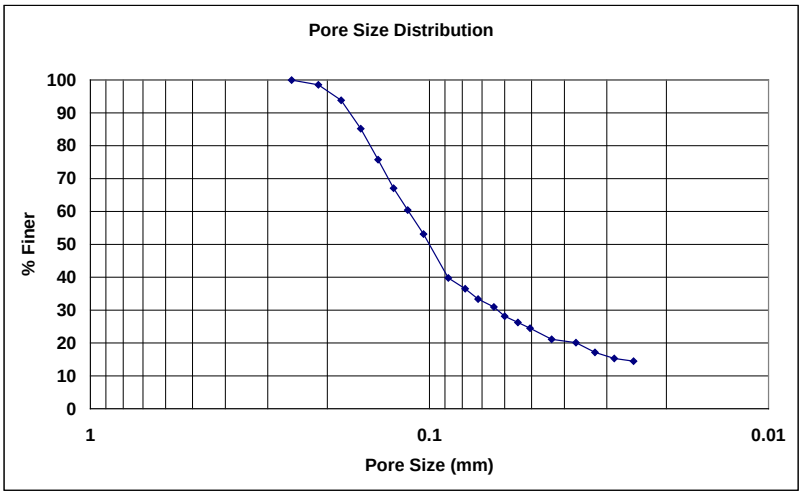

Figure B.104: MinOil-6 pore size distribution report.

Bubble Point Test

Auburn University - Department of Civil Engineering

date of test: 12/7/2000
test identification: MinOil-7
test performed by: David Howie
wetting fluid: mineral oil
ambient air temperature: 19.8 °C
porous media: NG-1 nonwoven geotextile
comments: testing to determine geotextile pore size distribution

Pore Size Calculation Parameters:
constant, C: 2860 mm/m
contact angle: 0 degrees
surface tension: 0.035 N/m

Dry Run

Recorded Data							Calculations				
Indirect Reading Rotameters				Direct Reading Rotameter Value (L/min)	Pressure at Rotameter Exit (psig)	Half of Manometer Reading (mm H20)	Manometer Reading (mm H20)	Manometer Pressure (Pa)	Pore Size (Diameter) (mm)	Indicated Airflow Rate (L/min)	True Airflow Rate (L/min)
First Rotameter Used		Second Rotameter Used									
Rotameter ID Number	Rotameter Value	Rotameter ID Number	Rotameter Value								
5	55				0.16	2	4	39.24	2.5509684	81.8	82.24397
5	68	5	55		0.25	6	12	117.72	0.8503228	183.8	185.3563
5	94	5	72		0.49	10	20	196.2	0.5101937	251	255.149
				350	0.07	14	28	274.68	0.3644241	350	350.8323
				400	0.08	18	36	353.16	0.2834409	400	401.087
				450	0.09	22	44	431.64	0.2319062	450	451.3754
				500	0.1	26	52	510.12	0.1962283	500	501.6978
				550	0.12	30	60	588.6	0.1700646	550	552.2403
				600	0.14	35	70	686.7	0.1457696	600	602.8504
				650	0.16	40	80	784.8	0.1275484	650	653.5278
				700	0.17	46	92	902.52	0.1109117	700	704.036
				800	0.23	56	112	1098.72	0.091106	800	806.2342
				900	0.28	69	138	1353.78	0.0739411	900	908.531
				1000	0.33	82	164	1608.84	0.0622187	1000	1011.162
				1100	0.38	96	192	1883.52	0.0531452	1100	1114.127
				1200	0.45	111	222	2177.82	0.0459634	1200	1218.229
				1300	0.53	127	254	2491.74	0.0401727	1300	1323.228
				1400	0.61	145	290	2844.9	0.0351858	1400	1428.752
				1600	0.7	195	390	3825.9	0.0261638	1600	1637.652

Wet Run

Recorded Data							Calculations				
Indirect Reading Rotameters				Direct Reading Rotameter Value (L/min)	Pressure at Rotameter Exit (psig)	Half of Manometer Reading (mm H20)	Manometer Reading (mm H20)	Manometer Pressure (Pa)	Pore Size (Diameter) (mm)	Indicated Airflow Rate (L/min)	True Airflow Rate (L/min)
First Rotameter Used		Second Rotameter Used									
Rotameter ID Number	Rotameter Value	Rotameter ID Number	Rotameter Value								
1	5					8	16	156.96	0.6377421	0.00316	0.00316
1	11					13	26	255.06	0.3924567	0.00847	0.00847
4	8				0.07	22	44	431.64	0.2319062	2.43	2.435779
4	80				0.5	26	52	510.12	0.1962283	30.4	30.91268
5	57				0.25	30	60	588.6	0.1700646	84.8	85.51805
5	97				0.57	34	68	667.08	0.150057	148	150.8421
5	81	5	67		0.45	38	76	745.56	0.1342615	222	225.3723
5	100	5	88		0.66	42	84	824.04	0.1214747	286	292.3499
				400	0.16	50	100	981	0.1020387	400	402.171
				500	0.19	56	112	1098.72	0.091106	500	503.2209
				550	0.21	61	122	1196.82	0.0836383	550	553.9146
				600	0.23	66	132	1294.92	0.0773021	600	604.6757
				650	0.25	72	144	1412.64	0.0708602	650	655.5039
				700	0.27	78	156	1530.36	0.0654094	700	706.3993
				800	0.33	89	178	1746.18	0.0573251	800	808.9298
				900	0.38	103	206	2020.86	0.0495334	900	911.5584
				1000	0.43	116	232	2275.92	0.0439822	1000	1014.52
				1100	0.49	132	264	2589.84	0.038651	1100	1118.183
				1200	0.56	148	296	2903.76	0.0344725	1200	1222.644
				1300	0.66	166	332	3256.92	0.0307346	1300	1328.863
				1400	0.74	186	372	3649.32	0.0274298	1400	1434.805
				1600	0.87	250	500	4905	0.0204077	1600	1646.666

Figure B.105: MinOil-7 recorded data and calculations.

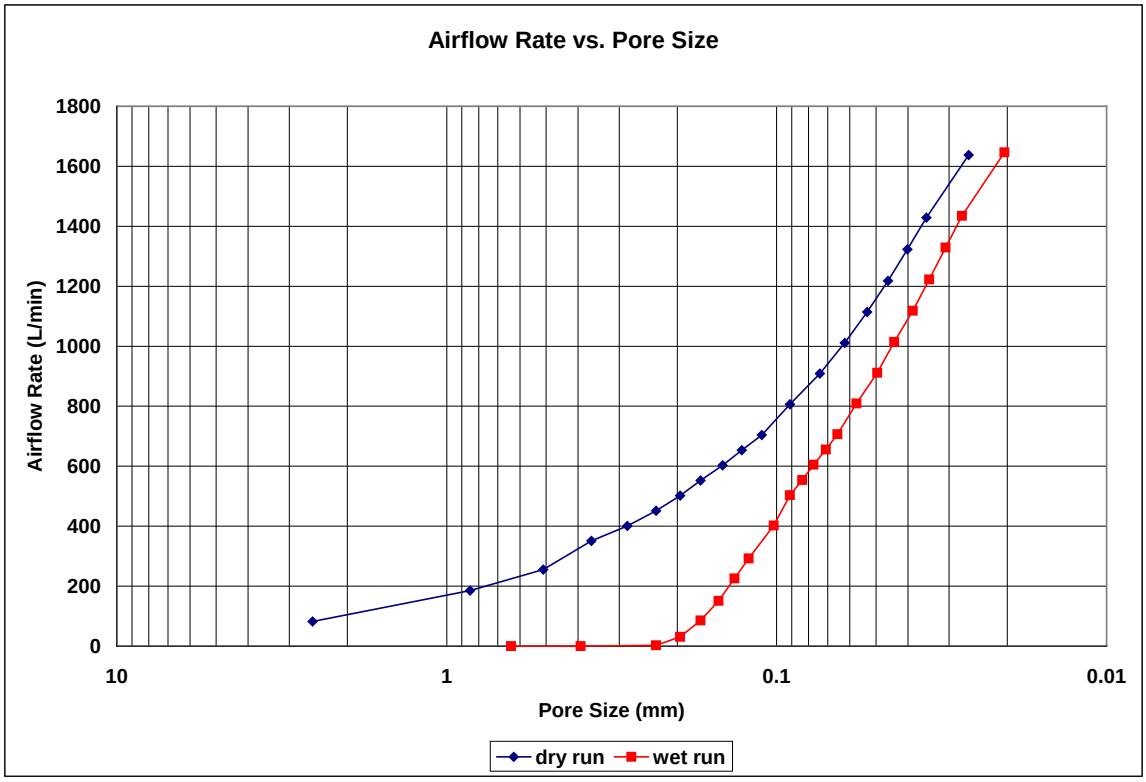

Figure B.106: MinOil-7 airflow rate vs. pore size for the wet and dry runs.

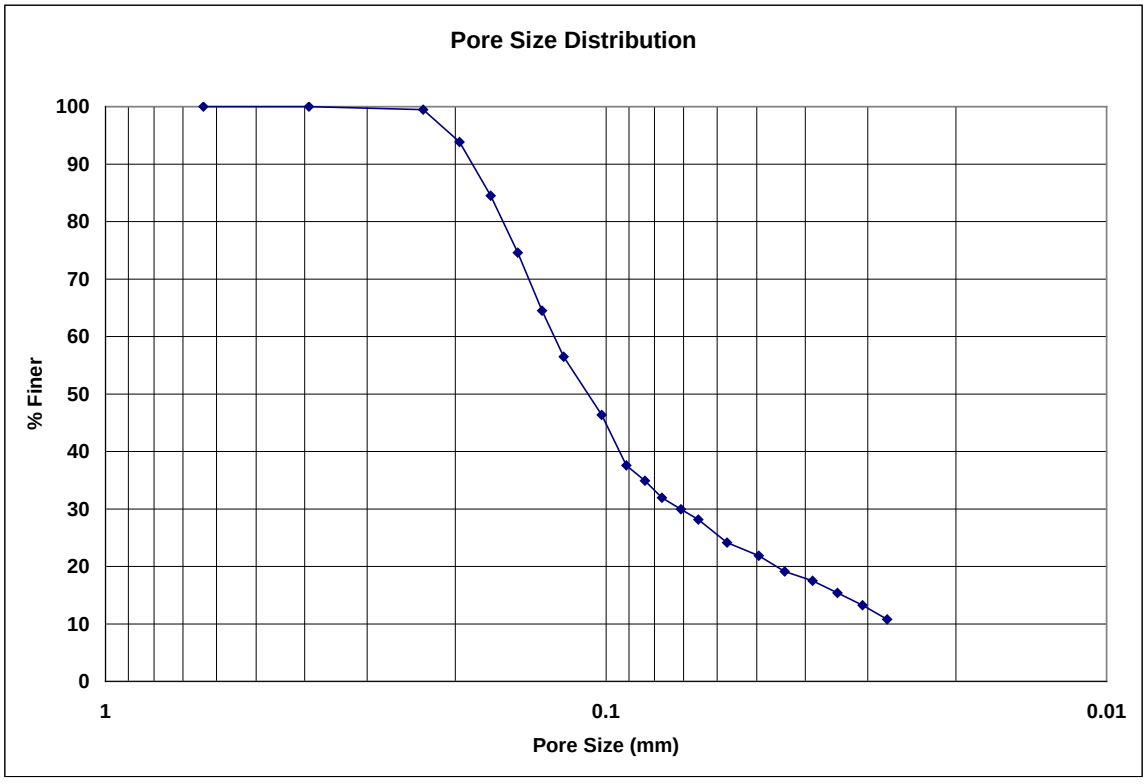

Figure B.107: MinOil-7 pore size distribution.

Bubble Point Test
Auburn University - Department of Civil Engineering

date of test: 12/7/2000
test identification: MinOil-7
test performed by: David Howie
wetting fluid: mineral oil
air temperature: 19.8 °C
porous media: NG-1 nonwoven geotextile
comments: testing to determine geotextile pore size distribution

Pore Size Calculation Parameters:
constant, C: 2860 mm/m
contact angle: 0 degrees
surface tension: 0.035 N/m

Pore Size at Selected % Finer

% Finer	Pore Size (mm)
98	0.22264
95	0.20360
90	0.18546
85	0.17143
80	0.16095
75	0.15086
70	0.14286
65	0.13504
60	0.12707
55	0.11861
50	0.10901
45	0.10034
40	0.09411
35	0.08394
30	0.07108
25	0.05902
20	0.04579
15	0.03377
10	---
5	---

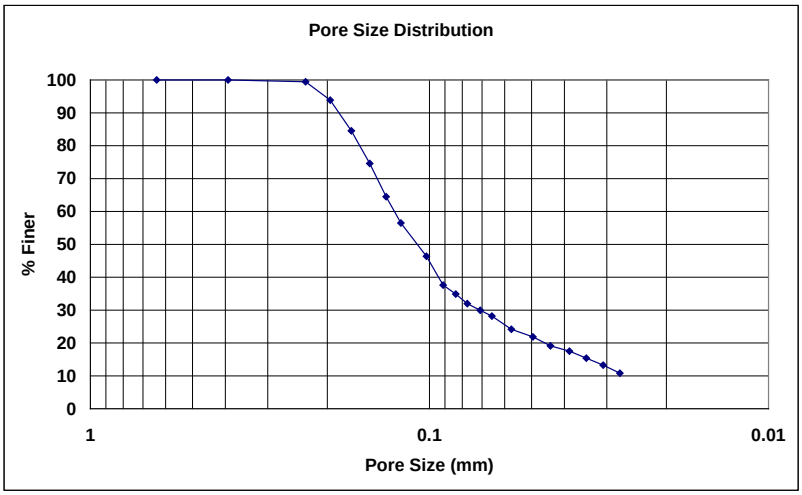

Figure B.108: MinOil-7 pore size distribution report.

Bubble Point Test
Auburn University - Department of Civil Engineering

date of test: 10/17/2002
test identification: MinOil-8
test performed by: Howie / Sims
wetting fluid: mineral oil
ambient air temperature: 21.5 °C
porous media: NG-1 nonwoven geotextile
comments: testing to determine geotextile pore size distribution

Pore Size Calculation Parameters:
constant, C: 2860 mm/m
contact angle: 0 degrees
surface tension: 0.035 N/m

Dry Run

Recorded Data							Calculations				
Indirect Reading Rotameters				Direct Reading Rotameter Value (L/min)	Pressure at Rotameter Exit (psig)	Half of Manometer Reading (mm H20)	Manometer Reading (mm H20)	Manometer Pressure (Pa)	Pore Size (Diameter) (mm)	Indicated Airflow Rate (L/min)	True Airflow Rate (L/min)
First Rotameter Used		Second Rotameter Used									
Rotameter ID Number	Rotameter Value	Rotameter ID Number	Rotameter Value								
5	23				0.03	1	2	19.62	5.1019368	35	35.0357
5	39				0.08	2	4	39.24	2.5509684	58	58.15761
5	63				0.2	4	8	78.48	1.2754842	94	94.6373
5	97				0.48	8	16	156.96	0.6377421	148	150.3969
5	74	5	61		0.31	12	24	235.44	0.4251614	201.9	204.0178
				300	0.06	19	38	372.78	0.268523	300	300.6116
				350	0.7	24	48	470.88	0.2125807	350	358.2364
				400	0.1	31	62	608.22	0.1645786	400	401.3582
				450	0.12	38	76	745.56	0.1342615	450	451.833
				500	0.14	45	90	882.9	0.1133764	500	502.3753
				550	0.17	53	106	1039.86	0.096263	550	553.1711
				600	0.19	62	124	1216.44	0.0822893	600	603.8651
				650	0.22	70	140	1373.4	0.0728848	650	654.8459
				700	0.25	80	160	1569.6	0.0637742	700	705.9273
				800	0.34	102	204	2001.24	0.050019	800	809.1988
				900	0.4	118	236	2315.16	0.0432368	900	912.1627
				1000	0.47	138	276	2707.56	0.0369706	1000	1015.861
				1100	0.55	164	328	3217.68	0.0311094	1100	1120.389
				1200	0.65	195	390	3825.9	0.0261638	1200	1226.244
				1300	0.76	225	450	4414.5	0.0226753	1300	1333.182
				1400	0.87	255	510	5003.1	0.0200076	1400	1440.833
				1600	1.1	355	710	6965.1	0.0143717	1600	1658.784

Wet Run

Recorded Data							Calculations				
Indirect Reading Rotameters				Direct Reading Rotameter Value (L/min)	Pressure at Rotameter Exit (psig)	Half of Manometer Reading (mm H20)	Manometer Reading (mm H20)	Manometer Pressure (Pa)	Pore Size (Diameter) (mm)	Indicated Airflow Rate (L/min)	True Airflow Rate (L/min)
First Rotameter Used		Second Rotameter Used									
Rotameter ID Number	Rotameter Value	Rotameter ID Number	Rotameter Value								
1	9					1	2	19.62	5.1019368	0.00636	0.00636
1	25					5	10	98.1	1.0203874	0.0352	0.0352
1	30					8	16	156.96	0.6377421	0.0478	0.0478
1	31					12	24	235.44	0.4251614	0.0505	0.0505
1	47					22	44	431.64	0.2319062	0.101	0.101
2	27					26	52	510.12	0.1962283	0.418	0.418
4	9				0.1	30	60	588.6	0.1700646	2.74	2.749304
5	32				0.17	36	72	706.32	0.1417205	47.9	48.17618
5	55				0.27	40	80	784.8	0.1275484	81.8	82.54781
5	93				0.56	46	92	902.52	0.1109117	141	143.6606
5	76	5	62		0.44	52	104	1020.24	0.0981142	206.5	209.5677
5	93	5	77		0.62	58	116	1137.96	0.0879644	257	262.3638
				350	0.24	67	134	1314.54	0.0761483	350	352.8456
				400	0.26	74	148	1451.88	0.0689451	400	403.5219
				450	0.28	82	164	1608.84	0.0622187	450	454.2655
				500	0.3	90	180	1765.8	0.0566882	500	505.0763
				550	0.33	98	196	1922.76	0.0520606	550	556.1392
				600	0.36	108	216	2118.96	0.0472402	600	607.3025
				650	0.39	119	238	2334.78	0.0428734	650	658.566
				700	0.42	130	260	2550.6	0.0392457	700	709.9296
				800	0.48	149	298	2923.38	0.0342412	800	812.9563
				900	0.55	170	340	3335.4	0.0300114	900	916.6821
				1000	0.63	194	388	3806.28	0.0262986	1000	1021.204
				1100	0.71	215	430	4218.3	0.0237299	1100	1126.251
				1200	0.81	246	492	4826.52	0.0207396	1200	1232.618
				1300	0.95	285	570	5591.7	0.0179015	1300	1341.349
				1400	1.07	316	632	6199.92	0.0161454	1400	1450.057
				1600	1.36	435	870	8534.7	0.0117286	1600	1672.377

Figure B.109: MinOil-8 recorded data and calculations.

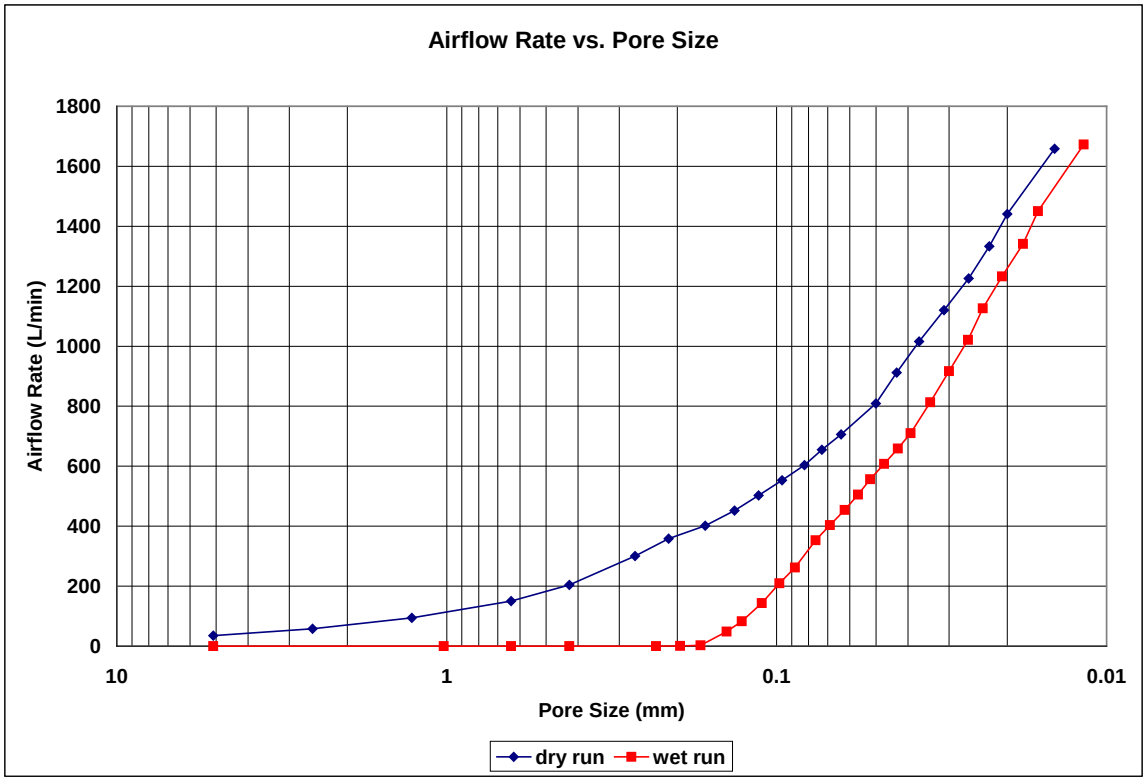

Figure B.110: MinOil-8 airflow rate vs. pore size for the wet and dry runs.

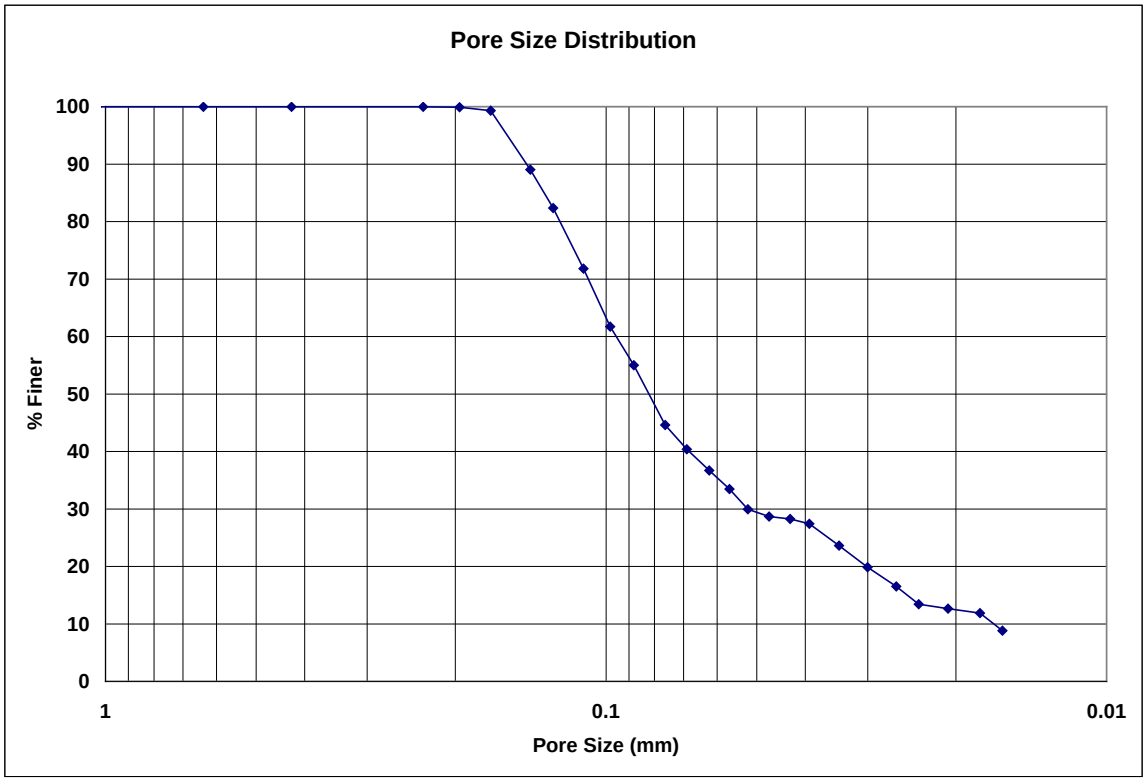

Figure B.111: MinOil-8 pore size distribution.

Bubble Point Test
Auburn University - Department of Civil Engineering

date of test: 10/17/2002
test identification: MinOil-8
test performed by: Howie / Sims
wetting fluid: mineral oil
air temperature: 21.5 °C
porous media: NG-1 nonwoven geotextile
comments: testing to determine geotextile pore size distribution

Pore Size Calculation Parameters:
constant, C: 2860 mm/m
contact angle: 0 degrees
surface tension: 0.035 N/m

Pore Size at Selected % Finer

% Finer	Pore Size (mm)
98	0.16646
95	0.15818
90	0.14438
85	0.13315
80	0.12382
75	0.11594
70	0.10861
65	0.10226
60	0.09549
55	0.08794
50	0.08226
45	0.07658
40	0.06823
35	0.05931
30	0.05213
25	0.03605
20	0.03017
15	0.02504
10	0.01682
5	---

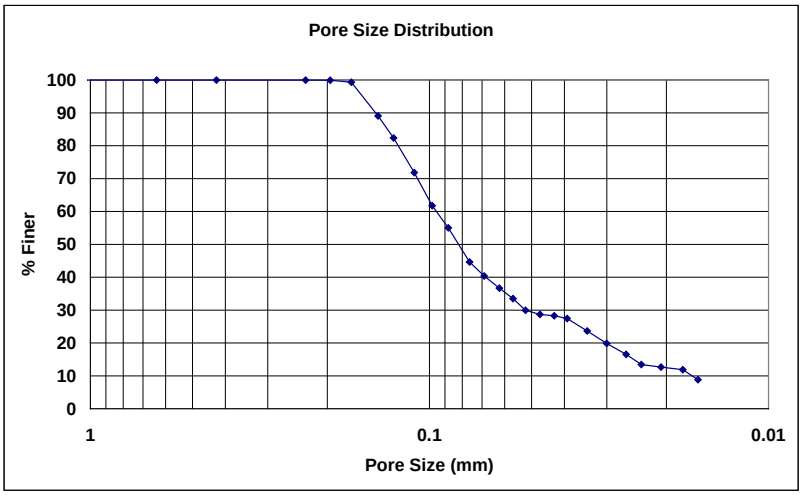

Figure B.112: MinOil-8 pore size distribution report.

Bubble Point Test

Auburn University - Department of Civil Engineering

date of test: 12/5/2002
test identification: MinOil-9
test performed by: Trent Sims
wetting fluid: mineral oil
ambient air temperature: 21 °C
porous media: NG-1 nonwoven geotextile
comments: testing to determine geotextile pore size distribution

Pore Size Calculation Parameters:
constant, C: 2860 mm/m
contact angle: 0 degrees
surface tension: 0.035 N/m

Dry Run

Recorded Data							Calculations				
Indirect Reading Rotameters				Direct Reading Rotameter Value (L/min)	Pressure at Rotameter Exit (psig)	Half of Manometer Reading (mm H20)	Manometer Reading (mm H20)	Manometer Pressure (Pa)	Pore Size (Diameter) (mm)	Indicated Airflow Rate (L/min)	True Airflow Rate (L/min)
First Rotameter Used		Second Rotameter Used									
Rotameter ID Number	Rotameter Value	Rotameter ID Number	Rotameter Value								
4	75				0.37	1	2	19.62	5.1019368	28.2	28.55269
5	45				0.09	2	4	39.24	2.5509684	66.8	67.00418
5	77				0.28	4	8	78.48	1.2754842	116	117.0996
5	59	5	48		0.18	6	12	117.72	0.8503228	159.2	160.1717
5	70	5	58		0.25	8	16	156.96	0.6377421	191.3	192.9198
5	79	5	65		0.32	10	20	196.2	0.5101937	216.1	218.4394
5	98	5	80		0.51	14	28	274.68	0.3644241	270	274.6437
				400	0.06	22	44	431.64	0.2319062	400	400.8155
				500	0.1	33	66	647.46	0.1546041	500	501.6978
				550	0.12	39	78	765.18	0.1308189	550	552.2403
				600	0.14	45	90	882.9	0.1133764	600	602.8504
				650	0.16	53	106	1039.86	0.096263	650	653.5278
				700	0.19	60	120	1177.2	0.0850323	700	704.5093
				800	0.25	74	148	1451.88	0.0689451	800	806.774
				900	0.31	89	178	1746.18	0.0573251	900	909.4403
				1000	0.36	106	212	2079.72	0.0481315	1000	1012.171
				1100	0.42	124	248	2432.88	0.0411447	1100	1115.604
				1200	0.5	141	282	2766.42	0.0361839	1200	1220.238
				1300	0.59	163	326	3198.06	0.0313002	1300	1325.832
				1400	0.68	186	372	3649.32	0.0274298	1400	1432.015
				1500	0.74	234	468	4591.08	0.0218031	1500	1537.292

Wet Run

Recorded Data							Calculations				
Indirect Reading Rotameters				Direct Reading Rotameter Value (L/min)	Pressure at Rotameter Exit (psig)	Half of Manometer Reading (mm H20)	Manometer Reading (mm H20)	Manometer Pressure (Pa)	Pore Size (Diameter) (mm)	Indicated Airflow Rate (L/min)	True Airflow Rate (L/min)
First Rotameter Used		Second Rotameter Used									
Rotameter ID Number	Rotameter Value	Rotameter ID Number	Rotameter Value								
1	2					1	2	19.62	5.1019368	0.00158	0.00158
1	4					2	4	39.24	2.5509684	0.00256	0.00256
1	7					4	8	78.48	1.2754842	0.00459	0.00459
1	25					6	12	117.72	0.8503228	0.0352	0.0352
1	29					8	16	156.96	0.6377421	0.0452	0.0452
1	31					10	20	196.2	0.5101937	0.0505	0.0505
1	35					12	24	235.44	0.4251614	0.0616	0.0616
1	39					14	28	274.68	0.3644241	0.0737	0.0737
1	40					18	36	353.16	0.2834409	0.0769	0.0769
2	78					25	50	490.5	0.2040775	1.628	1.628
4	68				0.39	30	60	588.6	0.1700646	25.2	25.5321
5	51				0.23	35	70	686.7	0.1457696	75.7	76.28991
5	88				0.49	40	80	784.8	0.1275484	133	135.1985
5	74	5	60		0.41	45	90	882.9	0.1133764	200.4	203.1755
5	93	5	76		0.59	50	100	981	0.1020387	255	260.067
				400	0.2	62	124	1216.44	0.0822893	400	402.7119
				450	0.22	68	136	1334.16	0.0750285	450	453.3548
				500	0.24	74	148	1451.88	0.0689451	500	504.0651
				550	0.26	80	160	1569.6	0.0637742	550	554.8426
				600	0.28	87	174	1706.94	0.058643	600	605.6873
				700	0.32	102	204	2001.24	0.050019	700	707.578
				800	0.39	117	234	2295.54	0.0436063	800	810.5428
				900	0.45	134	268	2629.08	0.0380742	900	913.6717
				1000	0.54	156	312	3060.72	0.0327047	1000	1018.202
				1100	0.59	192	384	3767.04	0.0265726	1100	1121.858
				1200	0.68	198	396	3884.76	0.0257674	1200	1227.441
				1300	0.79	226	452	4434.12	0.0225749	1300	1334.475
				1400	0.9	256	512	5022.72	0.0199294	1400	1442.221
				1600	1.03	330	660	6474.6	0.0154604	1600	1655.105

Figure B.113: MinOil-9 recorded data and calculations.

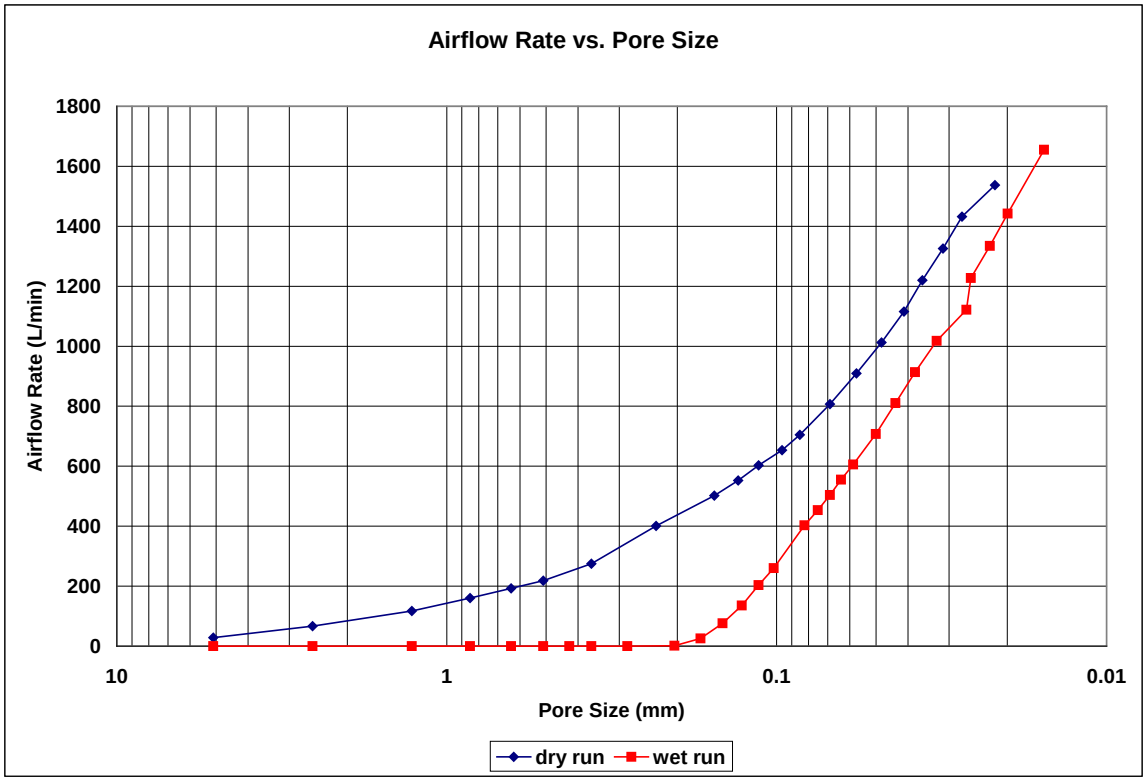

Figure B.114: MinOil-9 airflow rate vs. pore size for the wet and dry runs.

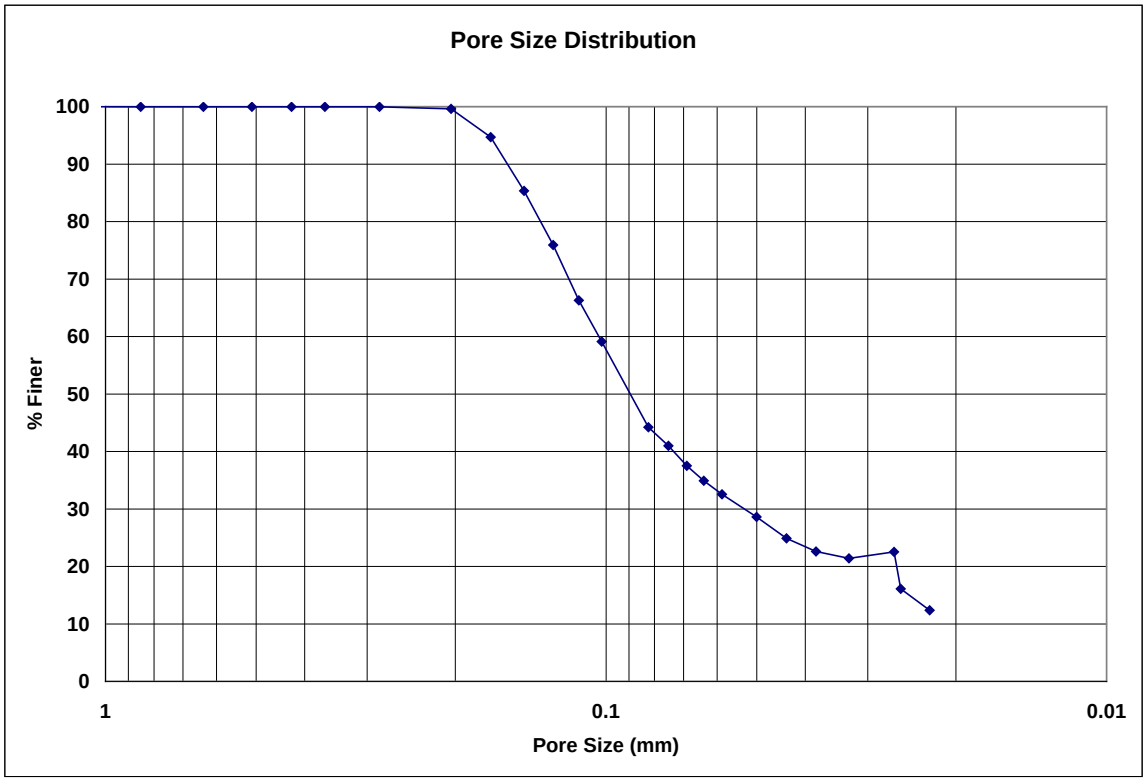

Figure B.115: MinOil-9 pore size distribution.

Bubble Point Test
Auburn University - Department of Civil Engineering

date of test: 12/5/2002
test identification: MinOil-9
test performed by: Trent Sims
wetting fluid: mineral oil
air temperature: 21 °C
porous media: NG-1 nonwoven geotextile
comments: testing to determine geotextile pore size distribution

Pore Size Calculation Parameters:
constant, C: 2860 mm/m
contact angle: 0 degrees
surface tension: 0.035 N/m

Pore Size at Selected % Finer

% Finer	Pore Size (mm)
98	0.19285
95	0.17215
90	0.15787
85	0.14511
80	0.13543
75	0.12618
70	0.11882
65	0.11132
60	0.10341
55	0.09656
50	0.08994
45	0.08332
40	0.07331
35	0.06395
30	0.05308
25	0.04379
20	0.02626
15	0.02482
10	---
5	---

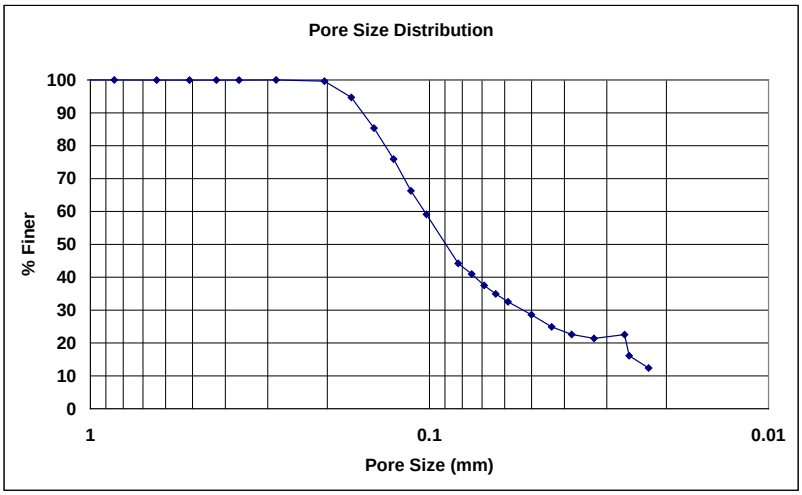

Figure B.116: MinOil-9 pore size distribution report.

Bubble Point Test

Auburn University - Department of Civil Engineering

date of test: 10/17/2002
test identification: MinOil-10
test performed by: Howie / Sims
wetting fluid: mineral oil
ambient air temperature: 21.5 °C
porous media: NG-1 nonwoven geotextile
comments: testing to determine geotextile pore size distribution

Pore Size Calculation Parameters:
constant, C: 2860 mm/m
contact angle: 0 degrees
surface tension: 0.035 N/m

Dry Run

Recorded Data							Calculations				
Indirect Reading Rotameters				Direct Reading Rotameter Value (L/min)	Pressure at Rotameter Exit (psig)	Half of Manometer Reading (mm H20)	Manometer Reading (mm H20)	Manometer Pressure (Pa)	Pore Size (Diameter) (mm)	Indicated Airflow Rate (L/min)	True Airflow Rate (L/min)
First Rotameter Used		Second Rotameter Used									
Rotameter ID Number	Rotameter Value	Rotameter ID Number	Rotameter Value								
4	73				0.37	1	2	19.62	5.1019368	27.3	27.64144
5	48				0.13	2	4	39.24	2.5509684	71.3	71.61458
5	78				0.31	4	8	78.48	1.2754842	118	119.2377
5	75	5	61		0.29	8	16	156.96	0.6377421	203.9	205.9014
5	85	5	70		0.39	10	20	196.2	0.5101937	234	237.0838
				400	0.06	20	40	392.4	0.2550968	400	400.8155
				500	0.09	26	52	510.12	0.1962283	500	501.5283
				600	0.13	41	82	804.42	0.1244375	600	602.6472
				650	0.15	46	92	902.52	0.1109117	650	653.3079
				700	0.17	54	108	1059.48	0.0944803	700	704.036
				800	0.2	64	128	1255.68	0.0797178	800	805.4238
				1000	0.29	94	188	1844.28	0.0542759	1000	1009.816
				1100	0.34	105	210	2060.1	0.0485899	1100	1112.648
				1200	0.41	122	244	2393.64	0.0418192	1200	1216.62
				1300	0.52	156	312	3060.72	0.0327047	1300	1322.793
				1400	0.71	164	328	3217.68	0.0311094	1400	1433.411
				1600	0.58	182	364	3570.84	0.0280326	1600	1631.259
				1800	0.99	306	612	6003.72	0.016673	1800	1859.625

Wet Run

Recorded Data							Calculations				
Indirect Reading Rotameters				Direct Reading Rotameter Value (L/min)	Pressure at Rotameter Exit (psig)	Half of Manometer Reading (mm H20)	Manometer Reading (mm H20)	Manometer Pressure (Pa)	Pore Size (Diameter) (mm)	Indicated Airflow Rate (L/min)	True Airflow Rate (L/min)
First Rotameter Used		Second Rotameter Used									
Rotameter ID Number	Rotameter Value	Rotameter ID Number	Rotameter Value								
1	24					6	12	117.72	0.8503228	0.0328	0.0328
1	25					8	16	156.96	0.6377421	0.0352	0.0352
1	27					10	20	196.2	0.5101937	0.0401	0.0401
1	28					14	28	274.68	0.3644241	0.0427	0.0427
2	23					20	40	392.4	0.2550968	0.338	0.338
4	97				0.71	30	60	588.6	0.1700646	37.8	38.70209
5	61				0.28	34	68	667.08	0.150057	90.9	91.76163
5	54	5	67		0.35	40	80	784.8	0.1275484	180.3	182.4338
5	68	5	83		0.48	44	88	863.28	0.1159531	227	230.6764
5	82	5	100		0.66	48	96	941.76	0.1062903	277	283.1501
				400	0.2	54	108	1059.48	0.0944803	400	402.7119
				450	0.21	62	124	1216.44	0.0822893	450	453.2029
				500	0.23	67	134	1314.54	0.0761483	500	503.8964
				550	0.25	73	146	1432.26	0.0698895	550	554.6572
				600	0.26	76	152	1491.12	0.0671307	600	605.2829
				650	0.28	83	166	1628.46	0.0614691	650	656.1613
				700	0.31	90	180	1765.8	0.0566882	700	707.3424
				800	0.35	104	208	2040.48	0.0490571	800	809.4678
				900	0.4	120	240	2354.4	0.0425161	900	912.1627
				1000	0.44	134	268	2629.08	0.0380742	1000	1014.856
				1100	0.5	150	300	2943	0.0340129	1100	1118.551
				1200	0.56	166	332	3256.92	0.0307346	1200	1222.644
				1300	0.71	198	396	3884.76	0.0257674	1300	1331.024
				1400	0.8	220	440	4316.4	0.0231906	1400	1437.591
				1600	0.92	284	568	5572.08	0.0179646	1600	1649.308
				1800	1.14	348	696	6827.76	0.0146607	1800	1868.493

Figure B.117: MinOil-10 recorded data and calculations.

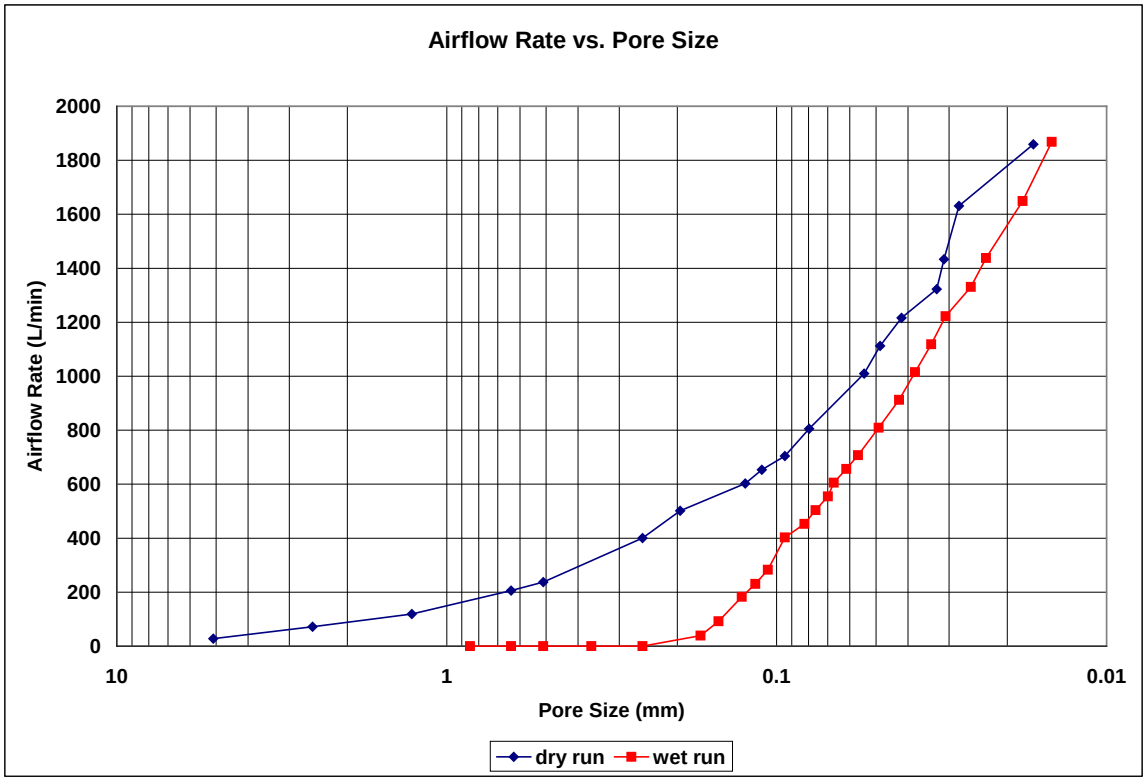

Figure B.118: MinOil-10 airflow rate vs. pore size for the wet and dry runs.

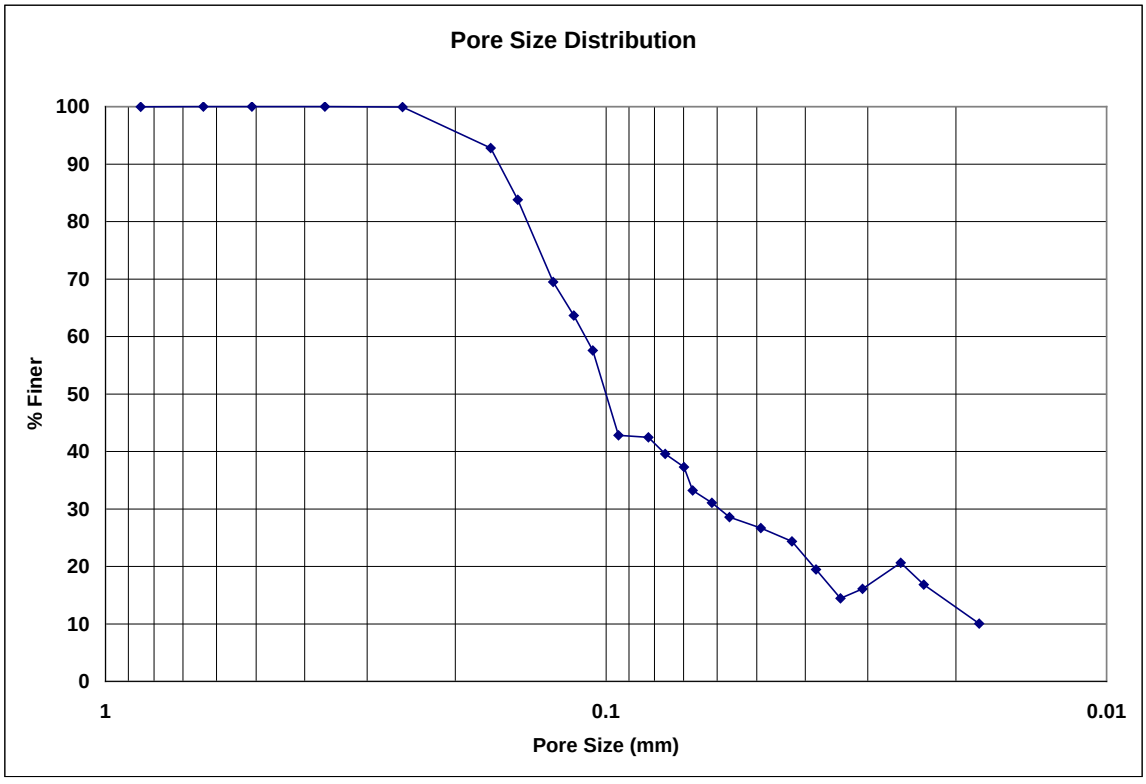

Figure B.119: MinOil-10 pore size distribution.

Bubble Point Test
Auburn University - Department of Civil Engineering

date of test: 10/17/2002
test identification: MinOil-10
test performed by: Howie / Sims
wetting fluid: mineral oil
air temperature: 21.5 °C
porous media: NG-1 nonwoven geotextile
comments: testing to determine geotextile pore size distribution

Pore Size Calculation Parameters:
constant, C: 2860 mm/m
contact angle: 0 degrees
surface tension: 0.035 N/m

Pore Size at Selected % Finer

% Finer	Pore Size (mm)
98	0.23217
95	0.19626
90	0.16382
85	0.15271
80	0.14407
75	0.13620
70	0.12833
65	0.11864
60	0.11014
55	0.10423
50	0.10023
45	0.09624
40	0.07703
35	0.06833
30	0.05940
25	0.04431
20	0.03855
15	0.03445
10	---
5	---

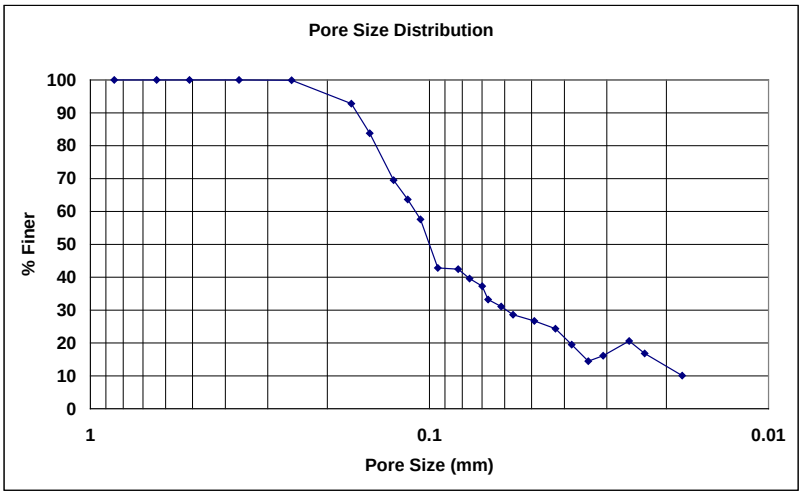

Figure B.120: MinOil-10 pore size distribution report.

B.4 Tests with 2-Ethyl Hexanol as the Wetting Fluid

Bubble Point Test
Auburn University - Department of Civil Engineering

date of test: 11/8/2006
test identification: 2EH-1
test performed by: David Hayes
wetting fluid: 2-ethyl hexanol
ambient air temperature: 21.4 °C
porous media: NG-1 nonwoven geotextile
comments: testing to determine geotextile pore size distribution

Pore Size Calculation Parameters:
constant, C: 2860 mm/m
contact angle: 0 degrees
surface tension: 0.0276 N/m

Dry Run

Recorded Data							Calculations				
Indirect Reading Rotameters				Direct Reading Rotameter Value (L/min)	Pressure at Rotameter Exit (psig)	Half of Manometer Reading (mm H20)	Manometer Reading (mm H20)	Manometer Pressure (Pa)	Pore Size (Diameter) (mm)	Indicated Airflow Rate (L/min)	True Airflow Rate (L/min)
First Rotameter Used		Second Rotameter Used									
Rotameter ID Number	Rotameter Value	Rotameter ID Number	Rotameter Value								
5	55				0.16	2	4	39.24	2.0116208	81.8	82.24397
5	82				0.35	4	8	78.48	1.0058104	124	125.4675
5	64	5	78		0.35	8	16	156.96	0.5029052	213.6	216.1279
5	74	5	91		0.47	10	20	196.2	0.4023242	249	252.9493
				350	0.07	16	32	313.92	0.2514526	350	350.8323
				400	0.08	20	40	392.4	0.2011621	400	401.087
				500	0.11	28	56	549.36	0.1436872	500	501.8673
				550	0.13	34	68	667.08	0.1183306	550	552.4266
				600	0.14	38	76	745.56	0.1058748	600	602.8504
				650	0.17	44	88	863.28	0.0914373	650	653.7477
				700	0.19	50	100	981	0.0804648	700	704.5093
				800	0.23	60	120	1177.2	0.067054	800	806.2342
				900	0.28	74	148	1451.88	0.0543681	900	908.531
				1000	0.33	86	172	1687.32	0.0467819	1000	1011.162
				1100	0.38	102	204	2001.24	0.0394435	1100	1114.127
				1200	0.45	118	236	2315.16	0.0340953	1200	1218.229
				1300	0.52	138	276	2707.56	0.0291539	1300	1322.793
				1400	0.58	154	308	3021.48	0.0261249	1400	1427.352
				1600	0.7	204	408	4002.48	0.0197218	1600	1637.652

Wet Run

Recorded Data							Calculations				
Indirect Reading Rotameters				Direct Reading Rotameter Value (L/min)	Pressure at Rotameter Exit (psig)	Half of Manometer Reading (mm H20)	Manometer Reading (mm H20)	Manometer Pressure (Pa)	Pore Size (Diameter) (mm)	Indicated Airflow Rate (L/min)	True Airflow Rate (L/min)
First Rotameter Used		Second Rotameter Used									
Rotameter ID Number	Rotameter Value	Rotameter ID Number	Rotameter Value								
2	81				0	2	4	39.24	2.0116208	1.7	1.7
4	8				0.03	4	8	78.48	1.0058104	2.43	2.432478
4	41				0.18	20	40	392.4	0.2011621	14.3	14.38728
5	45	5	56		0.29	24	48	470.88	0.1676351	150.1	151.5733
5	67	5	84		0.51	32	64	627.84	0.1257263	227	230.9042
				350	0.14	38	76	745.56	0.1058748	350	351.6627
				400	0.15	42	84	824.04	0.0957915	400	402.0356
				450	0.17	46	92	902.52	0.0874618	450	452.5946
				550	0.2	54	108	1059.48	0.0745045	550	553.7289
				600	0.22	60	120	1177.2	0.067054	600	604.4731
				650	0.22	66	132	1294.92	0.0609582	650	654.8459
				700	0.25	70	140	1373.4	0.0574749	700	705.9273
				800	0.32	80	160	1569.6	0.0502905	800	808.6606
				900	0.37	94	188	1844.28	0.0428004	900	911.2561
				1000	0.43	108	216	2118.96	0.0372522	1000	1014.52
				1100	0.5	124	248	2432.88	0.0324455	1100	1118.551
				1200	0.56	140	280	2746.8	0.0287374	1200	1222.644
				1300	0.65	162	324	3178.44	0.0248348	1300	1328.431
				1400	0.73	182	364	3570.84	0.0221057	1400	1434.341
				1600	0.81	240	480	4708.8	0.0167635	1600	1643.491

Figure B.121: 2EH-1 recorded data and calculations.

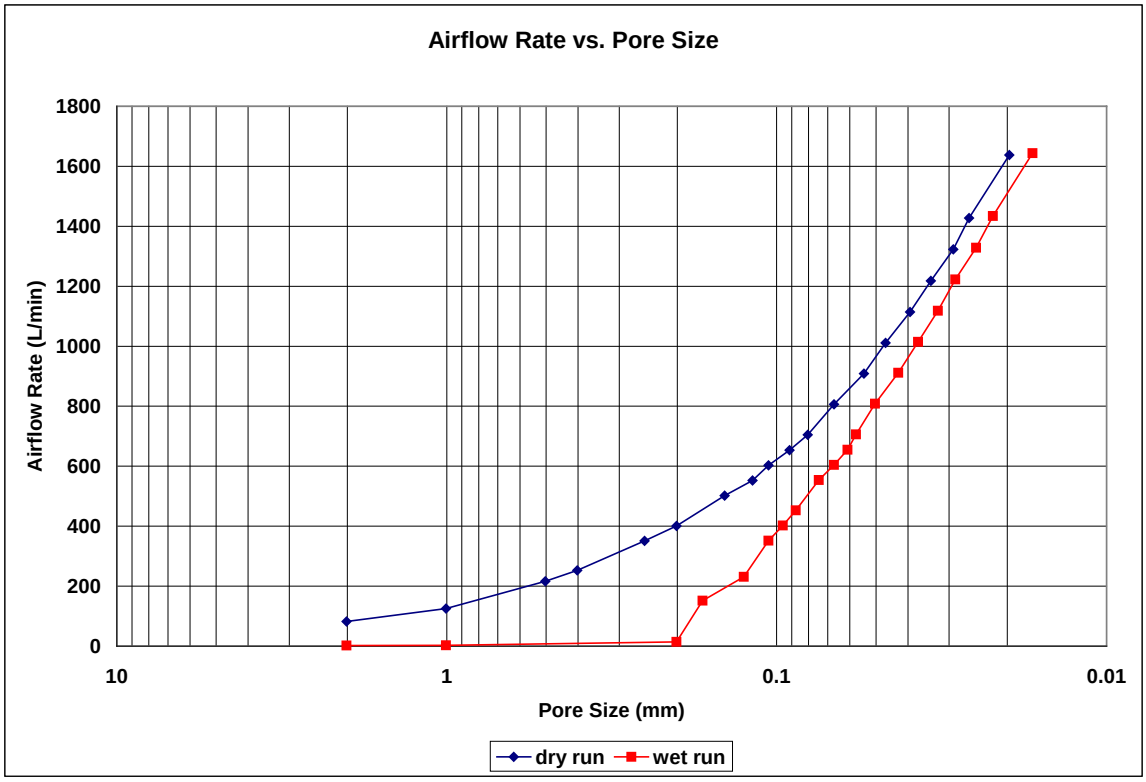

Figure B.122: 2EH-1 airflow rate vs. pore size for the wet and dry runs.

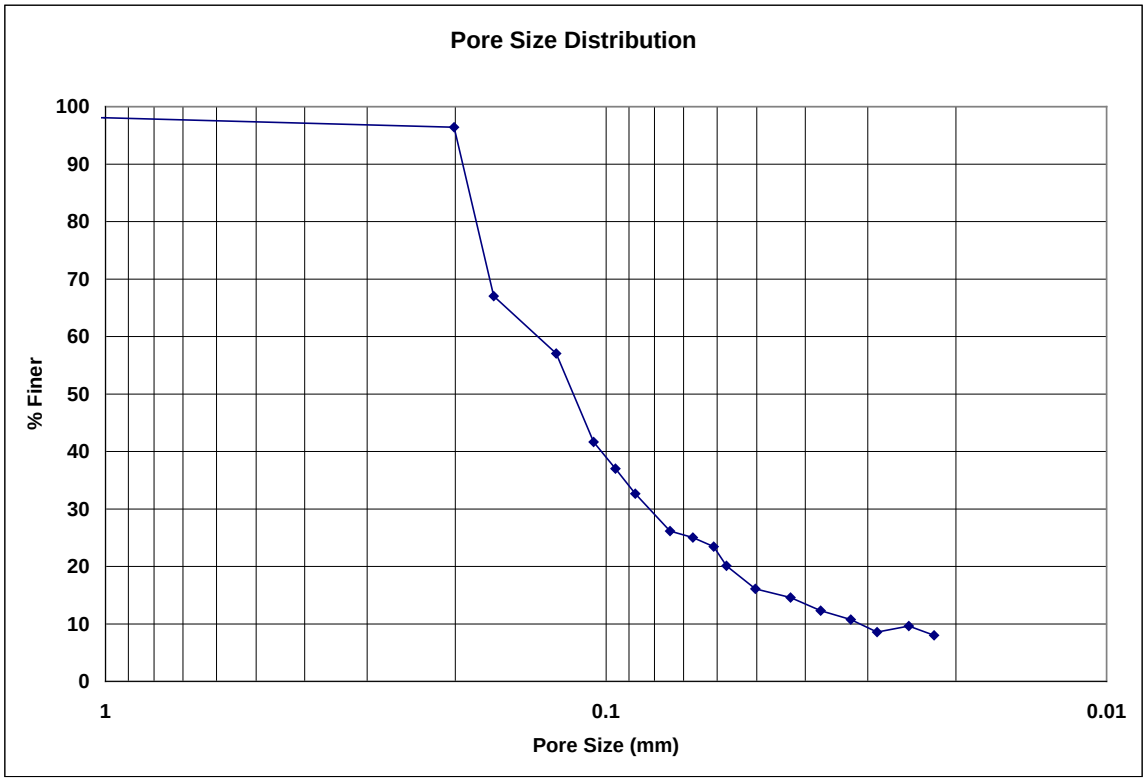

Figure B.123: 2EH-1 pore size distribution.

Bubble Point Test
Auburn University - Department of Civil Engineering

date of test:	11/8/2006	Pore Size Calculation Parameters:		
test identification:	2EH-1	constant, C:	2860	mm/m
test performed by:	David Hayes	contact angle:	0	degrees
wetting fluid:	2-ethyl hexanol	surface tension:	0.0276	N/m
air temperature:	21.4 °C			
porous media:	NG-1 nonwoven geotextile			
comments:	testing to determine geotextile pore size distribution			

Pore Size at Selected % Finer

% finer	pore size (mm)
98	0.97590
95	0.19955
90	0.19384
85	0.18813
80	0.18243
75	0.17672
70	0.17101
65	0.15907
60	0.13809
55	0.12307
50	0.11662
45	0.11017
40	0.10225
35	0.09192
30	0.08217
25	0.06696
20	0.05730
15	0.04482
10	0.03118
5	---

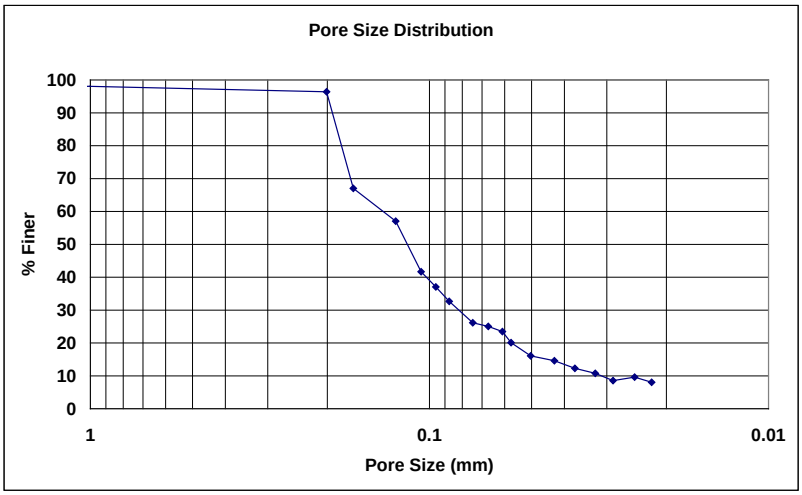

Figure B.124: 2EH-1 pore size distribution report.

Bubble Point Test

Auburn University - Department of Civil Engineering

date of test: 3/21/2007
test identification: 2EH-2
test performed by: David Hayes
wetting fluid: 2-ethyl hexanol
ambient air temperature: 21.5 °C
porous media: NG-1 nonwoven geotextile
comments: testing to determine geotextile pore size distribution

Pore Size Calculation Parameters:
constant, C: 2860 mm/m
contact angle: 0 degrees
surface tension: 0.0276 N/m

Dry Run

Recorded Data							Calculations				
Indirect Reading Rotameters				Direct Reading Rotameter Value (L/min)	Pressure at Rotameter Exit (psig)	Half of Manometer Reading (mm H20)	Manometer Reading (mm H20)	Manometer Pressure (Pa)	Pore Size (Diameter) (mm)	Indicated Airflow Rate (L/min)	True Airflow Rate (L/min)
First Rotameter Used		Second Rotameter Used									
Rotameter ID Number	Rotameter Value	Rotameter ID Number	Rotameter Value								
5	44				0.13	2	4	39.24	2.0116208	65.3	65.58811
5	71				0.28	4	8	78.48	1.0058104	106	107.0048
5	90				0.44	6	12	117.72	0.6705403	137	139.0352
5	63	5	51		0.26	8	16	156.96	0.5029052	169.7	171.1942
5	66	5	82		0.41	12	24	235.44	0.3352701	222.7	225.7843
5	79	5	97		0.57	16	32	313.92	0.2514526	267	272.1273
				350	0.08	22	44	431.64	0.1828746	350	350.9511
				400	0.1	28	56	549.36	0.1436872	400	401.3582
				450	0.12	34	68	667.08	0.1183306	450	451.833
				500	0.14	42	84	824.04	0.0957915	500	502.3753
				550	0.16	48	96	941.76	0.0838175	550	552.9851
				600	0.19	58	116	1137.96	0.0693662	600	603.8651
				650	0.22	64	128	1255.68	0.0628631	650	654.8459
				700	0.25	74	148	1451.88	0.0543681	700	705.9273
				800	0.29	88	176	1726.56	0.0457187	800	807.8526
				900	0.38	108	216	2118.96	0.0372522	900	911.5584
				1000	0.45	128	256	2511.36	0.0314316	1000	1015.191
				1100	0.54	150	300	2943	0.0268216	1100	1120.022
				1200	0.64	178	356	3492.36	0.0226025	1200	1225.844
				1300	0.73	202	404	3963.24	0.019917	1300	1331.888
				1400	0.82	228	456	4473.36	0.0176458	1400	1438.518
				1600	0.98	312	624	6121.44	0.012895	1600	1652.473

Wet Run

Recorded Data							Calculations				
Indirect Reading Rotameters				Direct Reading Rotameter Value (L/min)	Pressure at Rotameter Exit (psig)	Half of Manometer Reading (mm H20)	Manometer Reading (mm H20)	Manometer Pressure (Pa)	Pore Size (Diameter) (mm)	Indicated Airflow Rate (L/min)	True Airflow Rate (L/min)
First Rotameter Used		Second Rotameter Used									
Rotameter ID Number	Rotameter Value	Rotameter ID Number	Rotameter Value								
2	22					6	12	117.72	0.6705403	0.318	0.318
2	26					8	16	156.96	0.5029052	0.398	0.398
2	39					16	32	313.92	0.2514526	0.675	0.675
2	72					18	36	353.16	0.2235134	1.48	1.48
4	38				0.17	22	44	431.64	0.1828746	13.2	13.27611
5	36				0.15	26	52	510.12	0.1547401	53.6	53.87278
5	63				0.29	30	60	588.6	0.1341081	94	94.92268
5	97				0.57	36	72	706.32	0.1117567	148	150.8421
5	61	5	75		0.4	40	80	784.8	0.100581	203.9	206.6555
5	77	5	96		0.61	48	96	941.76	0.0838175	262	267.3808
				350	0.16	54	108	1059.48	0.0745045	350	351.8996
				400	0.19	60	120	1177.2	0.067054	400	402.5767
				450	0.21	66	132	1294.92	0.0609582	450	453.2029
				500	0.23	76	152	1491.12	0.0529374	500	503.8964
				550	0.25	82	164	1608.84	0.0490639	550	554.6572
				600	0.28	90	180	1765.8	0.0447027	600	605.6873
				650	0.3	98	196	1922.76	0.0410535	650	656.5992
				700	0.33	106	212	2079.72	0.0379551	700	707.8135
				800	0.41	124	248	2432.88	0.0324455	800	811.0797
				900	0.49	144	288	2825.28	0.0279392	900	914.877
				1000	0.57	166	332	3256.92	0.0242364	1000	1019.203
				1100	0.65	192	384	3767.04	0.0209544	1100	1124.057
				1200	0.75	220	440	4316.4	0.0182875	1200	1230.231
				1300	0.86	252	504	4944.24	0.0159652	1300	1337.487
				1400	0.99	290	580	5689.8	0.0138732	1400	1446.375
				1600	1.17	390	780	7651.8	0.010316	1600	1662.455

Figure B.125: 2EH-1 recorded data and calculations.

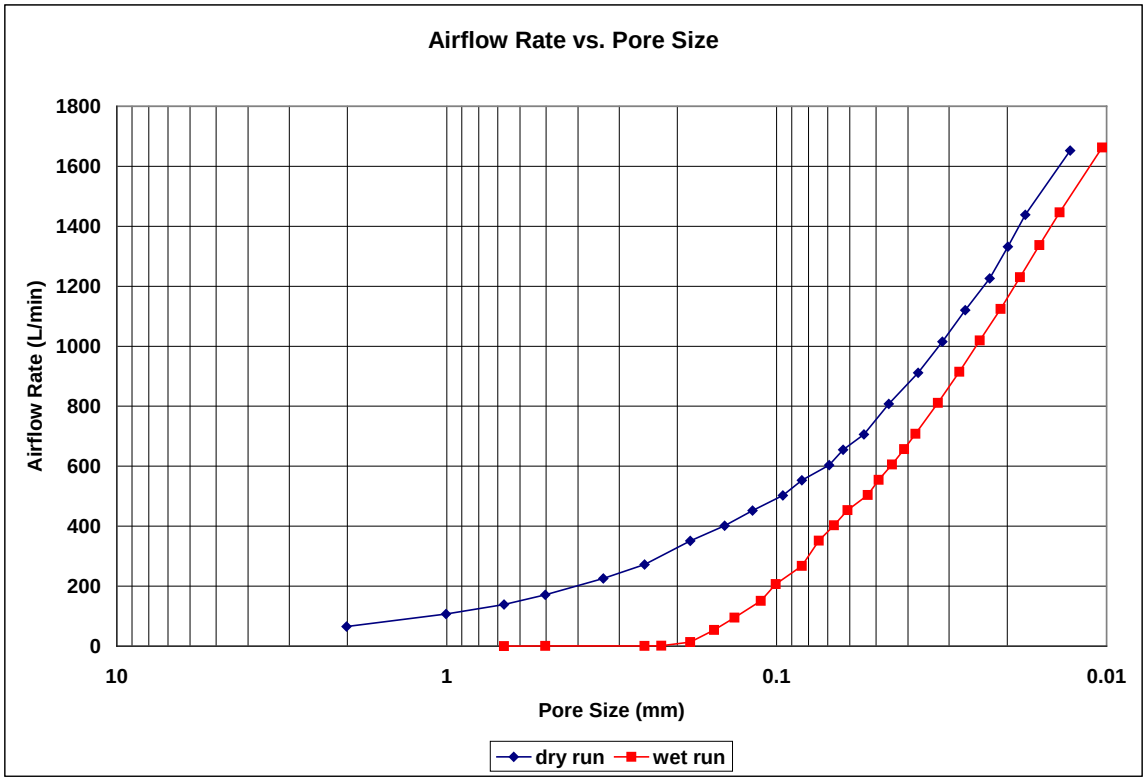

Figure B.126: 2EH-2 airflow rate vs. pore size for the wet and dry runs.

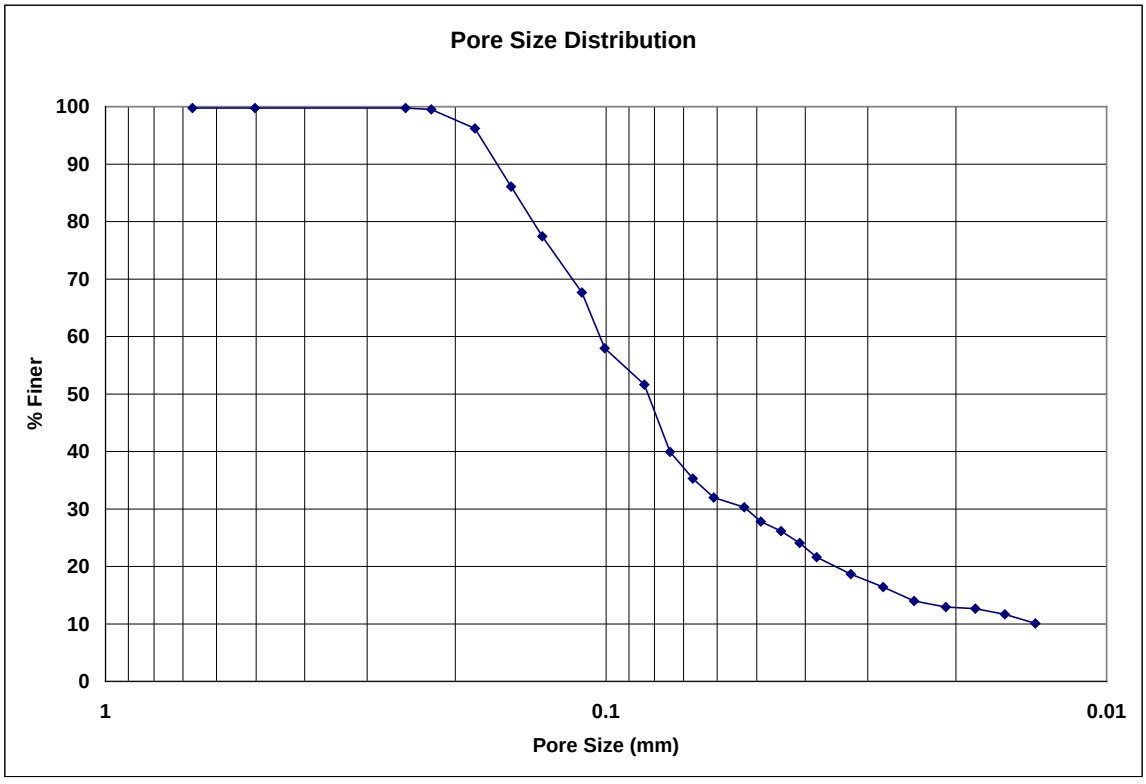

Figure B.127: 2EH-2 pore size distribution.

Bubble Point Test
Auburn University - Department of Civil Engineering

date of test: 3/21/2007
test identification: 2EH-2
test performed by: David Hayes
wetting fluid: 2-ethyl hexanol
air temperature: 21.5 °C
porous media: NG-1 nonwoven geotextile
comments: testing to determine geotextile pore size distribution

Pore Size Calculation Parameters:
constant, C: 2860 mm/m
contact angle: 0 degrees
surface tension: 0.0276 N/m

Pore Size at Selected % Finer

% finer	pore size (mm)
98	0.20485
95	0.17950
90	0.16561
85	0.15216
80	0.14025
75	0.12856
70	0.11710
65	0.10868
60	0.10292
55	0.09271
50	0.08251
45	0.07854
40	0.07456
35	0.06654
30	0.05249
25	0.04265
20	0.03495
15	0.02578
10	---
5	---

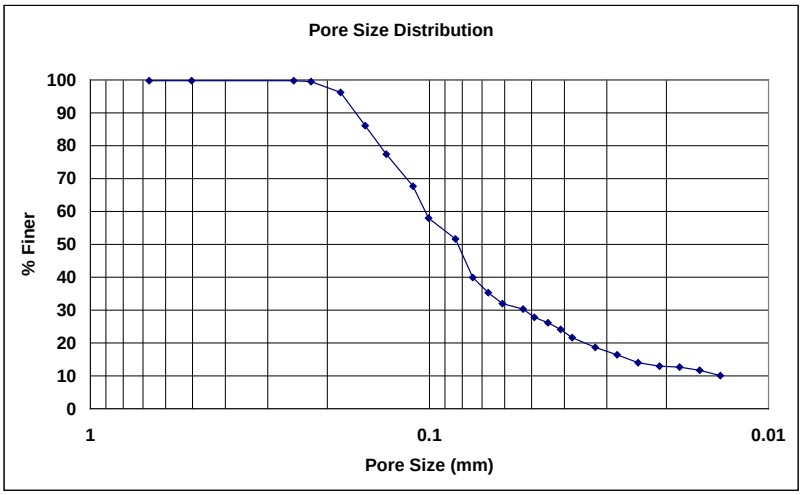

Figure B.128: 2EH-2 pore size distribution report.

Bubble Point Test

Auburn University - Department of Civil Engineering

date of test: 3/21/2007
test identification: 2EH-3
test performed by: David Hayes
wetting fluid: 2-ethyl hexanol
ambient air temperature: 21.5 °C
porous media: NG-1 nonwoven geotextile
comments: testing to determine geotextile pore size distribution

Pore Size Calculation Parameters:
constant, C: 2860 mm/m
contact angle: 0 degrees
surface tension: 0.0276 N/m

Dry Run

Recorded Data							Calculations				
Indirect Reading Rotameters				Direct Reading Rotameter Value (L/min)	Pressure at Rotameter Exit (psig)	Half of Manometer Reading (mm H20)	Manometer Reading (mm H20)	Manometer Pressure (Pa)	Pore Size (Diameter) (mm)	Indicated Airflow Rate (L/min)	True Airflow Rate (L/min)
First Rotameter Used		Second Rotameter Used									
Rotameter ID Number	Rotameter Value	Rotameter ID Number	Rotameter Value								
5	58				0.2	2	4	39.24	2.0116208	86.3	86.88509
5	86				0.4	4	8	78.48	1.0058104	130	131.7568
5	55	5	68		0.28	6	12	117.72	0.6705403	183.8	185.5422
5	64	5	80		0.37	8	16	156.96	0.5029052	216.6	219.309
5	72	5	90		0.47	10	20	196.2	0.4023242	245	248.8859
				350	0.08	16	32	313.92	0.2514526	350	350.9511
				400	0.09	20	40	392.4	0.2011621	400	401.2226
				450	0.1	24	48	470.88	0.1676351	450	451.528
				500	0.12	30	60	588.6	0.1341081	500	502.0367
				550	0.14	36	72	706.32	0.1117567	550	552.6128
				600	0.15	40	80	784.8	0.100581	600	603.0535
				650	0.17	46	92	902.52	0.0874618	650	653.7477
				700	0.2	54	108	1059.48	0.0745045	700	704.7458
				800	0.27	66	132	1294.92	0.0609582	800	807.3135
				900	0.32	80	160	1569.6	0.0502905	900	909.7432
				1000	0.39	96	192	1883.52	0.0419088	1000	1013.178
				1100	0.44	112	224	2197.44	0.0359218	1100	1116.341
				1200	0.51	128	256	2511.36	0.0314316	1200	1220.639
				1300	0.6	150	300	2943	0.0268216	1300	1326.265
				1400	0.67	170	340	3335.4	0.0236661	1400	1431.549
				1600	0.78	232	464	4551.84	0.0173416	1600	1641.9

Wet Run

Recorded Data							Calculations				
Indirect Reading Rotameters				Direct Reading Rotameter Value (L/min)	Pressure at Rotameter Exit (psig)	Half of Manometer Reading (mm H20)	Manometer Reading (mm H20)	Manometer Pressure (Pa)	Pore Size (Diameter) (mm)	Indicated Airflow Rate (L/min)	True Airflow Rate (L/min)
First Rotameter Used		Second Rotameter Used									
Rotameter ID Number	Rotameter Value	Rotameter ID Number	Rotameter Value								
2	17					4	8	78.48	1.0058104	0.221	0.221
2	32					12	24	235.44	0.3352701	0.52	0.52
4	35				0.16	18	36	353.16	0.2235134	12	12.06513
5	33				0.13	20	40	392.4	0.2011621	49.3	49.51751
5	77				0.37	26	52	510.12	0.1547401	116	117.4508
5	58	5	72		0.36	36	72	706.32	0.1117567	194.3	196.6648
5	80	5	98		0.63	38	76	745.56	0.1058748	270	275.725
				350	0.14	42	84	824.04	0.0957915	350	351.6627
				400	0.15	44	88	863.28	0.0914373	400	402.0356
				450	0.17	52	104	1020.24	0.07737	450	452.5946
				500	0.19	56	112	1098.72	0.0718436	500	503.2209
				550	0.21	62	124	1216.44	0.064891	550	553.9146
				600	0.23	66	132	1294.92	0.0609582	600	604.6757
				650	0.25	72	144	1412.64	0.0558784	650	655.5039
				700	0.27	80	160	1569.6	0.0502905	700	706.3993
				800	0.32	94	188	1844.28	0.0428004	800	808.6606
				900	0.39	110	220	2158.2	0.0365749	900	911.8606
				1000	0.44	122	244	2393.64	0.0329774	1000	1014.856
				1100	0.51	140	280	2746.8	0.0287374	1100	1118.919
				1200	0.59	160	320	3139.2	0.0251453	1200	1223.845
				1300	0.68	184	368	3610.08	0.0218654	1300	1329.728
				1400	0.77	210	420	4120.2	0.0191583	1400	1436.199
				1600	0.91	282	564	5532.84	0.0142668	1600	1648.78

Figure B.129: 2EH-3 recorded data and calculations.

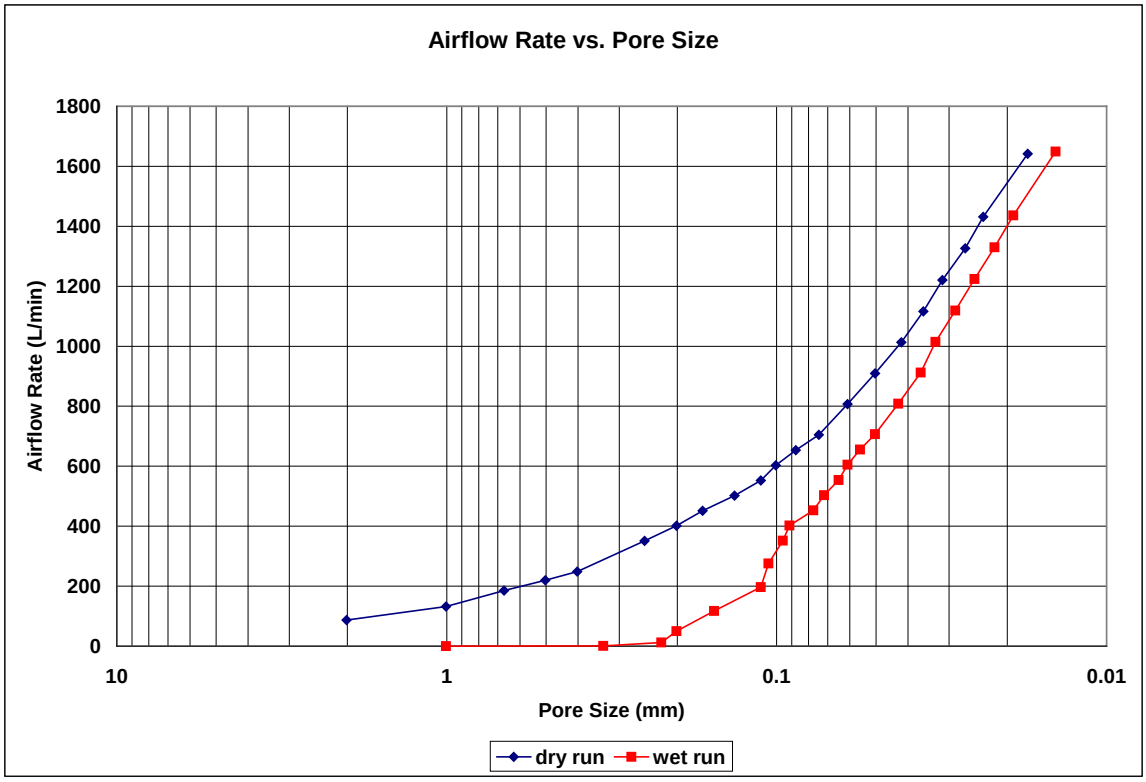

Figure B.130: 2EH-3 airflow rate vs. pore size for the wet and dry runs.

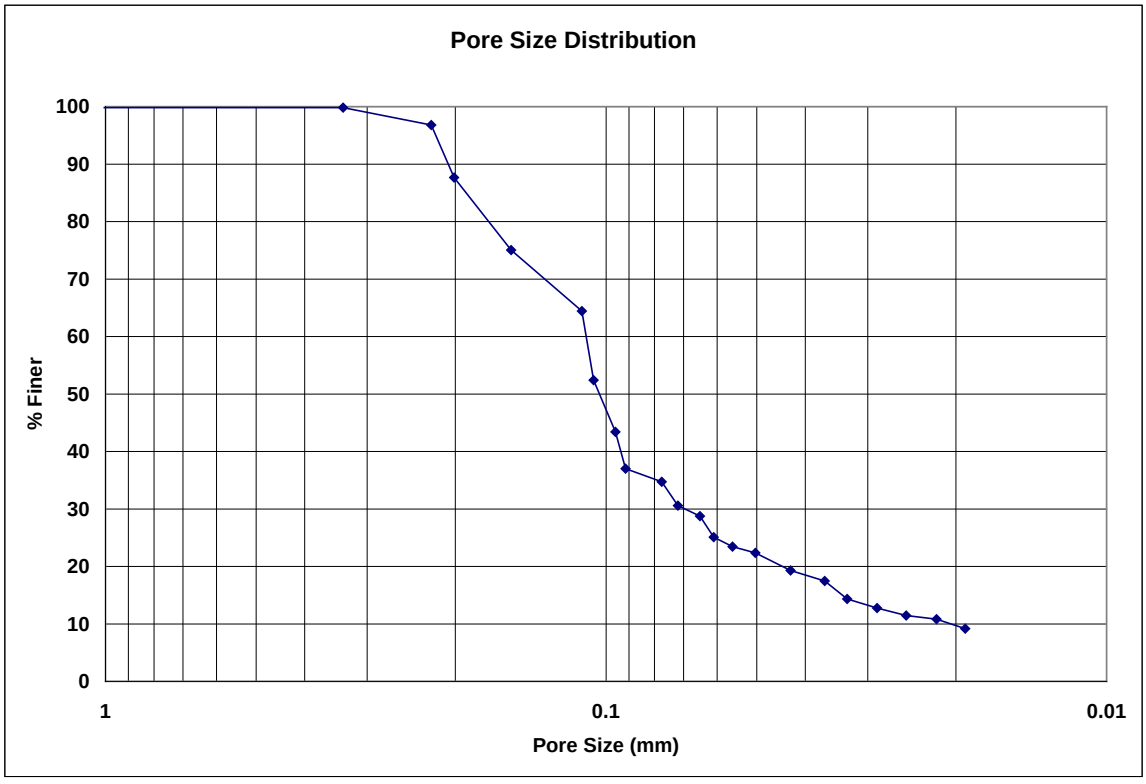

Figure B.131: 2EH-3 pore size distribution.

Bubble Point Test
Auburn University - Department of Civil Engineering

date of test: 3/21/2007
test identification: 2EH-3
test performed by: David Hayes
wetting fluid: 2-ethyl hexanol
air temperature: 21.5 °C
porous media: NG-1 nonwoven geotextile
comments: testing to determine geotextile pore size distribution

Pore Size Calculation Parameters:
constant, C: 2860 mm/m
contact angle: 0 degrees
surface tension: 0.0276 N/m

Pore Size at Selected % Finer

% finer	pore size (mm)
98	0.26752
95	0.21908
90	0.20688
85	0.19137
80	0.17294
75	0.15449
70	0.13431
65	0.11413
60	0.10960
55	0.10715
50	0.10319
45	0.09756
40	0.09346
35	0.07900
30	0.06963
25	0.06065
20	0.04450
15	0.03373
10	0.02049
5	---

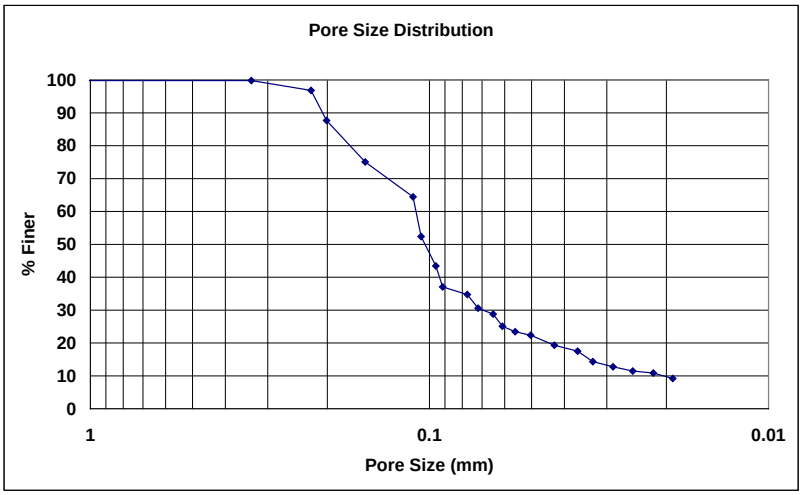

Figure B.132: 2EH-3 pore size distribution report.

Bubble Point Test

Auburn University - Department of Civil Engineering

date of test: 3/21/2007
test identification: 2EH-4
test performed by: David Hayes
wetting fluid: 2-ethyl hexanol
ambient air temperature: 21.5 °C
porous media: NG-1 nonwoven geotextile
comments: testing to determine geotextile pore size distribution

Pore Size Calculation Parameters:
constant, C: 2860 mm/m
contact angle: 0 degrees
surface tension: 0.0276 N/m

Dry Run

Recorded Data							Calculations				
Indirect Reading Rotameters				Direct Reading Rotameter Value (L/min)	Pressure at Rotameter Exit (psig)	Half of Manometer Reading (mm H20)	Manometer Reading (mm H20)	Manometer Pressure (Pa)	Pore Size (Diameter) (mm)	Indicated Airflow Rate (L/min)	True Airflow Rate (L/min)
First Rotameter Used		Second Rotameter Used									
Rotameter ID Number	Rotameter Value	Rotameter ID Number	Rotameter Value								
5	68				0.24	2	4	39.24	2.0116208	102	102.8293
5	92				0.44	4	8	78.48	1.0058104	140	142.0798
5	58	5	72		0.3	6	12	117.72	0.6705403	194.3	196.2726
5	69	5	85		0.42	8	16	156.96	0.5029052	232	235.2909
5	77	5	95		0.53	10	20	196.2	0.4023242	261	265.6634
				350	0.07	14	28	274.68	0.2873744	350	350.8323
				400	0.08	18	36	353.16	0.2235134	400	401.087
				450	0.1	22	44	431.64	0.1828746	450	451.528
				500	0.11	26	52	510.12	0.1547401	500	501.8673
				550	0.13	32	64	627.84	0.1257263	550	552.4266
				600	0.15	36	72	706.32	0.1117567	600	603.0535
				650	0.17	42	84	824.04	0.0957915	650	653.7477
				700	0.19	50	100	981	0.0804648	700	704.5093
				800	0.24	60	120	1177.2	0.067054	800	806.5042
				900	0.28	74	148	1451.88	0.0543681	900	908.531
				1000	0.35	88	176	1726.56	0.0457187	1000	1011.835
				1100	0.41	104	208	2040.48	0.038685	1100	1115.235
				1200	0.47	120	240	2354.4	0.033527	1200	1219.033
				1300	0.56	142	284	2786.04	0.0283327	1300	1324.53
				1400	0.63	158	316	3099.96	0.0254636	1400	1429.685
				1600	0.67	212	424	4159.44	0.0189776	1600	1636.056

Wet Run

Recorded Data							Calculations				
Indirect Reading Rotameters				Direct Reading Rotameter Value (L/min)	Pressure at Rotameter Exit (psig)	Half of Manometer Reading (mm H20)	Manometer Reading (mm H20)	Manometer Pressure (Pa)	Pore Size (Diameter) (mm)	Indicated Airflow Rate (L/min)	True Airflow Rate (L/min)
First Rotameter Used		Second Rotameter Used									
Rotameter ID Number	Rotameter Value	Rotameter ID Number	Rotameter Value								
2	17					4	8	78.48	1.0058104	0.221	0.221
2	45					12	24	235.44	0.3352701	0.811	0.811
4	46				0.2	18	36	353.16	0.2235134	16.2	16.30983
4	95				0.69	20	40	392.4	0.2011621	36.9	37.75609
5	64				0.27	24	48	470.88	0.1676351	95.6	96.47396
5	60	5	75		0.37	28	56	549.36	0.1436872	202.4	204.9314
5	73	5	95		0.57	34	68	667.08	0.1183306	255	259.8969
				350	0.12	36	72	706.32	0.1117567	350	351.4257
				400	0.14	40	80	784.8	0.100581	400	401.9002
				450	0.15	46	92	902.52	0.0874618	450	452.2901
				500	0.16	48	96	941.76	0.0838175	500	502.7137
				550	0.18	54	108	1059.48	0.0745045	550	553.3571
				600	0.2	60	120	1177.2	0.067054	600	604.0678
				650	0.22	64	128	1255.68	0.0628631	650	654.8459
				700	0.24	70	140	1373.4	0.0574749	700	705.6912
				800	0.3	82	164	1608.84	0.0490639	800	808.122
				900	0.35	92	184	1805.04	0.0437309	900	910.6513
				1000	0.39	106	212	2079.72	0.0379551	1000	1013.178
				1100	0.46	122	244	2393.64	0.0329774	1100	1117.078
				1200	0.52	138	276	2707.56	0.0291539	1200	1221.04
				1300	0.62	160	320	3139.2	0.0251453	1300	1327.132
				1400	0.7	182	364	3570.84	0.0221057	1400	1432.946
				1600	0.79	240	480	4708.8	0.0167635	1600	1642.431

Figure B.133: 2EH-4 recorded data and calculations.

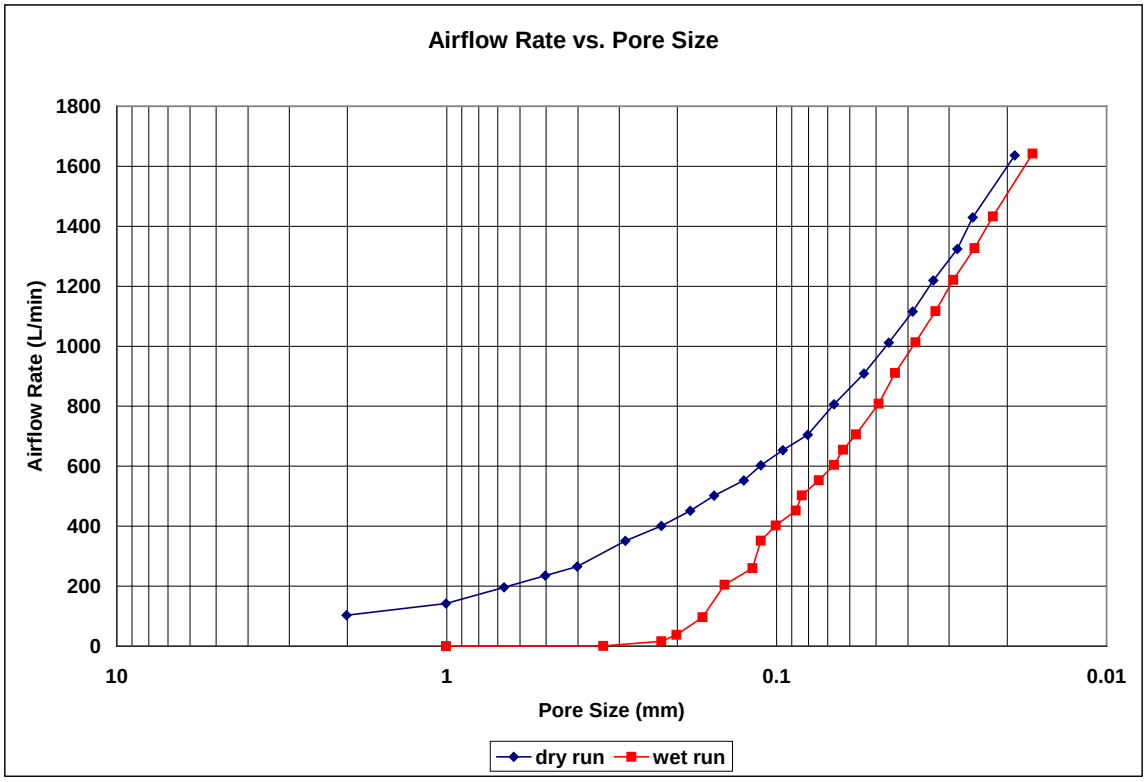

Figure B.134: 2EH-4 airflow rate vs. pore size for the wet and dry runs.

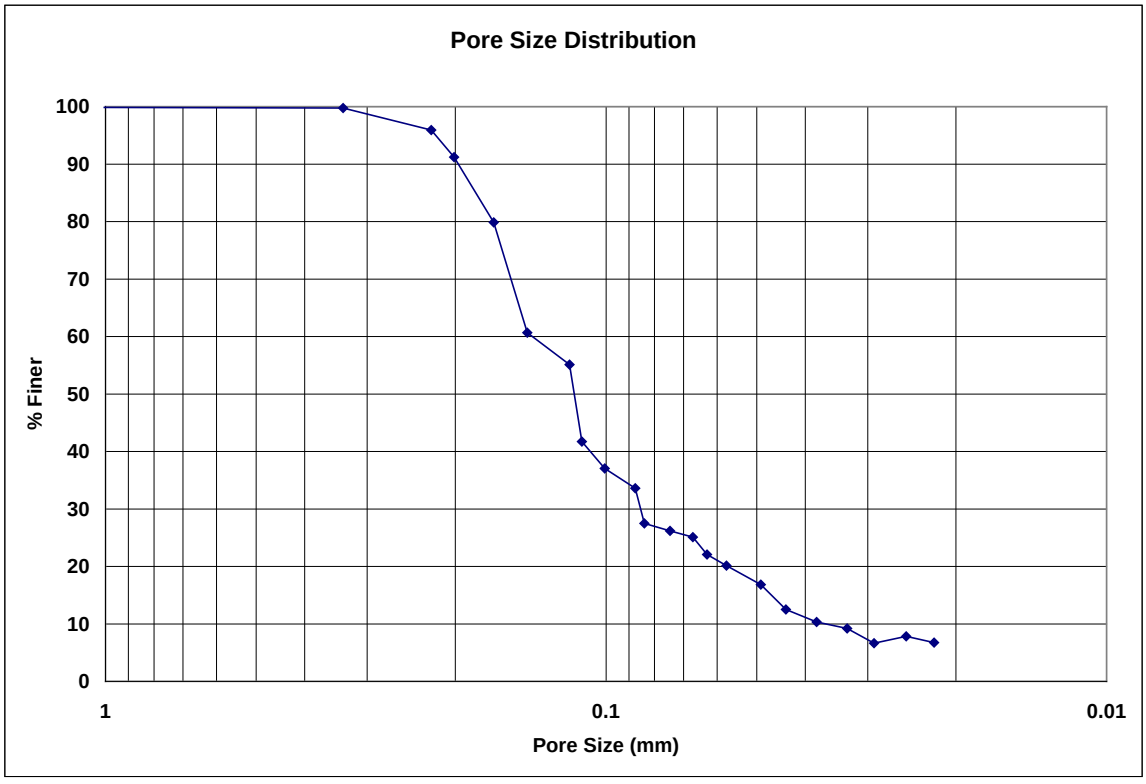

Figure B.135: 2EH-4 pore size distribution.

Bubble Point Test
Auburn University - Department of Civil Engineering

date of test:	3/21/2007	Pore Size Calculation Parameters:		
test identification:	2EH-4	constant, C:	2860	mm/m
test performed by:	David Hayes	contact angle:	0	degrees
wetting fluid:	2-ethyl hexanol	surface tension:	0.0276	N/m
air temperature:	21.5 °C			
porous media:	NG-1 nonwoven geotextile			
comments:	testing to determine geotextile pore size distribution			

Pore Size at Selected % Finer

% finer	pore size (mm)
98	0.28414
95	0.21911
90	0.19763
85	0.18285
80	0.16808
75	0.16158
70	0.15533
65	0.14909
60	0.14060
55	0.11827
50	0.11581
45	0.11336
40	0.10762
35	0.09273
30	0.08531
25	0.06692
20	0.05714
15	0.04678
10	0.03650
5	---

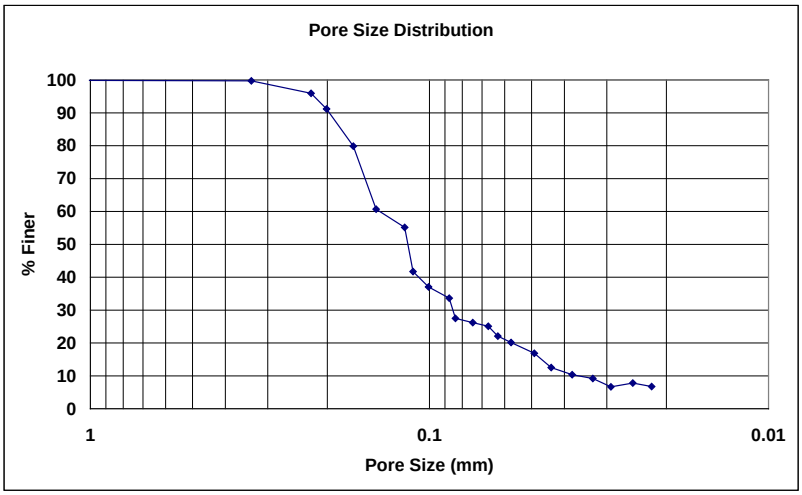

Figure B.136: 2EH-4 pore size distribution report.

Bubble Point Test

Auburn University - Department of Civil Engineering

date of test: 3/21/2007
test identification: 2EH-5
test performed by: David Hayes
wetting fluid: 2-ethyl hexanol
ambient air temperature: 21.5 °C
porous media: NG-1 nonwoven geotextile
comments: testing to determine geotextile pore size distribution

Pore Size Calculation Parameters:
constant, C: 2860 mm/m
contact angle: 0 degrees
surface tension: 0.0276 N/m

Dry Run

Recorded Data							Calculations				
Indirect Reading Rotameters				Direct Reading Rotameter Value (L/min)	Pressure at Rotameter Exit (psig)	Half of Manometer Reading (mm H20)	Manometer Reading (mm H20)	Manometer Pressure (Pa)	Pore Size (Diameter) (mm)	Indicated Airflow Rate (L/min)	True Airflow Rate (L/min)
First Rotameter Used		Second Rotameter Used									
Rotameter ID Number	Rotameter Value	Rotameter ID Number	Rotameter Value								
5	56				0.17	2	4	39.24	2.0116208	83.3	83.78028
5	85				0.37	4	8	78.48	1.0058104	129	130.6134
5	51	5	63		0.22	6	12	117.72	0.6705403	169.7	170.9651
5	62	5	77		0.33	8	16	156.96	0.5029052	208.5	210.8273
5	72	5	88		0.44	10	20	196.2	0.4023242	241	244.5802
				350	0.04	14	28	274.68	0.2873744	350	350.4759
				400	0.06	20	40	392.4	0.2011621	400	400.8155
				450	0.08	24	48	470.88	0.1676351	450	451.2228
				500	0.09	30	60	588.6	0.1341081	500	501.5283
				550	0.11	34	68	667.08	0.1183306	550	552.054
				600	0.13	40	80	784.8	0.100581	600	602.6472
				650	0.15	48	96	941.76	0.0838175	650	653.3079
				700	0.17	54	108	1059.48	0.0745045	700	704.036
				800	0.25	66	132	1294.92	0.0609582	800	806.774
				900	0.3	82	164	1608.84	0.0490639	900	909.1373
				1000	0.37	98	196	1922.76	0.0410535	1000	1012.507
				1100	0.43	114	228	2236.68	0.0352916	1100	1115.972
				1200	0.5	132	264	2589.84	0.0304791	1200	1220.238
				1300	0.59	154	308	3021.48	0.0261249	1300	1325.832
				1400	0.67	178	356	3492.36	0.0226025	1400	1431.549
				1600	0.76	234	468	4591.08	0.0171933	1600	1640.839

Wet Run

Recorded Data							Calculations				
Indirect Reading Rotameters				Direct Reading Rotameter Value (L/min)	Pressure at Rotameter Exit (psig)	Half of Manometer Reading (mm H20)	Manometer Reading (mm H20)	Manometer Pressure (Pa)	Pore Size (Diameter) (mm)	Indicated Airflow Rate (L/min)	True Airflow Rate (L/min)
First Rotameter Used		Second Rotameter Used									
Rotameter ID Number	Rotameter Value	Rotameter ID Number	Rotameter Value								
2	9					2	4	39.24	2.0116208	0.0764	0.0764
2	25					8	16	156.96	0.5029052	0.378	0.378
2	69					14	28	274.68	0.2873744	1.404	1.404
4	28				0.13	18	36	353.16	0.2235134	9.39	9.431429
5	51				0.2	22	44	431.64	0.1828746	75.7	76.21323
5	57	5	70		0.34	28	56	549.36	0.1436872	189.8	191.9824
5	78	5	91		0.54	34	68	667.08	0.1183306	256	260.6596
				350	0.13	40	80	784.8	0.100581	350	351.5442
				400	0.15	44	88	863.28	0.0914373	400	402.0356
				450	0.16	48	96	941.76	0.0838175	450	452.4424
				500	0.18	54	108	1059.48	0.0745045	500	503.0519
				550	0.19	58	116	1137.96	0.0693662	550	553.543
				600	0.21	64	128	1255.68	0.0628631	600	604.2705
				650	0.24	70	140	1373.4	0.0574749	650	655.2846
				700	0.25	76	152	1491.12	0.0529374	700	705.9273
				800	0.31	88	176	1726.56	0.0457187	800	808.3914
				900	0.36	100	200	1962	0.0402324	900	910.9538
				1000	0.41	116	232	2275.92	0.0346831	1000	1013.85
				1100	0.49	136	272	2668.32	0.0295827	1100	1118.183
				1200	0.57	154	308	3021.48	0.0261249	1200	1223.044
				1300	0.63	174	348	3413.88	0.0231221	1300	1327.565
				1400	0.73	196	392	3845.52	0.0205267	1400	1434.341
				1600	0.84	256	512	5022.72	0.0157158	1600	1645.079

Figure B.137: 2EH-5 recorded data and calculations.

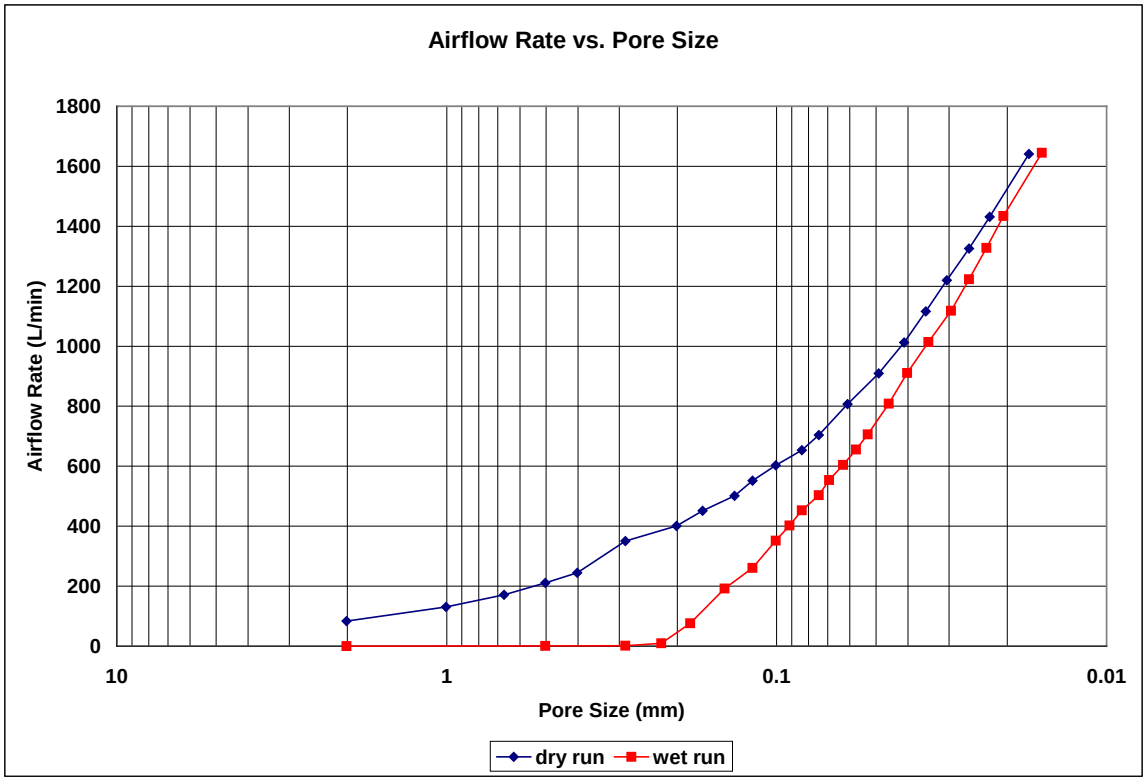

Figure B.138: 2EH-5 airflow rate vs. pore size for the wet and dry runs.

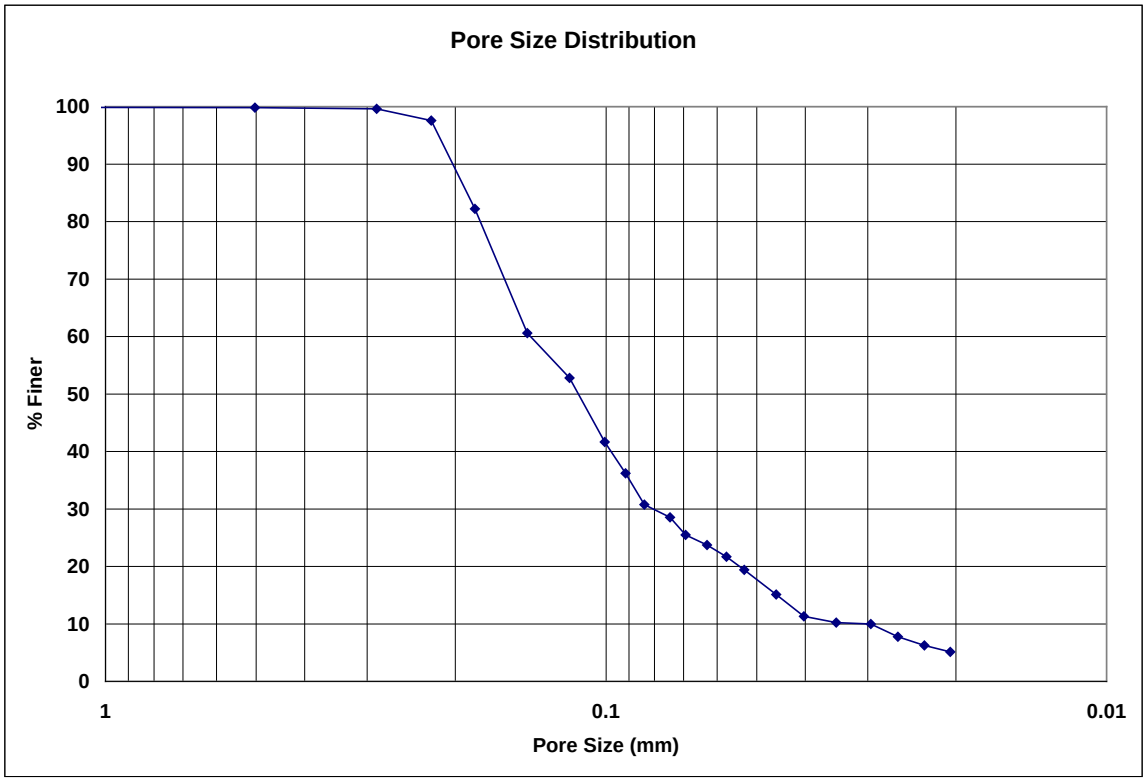

Figure B.139: 2EH-5 pore size distribution.

Bubble Point Test
Auburn University - Department of Civil Engineering

date of test: 3/21/2007
test identification: 2EH-5
test performed by: David Hayes
wetting fluid: 2-ethyl hexanol
air temperature: 21.5 °C
porous media: NG-1 nonwoven geotextile
comments: testing to determine geotextile pore size distribution

Pore Size Calculation Parameters:
constant, C: 2860 mm/m
contact angle: 0 degrees
surface tension: 0.0276 N/m

Pore Size at Selected % Finer

% finer	pore size (mm)
98	0.23710
95	0.21672
90	0.20349
85	0.19027
80	0.17888
75	0.16981
70	0.16075
65	0.15168
60	0.14177
55	0.12553
50	0.11389
45	0.10590
40	0.09779
35	0.08975
30	0.08066
25	0.06753
20	0.05413
15	0.04556
10	0.03026
5	---

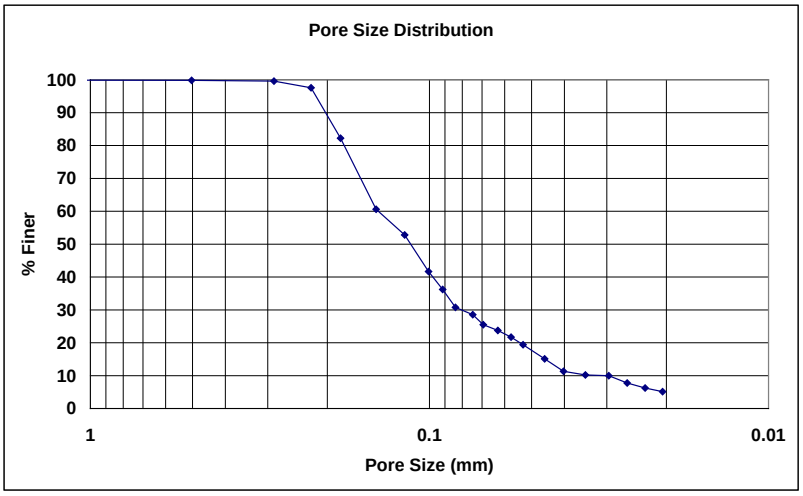

Figure B.140: 2EH-5 pore size distribution report.

Bubble Point Test
Auburn University - Department of Civil Engineering

date of test: 3/22/2007
test identification: 2EH-6
test performed by: David Hayes
wetting fluid: 2-ethyl hexanol
ambient air temperature: 21.3 °C
porous media: NG-1 nonwoven geotextile
comments: testing to determine geotextile pore size distribution

Pore Size Calculation Parameters:
constant, C: 2860 mm/m
contact angle: 0 degrees
surface tension: 0.0276 N/m

Dry Run											
Recorded Data							Calculations				
Indirect Reading Rotameters				Direct Reading Rotameter Value (L/min)	Pressure at Rotameter Exit (psig)	Half of Manometer Reading (mm H20)	Manometer Reading (mm H20)	Manometer Pressure (Pa)	Pore Size (Diameter) (mm)	Indicated Airflow Rate (L/min)	True Airflow Rate (L/min)
First Rotameter Used		Second Rotameter Used									
Rotameter ID Number	Rotameter Value	Rotameter ID Number	Rotameter Value								
5	73				0.01	2	4	39.24	2.0116208	110	110.0374
5	96				0.46	4	8	78.48	1.0058104	146	148.2668
5	58	5	72		0.18	6	12	117.72	0.6705403	194.3	195.486
5	67	5	83		0.23	8	16	156.96	0.5029052	225	226.7534
5	78	5	95		0.32	10	20	196.2	0.4023242	263	265.8472
				350	0.06	14	28	274.68	0.2873744	350	350.7136
				400	0.07	18	36	353.16	0.2235134	400	400.9512
				450	0.08	22	44	431.64	0.1828746	450	451.2228
				500	0.1	26	52	510.12	0.1547401	500	501.6978
				550	0.11	32	64	627.84	0.1257263	550	552.054
				600	0.13	38	76	745.56	0.1058748	600	602.6472
				650	0.15	42	84	824.04	0.0957915	650	653.3079
				700	0.17	50	100	981	0.0804648	700	704.036
				800	0.24	62	124	1216.44	0.064891	800	806.5042
				900	0.28	72	144	1412.64	0.0558784	900	908.531
				1000	0.34	86	172	1687.32	0.0467819	1000	1011.499
				1100	0.4	100	200	1962	0.0402324	1100	1114.866
				1200	0.46	118	236	2315.16	0.0340953	1200	1218.631
				1300	0.55	138	276	2707.56	0.0291539	1300	1324.096
				1400	0.62	156	312	3060.72	0.02579	1400	1429.219
				1600	0.67	208	416	4080.96	0.0193425	1600	1636.056

Wet Run											
Recorded Data							Calculations				
Indirect Reading Rotameters				Direct Reading Rotameter Value (L/min)	Pressure at Rotameter Exit (psig)	Half of Manometer Reading (mm H20)	Manometer Reading (mm H20)	Manometer Pressure (Pa)	Pore Size (Diameter) (mm)	Indicated Airflow Rate (L/min)	True Airflow Rate (L/min)
First Rotameter Used		Second Rotameter Used									
Rotameter ID Number	Rotameter Value	Rotameter ID Number	Rotameter Value								
2	14					4	8	78.48	1.0058104	0.164	0.164
2	19					6	12	117.72	0.6705403	0.259	0.259
2	42					12	24	235.44	0.3352701	0.743	0.743
4	57				0.29	20	40	392.4	0.2011621	20.6	20.8022
5	66				0.29	24	48	470.88	0.1676351	98.7	99.66882
5	65	5	80		0.43	30	60	588.6	0.1341081	218.1	221.2669
5	80	5	100		0.64	34	68	667.08	0.1183306	274	279.9011
				350	0.17	38	76	745.56	0.1058748	350	352.018
				400	0.18	42	84	824.04	0.0957915	400	402.4415
				450	0.2	46	92	902.52	0.0874618	450	453.0509
				500	0.2	50	100	981	0.0804648	500	503.3899
				550	0.22	54	108	1059.48	0.0745045	550	554.1004
				600	0.24	60	120	1177.2	0.067054	600	604.8781
				650	0.26	64	128	1255.68	0.0628631	650	655.7231
				700	0.28	70	140	1373.4	0.0574749	700	706.6352
				800	0.33	80	160	1569.6	0.0502905	800	808.9298
				900	0.38	90	180	1765.8	0.0447027	900	911.5584
				1000	0.41	104	208	2040.48	0.038685	1000	1013.85
				1100	0.48	118	236	2315.16	0.0340953	1100	1117.815
				1200	0.53	134	268	2629.08	0.0300242	1200	1221.441
				1300	0.61	152	304	2982.24	0.0264687	1300	1326.699
				1400	0.7	176	352	3453.12	0.0228593	1400	1432.946
				1600	0.78	236	472	4630.32	0.0170476	1600	1641.9

Figure B.141: 2EH-6 recorded data and calculations.

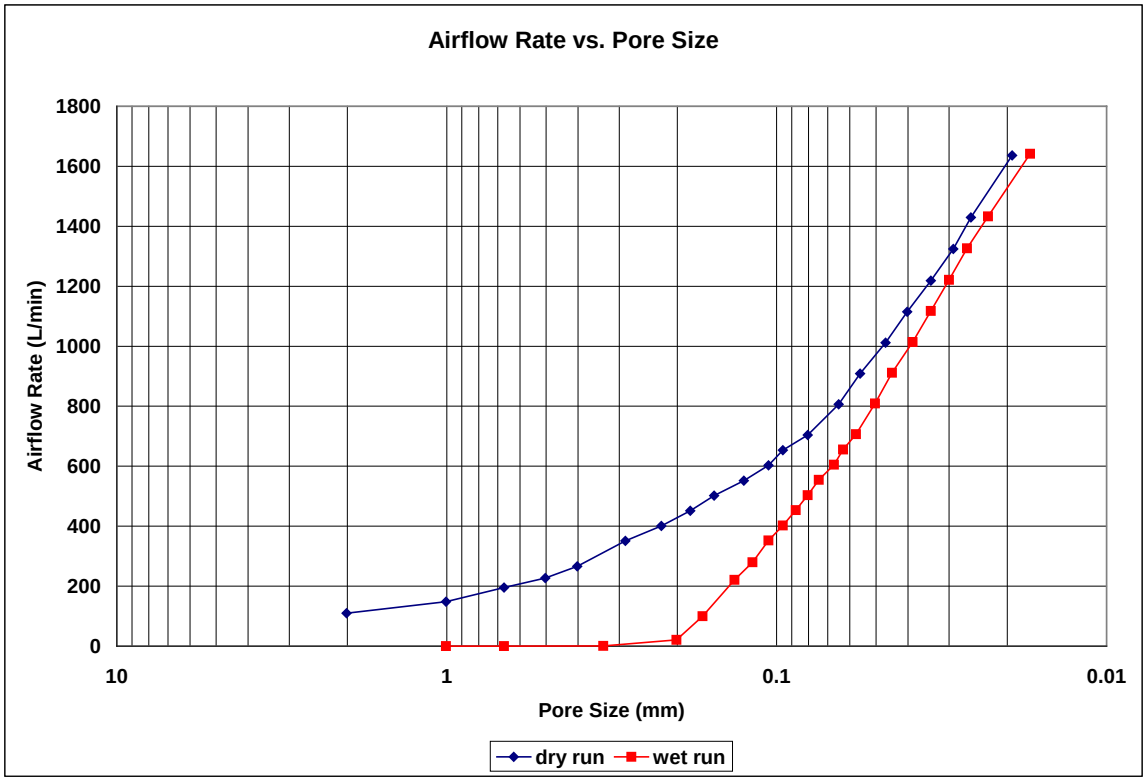

Figure B.142: 2EH-6 airflow rate vs. pore size for the wet and dry runs.

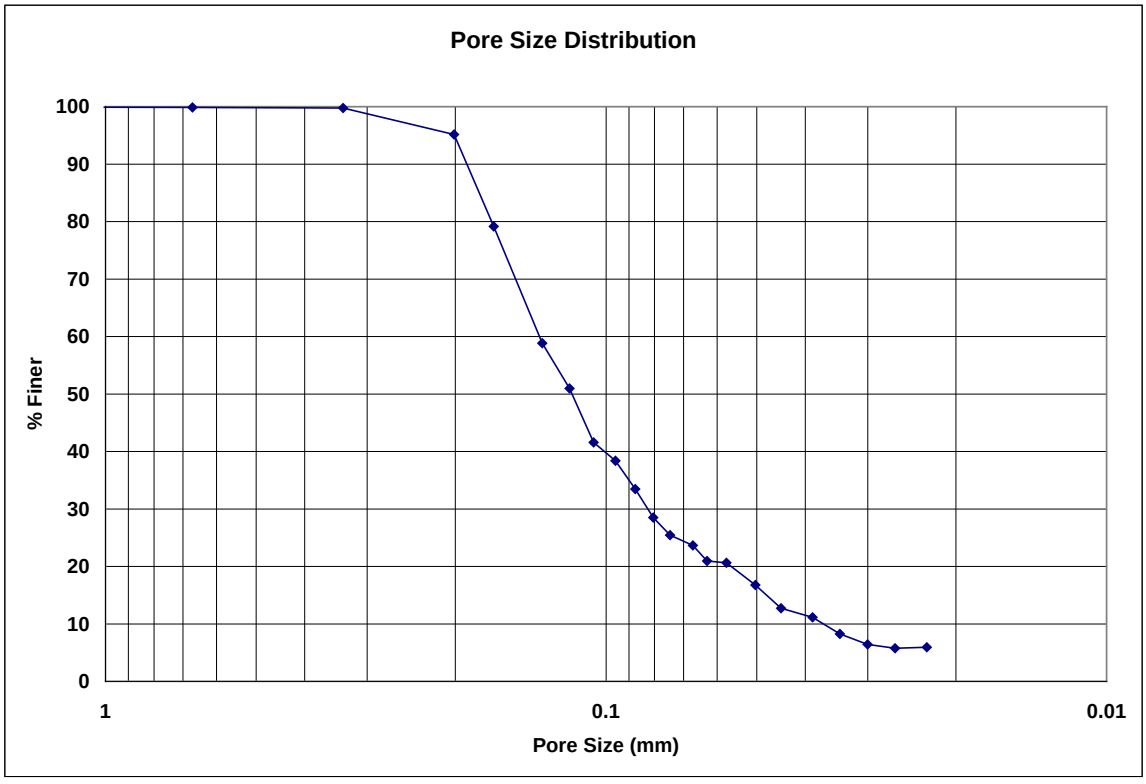

Figure B.143: 2EH-6 pore size distribution.

Bubble Point Test
Auburn University - Department of Civil Engineering

date of test: 3/22/2007
test identification: 2EH-6
test performed by: David Hayes
wetting fluid: 2-ethyl hexanol
air temperature: 21.3 °C
porous media: NG-1 nonwoven geotextile
comments: testing to determine geotextile pore size distribution

Pore Size Calculation Parameters:
constant, C: 2860 mm/m
contact angle: 0 degrees
surface tension: 0.0276 N/m

Pore Size at Selected % Finer

% finer	pore size (mm)
98	0.28403
95	0.20085
90	0.19036
85	0.17987
80	0.16937
75	0.16076
70	0.15251
65	0.14427
60	0.13603
55	0.12641
50	0.11704
45	0.11040
40	0.10085
35	0.09006
30	0.08258
25	0.07264
20	0.05628
15	0.04786
10	0.03685
5	---

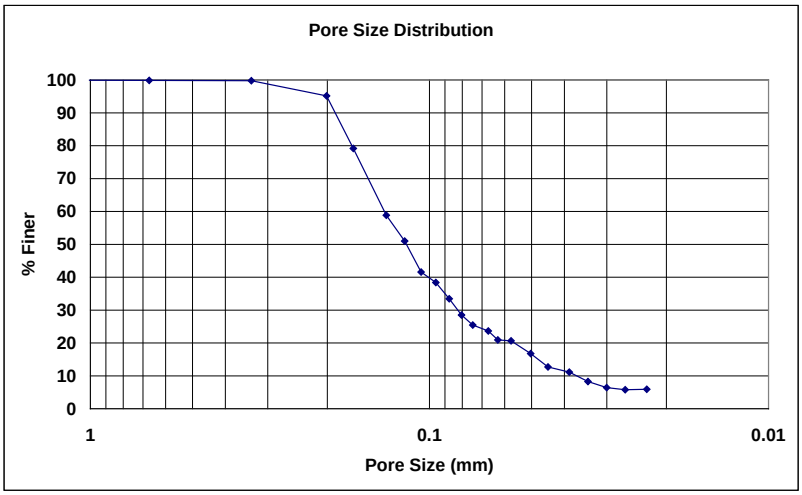

Figure B.144: 2EH-6 pore size distribution report.

Bubble Point Test

Auburn University - Department of Civil Engineering

date of test: 3/23/2007
test identification: 2EH-7
test performed by: David Hayes
wetting fluid: 2-ethyl hexanol
ambient air temperature: 21.3 °C
porous media: NG-1 nonwoven geotextile
comments: testing to determine geotextile pore size distribution

Pore Size Calculation Parameters:
constant, C: 2860 mm/m
contact angle: 0 degrees
surface tension: 0.0276 N/m

Dry Run

Recorded Data							Calculations				
Indirect Reading Rotameters				Direct Reading Rotameter Value (L/min)	Pressure at Rotameter Exit (psig)	Half of Manometer Reading (mm H20)	Manometer Reading (mm H20)	Manometer Pressure (Pa)	Pore Size (Diameter) (mm)	Indicated Airflow Rate (L/min)	True Airflow Rate (L/min)
First Rotameter Used		Second Rotameter Used									
Rotameter ID Number	Rotameter Value	Rotameter ID Number	Rotameter Value								
5	76				0.31	4	8	78.48	1.0058104	114	115.1958
5	50	5	62		0.18	6	12	117.72	0.6705403	166.7	167.7175
5	58	5	72		0.29	8	16	156.96	0.5029052	194.3	196.2072
5	67	5	82		0.38	10	20	196.2	0.4023242	224	226.8768
5	75	5	93		0.49	12	24	235.44	0.3352701	254	258.1986
				350	0.08	16	32	313.92	0.2514526	350	350.9511
				400	0.09	22	44	431.64	0.1828746	400	401.2226
				450	0.1	26	52	510.12	0.1547401	450	451.528
				500	0.12	30	60	588.6	0.1341081	500	502.0367
				550	0.14	36	72	706.32	0.1117567	550	552.6128
				600	0.16	42	84	824.04	0.0957915	600	603.2565
				650	0.17	48	96	941.76	0.0838175	650	653.7477
				700	0.2	56	112	1098.72	0.0718436	700	704.7458
				800	0.26	66	132	1294.92	0.0609582	800	807.0438
				900	0.32	82	164	1608.84	0.0490639	900	909.7432
				1000	0.38	96	192	1883.52	0.0419088	1000	1012.843
				1100	0.44	114	228	2236.68	0.0352916	1100	1116.341
				1200	0.51	132	264	2589.84	0.0304791	1200	1220.639
				1300	0.6	156	312	3060.72	0.02579	1300	1326.265
				1400	0.68	174	348	3413.88	0.0231221	1400	1432.015
				1600	0.77	240	480	4708.8	0.0167635	1600	1641.37

Wet Run

Recorded Data							Calculations				
Indirect Reading Rotameters				Direct Reading Rotameter Value (L/min)	Pressure at Rotameter Exit (psig)	Half of Manometer Reading (mm H20)	Manometer Reading (mm H20)	Manometer Pressure (Pa)	Pore Size (Diameter) (mm)	Indicated Airflow Rate (L/min)	True Airflow Rate (L/min)
First Rotameter Used		Second Rotameter Used									
Rotameter ID Number	Rotameter Value	Rotameter ID Number	Rotameter Value								
2	11					6	12	117.72	0.6705403	0.11	0.11
2	29					12	24	235.44	0.3352701	0.459	0.459
2	94					18	36	353.16	0.2235134	1.997	1.997
4	27				0.13	20	40	392.4	0.2011621	9.01	9.049752
5	78				0.39	28	56	549.36	0.1436872	118	119.5551
5	65	5	80		0.45	34	68	667.08	0.1183306	218.1	221.4131
5	80	5	100		0.65	38	76	745.56	0.1058748	274	279.9923
				350	0.15	42	84	824.04	0.0957915	350	351.7812
				400	0.16	46	92	902.52	0.0874618	400	402.171
				450	0.18	50	100	981	0.0804648	450	452.7467
				500	0.19	54	108	1059.48	0.0745045	500	503.2209
				550	0.21	60	120	1177.2	0.067054	550	553.9146
				600	0.23	64	128	1255.68	0.0628631	600	604.6757
				650	0.25	70	140	1373.4	0.0574749	650	655.5039
				700	0.26	76	152	1491.12	0.0529374	700	706.1633
				800	0.33	84	168	1648.08	0.0478957	800	808.9298
				900	0.37	96	192	1883.52	0.0419088	900	911.2561
				1000	0.43	114	228	2236.68	0.0352916	1000	1014.52
				1100	0.5	130	260	2550.6	0.030948	1100	1118.551
				1200	0.57	146	292	2864.52	0.0275564	1200	1223.044
				1300	0.66	170	340	3335.4	0.0236661	1300	1328.863
				1400	0.76	194	388	3806.28	0.0207384	1400	1435.734
				1600	0.86	258	516	5061.96	0.015594	1600	1646.138

Figure B.145: 2EH-7 recorded data and calculations.

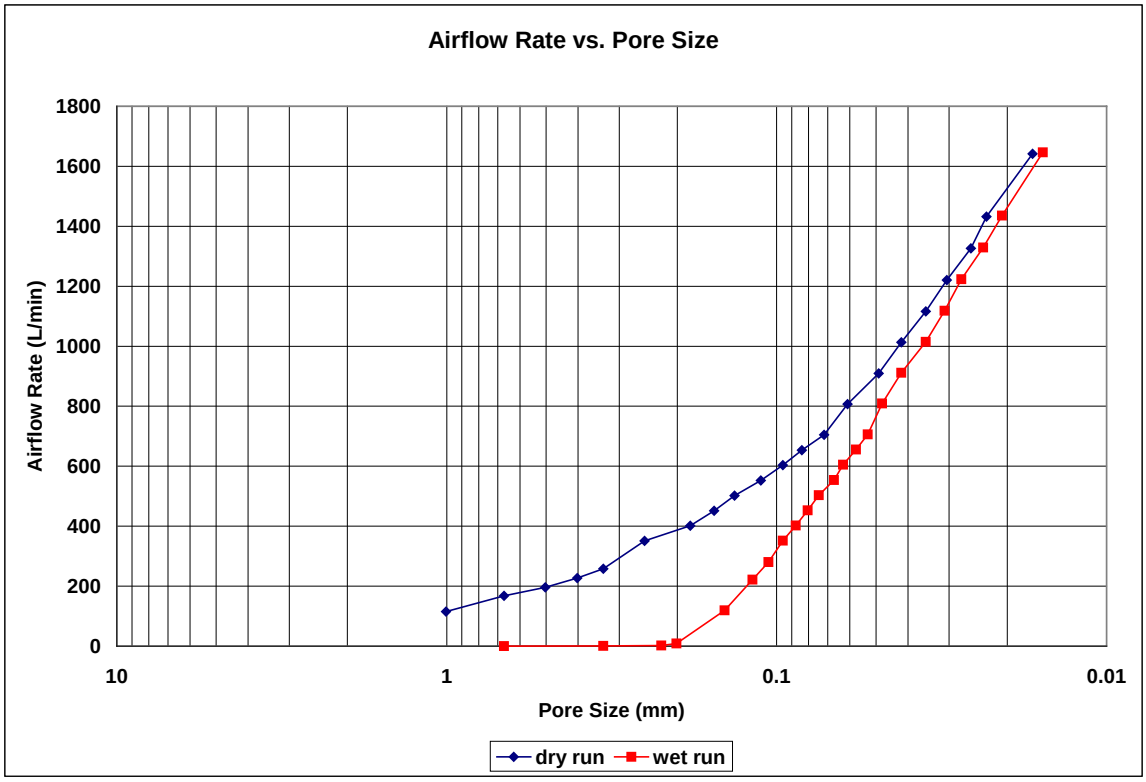

Figure B.146: 2EH-7 airflow rate vs. pore size for the wet and dry runs.

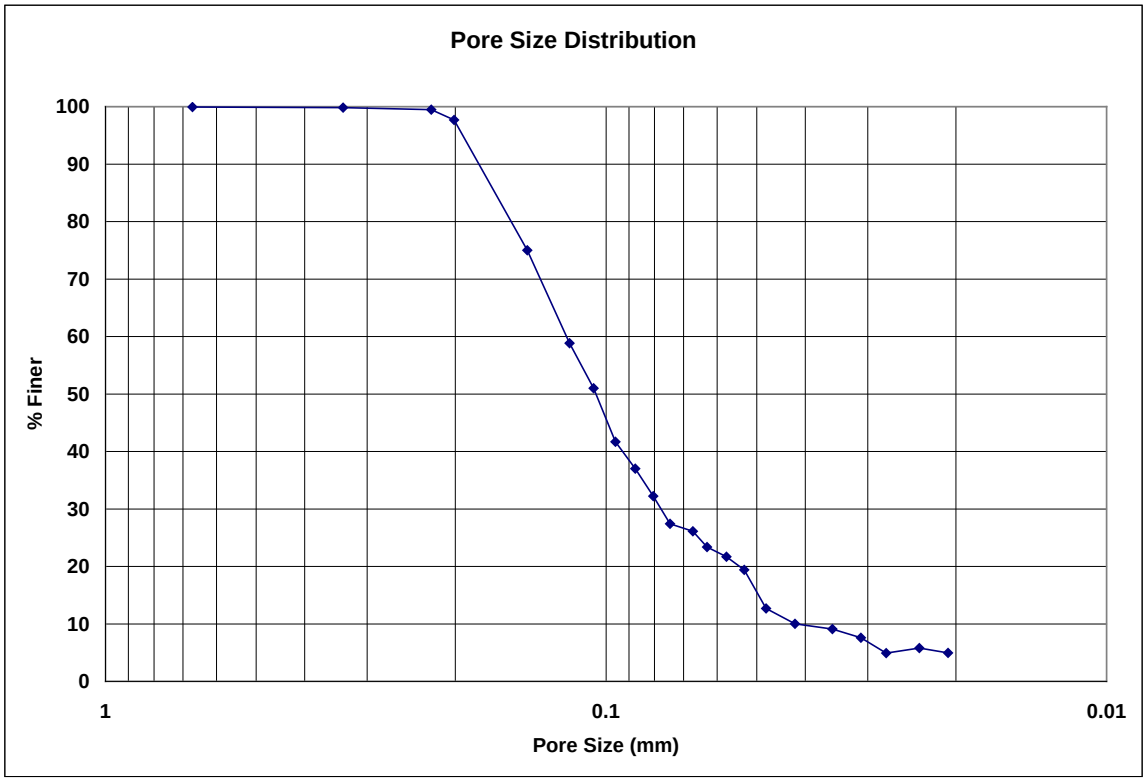

Figure B.147: 2EH-7 pore size distribution.

Bubble Point Test
Auburn University - Department of Civil Engineering

date of test: 3/23/2007
test identification: 2EH-7
test performed by: David Hayes
wetting fluid: 2-ethyl hexanol
air temperature: 21.3 °C
porous media: NG-1 nonwoven geotextile
comments: testing to determine geotextile pore size distribution

Pore Size Calculation Parameters:
constant, C: 2860 mm/m
contact angle: 0 degrees
surface tension: 0.0276 N/m

Pore Size at Selected % Finer

% finer	pore size (mm)
98	0.20531
95	0.19440
90	0.18171
85	0.16902
80	0.15633
75	0.14366
70	0.13583
65	0.12800
60	0.12017
55	0.11225
50	0.10480
45	0.09938
40	0.09279
35	0.08453
30	0.07770
25	0.06534
20	0.05410
15	0.04962
10	0.04169
5	0.02764

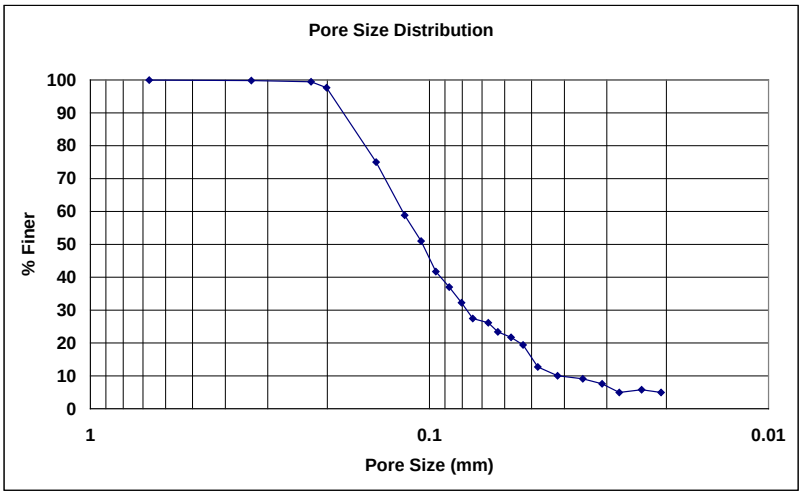

Figure B.148: 2EH-7 pore size distribution report.

Bubble Point Test

Auburn University - Department of Civil Engineering

date of test: 3/23/2007
test identification: 2EH-8
test performed by: David Hayes
wetting fluid: 2-ethyl hexanol
ambient air temperature: 21.3 °C
porous media: NG-1 nonwoven geotextile
comments: testing to determine geotextile pore size distribution

Pore Size Calculation Parameters:
constant, C: 2860 mm/m
contact angle: 0 degrees
surface tension: 0.0276 N/m

Dry Run

Recorded Data							Calculations				
Indirect Reading Rotameters				Direct Reading Rotameter Value (L/min)	Pressure at Rotameter Exit (psig)	Half of Manometer Reading (mm H20)	Manometer Reading (mm H20)	Manometer Pressure (Pa)	Pore Size (Diameter) (mm)	Indicated Airflow Rate (L/min)	True Airflow Rate (L/min)
First Rotameter Used		Second Rotameter Used									
Rotameter ID Number	Rotameter Value	Rotameter ID Number	Rotameter Value								
5	69				0.24	2	4	39.24	2.0116208	103	103.8374
5	90				0.41	4	8	78.48	1.0058104	137	138.8974
5	55	5	69		0.27	6	12	117.72	0.6705403	184.8	186.4894
5	66	5	81		0.38	8	16	156.96	0.5029052	220.7	223.5344
5	75	5	92		0.49	10	20	196.2	0.4023242	253	257.1821
				350	0.06	14	28	274.68	0.2873744	350	350.7136
				400	0.08	20	40	392.4	0.2011621	400	401.087
				450	0.09	22	44	431.64	0.1828746	450	451.3754
				500	0.11	30	60	588.6	0.1341081	500	501.8673
				550	0.12	34	68	667.08	0.1183306	550	552.2403
				600	0.14	40	80	784.8	0.100581	600	602.8504
				650	0.16	46	92	902.52	0.0874618	650	653.5278
				700	0.19	54	108	1059.48	0.0745045	700	704.5093
				800	0.25	64	128	1255.68	0.0628631	800	806.774
				900	0.3	80	160	1569.6	0.0502905	900	909.1373
				1000	0.36	94	188	1844.28	0.0428004	1000	1012.171
				1100	0.43	112	224	2197.44	0.0359218	1100	1115.972
				1200	0.49	130	260	2550.6	0.030948	1200	1219.836
				1300	0.58	152	304	2982.24	0.0264687	1300	1325.398
				1400	0.66	172	344	3374.64	0.0233909	1400	1431.084
				1600	0.75	236	472	4630.32	0.0170476	1600	1640.309

Wet Run

Recorded Data							Calculations				
Indirect Reading Rotameters				Direct Reading Rotameter Value (L/min)	Pressure at Rotameter Exit (psig)	Half of Manometer Reading (mm H20)	Manometer Reading (mm H20)	Manometer Pressure (Pa)	Pore Size (Diameter) (mm)	Indicated Airflow Rate (L/min)	True Airflow Rate (L/min)
First Rotameter Used		Second Rotameter Used									
Rotameter ID Number	Rotameter Value	Rotameter ID Number	Rotameter Value								
2	16					6	12	117.72	0.6705403	0.202	0.202
2	37					14	28	274.68	0.2873744	0.631	0.631
4	15				0.1	18	36	353.16	0.2235134	4.74	4.756095
4	83				0.54	22	44	431.64	0.1828746	31.7	32.27699
5	64				0.27	26	52	510.12	0.1547401	95.6	96.47396
5	58	5	72		0.34	30	60	588.6	0.1341081	194.3	196.5342
5	71	5	87		0.52	34	68	667.08	0.1183306	238	242.1729
				350	0.16	40	80	784.8	0.100581	350	351.8996
				400	0.17	44	88	863.28	0.0914373	400	402.3063
				450	0.18	48	96	941.76	0.0838175	450	452.7467
				500	0.2	54	108	1059.48	0.0745045	500	503.3899
				550	0.21	58	116	1137.96	0.0693662	550	553.9146
				600	0.23	64	128	1255.68	0.0628631	600	604.6757
				650	0.25	68	136	1334.16	0.0591653	650	655.5039
				700	0.27	74	148	1451.88	0.0543681	700	706.3993
				800	0.32	86	172	1687.32	0.0467819	800	808.6606
				900	0.35	100	200	1962	0.0402324	900	910.6513
				1000	0.42	112	224	2197.44	0.0359218	1000	1014.185
				1100	0.48	128	256	2511.36	0.0314316	1100	1117.815
				1200	0.56	148	296	2903.76	0.0271841	1200	1222.644
				1300	0.65	170	340	3335.4	0.0236661	1300	1328.431
				1400	0.73	192	384	3767.04	0.0209544	1400	1434.341
				1600	0.84	256	512	5022.72	0.0157158	1600	1645.079

Figure B.149: 2EH-8 recorded data and calculations.

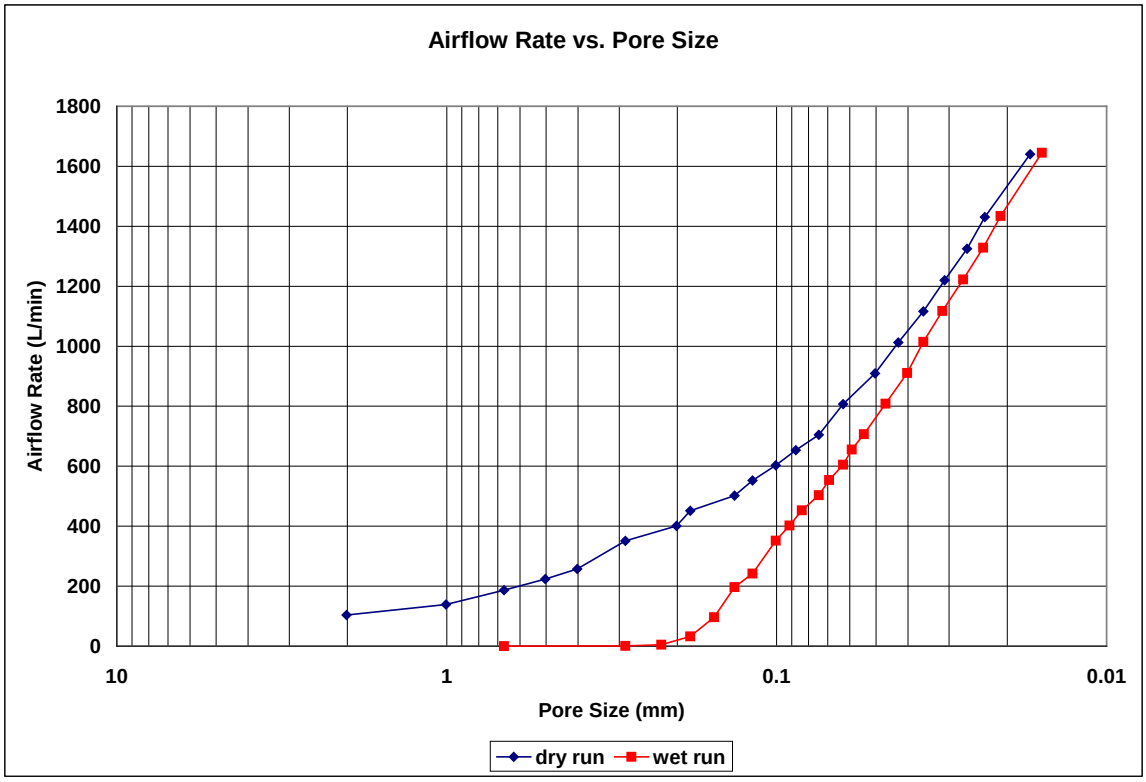

Figure B.150: 2EH-8 airflow rate vs. pore size for the wet and dry runs.

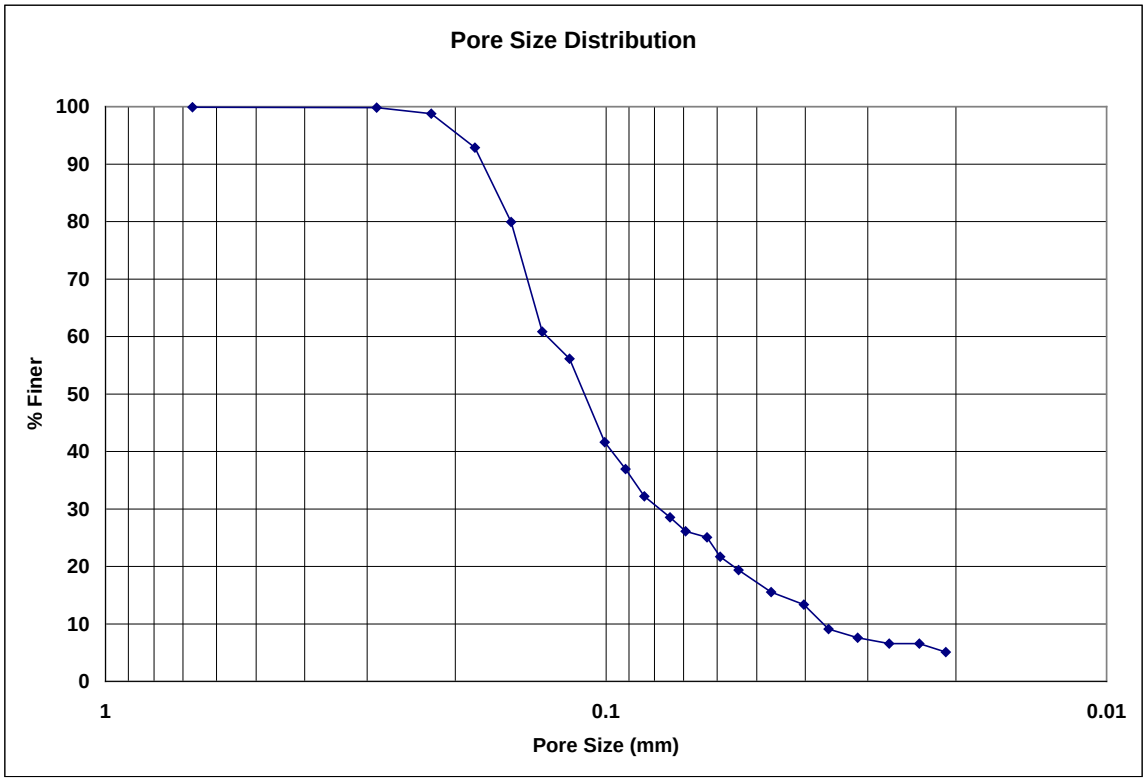

Figure B.151: 2EH-8 pore size distribution.

Bubble Point Test
Auburn University - Department of Civil Engineering

date of test: 3/23/2007
test identification: 2EH-8
test performed by: David Hayes
wetting fluid: 2-ethyl hexanol
air temperature: 21.3 °C
porous media: NG-1 nonwoven geotextile
comments: testing to determine geotextile pore size distribution

Pore Size Calculation Parameters:
constant, C: 2860 mm/m
contact angle: 0 degrees
surface tension: 0.0276 N/m

Pore Size at Selected % Finer

% finer	pore size (mm)
98	0.21820
95	0.19763
90	0.17667
85	0.16579
80	0.15491
75	0.14942
70	0.14401
65	0.13861
60	0.13129
55	0.11693
50	0.11082
45	0.10470
40	0.09739
35	0.08829
30	0.07820
25	0.06281
20	0.05570
15	0.04518
10	0.03682
5	---

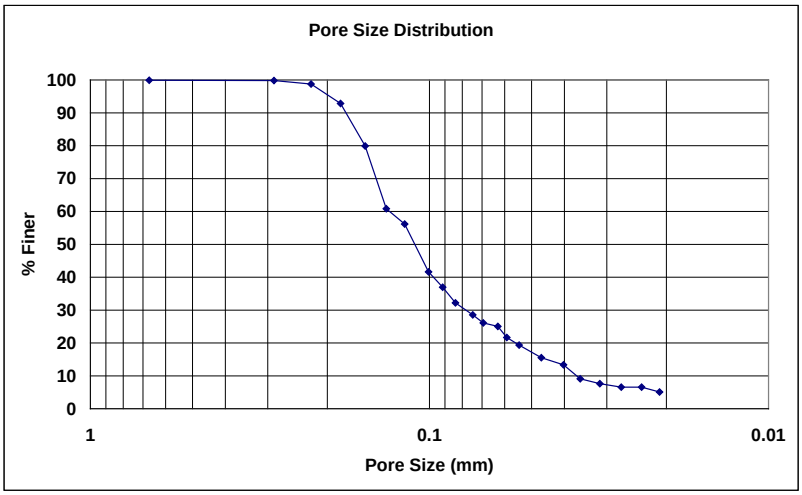

Figure B.152: 2EH-8 pore size distribution report.

Bubble Point Test
Auburn University - Department of Civil Engineering

date of test: 10/24/2002
test identification: 2EH 9
test performed by: David Howie
wetting fluid: 2-ethyl hexanol
ambient air temperature: 21 °C
porous media: NG-1 nonwoven geotextile
comments: testing to determine geotextile pore size distribution

Pore Size Calculation Parameters:
constant, C: 2860 mm/m
contact angle: 0 degrees
surface tension: 0.0276 N/m

Dry Run

Recorded Data							Calculations				
Indirect Reading Rotameters				Direct Reading Rotameter Value (L/min)	Pressure at Rotameter Exit (psig)	Half of Manometer Reading (mm H20)	Manometer Reading (mm H20)	Manometer Pressure (Pa)	Pore Size (Diameter) (mm)	Indicated Airflow Rate (L/min)	True Airflow Rate (L/min)
First Rotameter Used		Second Rotameter Used									
Rotameter ID Number	Rotameter Value	Rotameter ID Number	Rotameter Value								
5	38				0.08	1	2	19.62	4.0232416	56.5	56.65353
5	58				0.16	2	4	39.24	2.0116208	86.3	86.76839
5	87				0.38	4	8	78.48	1.0058104	132	133.6952
5	78	5	64		0.33	8	16	156.96	0.5029052	213.6	215.9842
				300	0.05	12	24	235.44	0.3352701	300	300.5098
				350	0.06	16	32	313.92	0.2514526	350	350.7136
				400	0.08	20	40	392.4	0.2011621	400	401.087
				450	0.09	24	48	470.88	0.1676351	450	451.3754
				500	0.11	30	60	588.6	0.1341081	500	501.8673
				550	0.12	34	68	667.08	0.1183306	550	552.2403
				600	0.14	40	80	784.8	0.100581	600	602.8504
				650	0.16	47	94	922.14	0.0856009	650	653.5278
				700	0.19	53	106	1039.86	0.0759102	700	704.5093
				800	0.24	65	130	1275.3	0.061896	800	806.5042
				900	0.28	77	154	1510.74	0.0522499	900	908.531
				1000	0.34	92	184	1805.04	0.0437309	1000	1011.499
				1100	0.39	106	212	2079.72	0.0379551	1100	1114.496
				1200	0.46	124	248	2432.88	0.0324455	1200	1218.631
				1300	0.55	146	292	2864.52	0.0275564	1300	1324.096
				1400	0.63	164	328	3217.68	0.024532	1400	1429.685
				1600	0.77	236	472	4630.32	0.0170476	1600	1641.37

Wet Run

Recorded Data							Calculations				
Indirect Reading Rotameters				Direct Reading Rotameter Value (L/min)	Pressure at Rotameter Exit (psig)	Half of Manometer Reading (mm H20)	Manometer Reading (mm H20)	Manometer Pressure (Pa)	Pore Size (Diameter) (mm)	Indicated Airflow Rate (L/min)	True Airflow Rate (L/min)
First Rotameter Used		Second Rotameter Used									
Rotameter ID Number	Rotameter Value	Rotameter ID Number	Rotameter Value								
1	8					2	4	39.24	2.0116208	0.00543	0.00543
1	32					12	24	235.44	0.3352701	0.0532	0.0532
2	41					18.5	37	362.97	0.2174725	0.72	0.72
4	9				0.07	20	40	392.4	0.2011621	2.74	2.746516
4	38				0.17	22	44	431.64	0.1828746	13.2	13.27611
4	94				0.67	24	48	470.88	0.1676351	36.5	37.32253
5	49				0.21	26	52	510.12	0.1547401	72.7	73.21744
5	74				0.36	28	56	549.36	0.1436872	111	112.351
				400	0.14	43	86	843.66	0.0935638	400	401.9002
				450	0.16	48	96	941.76	0.0838175	450	452.4424
				500	0.17	52	104	1020.24	0.07737	500	502.8828
				550	0.19	57	114	1118.34	0.0705832	550	553.543
				600	0.21	63	126	1236.06	0.063861	600	604.2705
				650	0.23	69	138	1353.78	0.0583078	650	655.0653
				700	0.25	75	150	1471.5	0.0536432	700	705.9273
				800	0.29	84	168	1648.08	0.0478957	800	807.8526
				900	0.34	96	192	1883.52	0.0419088	900	910.3487
				1000	0.39	110	220	2158.2	0.0365749	1000	1013.178
				1100	0.44	122	244	2393.64	0.0329774	1100	1116.341
				1200	0.5	140	280	2746.8	0.0287374	1200	1220.238
				1300	0.61	164	328	3217.68	0.024532	1300	1326.699
				1400	0.69	185	370	3629.7	0.0217473	1400	1432.48
				1600	0.86	265	530	5199.3	0.015182	1600	1646.138

Figure B.153: 2EH-9 recorded data and calculations.

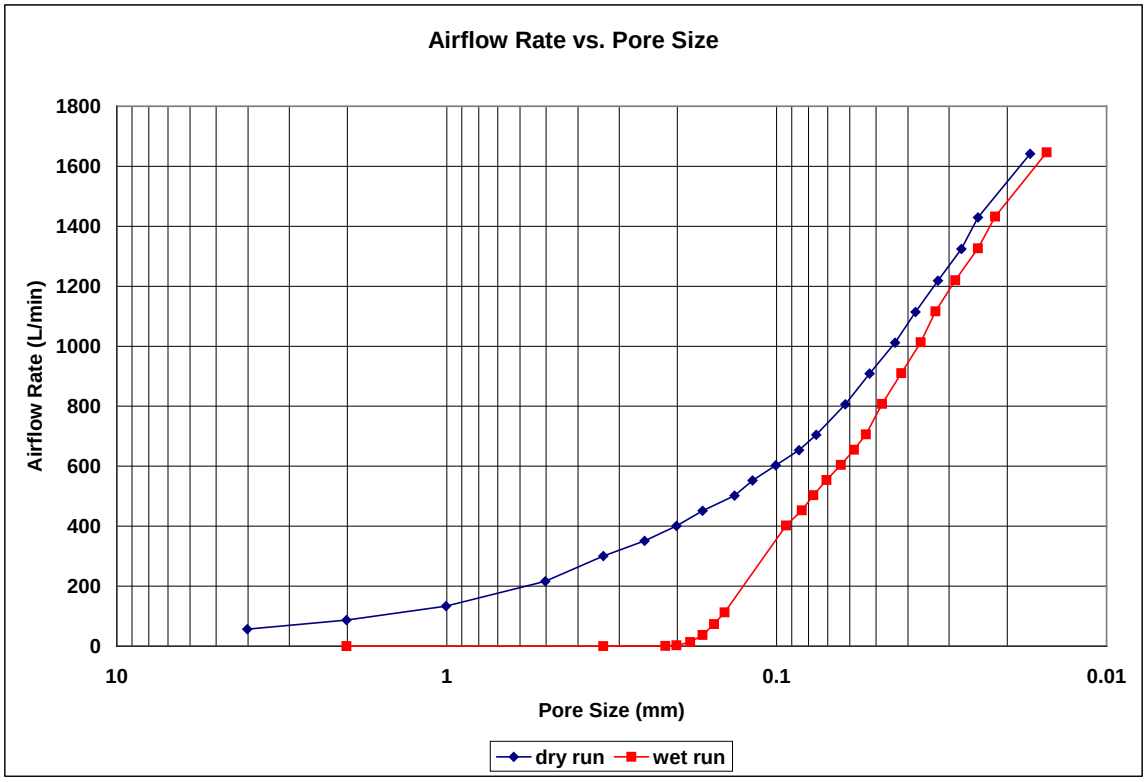

Figure B.154: 2EH-9 airflow rate vs. pore size for the wet and dry runs.

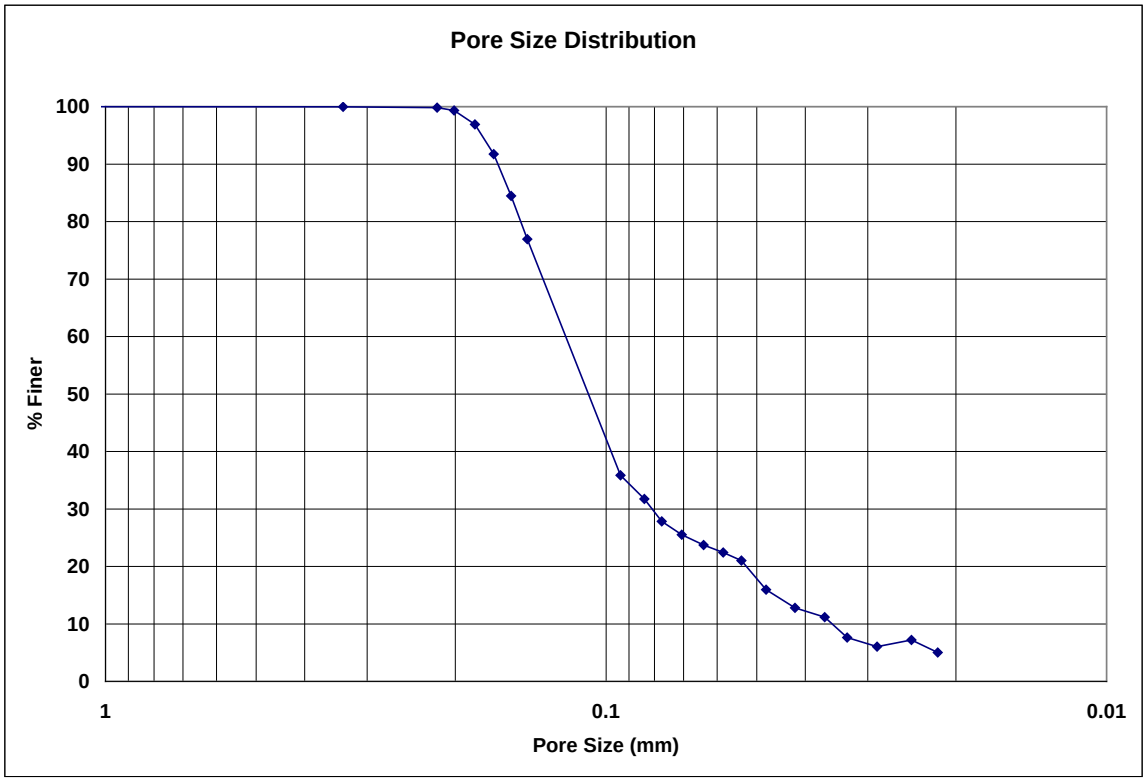

Figure B.155: 2EH-9 pore size distribution.

Bubble Point Test
Auburn University - Department of Civil Engineering

date of test: 10/24/2002
test identification: 2EH 9
test performed by: David Howie
wetting fluid: 2-ethyl hexanol
air temperature: 21 °C
porous media: NG-1 nonwoven geotextile
comments: testing to determine geotextile pore size distribution

Pore Size Calculation Parameters:
constant, C: 2860 mm/m
contact angle: 0 degrees
surface tension: 0.0276 N/m

Pore Size at Selected % Finer

% finer	pore size (mm)
98	0.19120
95	0.17727
90	0.16457
85	0.15572
80	0.14818
75	0.14131
70	0.13521
65	0.12911
60	0.12301
55	0.11691
50	0.11081
45	0.10471
40	0.09861
35	0.09153
30	0.08094
25	0.06862
20	0.05249
15	0.04609
10	0.03539
5	---

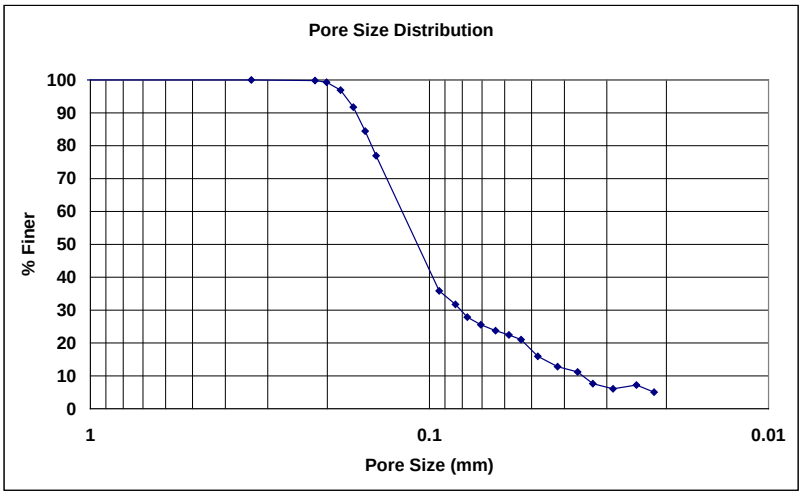

Figure B.156: 2EH-9 pore size distribution report.

Bubble Point Test
Auburn University - Department of Civil Engineering

date of test: 10/24/2002
test identification: 2EH 10
test performed by: David Howie
wetting fluid: 2-ethyl hexanol
ambient air temperature: 21 °C
porous media: NG-1 nonwoven geotextile
comments: testing to determine geotextile pore size distribution

Pore Size Calculation Parameters:
constant, C: 2860 mm/m
contact angle: 0 degrees
surface tension: 0.0276 N/m

Dry Run

Recorded Data							Calculations				
Indirect Reading Rotameters				Direct Reading Rotameter Value (L/min)	Pressure at Rotameter Exit (psig)	Half of Manometer Reading (mm H20)	Manometer Reading (mm H20)	Manometer Pressure (Pa)	Pore Size (Diameter) (mm)	Indicated Airflow Rate (L/min)	True Airflow Rate (L/min)
First Rotameter Used		Second Rotameter Used									
Rotameter ID Number	Rotameter Value	Rotameter ID Number	Rotameter Value								
5	36				0.07	1	2	19.62	4.0232416	53.6	53.72747
5	59				0.17	2	4	39.24	2.0116208	87.9	88.4068
5	89				0.4	4	8	78.48	1.0058104	135	136.8244
5	83	5	68		0.37	8	16	156.96	0.5029052	227	229.839
				300	0.07	11	22	215.82	0.3657492	300	300.7134
				350	0.08	14	28	274.68	0.2873744	350	350.9511
				400	0.09	18	36	353.16	0.2235134	400	401.2226
				450	0.1	22	44	431.64	0.1828746	450	451.528
				500	0.12	26	52	510.12	0.1547401	500	502.0367
				550	0.13	31	62	608.22	0.129782	550	552.4266
				600	0.15	36	72	706.32	0.1117567	600	603.0535
				650	0.17	42	84	824.04	0.0957915	650	653.7477
				700	0.19	48	96	941.76	0.0838175	700	704.5093
				800	0.22	58	116	1137.96	0.0693662	800	805.9642
				900	0.27	71	142	1393.02	0.0566654	900	908.2277
				1000	0.32	84	168	1648.08	0.0478957	1000	1010.826
				1100	0.37	98	196	1922.76	0.0410535	1100	1113.758
				1200	0.44	114	228	2236.68	0.0352916	1200	1217.827
				1300	0.53	134	268	2629.08	0.0300242	1300	1323.228
				1400	0.6	150	300	2943	0.0268216	1400	1428.286
				1600	0.72	215	430	4218.3	0.0187128	1600	1638.715

Wet Run

Recorded Data							Calculations				
Indirect Reading Rotameters				Direct Reading Rotameter Value (L/min)	Pressure at Rotameter Exit (psig)	Half of Manometer Reading (mm H20)	Manometer Reading (mm H20)	Manometer Pressure (Pa)	Pore Size (Diameter) (mm)	Indicated Airflow Rate (L/min)	True Airflow Rate (L/min)
First Rotameter Used		Second Rotameter Used									
Rotameter ID Number	Rotameter Value	Rotameter ID Number	Rotameter Value								
1	4					1	2	19.62	4.0232416	0.00256	0.00256
1	12					2	4	39.24	2.0116208	0.00967	0.00967
1	20					4	8	78.48	1.0058104	0.0234	0.0234
1	73					16	32	313.92	0.2514526	0.199	0.199
4	9				0.07	18.5	37	362.97	0.2174725	2.74	2.746516
4	69				0.38	22	44	431.64	0.1828746	25.6	25.92877
5	64				0.29	26	52	510.12	0.1547401	95.6	96.53839
5	94				0.54	28	56	549.36	0.1436872	143	145.6028
				400	0.16	42	84	824.04	0.0957915	400	402.171
				450	0.17	47	94	922.14	0.0856009	450	452.5946
				500	0.18	51	102	1000.62	0.0788871	500	503.0519
				550	0.2	55	110	1079.1	0.0731498	550	553.7289
				600	0.22	57	114	1118.34	0.0705832	600	604.4731
				650	0.23	62	124	1216.44	0.064891	650	655.0653
				800	0.28	73	146	1432.26	0.0551129	800	807.5831
				900	0.33	84	168	1648.08	0.0478957	900	910.046
				1000	0.37	96	192	1883.52	0.0419088	1000	1012.507
				1100	0.42	108	216	2118.96	0.0372522	1100	1115.604
				1200	0.49	126	252	2472.12	0.0319305	1200	1219.836
				1300	0.58	146	292	2864.52	0.0275564	1300	1325.398
				1400	0.65	164	328	3217.68	0.024532	1400	1430.618
				1600	0.78	230	460	4512.6	0.0174924	1600	1641.9

Figure B.157: 2EH-10 recorded data and calculations.

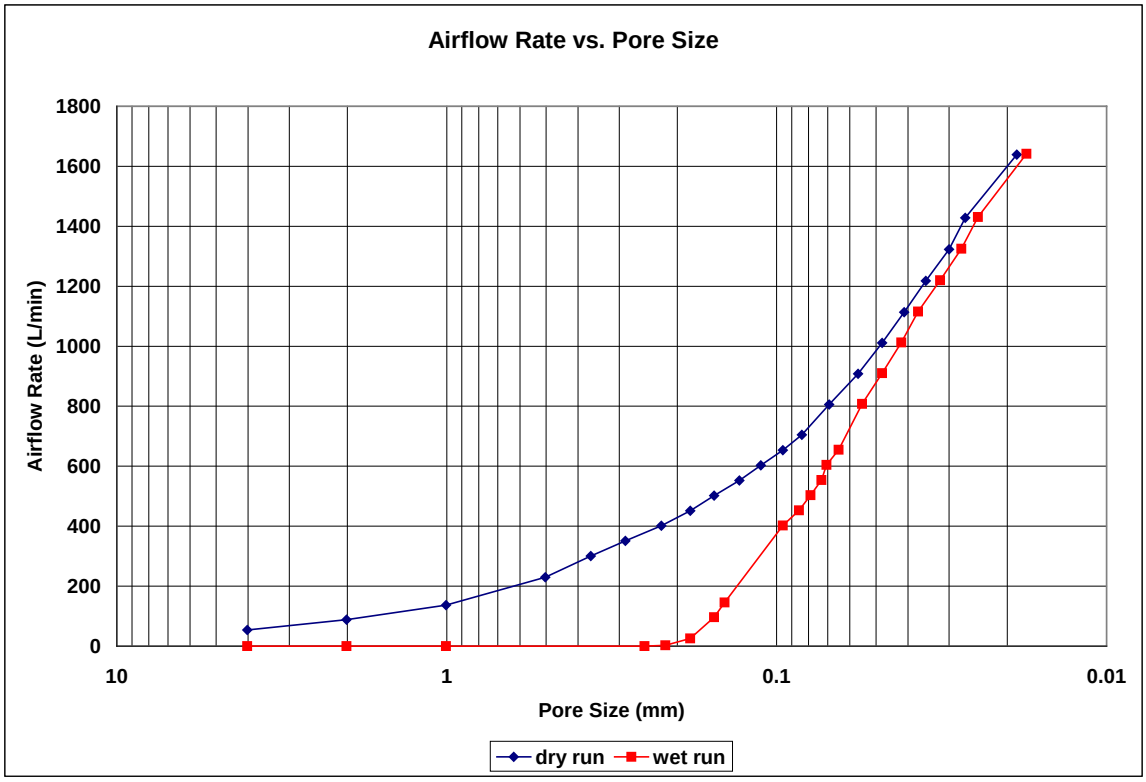

Figure B.158: 2EH-10 airflow rate vs. pore size for the wet and dry runs.

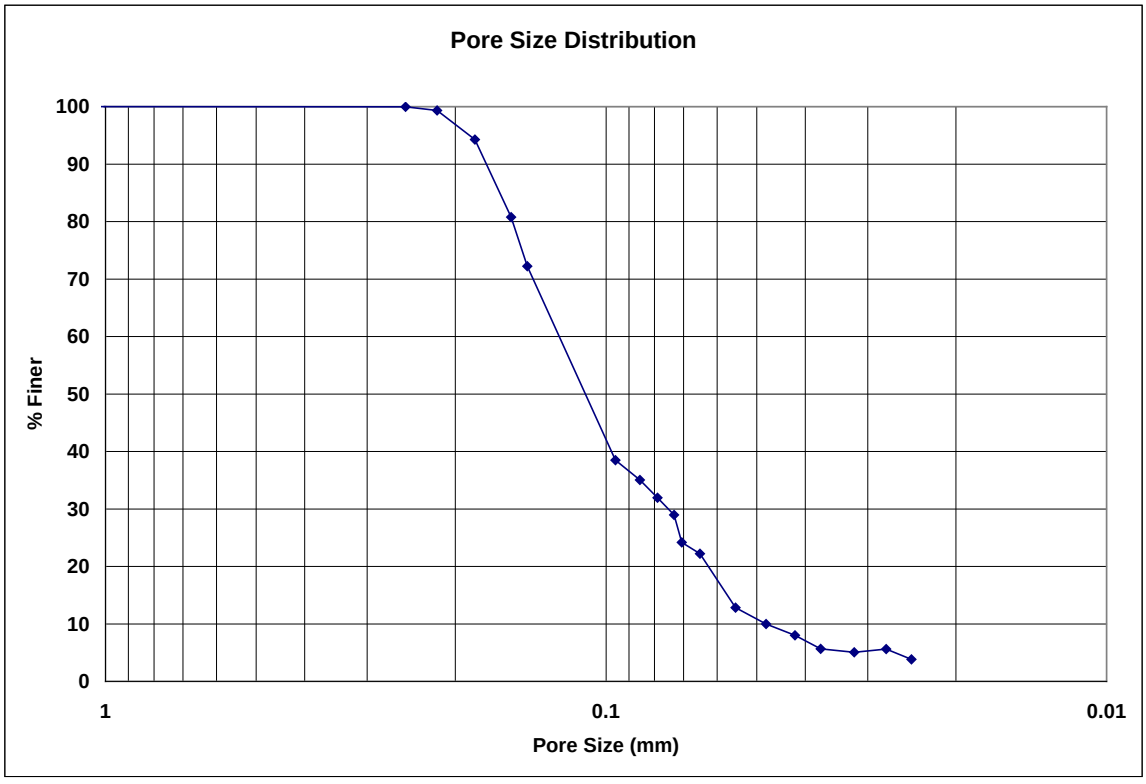

Figure B.159: 2EH-10 pore size distribution.

Bubble Point Test
Auburn University - Department of Civil Engineering

date of test: 10/24/2002
test identification: 2EH 10
test performed by: David Howie
wetting fluid: 2-ethyl hexanol
air temperature: 21 °C
porous media: NG-1 nonwoven geotextile
comments: testing to determine geotextile pore size distribution

Pore Size Calculation Parameters:
constant, C: 2860 mm/m
contact angle: 0 degrees
surface tension: 0.0276 N/m

Pore Size at Selected % Finer

% finer	pore size (mm)
98	0.20841
95	0.18794
90	0.17399
85	0.16356
80	0.15374
75	0.14727
70	0.14052
65	0.13342
60	0.12633
55	0.11923
50	0.11214
45	0.10504
40	0.09795
35	0.08547
30	0.07516
25	0.07102
20	0.06260
15	0.05738
10	0.04797
5	0.02652

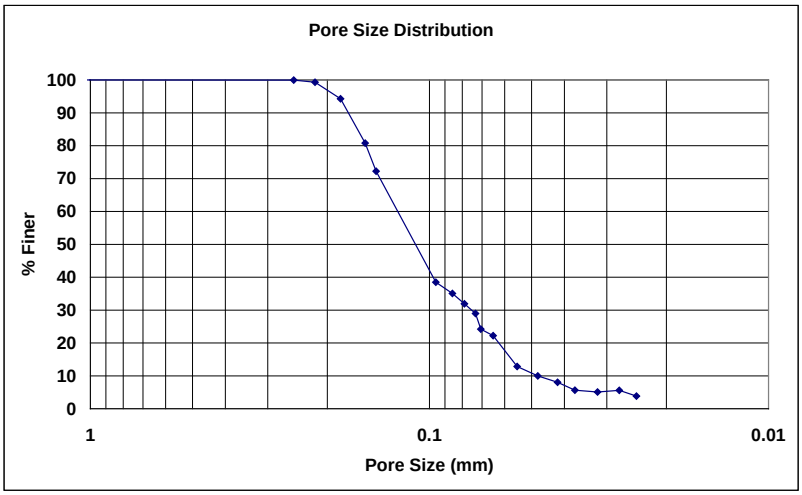

Figure B.160: 2EH-10 pore size distribution report.

B.5 Tests with Drakeol as the Wetting Fluid

Bubble Point Test
Auburn University - Department of Civil Engineering

date of test: 10/18/2006
test identification: drakeol 1
test performed by: David Hayes
wetting fluid: drakeol
ambient air temperature: 22.5 °C
porous media: NG-1 nonwoven geotextile
comments: testing to determine geotextile pore size distribution

Pore Size Calculation Parameters:
constant, C: 2860 mm/m
contact angle: 0 degrees
surface tension: 0.0347 N/m

Dry Run

Recorded Data							Calculations				
Indirect Reading Rotameters				Direct Reading Rotameter Value (L/min)	Pressure at Rotameter Exit (psig)	Half of Manometer Reading (mm H20)	Manometer Reading (mm H20)	Manometer Pressure (Pa)	Pore Size (Diameter) (mm)	Indicated Airflow Rate (L/min)	True Airflow Rate (L/min)
First Rotameter Used		Second Rotameter Used									
Rotameter ID Number	Rotameter Value	Rotameter ID Number	Rotameter Value								
5	50				0.12	2	4	39.24	2.529103	74.2	74.50224
5	74				0.27	4	8	78.48	1.2645515	111	112.0147
5	90				0.4	6	12	117.72	0.8430343	137	138.8514
5	57	5	73		0.28	10	20	196.2	0.5058206	194.8	196.6465
5	65	5	81		0.36	12	24	235.44	0.4215172	219.1	221.7666
5	77	5	94		0.5	16	32	313.92	0.3161379	259	263.3679
				350	0.06	22	44	431.64	0.2299185	350	350.7136
				400	0.08	28	56	549.36	0.1806502	400	401.087
				450	0.1	34	68	667.08	0.1487708	450	451.528
				550	0.14	48	96	941.76	0.1053793	550	552.6128
				600	0.17	58	116	1137.96	0.0872104	600	603.4594
				650	0.2	64	128	1255.68	0.0790345	650	654.4068
				700	0.23	76	152	1491.12	0.0665553	700	705.4549
				800	0.32	90	180	1765.8	0.0562023	800	808.6606
				900	0.37	112	224	2197.44	0.0451626	900	911.2561
				1000	0.46	132	264	2589.84	0.0383197	1000	1015.526
				1100	0.54	156	312	3060.72	0.0324244	1100	1120.022
				1200	0.64	182	364	3570.84	0.0277923	1200	1225.844
				1300	0.73	208	416	4080.96	0.0243183	1300	1331.888
				1400	0.85	240	480	4708.8	0.0210759	1400	1439.907
				1600	0.99	320	640	6278.4	0.0158069	1600	1653

Wet Run

Recorded Data							Calculations				
Indirect Reading Rotameters				Direct Reading Rotameter Value (L/min)	Pressure at Rotameter Exit (psig)	Half of Manometer Reading (mm H20)	Manometer Reading (mm H20)	Manometer Pressure (Pa)	Pore Size (Diameter) (mm)	Indicated Airflow Rate (L/min)	True Airflow Rate (L/min)
First Rotameter Used		Second Rotameter Used									
Rotameter ID Number	Rotameter Value	Rotameter ID Number	Rotameter Value								
2	89				0	2	4	39.24	2.529103	1.886	1.886
4	8				0.03	4	8	78.48	1.2645515	2.43	2.432478
4	47				0.24	30	60	588.6	0.1686069	16.6	16.73496
5	46				0.21	38	76	745.56	0.1331107	68.3	68.78613
5	82				0.45	42	84	824.04	0.1204335	124	125.8837
5	51	5	64		0.35	46	92	902.52	0.109961	171.3	173.3273
5	77	5	95		0.64	58	116	1137.96	0.0872104	261	266.6211
				350	0.2	64	128	1255.68	0.0790345	350	352.3729
				400	0.23	74	148	1451.88	0.0683541	400	403.1171
				450	0.24	80	160	1569.6	0.0632276	450	453.6586
				500	0.27	88	176	1726.56	0.0574796	500	504.5709
				550	0.31	98	196	1922.76	0.0516143	550	555.7691
				600	0.33	108	216	2118.96	0.0468352	600	606.6973
				650	0.37	118	236	2315.16	0.0428662	650	658.1294
				700	0.4	130	260	2550.6	0.0389093	700	709.4599
				800	0.48	150	300	2943	0.0337214	800	812.9563
				900	0.56	170	340	3335.4	0.0297542	900	916.9826
				1000	0.6	196	392	3845.52	0.0258072	1000	1020.204
				1100	0.76	222	444	4355.64	0.0227847	1100	1128.077
				1200	0.85	254	508	4983.48	0.0199142	1200	1234.206
				1300	0.98	292	584	5729.04	0.0173226	1300	1342.634
				1400	1.09	324	648	6356.88	0.0156117	1400	1450.977
				1600	1.28	476	952	9339.12	0.0106265	1600	1668.206

Figure B.161: Drakeol-1 recorded data and calculations.

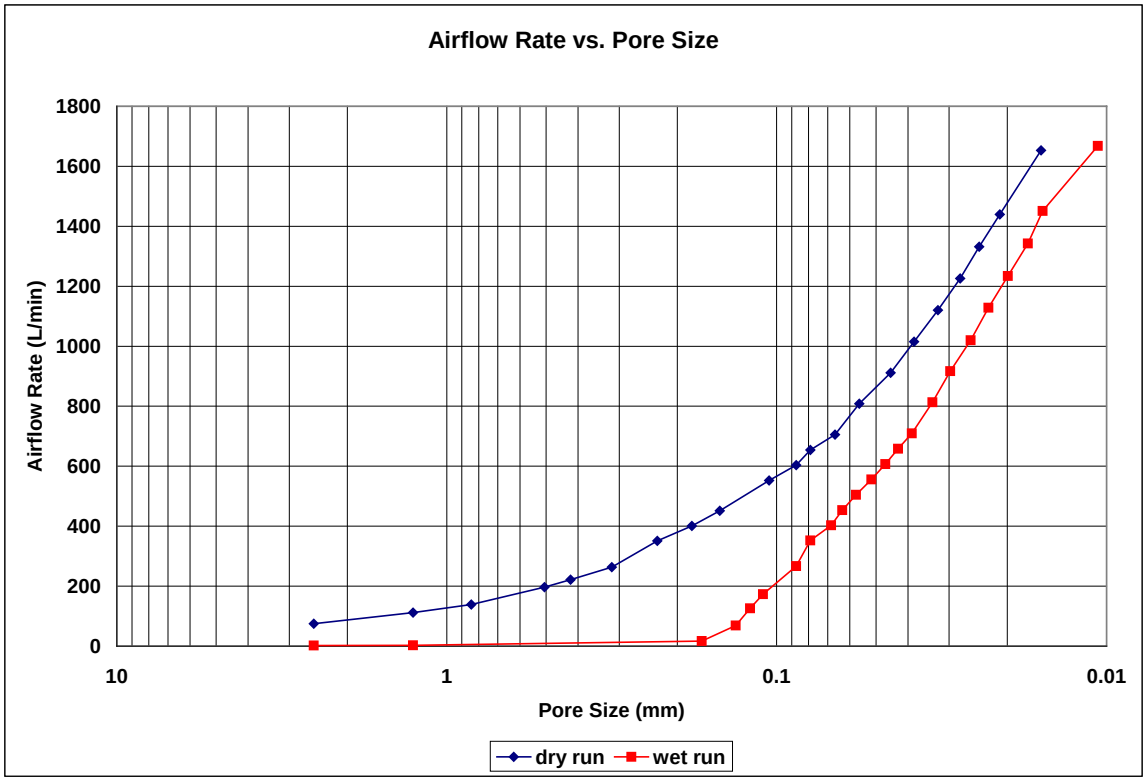

Figure B.162: Drakeol-1 airflow rate vs. pore size for the wet and dry runs.

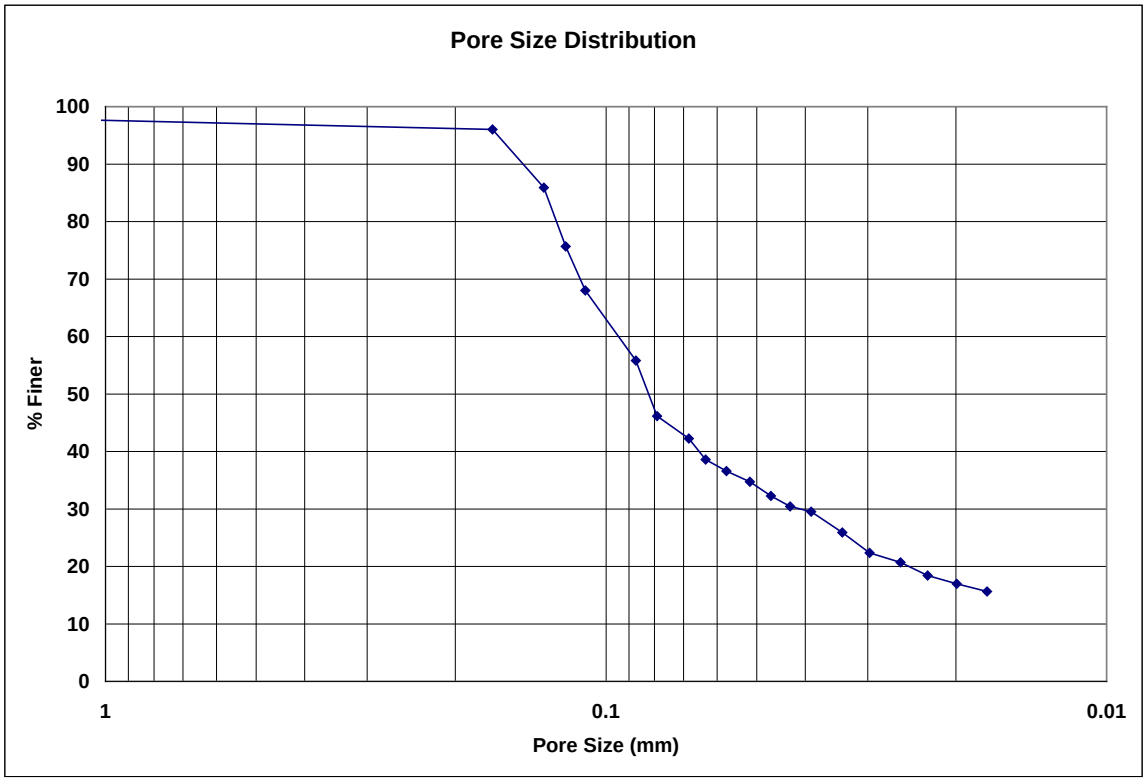

Figure B.163: Drakeol-1 pore size distribution.

Bubble Point Test
Auburn University - Department of Civil Engineering

date of test: 10/18/2006
test identification: drakeol 1
test performed by: David Hayes
wetting fluid: drakeol
air temperature: 22.5 °C
porous media: NG-1 nonwoven geotextile
comments: testing to determine geotextile pore size distribution

Pore Size Calculation Parameters:
constant, C: 2860 mm/m
contact angle: 0 degrees
surface tension: 0.0347 N/m

Pore Size at Selected % Finer

% finer	pore size (mm)
98	---
95	0.16504
90	0.14749
85	0.13199
80	0.12579
75	0.11951
70	0.11267
65	0.10433
60	0.09501
55	0.08652
50	0.08229
45	0.07587
40	0.06521
35	0.05250
30	0.04096
25	0.03272
20	0.02488
15	---
10	---
5	---

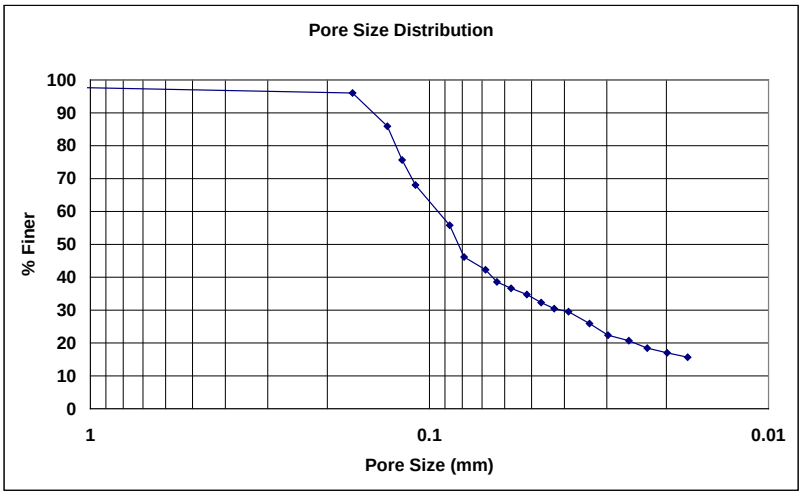

Figure B.164: Drakeol-1 pore size distribution report.

Bubble Point Test
Auburn University - Department of Civil Engineering

date of test: 10/4/2006
test identification: drakeol 2
test performed by: David Hayes
wetting fluid: Drakeol
ambient air temperature: 19.4 °C
porous media: NG-1 nonwoven geotextile
comments: testing to determine geotextile pore size distribution

Pore Size Calculation Parameters:
constant, C: 2860 mm/m
contact angle: 0 degrees
surface tension: 0.0347 N/m

Dry Run											
Recorded Data							Calculations				
Indirect Reading Rotameters				Direct Reading Rotameter Value (L/min)	Pressure at Rotameter Exit (psig)	Half of Manometer Reading (mm H20)	Manometer Reading (mm H20)	Manometer Pressure (Pa)	Pore Size (Diameter) (mm)	Indicated Airflow Rate (L/min)	True Airflow Rate (L/min)
First Rotameter Used		Second Rotameter Used									
Rotameter ID Number	Rotameter Value	Rotameter ID Number	Rotameter Value								
5	51				0.14	2	4	39.24	2.529103	75.7	76.05962
5	77				0.31	4	8	78.48	1.2645515	116	117.2167
5	96				0.48	6	12	117.72	0.8430343	146	148.3645
5	51	5	70		0.33	8	16	156.96	0.6322757	180.7	182.717
5	64	5	80		0.4	10	20	196.2	0.5058206	216.6	219.5272
5	77	5	95		0.56	14	28	274.68	0.3613004	261	265.925
				350	0.1	20	40	392.4	0.2529103	350	351.1885
				400	0.12	24	48	470.88	0.2107586	400	401.6293
				500	0.16	38	76	745.56	0.1331107	500	502.7137
				550	0.18	42	84	824.04	0.1204335	550	553.3571
				600	0.2	50	100	981	0.1011641	600	604.0678
				650	0.22	58	116	1137.96	0.0872104	650	654.8459
				700	0.25	66	132	1294.92	0.0766395	700	705.9273
				800	0.31	80	160	1569.6	0.0632276	800	808.3914
				900	0.37	96	192	1883.52	0.0526896	900	911.2561
				1000	0.43	112	224	2197.44	0.0451626	1000	1014.52
				1100	0.49	130	260	2550.6	0.0389093	1100	1118.183
				1200	0.58	154	308	3021.48	0.0328455	1200	1223.444
				1300	0.66	178	356	3492.36	0.0284169	1300	1328.863
				1400	0.74	200	400	3924	0.025291	1400	1434.805
				1600	0.92	228	456	4473.36	0.0221851	1600	1649.308

Wet Run											
Recorded Data							Calculations				
Indirect Reading Rotameters				Direct Reading Rotameter Value (L/min)	Pressure at Rotameter Exit (psig)	Half of Manometer Reading (mm H20)	Manometer Reading (mm H20)	Manometer Pressure (Pa)	Pore Size (Diameter) (mm)	Indicated Airflow Rate (L/min)	True Airflow Rate (L/min)
First Rotameter Used		Second Rotameter Used									
Rotameter ID Number	Rotameter Value	Rotameter ID Number	Rotameter Value								
2	89					2	4	39.24	2.529103	1.886	1.886
4	8				0.03	4	8	78.48	1.2645515	2.43	2.432478
4	21				0.11	22	44	431.64	0.2299185	6.8	6.825395
4	79				0.52	32	64	627.84	0.1580689	29.9	30.42425
5	44				0.19	36	72	706.32	0.1405057	65.3	65.72065
5	92				0.53	44	88	863.28	0.1149592	140	142.5015
5	61	5	75		0.44	50	100	981	0.1011641	203.9	206.9291
5	81	5	100		0.7	58	116	1137.96	0.0872104	275	281.4715
				350	0.2	64	128	1255.68	0.0790345	350	352.3729
				400	0.22	68	136	1334.16	0.0743854	400	402.9821
				450	0.25	80	160	1569.6	0.0632276	450	453.8104
				600	0.32	100	200	1962	0.0505821	600	606.4955
				650	0.35	112	224	2197.44	0.0451626	650	657.6926
				700	0.38	122	244	2393.64	0.0414607	700	708.9899
				800	0.46	138	276	2707.56	0.0366537	800	812.4206
				900	0.55	166	332	3256.92	0.0304711	900	916.6821
				1000	0.64	190	380	3727.8	0.0266221	1000	1021.537
				1100	0.72	216	432	4237.92	0.0234176	1100	1126.617
				1200	0.84	246	492	4826.52	0.0205618	1200	1233.809
				1300	0.94	278	556	5454.36	0.018195	1300	1340.921
				1400	1.06	312	624	6121.44	0.0162122	1400	1449.598

Figure B.165: Drakeol-2 recorded data and calculations.

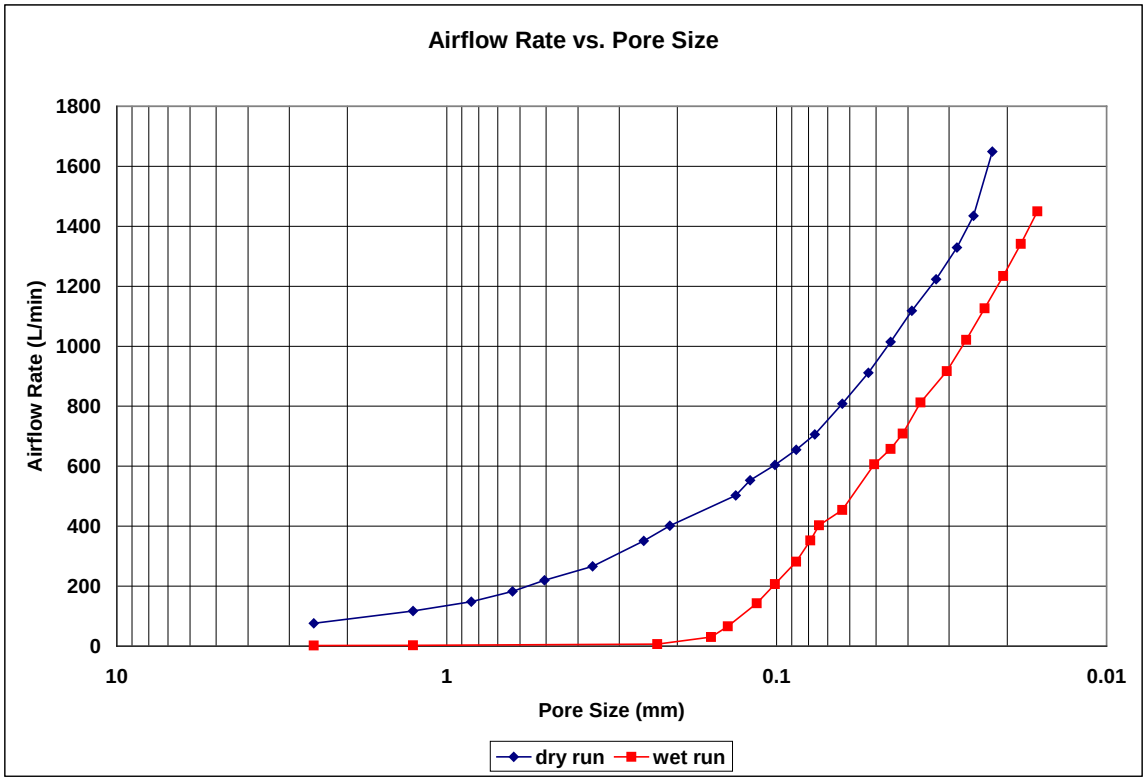

Figure B.166: Drakeol-2 airflow rate vs. pore size for the wet and dry runs.

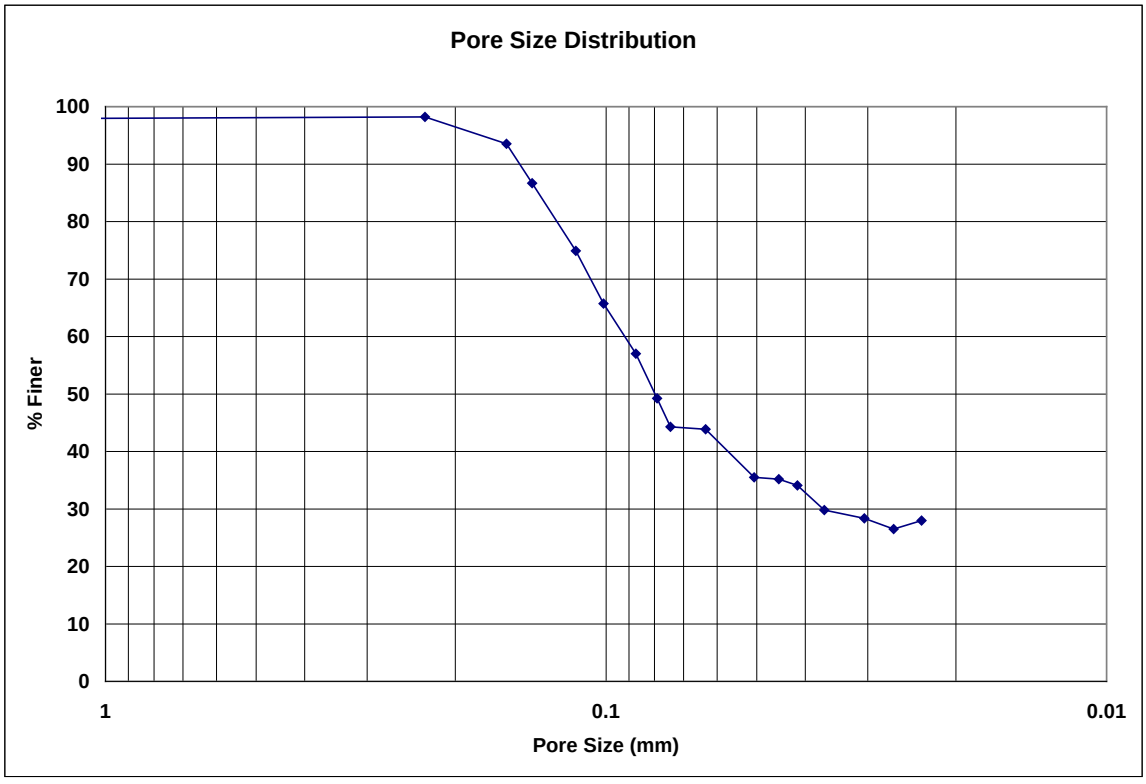

Figure B.167: Drakeol-2 pore size distribution.

Bubble Point Test
Auburn University - Department of Civil Engineering

date of test: 10/4/2006
test identification: drakeol 2
test performed by: David Hayes
wetting fluid: Drakeol
air temperature: 19.4 °C
porous media: NG-1 nonwoven geotextile
comments: testing to determine geotextile pore size distribution

Pore Size Calculation Parameters:
constant, C: 2860 mm/m
contact angle: 0 degrees
surface tension: 0.0347 N/m

Pore Size at Selected % Finer

% finer	pore size (mm)
98	0.22688
95	0.18070
90	0.14903
85	0.13688
80	0.12603
75	0.11517
70	0.10758
65	0.09997
60	0.09198
55	0.08509
50	0.07982
45	0.07506
40	0.05739
35	0.04457
30	0.03687
25	---
20	---
15	---
10	---
5	---

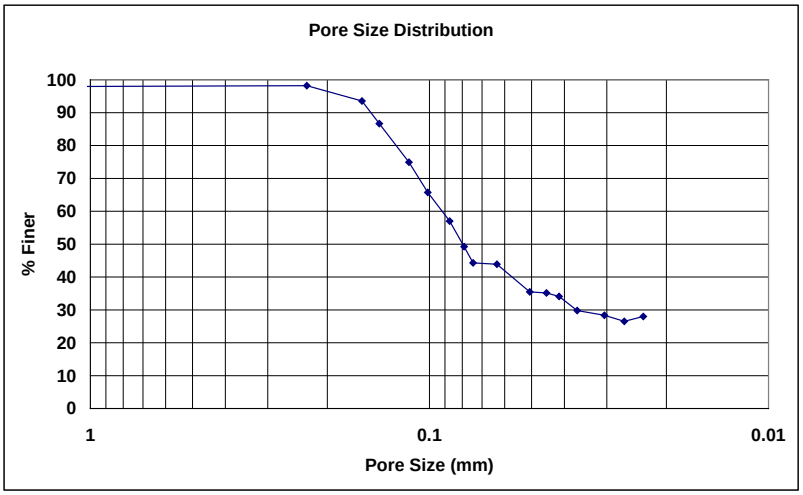

Figure B.168: Drakeol-2 pore size distribution report.

Bubble Point Test
Auburn University - Department of Civil Engineering

date of test: 10/2/2006
test identification: drakeol 3
test performed by: David Hayes
wetting fluid: Drakeol
ambient air temperature: 19.4 °C
porous media: NG-1 nonwoven geotextile
comments: testing to determine geotextile pore size distribution

Pore Size Calculation Parameters:
constant, C: 2860 mm/m
contact angle: 0 degrees
surface tension: 0.0347 N/m

Dry Run

Recorded Data							Calculations				
Indirect Reading Rotameters				Direct Reading Rotameter Value (L/min)	Pressure at Rotameter Exit (psig)	Half of Manometer Reading (mm H20)	Manometer Reading (mm H20)	Manometer Pressure (Pa)	Pore Size (Diameter) (mm)	Indicated Airflow Rate (L/min)	True Airflow Rate (L/min)
First Rotameter Used		Second Rotameter Used									
Rotameter ID Number	Rotameter Value	Rotameter ID Number	Rotameter Value								
5	63				0.16	2	4	39.24	2.529103	94	94.51018
5	89				0.36	4	8	78.48	1.2645515	135	136.6431
5	55	5	67		0.21	6	12	117.72	0.8430343	181.8	183.094
5	64	5	78		0.3	10	20	196.2	0.5058206	213.6	215.7686
5	82	5	99		0.51	14	28	274.68	0.3613004	275	279.7297
				350	0.03	18	36	353.16	0.2810114	350	350.357
				400	0.05	22	44	431.64	0.2299185	400	400.6797
				450	0.06	26	52	510.12	0.1945464	450	450.9174
				500	0.08	32	64	627.84	0.1580689	500	501.3587
				550	0.1	38	76	745.56	0.1331107	550	551.8676
				600	0.12	44	88	863.28	0.1149592	600	602.444
				650	0.13	48	96	941.76	0.1053793	650	652.8678
				700	0.16	58	116	1137.96	0.0872104	700	703.7992
				800	0.25	68	136	1334.16	0.0743854	800	806.774
				900	0.29	82	164	1608.84	0.0616854	900	908.8342
				1000	0.35	96	192	1883.52	0.0526896	1000	1011.835
				1100	0.41	114	228	2236.68	0.0443702	1100	1115.235
				1200	0.49	134	268	2629.08	0.0377478	1200	1219.836
				1300	0.57	152	304	2982.24	0.0332777	1300	1324.964
				1400	0.65	170	340	3335.4	0.0297542	1400	1430.618
				1600	0.74	240	480	4708.8	0.0210759	1600	1639.778

Wet Run

Recorded Data							Calculations				
Indirect Reading Rotameters				Direct Reading Rotameter Value (L/min)	Pressure at Rotameter Exit (psig)	Half of Manometer Reading (mm H20)	Manometer Reading (mm H20)	Manometer Pressure (Pa)	Pore Size (Diameter) (mm)	Indicated Airflow Rate (L/min)	True Airflow Rate (L/min)
First Rotameter Used		Second Rotameter Used									
Rotameter ID Number	Rotameter Value	Rotameter ID Number	Rotameter Value								
2	92					2	4	39.24	2.529103	1.953	1.953
4	9				0.02	4	8	78.48	1.2645515	2.74	2.741863
4	25				0.1	18	36	353.16	0.2810114	8.27	8.298082
4	32				0.15	26	52	510.12	0.1945464	10.9	10.95547
5	32				0.14	34	68	667.08	0.1487708	47.9	48.12755
5	93				0.53	44	88	863.28	0.1149592	141	143.5193
5	35	5	69		0.37	48	96	941.76	0.1053793	155.2	157.1411
5	72	5	88		0.56	54	108	1059.48	0.0936705	241	245.5476
				350	0.19	64	128	1255.68	0.0790345	350	352.2546
				400	0.2	68	136	1334.16	0.0743854	400	402.7119
				450	0.23	78	156	1530.36	0.0648488	450	453.5067
				500	0.25	84	168	1648.08	0.0602167	500	504.2338
				600	0.3	102	204	2001.24	0.0495903	600	606.0915
				650	0.33	112	224	2197.44	0.0451626	650	657.2554
				700	0.37	120	240	2354.4	0.0421517	700	708.7548
				800	0.42	138	276	2707.56	0.0366537	800	811.3481
				900	0.5	166	332	3256.92	0.0304711	900	915.1781
				1000	0.56	184	368	3610.08	0.0274902	1000	1018.87
				1100	0.65	204	408	4002.48	0.0247951	1100	1124.057
				1200	0.74	240	480	4708.8	0.0210759	1200	1229.833
				1300	0.84	272	544	5336.64	0.0185963	1300	1336.627
				1400	0.96	304	608	5964.48	0.0166388	1400	1444.991
				1600	1.22	424	848	8318.88	0.0119297	1600	1665.071

Figure B.169: Drakeol-3 recorded data and calculations.

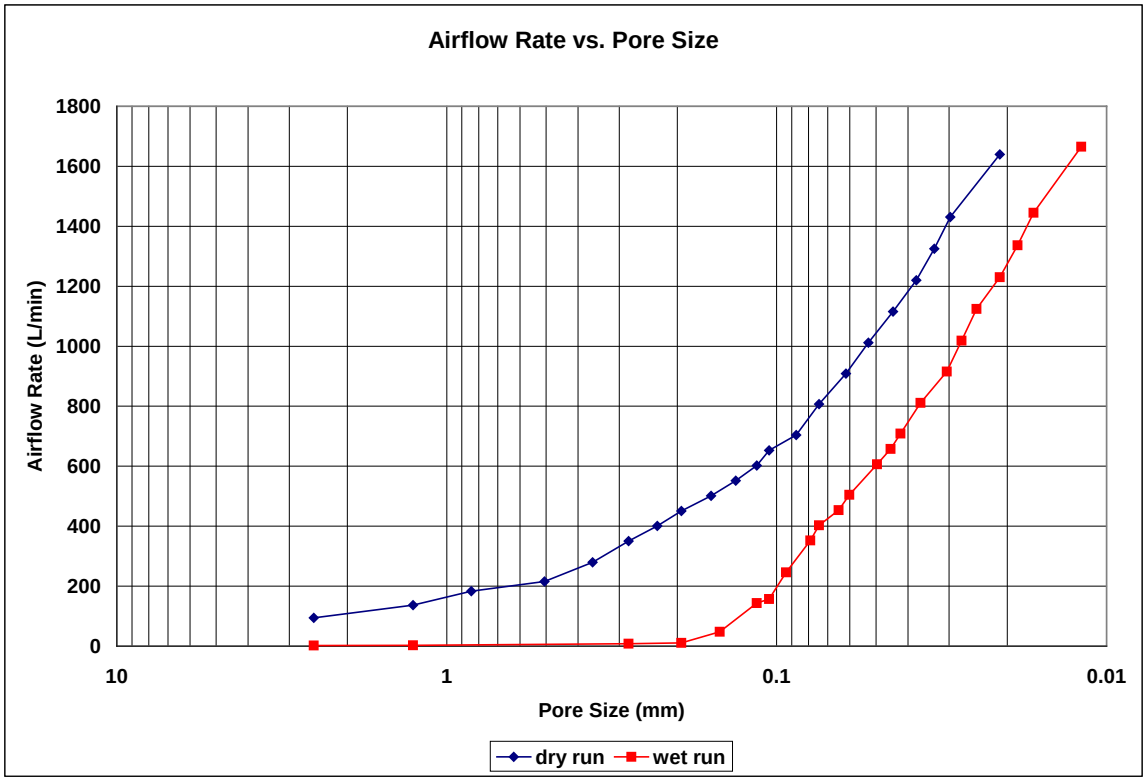

Figure B.170: Drakeol-3 airflow rate vs. pore size for the wet and dry runs.

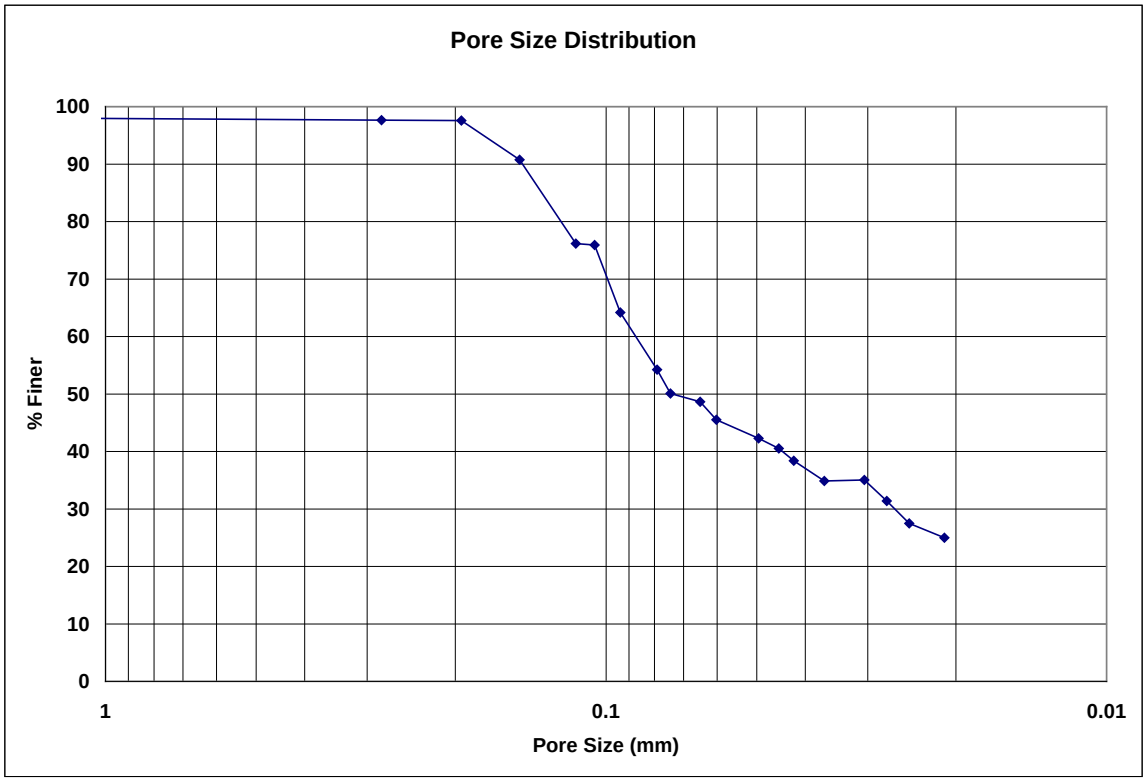

Figure B.171: Drakeol-3 pore size distribution.

Bubble Point Test
Auburn University - Department of Civil Engineering

date of test: 10/2/2006
test identification: drakeol 3
test performed by: David Hayes
wetting fluid: Drakeol
air temperature: 19.4 °C
porous media: NG-1 nonwoven geotextile
comments: testing to determine geotextile pore size distribution

Pore Size Calculation Parameters:
constant, C: 2860 mm/m
contact angle: 0 degrees
surface tension: 0.0347 N/m

Pore Size at Selected % Finer

% finer	pore size (mm)
98	---
95	0.17730
90	0.14704
85	0.13543
80	0.12383
75	0.10445
70	0.09946
65	0.09448
60	0.08752
55	0.08018
50	0.07382
45	0.05848
40	0.04441
35	0.03687
30	0.02653
25	---
20	---
15	---
10	---
5	---

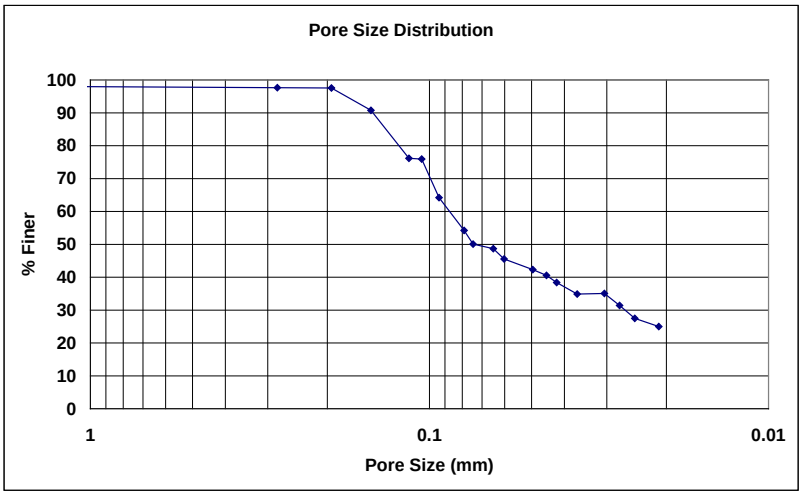

Figure B.172: Drakeol-3 pore size distribution report.

Bubble Point Test

Auburn University - Department of Civil Engineering

date of test: 10/4/2006
test identification: drakeol 4
test performed by: David Hayes
wetting fluid: Drakeol
ambient air temperature: 20 °C
porous media: NG-1 nonwoven geotextile
comments: testing to determine geotextile pore size distribution

Pore Size Calculation Parameters:
constant, C: 2860 mm/m
contact angle: 0 degrees
surface tension: 0.0347 N/m

Dry Run

Recorded Data							Calculations				
Indirect Reading Rotameters				Direct Reading Rotameter Value (L/min)	Pressure at Rotameter Exit (psig)	Half of Manometer Reading (mm H20)	Manometer Reading (mm H20)	Manometer Pressure (Pa)	Pore Size (Diameter) (mm)	Indicated Airflow Rate (L/min)	True Airflow Rate (L/min)
First Rotameter Used		Second Rotameter Used									
Rotameter ID Number	Rotameter Value	Rotameter ID Number	Rotameter Value								
5	52				0.14	2	4	39.24	2.529103	77.2	77.56675
5	86				0.32	4	8	78.48	1.2645515	130	131.4073
5	51	5	63		0.22	6	12	117.72	0.8430343	169.7	170.9651
5	68	5	85		0.4	10	20	196.2	0.5058206	231	234.1218
5	76	5	94		0.5	12	24	235.44	0.4215172	257	261.3342
				350	0.08	18	36	353.16	0.2810114	350	350.9511
				400	0.09	22	44	431.64	0.2299185	400	401.2226
				450	0.1	26	52	510.12	0.1945464	450	451.528
				550	0.14	36	72	706.32	0.1405057	550	552.6128
				600	0.16	42	84	824.04	0.1204335	600	603.2565
				650	0.17	48	96	941.76	0.1053793	650	653.7477
				700	0.19	54	108	1059.48	0.0936705	700	704.5093
				800	0.27	68	136	1334.16	0.0743854	800	807.3135
				900	0.32	82	164	1608.84	0.0616854	900	909.7432
				1000	0.38	98	196	1922.76	0.0516143	1000	1012.843
				1100	0.44	114	228	2236.68	0.0443702	1100	1116.341
				1200	0.52	132	264	2589.84	0.0383197	1200	1221.04
				1300	0.59	154	308	3021.48	0.0328455	1300	1325.832
				1400	0.67	170	340	3335.4	0.0297542	1400	1431.549
				1600	0.77	244	488	4787.28	0.0207304	1600	1641.37

Wet Run

Recorded Data							Calculations				
Indirect Reading Rotameters				Direct Reading Rotameter Value (L/min)	Pressure at Rotameter Exit (psig)	Half of Manometer Reading (mm H20)	Manometer Reading (mm H20)	Manometer Pressure (Pa)	Pore Size (Diameter) (mm)	Indicated Airflow Rate (L/min)	True Airflow Rate (L/min)
First Rotameter Used		Second Rotameter Used									
Rotameter ID Number	Rotameter Value	Rotameter ID Number	Rotameter Value								
2	81					2	4	39.24	2.529103	1.7	1.7
4	9				0.02	4	8	78.48	1.2645515	2.74	2.741863
4	13				0.04	8	16	156.96	0.6322757	4.07	4.075534
4	23				0.1	20	40	392.4	0.2529103	7.54	7.565603
4	97				0.73	32	64	627.84	0.1580689	37.8	38.7272
5	55				0.16	36	72	706.32	0.1405057	81.8	82.24397
5	97				0.35	42	84	824.04	0.1204335	148	149.7515
5	78	5	91		0.58	50	100	981	0.1011641	256	261.0015
				350	0.18	58	116	1137.96	0.0872104	350	352.1363
				400	0.2	64	128	1255.68	0.0790345	400	402.7119
				450	0.23	72	144	1412.64	0.0702529	450	453.5067
				500	0.24	76	152	1491.12	0.0665553	500	504.0651
				650	0.33	100	200	1962	0.0505821	650	657.2554
				700	0.36	108	216	2118.96	0.0468352	700	708.5196
				800	0.45	126	252	2472.12	0.0401445	800	812.1526
				900	0.51	144	288	2825.28	0.0351264	900	915.4791
				1000	0.59	166	332	3256.92	0.0304711	1000	1019.871
				1100	0.65	186	372	3649.32	0.0271947	1100	1124.057
				1200	0.76	214	428	4198.68	0.0236365	1200	1230.63
				1300	0.86	242	484	4748.04	0.0209017	1300	1337.487
				1400	0.96	270	540	5297.4	0.0187341	1400	1444.991

Figure B.173: Drakeol-4 recorded data and calculations.

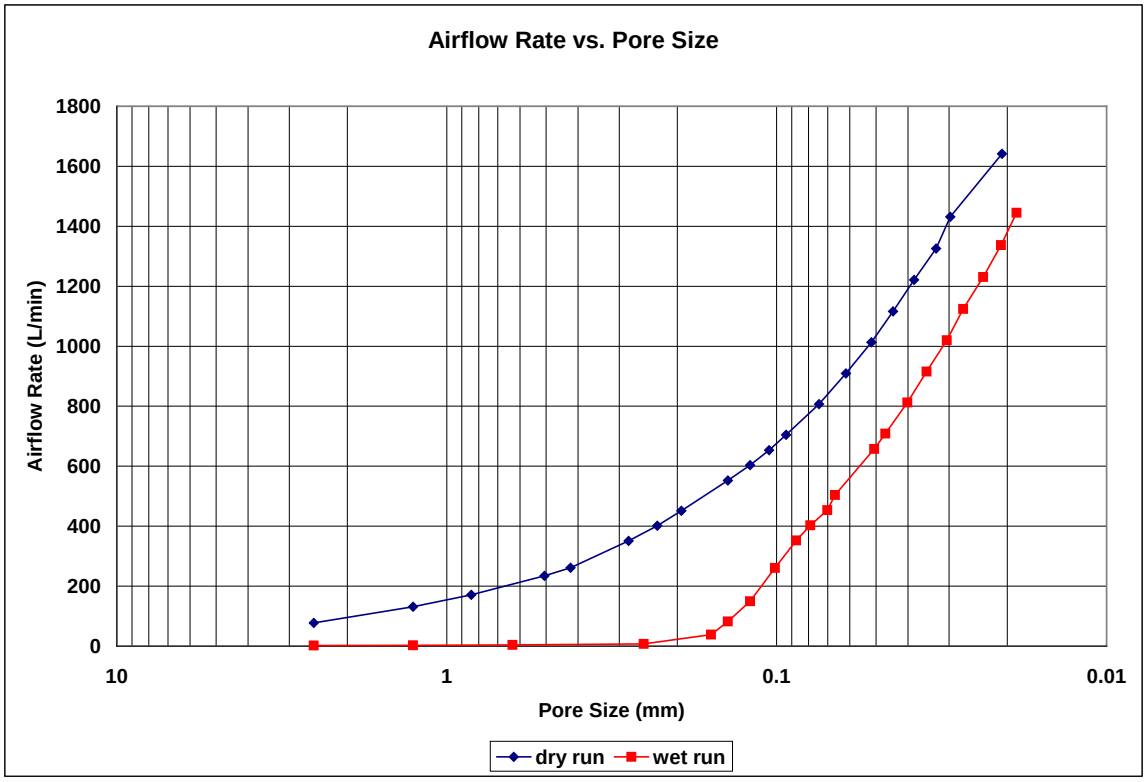

Figure B.174: Drakeol-4 airflow rate vs. pore size for the wet and dry runs.

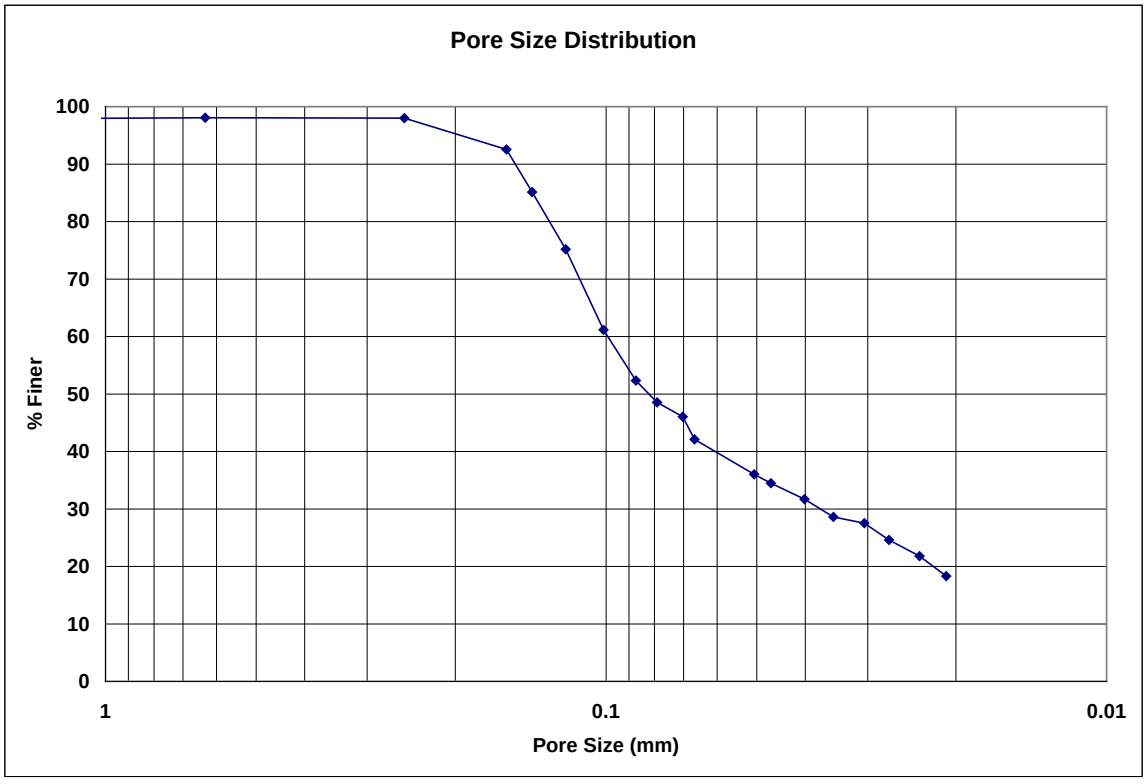

Figure B.175: Drakeol-4 pore size distribution.

Bubble Point Test
Auburn University - Department of Civil Engineering

date of test: 10/4/2006
test identification: drakeol 4
test performed by: David Hayes
wetting fluid: Drakeol
air temperature: 20 °C
porous media: NG-1 nonwoven geotextile
comments: testing to determine geotextile pore size distribution

Pore Size Calculation Parameters:
constant, C: 2860 mm/m
contact angle: 0 degrees
surface tension: 0.0347 N/m

Pore Size at Selected % Finer

% finer	pore size (mm)
98	0.25288
95	0.20070
90	0.15204
85	0.14027
80	0.13017
75	0.12019
70	0.11332
65	0.10644
60	0.09933
55	0.09141
50	0.08217
45	0.06927
40	0.06103
35	0.04811
30	0.03738
25	0.02763
20	0.02222
15	---
10	---
5	---

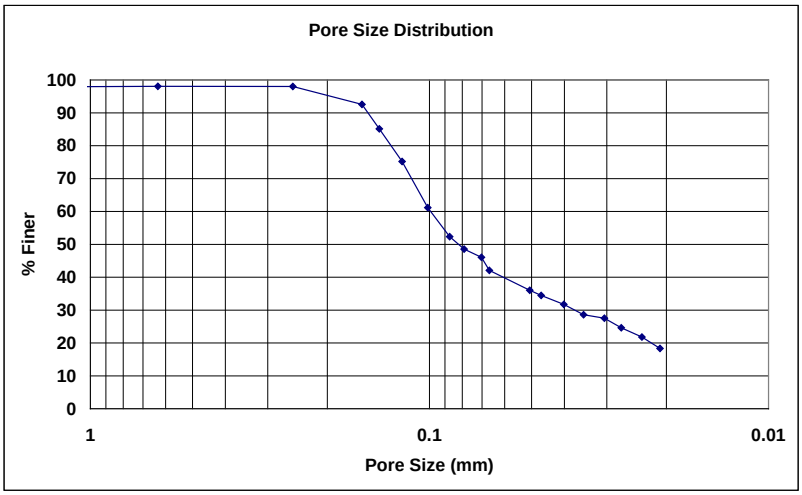

Figure B.176: Drakeol-4 pore size distribution report.

Bubble Point Test

Auburn University - Department of Civil Engineering

date of test: 10/18/2006
test identification: drakeol 5
test performed by: David Hayes
wetting fluid: drakeol
ambient air temperature: 22.5 °C
porous media: NG-1 nonwoven geotextile
comments: testing to determine geotextile pore size distribution

Pore Size Calculation Parameters:
constant, C: 2860 mm/m
contact angle: 0 degrees
surface tension: 0.0347 N/m

Dry Run

Recorded Data							Calculations				
Indirect Reading Rotameters				Direct Reading Rotameter Value (L/min)	Pressure at Rotameter Exit (psig)	Half of Manometer Reading (mm H20)	Manometer Reading (mm H20)	Manometer Pressure (Pa)	Pore Size (Diameter) (mm)	Indicated Airflow Rate (L/min)	True Airflow Rate (L/min)
First Rotameter Used		Second Rotameter Used									
Rotameter ID Number	Rotameter Value	Rotameter ID Number	Rotameter Value								
5	43				0.08	2	4	39.24	2.529103	63.8	63.97337
5	73				0.25	4	8	78.48	1.2645515	110	110.9314
5	85				0.36	6	12	117.72	0.8430343	129	130.57
5	57	5	71		0.3	10	20	196.2	0.5058206	190.8	192.7371
5	72	5	95		0.52	16	32	313.92	0.3161379	253	257.4359
				350	0.06	22	44	431.64	0.2299185	350	350.7136
				400	0.08	28	56	549.36	0.1806502	400	401.087
				450	0.09	34	68	667.08	0.1487708	450	451.3754
				550	0.14	48	96	941.76	0.1053793	550	552.6128
				600	0.16	56	112	1098.72	0.0903251	600	603.2565
				650	0.19	64	128	1255.68	0.0790345	650	654.1872
				700	0.22	72	144	1412.64	0.0702529	700	705.2186
				800	0.32	88	176	1726.56	0.0574796	800	808.6606
				900	0.38	106	212	2079.72	0.0477189	900	911.5584
				1000	0.47	128	256	2511.36	0.0395172	1000	1015.861
				1100	0.53	148	296	2903.76	0.0341771	1100	1119.654
				1200	0.63	172	344	3374.64	0.0294082	1200	1225.445
				1300	0.72	196	392	3845.52	0.0258072	1300	1331.456
				1400	0.81	222	444	4355.64	0.0227847	1400	1438.054
				1600	0.97	302	604	5925.24	0.016749	1600	1651.946

Wet Run

Recorded Data							Calculations				
Indirect Reading Rotameters				Direct Reading Rotameter Value (L/min)	Pressure at Rotameter Exit (psig)	Half of Manometer Reading (mm H20)	Manometer Reading (mm H20)	Manometer Pressure (Pa)	Pore Size (Diameter) (mm)	Indicated Airflow Rate (L/min)	True Airflow Rate (L/min)
First Rotameter Used		Second Rotameter Used									
Rotameter ID Number	Rotameter Value	Rotameter ID Number	Rotameter Value								
2	89					2	4	39.24	2.529103	1.886	1.886
4	12				0.04	8	16	156.96	0.6322757	3.74	3.745085
4	17				0.07	14	28	274.68	0.3613004	5.41	5.422866
4	20				0.09	20	40	392.4	0.2529103	6.44	6.459684
4	26				0.13	26	52	510.12	0.1945464	8.64	8.67812
4	51				0.25	30	60	588.6	0.1686069	18.2	18.35411
5	54				0.25	36	72	706.32	0.1405057	80.3	80.97994
5	80				0.41	42	84	824.04	0.1204335	121	122.6758
5	58	5	72		0.39	46	92	902.52	0.109961	194.3	196.8606
5	73	5	98		0.65	56	112	1098.72	0.0903251	259	264.6643
				400	0.22	68	136	1334.16	0.0743854	400	402.9821
				450	0.24	80	160	1569.6	0.0632276	450	453.6586
				500	0.26	84	168	1648.08	0.0602167	500	504.4024
				550	0.29	92	184	1805.04	0.0549805	550	555.3987
				600	0.32	102	204	2001.24	0.0495903	600	606.4955
				650	0.36	112	224	2197.44	0.0451626	650	657.911
				700	0.38	122	244	2393.64	0.0414607	700	708.9899
				800	0.46	140	280	2746.8	0.03613	800	812.4206
				900	0.53	158	316	3099.96	0.032014	900	916.0808
				1000	0.6	182	364	3570.84	0.0277923	1000	1020.204
				1100	0.71	210	420	4120.2	0.0240867	1100	1126.251
				1200	0.79	232	464	4551.84	0.0218026	1200	1231.823
				1300	0.92	268	536	5258.16	0.0188739	1300	1340.063
				1400	1.03	300	600	5886	0.0168607	1400	1448.217
				1600	1.22	402	804	7887.24	0.0125826	1600	1665.071

Figure B.177: Drakeol-5 recorded data and calculations.

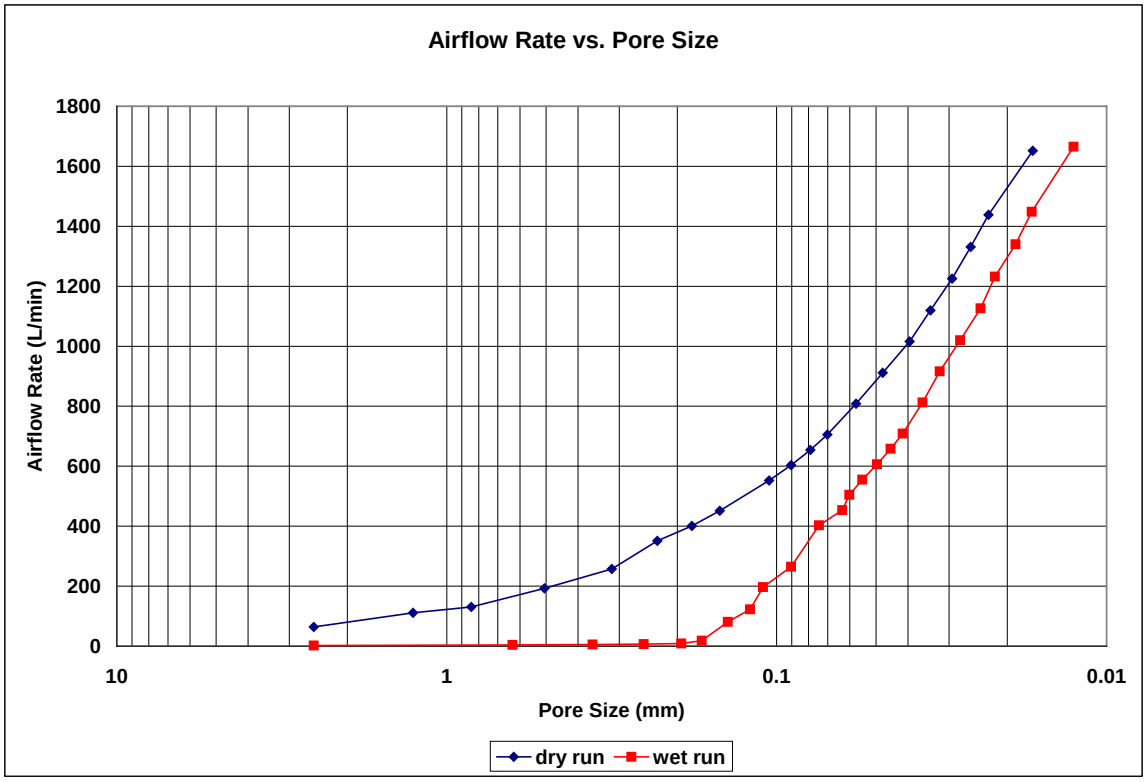

Figure B.178: Drakeol-5 airflow rate vs. pore size for the wet and dry runs.

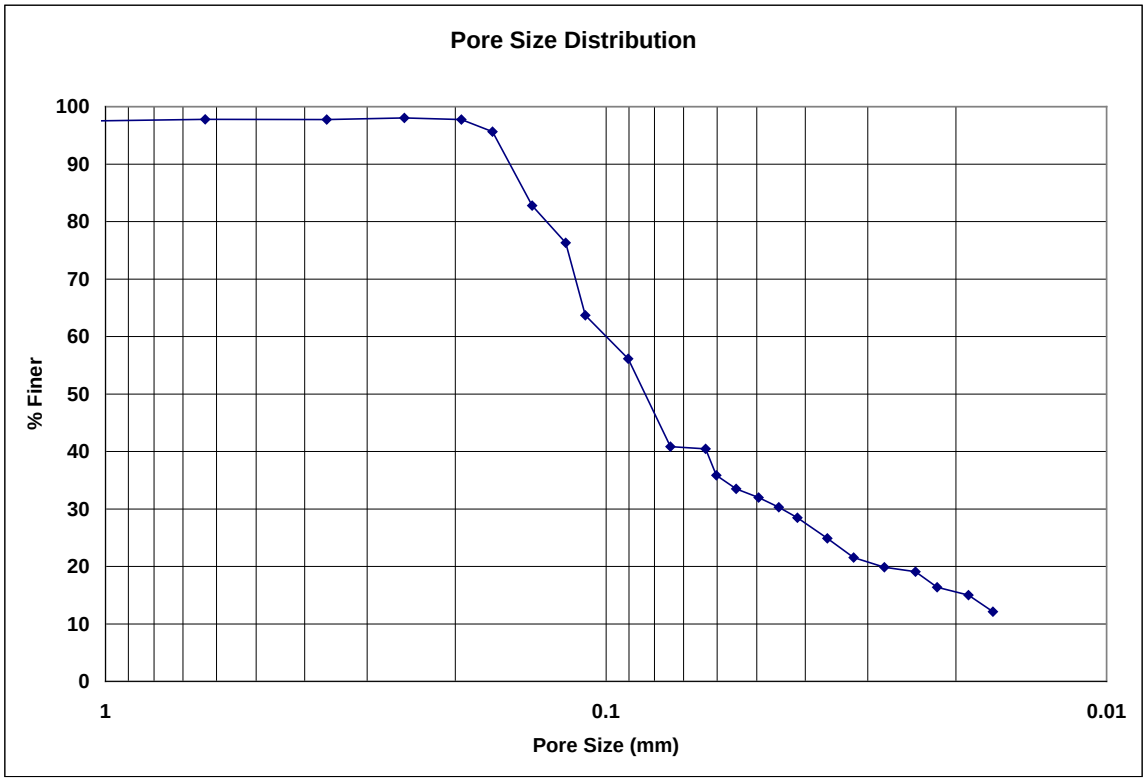

Figure B.179: Drakeol-5 pore size distribution.

Bubble Point Test
Auburn University - Department of Civil Engineering

date of test:	10/18/2006	Pore Size Calculation Parameters:	
test identification:	drakeol 5	constant, C:	2860 mm/m
test performed by:	David Hayes	contact angle:	0 degrees
wetting fluid:	drakeol	surface tension:	0.0347 N/m
air temperature:	22.5 °C		
porous media:	NG-1 nonwoven geotextile		
comments:	testing to determine geotextile pore size distribution		

Pore Size at Selected % Finer

% finer	pore size (mm)
98	0.24899
95	0.16723
90	0.15628
85	0.14533
80	0.13188
75	0.11936
70	0.11521
65	0.11106
60	0.10040
55	0.08915
50	0.08394
45	0.07872
40	0.06292
35	0.05831
30	0.04454
25	0.03629
20	0.02815
15	0.01887
10	---
5	---

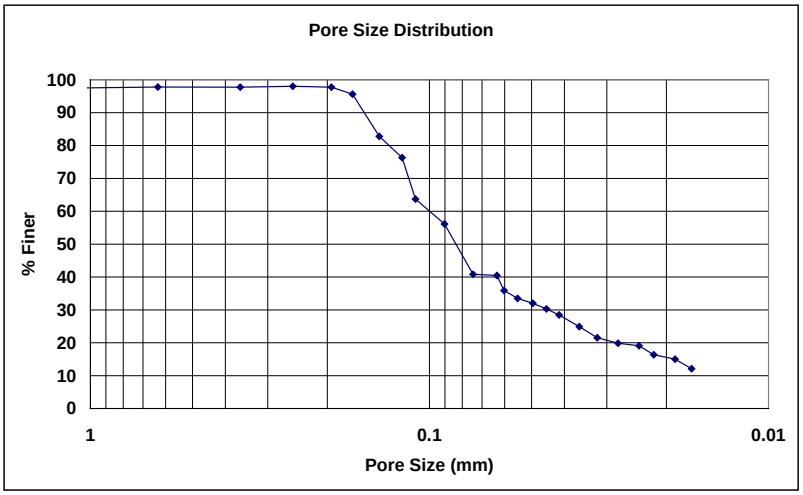

Figure B.180: Drakeol-5 pore size distribution report.

Bubble Point Test
Auburn University - Department of Civil Engineering

date of test: 10/18/2006
test identification: drakeol 6
test performed by: David Hayes
wetting fluid: Drakeol
ambient air temperature: 22.5 °C
porous media: NG-1 nonwoven geotextile
comments: testing to determine geotextile pore size distribution

Pore Size Calculation Parameters:
constant, C: 2860 mm/m
contact angle: 0 degrees
surface tension: 0.0347 N/m

Dry Run											
Recorded Data							Calculations				
Indirect Reading Rotameters				Direct Reading Rotameter Value (L/min)	Pressure at Rotameter Exit (psig)	Half of Manometer Reading (mm H20)	Manometer Reading (mm H20)	Manometer Pressure (Pa)	Pore Size (Diameter) (mm)	Indicated Airflow Rate (L/min)	True Airflow Rate (L/min)
First Rotameter Used		Second Rotameter Used									
Rotameter ID Number	Rotameter Value	Rotameter ID Number	Rotameter Value								
5	51				0.11	2	4	39.24	2.529103	75.7	75.9827
5	80				0.3	4	8	78.48	1.2645515	121	122.2285
5	59	5	73		0.27	8	16	156.96	0.6322757	197.9	199.7092
5	70	5	86		0.4	10	20	196.2	0.5058206	235	238.1758
				350	0.05	18	36	353.16	0.2810114	350	350.5947
				400	0.07	22	44	431.64	0.2299185	400	400.9512
				450	0.08	26	52	510.12	0.1945464	450	451.2228
				550	0.12	36	72	706.32	0.1405057	550	552.2403
				600	0.14	42	84	824.04	0.1204335	600	602.8504
				650	0.16	48	96	941.76	0.1053793	650	653.5278
				700	0.18	56	112	1098.72	0.0903251	700	704.2727
				800	0.22	68	136	1334.16	0.0743854	800	805.9642
				900	0.27	82	164	1608.84	0.0616854	900	908.2277
				1000	0.33	100	200	1962	0.0505821	1000	1011.162
				1100	0.39	116	232	2275.92	0.0436052	1100	1114.496
				1200	0.52	136	272	2668.32	0.0371927	1200	1221.04
				1300	0.58	158	316	3099.96	0.032014	1300	1325.398
				1400	0.67	174	348	3413.88	0.0290701	1400	1431.549

Wet Run											
Recorded Data							Calculations				
Indirect Reading Rotameters				Direct Reading Rotameter Value (L/min)	Pressure at Rotameter Exit (psig)	Half of Manometer Reading (mm H20)	Manometer Reading (mm H20)	Manometer Pressure (Pa)	Pore Size (Diameter) (mm)	Indicated Airflow Rate (L/min)	True Airflow Rate (L/min)
First Rotameter Used		Second Rotameter Used									
Rotameter ID Number	Rotameter Value	Rotameter ID Number	Rotameter Value								
2	79					2	4	39.24	2.529103	1.652	1.652
4	8				0.01	4	8	78.48	1.2645515	2.43	2.430826
4	11				0.02	6	12	117.72	0.8430343	3.41	3.412319
4	23				0.1	22	44	431.64	0.2299185	7.54	7.565603
4	95				0.69	30	60	588.6	0.1686069	36.9	37.75609
5	52				0.2	32	64	627.84	0.1580689	77.2	77.7234
5	52	5	63		0.34	40	80	784.8	0.1264551	171.2	173.1685
5	70	5	87		0.54	46	92	902.52	0.109961	237	241.3138
				350	0.15	50	100	981	0.1011641	350	351.7812
				400	0.17	58	116	1137.96	0.0872104	400	402.3063
				450	0.19	69	138	1353.78	0.0733073	450	452.8988
				550	0.24	78	156	1530.36	0.0648488	550	554.4716
				600	0.26	84	168	1648.08	0.0602167	600	605.2829
				650	0.29	92	184	1805.04	0.0549805	650	656.3803
				700	0.31	100	200	1962	0.0505821	700	707.3424
				800	0.38	110	220	2158.2	0.0459837	800	810.2742
				900	0.45	130	260	2550.6	0.0389093	900	913.6717
				1000	0.53	150	300	2943	0.0337214	1000	1017.868
				1100	0.6	170	340	3335.4	0.0297542	1100	1122.224
				1200	0.69	192	384	3767.04	0.0263448	1200	1227.84
				1300	0.78	220	440	4316.4	0.0229918	1300	1334.044
				1400	0.87	244	488	4787.28	0.0207304	1400	1440.833
				1600	1	316	632	6199.92	0.016007	1600	1653.526

Figure B.181: Drakeol-6 recorded data and calculations.

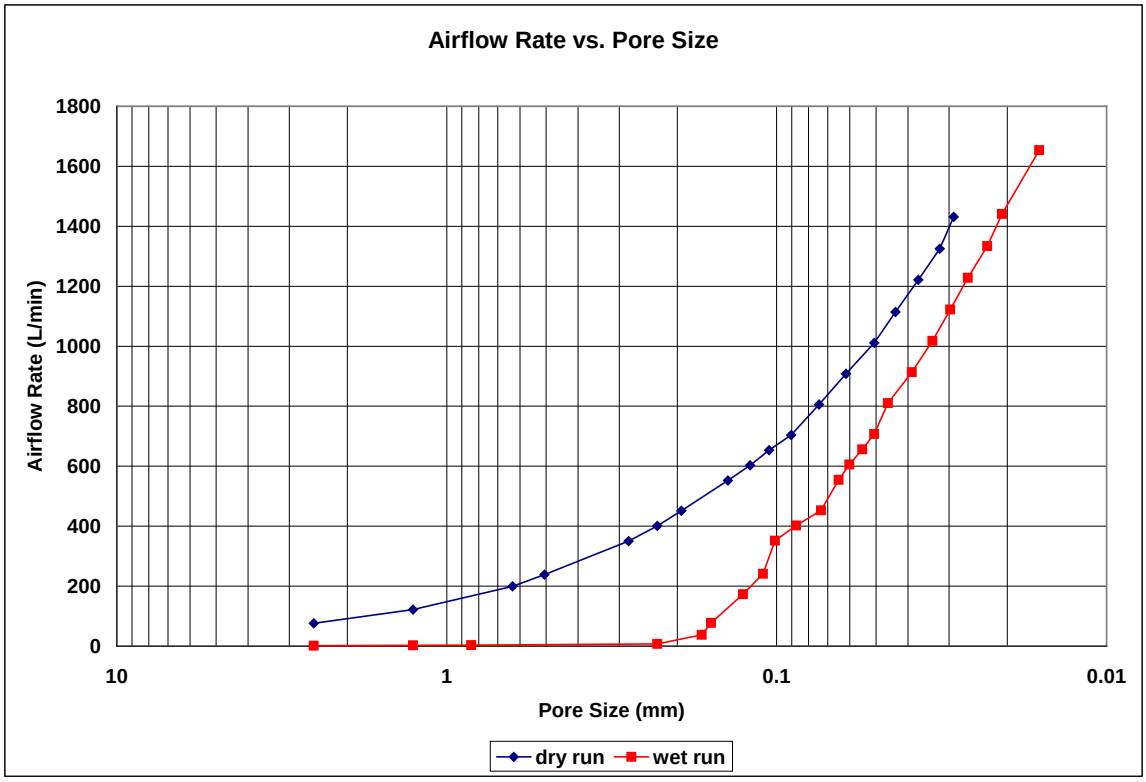

Figure B.182: Drakeol-6 airflow rate vs. pore size for the wet and dry runs.

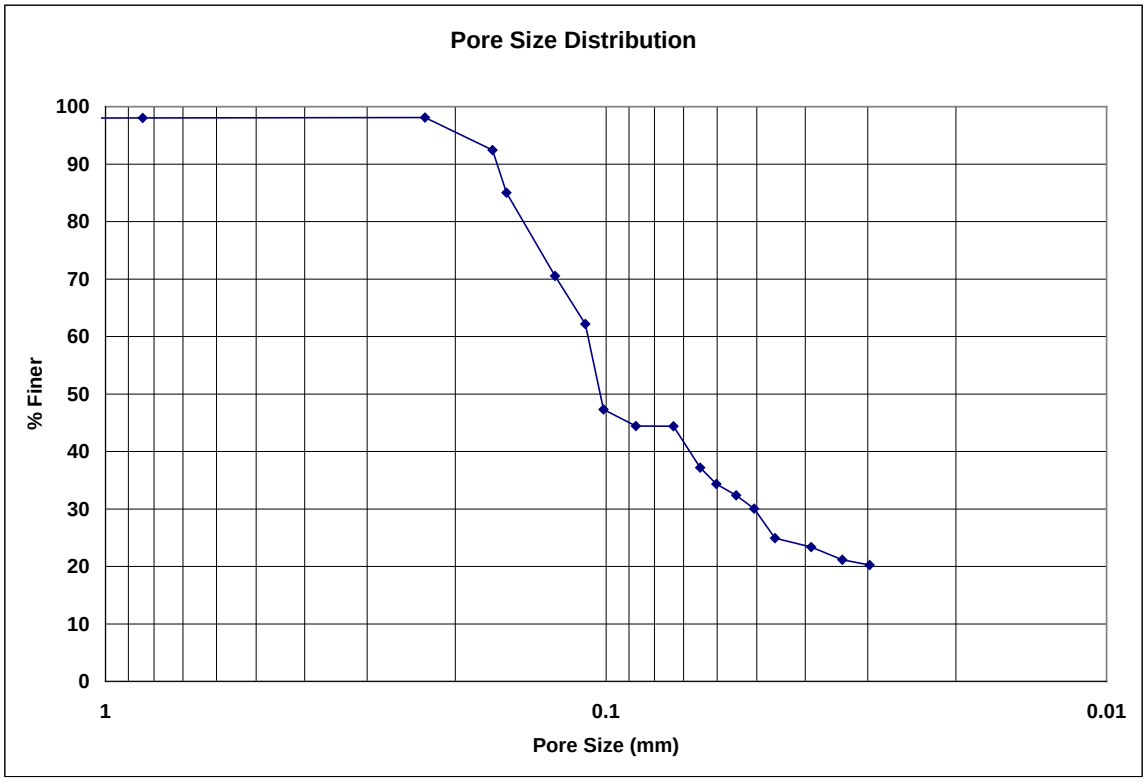

Figure B.183: Drakeol-6 pore size distribution.

Bubble Point Test
Auburn University - Department of Civil Engineering

date of test: 10/18/2006
test identification: drakeol 6
test performed by: David Hayes
wetting fluid: Drakeol
air temperature: 22.5 °C
porous media: NG-1 nonwoven geotextile
comments: testing to determine geotextile pore size distribution

Pore Size Calculation Parameters:
constant, C: 2860 mm/m
contact angle: 0 degrees
surface tension: 0.0347 N/m

Pore Size at Selected % Finer

% finer	pore size (mm)
98	0.22870
95	0.19625
90	0.16513
85	0.15799
80	0.14709
75	0.13619
70	0.12540
65	0.11553
60	0.10867
55	0.10571
50	0.10275
45	0.08991
40	0.06814
35	0.06129
30	0.05054
25	0.04605
20	---
15	---
10	---
5	---

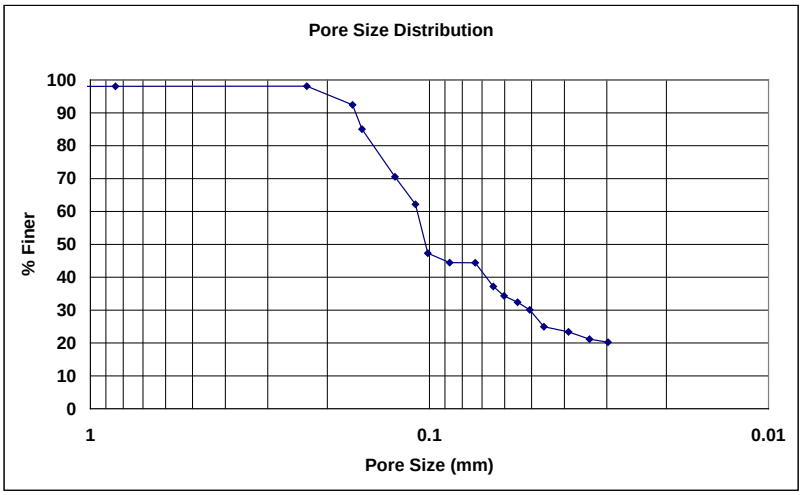

Figure B.184: Drakeol-6 pore size distribution report.

Bubble Point Test
Auburn University - Department of Civil Engineering

date of test: 10/18/2006
test identification: drakeol 7
test performed by: David Hayes
wetting fluid: Drakeol
ambient air temperature: 22.5 °C
porous media: NG-1 nonwoven geotextile
comments: testing to determine geotextile pore size distribution

Pore Size Calculation Parameters:
constant, C: 2860 mm/m
contact angle: 0 degrees
surface tension: 0.0347 N/m

Dry Run

Recorded Data							Calculations				
Indirect Reading Rotameters				Direct Reading Rotameter Value (L/min)	Pressure at Rotameter Exit (psig)	Half of Manometer Reading (mm H20)	Manometer Reading (mm H20)	Manometer Pressure (Pa)	Pore Size (Diameter) (mm)	Indicated Airflow Rate (L/min)	True Airflow Rate (L/min)
First Rotameter Used		Second Rotameter Used									
Rotameter ID Number	Rotameter Value	Rotameter ID Number	Rotameter Value								
5	45				0.09	2	4	39.24	2.529103	66.8	67.00418
5	72				0.25	4	8	78.48	1.2645515	108	108.9145
5	88				0.38	6	12	117.72	0.8430343	133	134.7081
5	61	5	75		0.33	10	20	196.2	0.5058206	203.9	206.176
5	68	5	83		0.4	12	24	235.44	0.4215172	227	230.0677
5	80	5	100		0.57	16	32	313.92	0.3161379	274	279.2617
				350	0.05	20	40	392.4	0.2529103	350	350.5947
				400	0.07	26	52	510.12	0.1945464	400	400.9512
				450	0.08	32	64	627.84	0.1580689	450	451.2228
				550	0.12	44	88	863.28	0.1149592	550	552.2403
				600	0.15	52	104	1020.24	0.0972732	600	603.0535
				650	0.17	58	116	1137.96	0.0872104	650	653.7477
				700	0.2	66	132	1294.92	0.0766395	700	704.7458
				800	0.29	84	168	1648.08	0.0602167	800	807.8526
				900	0.35	100	200	1962	0.0505821	900	910.6513
				1000	0.41	120	240	2354.4	0.0421517	1000	1013.85
				1100	0.5	141	282	2766.42	0.0358738	1100	1118.551
				1200	0.59	166	332	3256.92	0.0304711	1200	1223.845
				1300	0.69	170	340	3335.4	0.0297542	1300	1330.16
				1400	0.78	214	428	4198.68	0.0236365	1400	1436.663
				1600	0.91	290	580	5689.8	0.0174421	1600	1648.78

Wet Run

Recorded Data							Calculations				
Indirect Reading Rotameters				Direct Reading Rotameter Value (L/min)	Pressure at Rotameter Exit (psig)	Half of Manometer Reading (mm H20)	Manometer Reading (mm H20)	Manometer Pressure (Pa)	Pore Size (Diameter) (mm)	Indicated Airflow Rate (L/min)	True Airflow Rate (L/min)
First Rotameter Used		Second Rotameter Used									
Rotameter ID Number	Rotameter Value	Rotameter ID Number	Rotameter Value								
2	89				0	2	4	39.24	2.529103	1.886	1.886
4	8				0.03	4	8	78.48	1.2645515	2.43	2.432478
4	11				0.03	6	12	117.72	0.8430343	3.41	3.413478
4	23				0.11	22	44	431.64	0.2299185	7.54	7.568158
5	31				0.12	32	64	627.84	0.1580689	46.4	46.589
5	72				0.34	40	80	784.8	0.1264551	108	109.2418
5	67	5	82		0.48	50	100	981	0.1011641	224	227.6278
5	81	5	100		0.67	56	112	1098.72	0.0903251	275	281.1972
				350	0.16	58	116	1137.96	0.0872104	350	351.8996
				400	0.19	66	132	1294.92	0.0766395	400	402.5767
				450	0.21	72	144	1412.64	0.0702529	450	453.2029
				500	0.23	80	160	1569.6	0.0632276	500	503.8964
				550	0.26	88	176	1726.56	0.0574796	550	554.8426
				600	0.28	96	192	1883.52	0.0526896	600	605.6873
				650	0.32	106	212	2079.72	0.0477189	650	657.0367
				700	0.35	116	232	2275.92	0.0436052	700	708.2843
				800	0.41	128	256	2511.36	0.0395172	800	811.0797
				900	0.49	150	300	2943	0.0337214	900	914.877
				1000	0.57	170	340	3335.4	0.0297542	1000	1019.203
				1100	0.65	192	384	3767.04	0.0263448	1100	1124.057
				1200	0.76	220	440	4316.4	0.0229918	1200	1230.63
				1300	0.84	248	496	4865.76	0.020396	1300	1336.627
				1400	0.97	280	560	5493.6	0.018065	1400	1445.453
				1600	1.11	366	732	7180.92	0.0138202	1600	1659.309

Figure B.185: Drakeol-7 recorded data and calculations.

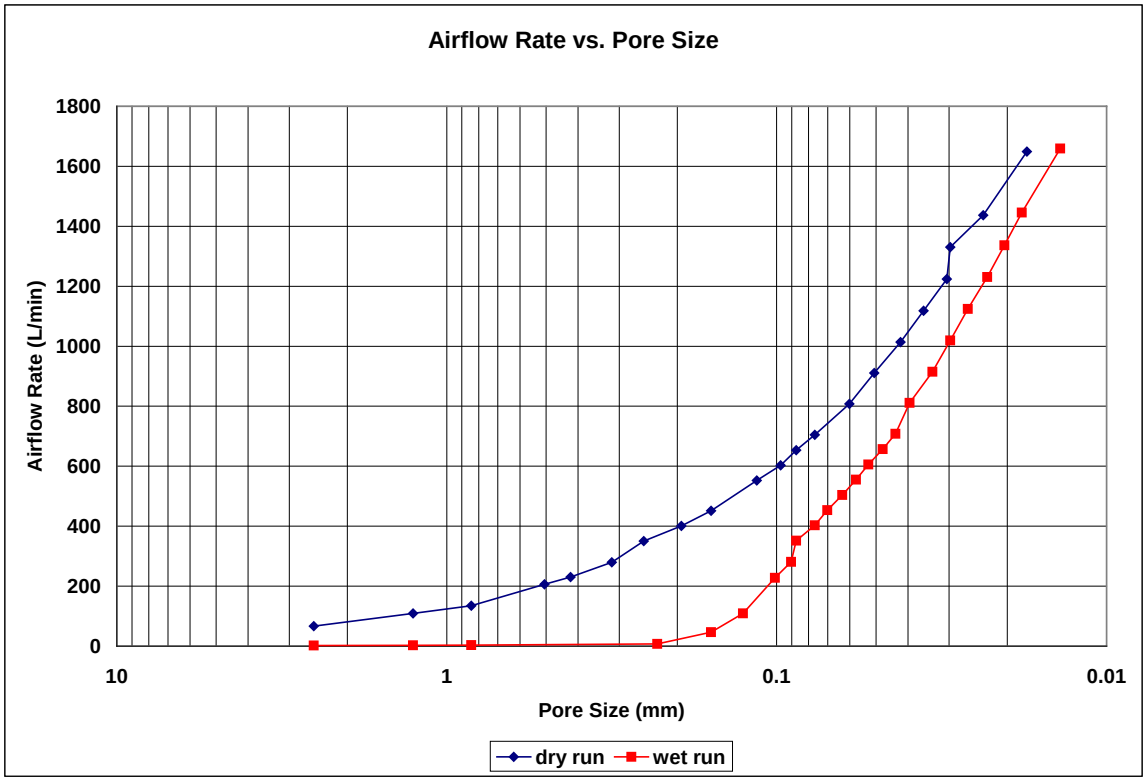

Figure B.186: Drakeol-7 airflow rate vs. pore size for the wet and dry runs.

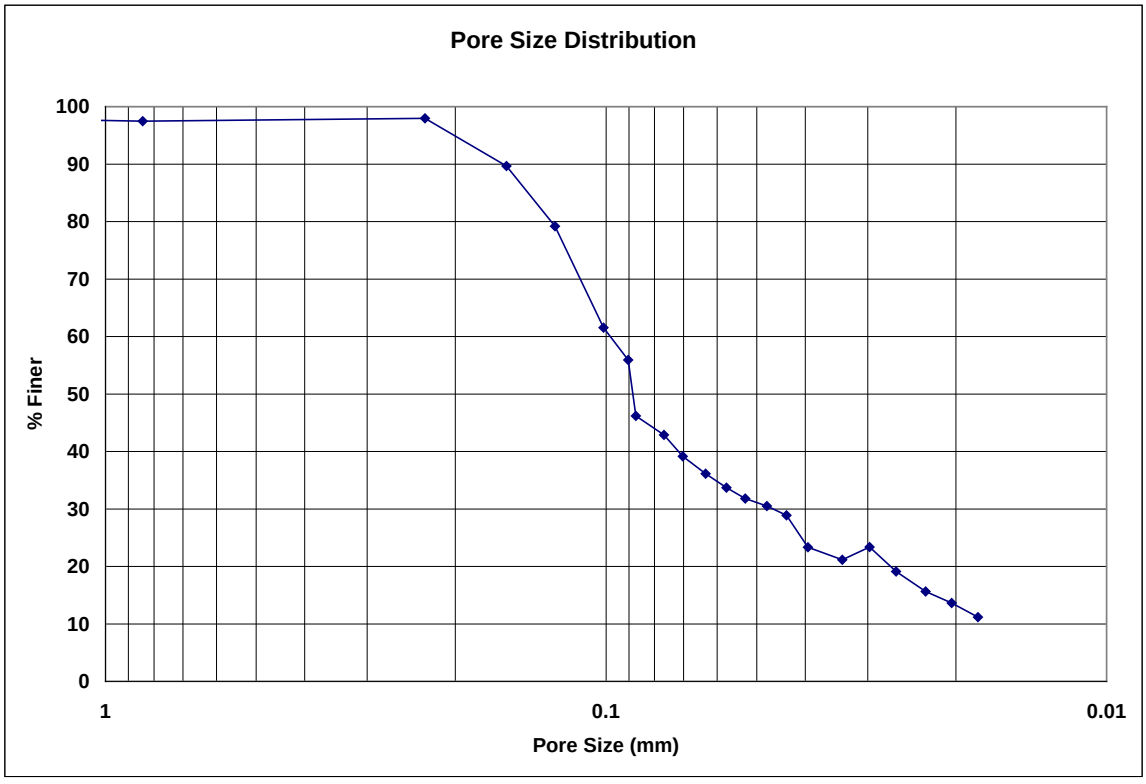

Figure B.187: Drakeol-7 pore size distribution.

Bubble Point Test
Auburn University - Department of Civil Engineering

date of test: 10/18/2006
test identification: drakeol 7
test performed by: David Hayes
wetting fluid: Drakeol
air temperature: 22.5 °C
porous media: NG-1 nonwoven geotextile
comments: testing to determine geotextile pore size distribution

Pore Size Calculation Parameters:
constant, C: 2860 mm/m
contact angle: 0 degrees
surface tension: 0.0347 N/m

Pore Size at Selected % Finer

% finer	pore size (mm)
98	---
95	0.20427
90	0.16089
85	0.14395
80	0.12886
75	0.12044
70	0.11328
65	0.10612
60	0.09819
55	0.09003
50	0.08843
45	0.08345
40	0.07170
35	0.06054
30	0.04640
25	0.04075
20	0.02706
15	0.02217
10	---
5	---

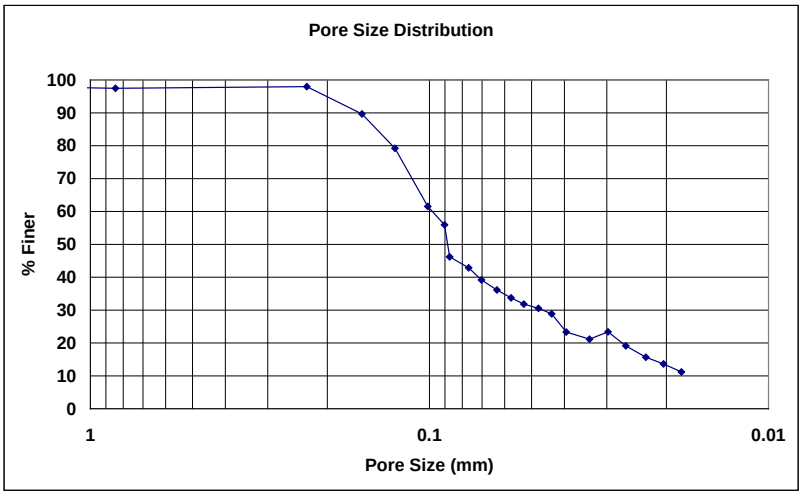

Figure B.188: Drakeol-7 pore size distribution report.

Bubble Point Test

Auburn University - Department of Civil Engineering

date of test: 10/18/2006
test identification: drakeol 8
test performed by: David Hayes
wetting fluid: Drakeol
ambient air temperature: 22.5 °C
porous media: NG-1 nonwoven geotextile
comments: testing to determine geotextile pore size distribution

Pore Size Calculation Parameters:
constant, C: 2860 mm/m
contact angle: 0 degrees
surface tension: 0.0347 N/m

Dry Run

Recorded Data							Calculations				
Indirect Reading Rotameters				Direct Reading Rotameter Value (L/min)	Pressure at Rotameter Exit (psig)	Half of Manometer Reading (mm H20)	Manometer Reading (mm H20)	Manometer Pressure (Pa)	Pore Size (Diameter) (mm)	Indicated Airflow Rate (L/min)	True Airflow Rate (L/min)
First Rotameter Used		Second Rotameter Used									
Rotameter ID Number	Rotameter Value	Rotameter ID Number	Rotameter Value								
5	42				0.09	2	4	39.24	2.529103	62.4	62.59073
5	70				0.24	4	8	78.48	1.2645515	105	105.8537
5	90				0.4	6	12	117.72	0.8430343	137	138.8514
5	62	5	77		0.35	10	20	196.2	0.5058206	208.5	210.9675
5	70	5	85		0.43	12	24	235.44	0.4215172	234	237.3978
5	75	5	93		0.51	14	28	274.68	0.3613004	254	258.3686
				350	0.07	20	40	392.4	0.2529103	350	350.8323
				400	0.09	24	48	470.88	0.2107586	400	401.2226
				450	0.1	30	60	588.6	0.1686069	450	451.528
				550	0.14	40	80	784.8	0.1264551	550	552.6128
				600	0.16	48	96	941.76	0.1053793	600	603.2565
				650	0.18	56	112	1098.72	0.0903251	650	653.9675
				700	0.2	64	128	1255.68	0.0790345	700	704.7458
				800	0.28	80	160	1569.6	0.0632276	800	807.5831
				900	0.34	94	188	1844.28	0.0538107	900	910.3487
				1000	0.4	114	228	2236.68	0.0443702	1000	1013.514
				1100	0.47	130	260	2550.6	0.0389093	1100	1117.447
				1200	0.56	154	308	3021.48	0.0328455	1200	1222.644
				1300	0.64	174	348	3413.88	0.0290701	1300	1327.998
				1400	0.74	202	404	3963.24	0.0250406	1400	1434.805

Wet Run

Recorded Data							Calculations				
Indirect Reading Rotameters				Direct Reading Rotameter Value (L/min)	Pressure at Rotameter Exit (psig)	Half of Manometer Reading (mm H20)	Manometer Reading (mm H20)	Manometer Pressure (Pa)	Pore Size (Diameter) (mm)	Indicated Airflow Rate (L/min)	True Airflow Rate (L/min)
First Rotameter Used		Second Rotameter Used									
Rotameter ID Number	Rotameter Value	Rotameter ID Number	Rotameter Value								
2	91					2	4	39.24	2.529103	1.931	1.931
4	9					4	8	78.48	1.2645515	2.74	2.74
4	11				0.01	6	12	117.72	0.8430343	3.41	3.41116
4	46				0.2	22	44	431.64	0.2299185	16.2	16.30983
5	30				0.13	32	64	627.84	0.1580689	45	45.19854
5	84				0.44	40	80	784.8	0.1264551	127	128.8867
5	50	5	62		0.33	50	100	981	0.1011641	166.7	168.5607
				350	0.18	56	112	1098.72	0.0903251	350	352.1363
				400	0.2	58	116	1137.96	0.0872104	400	402.7119
				450	0.22	66	132	1294.92	0.0766395	450	453.3548
				500	0.23	72	144	1412.64	0.0702529	500	503.8964
				550	0.25	80	160	1569.6	0.0632276	550	554.6572
				600	0.28	88	176	1726.56	0.0574796	600	605.6873
				650	0.3	96	192	1883.52	0.0526896	650	656.5992
				700	0.32	106	212	2079.72	0.0477189	700	707.578
				800	0.43	116	232	2275.92	0.0436052	800	811.6163
				900	0.51	128	256	2511.36	0.0395172	900	915.4791
				1000	0.58	150	300	2943	0.0337214	1000	1019.537
				1100	0.66	170	340	3335.4	0.0297542	1100	1124.423
				1200	0.76	192	384	3767.04	0.0263448	1200	1230.63
				1300	0.86	220	440	4316.4	0.0229918	1300	1337.487
				1400	0.97	248	496	4865.76	0.020396	1400	1445.453
				1600	1.1	280	560	5493.6	0.018065	1600	1658.784

Figure B.189: Drakeol-8 recorded data and calculations.

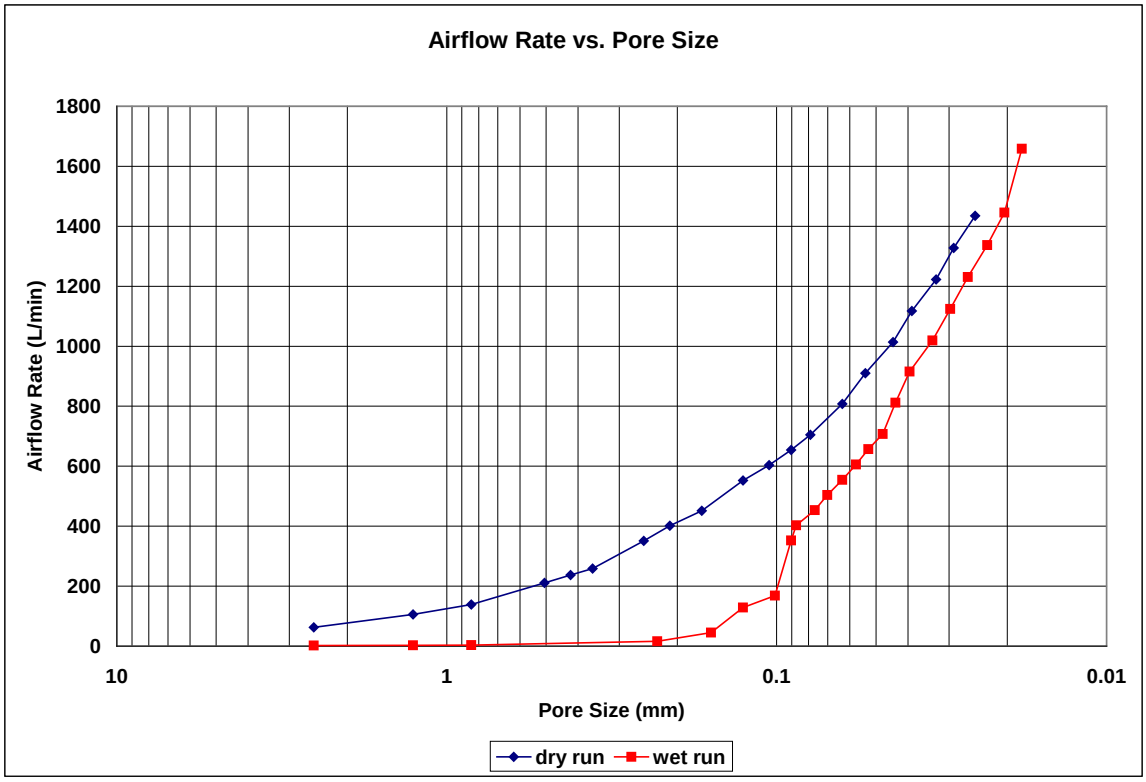

Figure B.190: Drakeol-8 airflow rate vs. pore size for the wet and dry runs.

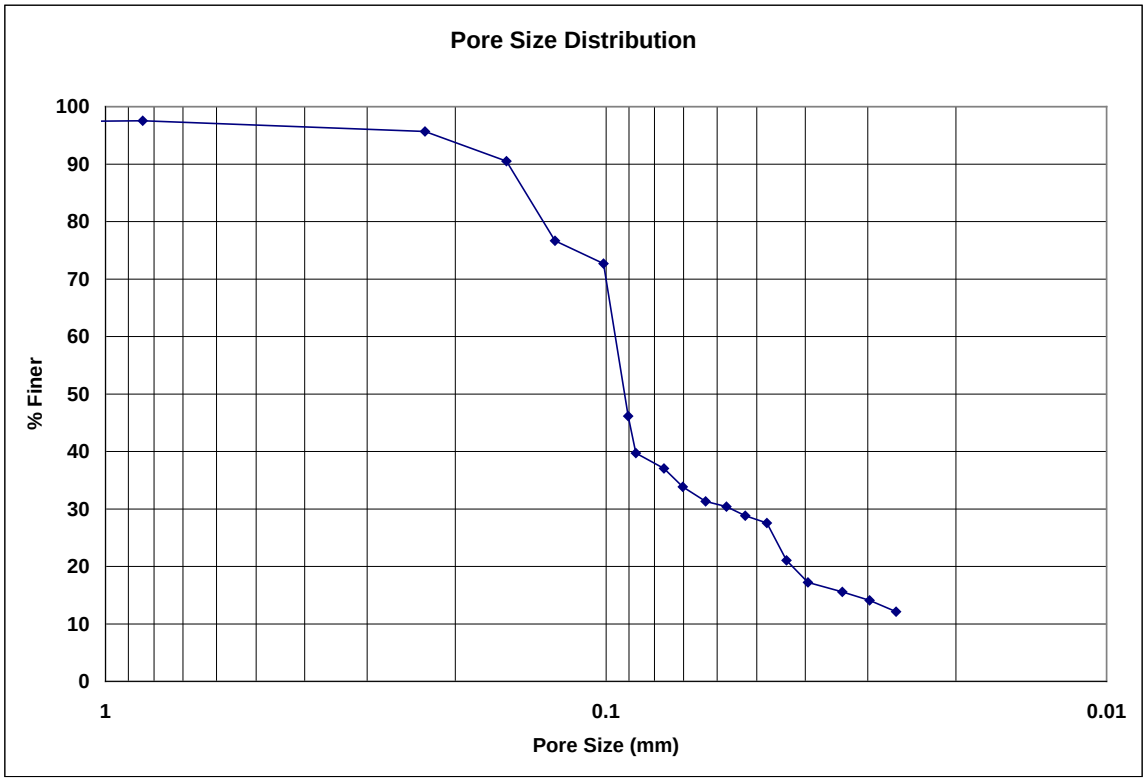

Figure B.191: Drakeol-8 pore size distribution.

Bubble Point Test
Auburn University - Department of Civil Engineering

date of test: 10/18/2006
test identification: drakeol 8
test performed by: David Hayes
wetting fluid: Drakeol
air temperature: 22.5 °C
porous media: NG-1 nonwoven geotextile
comments: testing to determine geotextile pore size distribution

Pore Size Calculation Parameters:
constant, C: 2860 mm/m
contact angle: 0 degrees
surface tension: 0.0347 N/m

Pore Size at Selected % Finer

% finer	pore size (mm)
98	---
95	0.22034
90	0.15688
85	0.14546
80	0.13404
75	0.11579
70	0.10006
65	0.09802
60	0.09598
55	0.09394
50	0.09190
45	0.08977
40	0.08735
35	0.07252
30	0.05625
25	0.04610
20	0.04248
15	0.03220
10	---
5	---

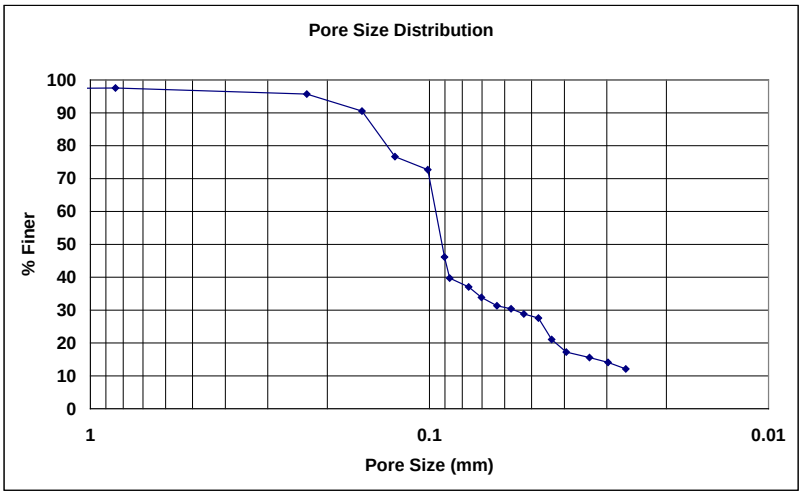

Figure B.192: Drakeol-8 pore size distribution report.

Bubble Point Test

Auburn University - Department of Civil Engineering

date of test: 10/18/2006
test identification: drakeol 9
test performed by: David Hayes
wetting fluid: Drakeol
ambient air temperature: 22.5 °C
porous media: NG-1 nonwoven geotextile
comments: testing to determine geotextile pore size distribution

Pore Size Calculation Parameters:
constant, C: 2860 mm/m
contact angle: 0 degrees
surface tension: 0.0347 N/m

Dry Run

Recorded Data							Calculations				
Indirect Reading Rotameters				Direct Reading Rotameter Value (L/min)	Pressure at Rotameter Exit (psig)	Half of Manometer Reading (mm H20)	Manometer Reading (mm H20)	Manometer Pressure (Pa)	Pore Size (Diameter) (mm)	Indicated Airflow Rate (L/min)	True Airflow Rate (L/min)
First Rotameter Used		Second Rotameter Used									
Rotameter ID Number	Rotameter Value	Rotameter ID Number	Rotameter Value								
5	45				0.09	2	4	39.24	2.529103	66.8	67.00418
5	75				0.26	4	8	78.48	1.2645515	113	113.9949
5	46	5	57		0.18	6	12	117.72	0.8430343	153.1	154.0345
5	63	5	78		0.34	10	20	196.2	0.5058206	212	214.4377
5	76	5	95		0.5	14	28	274.68	0.3613004	259	263.3679
				350	0.07	20	40	392.4	0.2529103	350	350.8323
				400	0.09	26	52	510.12	0.1945464	400	401.2226
				450	0.11	32	64	627.84	0.1580689	450	451.6805
				500	0.13	38	76	745.56	0.1331107	500	502.206
				550	0.15	46	92	902.52	0.109961	550	552.799
				600	0.17	52	104	1020.24	0.0972732	600	603.4594
				650	0.2	60	120	1177.2	0.0843034	650	654.4068
				700	0.23	70	140	1373.4	0.0722601	700	705.4549
				800	0.32	86	172	1687.32	0.0588163	800	808.6606
				900	0.37	100	200	1962	0.0505821	900	911.2561
				1000	0.44	118	236	2315.16	0.0428662	1000	1014.856
				1100	0.5	136	272	2668.32	0.0371927	1100	1118.551
				1200	0.59	160	320	3139.2	0.0316138	1200	1223.845
				1300	0.68	186	372	3649.32	0.0271947	1300	1329.728
				1400	0.77	208	416	4080.96	0.0243183	1400	1436.199
				1600	0.92	296	592	5807.52	0.0170885	1600	1649.308

Wet Run

Recorded Data							Calculations				
Indirect Reading Rotameters				Direct Reading Rotameter Value (L/min)	Pressure at Rotameter Exit (psig)	Half of Manometer Reading (mm H20)	Manometer Reading (mm H20)	Manometer Pressure (Pa)	Pore Size (Diameter) (mm)	Indicated Airflow Rate (L/min)	True Airflow Rate (L/min)
First Rotameter Used		Second Rotameter Used									
Rotameter ID Number	Rotameter Value	Rotameter ID Number	Rotameter Value								
2	19					6	12	117.72	0.8430343	0.259	0.259
2	35					16	32	313.92	0.3161379	0.586	0.586
2	44					20	40	392.4	0.2529103	0.788	0.788
2	98					24	48	470.88	0.2107586	2.084	2.084
4	43				0.21	30	60	588.6	0.1686069	15.1	15.20747
4	100				0.8	34	68	667.08	0.1487708	39.2	40.25254
5	65				0.32	38	76	745.56	0.1331107	97.1	98.15118
5	52	5	65		0.36	44	88	863.28	0.1149592	174.3	176.4214
5	84	5	68		0.53	50	100	981	0.1011641	229	233.0917
5	100	5	80		0.7	56	112	1098.72	0.0903251	274	280.4479
				400	0.22	64	128	1255.68	0.0790345	400	402.9821
				450	0.24	70	140	1373.4	0.0722601	450	453.6586
				500	0.27	80	160	1569.6	0.0632276	500	504.5709
				550	0.29	86	172	1687.32	0.0588163	550	555.3987
				600	0.32	98	196	1922.76	0.0516143	600	606.4955
				650	0.35	106	212	2079.72	0.0477189	650	657.6926
				700	0.38	116	232	2275.92	0.0436052	700	708.9899
				800	0.46	130	260	2550.6	0.0389093	800	812.4206
				900	0.53	150	300	2943	0.0337214	900	916.0808
				1000	0.61	172	344	3374.64	0.0294082	1000	1020.537
				1100	0.7	198	396	3884.76	0.0255465	1100	1125.886
				1200	0.81	226	452	4434.12	0.0223814	1200	1232.618
				1300	0.92	256	512	5022.72	0.0197586	1300	1340.063
				1400	1.02	284	568	5572.08	0.0178106	1400	1447.757

Figure B.193: Drakeol-9 recorded data and calculations.

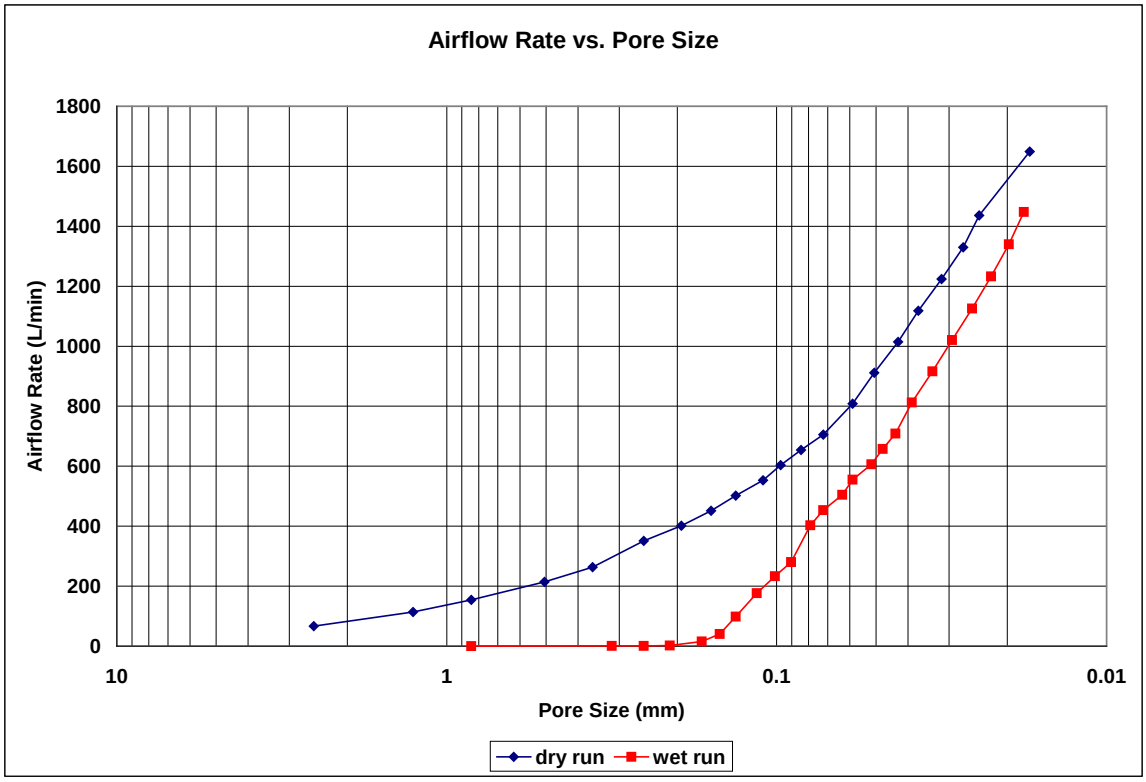

Figure B.194: Drakeol-9 airflow rate vs. pore size for the wet and dry runs.

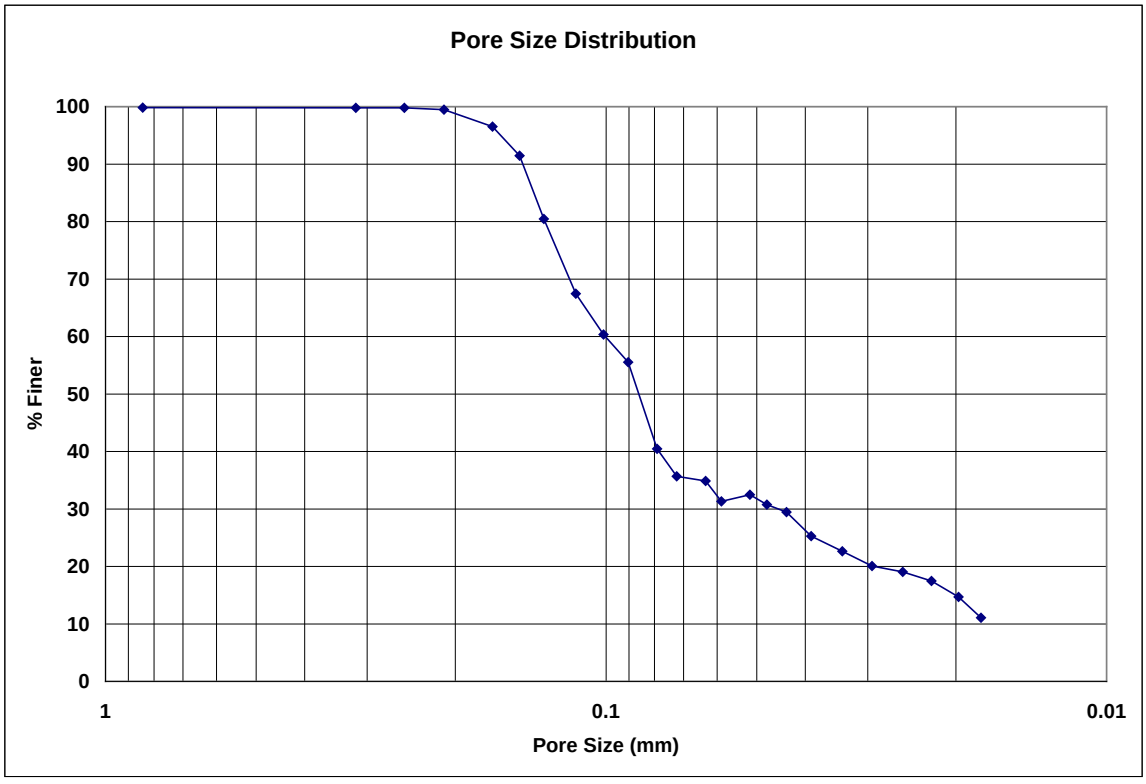

Figure B.195: Drakeol-9 pore size distribution.

Bubble Point Test
Auburn University - Department of Civil Engineering

date of test:	10/18/2006	Pore Size Calculation Parameters:		
test identification:	drakeol 9	constant, C:	2860	mm/m
test performed by:	David Hayes	contact angle:	0	degrees
wetting fluid:	Drakeol	surface tension:	0.0347	N/m
air temperature:	22.5 °C			
porous media:	NG-1 nonwoven geotextile			
comments:	testing to determine geotextile pore size distribution			

Pore Size at Selected % Finer

% finer	pore size (mm)
98	0.18981
95	0.16266
90	0.14671
85	0.13959
80	0.13247
75	0.12550
70	0.11853
65	0.11021
60	0.10037
55	0.08992
50	0.08618
45	0.08244
40	0.07839
35	0.06459
30	0.04535
25	0.03837
20	0.02917
15	0.02006
10	---
5	---

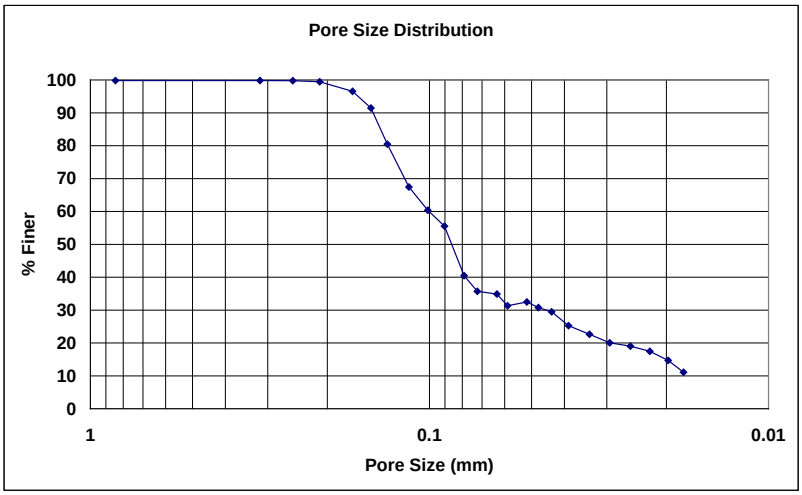

Figure B.196: Drakeol-9 pore size distribution report.

Bubble Point Test

Auburn University - Department of Civil Engineering

date of test: 4/10/2002
test identification: Drakeol 10
test performed by: David Howie
wetting fluid: Drakeol
ambient air temperature: 21 °C
porous media: NG-1 nonwoven geotextile
comments: testing to determine geotextile pore size distribution

Pore Size Calculation Parameters:
constant, C: 2860 mm/m
contact angle: 0 degrees
surface tension: 0.0347 N/m

Dry Run

Recorded Data							Calculations				
Indirect Reading Rotameters				Direct Reading Rotameter Value (L/min)	Pressure at Rotameter Exit (psig)	Half of Manometer Reading (mm H20)	Manometer Reading (mm H20)	Manometer Pressure (Pa)	Pore Size (Diameter) (mm)	Indicated Airflow Rate (L/min)	True Airflow Rate (L/min)
First Rotameter Used		Second Rotameter Used									
Rotameter ID Number	Rotameter Value	Rotameter ID Number	Rotameter Value								
4	76				0.36	1	2	19.62	5.0582059	28.6	28.94809
5	44				0.09	2	4	39.24	2.529103	65.3	65.49959
5	72				0.25	4	8	78.48	1.2645515	108	108.9145
5	95				0.49	6	12	117.72	0.8430343	145	147.3969
5	77	5	64		0.32	10	20	196.2	0.5058206	211.6	213.8907
5	99	5	81		0.54	15	30	294.3	0.3372137	273	277.9691
				400	0.09	24	48	470.88	0.2107586	400	401.2226
				600	0.16	47	94	922.14	0.1076214	600	603.2565
				700	0.21	63	126	1236.06	0.080289	700	704.9823
				800	0.29	78	156	1530.36	0.0648488	800	807.8526
				1000	0.4	110	220	2158.2	0.0459837	1000	1013.514
				1200	0.56	149	298	2923.38	0.0339477	1200	1222.644
				1400	0.73	193	386	3786.66	0.0262083	1400	1434.341
				1600	0.82	260	520	5101.2	0.0194546	1600	1644.02
				1800	1.03	325	650	6376.5	0.0155637	1800	1861.994

Wet Run

Recorded Data							Calculations				
Indirect Reading Rotameters				Direct Reading Rotameter Value (L/min)	Pressure at Rotameter Exit (psig)	Half of Manometer Reading (mm H20)	Manometer Reading (mm H20)	Manometer Pressure (Pa)	Pore Size (Diameter) (mm)	Indicated Airflow Rate (L/min)	True Airflow Rate (L/min)
First Rotameter Used		Second Rotameter Used									
Rotameter ID Number	Rotameter Value	Rotameter ID Number	Rotameter Value								
1	12					4	8	78.48	1.2645515	0.00967	0.00967
1	22					6	12	117.72	0.8430343	0.028	0.028
1	23					10	20	196.2	0.5058206	0.0304	0.0304
1	35					15	30	294.3	0.3372137	0.0616	0.0616
1	50					20	40	392.4	0.2529103	0.111	0.111
5	31				0.19	30	60	588.6	0.1686069	46.4	46.6989
5	74				0.37	40	80	784.8	0.1264551	111	112.3883
5	84	5	69		0.51	50	100	981	0.1011641	230	233.9558
				400	0.2	64	128	1255.68	0.0790345	400	402.7119
				500	0.03	75	150	1471.5	0.0674427	500	500.5099
				600	0.08	88	176	1726.56	0.0574796	600	601.6304
				700	0.33	102	204	2001.24	0.0495903	700	707.8135
				800	0.4	117	234	2295.54	0.0432325	800	810.8113
				1000	0.53	143	286	2805.66	0.0353721	1000	1017.868
				1200	0.69	195	390	3825.9	0.0259395	1200	1227.84
				1400	0.87	245	490	4806.9	0.0206457	1400	1440.833
				1600	1.04	325	650	6376.5	0.0155637	1600	1655.631
				1800	1.28	400	800	7848	0.0126455	1800	1876.732

Figure B.197: Drakeol-10 recorded data and calculations.

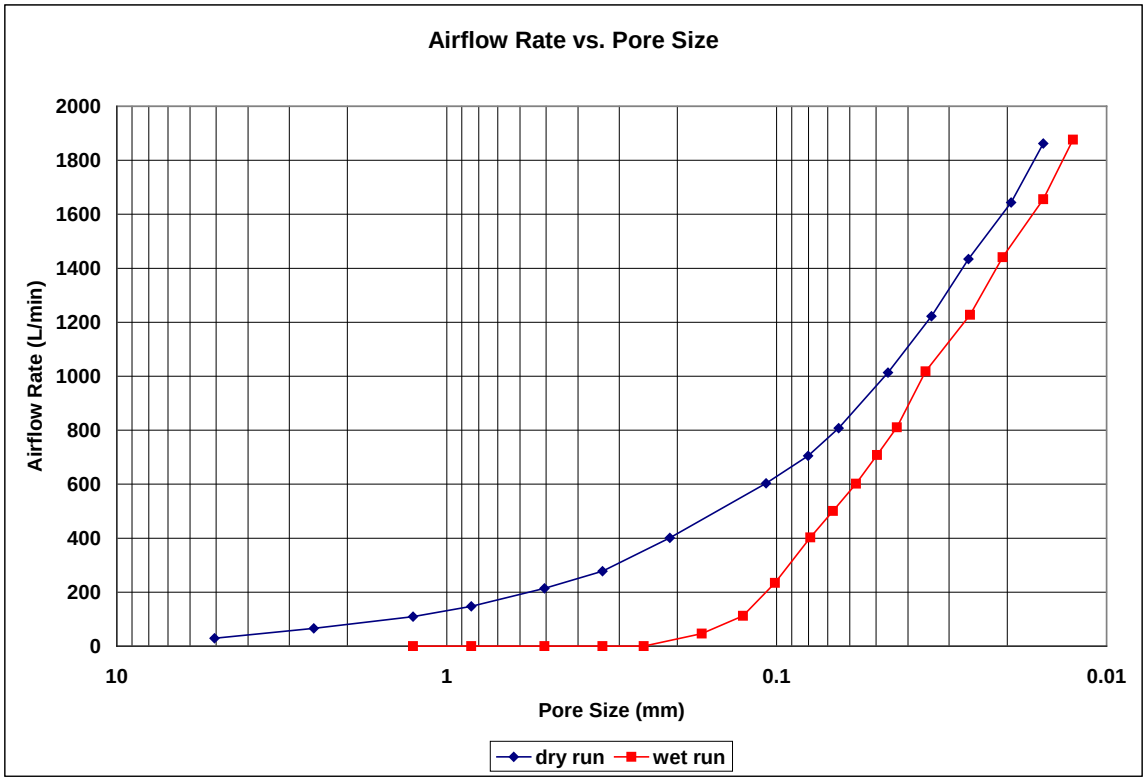

Figure B.198: Drakeol-10 airflow rate vs. pore size for the wet and dry runs.

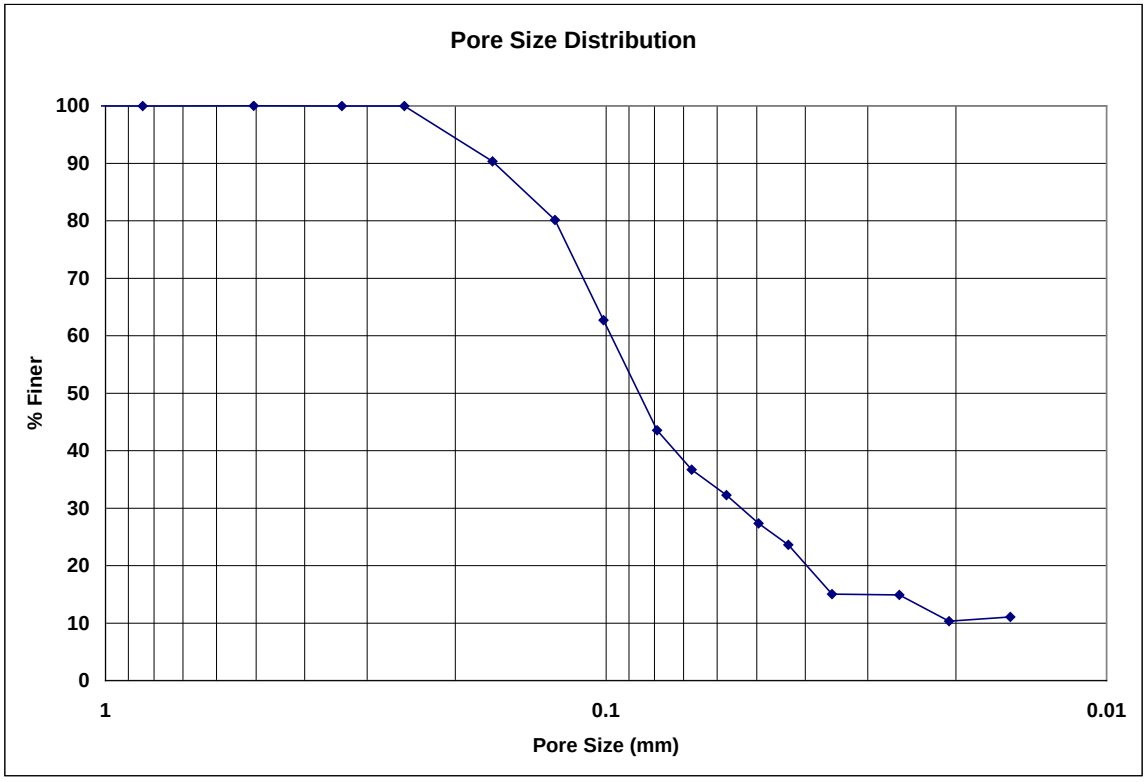

Figure B.199: Drakeol-10 pore size distribution.

Bubble Point Test
Auburn University - Department of Civil Engineering

date of test: 4/10/2002
test identification: Drakeol 10
test performed by: David Howie
wetting fluid: Drakeol
air temperature: 21 °C
porous media: NG-1 nonwoven geotextile
comments: testing to determine geotextile pore size distribution

Pore Size Calculation Parameters:
constant, C: 2860 mm/m
contact angle: 0 degrees
surface tension: 0.0347 N/m

Pore Size at Selected % Finer

% finer	pore size (mm)
98	0.23566
95	0.20937
90	0.16717
85	0.14649
80	0.12623
75	0.11898
70	0.11174
65	0.10449
60	0.09804
55	0.09227
50	0.08649
45	0.08071
40	0.07304
35	0.06364
30	0.05385
25	0.04561
20	0.03993
15	0.03340
10	---
5	---

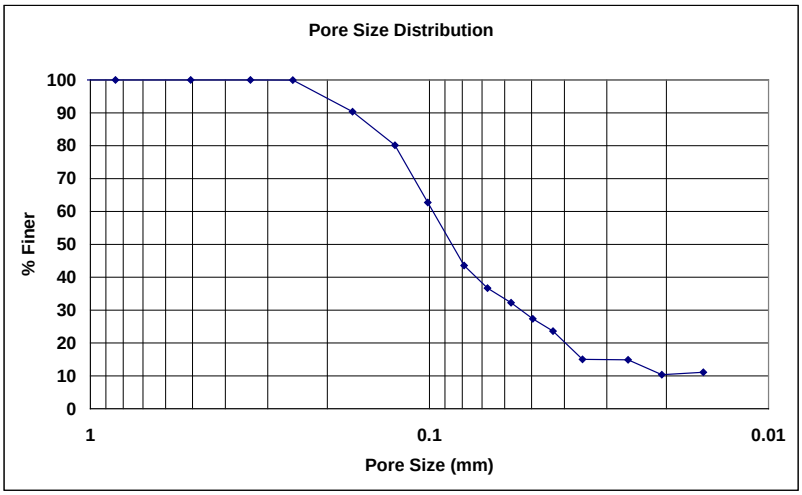

Figure B.200: Drakeol-10 pore size distribution report.

B.6 Tests with Glycerin as the Wetting Fluid

Bubble Point Test
Auburn University - Department of Civil Engineering

date of test: 11/9/2006
test identification: glycerin 1
test performed by: David Hayes
wetting fluid: glycerin
ambient air temperature: 21.2 °C
porous media: NG-1 nonwoven geotextile
comments: testing to determine geotextile pore size distribution

Pore Size Calculation Parameters:
constant, C: 2860 mm/m
contact angle: 34.51 degrees
surface tension: 0.0634 N/m

Dry Run

Recorded Data							Calculations				
Indirect Reading Rotameters				Direct Reading Rotameter Value (L/min)	Pressure at Rotameter Exit (psig)	Half of Manometer Reading (mm H20)	Manometer Reading (mm H20)	Manometer Pressure (Pa)	Pore Size (Diameter) (mm)	Indicated Airflow Rate (L/min)	True Airflow Rate (L/min)
First Rotameter Used		Second Rotameter Used									
Rotameter ID Number	Rotameter Value	Rotameter ID Number	Rotameter Value								
5	50				0.13	2	4	39.24	3.8077454	74.2	74.52737
5	81				0.32	4	8	78.48	1.9038727	122	123.3207
5	60	5	75		0.32	8	16	156.96	0.9519364	202.4	204.5911
5	68	5	85		0.41	10	20	196.2	0.7615491	231	234.1993
5	75	5	93		0.5	12	24	235.44	0.6346242	254	258.2836
				350	0.05	18	36	353.16	0.4230828	350	350.5947
				400	0.06	22	44	431.64	0.3461587	400	400.8155
				450	0.08	28	56	549.36	0.2719818	450	451.2228
				500	0.09	32	64	627.84	0.2379841	500	501.5283
				600	0.13	44	88	863.28	0.1730793	600	602.6472
				650	0.15	50	100	981	0.1523098	650	653.3079
				700	0.18	58	116	1137.96	0.1313016	700	704.2727
				800	0.28	68	136	1334.16	0.1119925	800	807.5831
				900	0.33	82	164	1608.84	0.0928718	900	910.046
				1000	0.4	104	208	2040.48	0.0732259	1000	1013.514
				1100	0.46	120	240	2354.4	0.0634624	1100	1117.078
				1200	0.54	140	280	2746.8	0.0543964	1200	1221.842
				1300	0.62	160	320	3139.2	0.0475968	1300	1327.132
				1400	0.71	184	368	3610.08	0.0413885	1400	1433.411
				1600	0.81	244	488	4787.28	0.031211	1600	1643.491

Wet Run

Recorded Data							Calculations				
Indirect Reading Rotameters				Direct Reading Rotameter Value (L/min)	Pressure at Rotameter Exit (psig)	Half of Manometer Reading (mm H20)	Manometer Reading (mm H20)	Manometer Pressure (Pa)	Pore Size (Diameter) (mm)	Indicated Airflow Rate (L/min)	True Airflow Rate (L/min)
First Rotameter Used		Second Rotameter Used									
Rotameter ID Number	Rotameter Value	Rotameter ID Number	Rotameter Value								
2	84				0	2	4	39.24	3.8077454	1.771	1.771
4	8				0.03	4	8	78.48	1.9038727	2.43	2.432478
4	23				0.13	28	56	549.36	0.2719818	7.54	7.573267
4	78				0.15	50	100	981	0.1523098	29.5	29.65013
5	81				0.51	64	128	1255.68	0.118992	122	124.0983
5	67	5	76		0.51	68	136	1334.16	0.1119925	214	217.6806
5	85	5	68		0.59	70	140	1373.4	0.1087927	231	235.5901
				450	0.27	80	160	1569.6	0.0951936	450	454.1138
				550	0.33	100	200	1962	0.0761549	550	556.1392
				600	0.36	102	204	2001.24	0.0746617	600	607.3025
				650	0.38	110	220	2158.2	0.0692317	650	658.3478
				700	0.42	122	244	2393.64	0.0624221	700	709.9296
				800	0.5	140	280	2746.8	0.0543964	800	813.4917
				900	0.58	158	316	3099.96	0.0481993	900	917.5833
				1000	0.62	178	356	3492.36	0.0427837	1000	1020.871
				1100	0.73	198	396	3884.76	0.0384621	1100	1126.982
				1200	0.82	220	440	4316.4	0.0346159	1200	1233.015
				1300	0.92	244	488	4787.28	0.031211	1300	1340.063
				1400	1.01	260	520	5101.2	0.0292903	1400	1447.296

Figure B.201: Glycerin-1 recorded data and calculations.

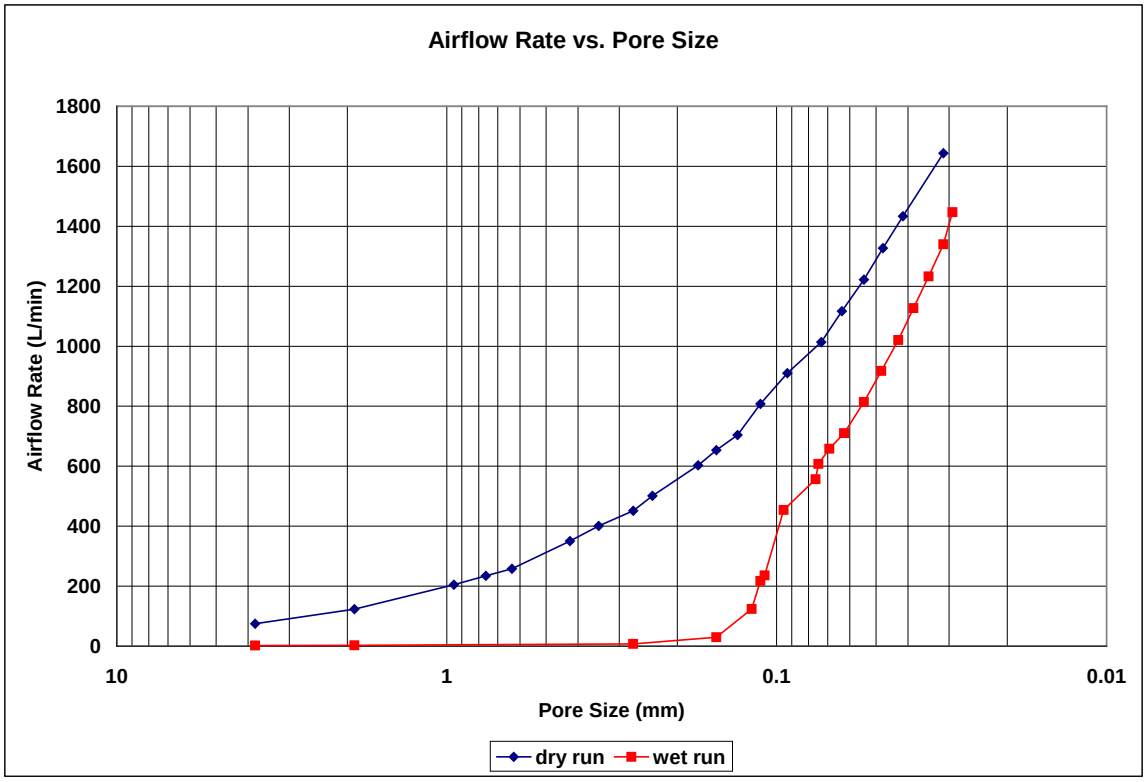

Figure B.202: Glycerin-1 airflow rate vs. pore size for the wet and dry runs.

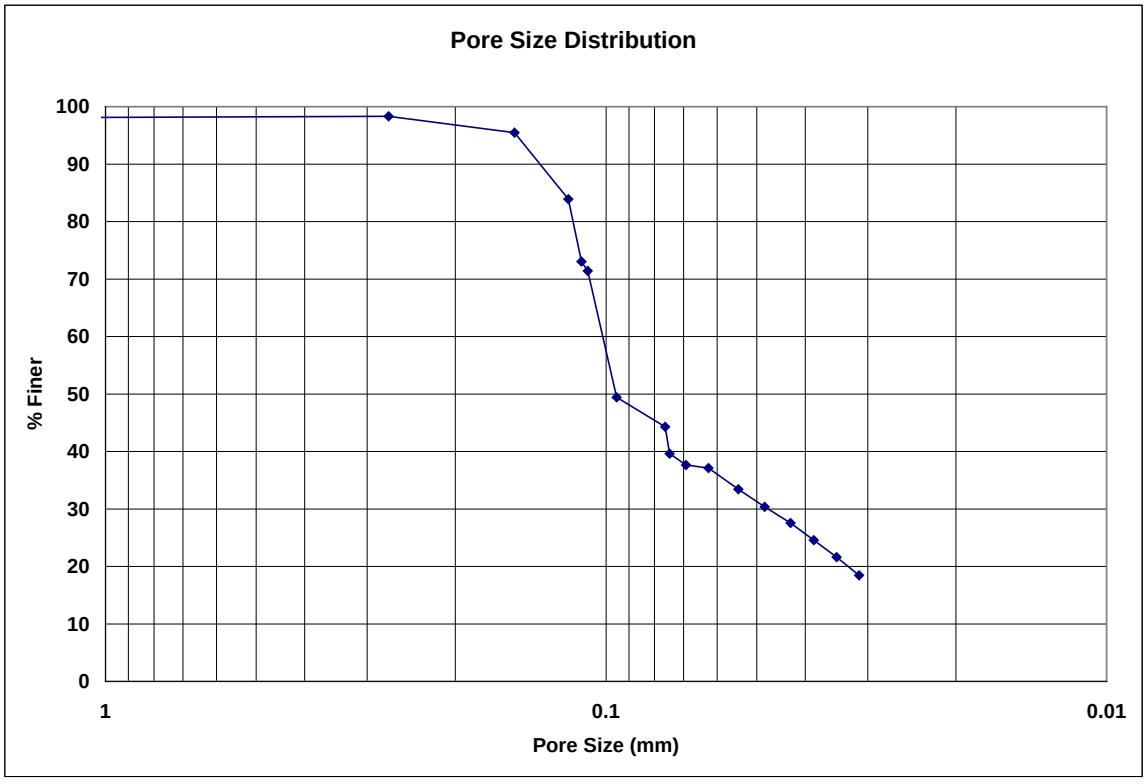

Figure B.203: Glycerin-1 pore size distribution.

Bubble Point Test
Auburn University - Department of Civil Engineering

date of test: 11/9/2006
test identification: glycerin 1
test performed by: David Hayes
wetting fluid: glycerin
air temperature: 21.2 °C
porous media: NG-1 nonwoven geotextile
comments: testing to determine geotextile pore size distribution

Pore Size Calculation Parameters:
constant, C: 2860 mm/m
contact angle: 34.51 degrees
surface tension: 0.0634 N/m

Pore Size at Selected % Finer

% finer	pore size (mm)
98	0.25852
95	0.15098
90	0.13659
85	0.12220
80	0.11648
75	0.11325
70	0.10791
65	0.10482
60	0.10173
55	0.09865
50	0.09556
45	0.07883
40	0.07478
35	0.05782
30	0.04748
25	0.03910
20	0.03287
15	---
10	---
5	---

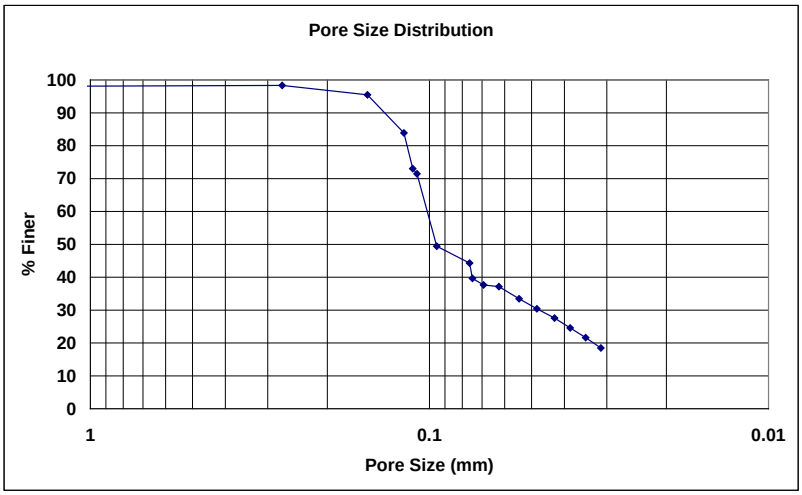

Figure B.204: Glycerin-1 pore size distribution report.

Bubble Point Test

Auburn University - Department of Civil Engineering

date of test: 1/7/2007
test identification: glycerin 2
test performed by: David Hayes
wetting fluid: glycerin
ambient air temperature: 21.5 °C
porous media: NG-1 nonwoven geotextile
comments: testing to determine geotextile pore size distribution

Pore Size Calculation Parameters:
constant, C: 2860 mm/m
contact angle: 34.51 degrees
surface tension: 0.0634 N/m

Dry Run

Recorded Data							Calculations				
Indirect Reading Rotameters				Direct Reading Rotameter Value (L/min)	Pressure at Rotameter Exit (psig)	Half of Manometer Reading (mm H20)	Manometer Reading (mm H20)	Manometer Pressure (Pa)	Pore Size (Diameter) (mm)	Indicated Airflow Rate (L/min)	True Airflow Rate (L/min)
First Rotameter Used		Second Rotameter Used									
Rotameter ID Number	Rotameter Value	Rotameter ID Number	Rotameter Value								
5	55				0.15	2	4	39.24	3.8077454	81.8	82.21629
5	83				0.34	4	8	78.48	1.9038727	125	126.4373
5	51	5	63		0.23	6	12	117.72	1.2692485	169.7	171.0224
5	59	5	72		0.3	8	16	156.96	0.9519364	195.9	197.8889
5	67	5	83		0.39	10	20	196.2	0.7615491	225	227.9652
5	81	5	100		0.58	14	28	274.68	0.5439636	275	280.3727
				400	0.11	22	44	431.64	0.3461587	400	401.4938
				450	0.13	28	56	549.36	0.2719818	450	451.9854
				550	0.16	38	76	745.56	0.2004077	550	552.9851
				600	0.18	44	88	863.28	0.1730793	600	603.6623
				650	0.21	52	104	1020.24	0.1464517	650	654.6264
				700	0.23	60	120	1177.2	0.1269248	700	705.4549
				800	0.3	72	144	1412.64	0.1057707	800	808.122
				900	0.36	88	176	1726.56	0.0865397	900	910.9538
				1000	0.42	104	208	2040.48	0.0732259	1000	1014.185
				1100	0.49	122	244	2393.64	0.0624221	1100	1118.183
				1200	0.57	146	292	2864.52	0.0521609	1200	1223.044
				1300	0.66	166	332	3256.92	0.0458765	1300	1328.863
				1400	0.76	192	384	3767.04	0.039664	1400	1435.734
				1600	0.86	258	516	5061.96	0.0295174	1600	1646.138

Wet Run

Recorded Data							Calculations				
Indirect Reading Rotameters				Direct Reading Rotameter Value (L/min)	Pressure at Rotameter Exit (psig)	Half of Manometer Reading (mm H20)	Manometer Reading (mm H20)	Manometer Pressure (Pa)	Pore Size (Diameter) (mm)	Indicated Airflow Rate (L/min)	True Airflow Rate (L/min)
First Rotameter Used		Second Rotameter Used									
Rotameter ID Number	Rotameter Value	Rotameter ID Number	Rotameter Value								
1	81				0	6	12	117.72	1.2692485	0.2293	0.2293
1	97				0	8	16	156.96	0.9519364	0.3054	0.3054
2	32				0	18	36	353.16	0.4230828	0.52	0.52
2	41				0	24	48	470.88	0.3173121	0.72	0.72
2	46				0	30	60	588.6	0.2538497	0.834	0.834
4	87				0.65	50	100	981	0.1523098	33.4	34.13045
5	82				0.46	60	120	1177.2	0.1269248	124	125.9252
5	74	5	93		0.63	70	140	1373.4	0.1087927	252	257.3434
				550	0.29	90	180	1765.8	0.0846166	550	555.3987
				700	0.38	118	236	2315.16	0.0645381	700	708.9899
				800	0.43	132	264	2589.84	0.0576931	800	811.6163
				900	0.51	150	300	2943	0.0507699	900	915.4791
				1000	0.56	164	328	3217.68	0.0464359	1000	1018.87
				1100	0.64	190	380	3727.8	0.0400815	1100	1123.69
				1200	0.72	206	412	4041.72	0.0369684	1200	1229.036
				1300	0.83	240	480	4708.8	0.0317312	1300	1336.197
				1400	0.91	262	524	5140.44	0.0290668	1400	1442.683

Figure B.205: Glycerin-2 recorded data and calculations.

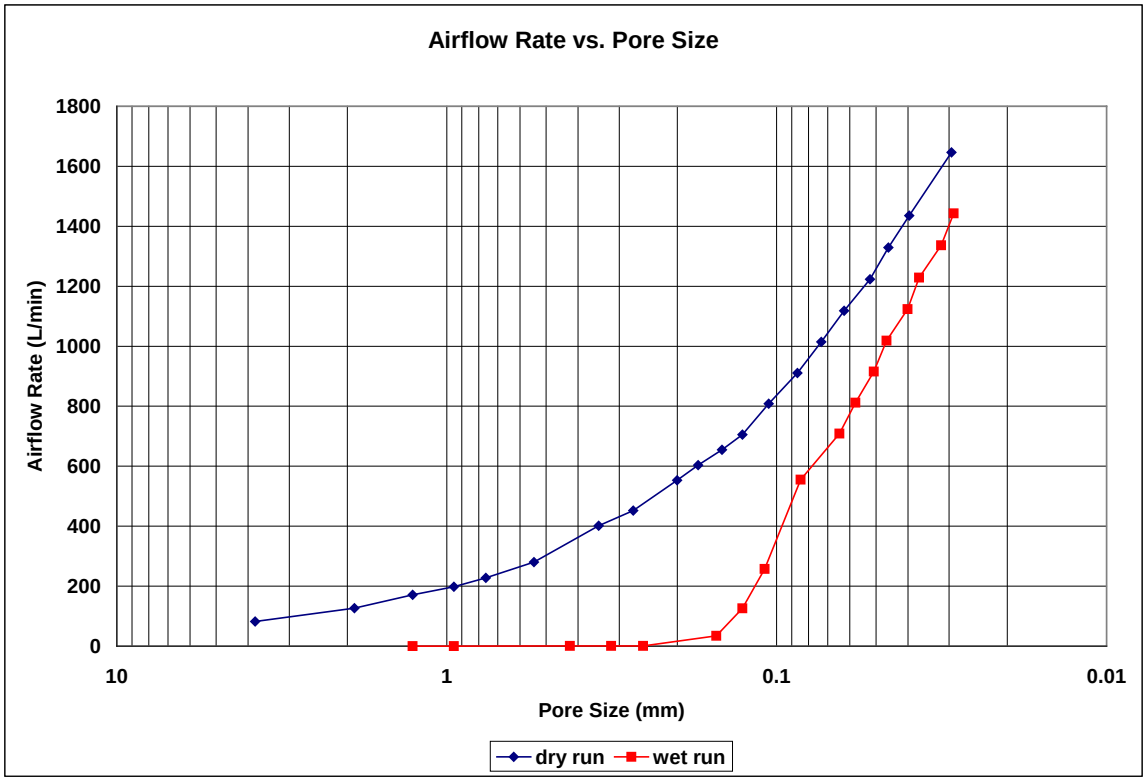

Figure B.206: Glycerin-2 airflow rate vs. pore size for the wet and dry runs.

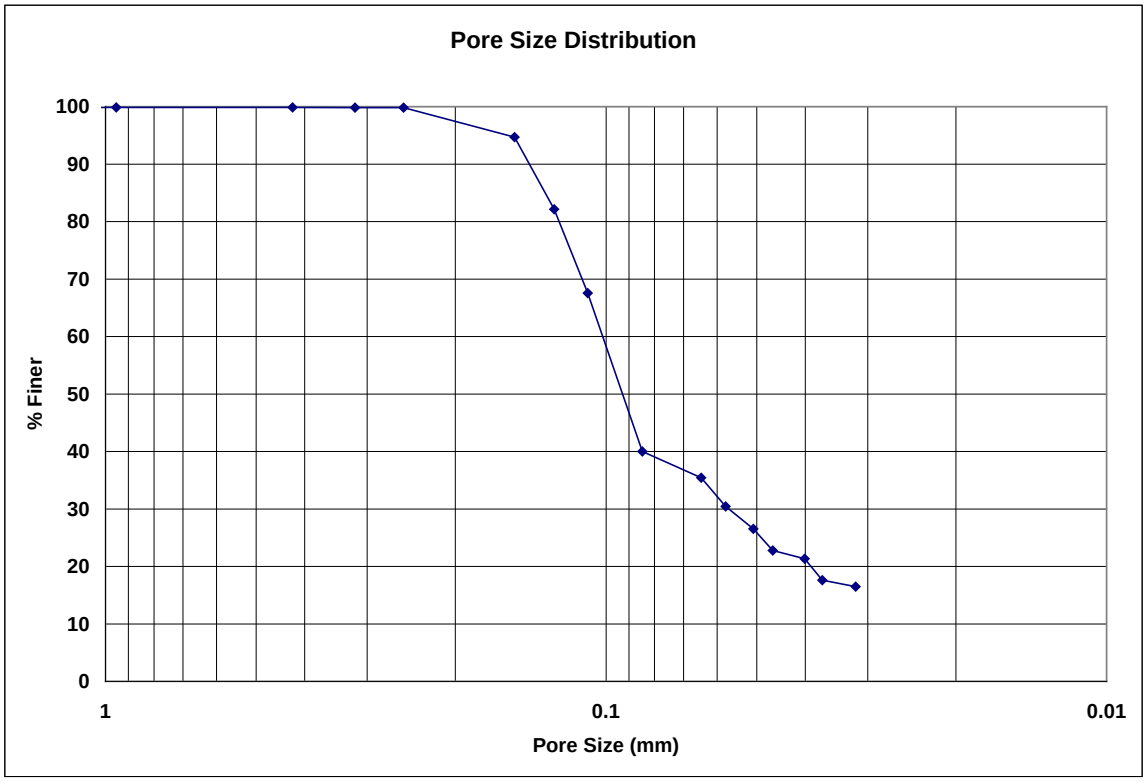

Figure B.207: Glycerin-2 pore size distribution.

Bubble Point Test
Auburn University - Department of Civil Engineering

date of test: 1/7/2007
test identification: glycerin 2
test performed by: David Hayes
wetting fluid: glycerin
air temperature: 21.5 °C
porous media: NG-1 nonwoven geotextile
comments: testing to determine geotextile pore size distribution

Pore Size Calculation Parameters:
constant, C: 2860 mm/m
contact angle: 34.51 degrees
surface tension: 0.0634 N/m

Pore Size at Selected % Finer

% finer	pore size (mm)
98	0.21772
95	0.15834
90	0.14281
85	0.13269
80	0.12425
75	0.11804
70	0.11182
65	0.10654
60	0.10215
55	0.09777
50	0.09338
45	0.08899
40	0.08456
35	0.06397
30	0.05694
25	0.04899
20	0.03896
15	---
10	---
5	---

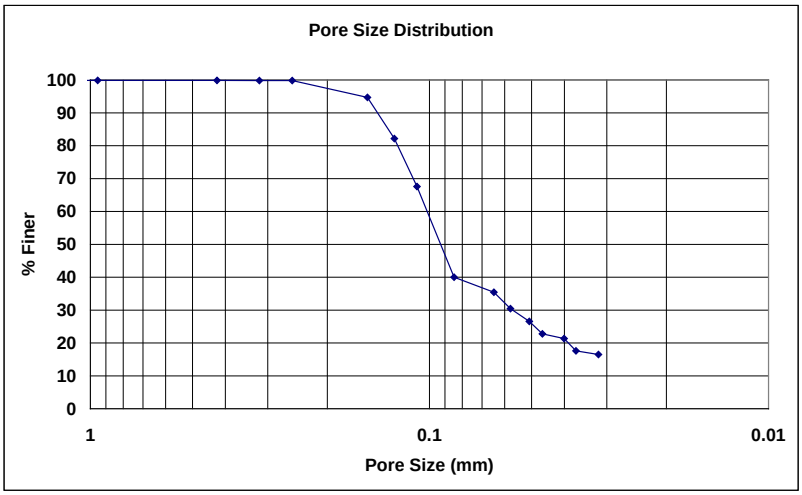

Figure B.208: Glycerin-2 pore size distribution report.

Bubble Point Test
Auburn University - Department of Civil Engineering

date of test: 2/8/2007
test identification: glycerin 3
test performed by: David Hayes
wetting fluid: glycerin
ambient air temperature: 21.5 °C
porous media: NG-1 nonwoven geotextile
comments: testing to determine geotextile pore size distribution

Pore Size Calculation Parameters:
constant, C: 2860 mm/m
contact angle: 34.51 degrees
surface tension: 0.0634 N/m

Dry Run

Recorded Data							Calculations				
Indirect Reading Rotameters				Direct Reading Rotameter Value (L/min)	Pressure at Rotameter Exit (psig)	Half of Manometer Reading (mm H20)	Manometer Reading (mm H20)	Manometer Pressure (Pa)	Pore Size (Diameter) (mm)	Indicated Airflow Rate (L/min)	True Airflow Rate (L/min)
First Rotameter Used		Second Rotameter Used									
Rotameter ID Number	Rotameter Value	Rotameter ID Number	Rotameter Value								
5	51				0.11	2	4	39.24	3.8077454	75.7	75.9827
5	79				0.29	4	8	78.48	1.9038727	119	120.1681
5	56	5	70		0.27	8	16	156.96	0.9519364	188.3	190.0214
5	65	5	81		0.35	10	20	196.2	0.7615491	219.1	221.693
5	72	5	90		0.45	12	24	235.44	0.6346242	245	248.7217
				400	0.08	24	48	470.88	0.3173121	400	401.087
				450	0.1	30	60	588.6	0.2538497	450	451.528
				500	0.12	36	72	706.32	0.2115414	500	502.0367
				600	0.16	48	96	941.76	0.1586561	600	603.2565
				650	0.17	54	108	1059.48	0.1410276	650	653.7477
				700	0.2	62	124	1216.44	0.1228305	700	704.7458
				800	0.26	76	152	1491.12	0.1002038	800	807.0438
				900	0.32	92	184	1805.04	0.0827771	900	909.7432
				1000	0.4	110	220	2158.2	0.0692317	1000	1013.514
				1100	0.45	126	252	2472.12	0.0604404	1100	1116.71
				1200	0.54	154	308	3021.48	0.0494512	1200	1221.842
				1300	0.64	178	356	3492.36	0.0427837	1300	1327.998
				1400	0.73	200	400	3924	0.0380775	1400	1434.341

Wet Run

Recorded Data							Calculations				
Indirect Reading Rotameters				Direct Reading Rotameter Value (L/min)	Pressure at Rotameter Exit (psig)	Half of Manometer Reading (mm H20)	Manometer Reading (mm H20)	Manometer Pressure (Pa)	Pore Size (Diameter) (mm)	Indicated Airflow Rate (L/min)	True Airflow Rate (L/min)
First Rotameter Used		Second Rotameter Used									
Rotameter ID Number	Rotameter Value	Rotameter ID Number	Rotameter Value								
2	65				0	2	4	39.24	3.8077454	1.302	1.302
2	93				0	4	8	78.48	1.9038727	1.975	1.975
4	8				0.02	6	12	117.72	1.2692485	2.43	2.431652
4	20				0.13	36	72	706.32	0.2115414	6.44	6.468414
4	30				0.18	44	88	863.28	0.1730793	10.1	10.16165
4	52				0.29	50	100	981	0.1523098	18.6	18.78257
5	85				0.53	58	116	1137.96	0.1313016	129	131.3049
5	67	5	83		0.58	70	140	1373.4	0.1087927	225	229.3958
				350	0.23	80	160	1569.6	0.0951936	350	352.7275
				400	0.25	88	176	1726.56	0.0865397	400	403.387
				500	0.3	100	200	1962	0.0761549	500	505.0763
				550	0.33	108	216	2118.96	0.0705138	550	556.1392
				600	0.35	114	228	2236.68	0.0668026	600	607.1008
				650	0.36	120	240	2354.4	0.0634624	650	657.911
				700	0.4	132	264	2589.84	0.0576931	700	709.4599
				800	0.5	150	300	2943	0.0507699	800	813.4917
				900	0.58	170	340	3335.4	0.044797	900	917.5833
				1000	0.65	190	380	3727.8	0.0400815	1000	1021.87
				1100	0.73	214	428	4198.68	0.0355864	1100	1126.982
				1200	0.83	244	488	4787.28	0.031211	1200	1233.412
				1300	0.94	270	540	5297.4	0.0282055	1300	1340.921
				1400	1.02	300	600	5886	0.025385	1400	1447.757

Figure B.209: Glycerin-3 recorded data and calculations.

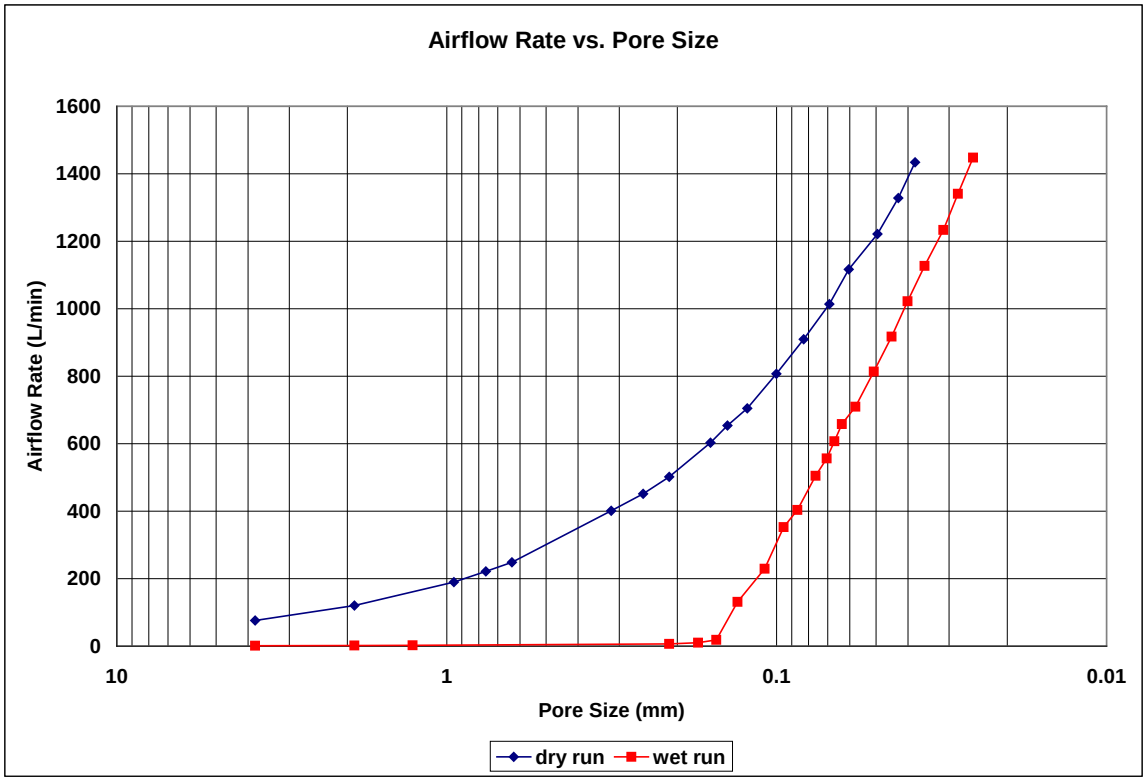

Figure B.210: Glycerin-3 airflow rate vs. pore size for the wet and dry runs.

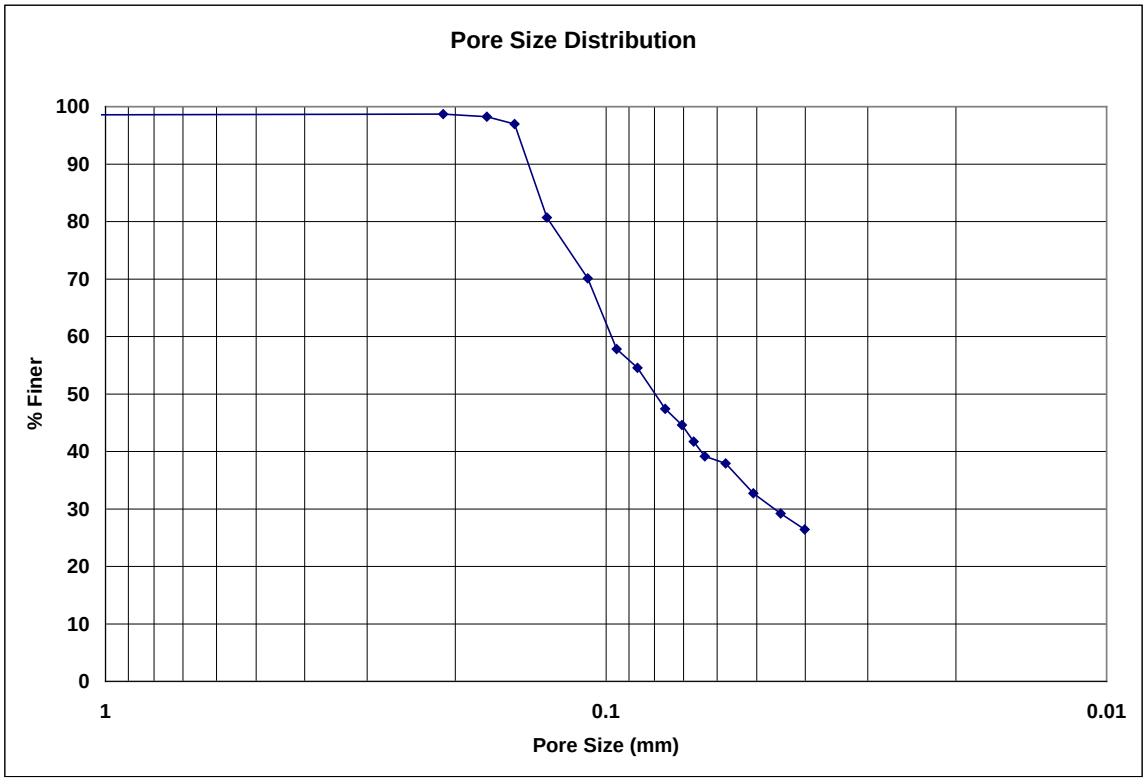

Figure B.211: Glycerin-3 pore size distribution.

Bubble Point Test
Auburn University - Department of Civil Engineering

date of test:	2/8/2007	Pore Size Calculation Parameters:		
test identification:	glycerin 3	constant, C:	2860	mm/m
test performed by:	David Hayes	contact angle:	34.51	degrees
wetting fluid:	glycerin	surface tension:	0.0634	N/m
air temperature:	21.5 °C			
porous media:	NG-1 nonwoven geotextile			
comments:	testing to determine geotextile pore size distribution			

Pore Size at Selected % Finer

% finer	pore size (mm)
98	0.16920
95	0.14975
90	0.14329
85	0.13683
80	0.12977
75	0.11913
70	0.10864
65	0.10311
60	0.09759
55	0.08772
50	0.07992
45	0.07133
40	0.06456
35	0.05380
30	0.04616
25	---
20	---
15	---
10	---
5	---

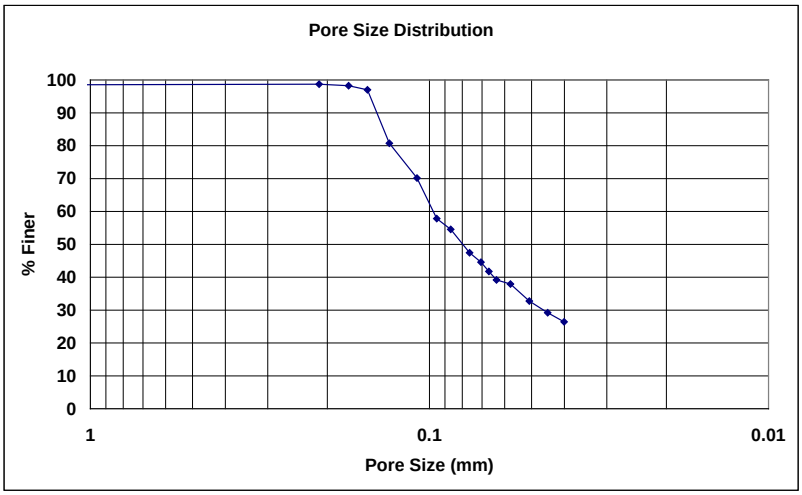

Figure B.212: Glycerin-3 pore size distribution report.

Bubble Point Test

Auburn University - Department of Civil Engineering

date of test: 2/8/2007
test identification: glycerin 4
test performed by: David Hayes
wetting fluid: glycerin
ambient air temperature: 20 °C
porous media: NG-1 nonwoven geotextile
comments: testing to determine geotextile pore size distribution

Pore Size Calculation Parameters:
constant, C: 2860 mm/m
contact angle: 34.51 degrees
surface tension: 0.0634 N/m

Dry Run

Recorded Data							Calculations				
Indirect Reading Rotameters				Direct Reading Rotameter Value (L/min)	Pressure at Rotameter Exit (psig)	Half of Manometer Reading (mm H20)	Manometer Reading (mm H20)	Manometer Pressure (Pa)	Pore Size (Diameter) (mm)	Indicated Airflow Rate (L/min)	True Airflow Rate (L/min)
First Rotameter Used		Second Rotameter Used									
Rotameter ID Number	Rotameter Value	Rotameter ID Number	Rotameter Value								
5	37				0.11	2	4	39.24	3.8077454	55.1	55.30577
5	62				0.22	4	8	78.48	1.9038727	92.5	93.18961
5	77				0.33	6	12	117.72	1.2692485	116	117.2948
5	94				0.48	8	16	156.96	0.9519364	143	145.3159
5	51	5	65		0.24	10	20	196.2	0.7615491	172.8	174.2049
5	78	5	96		0.54	20	40	392.4	0.3807745	264	268.8052
				350	0.08	26	52	510.12	0.2929035	350	350.9511
				400	0.1	34	68	667.08	0.223985	400	401.3582
				450	0.12	40	80	784.8	0.1903873	450	451.833
				500	0.15	48	96	941.76	0.1586561	500	502.5445
				550	0.17	58	116	1137.96	0.1313016	550	553.1711
				600	0.2	66	132	1294.92	0.1153862	600	604.0678
				650	0.23	76	152	1491.12	0.1002038	650	655.0653
				700	0.28	90	180	1765.8	0.0846166	700	706.6352
				800	0.36	110	220	2158.2	0.0692317	800	809.7367
				900	0.44	130	260	2550.6	0.0585807	900	913.3701
				1000	0.52	154	308	3021.48	0.0494512	1000	1017.533
				1100	0.61	180	360	3531.6	0.0423083	1100	1122.591
				1200	0.71	208	416	4080.96	0.0366129	1200	1228.638
				1300	0.82	240	480	4708.8	0.0317312	1300	1335.766
				1400	0.94	276	552	5415.12	0.0275924	1400	1444.068
				1600	1.16	384	768	7534.08	0.019832	1600	1661.931

Wet Run

Recorded Data							Calculations				
Indirect Reading Rotameters				Direct Reading Rotameter Value (L/min)	Pressure at Rotameter Exit (psig)	Half of Manometer Reading (mm H20)	Manometer Reading (mm H20)	Manometer Pressure (Pa)	Pore Size (Diameter) (mm)	Indicated Airflow Rate (L/min)	True Airflow Rate (L/min)
First Rotameter Used		Second Rotameter Used									
Rotameter ID Number	Rotameter Value	Rotameter ID Number	Rotameter Value								
2	15				0	2	4	39.24	3.8077454	0.183	0.183
2	17				0	4	8	78.48	1.9038727	0.221	0.221
2	50				0	6	12	117.72	1.2692485	0.928	0.928
2	60				0	36	72	706.32	0.2115414	1.173	1.173
5	72				0	44	88	863.28	0.1730793	108	108
5	62	5	76		0.51	50	100	981	0.1523098	206.5	210.0516
				350	0.27	58	116	1137.96	0.1313016	350	353.1997
				400	0.31	70	140	1373.4	0.1087927	400	404.1957
				450	0.34	80	160	1569.6	0.0951936	450	455.1743
				500	0.38	88	176	1726.56	0.0865397	500	506.4214
				550	0.43	100	200	1962	0.0761549	550	557.9862
				600	0.48	108	216	2118.96	0.0705138	600	609.7172
				650	0.51	114	228	2236.68	0.0668026	650	661.1794
				700	0.56	120	240	2354.4	0.0634624	700	713.2087
				800	0.64	132	264	2589.84	0.0576931	800	817.2294
				900	0.75	150	300	2943	0.0507699	900	922.6736
				1000	0.87	170	340	3335.4	0.044797	1000	1029.166
				1100	0.97	190	380	3727.8	0.0400815	1100	1135.713
				1200	1.09	214	428	4198.68	0.0355864	1200	1243.694
				1300	1.23	244	488	4787.28	0.031211	1300	1353.295
				1400	1.34	270	540	5297.4	0.0282055	1400	1462.418

Figure B.213: Glycerin-4 recorded data and calculations.

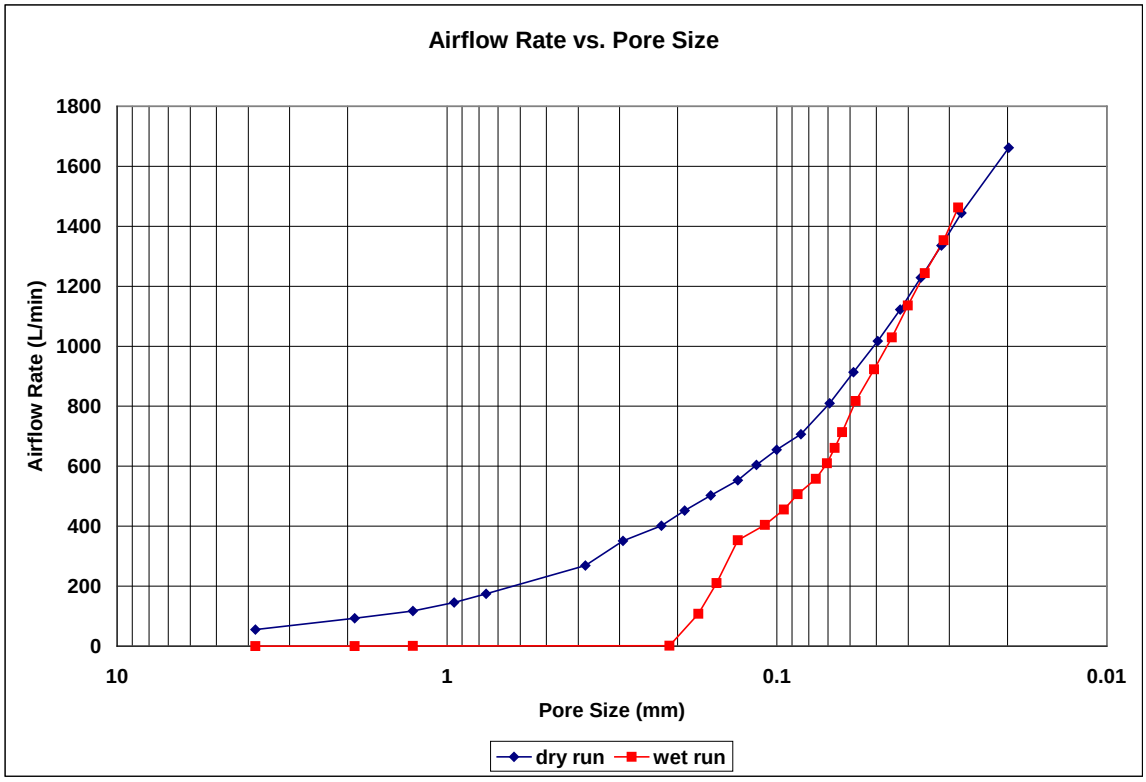

Figure B.214: Glycerin-4 airflow rate vs. pore size for the wet and dry runs.

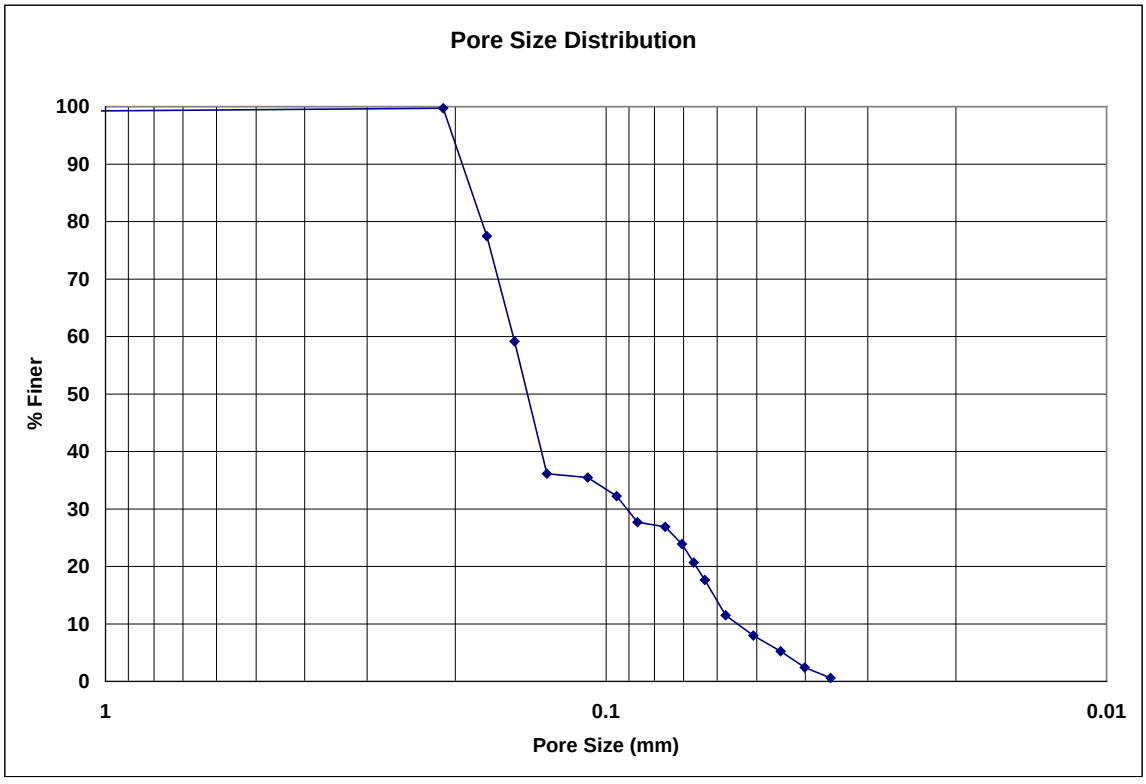

Figure B.215: Glycerin-4 pore size distribution.

Bubble Point Test
Auburn University - Department of Civil Engineering

date of test:	2/8/2007	Pore Size Calculation Parameters:		
test identification:	glycerin 4	constant, C:	2860	mm/m
test performed by:	David Hayes	contact angle:	34.51	degrees
wetting fluid:	glycerin	surface tension:	0.0634	N/m
air temperature:	20 °C			
porous media:	NG-1 nonwoven geotextile			
comments:	testing to determine geotextile pore size distribution			

Pore Size at Selected % Finer

% finer	pore size (mm)
98	0.20857
95	0.20338
90	0.19473
85	0.18609
80	0.17744
75	0.17027
70	0.16460
65	0.15893
60	0.15327
55	0.14851
50	0.14395
45	0.13938
40	0.13482
35	0.10688
30	0.09095
25	0.07259
20	0.06607
15	0.06098
10	0.05475
5	0.04441

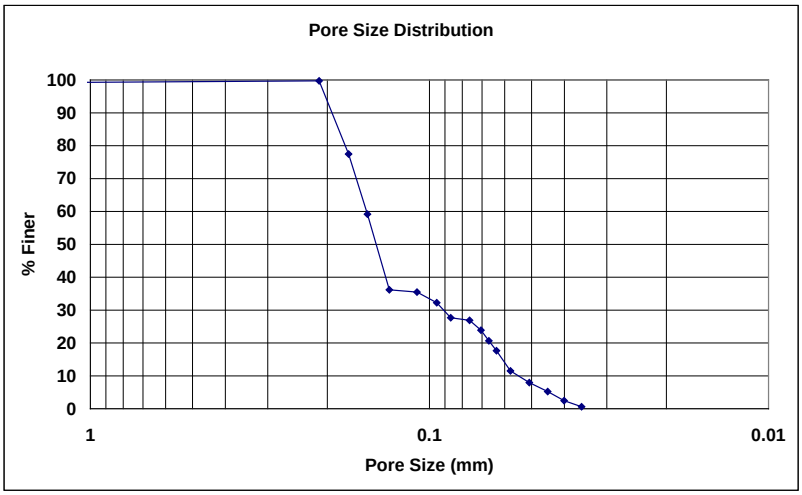

Figure B.216: Glycerin-4 pore size distribution report.

Bubble Point Test

Auburn University - Department of Civil Engineering

date of test: 2/8/2007
test identification: glycerin 5
test performed by: David Hayes
wetting fluid: glycerin
ambient air temperature: 20 °C
porous media: NG-1 nonwoven geotextile
comments: testing to determine geotextile pore size distribution

Pore Size Calculation Parameters:
constant, C: 2860 mm/m
contact angle: 34.51 degrees
surface tension: 0.0634 N/m

Dry Run

Recorded Data							Calculations				
Indirect Reading Rotameters				Direct Reading Rotameter Value (L/min)	Pressure at Rotameter Exit (psig)	Half of Manometer Reading (mm H20)	Manometer Reading (mm H20)	Manometer Pressure (Pa)	Pore Size (Diameter) (mm)	Indicated Airflow Rate (L/min)	True Airflow Rate (L/min)
First Rotameter Used		Second Rotameter Used									
Rotameter ID Number	Rotameter Value	Rotameter ID Number	Rotameter Value								
5	44				0.09	2	4	39.24	3.8077454	65.3	65.49959
5	72				0.24	4	8	78.48	1.9038727	108	108.8781
5	85				0.36	6	12	117.72	1.2692485	129	130.57
5	51	5	63		0.23	8	16	156.96	0.9519364	169.7	171.0224
5	64	5	80		0.37	12	24	235.44	0.6346242	216.6	219.309
5	76	5	94		0.51	16	32	313.92	0.4759682	257	261.4202
				350	0.09	24	48	470.88	0.3173121	350	351.0698
				450	0.12	34	68	667.08	0.223985	450	451.833
				500	0.15	42	84	824.04	0.1813212	500	502.5445
				550	0.17	50	100	981	0.1523098	550	553.1711
				600	0.19	56	112	1098.72	0.1359909	600	603.8651
				650	0.22	66	132	1294.92	0.1153862	650	654.8459
				700	0.25	76	152	1491.12	0.1002038	700	705.9273
				800	0.31	94	188	1844.28	0.0810159	800	808.3914
				900	0.37	102	204	2001.24	0.0746617	900	911.2561
				1000	0.45	132	264	2589.84	0.0576931	1000	1015.191
				1100	0.52	156	312	3060.72	0.0488172	1100	1119.287
				1200	0.61	180	360	3531.6	0.0423083	1200	1224.645
				1300	0.71	210	420	4120.2	0.0362642	1300	1331.024
				1400	0.81	238	476	4669.56	0.0319979	1400	1438.054
				1600	1.08	340	680	6670.8	0.0223985	1600	1657.734

Wet Run

Recorded Data							Calculations				
Indirect Reading Rotameters				Direct Reading Rotameter Value (L/min)	Pressure at Rotameter Exit (psig)	Half of Manometer Reading (mm H20)	Manometer Reading (mm H20)	Manometer Pressure (Pa)	Pore Size (Diameter) (mm)	Indicated Airflow Rate (L/min)	True Airflow Rate (L/min)
First Rotameter Used		Second Rotameter Used									
Rotameter ID Number	Rotameter Value	Rotameter ID Number	Rotameter Value								
2	20				0	2	4	39.24	3.8077454	0.279	0.279
2	49				0	4	8	78.48	1.9038727	0.904	0.904
2	81				0	6	12	117.72	1.2692485	1.7	1.7
4	78				0.56	36	72	706.32	0.2115414	29.5	30.05665
5	43				0.25	44	88	863.28	0.1730793	63.8	64.34023
5	88				0.58	50	100	981	0.1523098	133	135.5984
5	66	5	82		0.58	58	116	1137.96	0.1313016	222.7	227.0509
				400	0.33	70	140	1373.4	0.1087927	400	404.4649
				450	0.36	80	160	1569.6	0.0951936	450	455.4769
				500	0.39	88	176	1726.56	0.0865397	500	506.5892
				550	0.44	100	200	1962	0.0761549	550	558.1706
				600	0.48	108	216	2118.96	0.0705138	600	609.7172
				650	0.51	114	228	2236.68	0.0668026	650	661.1794
				700	0.56	120	240	2354.4	0.0634624	700	713.2087
				800	0.63	132	264	2589.84	0.0576931	800	816.963
				900	0.71	150	300	2943	0.0507699	900	921.4784
				1000	0.8	170	340	3335.4	0.044797	1000	1026.85
				1100	0.92	190	380	3727.8	0.0400815	1100	1133.899
				1200	1.02	214	428	4198.68	0.0355864	1200	1240.934
				1300	1.12	244	488	4787.28	0.031211	1300	1348.615
				1400	1.24	270	540	5297.4	0.0282055	1400	1457.852

Figure B.217: Glycerin-5 recorded data and calculations.

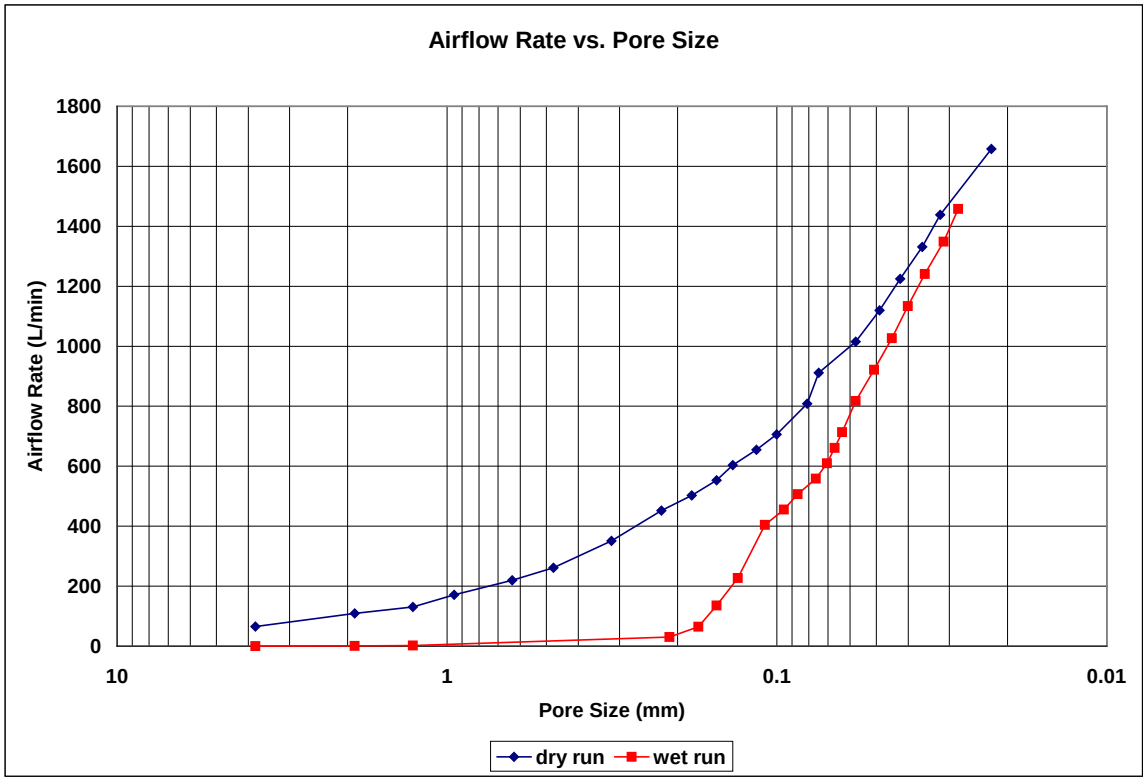

Figure B.218: Glycerin-5 airflow rate vs. pore size for the wet and dry runs.

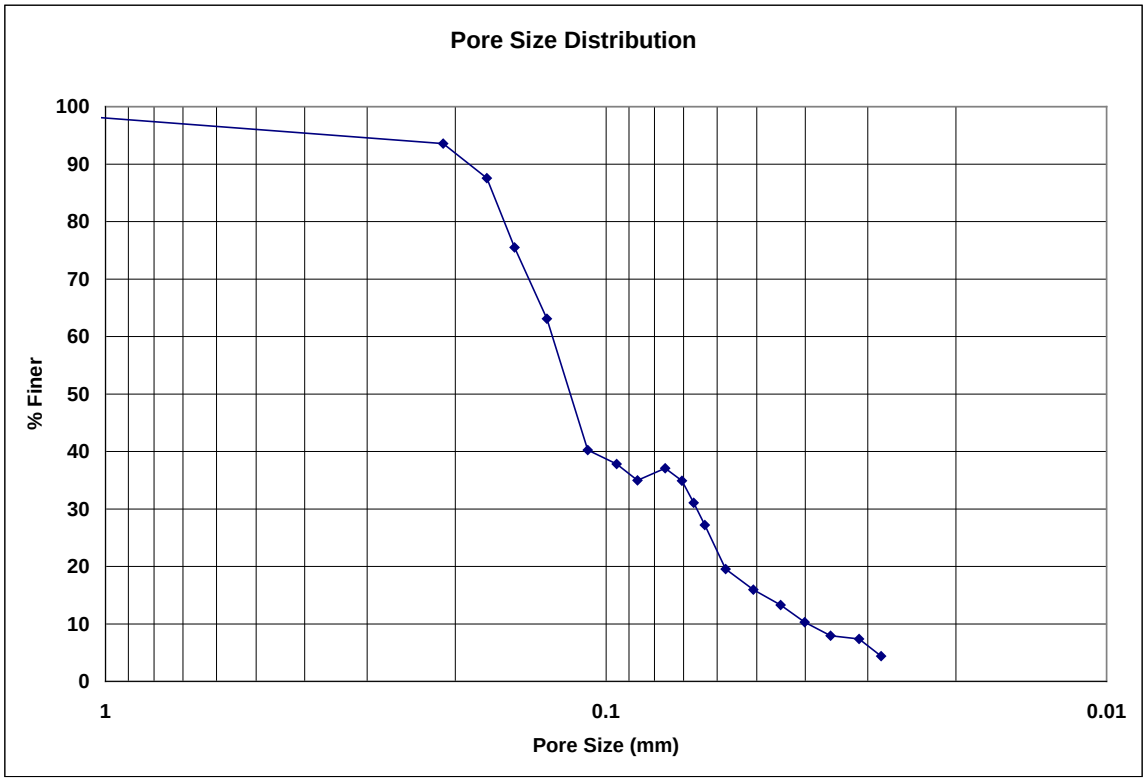

Figure B.219: Glycerin-5 pore size distribution.

Bubble Point Test
Auburn University - Department of Civil Engineering

date of test:	2/8/2007		Pore Size Calculation Parameters:		
test identification:	glycerin 5		constant, C:	2860	mm/m
test performed by:	David Hayes		contact angle:	34.51	degrees
wetting fluid:	glycerin		surface tension:	0.0634	N/m
air temperature:	20	°C			
porous media:	NG-1 nonwoven geotextile				
comments:	testing to determine geotextile pore size distribution				

Pore Size at Selected % Finer

% finer	pore size (mm)
98	1.12559
95	0.50817
90	0.18875
85	0.16868
80	0.16008
75	0.15148
70	0.14300
65	0.13451
60	0.12824
55	0.12331
50	0.11839
45	0.11346
40	0.10734
35	0.08666
30	0.06587
25	0.06180
20	0.05805
15	0.04862
10	0.03954
5	0.02882

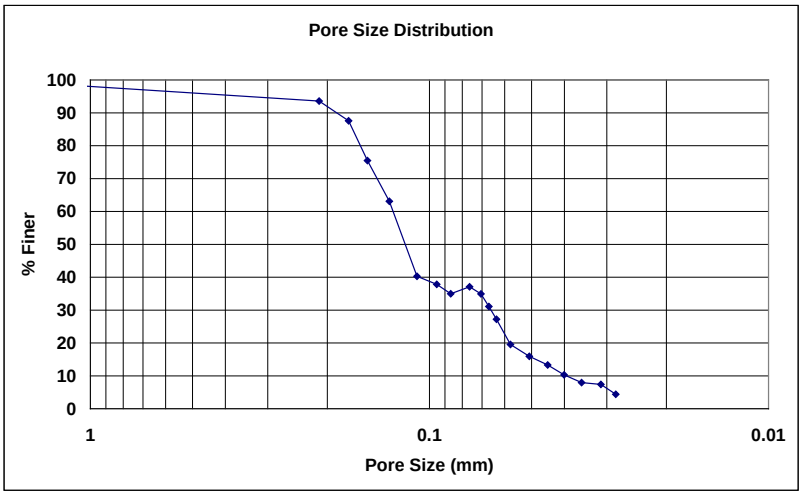

Figure B.220: Glycerin-5 pore size distribution report.

Bubble Point Test

Auburn University - Department of Civil Engineering

date of test: 2/8/2007
test identification: glycerin 6
test performed by: David Hayes
wetting fluid: glycerin
ambient air temperature: 20 °C
porous media: NG-1 nonwoven geotextile
comments: testing to determine geotextile pore size distribution

Pore Size Calculation Parameters:
constant, C: 2860 mm/m
contact angle: 34.51 degrees
surface tension: 0.0634 N/m

Dry Run

Recorded Data							Calculations				
Indirect Reading Rotameters				Direct Reading Rotameter Value (L/min)	Pressure at Rotameter Exit (psig)	Half of Manometer Reading (mm H20)	Manometer Reading (mm H20)	Manometer Pressure (Pa)	Pore Size (Diameter) (mm)	Indicated Airflow Rate (L/min)	True Airflow Rate (L/min)
First Rotameter Used		Second Rotameter Used									
Rotameter ID Number	Rotameter Value	Rotameter ID Number	Rotameter Value								
5	50				0.1	2	4	39.24	3.8077454	74.2	74.45195
5	74				0.25	4	8	78.48	1.9038727	111	111.9399
5	95				0.43	6	12	117.72	1.2692485	145	147.1055
5	54	5	68		0.15	8	16	156.96	0.9519364	182.3	183.2277
5	68	5	84		0.24	12	24	235.44	0.6346242	229	230.8618
5	80	5	100		0.54	16	32	313.92	0.4759682	274	278.9873
				350	0.05	20	40	392.4	0.3807745	350	350.5947
				400	0.07	26	52	510.12	0.2929035	400	400.9512
				450	0.08	32	64	627.84	0.2379841	450	451.2228
				500	0.1	36	72	706.32	0.2115414	500	501.6978
				550	0.15	44	88	863.28	0.1730793	550	552.799
				600	0.18	52	104	1020.24	0.1464517	600	603.6623
				650	0.21	60	120	1177.2	0.1269248	650	654.6264
				700	0.23	68	136	1334.16	0.1119925	700	705.4549
				800	0.29	82	164	1608.84	0.0928718	800	807.8526
				900	0.35	98	196	1922.76	0.0777091	900	910.6513
				1000	0.41	116	232	2275.92	0.0656508	1000	1013.85
				1100	0.48	136	272	2668.32	0.0559963	1100	1117.815
				1200	0.58	162	324	3178.44	0.0470092	1200	1223.444
				1300	0.67	188	376	3688.56	0.0405079	1300	1329.296
				1400	0.75	216	432	4237.92	0.0352569	1400	1435.27
				1600	0.87	276	552	5415.12	0.0275924	1600	1646.666

Wet Run

Recorded Data							Calculations				
Indirect Reading Rotameters				Direct Reading Rotameter Value (L/min)	Pressure at Rotameter Exit (psig)	Half of Manometer Reading (mm H20)	Manometer Reading (mm H20)	Manometer Pressure (Pa)	Pore Size (Diameter) (mm)	Indicated Airflow Rate (L/min)	True Airflow Rate (L/min)
First Rotameter Used		Second Rotameter Used									
Rotameter ID Number	Rotameter Value	Rotameter ID Number	Rotameter Value								
2	37				0	20	40	392.4	0.3807745	0.631	0.631
2	60				0	36	72	706.32	0.2115414	1.173	1.173
4	8				0.12	40	80	784.8	0.1903873	2.43	2.439898
4	53				0.32	46	92	902.52	0.1655541	19	19.20569
5	34				0.21	52	104	1020.24	0.1464517	50.7	51.06086
5	56				0.32	60	120	1177.2	0.1269248	83.3	84.20179
5	62	5	76		0.5	66	132	1294.92	0.1153862	206.5	209.9825
5	76	5	93		0.68	80	160	1569.6	0.0951936	255	260.8313
				350	0.26	80	160	1569.6	0.0951936	350	353.0817
				400	0.29	92	184	1805.04	0.0827771	400	403.9263
				450	0.32	102	204	2001.24	0.0746617	450	454.8716
				500	0.4	124	248	2432.88	0.0614152	500	506.7571
				600	0.42	140	280	2746.8	0.0543964	600	608.5111
				650	0.46	148	296	2903.76	0.051456	650	660.0917
				700	0.51	162	324	3178.44	0.0470092	700	712.0393
				800	0.56	172	344	3374.64	0.0442761	800	815.0957
				900	0.65	200	400	3924	0.0380775	900	919.6827
				1000	0.75	222	444	4355.64	0.034304	1000	1025.193
				1100	0.83	242	484	4748.04	0.031469	1100	1130.628
				1200	0.88	260	520	5101.2	0.0292903	1200	1235.396
				1300	0.98	290	580	5689.8	0.0262603	1300	1342.634
				1400	1.11	320	640	6278.4	0.0237984	1400	1451.895

Figure B.221: Glycerin-6 recorded data and calculations.

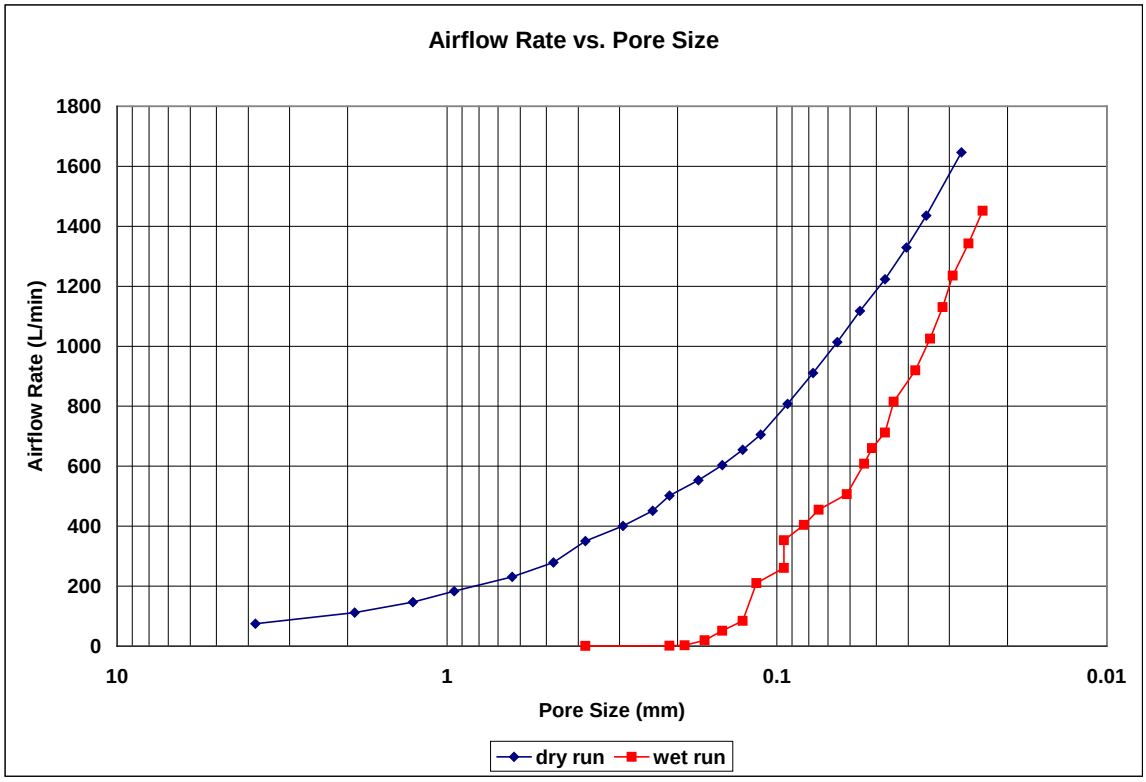

Figure B.222: Glycerin-6 airflow rate vs. pore size for the wet and dry runs.

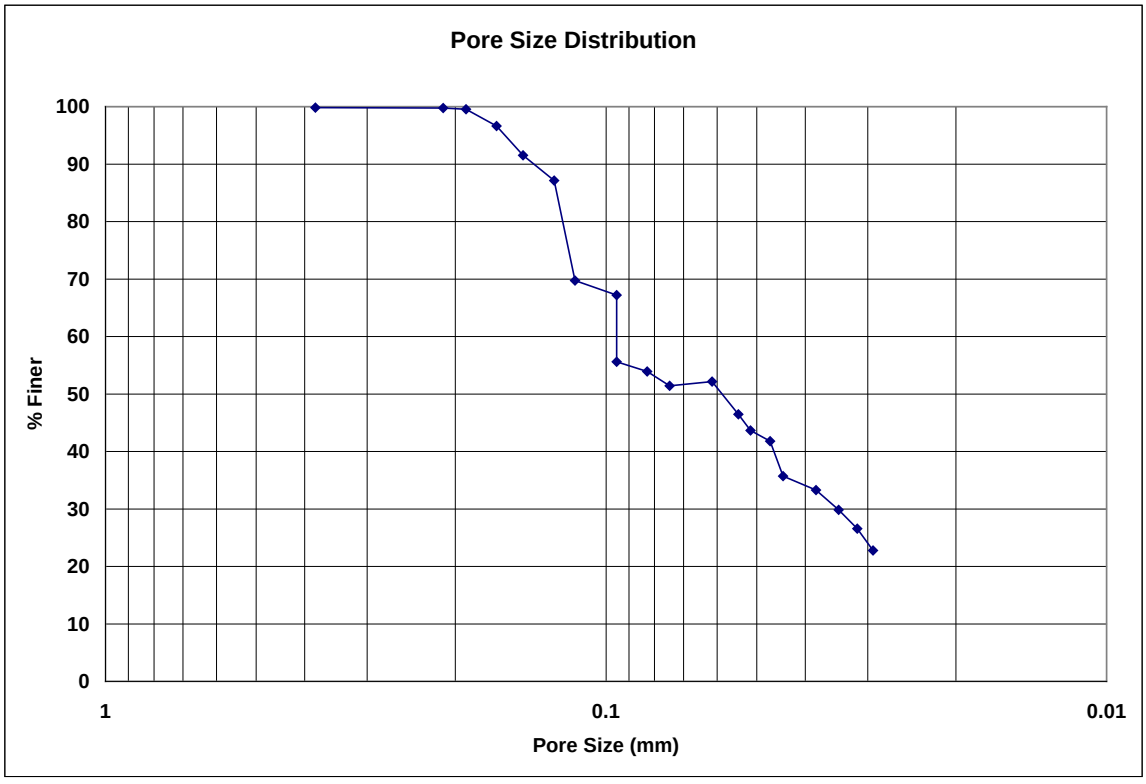

Figure B.223: Glycerin-6 pore size distribution.

Bubble Point Test
Auburn University - Department of Civil Engineering

date of test: 2/8/2007
test identification: glycerin 6
test performed by: David Hayes
wetting fluid: glycerin
air temperature: 20 °C
porous media: NG-1 nonwoven geotextile
comments: testing to determine geotextile pore size distribution

Pore Size Calculation Parameters:
constant, C: 2860 mm/m
contact angle: 34.51 degrees
surface tension: 0.0634 N/m

Pore Size at Selected % Finer

% finer	pore size (mm)
98	0.17732
95	0.15948
90	0.13962
85	0.12551
80	0.12219
75	0.11888
70	0.11556
65	0.09519
60	0.09519
55	0.09075
50	0.05875
45	0.05287
40	0.04620
35	0.04246
30	0.03446
25	0.03057
20	---
15	---
10	---
5	---

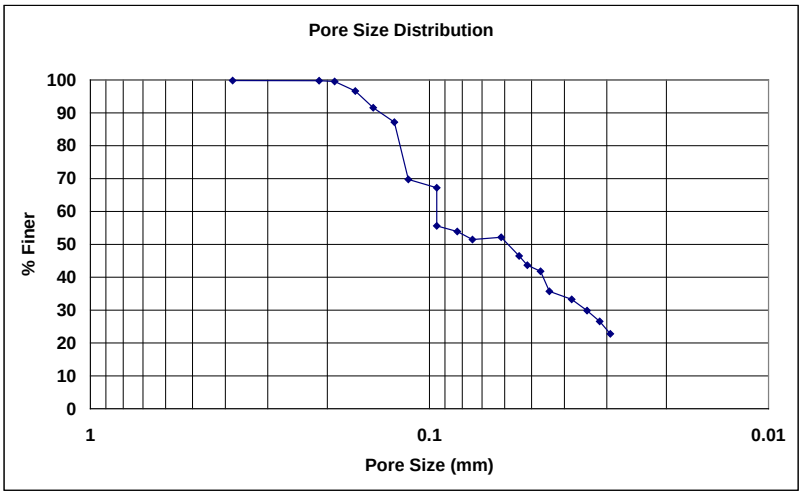

Figure B.224: Glycerin-6 pore size distribution report.

Bubble Point Test

Auburn University - Department of Civil Engineering

date of test: 2/9/2007
test identification: glycerin 7
test performed by: David Hayes
wetting fluid: glycerin
ambient air temperature: 19.8 °C
porous media: NG-1 nonwoven geotextile
comments: testing to determine geotextile pore size distribution

Pore Size Calculation Parameters:
constant, C: 2860 mm/m
contact angle: 34.51 degrees
surface tension: 0.0634 N/m

Dry Run

Recorded Data							Calculations				
Indirect Reading Rotameters				Direct Reading Rotameter Value (L/min)	Pressure at Rotameter Exit (psig)	Half of Manometer Reading (mm H20)	Manometer Reading (mm H20)	Manometer Pressure (Pa)	Pore Size (Diameter) (mm)	Indicated Airflow Rate (L/min)	True Airflow Rate (L/min)
First Rotameter Used		Second Rotameter Used									
Rotameter ID Number	Rotameter Value	Rotameter ID Number	Rotameter Value								
5	50				0.12	2	4	39.24	3.8077454	74.2	74.50224
5	75				0.28	4	8	78.48	1.9038727	113	114.0711
5	90				0.41	6	12	117.72	1.2692485	137	138.8974
5	60	5	74		0.32	10	20	196.2	0.7615491	200.4	202.5695
5	72	5	90		0.47	14	28	274.68	0.5439636	245	248.8859
				400	0.11	28	56	549.36	0.2719818	400	401.4938
				450	0.13	32	64	627.84	0.2379841	450	451.9854
				500	0.15	40	80	784.8	0.1903873	500	502.5445
				550	0.17	46	92	902.52	0.1655541	550	553.1711
				600	0.2	54	108	1059.48	0.1410276	600	604.0678
				650	0.23	64	128	1255.68	0.118992	650	655.0653
				700	0.26	74	148	1451.88	0.102912	700	706.1633
				800	0.31	88	176	1726.56	0.0865397	800	808.3914
				900	0.37	108	216	2118.96	0.0705138	900	911.2561
				1000	0.44	128	256	2511.36	0.059496	1000	1014.856
				1100	0.51	150	300	2943	0.0507699	1100	1118.919
				1200	0.6	178	356	3492.36	0.0427837	1200	1224.245
				1300	0.7	206	412	4041.72	0.0369684	1300	1330.592
				1400	0.79	236	472	4630.32	0.032269	1400	1437.127

Wet Run

Recorded Data							Calculations				
Indirect Reading Rotameters				Direct Reading Rotameter Value (L/min)	Pressure at Rotameter Exit (psig)	Half of Manometer Reading (mm H20)	Manometer Reading (mm H20)	Manometer Pressure (Pa)	Pore Size (Diameter) (mm)	Indicated Airflow Rate (L/min)	True Airflow Rate (L/min)
First Rotameter Used		Second Rotameter Used									
Rotameter ID Number	Rotameter Value	Rotameter ID Number	Rotameter Value								
2	14				0	4	8	78.48	1.9038727	0.164	0.164
2	47				0	24	48	470.88	0.3173121	0.858	0.858
2	81				0	34	68	667.08	0.223985	1.7	1.7
5	52	5	65		0.35	56	112	1098.72	0.1359909	174.3	176.3628
5	75	5	93		0.63	72	144	1412.64	0.1057707	254	259.3858
				350	0.18	80	160	1569.6	0.0951936	350	352.1363
				400	0.23	92	184	1805.04	0.0827771	400	403.1171
				450	0.25	100	200	1962	0.0761549	450	453.8104
				550	0.32	120	240	2354.4	0.0634624	550	555.9542
				600	0.36	132	264	2589.84	0.0576931	600	607.3025
				650	0.39	142	284	2786.04	0.0536302	650	658.566
				700	0.43	154	308	3021.48	0.0494512	700	710.1643
				800	0.5	180	360	3531.6	0.0423083	800	813.4917
				900	0.55	190	380	3727.8	0.0400815	900	916.6821
				1000	0.64	220	440	4316.4	0.0346159	1000	1021.537
				1100	0.75	244	488	4787.28	0.031211	1100	1127.712
				1200	0.85	272	544	5336.64	0.0279981	1200	1234.206
				1300	0.95	302	604	5925.24	0.0252169	1300	1341.349
				1400	1.08	340	680	6670.8	0.0223985	1400	1450.517

Figure B.225: Glycerin-7 recorded data and calculations.

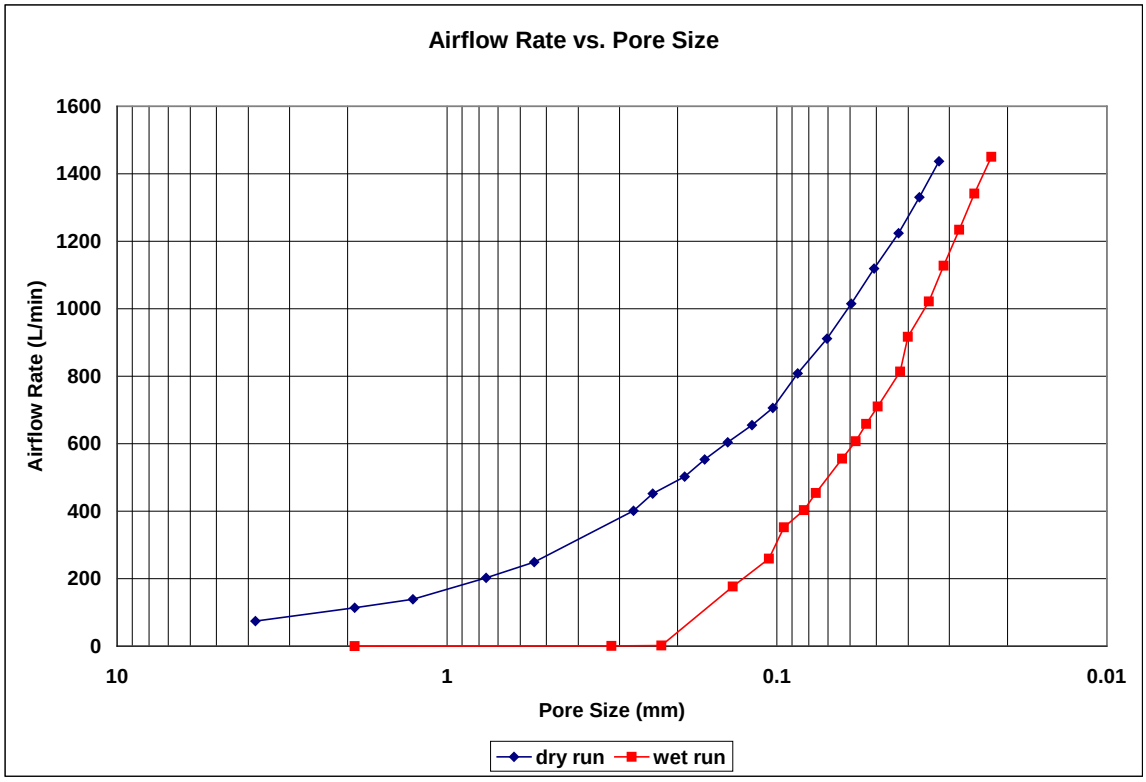

Figure B.226: Glycerin-7 airflow rate vs. pore size for the wet and dry runs.

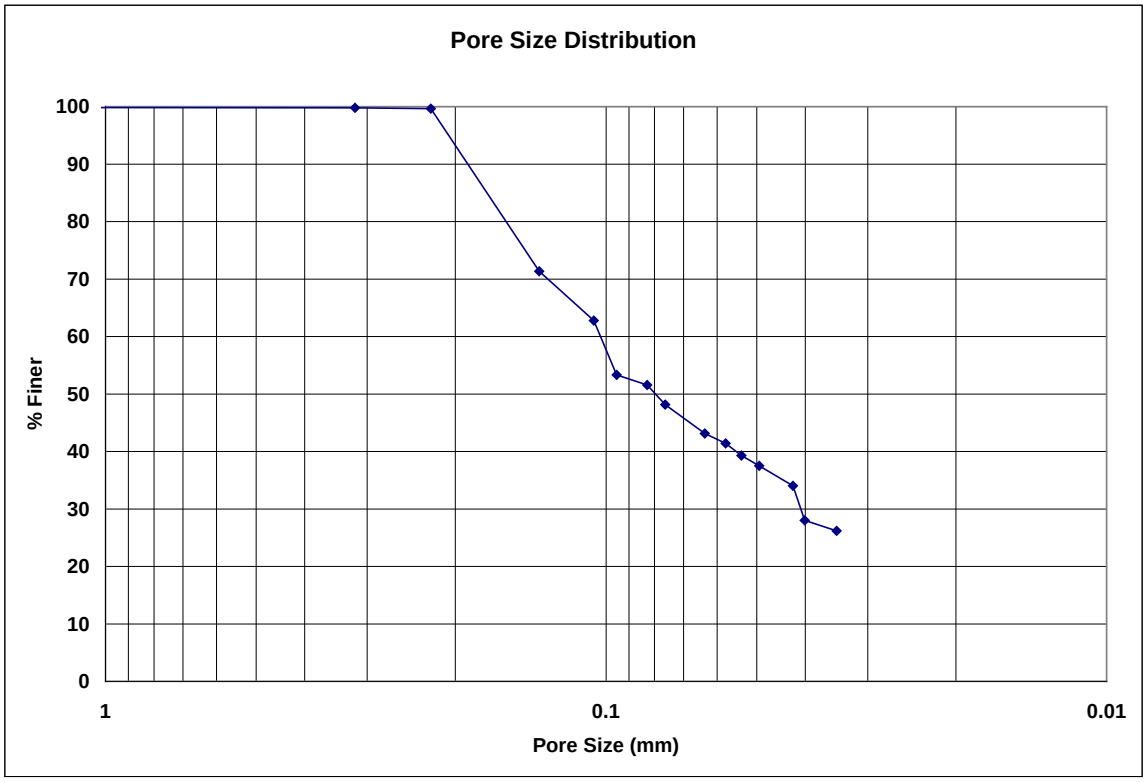

Figure B.227: Glycerin-7 pore size distribution.

Bubble Point Test
Auburn University - Department of Civil Engineering

date of test: 2/9/2007
test identification: glycerin 7
test performed by: David Hayes
wetting fluid: glycerin
air temperature: 19.8 °C
porous media: NG-1 nonwoven geotextile
comments: testing to determine geotextile pore size distribution

Pore Size Calculation Parameters:
constant, C: 2860 mm/m
contact angle: 34.51 degrees
surface tension: 0.0634 N/m

Pore Size at Selected % Finer

% finer	pore size (mm)
98	0.21889
95	0.20956
90	0.19400
85	0.17844
80	0.16289
75	0.14733
70	0.13120
65	0.11357
60	0.10265
55	0.09707
50	0.07974
45	0.06820
40	0.05499
35	0.04432
30	0.04081
25	---
20	---
15	---
10	---
5	---

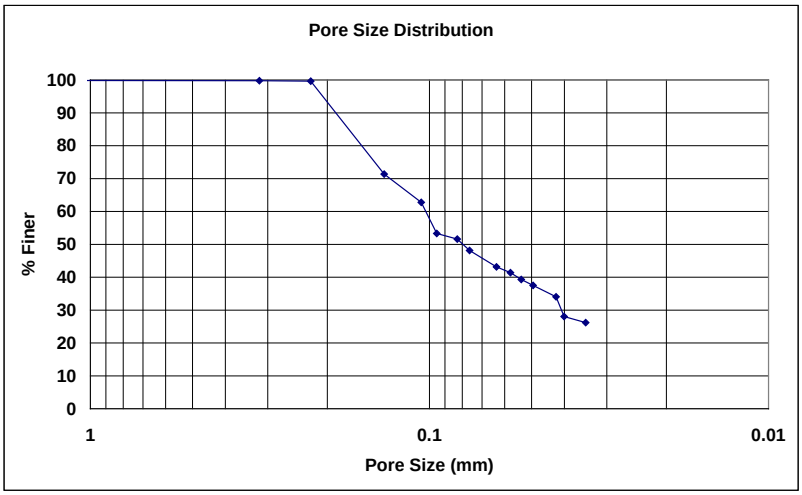

Figure B.228: Glycerin-7 pore size distribution report.

Bubble Point Test

Auburn University - Department of Civil Engineering

date of test: 2/9/2007
test identification: glycerin 8
test performed by: David Hayes
wetting fluid: glycerin
ambient air temperature: 19.8 °C
porous media: NG-1 nonwoven geotextile
comments: testing to determine geotextile pore size distribution

Pore Size Calculation Parameters:
constant, C: 2860 mm/m
contact angle: 34.51 degrees
surface tension: 0.0634 N/m

Dry Run

Recorded Data							Calculations				
Indirect Reading Rotameters				Direct Reading Rotameter Value (L/min)	Pressure at Rotameter Exit (psig)	Half of Manometer Reading (mm H20)	Manometer Reading (mm H20)	Manometer Pressure (Pa)	Pore Size (Diameter) (mm)	Indicated Airflow Rate (L/min)	True Airflow Rate (L/min)
First Rotameter Used		Second Rotameter Used									
Rotameter ID Number	Rotameter Value	Rotameter ID Number	Rotameter Value								
5	40				0.08	2	4	39.24	3.8077454	59.4	59.56141
5	68				0.22	4	8	78.48	1.9038727	102	102.7604
5	87				0.38	6	12	117.72	1.2692485	132	133.6952
5	56	5	70		0.28	10	20	196.2	0.7615491	188.3	190.0849
5	70	5	86		0.43	14	28	274.68	0.5439636	235	238.4123
				350	0.06	22	44	431.64	0.3461587	350	350.7136
				400	0.08	28	56	549.36	0.2719818	400	401.087
				450	0.09	34	68	667.08	0.223985	450	451.3754
				500	0.12	40	80	784.8	0.1903873	500	502.0367
				550	0.14	48	96	941.76	0.1586561	550	552.6128
				600	0.17	56	112	1098.72	0.1359909	600	603.4594
				650	0.2	66	132	1294.92	0.1153862	650	654.4068
				700	0.23	76	152	1491.12	0.1002038	700	705.4549
				800	0.29	90	180	1765.8	0.0846166	800	807.8526
				900	0.37	108	216	2118.96	0.0705138	900	911.2561
				1000	0.44	130	260	2550.6	0.0585807	1000	1014.856
				1100	0.52	152	304	2982.24	0.0501019	1100	1119.287
				1200	0.62	180	360	3531.6	0.0423083	1200	1225.045
				1300	0.72	206	412	4041.72	0.0369684	1300	1331.456
				1400	0.83	238	476	4669.56	0.0319979	1400	1438.981

Wet Run

Recorded Data							Calculations				
Indirect Reading Rotameters				Direct Reading Rotameter Value (L/min)	Pressure at Rotameter Exit (psig)	Half of Manometer Reading (mm H20)	Manometer Reading (mm H20)	Manometer Pressure (Pa)	Pore Size (Diameter) (mm)	Indicated Airflow Rate (L/min)	True Airflow Rate (L/min)
First Rotameter Used		Second Rotameter Used									
Rotameter ID Number	Rotameter Value	Rotameter ID Number	Rotameter Value								
2	20				0	6	12	117.72	1.2692485	0.279	0.279
2	40				0	20	40	392.4	0.3807745	0.698	0.698
2	62				0	40	80	784.8	0.1903873	1.224	1.224
4	93				0.74	50	100	981	0.1523098	36.1	36.99748
5	83				0.52	62	124	1216.44	0.1228305	125	127.1917
5	58	5	72		0.48	70	140	1373.4	0.1087927	194.3	197.4468
				350	0.24	74	148	1451.88	0.102912	350	352.8456
				400	0.28	86	172	1687.32	0.0885522	400	403.7916
				500	0.35	108	216	2118.96	0.0705138	500	505.9174
				550	0.39	124	248	2432.88	0.0614152	550	557.2482
				600	0.43	140	280	2746.8	0.0543964	600	608.7123
				700	0.52	164	328	3217.68	0.0464359	700	712.2734
				800	0.58	186	372	3649.32	0.0409435	800	815.6296
				900	0.71	204	408	4002.48	0.0373308	900	921.4784
				1000	0.8	230	460	4512.6	0.0331108	1000	1026.85
				1100	0.9	258	516	5061.96	0.0295174	1100	1133.173
				1200	1	284	568	5572.08	0.0268151	1200	1240.145
				1300	1.13	320	640	6278.4	0.0237984	1300	1349.041
				1400	1.24	360	720	7063.2	0.0211541	1400	1457.852

Figure B.229: Glycerin-8 recorded data and calculations.

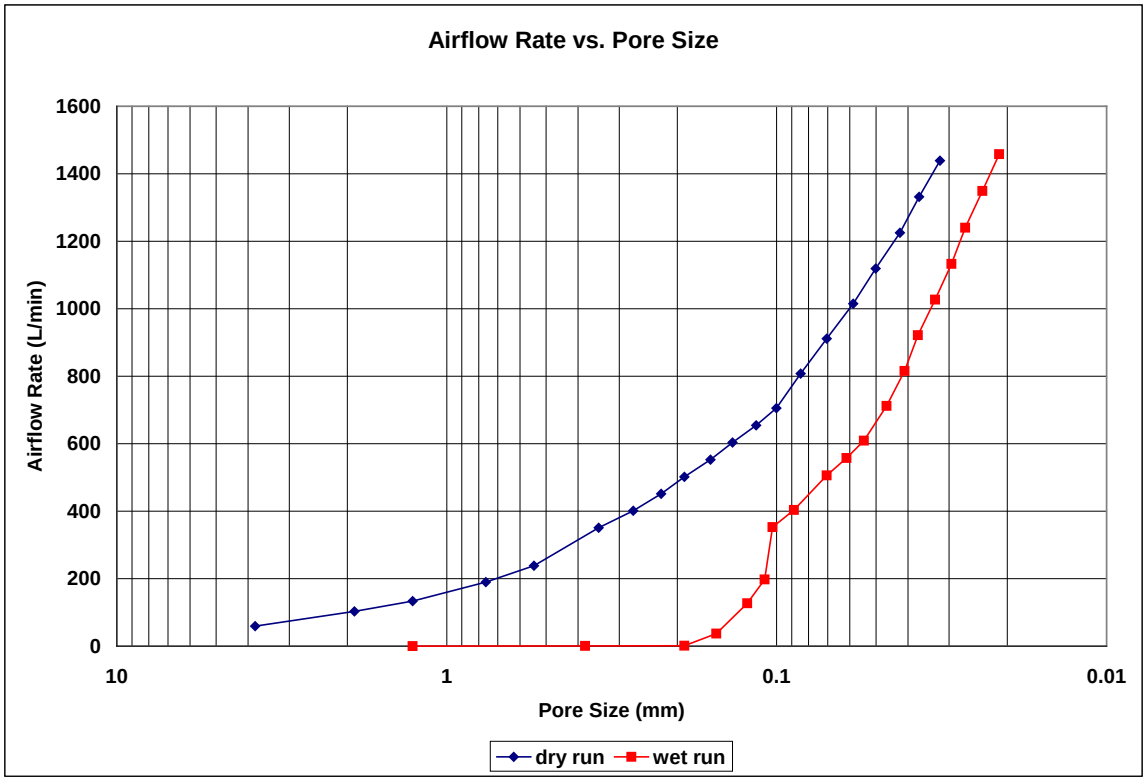

Figure B.230: Glycerin-8 airflow rate vs. pore size for the wet and dry runs.

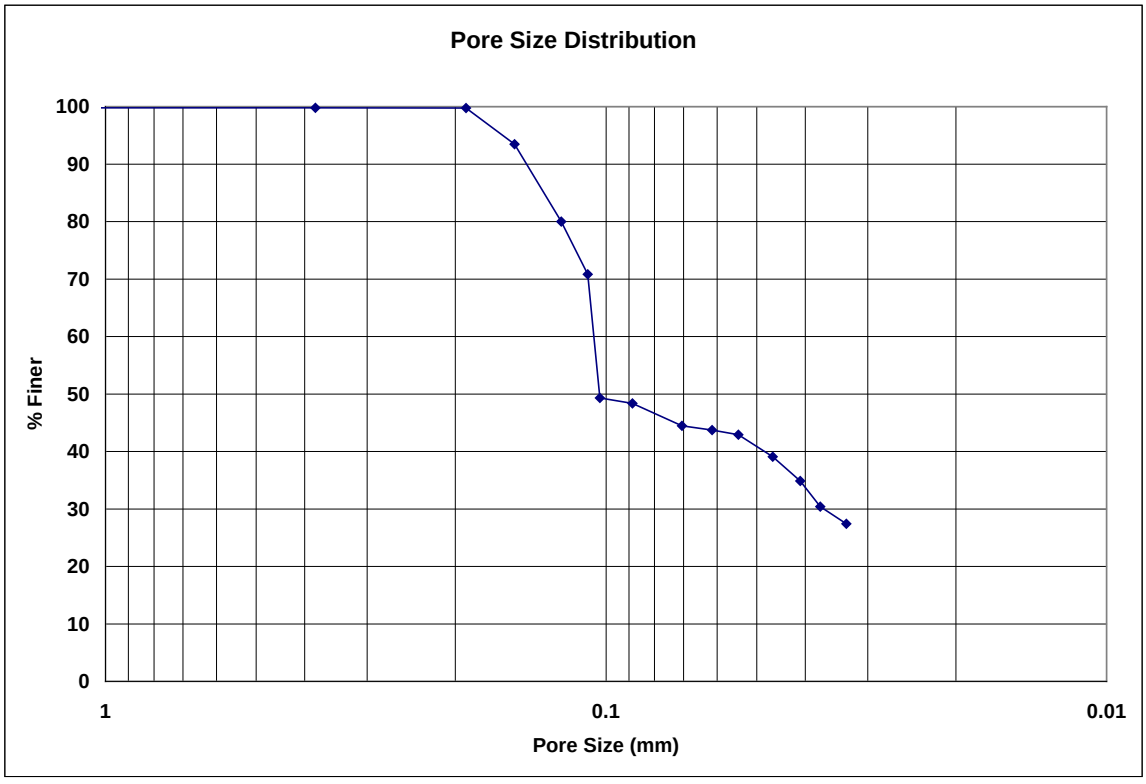

Figure B.231: Glycerin-8 pore size distribution.

Bubble Point Test
Auburn University - Department of Civil Engineering

date of test: 2/9/2007
test identification: glycerin 8
test performed by: David Hayes
wetting fluid: glycerin
air temperature: 19.8 °C
porous media: NG-1 nonwoven geotextile
comments: testing to determine geotextile pore size distribution

Pore Size Calculation Parameters:
constant, C: 2860 mm/m
contact angle: 34.51 degrees
surface tension: 0.0634 N/m

Pore Size at Selected % Finer

% finer	pore size (mm)
98	0.17974
95	0.16156
90	0.14471
85	0.13377
80	0.12283
75	0.11519
70	0.10857
65	0.10720
60	0.10583
55	0.10446
50	0.10310
45	0.07292
40	0.04836
35	0.04112
30	0.03675
25	---
20	---
15	---
10	---
5	---

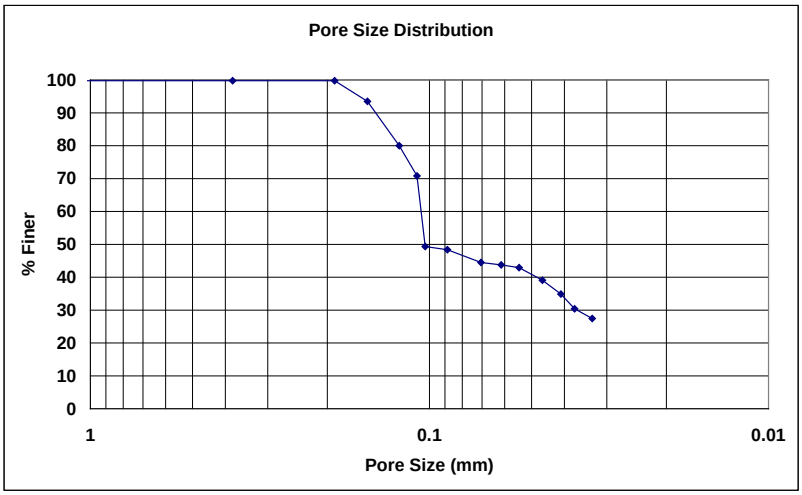

Figure B.232: Glycerin-8 pore size distribution report.

Bubble Point Test

Auburn University - Department of Civil Engineering

date of test: 2/9/2007
test identification: glycerin 9
test performed by: David Hayes
wetting fluid: glycerin
ambient air temperature: 19.8 °C
porous media: NG-1 nonwoven geotextile
comments: testing to determine geotextile pore size distribution

Pore Size Calculation Parameters:
constant, C: 2860 mm/m
contact angle: 34.51 degrees
surface tension: 0.0634 N/m

Dry Run

Recorded Data							Calculations				
Indirect Reading Rotameters				Direct Reading Rotameter Value (L/min)	Pressure at Rotameter Exit (psig)	Half of Manometer Reading (mm H20)	Manometer Reading (mm H20)	Manometer Pressure (Pa)	Pore Size (Diameter) (mm)	Indicated Airflow Rate (L/min)	True Airflow Rate (L/min)
First Rotameter Used		Second Rotameter Used									
Rotameter ID Number	Rotameter Value	Rotameter ID Number	Rotameter Value								
5	50				0.15	2	4	39.24	3.8077454	74.2	74.57761
5	76				0.31	4	8	78.48	1.9038727	114	115.1958
5	93				0.46	6	12	117.72	1.2692485	141	143.1891
5	60	5	75		0.34	10	20	196.2	0.7615491	202.4	204.7273
5	75	5	93		0.52	14	28	274.68	0.5439636	254	258.4535
				350	0.07	20	40	392.4	0.3807745	350	350.8323
				400	0.09	26	52	510.12	0.2929035	400	401.2226
				450	0.11	30	60	588.6	0.2538497	450	451.6805
				500	0.13	38	76	745.56	0.2004077	500	502.206
				550	0.15	44	88	863.28	0.1730793	550	552.799
				600	0.18	52	104	1020.24	0.1464517	600	603.6623
				650	0.2	60	120	1177.2	0.1269248	650	654.4068
				700	0.24	70	140	1373.4	0.1087927	700	705.6912
				800	0.29	84	168	1648.08	0.0906606	800	807.8526
				900	0.35	102	204	2001.24	0.0746617	900	910.6513
				1000	0.42	120	240	2354.4	0.0634624	1000	1014.185
				1100	0.48	140	280	2746.8	0.0543964	1100	1117.815
				1200	0.57	162	324	3178.44	0.0470092	1200	1223.044
				1300	0.68	192	384	3767.04	0.039664	1300	1329.728
				1400	0.78	220	440	4316.4	0.0346159	1400	1436.663

Wet Run

Recorded Data							Calculations				
Indirect Reading Rotameters				Direct Reading Rotameter Value (L/min)	Pressure at Rotameter Exit (psig)	Half of Manometer Reading (mm H20)	Manometer Reading (mm H20)	Manometer Pressure (Pa)	Pore Size (Diameter) (mm)	Indicated Airflow Rate (L/min)	True Airflow Rate (L/min)
First Rotameter Used		Second Rotameter Used									
Rotameter ID Number	Rotameter Value	Rotameter ID Number	Rotameter Value								
2	15				0	4	8	78.48	1.9038727	0.183	0.183
2	38				0	16	32	313.92	0.4759682	0.653	0.653
2	55				0	32	64	627.84	0.2379841	1.049	1.049
4	55				0.32	40	80	784.8	0.1903873	19.8	20.01435
5	52				0.3	52	104	1020.24	0.1464517	77.2	77.98378
5	98				0.66	56	112	1098.72	0.1359909	149	152.3082
5	63	5	78		0.52	68	136	1334.16	0.1119925	212	215.7171
				350	0.24	72	144	1412.64	0.1057707	350	352.8456
				400	0.28	84	168	1648.08	0.0906606	400	403.7916
				450	0.31	98	196	1922.76	0.0777091	450	454.7201
				550	0.38	120	240	2354.4	0.0634624	550	557.0635
				600	0.4	124	248	2432.88	0.0614152	600	608.1085
				650	0.43	140	280	2746.8	0.0543964	650	659.4383
				700	0.47	150	300	2943	0.0507699	700	711.1024
				800	0.52	168	336	3296.16	0.0453303	800	814.0267
				900	0.6	190	380	3727.8	0.0400815	900	918.1837
				1000	0.7	210	420	4120.2	0.0362642	1000	1023.533
				1100	0.78	230	460	4512.6	0.0331108	1100	1128.806
				1200	0.87	252	504	4944.24	0.0302202	1200	1235
				1300	0.97	282	564	5532.84	0.0270053	1300	1342.206
				1400	1.08	320	640	6278.4	0.0237984	1400	1450.517

Figure B.233: Glycerin-9 recorded data and calculations.

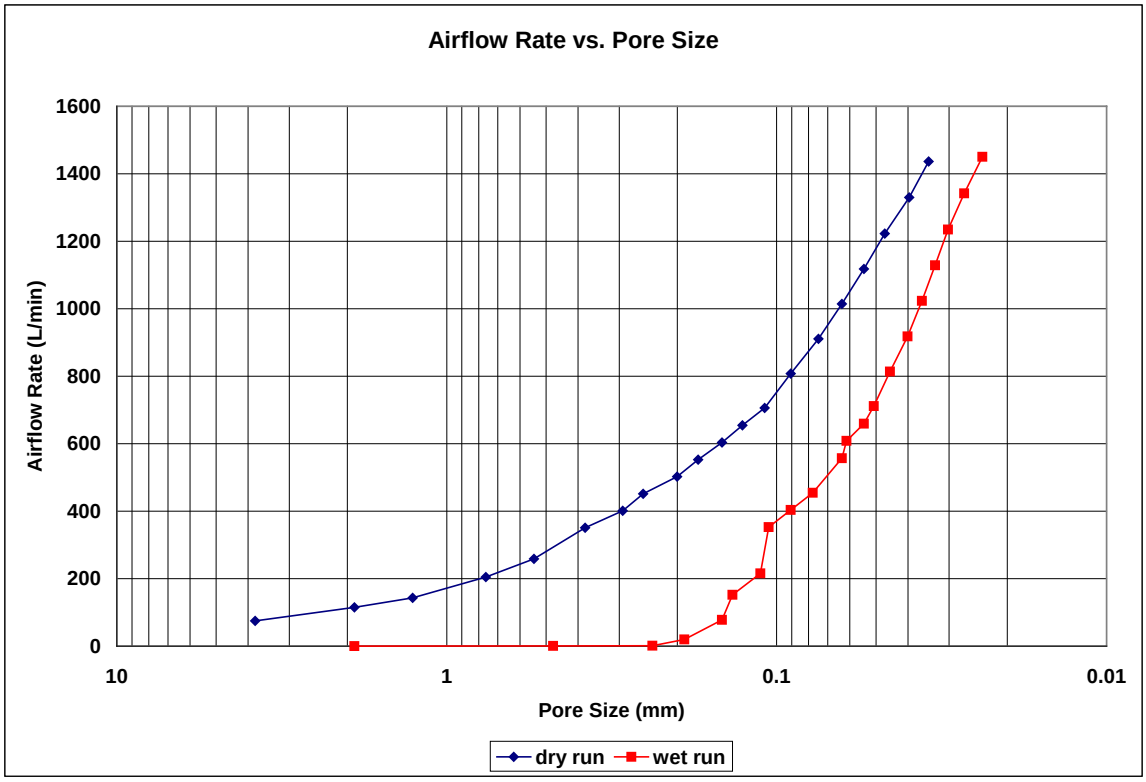

Figure B.234: Glycerin-9 airflow rate vs. pore size for the wet and dry runs.

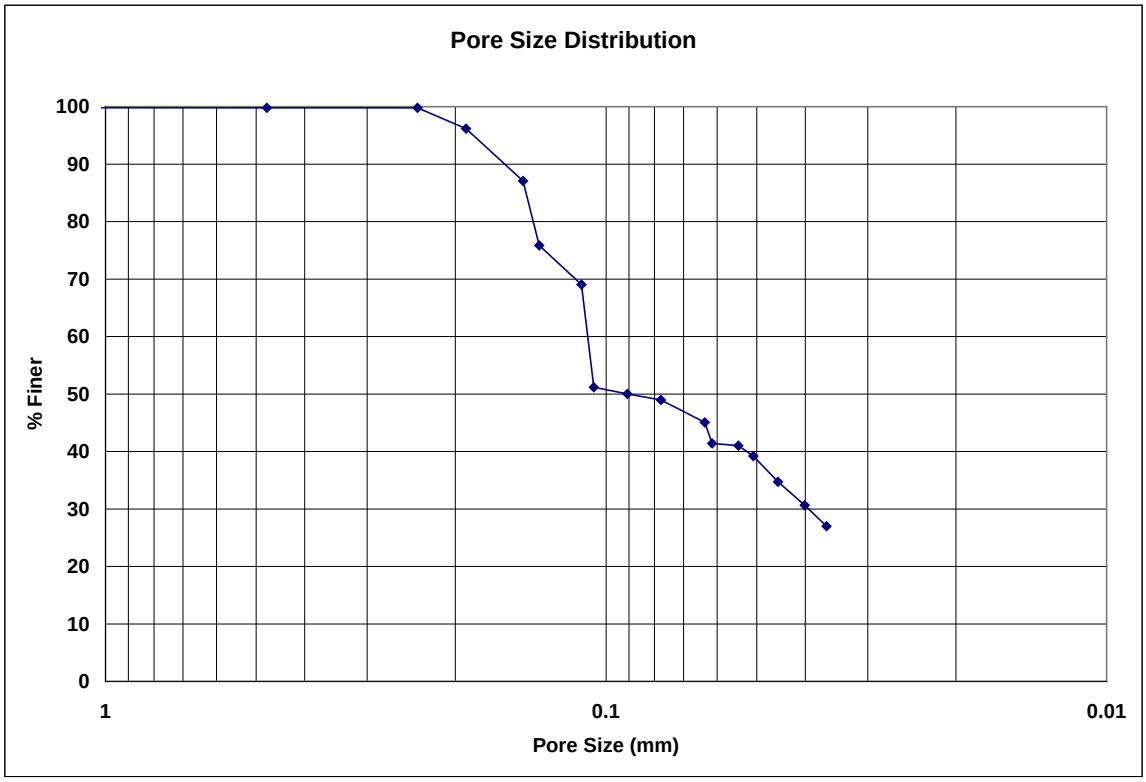

Figure B.235: Glycerin-9 pore size distribution.

Bubble Point Test
Auburn University - Department of Civil Engineering

date of test: 2/9/2007
test identification: glycerin 9
test performed by: David Hayes
wetting fluid: glycerin
air temperature: 19.8 °C
porous media: NG-1 nonwoven geotextile
comments: testing to determine geotextile pore size distribution

Pore Size Calculation Parameters:
constant, C: 2860 mm/m
contact angle: 34.51 degrees
surface tension: 0.0634 N/m

Pore Size at Selected % Finer

% finer	pore size (mm)
98	0.21463
95	0.18479
90	0.16058
85	0.14451
80	0.13985
75	0.13298
70	0.11539
65	0.11059
60	0.10884
55	0.10710
50	0.09045
45	0.06342
40	0.05238
35	0.04564
30	0.03942
25	---
20	---
15	---
10	---
5	---

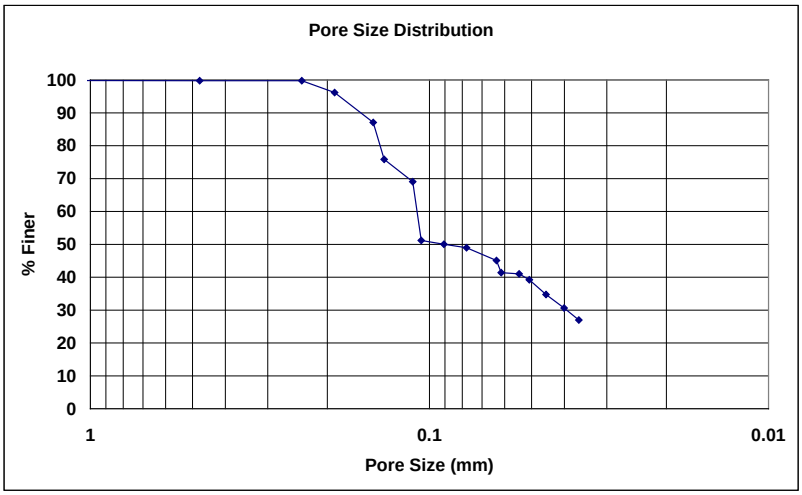

Figure B.236: Glycerin-9 pore size distribution report.

Bubble Point Test

Auburn University - Department of Civil Engineering

date of test: 2/11/2007
test identification: glycerin 10
test performed by: David Hayes
wetting fluid: glycerin
ambient air temperature: 19.8 °C
porous media: NG-1 nonwoven geotextile
comments: testing to determine geotextile pore size distribution

Pore Size Calculation Parameters:
constant, C: 2860 mm/m
contact angle: 34.51 degrees
surface tension: 0.0634 N/m

Dry Run

Recorded Data							Calculations				
Indirect Reading Rotameters				Direct Reading Rotameter Value (L/min)	Pressure at Rotameter Exit (psig)	Half of Manometer Reading (mm H20)	Manometer Reading (mm H20)	Manometer Pressure (Pa)	Pore Size (Diameter) (mm)	Indicated Airflow Rate (L/min)	True Airflow Rate (L/min)
First Rotameter Used		Second Rotameter Used									
Rotameter ID Number	Rotameter Value	Rotameter ID Number	Rotameter Value								
5	49				0.12	2	4	39.24	3.8077454	72.7	72.99613
5	74				0.27	4	8	78.48	1.9038727	111	112.0147
5	93				0.44	6	12	117.72	1.2692485	141	143.0946
5	52	5	65		0.22	8	16	156.96	0.9519364	174.3	175.5994
5	60	5	73		0.29	10	20	196.2	0.7615491	199.4	201.3573
5	73	5	91		0.45	14	28	274.68	0.5439636	248	251.7673
				350	0.04	22	44	431.64	0.3461587	350	350.4759
				400	0.06	26	52	510.12	0.2929035	400	400.8155
				450	0.08	32	64	627.84	0.2379841	450	451.2228
				500	0.1	38	76	745.56	0.2004077	500	501.6978
				550	0.12	46	92	902.52	0.1655541	550	552.2403
				600	0.15	54	108	1059.48	0.1410276	600	603.0535
				650	0.17	62	124	1216.44	0.1228305	650	653.7477
				700	0.21	72	144	1412.64	0.1057707	700	704.9823
				800	0.28	86	172	1687.32	0.0885522	800	807.5831
				900	0.35	106	212	2079.72	0.0718443	900	910.6513
				1000	0.42	124	248	2432.88	0.0614152	1000	1014.185
				1100	0.49	146	292	2864.52	0.0521609	1100	1118.183
				1200	0.6	174	348	3413.88	0.0437672	1200	1224.245
				1300	0.69	200	400	3924	0.0380775	1300	1330.16
				1400	0.79	226	452	4434.12	0.0336969	1400	1437.127

Wet Run

Recorded Data							Calculations				
Indirect Reading Rotameters				Direct Reading Rotameter Value (L/min)	Pressure at Rotameter Exit (psig)	Half of Manometer Reading (mm H20)	Manometer Reading (mm H20)	Manometer Pressure (Pa)	Pore Size (Diameter) (mm)	Indicated Airflow Rate (L/min)	True Airflow Rate (L/min)
First Rotameter Used		Second Rotameter Used									
Rotameter ID Number	Rotameter Value	Rotameter ID Number	Rotameter Value								
2	14					4	8	78.48	1.9038727	0.164	0.164
2	45					26	52	510.12	0.2929035	0.811	0.811
2	79					32	64	627.84	0.2379841	1.652	1.652
4	73				0.49	42	84	824.04	0.1813212	27.3	27.75127
5	66				0.37	44	88	863.28	0.1730793	98.7	99.93442
5	83				0.51	50	100	981	0.1523098	125	127.1499
5	53	5	67		0.43	58	116	1137.96	0.1313016	178.8	181.3963
5	78	5	96		0.72	70	140	1373.4	0.1087927	264	270.388
				350	0.24	80	160	1569.6	0.0951936	350	352.8456
				400	0.28	90	180	1765.8	0.0846166	400	403.7916
				450	0.3	100	200	1962	0.0761549	450	454.5686
				500	0.33	106	212	2079.72	0.0718443	500	505.5811
				550	0.36	118	236	2315.16	0.0645381	550	556.694
				600	0.4	130	260	2550.6	0.0585807	600	608.1085
				650	0.43	140	280	2746.8	0.0543964	650	659.4383
				700	0.47	154	308	3021.48	0.0494512	700	711.1024
				800	0.54	172	344	3374.64	0.0442761	800	814.5614
				900	0.6	196	392	3845.52	0.0388545	900	918.1837
				1000	0.7	218	436	4277.16	0.0349334	1000	1023.533
				1100	0.8	242	484	4748.04	0.031469	1100	1129.535
				1200	0.91	268	536	5258.16	0.028416	1200	1236.585
				1300	1	302	604	5925.24	0.0252169	1300	1343.49
				1400	1.14	332	664	6513.84	0.0229382	1400	1453.272

Figure B.237: Glycerin-10 recorded data and calculations.

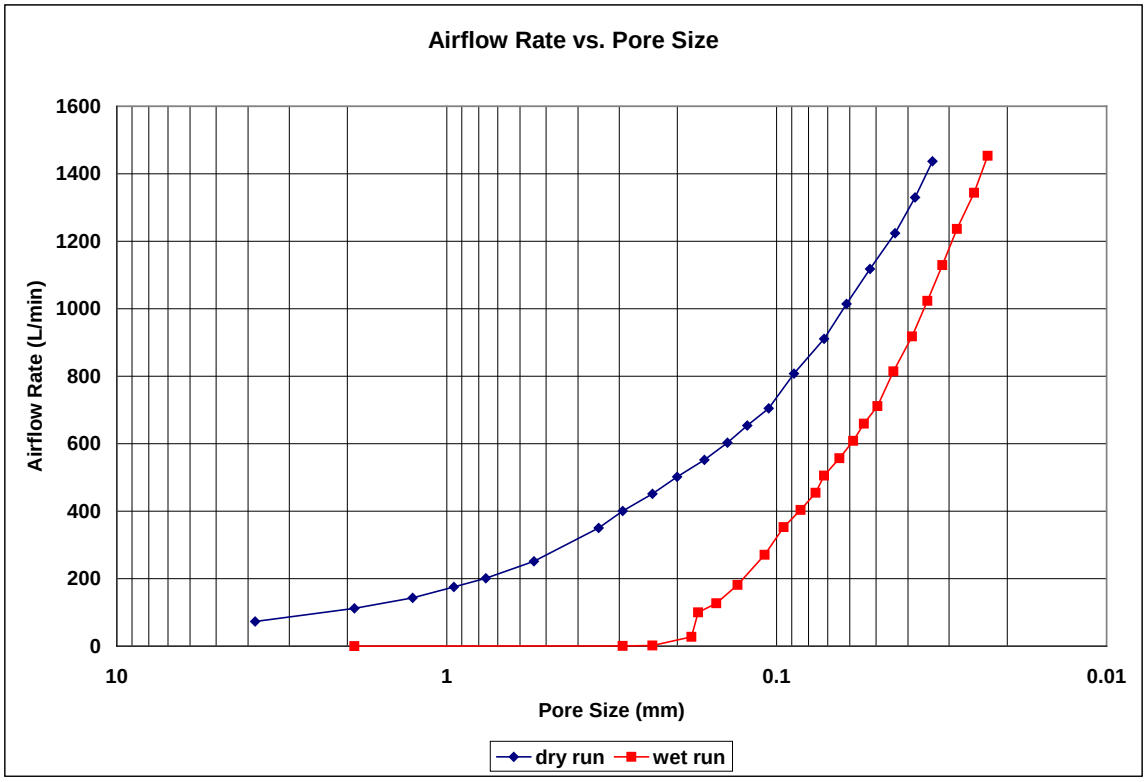

Figure B.238: Glycerin-10 airflow rate vs. pore size for the wet and dry runs.

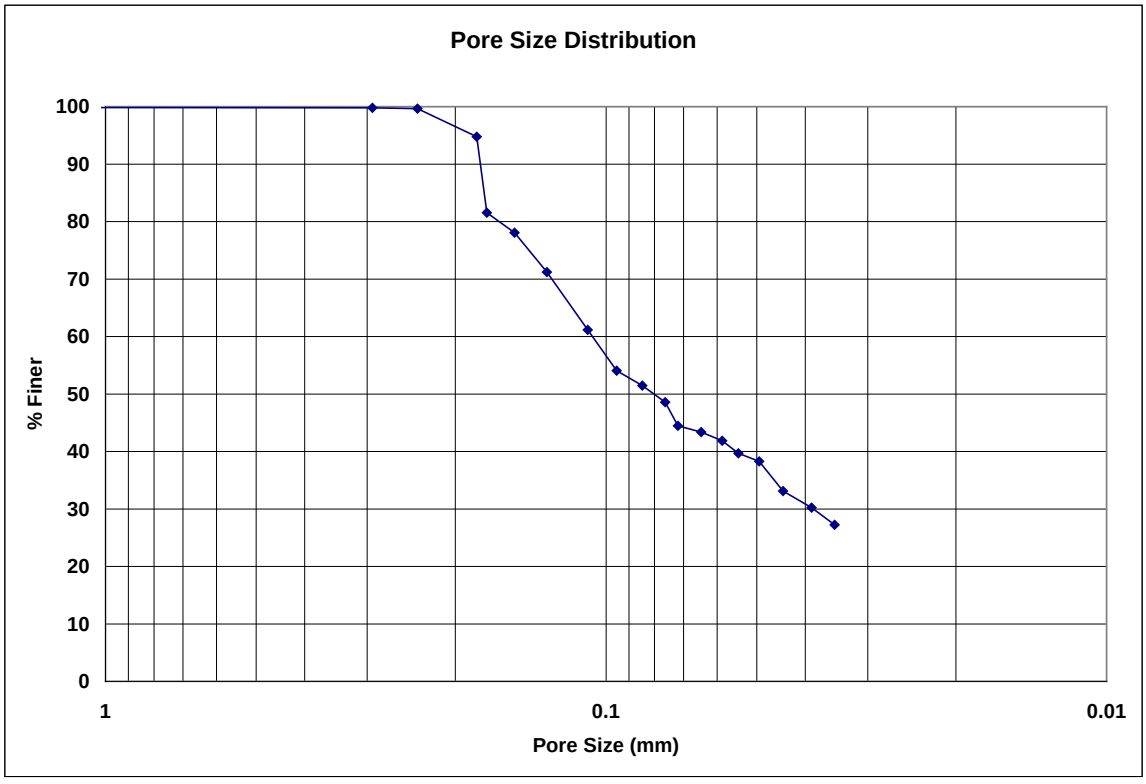

Figure B.239: Glycerin-10 pore size distribution.

Bubble Point Test
Auburn University - Department of Civil Engineering

date of test: 2/11/2007
test identification: glycerin 10
test performed by: David Hayes
wetting fluid: glycerin
air temperature: 19.8 °C
porous media: NG-1 nonwoven geotextile
comments: testing to determine geotextile pore size distribution

Pore Size Calculation Parameters:
constant, C: 2860 mm/m
contact angle: 34.51 degrees
surface tension: 0.0634 N/m

Pore Size at Selected % Finer

% finer	pore size (mm)
98	0.21900
95	0.18414
90	0.17835
85	0.17524
80	0.16388
75	0.14291
70	0.12859
65	0.11741
60	0.10659
55	0.09700
50	0.08033
45	0.07239
40	0.05502
35	0.04616
30	0.03857
25	---
20	---
15	---
10	---
5	---

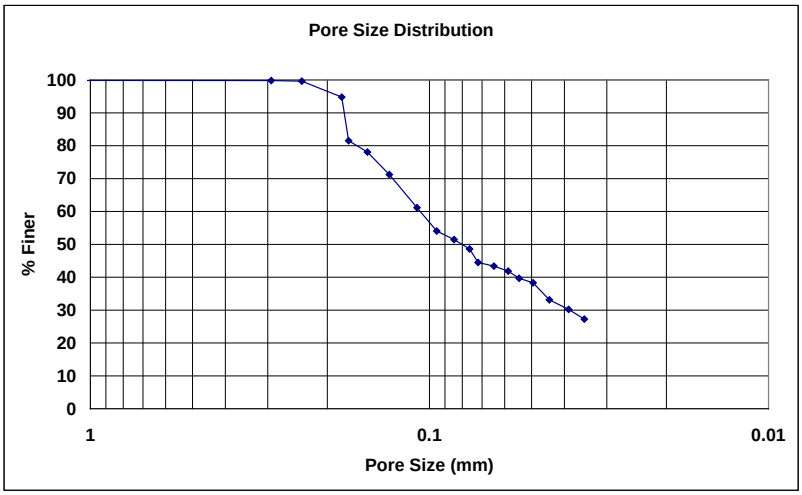

Figure B.240: Glycerin-10 pore size distribution report.

Appendix C: ANOVA Calculations for NG-1 Nonwoven Geotextile Mean Pore Sizes at Selected Opening Sizes

C.1 98% Opening Size (O_{98}, 98% Finer)

	% Finer	98				
	number of treatments, k	6				
	grand average, y	0.20887				
treatment:	water	Porewick	mineral oil	2EH	Drakeol	glycerin
test	pore size (mm)	pore size (mm)	pore size (mm)	pore size (mm)	pore size (mm)	pore size (mm)
1	0.12191	---	---	---	---	0.25852
2	---	---	0.21405	0.20485	0.22688	0.21772
3	0.20251	---	0.18212	0.26752	---	0.16920
4	0.16537	---	0.22170	0.28414	0.25288	0.20857
5	0.23077	0.18347	0.23077	0.23710	0.24899	---
6	0.16887	0.16269	0.20917	0.28403	0.22870	0.17732
7	0.18402	0.19233	0.22264	0.20531	---	0.21889
8	0.14265	0.21304	0.16646	0.21820	---	0.17974
9	---	0.21666	0.19285	0.19120	---	0.21463
10	0.16847	0.22593	0.23217	0.20841	0.23566	0.21900
n_t	8	6	9	9	5	9
n_t-1	7	5	8	8	4	8
mean, y_t	0.17307	0.19902	0.20799	0.23342	0.23862	0.20707
variance, s^2_t	0.00114	0.00057	0.00052	0.00132	0.00014	0.00077
$(n_t-1)s^2_t$	0.00796	0.00284	0.00417	0.01056	0.00056	0.00617
$n_t(y_t-y)$	0.01025	0.00058	0.00001	0.00542	0.00442	0.00003

between-treatment variance, s^2_b	0.00414
within-treatment variance, s^2_w	0.00081
Fratio	5.14
v_1	5
v_2	40
α	0.05
critical value, $F(v_1,v_2,\alpha)$	2.45
Fratio	5.14
critical value, $F(v_1,v_2,\alpha)$	2.45

ANOVA Test Result:	means are significantly different
significance level:	0.05
confidence level:	95 %

Figure C.1: ANOVA test for O_{98}, significance level = 0.05

	% Finer	98				
number of treatments, k		6				
grand average, y		0.20887				
treatment:	water pore size	Porewick pore size	mineral oil pore size	2EH pore size	Drakeol pore size	glycerin pore size
test	(mm)	(mm)	(mm)	(mm)	(mm)	(mm)
1	0.12191	---	---	---	---	0.25852
2	---	---	0.21405	0.20485	0.22688	0.21772
3	0.20251	---	0.18212	0.26752	---	0.16920
4	0.16537	---	0.22170	0.28414	0.25288	0.20857
5	0.23077	0.18347	0.23077	0.23710	0.24899	---
6	0.16887	0.16269	0.20917	0.28403	0.22870	0.17732
7	0.18402	0.19233	0.22264	0.20531	---	0.21889
8	0.14265	0.21304	0.16646	0.21820	---	0.17974
9	---	0.21666	0.19285	0.19120	---	0.21463
10	0.16847	0.22593	0.23217	0.20841	0.23566	0.21900
n_t	8	6	9	9	5	9
n_t-1	7	5	8	8	4	8
mean, y_t	0.17307	0.19902	0.20799	0.23342	0.23862	0.20707
variance, s^2_t	0.00114	0.00057	0.00052	0.00132	0.00014	0.00077
$(n_t-1)s^2_t$	0.00796	0.00284	0.00417	0.01056	0.00056	0.00617
$n_t(y_t-y)$	0.01025	0.00058	0.00001	0.00542	0.00442	0.00003

between-treatment variance, s^2_b	0.00414
within-treatment variance, s^2_w	0.00081
Fratio	5.14
v_1	5
v_2	40
α	0.01
critical value, $F(v_1,v_2,\alpha)$	3.51
Fratio	5.14
critical value, $F(v_1,v_2,\alpha)$	3.51

ANOVA Test Result:	means are significantly different
significance level:	0.01
confidence level:	99 %

Figure C.2: ANOVA test for O_{98}, significance level = 0.01

C.2 95% Opening Size (O_{95}, 95% Finer)

	% Finer	95				
	number of treatments, k	6				
	grand average, y	0.18289				
treatment:	water	Porewick	mineral oil	2EH	Drakeol	glycerin
	pore size	pore size	pore size	pore size	pore size	pore size
test	(mm)	(mm)	(mm)	(mm)	(mm)	(mm)
1	0.11836	0.16527	0.16894	0.19955	0.16504	0.15098
2	0.16849	0.19192	0.19612	0.17950	0.18070	0.15834
3	0.20095	---	0.17067	0.21908	0.17730	0.14975
4	0.12366	0.23171	0.19916	0.21911	0.20070	0.20338
5	0.20028	0.16511	0.21918	0.21672	0.16723	---
6	0.16694	0.15100	0.18991	0.20085	0.19625	0.15948
7	0.18173	0.18328	0.20360	0.19440	0.20427	0.20956
8	0.13427	0.18913	0.15818	0.19763	0.22034	0.16156
9	0.16761	0.19149	0.17215	0.17727	0.16266	0.18479
10	0.15747	0.20678	0.19626	0.18794	0.20937	0.18414
n_t	10	9	10	10	10	9
n_t-1	9	8	9	9	9	8
mean, y_t	0.16198	0.18619	0.18742	0.19920	0.18839	0.17355
variance, s^2_t	0.00085	0.00059	0.00036	0.00024	0.00042	0.00051
$(n_t-1)s^2_t$	0.00763	0.00469	0.00328	0.00212	0.00376	0.00407
$n_t(y_t-y)$	0.00437	0.00010	0.00021	0.00266	0.00030	0.00078

between-treatment variance, s^2_b	0.00168
within-treatment variance, s^2_w	0.00049
Fratio	3.43
v_1	5
v_2	52
α	0.05
critical value, $F(v_1,v_2,\alpha)$	2.39
Fratio	3.43
critical value, $F(v_1,v_2,\alpha)$	2.39

ANOVA Test Result:	means are significantly different
significance level:	0.05
confidence level:	95 %

Figure C.3: ANOVA test for O_{95}, significance level = 0.05

% Finer	95					
number of treatments, k	6					
grand average, y	0.18289					
treatment:	water pore size	Porewick pore size	mineral oil pore size	2EH pore size	Drakeol pore size	glycerin pore size
test	(mm)	(mm)	(mm)	(mm)	(mm)	(mm)
1	0.11836	0.16527	0.16894	0.19955	0.16504	0.15098
2	0.16849	0.19192	0.19612	0.17950	0.18070	0.15834
3	0.20095	---	0.17067	0.21908	0.17730	0.14975
4	0.12366	0.23171	0.19916	0.21911	0.20070	0.20338
5	0.20028	0.16511	0.21918	0.21672	0.16723	---
6	0.16694	0.15100	0.18991	0.20085	0.19625	0.15948
7	0.18173	0.18328	0.20360	0.19440	0.20427	0.20956
8	0.13427	0.18913	0.15818	0.19763	0.22034	0.16156
9	0.16761	0.19149	0.17215	0.17727	0.16266	0.18479
10	0.15747	0.20678	0.19626	0.18794	0.20937	0.18414
n_t	10	9	10	10	10	9
n_t-1	9	8	9	9	9	8
mean, y_t	0.16198	0.18619	0.18742	0.19920	0.18839	0.17355
variance, s^2_t	0.00085	0.00059	0.00036	0.00024	0.00042	0.00051
$(n_t-1)s^2_t$	0.00763	0.00469	0.00328	0.00212	0.00376	0.00407
$n_t(y_t-y)$	0.00437	0.00010	0.00021	0.00266	0.00030	0.00078

between-treatment variance, s^2_b	0.00168
within-treatment variance, s^2_w	0.00049
Fratio	3.43
v_1	5
v_2	52
α	0.01
critical value, $F(v_1,v_2,\alpha)$	3.39
Fratio	3.43
critical value, $F(v_1,v_2,\alpha)$	3.39

ANOVA Test Result:	means are significantly different
significance level:	0.01
confidence level:	99 %

Figure C.4: ANOVA test for O_{95}, significance level = 0.01

C.3 90% Opening Size (O_{90}, 90% Finer)

	% Finer	90				
	number of treatments, k	6				
	grand average, y	0.16675				
treatment:	water	Porewick	mineral oil	2EH	Drakeol	glycerin
	pore size	pore size	pore size	pore size	pore size	pore size
test	(mm)	(mm)	(mm)	(mm)	(mm)	(mm)
1	0.11677	0.15104	0.14966	0.19384	0.14749	0.13659
2	0.16771	0.17466	0.18355	0.16561	0.14903	0.14281
3	0.19836	0.18388	0.16070	0.20688	0.14704	0.14329
4	0.11130	0.18936	0.18428	0.19763	0.15204	0.19473
5	0.19622	0.15402	0.19985	0.20349	0.15628	0.18875
6	0.16371	0.14506	0.17219	0.19036	0.16513	0.13962
7	0.17793	0.16818	0.18546	0.18171	0.16089	0.19400
8	0.13256	0.17241	0.14438	0.17667	0.15688	0.14471
9	0.16520	0.18094	0.15787	0.16457	0.14671	0.16058
10	0.13915	0.18795	0.16382	0.17399	0.16717	0.17835
n_t	10	10	10	10	10	10
n_t-1	9	9	9	9	9	9
mean, y_t	0.15689	0.17075	0.17018	0.18548	0.15487	0.16234
variance, s^2_t	0.00095	0.00025	0.00032	0.00023	0.00006	0.00058
$(n_t-1)s^2_t$	0.00854	0.00227	0.00286	0.00208	0.00052	0.00524
$n_t(y_t-y)$	0.00097	0.00016	0.00012	0.00351	0.00141	0.00019

between-treatment variance, s^2_b	0.00127
within-treatment variance, s^2_w	0.00040
Fratio	3.19
v_1	5
v_2	54
α	0.05
critical value, $F(v_1,v_2,\alpha)$	2.39
Fratio	3.19
critical value, $F(v_1,v_2,\alpha)$	2.39

ANOVA Test Result:	means are significantly different
significance level:	0.05
confidence level:	95 %

Figure C.5: ANOVA test for O_{90}, significance level = 0.05

	% Finer	90				
number of treatments, k		6				
grand average, y		0.16675				
treatment:	water pore size	Porewick pore size	mineral oil pore size	2EH pore size	Drakeol pore size	glycerin pore size
test	(mm)	(mm)	(mm)	(mm)	(mm)	(mm)
1	0.11677	0.15104	0.14966	0.19384	0.14749	0.13659
2	0.16771	0.17466	0.18355	0.16561	0.14903	0.14281
3	0.19836	0.18388	0.16070	0.20688	0.14704	0.14329
4	0.11130	0.18936	0.18428	0.19763	0.15204	0.19473
5	0.19622	0.15402	0.19985	0.20349	0.15628	0.18875
6	0.16371	0.14506	0.17219	0.19036	0.16513	0.13962
7	0.17793	0.16818	0.18546	0.18171	0.16089	0.19400
8	0.13256	0.17241	0.14438	0.17667	0.15688	0.14471
9	0.16520	0.18094	0.15787	0.16457	0.14671	0.16058
10	0.13915	0.18795	0.16382	0.17399	0.16717	0.17835
n_t	10	10	10	10	10	10
n_t-1	9	9	9	9	9	9
mean, y_t	0.15689	0.17075	0.17018	0.18548	0.15487	0.16234
variance, s^2_t	0.00095	0.00025	0.00032	0.00023	0.00006	0.00058
$(n_t-1)s^2_t$	0.00854	0.00227	0.00286	0.00208	0.00052	0.00524
$n_t(y_t-y)$	0.00097	0.00016	0.00012	0.00351	0.00141	0.00019

between-treatment variance, s^2_b	0.00127
within-treatment variance, s^2_w	0.00040
Fratio	3.19
v_1	5
v_2	54
α	0.01
critical value, $F(v_1,v_2,\alpha)$	3.38
Fratio	3.19
critical value, $F(v_1,v_2,\alpha)$	3.38

ANOVA Test Result:	means are not significantly different
significance level:	0.01
confidence level:	99 %

Figure C.6: ANOVA test for O_{90}, significance level = 0.01

C.4 85% Opening Size (O_{85}, 85% Finer)

	% Finer	85				
	number of treatments, k	6				
	grand average, y	0.15599				
treatment:	water	Porewick	mineral oil	2EH	Drakeol	glycerin
	pore size	pore size	pore size	pore size	pore size	pore size
test	(mm)	(mm)	(mm)	(mm)	(mm)	(mm)
1	0.11518	0.14070	0.13736	0.18813	0.13199	0.12220
2	0.16692	0.15741	0.16929	0.15216	0.13688	0.13269
3	0.19576	0.17005	0.14821	0.19137	0.13543	0.13683
4	0.10906	0.16157	0.17132	0.18285	0.14027	0.18609
5	0.19217	0.14518	0.18117	0.19027	0.14533	0.16868
6	0.16049	0.14409	0.15913	0.17987	0.15799	0.12551
7	0.17412	0.16474	0.17143	0.16902	0.14395	0.17844
8	0.13085	0.16029	0.13315	0.16579	0.14546	0.13377
9	0.16279	0.17039	0.14511	0.15572	0.13959	0.14451
10	0.12496	0.17746	0.15271	0.16356	0.14649	0.17524
n_t	10	10	10	10	10	10
n_t-1	9	9	9	9	9	9
mean, y_t	0.15323	0.15919	0.15689	0.17387	0.14234	0.15040
variance, s^2_t	0.00098	0.00015	0.00026	0.00021	0.00005	0.00058
$(n_t-1)s^2_t$	0.00879	0.00138	0.00234	0.00189	0.00048	0.00524
$n_t(y_t-y)$	0.00008	0.00010	0.00001	0.00320	0.00186	0.00031

between-treatment variance, s^2_b	0.00111
within-treatment variance, s^2_w	0.00037
Fratio	2.98
v_1	5
v_2	54
α	0.05
critical value, $F(v_1,v_2,\alpha)$	2.39
Fratio	2.98
critical value, $F(v_1,v_2,\alpha)$	2.39

ANOVA Test Result:	means are significantly different
significance level:	0.05
confidence level:	95 %

Figure C.7: ANOVA test for O_{85}, significance level = 0.05

	% Finer	85				
number of treatments, k		6				
grand average, y		0.15599				
treatment:	water pore size	Porewick pore size	mineral oil pore size	2EH pore size	Drakeol pore size	glycerin pore size
test	(mm)	(mm)	(mm)	(mm)	(mm)	(mm)
1	0.11518	0.14070	0.13736	0.18813	0.13199	0.12220
2	0.16692	0.15741	0.16929	0.15216	0.13688	0.13269
3	0.19576	0.17005	0.14821	0.19137	0.13543	0.13683
4	0.10906	0.16157	0.17132	0.18285	0.14027	0.18609
5	0.19217	0.14518	0.18117	0.19027	0.14533	0.16868
6	0.16049	0.14409	0.15913	0.17987	0.15799	0.12551
7	0.17412	0.16474	0.17143	0.16902	0.14395	0.17844
8	0.13085	0.16029	0.13315	0.16579	0.14546	0.13377
9	0.16279	0.17039	0.14511	0.15572	0.13959	0.14451
10	0.12496	0.17746	0.15271	0.16356	0.14649	0.17524
n_t	10	10	10	10	10	10
n_t-1	9	9	9	9	9	9
mean, y_t	0.15323	0.15919	0.15689	0.17387	0.14234	0.15040
variance, s^2_t	0.00098	0.00015	0.00026	0.00021	0.00005	0.00058
$(n_t-1)s^2_t$	0.00879	0.00138	0.00234	0.00189	0.00048	0.00524
$n_t(y_t-y)$	0.00008	0.00010	0.00001	0.00320	0.00186	0.00031

between-treatment variance, s^2_b	0.00111
within-treatment variance, s^2_w	0.00037
Fratio	2.98
v_1	5
v_2	54
α	0.01
critical value, $F(v_1,v_2,\alpha)$	3.38
Fratio	2.98
critical value, $F(v_1,v_2,\alpha)$	3.38

ANOVA Test Result:	means are not significantly different
significance level:	0.01
confidence level:	99 %

Figure C.8: ANOVA test for O_{85}, significance level = 0.01

C.5 80% Opening Size (O_{80}, 80% Finer)

	% Finer	80				
	number of treatments, k	6				
	grand average, y	0.14730				
treatment:	water	Porewick	mineral oil	2EH	Drakeol	glycerin
test	pore size (mm)	pore size (mm)	pore size (mm)	pore size (mm)	pore size (mm)	pore size (mm)
1	0.11358	0.13265	0.12595	0.18243	0.12579	0.11648
2	0.16614	0.14304	0.15993	0.14025	0.12603	0.12425
3	0.19317	0.15622	0.13926	0.17294	0.12383	0.12977
4	0.10681	0.15070	0.16043	0.16808	0.13017	0.17744
5	0.18811	0.14287	0.16918	0.17888	0.13188	0.16008
6	0.15726	0.14312	0.14970	0.16937	0.14709	0.12219
7	0.17031	0.16267	0.16095	0.15633	0.12886	0.16289
8	0.12914	0.15063	0.12382	0.15491	0.13404	0.12283
9	0.16039	0.16451	0.13543	0.14818	0.13247	0.13985
10	0.11961	0.16697	0.14407	0.15374	0.12623	0.16388
n_t	10	10	10	10	10	10
n_t-1	9	9	9	9	9	9
mean, y_t	0.15045	0.15134	0.14687	0.16251	0.13064	0.14197
variance, s^2_t	0.00097	0.00013	0.00025	0.00019	0.00004	0.00049
$(n_t-1)s^2_t$	0.00870	0.00113	0.00222	0.00173	0.00040	0.00438
$n_t(y_t-y)$	0.00010	0.00016	0.00000	0.00231	0.00277	0.00028

between-treatment variance, s^2_b	0.00113
within-treatment variance, s^2_w	0.00034
F ratio	3.28
v_1	5
v_2	54
α	0.05
critical value, $F(v_1,v_2,\alpha)$	2.39
Fratio	3.28
critical value, $F(v_1,v_2,\alpha)$	2.39

ANOVA Test Result:	means are significantly different
significance level:	0.05
confidence level:	95 %

Figure C.9: ANOVA test for O_{80}, significance level = 0.05

	% Finer	80				
number of treatments, k		6				
grand average, y		0.14730				
treatment:	water pore size	Porewick pore size	mineral oil pore size	2EH pore size	Drakeol pore size	glycerin pore size
test	(mm)	(mm)	(mm)	(mm)	(mm)	(mm)
1	0.11358	0.13265	0.12595	0.18243	0.12579	0.11648
2	0.16614	0.14304	0.15993	0.14025	0.12603	0.12425
3	0.19317	0.15622	0.13926	0.17294	0.12383	0.12977
4	0.10681	0.15070	0.16043	0.16808	0.13017	0.17744
5	0.18811	0.14287	0.16918	0.17888	0.13188	0.16008
6	0.15726	0.14312	0.14970	0.16937	0.14709	0.12219
7	0.17031	0.16267	0.16095	0.15633	0.12886	0.16289
8	0.12914	0.15063	0.12382	0.15491	0.13404	0.12283
9	0.16039	0.16451	0.13543	0.14818	0.13247	0.13985
10	0.11961	0.16697	0.14407	0.15374	0.12623	0.16388
n_t	10	10	10	10	10	10
n_t-1	9	9	9	9	9	9
mean, y_t	0.15045	0.15134	0.14687	0.16251	0.13064	0.14197
variance, s^2_t	0.00097	0.00013	0.00025	0.00019	0.00004	0.00049
$(n_t-1)s^2_t$	0.00870	0.00113	0.00222	0.00173	0.00040	0.00438
$n_t(y_t-y)$	0.00010	0.00016	0.00000	0.00231	0.00277	0.00028

between-treatment variance, s^2_b	0.00113
within-treatment variance, s^2_w	0.00034
F ratio	3.28
v_1	5
v_2	54
α	0.01
critical value, $F(v_1,v_2,\alpha)$	3.38
Fratio	3.28
critical value, $F(v_1,v_2,\alpha)$	3.38

ANOVA Test Result:	means are not significantly different
significance level:	0.01
confidence level:	99 %

Figure C.10: ANOVA test for O_{80}, significance level = 0.01

C.6 75% Opening Size (O_{75}, 75% Finer)

	% Finer	75				
	number of treatments, k	6				
	grand average, y	0.13950				
treatment:	water	Porewick	mineral oil	2EH	Drakeol	glycerin
	pore size	pore size	pore size	pore size	pore size	pore size
test	(mm)	(mm)	(mm)	(mm)	(mm)	(mm)
1	0.11199	0.12459	0.11808	0.17672	0.11951	0.11325
2	0.16535	0.13467	0.15184	0.12856	0.11517	0.11804
3	0.19057	0.14240	0.13096	0.15449	0.10445	0.11913
4	0.10456	0.13984	0.14980	0.16158	0.12019	0.17027
5	0.18406	0.14057	0.15802	0.16981	0.11936	0.15148
6	0.15403	0.14215	0.14047	0.16076	0.13619	0.11888
7	0.16650	0.16061	0.15086	0.14366	0.12044	0.14733
8	0.12742	0.14522	0.11594	0.14942	0.11579	0.11519
9	0.15798	0.16126	0.12618	0.14131	0.12550	0.13298
10	0.11426	0.16501	0.13620	0.14727	0.11898	0.14291
n_t	10	10	10	10	10	10
n_t-1	9	9	9	9	9	9
mean, y_t	0.14767	0.14563	0.13783	0.15336	0.11956	0.13295
variance, s^2_t	0.00096	0.00017	0.00022	0.00021	0.00006	0.00037
$(n_t-1)s^2_t$	0.00864	0.00149	0.00198	0.00185	0.00058	0.00336
$n_t(y_t-y)$	0.00067	0.00038	0.00003	0.00192	0.00398	0.00043

between-treatment variance, s^2_b	0.00148
within-treatment variance, s^2_w	0.00033
F ratio	4.47
v_1	5
v_2	54
α	0.05
critical value, $F(v_1,v_2,\alpha)$	2.39
Fratio	4.47
critical value, $F(v_1,v_2,\alpha)$	2.39

ANOVA Test Result:	means are significantly different
significance level:	0.05
confidence level:	95 %

Figure C.11: ANOVA test for O_{75}, significance level = 0.05

	% Finer	75				
number of treatments, k		6				
grand average, y		0.13950				
treatment:	water pore size	Porewick pore size	mineral oil pore size	2EH pore size	Drakeol pore size	glycerin pore size
test	(mm)	(mm)	(mm)	(mm)	(mm)	(mm)
1	0.11199	0.12459	0.11808	0.17672	0.11951	0.11325
2	0.16535	0.13467	0.15184	0.12856	0.11517	0.11804
3	0.19057	0.14240	0.13096	0.15449	0.10445	0.11913
4	0.10456	0.13984	0.14980	0.16158	0.12019	0.17027
5	0.18406	0.14057	0.15802	0.16981	0.11936	0.15148
6	0.15403	0.14215	0.14047	0.16076	0.13619	0.11888
7	0.16650	0.16061	0.15086	0.14366	0.12044	0.14733
8	0.12742	0.14522	0.11594	0.14942	0.11579	0.11519
9	0.15798	0.16126	0.12618	0.14131	0.12550	0.13298
10	0.11426	0.16501	0.13620	0.14727	0.11898	0.14291
n_t	10	10	10	10	10	10
n_t-1	9	9	9	9	9	9
mean, y_t	0.14767	0.14563	0.13783	0.15336	0.11956	0.13295
variance, s^2_t	0.00096	0.00017	0.00022	0.00021	0.00006	0.00037
$(n_t-1)s^2_t$	0.00864	0.00149	0.00198	0.00185	0.00058	0.00336
$n_t(y_t-y)$	0.00067	0.00038	0.00003	0.00192	0.00398	0.00043

between-treatment variance, s^2_b	0.00148
within-treatment variance, s^2_w	0.00033
F ratio	4.47
v_1	5
v_2	54
α	0.01
critical value, $F(v_1,v_2,\alpha)$	3.38
Fratio	4.47
critical value, $F(v_1,v_2,\alpha)$	3.38

ANOVA Test Result:	means are significantly different
significance level:	0.01
confidence level:	99 %

Figure C.12: ANOVA test for O_{75}, significance level = 0.01

C.7 70% Opening Size (O_{70}, 70% Finer)

	% Finer	70				
	number of treatments, k	6				
	grand average, y	0.13254				
treatment:	water	Porewick	mineral oil	2EH	Drakeol	glycerin
test	pore size (mm)	pore size (mm)	pore size (mm)	pore size (mm)	pore size (mm)	pore size (mm)
1	0.11040	0.11655	0.11020	0.17101	0.11267	0.10791
2	0.16457	0.12630	0.14381	0.11710	0.10758	0.11182
3	0.18798	0.12914	0.12350	0.13431	0.09946	0.10864
4	0.10231	0.12898	0.14091	0.15533	0.11332	0.16460
5	0.18000	0.13827	0.15044	0.16075	0.11521	0.14300
6	0.15081	0.14119	0.13233	0.15251	0.12540	0.11556
7	0.16269	0.15854	0.14286	0.13583	0.11328	0.13120
8	0.12571	0.14412	0.10861	0.14401	0.10006	0.10857
9	0.15557	0.15801	0.11882	0.13521	0.11853	0.11539
10	0.10891	0.16338	0.12833	0.14052	0.11174	0.12859
n_t	10	10	10	10	10	10
n_t-1	9	9	9	9	9	9
mean, y_t	0.14490	0.14045	0.12998	0.14466	0.11172	0.12353
variance, s^2_t	0.00096	0.00025	0.00021	0.00024	0.00006	0.00035
$(n_t-1)s^2_t$	0.00861	0.00221	0.00192	0.00218	0.00055	0.00311
$n_t(y_t-y)$	0.00153	0.00063	0.00007	0.00147	0.00433	0.00081

between-treatment variance, s^2_b	0.00177
within-treatment variance, s^2_w	0.00034
Fratio	5.13
v_1	5
v_2	54
α	0.05
critical value, $F(v_1,v_2,\alpha)$	2.39
Fratio	5.13
critical value, $F(v_1,v_2,\alpha)$	2.39

ANOVA Test Result:	means are significantly different
significance level:	0.05
confidence level:	95 %

Figure C.13: ANOVA test for O_{70}, significance level = 0.05

% Finer	70					
number of treatments, k	6					
grand average, y	0.13254					
treatment:	water pore size	Porewick pore size	mineral oil pore size	2EH pore size	Drakeol pore size	glycerin pore size
test	(mm)	(mm)	(mm)	(mm)	(mm)	(mm)
1	0.11040	0.11655	0.11020	0.17101	0.11267	0.10791
2	0.16457	0.12630	0.14381	0.11710	0.10758	0.11182
3	0.18798	0.12914	0.12350	0.13431	0.09946	0.10864
4	0.10231	0.12898	0.14091	0.15533	0.11332	0.16460
5	0.18000	0.13827	0.15044	0.16075	0.11521	0.14300
6	0.15081	0.14119	0.13233	0.15251	0.12540	0.11556
7	0.16269	0.15854	0.14286	0.13583	0.11328	0.13120
8	0.12571	0.14412	0.10861	0.14401	0.10006	0.10857
9	0.15557	0.15801	0.11882	0.13521	0.11853	0.11539
10	0.10891	0.16338	0.12833	0.14052	0.11174	0.12859
n_t	10	10	10	10	10	10
n_t-1	9	9	9	9	9	9
mean, y_t	0.14490	0.14045	0.12998	0.14466	0.11172	0.12353
variance, s^2_t	0.00096	0.00025	0.00021	0.00024	0.00006	0.00035
$(n_t-1)s^2_t$	0.00861	0.00221	0.00192	0.00218	0.00055	0.00311
$n_t(y_t-y)$	0.00153	0.00063	0.00007	0.00147	0.00433	0.00081

between-treatment variance, s^2_b	0.00177
within-treatment variance, s^2_w	0.00034
Fratio	5.13
v_1	5
v_2	54
α	0.01
critical value, $F(v_1,v_2,\alpha)$	3.38
Fratio	5.13
critical value, $F(v_1,v_2,\alpha)$	3.38

ANOVA Test Result:	means are significantly different
significance level:	0.01
confidence level:	99 %

Figure C.14: ANOVA test for O_{70}, significance level = 0.01

C.8 65% Opening Size (O_{65}, 65% Finer)

% Finer	65					
number of treatments, k	6					
grand average, y	0.12606					
treatment:	water	Porewick	mineral oil	2EH	Drakeol	glycerin
test	pore size (mm)	pore size (mm)	pore size (mm)	pore size (mm)	pore size (mm)	pore size (mm)
1	0.10881	0.10975	0.10259	0.15907	0.10433	0.10482
2	0.16378	0.11793	0.13578	0.10868	0.09997	0.10654
3	0.18539	0.12319	0.11529	0.11413	0.09448	0.10311
4	0.10006	0.11811	0.13201	0.14909	0.10644	0.15893
5	0.17595	0.13596	0.14286	0.15168	0.11106	0.13451
6	0.14758	0.14022	0.12396	0.14427	0.11553	0.09519
7	0.15888	0.15647	0.13504	0.12800	0.10612	0.11357
8	0.12400	0.14302	0.10226	0.13861	0.09802	0.10720
9	0.15316	0.15476	0.11132	0.12911	0.11021	0.11059
10	0.10640	0.16174	0.11864	0.13342	0.10449	0.11741
n_t	10	10	10	10	10	10
n_t-1	9	9	9	9	9	9
mean, y_t	0.14240	0.13611	0.12198	0.13561	0.10507	0.11519
variance, s^2_t	0.00093	0.00033	0.00020	0.00026	0.00004	0.00035
$(n_t-1)s^2_t$	0.00840	0.00300	0.00184	0.00237	0.00036	0.00311
$n_t(y_t-y)$	0.00267	0.00101	0.00017	0.00091	0.00441	0.00118

between-treatment variance, s^2_b	0.00207
within-treatment variance, s^2_w	0.00035
Fratio	5.86
v_1	5
v_2	54
α	0.05
critical value, $F(v_1,v_2,\alpha)$	2.39
Fratio	5.86
critical value, $F(v_1,v_2,\alpha)$	2.39

ANOVA Test Result:	means are significantly different
significance level:	0.05
confidence level:	95 %

Figure C.15: ANOVA test for O_{65}, significance level = 0.05

% Finer	65					
number of treatments, k	6					
grand average, y	0.12606					
treatment:	water pore size	Porewick pore size	mineral oil pore size	2EH pore size	Drakeol pore size	glycerin pore size
test	(mm)	(mm)	(mm)	(mm)	(mm)	(mm)
1	0.10881	0.10975	0.10259	0.15907	0.10433	0.10482
2	0.16378	0.11793	0.13578	0.10868	0.09997	0.10654
3	0.18539	0.12319	0.11529	0.11413	0.09448	0.10311
4	0.10006	0.11811	0.13201	0.14909	0.10644	0.15893
5	0.17595	0.13596	0.14286	0.15168	0.11106	0.13451
6	0.14758	0.14022	0.12396	0.14427	0.11553	0.09519
7	0.15888	0.15647	0.13504	0.12800	0.10612	0.11357
8	0.12400	0.14302	0.10226	0.13861	0.09802	0.10720
9	0.15316	0.15476	0.11132	0.12911	0.11021	0.11059
10	0.10640	0.16174	0.11864	0.13342	0.10449	0.11741
n_t	10	10	10	10	10	10
n_t-1	9	9	9	9	9	9
mean, y_t	0.14240	0.13611	0.12198	0.13561	0.10507	0.11519
variance, s^2_t	0.00093	0.00033	0.00020	0.00026	0.00004	0.00035
$(n_t-1)s^2_t$	0.00840	0.00300	0.00184	0.00237	0.00036	0.00311
$n_t(y_t-y)$	0.00267	0.00101	0.00017	0.00091	0.00441	0.00118

between-treatment variance, s^2_b	0.00207
within-treatment variance, s^2_w	0.00035
Fratio	5.86
v_1	5
v_2	54
α	0.01
critical value, $F(v_1,v_2,\alpha)$	3.38
Fratio	5.86
critical value, $F(v_1,v_2,\alpha)$	3.38

ANOVA Test Result:	means are significantly different
significance level:	0.01
confidence level:	99 %

Figure C.16: ANOVA test for O_{65}, significance level = 0.01

C.9 60% Opening Size (O_{60}, 60% Finer)

	% Finer	60				
	number of treatments, k	6				
	grand average, y	0.12018				
treatment:	water	Porewick	mineral oil	2EH	Drakeol	glycerin
	pore size	pore size	pore size	pore size	pore size	pore size
test	(mm)	(mm)	(mm)	(mm)	(mm)	(mm)
1	0.10722	0.10295	0.09526	0.13809	0.09501	0.10173
2	0.16300	0.11163	0.12776	0.10292	0.09198	0.10215
3	0.18279	0.11723	0.10771	0.10960	0.08752	0.09759
4	0.09781	0.11398	0.12298	0.14060	0.09933	0.15327
5	0.17189	0.13366	0.13040	0.14177	0.10040	0.12824
6	0.14436	0.13925	0.11530	0.13603	0.10867	0.09519
7	0.15508	0.15440	0.12707	0.12017	0.09819	0.10265
8	0.12229	0.14192	0.09549	0.13129	0.09598	0.10583
9	0.15075	0.15151	0.10341	0.12301	0.10037	0.10884
10	0.10595	0.16010	0.11014	0.12633	0.09804	0.10659
n_t	10	10	10	10	10	10
n_t-1	9	9	9	9	9	9
mean, y_t	0.14011	0.13266	0.11355	0.12698	0.09755	0.11021
variance, s^2_t	0.00090	0.00040	0.00017	0.00017	0.00003	0.00031
$(n_t-1)s^2_t$	0.00807	0.00362	0.00157	0.00157	0.00028	0.00279
$n_t(y_t-y)$	0.00397	0.00156	0.00044	0.00046	0.00512	0.00099

between-treatment variance, s^2_b	0.00251
within-treatment variance, s^2_w	0.00033
F ratio	7.57
v_1	5
v_2	54
α	0.05
critical value, $F(v_1,v_2,\alpha)$	2.39
Fratio	7.57
critical value, $F(v_1,v_2,\alpha)$	2.39

ANOVA Test Result:	means are significantly different
significance level:	0.05
confidence level:	95 %

Figure C.17: ANOVA test for O_{60}, significance level = 0.05

	% Finer	60				
	number of treatments, k	6				
	grand average, y	0.12018				
treatment:	water	Porewick	mineral oil	2EH	Drakeol	glycerin
	pore size	pore size	pore size	pore size	pore size	pore size
test	(mm)	(mm)	(mm)	(mm)	(mm)	(mm)
1	0.10722	0.10295	0.09526	0.13809	0.09501	0.10173
2	0.16300	0.11163	0.12776	0.10292	0.09198	0.10215
3	0.18279	0.11723	0.10771	0.10960	0.08752	0.09759
4	0.09781	0.11398	0.12298	0.14060	0.09933	0.15327
5	0.17189	0.13366	0.13040	0.14177	0.10040	0.12824
6	0.14436	0.13925	0.11530	0.13603	0.10867	0.09519
7	0.15508	0.15440	0.12707	0.12017	0.09819	0.10265
8	0.12229	0.14192	0.09549	0.13129	0.09598	0.10583
9	0.15075	0.15151	0.10341	0.12301	0.10037	0.10884
10	0.10595	0.16010	0.11014	0.12633	0.09804	0.10659
n_t	10	10	10	10	10	10
n_t-1	9	9	9	9	9	9
mean, y_t	0.14011	0.13266	0.11355	0.12698	0.09755	0.11021
variance, s^2_t	0.00090	0.00040	0.00017	0.00017	0.00003	0.00031
$(n_t-1)s^2_t$	0.00807	0.00362	0.00157	0.00157	0.00028	0.00279
$n_t(y_t-y)$	0.00397	0.00156	0.00044	0.00046	0.00512	0.00099

between-treatment variance, s^2_b	0.00251
within-treatment variance, s^2_w	0.00033
F ratio	7.57
v_1	5
v_2	54
α	0.01
critical value, $F(v_1,v_2,\alpha)$	3.38
Fratio	7.57
critical value, $F(v_1,v_2,\alpha)$	3.38

ANOVA Test Result:	means are significantly different
significance level:	0.01
confidence level:	99 %

Figure C.18: ANOVA test for O_{60}, significance level = 0.01

C.10 55% Opening Size (O_{55}, 55% Finer)

		% Finer	55			
number of treatments, k		6				
grand average, y		0.11413				
treatment:	water	Porewick	mineral oil	2EH	Drakeol	glycerin
	pore size	pore size	pore size	pore size	pore size	pore size
test	(mm)	(mm)	(mm)	(mm)	(mm)	(mm)
1	0.10562	0.09615	0.08964	0.12307	0.08652	0.09865
2	0.16221	0.10571	0.12027	0.09271	0.08509	0.09777
3	0.18020	0.11128	0.10099	0.10715	0.08018	0.08772
4	0.09556	0.11092	0.11454	0.11827	0.09141	0.14851
5	0.16784	0.13135	0.12129	0.12553	0.08915	0.12331
6	0.14113	0.13828	0.10716	0.12641	0.10571	0.09075
7	0.15127	0.15233	0.11861	0.11225	0.09003	0.09707
8	0.12058	0.14081	0.08794	0.11693	0.09394	0.10446
9	0.14834	0.14826	0.09656	0.11691	0.08992	0.10710
10	0.10549	0.15846	0.10423	0.11923	0.09227	0.09700
n_t	10	10	10	10	10	10
n_t-1	9	9	9	9	9	9
mean, y_t	0.13782	0.12936	0.10612	0.11585	0.09042	0.10523
variance, s^2_t	0.00086	0.00048	0.00015	0.00010	0.00004	0.00033
$(n_t-1)s^2_t$	0.00776	0.00428	0.00138	0.00090	0.00040	0.00295
$n_t(y_t-y)$	0.00561	0.00232	0.00064	0.00003	0.00562	0.00079

between-treatment variance, s^2_b	0.00300
within-treatment variance, s^2_w	0.00033
Fratio	9.18
v_1	5
v_2	54
α	0.05
critical value, $F(v_1,v_2,\alpha)$	2.39
Fratio	9.18
critical value, $F(v_1,v_2,\alpha)$	2.39

ANOVA Test Result:	means are significantly different
significance level:	0.05
confidence level:	95 %

Figure C.19: ANOVA test for O_{55}, significance level = 0.05

		% Finer	55			
number of treatments, k		6				
grand average, y		0.11413				
treatment:	water pore size	Porewick pore size	mineral oil pore size	2EH pore size	Drakeol pore size	glycerin pore size
test	(mm)	(mm)	(mm)	(mm)	(mm)	(mm)
1	0.10562	0.09615	0.08964	0.12307	0.08652	0.09865
2	0.16221	0.10571	0.12027	0.09271	0.08509	0.09777
3	0.18020	0.11128	0.10099	0.10715	0.08018	0.08772
4	0.09556	0.11092	0.11454	0.11827	0.09141	0.14851
5	0.16784	0.13135	0.12129	0.12553	0.08915	0.12331
6	0.14113	0.13828	0.10716	0.12641	0.10571	0.09075
7	0.15127	0.15233	0.11861	0.11225	0.09003	0.09707
8	0.12058	0.14081	0.08794	0.11693	0.09394	0.10446
9	0.14834	0.14826	0.09656	0.11691	0.08992	0.10710
10	0.10549	0.15846	0.10423	0.11923	0.09227	0.09700
n_t	10	10	10	10	10	10
n_t-1	9	9	9	9	9	9
mean, y_t	0.13782	0.12936	0.10612	0.11585	0.09042	0.10523
variance, s^2_t	0.00086	0.00048	0.00015	0.00010	0.00004	0.00033
$(n_t-1)s^2_t$	0.00776	0.00428	0.00138	0.00090	0.00040	0.00295
$n_t(y_t-y)$	0.00561	0.00232	0.00064	0.00003	0.00562	0.00079

between-treatment variance, s^2_b	0.00300
within-treatment variance, s^2_w	0.00033
Fratio	9.18
v_1	5
v_2	54
α	0.01
critical value, $F(v_1,v_2,\alpha)$	3.38
Fratio	9.18
critical value, $F(v_1,v_2,\alpha)$	3.38

ANOVA Test Result:	means are significantly different
significance level:	0.01
confidence level:	99 %

Figure C.20: ANOVA test for O_{55}, significance level = 0.01

C.11 50% Opening Size (O_{50}, 50% Finer)

		% Finer	50			
number of treatments, k		6				
grand average, y		0.10834				
treatment:	water	Porewick	mineral oil	2EH	Drakeol	glycerin
test	pore size (mm)	pore size (mm)	pore size (mm)	pore size (mm)	pore size (mm)	pore size (mm)
1	0.10403	0.08935	0.08627	0.11662	0.08229	0.09556
2	0.16143	0.09979	0.11211	0.08251	0.07982	0.09338
3	0.17761	0.10533	0.09364	0.10319	0.07382	0.07992
4	0.09332	0.10786	0.10841	0.11581	0.08217	0.14395
5	0.16378	0.12905	0.11335	0.11389	0.08394	0.11839
6	0.13790	0.13731	0.10033	0.11704	0.10275	0.05875
7	0.14746	0.15026	0.10901	0.10480	0.08843	0.07974
8	0.11887	0.13971	0.08226	0.11082	0.09190	0.10310
9	0.14593	0.14501	0.08994	0.11081	0.08618	0.09045
10	0.10504	0.15682	0.10023	0.11214	0.08649	0.08033
n_t	10	10	10	10	10	10
n_t-1	9	9	9	9	9	9
mean, y_t	0.13554	0.12605	0.09956	0.10876	0.08578	0.09436
variance, s^2_t	0.00083	0.00056	0.00012	0.00011	0.00006	0.00056
$(n_t-1)s^2_t$	0.00748	0.00501	0.00112	0.00096	0.00054	0.00502
$n_t(y_t-y)$	0.00740	0.00314	0.00077	0.00000	0.00509	0.00196

between-treatment variance, s^2_b	0.00367
within-treatment variance, s^2_w	0.00037
Fratio	9.85
v_1	5
v_2	54
α	0.05
critical value, $F(v_1,v_2,\alpha)$	2.39
Fratio	9.85
critical value, $F(v_1,v_2,\alpha)$	2.39

ANOVA Test Result:	means are significantly different
significance level:	0.05
confidence level:	95 %

Figure C.21: ANOVA test for O_{50}, significance level = 0.05

		% Finer	50			
number of treatments, k		6				
grand average, y		0.10834				
treatment:	water pore size	Porewick pore size	mineral oil pore size	2EH pore size	Drakeol pore size	glycerin pore size
test	(mm)	(mm)	(mm)	(mm)	(mm)	(mm)
1	0.10403	0.08935	0.08627	0.11662	0.08229	0.09556
2	0.16143	0.09979	0.11211	0.08251	0.07982	0.09338
3	0.17761	0.10533	0.09364	0.10319	0.07382	0.07992
4	0.09332	0.10786	0.10841	0.11581	0.08217	0.14395
5	0.16378	0.12905	0.11335	0.11389	0.08394	0.11839
6	0.13790	0.13731	0.10033	0.11704	0.10275	0.05875
7	0.14746	0.15026	0.10901	0.10480	0.08843	0.07974
8	0.11887	0.13971	0.08226	0.11082	0.09190	0.10310
9	0.14593	0.14501	0.08994	0.11081	0.08618	0.09045
10	0.10504	0.15682	0.10023	0.11214	0.08649	0.08033
n_t	10	10	10	10	10	10
n_t-1	9	9	9	9	9	9
mean, y_t	0.13554	0.12605	0.09956	0.10876	0.08578	0.09436
variance, s^2_t	0.00083	0.00056	0.00012	0.00011	0.00006	0.00056
$(n_t-1)s^2_t$	0.00748	0.00501	0.00112	0.00096	0.00054	0.00502
$n_t(y_t-y)$	0.00740	0.00314	0.00077	0.00000	0.00509	0.00196

between-treatment variance, s^2_b	0.00367
within-treatment variance, s^2_w	0.00037
Fratio	9.85
v_1	5
v_2	54
α	0.01
critical value, $F(v_1,v_2,\alpha)$	3.38
Fratio	9.85
critical value, $F(v_1,v_2,\alpha)$	3.38

ANOVA Test Result:	means are significantly different
significance level:	0.01
confidence level:	99 %

Figure C.22: ANOVA test for O_{50}, significance level = 0.01

C.12 45% Opening Size (O_{45}, 45% Finer)

		% Finer	45			
number of treatments, k		6				
grand average, y		0.10210				
treatment:	water	Porewick	mineral oil	2EH	Drakeol	glycerin
	pore size	pore size	pore size	pore size	pore size	pore size
test	(mm)	(mm)	(mm)	(mm)	(mm)	(mm)
1	0.10244	0.08256	0.08289	0.11017	0.07587	0.07883
2	0.16064	0.09387	0.10225	0.07854	0.07506	0.08899
3	0.17501	0.09937	0.08535	0.09756	0.05848	0.07133
4	0.09107	0.10480	0.10055	0.11336	0.06927	0.13938
5	0.15973	0.12674	0.10899	0.10590	0.07872	0.11346
6	0.13468	0.13634	0.09428	0.11040	0.08991	0.05287
7	0.14365	0.14819	0.10034	0.09938	0.08345	0.06820
8	0.11716	0.13861	0.07658	0.10470	0.08977	0.07292
9	0.14352	0.14176	0.08332	0.10471	0.08244	0.06342
10	0.10459	0.15518	0.09624	0.10504	0.08071	0.07239
n_t	10	10	10	10	10	10
n_t-1	9	9	9	9	9	9
mean, y_t	0.13325	0.12274	0.09308	0.10298	0.07837	0.08218
variance, s^2_t	0.00080	0.00065	0.00011	0.00010	0.00009	0.00067
$(n_t-1)s^2_t$	0.00722	0.00583	0.00099	0.00087	0.00081	0.00601
$n_t(y_t-y)$	0.00970	0.00426	0.00081	0.00001	0.00563	0.00397

between-treatment variance, s^2_b	0.00488
within-treatment variance, s^2_w	0.00040
Fratio	12.12
v_1	5
v_2	54
α	0.05
critical value, $F(v_1,v_2,\alpha)$	2.39
Fratio	12.12
critical value, $F(v_1,v_2,\alpha)$	2.39

ANOVA Test Result:	means are significantly different
significance level:	0.05
confidence level:	95 %

Figure C.23: ANOVA test for O_{45}, significance level = 0.01

		% Finer	45			
number of treatments, k		6				
grand average, y		0.10210				
treatment:	water pore size	Porewick pore size	mineral oil pore size	2EH pore size	Drakeol pore size	glycerin pore size
test	(mm)	(mm)	(mm)	(mm)	(mm)	(mm)
1	0.10244	0.08256	0.08289	0.11017	0.07587	0.07883
2	0.16064	0.09387	0.10225	0.07854	0.07506	0.08899
3	0.17501	0.09937	0.08535	0.09756	0.05848	0.07133
4	0.09107	0.10480	0.10055	0.11336	0.06927	0.13938
5	0.15973	0.12674	0.10899	0.10590	0.07872	0.11346
6	0.13468	0.13634	0.09428	0.11040	0.08991	0.05287
7	0.14365	0.14819	0.10034	0.09938	0.08345	0.06820
8	0.11716	0.13861	0.07658	0.10470	0.08977	0.07292
9	0.14352	0.14176	0.08332	0.10471	0.08244	0.06342
10	0.10459	0.15518	0.09624	0.10504	0.08071	0.07239
n_t	10	10	10	10	10	10
n_t-1	9	9	9	9	9	9
mean, y_t	0.13325	0.12274	0.09308	0.10298	0.07837	0.08218
variance, s^2_t	0.00080	0.00065	0.00011	0.00010	0.00009	0.00067
$(n_t-1)s^2_t$	0.00722	0.00583	0.00099	0.00087	0.00081	0.00601
$n_t(y_t-y)$	0.00970	0.00426	0.00081	0.00001	0.00563	0.00397

between-treatment variance, s^2_b	0.00488
within-treatment variance, s^2_w	0.00040
Fratio	12.12
v_1	5
v_2	54
α	0.01
critical value, $F(v_1,v_2,\alpha)$	3.38
Fratio	12.12
critical value, $F(v_1,v_2,\alpha)$	3.38

ANOVA Test Result:	means are significantly different
significance level:	0.01
confidence level:	99 %

Figure C.24: ANOVA test for O_{45}, significance level = 0.01

C.13 40% Opening Size (O_{40}, 40% Finer)

		% Finer	40			
number of treatments, k		6				
grand average, y		0.09477				
treatment:	water pore size	Porewick pore size	mineral oil pore size	2EH pore size	Drakeol pore size	glycerin pore size
test	(mm)	(mm)	(mm)	(mm)	(mm)	(mm)
1	0.10085	0.07732	0.06916	0.10225	0.06521	0.07478
2	0.15986	0.08795	0.09072	0.07456	0.05739	0.08456
3	0.17242	0.09342	0.07581	0.09346	0.04441	0.06456
4	0.08882	0.10174	0.09191	0.10762	0.06103	0.13482
5	0.15567	0.12444	0.09617	0.09779	0.06292	0.10734
6	0.13145	0.13537	0.08823	0.10085	0.06814	0.04620
7	0.13984	0.14612	0.09411	0.09279	0.07170	0.05499
8	0.11544	0.13751	0.06823	0.09739	0.08735	0.04836
9	0.14111	0.13851	0.07331	0.09861	0.07839	0.05238
10	0.10413	0.15354	0.07703	0.09795	0.07304	0.05502
n_t	10	10	10	10	10	10
n_t-1	9	9	9	9	9	9
mean, y_t	0.13096	0.11959	0.08247	0.09633	0.06696	0.07230
variance, s^2_t	0.00078	0.00073	0.00012	0.00008	0.00014	0.00084
$(n_t-1)s^2_t$	0.00699	0.00660	0.00105	0.00069	0.00126	0.00760
$n_t(y_t-y)$	0.01310	0.00616	0.00151	0.00002	0.00773	0.00505

between-treatment variance, s^2_b	0.00672
within-treatment variance, s^2_w	0.00045
Fratio	14.99
v_1	5
v_2	54
α	0.05
critical value, $F(v_1,v_2,\alpha)$	2.39
Fratio	14.99
critical value, $F(v_1,v_2,\alpha)$	2.39

ANOVA Test Result:	means are significantly different
significance level:	0.05
confidence level:	95 %

Figure C.25: ANOVA test for O_{40}, significance level = 0.05

		% Finer	40			
number of treatments, k		6				
grand average, y		0.09477				
treatment:	water pore size	Porewick pore size	mineral oil pore size	2EH pore size	Drakeol pore size	glycerin pore size
test	(mm)	(mm)	(mm)	(mm)	(mm)	(mm)
1	0.10085	0.07732	0.06916	0.10225	0.06521	0.07478
2	0.15986	0.08795	0.09072	0.07456	0.05739	0.08456
3	0.17242	0.09342	0.07581	0.09346	0.04441	0.06456
4	0.08882	0.10174	0.09191	0.10762	0.06103	0.13482
5	0.15567	0.12444	0.09617	0.09779	0.06292	0.10734
6	0.13145	0.13537	0.08823	0.10085	0.06814	0.04620
7	0.13984	0.14612	0.09411	0.09279	0.07170	0.05499
8	0.11544	0.13751	0.06823	0.09739	0.08735	0.04836
9	0.14111	0.13851	0.07331	0.09861	0.07839	0.05238
10	0.10413	0.15354	0.07703	0.09795	0.07304	0.05502
n_t	10	10	10	10	10	10
n_t-1	9	9	9	9	9	9
mean, y_t	0.13096	0.11959	0.08247	0.09633	0.06696	0.07230
variance, s^2_t	0.00078	0.00073	0.00012	0.00008	0.00014	0.00084
$(n_t-1)s^2_t$	0.00699	0.00660	0.00105	0.00069	0.00126	0.00760
$n_t(y_t-y)$	0.01310	0.00616	0.00151	0.00002	0.00773	0.00505

between-treatment variance, s^2_b	0.00672
within-treatment variance, s^2_w	0.00045
Fratio	14.99
v_1	5
v_2	54
α	0.01
critical value, $F(v_1,v_2,\alpha)$	3.38
Fratio	14.99
critical value, $F(v_1,v_2,\alpha)$	3.38

ANOVA Test Result:	means are significantly different
significance level:	0.01
confidence level:	99 %

Figure C.26: ANOVA test for O_{40}, significance level = 0.01

C.14 35% Opening Size (O_{35}, 35% Finer)

		% Finer	35			
number of treatments, k		6				
grand average, y		0.08661				
treatment:	water	Porewick	mineral oil	2EH	Drakeol	glycerin
	pore size	pore size	pore size	pore size	pore size	pore size
test	(mm)	(mm)	(mm)	(mm)	(mm)	(mm)
1	0.09926	0.07587	0.06185	0.09192	0.05250	0.05782
2	0.15907	0.08270	0.08254	0.06654	0.04457	0.06397
3	0.16983	0.08747	0.06780	0.07900	0.03687	0.05380
4	0.08657	0.09868	0.08176	0.09273	0.04811	0.10688
5	0.15162	0.12213	0.08478	0.08975	0.05831	0.08666
6	0.12823	0.13441	0.07535	0.09006	0.06129	0.04246
7	0.13603	0.14405	0.08394	0.08453	0.06054	0.04432
8	0.11373	0.13640	0.05931	0.08829	0.07252	0.04112
9	0.13871	0.13526	0.06395	0.09153	0.06459	0.04564
10	0.10368	0.15190	0.06833	0.08547	0.06364	0.04616
n_t	10	10	10	10	10	10
n_t-1	9	9	9	9	9	9
mean, y_t	0.12867	0.11689	0.07296	0.08598	0.05629	0.05888
variance, s^2_t	0.00075	0.00079	0.00010	0.00006	0.00011	0.00047
$(n_t-1)s^2_t$	0.00678	0.00707	0.00087	0.00058	0.00103	0.00426
$n_t(y_t-y)$	0.01769	0.00917	0.00186	0.00000	0.00919	0.00769

between-treatment variance, s^2_b	0.00912
within-treatment variance, s^2_w	0.00038
Fratio	23.92
v_1	5
v_2	54
α	0.05
critical value, $F(v_1,v_2,\alpha)$	2.39
Fratio	23.92
critical value, $F(v_1,v_2,\alpha)$	2.39

ANOVA Test Result:	means are significantly different
significance level:	0.05
confidence level:	95 %

Figure C.27: ANOVA test for O_{35}, significance level = 0.05

		% Finer	35			
number of treatments, k		6				
grand average, y		0.08661				
treatment:	water pore size	Porewick pore size	mineral oil pore size	2EH pore size	Drakeol pore size	glycerin pore size
test	(mm)	(mm)	(mm)	(mm)	(mm)	(mm)
1	0.09926	0.07587	0.06185	0.09192	0.05250	0.05782
2	0.15907	0.08270	0.08254	0.06654	0.04457	0.06397
3	0.16983	0.08747	0.06780	0.07900	0.03687	0.05380
4	0.08657	0.09868	0.08176	0.09273	0.04811	0.10688
5	0.15162	0.12213	0.08478	0.08975	0.05831	0.08666
6	0.12823	0.13441	0.07535	0.09006	0.06129	0.04246
7	0.13603	0.14405	0.08394	0.08453	0.06054	0.04432
8	0.11373	0.13640	0.05931	0.08829	0.07252	0.04112
9	0.13871	0.13526	0.06395	0.09153	0.06459	0.04564
10	0.10368	0.15190	0.06833	0.08547	0.06364	0.04616
n_t	10	10	10	10	10	10
n_t-1	9	9	9	9	9	9
mean, y_t	0.12867	0.11689	0.07296	0.08598	0.05629	0.05888
variance, s^2_t	0.00075	0.00079	0.00010	0.00006	0.00011	0.00047
$(n_t-1)s^2_t$	0.00678	0.00707	0.00087	0.00058	0.00103	0.00426
$n_t(y_t-y)$	0.01769	0.00917	0.00186	0.00000	0.00919	0.00769

between-treatment variance, s^2_b	0.00912
within-treatment variance, s^2_w	0.00038
Fratio	23.92
v_1	5
v_2	54
α	0.01
critical value, $F(v_1,v_2,\alpha)$	3.38
Fratio	23.92
critical value, $F(v_1,v_2,\alpha)$	3.38

ANOVA Test Result:	means are significantly different
significance level:	0.01
confidence level:	99 %

Figure C.28: ANOVA test for O_{35}, significance level = 0.01

C.15 30% Opening Size (O_{30}, 30% Finer)

		% Finer	30			
number of treatments, k		6				
grand average, y		0.07888				
treatment:	water	Porewick	mineral oil	2EH	Drakeol	glycerin
	pore size	pore size	pore size	pore size	pore size	pore size
test	(mm)	(mm)	(mm)	(mm)	(mm)	(mm)
1	0.09766	0.07441	0.05293	0.08217	0.04096	0.04748
2	0.15829	0.07994	0.07210	0.05249	0.03687	0.05694
3	0.16723	0.08151	0.05629	0.06963	0.02653	0.04616
4	0.08432	0.09562	0.06999	0.08531	0.03738	0.09095
5	0.14756	0.11983	0.07397	0.08066	0.04454	0.06587
6	0.12500	0.13344	0.06305	0.08258	0.05054	0.03446
7	0.13223	0.14199	0.07108	0.07770	0.04640	0.04081
8	0.11202	0.13530	0.05213	0.07820	0.05625	0.03675
9	0.13630	0.13202	0.05308	0.08094	0.04535	0.03942
10	0.10323	0.15027	0.05940	0.07516	0.05385	0.03857
n_t	10	10	10	10	10	10
n_t-1	9	9	9	9	9	9
mean, y_t	0.12638	0.11443	0.06240	0.07648	0.04387	0.04974
variance, s^2_t	0.00073	0.00082	0.00008	0.00009	0.00008	0.00030
$(n_t-1)s^2_t$	0.00661	0.00741	0.00069	0.00081	0.00071	0.00274
$n_t(y_t-y)$	0.02256	0.01264	0.00272	0.00006	0.01226	0.00849

between-treatment variance, s^2_b	0.01175
within-treatment variance, s^2_w	0.00035
Fratio	33.45
v_1	5
v_2	54
α	0.05
critical value, $F(v_1,v_2,\alpha)$	2.39
Fratio	33.45
critical value, $F(v_1,v_2,\alpha)$	2.39

ANOVA Test Result:	means are significantly different
significance level:	0.05
confidence level:	95 %

Figure C.29: ANOVA test for O_{30}, significance level = 0.05

		% Finer	30			
number of treatments, k		6				
grand average, y		0.07888				
treatment:	water pore size	Porewick pore size	mineral oil pore size	2EH pore size	Drakeol pore size	glycerin pore size
test	(mm)	(mm)	(mm)	(mm)	(mm)	(mm)
1	0.09766	0.07441	0.05293	0.08217	0.04096	0.04748
2	0.15829	0.07994	0.07210	0.05249	0.03687	0.05694
3	0.16723	0.08151	0.05629	0.06963	0.02653	0.04616
4	0.08432	0.09562	0.06999	0.08531	0.03738	0.09095
5	0.14756	0.11983	0.07397	0.08066	0.04454	0.06587
6	0.12500	0.13344	0.06305	0.08258	0.05054	0.03446
7	0.13223	0.14199	0.07108	0.07770	0.04640	0.04081
8	0.11202	0.13530	0.05213	0.07820	0.05625	0.03675
9	0.13630	0.13202	0.05308	0.08094	0.04535	0.03942
10	0.10323	0.15027	0.05940	0.07516	0.05385	0.03857
n_t	10	10	10	10	10	10
n_t-1	9	9	9	9	9	9
mean, y_t	0.12638	0.11443	0.06240	0.07648	0.04387	0.04974
variance, s^2_t	0.00073	0.00082	0.00008	0.00009	0.00008	0.00030
$(n_t-1)s^2_t$	0.00661	0.00741	0.00069	0.00081	0.00071	0.00274
$n_t(y_t-y)$	0.02256	0.01264	0.00272	0.00006	0.01226	0.00849

between-treatment variance, s^2_b	0.01175
within-treatment variance, s^2_w	0.00035
Fratio	33.45
v_1	5
v_2	54
α	0.01
critical value, $F(v_1,v_2,\alpha)$	3.38
Fratio	33.45
critical value, $F(v_1,v_2,\alpha)$	3.38

ANOVA Test Result:	means are significantly different
significance level:	0.01
confidence level:	99 %

Figure C.30: ANOVA test for O_{30}, significance level = 0.01

C.16 25% Opening Size (O_{25}, 25% Finer)

		% Finer	25			
number of treatments, k		6				
grand average, y		0.07689				
treatment:	water	Porewick	mineral oil	2EH	Drakeol	glycerin
	pore size	pore size	pore size	pore size	pore size	pore size
test	(mm)	(mm)	(mm)	(mm)	(mm)	(mm)
1	0.09607	0.07296	0.04262	0.06696	0.03272	0.03910
2	0.15750	0.07717	0.06232	0.04265	---	0.04899
3	0.16464	0.07602	0.04575	0.06065	---	---
4	0.08207	0.09256	0.05698	0.06692	0.02763	0.07259
5	0.14350	0.11752	0.05980	0.06753	0.03629	0.06180
6	0.12177	0.13247	0.05181	0.07264	0.04605	0.03057
7	0.12842	0.13992	0.05902	0.06534	0.04075	---
8	0.11031	0.13420	0.03605	0.06281	0.04610	---
9	0.13389	0.12856	0.04379	0.06862	0.03837	---
10	0.10277	0.14863	0.04431	0.07102	0.04561	---
n_t	10	10	10	10	8	5
n_t-1	9	9	9	9	7	4
mean, y_t	0.12410	0.11200	0.05024	0.06451	0.03919	0.05061
variance, s^2_t	0.00072	0.00086	0.00008	0.00007	0.00005	0.00029
$(n_t-1)s^2_t$	0.00645	0.00775	0.00072	0.00064	0.00032	0.00115
$n_t(y_t-y)$	0.02228	0.01233	0.00710	0.00153	0.01137	0.00345

between-treatment variance, s^2_b	0.01161
within-treatment variance, s^2_w	0.00036
Fratio	32.05
v_1	5
v_2	47
α	0.05
critical value, $F(v_1,v_2,\alpha)$	2.41
Fratio	32.05
critical value, $F(v_1,v_2,\alpha)$	2.41

ANOVA Test Result:	means are significantly different
significance level:	0.05
confidence level:	95 %

Figure C.31: ANOVA test for O_{25}, significance level = 0.05

		% Finer	25			
number of treatments, k		6				
grand average, y		0.07689				
treatment:	water pore size	Porewick pore size	mineral oil pore size	2EH pore size	Drakeol pore size	glycerin pore size
test	(mm)	(mm)	(mm)	(mm)	(mm)	(mm)
1	0.09607	0.07296	0.04262	0.06696	0.03272	0.03910
2	0.15750	0.07717	0.06232	0.04265	---	0.04899
3	0.16464	0.07602	0.04575	0.06065	---	---
4	0.08207	0.09256	0.05698	0.06692	0.02763	0.07259
5	0.14350	0.11752	0.05980	0.06753	0.03629	0.06180
6	0.12177	0.13247	0.05181	0.07264	0.04605	0.03057
7	0.12842	0.13992	0.05902	0.06534	0.04075	---
8	0.11031	0.13420	0.03605	0.06281	0.04610	---
9	0.13389	0.12856	0.04379	0.06862	0.03837	---
10	0.10277	0.14863	0.04431	0.07102	0.04561	---
n_t	10	10	10	10	8	5
n_t-1	9	9	9	9	7	4
mean, y_t	0.12410	0.11200	0.05024	0.06451	0.03919	0.05061
variance, s^2_t	0.00072	0.00086	0.00008	0.00007	0.00005	0.00029
$(n_t-1)s^2_t$	0.00645	0.00775	0.00072	0.00064	0.00032	0.00115
$n_t(y_t-y)$	0.02228	0.01233	0.00710	0.00153	0.01137	0.00345

between-treatment variance, s^2_b	0.01161
within-treatment variance, s^2_w	0.00036
Fratio	32.05
v_1	5
v_2	47
α	0.01
critical value, $F(v_1,v_2,\alpha)$	3.43
Fratio	32.05
critical value, $F(v_1,v_2,\alpha)$	3.43

ANOVA Test Result:	means are significantly different
significance level:	0.01
confidence level:	99 %

Figure C.32: ANOVA test for O_{25}, significance level = 0.01